Aero-dynam-ics

N. F. Krasnov

1

Fundamentals of Theory. Aerodynamics of an Airfoil and a Wing

Mir Publishers

Aero-dynam-ics

N. F. Krasnov

1

This textbook deals with the general laws of the flow of a fluid and with the application of aerodynamics in rocketry and modern aviation. The book is in two parts, each forming a separate volume. The first concerns the fundamental concepts and definitions of aerodynamics and the theory of flow over an airfoil or a wing, including unsteady flow, the features of gas flows at high velocities, and the thermodynamic properties of a gas at high temperatures and pressures. It considers in detail the kinematics and dynamics of a gas in the general case for a complicated model of chemically reacting viscous compressible fluids, the theory of shocks, and the method of characteristics, which is used very widely in aerodynamics. Methods for calculating the stationary aerodynamic characteristics of airfoils and wings and for finding the stability derivatives of lifting surfaces are also dealt with.

The second part describes the aerodynamic design of craft and their individual parts. The textbook was designed for use in a two-semester course in aerodynamics, although the first part can be used independently by those interested in individual areas of theoretical aerodynamics.

The book is the result of the author's experience of teaching aerodynamics at the Bauman Higher Engineering College in Moscow, USSR. Intended for college and junior-college students, it will also be a useful aid to engineers in research institutions, design departments, and industrial enterprises.

Aerodynamics
N.F. Krasnov
1

Aerodynamics
N.F. Krasnov

Aero-dynamics 1

Н. Ф. Краснов

Аэродинамика

Часть I

Основы теории
Аэродинамика профиля и крыла

Издательство
«Высшая школа»
Москва

Aerodynamics

1

N. F. Krasnov

Fundamentals of Theory. Aerodynamics of an Airfoil and a Wing

Translated from the Russian by
G. Leib

Mir Publishers Moscow

First published 1985
Revised from the 1980 Russian edition

На английском языке

© Издательство «Высшая школа», 1980
© English translation, Mir Publishers, 1985

Preface

Aerodynamics is the theoretical foundation of aeronautical, rocket, space, and artillery engineering and the cornerstone of the aerodynamic design of modern craft. The fundamentals of aerodynamics are used in studying the external flow over various bodies or the motion of air (a gas) inside various objects. Engineering success in the fields of aviation, artillery, rocketry, space flight, motor vehicle transport, and so on, i.e. fields that pertain to the flow of air or a gas in some form or other, depends on a firm knowledge of aerodynamics.

The present textbook, in addition to the general laws of flow of a fluid, treats the application of aerodynamics, chiefly in rocketry and modern high-speed aviation. The book consists of two parts, each forming a separate volume. The first of them concerns the fundamental concepts and definitions of aerodynamics and the theory of flow over an airfoil and a wing, including an unsteady flow (Chapters 1-9), while the second describes the aerodynamic design of craft and their individual parts (Chapters 10-15). The two parts are designed for use in a two-semester course of aerodynamics, although the first part can be used independently by those interested in individual problems of theoretical aerodynamics.

A sound theoretical background is important to the study of any subject because creative solutions of practical problems, scientific research, and discoveries are impossible without it. Students should therefore devote special attention to the first five chapters, which deal with the fundamental concepts and definitions of aerodynamics, the kinematics of a fluid, the fundamentals of fluid dynamics, the theory of shocks, and the method of characteristics used widely in investigating supersonic flows. Chapters 6 and 7, which relate to the flow over airfoils, are also important to a fundamental understanding of the subject. These chapters contain a fairly complete discussion of the general theory of flow of a gas in two-dimensional space (the theory of two-dimensional flow). The information on the supersonic steady flow over a wing in Chapter 8 relates directly to these materials. The aerodynamic design of most modern craft is based on studies of such flow.

One of the most topical areas of modern aerodynamic research is the study of optimal aerodynamic configurations of craft and their separate (isolated) parts (the fuselage, wing, empennage). Therefore, a small section (6.5) that defines a finite-span wing with the most advantageous planform in an incompressible flow has been included here. This section presents important practical and methodological information on the conversion of the aerodynamic coefficients of a wing from one aspect ratio to another.

The study of non-stationary gas flows is a rather well developed field of modern theoretical and practical aerodynamics. The results of this study are widely used in calculating the effect of aerodynamic forces and moments on

craft whose motion is generally characterized by non-uniformity, and the non-stationary aerodynamic characteristics thus calculated are used in the dynamics of craft when studying their flight stability. Chapter 9 concerns the general relations of the aerodynamic coefficients in unsteady flow. Aerodynamic derivatives (stability derivatives) are analysed, as is the concept of dynamic stability. Unsteady flow over a wing is also considered. The most important section of this chapter is devoted to numerical methods of calculating the stability derivatives of a lifting surface of arbitrary planform, generally with a curved leading edge (i.e. with variable sweep along the span). Both exact and approximate methods of determining the non-stationary aerodynamic characteristics of a wing are given.

A special place in the book is devoted to the most important theoretical and applied problems of high-speed aerodynamics, including the thermodynamic and kinetic parameters of dissociating gases, the equations of motion and energy, and the theory of shocks and its relation to the physicochemical properties of gases at high temperatures. Considerable attention is given to shock waves (shocks), which are a manifestation of the specific properties of supersonic flows. The concept of the thickness of a shock is discussed, and the book includes graphs of the functions characterizing changes in the parameters of a gas as it passes through a shock.

Naturally, a textbook cannot reflect the entire diversity of problems facing the science of aerodynamics. I have tried to provide the scientific information for specialists in the field of aeronautic and rocket engineering. This information, if mastered in its entirety, should be sufficient for young specialists to cope independently with other practical aerodynamic problems that may appear. Among these problems, not reflected in the book, are magnetogasdynamic investigations, the application of the method of characteristics to three-dimensional gas flows, and experimental aerodynamics. I will be happy if study of this textbook leads students to a more comprehensive, independent investigation of modern aerodynamics.

The book is the result of my experience teaching courses in aerodynamics at the N.E. Bauman Higher Engineering College in Moscow, USSR. Intended for college and junior-college students, it will also be a useful aid to specialists in research institutions, design departments, and industrial enterprises.

All physical quantities are given according to the International System of Units (SI).

In preparing the third Russian edition of the book, which the present English edition has been translated from, I took account of readers' remarks and of the valuable suggestions made by the reviewer, professor A.M. Mkhiteryan, to whom I express my profound gratitude.

Nikolai F. Krasnov

Contents

Preface 5
Introduction 13

Chapter 1 25
Basic Information from Aerodynamics

1.1. Forces Acting on a Moving Body 25
Surface Force 25
Property of Pressures in an Ideal Fluid 26
Influence of Viscosity on the Flow of a Fluid 28
1.2. Resultant Force Action 36
Components of Aerodynamic Forces and Moments 36
Conversion of Aerodynamic Forces and Moments from One Coordinate System to Another 40
1.3. Determination of Aerodynamic Forces and Moments According to the Known Distribution of the Pressure and Shear Stress. Aerodynamic Coefficients 41
Aerodynamic Forces and Moments and Their Coefficients 41
1.4. Static Equilibrium and Static Stability 52
Concept of Equilibrium and Stability 52
Static Longitudinal Stability 53
Static Lateral Stability 57
1.5. Features of Gas Flow at High Speeds 58
Compressibility of a Gas 58
Heating of a Gas 59
State of Air at High Temperatures 65

Chapter 2
Kinematics of a Fluid

2.1. Approaches to the Kinematic Investigation of a Fluid 71
Lagrangian Approach 71
Eulerian Approach 72
Streamlines and Pathlines 73
2.2. Analysis of Fluid Particle Motion 74
2.3. Vortex-Free Motion of a Fluid 79

2.4. Continuity Equation 80
General Form of the Equation 80
Cartesian Coordinate System 81
Curvilinear Coordinate System 82
Continuity Equation of Gas Flow along a Curved Surface 86
Flow Rate Equation 88
2.5. Stream Function 89
2.6. Vortex Lines 90
2.7. Velocity Circulation 91
Concept 91
Stokes Theorem 92
Vortex-Induced Velocities 94
2.8. Complex Potential 96
2.9. Kinds of Fluid Flows 97
Parallel Flow 98
Two-Dimensional Point Source and Sink 98
Three-Dimensional Source and Sink 100
Doublet 100
Circulation Flow (Vortex) 103

Chapter 3
Fundamentals of Fluid Dynamics

3.1. Equations of Motion of a Viscous Fluid 106
Cartesian Coordinates 106
Vector Form of the Equations of Motion 113
Curvilinear Coordinates 114
Cylindrical Coordinates 116
Spherical Coordinates 118
Equations of Two-Dimensional Flow of a Gas Near a Curved Surface 120
3.2. Equations of Energy and Diffusion of a Gas 121
Diffusion Equation 121
Energy Equation 124
3.3. System of Equations of Gas Dynamics. Initial and Boundary Conditions 129
3.4. Integrals of Motion for an Ideal Fluid 134
3.5. Aerodynamic Similarity 138
Concept of Similarity 138
Similarity Criteria Taking Account of the Viscosity and Heat Conduction 141
3.6. Isentropic Gas Flows 149
Configuration of Gas Jet 149
Flow Velocity 150
Pressure, Density, and Temperature 152
Flow of a Gas from a Reservoir 154

Chapter 4
Shock Wave Theory

4.1. Physical Nature of Shock Wave Formation 159
4.2. General Equations for a Shock 162
Oblique Shock 163
Normal Shock 168
4.3. Shock in the Flow of a Gas with

Constant Specific Heats 169
System of Equations 169
Formulas for Calculating the Parameters of a Gas Behind a Shock 170
Oblique Shock Angle 176
4.4. Hodograph 179
4.5. A Normal Shock in the Flow of a Gas with Constant Specific Heats 184
4.6. A Shock at Hypersonic Velocities and Constant Specific Heats of a Gas 186
4.7. A Shock in a Flow of a Gas with Varying Specific Heats and with Dissociation and Ionization 188
4.8. Relaxation Phenomena 193
Non-Equilibrium Flows 193
Equilibrium Processes 195
Relaxation Effects in Shock Waves 196

Chapter 5
Method of Characteristics

5.1. Equations for the Velocity Potential and Stream Function 200
5.2. The Cauchy Problem 205
5.3. Characteristics 209
Compatibility Conditions 209
Determination of Characteristics 209
Orthogonality of Characteristics 213
Transformation of the Equations for Characteristics in a Hodograph 214
Equations for Characteristics in a Hodograph for Particular Cases of Gas Flow 219
5.4. Outline of Solution of Gas-Dynamic Problems According to the Method of Characteristics 222
5.5. Application of the Method of Characteristics to the Solution of the Problem on Shaping the Nozzles of Supersonic Wind Tunnels 230

Chapter 6
Airfoil and Finite-Span Wing in an Incompressible Flow

6.1. Thin Airfoil in an Incompressible Flow 234
6.2. Transverse Flow over a Thin Plate 240
6.3. Thin Plate at an Angle of Attack 243
6.4. Finite-Span Wing in an Incompressible Flow 249
6.5. Wing with Optimal Planform 258
Conversion of Coefficients c_y and $c_{x,i}$ from One Wing Aspect Ratio to Another 258

Chapter 7
An Airfoil In a Compressible Flow

7.1. Subsonic Flow over a Thin Airfoil 264
Linearization of the Equation for the Velocity Potential 264
Relation Between the Parameters of a Compressible and Incompressible Fluid Flow over a Thin Airfoil 266
7.2. Khristianovich Method 269
Content of the Method 269

Conversion of the Pressure Coefficient for an Incompressible Fluid to the Number $M_\infty > 0$ 271
Conversion of the Pressure Coefficient from $M_{\infty 1} > 0$ to $M_{\infty 2} > 0$ 272
Determination of the Critical Number M 273
Aerodynamic Coefficients 274
7.3. Flow at Supercritical Velocity over an Airfoil ($M_\infty > M_{\infty,cr}$) 274
7.4. Supersonic Flow of a Gas with Constant Specific Heats over a Thin Plate 278
7.5. Parameters of a Supersonic Flow over an Airfoil with an Arbitrary Configuration 285
Use of the Method of Characteristics 285
Hypersonic Flow over a Thin Airfoil 291
Nearly Uniform Flow over a Thin Airfoil 293
Aerodynamic Forces and Their Coefficients 293
7.6. Sideslipping Wing Airfoil 298
Definition of a Sideslipping Wing 299
Aerodynamic Characteristics of a Sideslipping Wing Airfoil 301
Suction Force 305

Chapter 8
A Wing in a Supersonic Flow

8.1. Linearized Theory of Supersonic Flow over a Finite-Span Wing 308
Linearization of the Equation for the Potential Function 308
Boundary Conditions 310
Components of the Total Values of the Velocity Potentials and Aerodynamic Coefficients 313
Features of Supersonic Flow over Wings 315
8.2. Method of Sources 317
8.3. Wing with a Symmetric Airfoil and Triangular Planform ($\alpha = 0, c_{y_a} = 0$) 321
Flow over a Wing Panel with a Subsonic Leading Edge 321
Triangular Wing Symmetric about the x-Axis with Subsonic Leading Edges 326
Semi-Infinite Wing with a Supersonic Edge 328
Triangular Wing Symmetric about the x-Axis with Supersonic Leading Edges 330
8.4. Flow over a Tetragonal Symmetric Airfoil Wing with Subsonic Edges at a Zero Angle of Attack 331
8.5. Flow over a Tetragonal Symmetric Airfoil Wing with Edges of Different Kinds (Subsonic and Supersonic) 343

Leading and Middle Edges are Subsonic, Trailing Edge is Supersonic 343
Leading Edge is Subsonic, Middle and Trailing Edges are Supersonic 345
Wing with All Supersonic Edges 346
General Relation for Calculating the Drag 350
8.6. Field of Application of the Source Method 351
8.7. Doublet Distribution Method 353
8.8. Flow over a Triangular Wing with Subsonic Leading Edges 355
8.9. Flow over a Hexagonal Wing with Subsonic Leading and Supersonic Trailing Edges 366
8.10. Flow over a Hexagonal Wing with Supersonic Leading and Trailing Edges 372
8.11. Drag of Wings with Subsonic Leading Edges 381
8.12. Aerodynamic Characteristics of a Rectangular Wing 385
8.13. Reverse-Flow Method 391

Chapter 9
Aerodynamic Characteristics of Craft in Unsteady Motion

9.1. General Relations for the Aerodynamic Coefficients 395
9.2. Analysis of Stability Derivatives and Aerodynamic Coefficients 398
9.3. Conversion of Stability Derivatives upon a Change in the Position of the Force Reduction Centre 404
9.4. Particular Cases of Motion 406
Longitudinal and Lateral Motions 406
Motion of the Centre of Mass and Rotation about It 407
Pitching Motion 408
9.5. Dynamic Stability 410
Definition 410
Stability Characteristics 413
9.6. Basic Relations for Unsteady Flow 416
Aerodynamic Coefficients 416
Cauchy-Lagrange Integral 420
Wave Equation 423
9.7. Basic Methods of Solving Non-Stationary Problems 425
Method of Sources 425
Vortex Theory 428
9.8. Numerical Method of Calculating the Stability Derivatives for a Wing in an Incompressible Flow 431
Velocity Field of an Oblique Horseshoe Vortex 431
Vortex Model of a Wing 436
Calculation of Circulatory Flow 439
Aerodynamic Characteristics 446
Deformation of a Wing Surface 451

Influence of Compressibility (the Number M_∞) on Non-Stationary Flow 452
9.9. Unsteady Supersonic Flow over a Wing 456
9.10. Properties of Aerodynamic Derivatives 478
9.11. Approximate Methods for Determining the Non-Stationary Aerodynamic Characteristics 488
Hypotheses of Harmonicity and Stationarity 488
Tangent-Wedge Method 489

References 493
Supplementary Reading 494
Name Index 495
Subject Index 497

Introduction

Aerodynamics is a complex word originating from the Greek words αηρ (air) and δθναμισ (power). This name has been given to a science that, being a part of mechanics—the science of the motion of bodies in general—studies the laws of motion of air depending on the acting forces and on their basis establishes special laws of the interaction between air and a solid body moving in it.

The practical problems confronting mankind in connection with flights in heavier-than-air craft provided an impetus to the development of aerodynamics as a science. These problems were associated with the determination of the forces and moments (what we call the aerodynamic forces and moments) acting on moving bodies. The main task in investigating the action of forces was calculation of the buoyancy, or lift, force.

At the beginning of its development, aerodynamics dealt with the investigation of the motion of air at quite low speeds because aircraft at that time had a low flight speed. It is quite natural that aerodynamics was founded theoretically on **hydrodynamics**—the science dealing with the motion of a dropping (incompressible) liquid. The cornerstones of this science were laid in the 18th century by L. Euler (1707-1783) and D. Bernoulli (1700-1782), members of the Russian Academy of Sciences. In his scientific treatise "The General Principles of Motion of Fluids" (in Russian—1755), Euler for the first time derived the fundamental differential equations of motion of ideal (non-viscous) fluids. The fundamental equation of hydrodynamics establishing the relation between the pressure and speed in a flow of an incompressible fluid was discovered by Bernoulli. He published this equation in 1738 in his works "Fluid Mechanics" (in Russian).

At low flight speeds, the influence on the nature of motion of air of such its important property as compressibility is negligibly small. But the development of artillery—rifle and rocket—and high-speed aircraft moved to the forefront the task of studying the laws

of motion of air or in general of a gas at high speeds. It was found that if the forces acting on a body moving at a high speed are calculated on the basis of the laws of motion of air at low speeds, they may differ greatly from the actual forces. It became necessary to seek the explanation of this phenomenon in the nature itself of the motion of air at high speeds. It consists in a change in its density depending on the pressure, which may be quite considerable at such speeds. It is exactly this change that underlies the property of compressibility of a gas.

Compressibility causes a change in the internal energy of a gas, which must be considered when calculating the parameters determining the motion of the fluid. The change in the internal energy associated with the parameters of state and the work that a compressed gas can do upon expansion is determined by the first law of thermodynamics. Hence, thermodynamic relations were used in the aerodynamics of a compressible gas.

A liquid and air (a gas) differ from each other in their physical properties owing to their molecular structure being different. Digressing from these features, we can take into account only the basic difference between a liquid and a gas associated with the degree of their compressibility. Accordingly, in **aerohydromechanics,** which deals with the motion of liquids and gases, it is customary to use the term **fluid** to designate both a liquid and a gas, distinguishing between an incompressible and a compressible fluid when necessary.

Aerohydromechanics treats laws of motion common to both liquids and gases, which made it expedient and possible to combine the studying of these laws within the bounds of a single science of aerodynamics (or aeromechanics). In addition to the general laws characterizing the motion of fluids, there are laws obeyed only by a gas or only by a liquid.

Fluid mechanics studies the motion of fluids at a low speed at which a gas behaves practically like an incompressible liquid. In these conditions, the enthalpy of a gas is large in comparison with its kinetic energy, and one does not have to take account of the change in the enthalpy with a change in the speed of the flow, i.e. with a change in the kinetic energy of the fluid. This is why there is no need to use thermodynamic concepts and relations in low-speed aerodynamics (hydrodynamics). The mechanics of a gas differs from that of a liquid when the gas has a high speed. At such speeds, a gas flowing over a craft experiences not only a change in its density, but also an increase in its temperature that may result in various physicochemical transformations in it. A substantial part of the kinetic energy associated with the speed of a flight is converted into heat and chemical energy.

All these features of motion of a gas resulted in the appearance of **high-speed aerodynamics** or **gas dynamics**—a special branch of

aerodynamics studying the laws of motion of air (a gas) at high subsonic and supersonic speeds, and also the laws of interaction between a gas and a body travelling in it at such speeds.

One of the founders of gas dynamics was academician S. Chaplygin (1869-1942), who in 1902 published an outstanding scientific work "On Gas Jets" (in Russian). Equations are derived in this work that form the theoretical foundation of modern gas dynamics and entered the world's science under the name of the Chaplygin equations.

The development of theoretical aerodynamics was attended by the creation of **experimental aerodynamics** devoted to the experimental investigation of the interaction between a body and a gas flow past it with the aid of various technical means such as a wind tunnel that imitate the flow of aircraft.

Under the guidance of professor N. Zhukovsky (1847-1921), the first aerodynamic laboratories in Russia were erected (at the Moscow State University, the Moscow Higher Technical College, and at Kuchino, near Moscow). In 1918, the Central Aerohydrodynamic Institute (TsAGI) was organized by Zhukovsky's initiative with the direct aid of V. Lenin. At present it is one of the major world centres fo the science of aerodynamics bearing the name of N. Zhukovsky.

The development of aviation, artillery, and rocketry, and the maturing of the theoretical fundamentals of aerodynamics changed the nature of aerodynamic installations, from the first, comparatively small and low-speed wind tunnels up to the giant high-speed tunnels of TsAGI (1940) and modern hypersonic installations, and also special facilities in which a supersonic flow of a heated gas is artificially created (what we call high-temperature tunnels, shock tunnels, plasma installations, etc.).

The nature of the interaction between a gas and a body moving in it may vary. At low speeds, the interaction is mainly of a force nature. With a growth in the speed, the force interaction is attended by heating of the surface owing to heat transfer from the gas to the body: this gives rise to **thermal interaction**. At very high speeds, aerodynamic heating is so great that it may lead to failure of the material of a craft wall because of its fusion or sublimation and, as a result, to the entrainment of the destroyed material (ablation) and to a change in the nature of heating of the wall. Aerodynamic heating may also cause **chemical interaction** between a solid wall and the gas flowing over it, as a result of which the same effect of ablation appears. High flight speeds may also cause ablation as a result of **mechanical interaction** between the gas and a moving body consisting in erosion of the material of a wall and damage to its structure.

The investigation of all kinds of interaction between a gas and a craft allows one to perform aerodynamic calculations associated with the evaluation of the quantitative criteria of this interaction,

namely, with determination of the aerodynamic forces and moments, heat transfer, and ablation. As posed at present, this problem consists not only in determining the overall aerodynamic quantities (the total lift force or drag, the total heat flux from the gas to a surface, etc.), but also in evaluating the distribution of the aerodynamic properties—dynamic and thermal—over a surface of an aircraft moving through a gas (the pressure and shearing stress of friction, local heat fluxes, local ablation).

The solution of such a problem requires a deeper investigation of the flow of a gas than is needed to determine the overall aerodynamic action. It consists in determining the properties of the gas characterizing its flow at each point of the space it occupies and at each instant.

The modern methods of studying the flow of a gas are based on a number of principles and hypotheses established in aerodynamics. One of them is the **continuum hypothesis**—the assumption of the continuity of a gas flow according to which we may disregard the intermolecular distances and molecular movements and consider the continuous changes of the basic properties of a gas in space and in time. This hypothesis follows from the condition consisting in that the free path of molecules and the amplitude of their vibrational motion are sufficiently small in comparison with the linear dimensions characterizing flow around a body, for example the wing span and the diameter or length of the fuselage (or body).

The introduced continuum hypothesis should not contradict the concept of the compressibility of a gas, although the latter should seem to be incompressible in the absence of intermolecular distances. The reality of a compressible continuum follows from the circumstance that the existence of intermolecular distances may be disregarded in many investigations, but at the same time one may assume the possibility of the concentration (density) varying as a result of a change in the magnitude of these distances.

In aerodynamic investigations, the interaction between a gas and a body moving in it is based on the **principle of inverted flow** according to which a system consisting of a gas (air) at rest and a moving body is replaced with a system consisting of a moving gas and a body at rest. When one system is replaced with the other, the condition must be satisfied that the free-stream speed of the gas relative to the body at rest equals the speed of this body in the gas at rest. The principle of inverted motion follows from the general principle of relativity of classical mechanics according to which forces do not depend on which of two interacting bodies (in our case the gas or craft) is at rest and which is performing uniform rectilinear motion.

The system of differential equations underlying the solution of problems of flow over objects is customarily treated separately in

modern aerodynamics for two basic kinds of motion: free (inviscid) flow and flow in a thin layer of the gas adjacent to a wall or boundary—in the boundary layer, where motion is considered with account taken of viscosity. This division of a flow is based on the **hypothesis of the absence of the reverse influence of the boundary layer on the free flow.** According to this hypothesis, the parameters of inviscid flow, i.e. on the outer surface of the boundary layer, are the same as on a wall in the absence of this layer.

The finding of the aerodynamic parameters of craft in unsteady motion characterized by a change in the kinematic parameters with time is usually a very intricate task. Simplified ways of solving this problem are used for practical purposes. Such simplification is possible when the change occurs sufficiently slowly. This is characteristic of many craft. When determining their aerodynamic characteristics, we can proceed from the **hypothesis of steadiness** in accordance with which these characteristics in unsteady motion are assumed to be the same as in steady motion, and are determined by the kinematic parameters of this motion at a given instant.

When performing aerodynamic experiments and calculations, account must be taken of various circumstances associated with the physical similitude of the flow phenomena being studied. Aerodynamic calculations of full-scale craft (rockets, airplanes) are based on preliminary widespread investigations (theoretical and experimental) of flow over models. The conditions that must be observed in such investigations on models are found in the theory of dynamic similitude, and typical and convenient parameters determining the basic conditions of the processes being studied are established. They are called **dimensionless numbers or similarity criteria.** The modern problems of similarity and also the theory of dimensions widely used in aerodynamics are set out in a fundamental work of academician L. Sedov titled "Similarity and Dimensional Methods in Mechanics" [1].

Aerodynamics, figuratively speaking, is a multibranch science. In accordance with the needs of the rapidly developing aviation, rocket, and cosmic engineering, more or less clearly expressed basic scientific trends have taken shape in aerodynamics. They are associated with the aerodynamic investigations of craft as a whole and their individual structural elements, and also of the most characteristic kinds of gas flows and processes attending the flow over a body. It is quite natural that any classification of aerodynamics is conditional to a certain extent because all these trends or part of them are interrelated. Nevertheless, such a "branch" specialization of the aerodynamic science is of a practical interest.

The two main paths along which modern aerodynamics is developing can be determined. The first of them is what is called **force aerodynamics** occupied in solving problems connected with the

force action of a fluid, i.e. in finding the distribution of the pressure and shearing stress over the surface of a craft, and also with the distribution of the resultant aerodynamic forces and moments. The data obtained are used for strength analysis of a craft as a whole and of individual elements thereof, and also for determining its flight characteristics. The second path includes problems of **aerothermodynamics** and **aerodynamic heating**—a science combining aerodynamics, thermodynamics, and heat transfer and studying flow over bodies in connection with thermal interaction. As a result of these investigations, we find the heat fluxes from a gas to a wall and determine its temperature. These data are needed in analysing the strength and designing the cooling of craft. At the same time, the taking into account of the changes in the properties of a gas flowing over a body under the influence of high temperatures allows us to determine more precisely the quantitative criteria of force interaction of both the external flow and of the boundary layer.

All these problems are of a paramount importance for very high air speeds at which the thermal processes are very intensive. Even greater complications are introduced into the solution of such problems, however, because it is associated with the need to take into consideration the chemical processes occurring in the gas, and also the influence of chemical interaction between the gas and the material of the wall.

If we have in view the range of air speeds from low subsonic to very high supersonic ones, then, as already indicated, we can separate the following basic regions in the science of investigating flow: aerodynamics of an incompressible fluid, or fluid mechanics (the Mach number of the flow is $M = 0$), and high-speed aerodynamics. The latter, in turn, is divided into **subsonic** ($M < 1$), **transonic** ($M \approx 1$), **supersonic** ($M > 1$) and **hypersonic** ($M \gg 1$) **aerodynamics.** It must be noted that each of these branches studies flow processes that are characterized by certain specific features of flows with the indicated Mach numbers. This is why the investigation of such flows can be based on a different mathematical foundation.

We have already indicated that aerodynamic investigations are based on a division of the flow near bodies into two kinds: free (external) inviscid flow and the boundary layer. An independent section of aerodynamics is devoted to each of them.

Aerodynamics of an ideal fluid studies a free flow and investigates the distribution of the parameters in inviscid flow over a body that are treated as parameters on the boundary layer edge and, consequently, are the boundary conditions for solving the differential equations of this layer. The inviscid parameters include the pressure. If we know its distribution, we can find the relevant resultant forces and moments. Aerodynamics of an ideal fluid is based on Euler's fundamental equations.

Aerodynamics of a boundary layer is one of the broadest and most developed sections of the science of a fluid in motion. It studies viscous gas flow in a boundary layer. The solution of the problem of flow in a boundary layer makes it possible to find the distribution of the shearing stresses and, consequently, of the resultant aerodynamic forces and moments caused by friction. It also makes it possible to calculate the transfer of heat from the gas flowing over a body to a boundary. The conclusions of the boundary layer theory can also be used for correcting the solution on inviscid flow, particularly for finding the correction to the pressure distribution due to the influence of the boundary layer.

The modern theory of the boundary layer is based on fundamental investigations of A. Navier, G. Stokes, O. Reynolds, L. Prandtl, and T. von Kármán. A substantial contribution to the development of the boundary layer theory was made by the Soviet scientists A. Dorodnitsyn, L. Loitsyansky, A. Melnikov, N. Kochin, G. Petrov, V. Struminsky, and others. They created a harmonious theory of the boundary layer in a compressible gas, worked out methods of calculating the flow of a viscous fluid over various bodies (two- and three-dimensional), investigated problems of the transition of a laminar boundary layer into a turbulent one, and studied the complicated problems of turbulent motion.

In aerodynamic investigations involving low airspeeds, the thermal processes in the boundary layer do not have to be taken into account because of their low intensity. When high speeds are involved, however, account must be taken of heat transfer and of the influence of the high boundary layer temperatures on friction. It is quite natural that abundant attention is being given to the solution of such problems, especially recently. In the Soviet Union, professors L. Kalikhman, I. Kibel, V. Iyevlev and others are developing the gas-dynamic theory of heat transfer, studying the viscous flow over various bodies at high temperatures of the boundary layer. Similar problems are also being solved by a number of foreign scientists.

At hypersonic flow speeds, the problems of aerodynamic heating are not the only ones. That ionization occurs at such speeds because of the high temperatures and the gas begins to conduct electricity causes new problems associated with control of the plasma flow with the aid of a magnetic field. When describing the processes of interaction of a moving body with plasma, the relevant aerodynamic calculations must take into account electromagnetic forces in addition to gas-dynamic ones. These problems are studied in **magnetogasdynamics.**

The motion of fluids in accordance with the continuum hypothesis set out above is considered in a special branch of aerodynamics—**continuum aerodynamics.** Many theoretical problems of this branch

of aerodynamics are treated in a fundamental work of L. Sedov: "Continuum Mechanics" (in Russian—a textbook for universities) [2]. It must be noted that the continuum hypothesis holds only for conditions of flight at low altitudes, i.e. in sufficiently dense layers of the atmosphere where the mean free path of the air molecules is small. At high altitudes in conditions of a greatly rarefied atmosphere, the free path of molecules becomes quite significant, and the air can no longer be considered as a continuum. This is why the conclusions of continuum aerodynamics are not valid for such conditions.

The interaction of a rarefied gas with a body moving in it is studied in a special branch of aerodynamics—**aerodynamics of rarefied gases.** The rapid development of this science during recent years is due to the progress in space exploration with the aid of artificial satellites of the Earth and rocket-propelled vehicles, as well as in various types of rocket systems (ballistic, intercontinental, global missiles, etc.) performing flights near the earth at very high altitudes.

The conditions of flow over craft and, consequently, their aerodynamic characteristics vary depending on how the parameters of the gas change at fixed points on a surface. A broad class of flow problems of a practical significance can be solved, as already noted, in steady-state aerodynamics, presuming that the parameters are independent of the time at these points. When studying flight stability, however, account must be taken of the unsteady nature of flow due to the non-uniform airspeed, and of vibrations or rotation of the craft, because in these conditions the flow over a body is characterized by a local change in its parameters with time. The investigation of this kind of flow relates to **unsteady aerodynamics.**

We have considered a classification of modern aerodynamics by the kinds of gas flows. It is obvious that within the confines of each of these branches of aerodynamics, flow is studied as applied to various configurations of craft or their parts. In addition to such a classification, of interest are the branches of modern aerodynamics for which the configuration of a craft or its individual elements is the determining factor.

As regards its aerodynamic scheme, a modern aircraft in the generalized form is a combination of a hull (fuselage), wings, a tail unit (empennage), elevators, and rudders. When performing aerodynamic calculations of such combinations, one must take into account the effects of **aerodynamic interference**—the aerodynamic interaction between all these elements of an aircraft. Accordingly, in particular, the overall aerodynamic characteristics such as the lift force, drag, or moment must be evaluated as the sum of similar characteristics of the isolated hull, wings, tail unit, elevators, and rudders with corrections made for this interaction.

Hence, this scheme of aerodynamic calculations presumes a knowl-

edge of the aerodynamic characteristics of the separate constituent parts of an aircraft.

Aerodynamic calculations of the lifting planes of wings is the subject of a special branch of the aerodynamic science—**wing aerodynamics.** The outstanding Russian scientists and mechanics N. Zhukovsky (Joukowski) and S. Chaplygin are by right considered to be the founders of the aerodynamic theory of a wing.

The beginning of the 20th century was noted by the remarkable discovery by Zhukovsky of the nature of the lift force of a wing; he derived a formula for calculating this force that bears his name. His work on the bound vortices that are a hydrodynamic model of a wing was far ahead of his time. The series of wing profiles (Zhukovsky wing profiles) he developed were widely used in designing airplanes.

Academician S. Chaplygin is the author of many prominent works on wing aerodynamics. In 1910 in his work "On the Pressure of a Parallel Flow on Obstacles" (in Russian), he laid the foundations of the theory of an infinite-span wing. In 1922, he published the scientific work "The Theory of a Monoplane Wing" (in Russian) that sets out the theory of a number of wing profiles (Chaplygin wing profiles) and also develops the theory of stability of a monoplane wing. Chaplygin is the founder of the theory of a finite-span wing.

The fundamental ideas of Zhukovsky and Chaplygin were developed in the works of Soviet scientists specializing in aerodynamics. Associate member of the USSR Academy of Sciences V. Golubev (1884-1954) investigated the flow past short-span wings and various kinds of high-lift devices. Important results in the potential wing theory were obtained by academician M. Keldysh (1911-1978), and also by academicians M. Lavrentyev and L. Sedov. Academician A. Dorodnitsyn summarized the theory of the lifting (loaded) line for a side-slipping wing.

Considerable achievements in the theory of subsonic gas flows belong to M. Keldysh and F. Frankl, who strictly formulated the problem of a compressible flow past a wing and generalized the Kutta-Zhukovsky theorem for this case.

Academician S. Khristianovich in his work "The Flow of a Gas Past a Body at High Subsonic Speeds" (in Russian) [3] developed an original and very effective method for taking into account the influence of compressibility on the flow over airfoils of an arbitrary configuration.

The foreign scientists L. Prandtl (Germany) and H. Glauert (Great Britain) studied the problem of the influence of compressibility on flow past wings. They created an approximate theory of a thin wing in a subsonic flow at a small angle of attack. The results they obtained can be considered as particular c ses of the general theory of flow developed by Khristianovich.

A great contribution to the aerodynamics of a wing was made by academician A. Nekrasov (1883-1954), who developed a harmonious theory of a lifting plane in an unsteady flow. Keldysh and Lavrentyev solved the important problem on the flow over a vibrating airfoil by generalizing Chaplygin's method for a wing with varying circulation. Academician Sedov established general formulas for unsteady aerodynamic forces and moments acting on an arbitrarily moving wing.

Professors F. Frankl, E. Krasilshchikova, and S. Falkovich developed the theory of steady and unsteady supersonic flow over thin wings of various configurations.

Important results in studying unsteady aerodynamics of a wing were obtained by professor S. Belotserkovsky, who widely used numerical methods and computers.

The results of aerodynamic investigations of wings can be applied to the calculation of the aerodynamic characteristics of the tail unit, and also of elevators and rudders shaped like a wing. The specific features of flow over separate kinds of aerodynamic elevators and rudders and the presence of other kinds of controls resulted in the appearance of a special branch of modern aerodynamics—the **aerodynamics of controls.**

Modern rocket-type craft often have the configuration of bodies of revolution or are close to them. Combined rocket systems of the type "hull-wing-tail unit" have a hull (body of revolution) as the main component of the aerodynamic system. This explains why the **aerodynamics of hulls (bodies of revolution)**, which has become one of the important branches of today's aerodynamic science, has seen intensive development in recent years.

A major contribution to the development of aerodynamics of bodies of revolution was made by professors F. Frankl and E. Karpovich, who published an interesting scientific work "The Gas Dynamics of Slender Bodies" (in Russian).

The Soviet scientists I. Kibel and F. Frankl, who specialized in aerodynamics, developed the method of characteristics that made it possible to perform effective calculations of axisymmetric supersonic flow past pointed bodies of revolution of an arbitrary thickness.

A group of scientific workers of the Institute of Mathematics of the USSR Academy of Sciences (K. Babenko, G. Voskresensky, and others) developed a method for the numerical calculation of three-dimensional supersonic flow over slender bodies in the general case when chemical reactions in the flow are taken into account. The important problem on the supersonic flow over a slender cone was solved by the foreign specialists in aerodynamics G. Taylor (Great Britain) and Z. Copal (USA).

The intensive development of modern mathematics and computers and the improvement on this basis of the methods of aerodynamic

investigations lead to greater and greater success in solving many complicated problems of aerodynamics including the determination of the overall aerodynamic characteristics of a craft. Among them are the aerodynamic derivatives at subsonic speeds, the finding of which a work of S. Belotserkovsky and B. Skripach [4] is devoted to. In addition, approximate methods came into use for appraising the effect of aerodynamic interference and calculating the relevant corrections to aerodynamic characteristics when the latter were obtained in the form of an additive sum of the relevant characteristics of the individual (isolated) elements of a craft. The solution of such problems is the subject of a special branch of the aerodynamic science—**interference aerodynamics.**

At low supersonic speeds, aerodynamic heating is comparatively small and cannot lead to destruction of a craft member. The main problem solved in the given case is associated with the choice of the cooling for maintaining the required boundary temperature. More involved problems appear for very high airspeeds when a moving body has a tremendous store of kinetic energy. For example, if a craft has an orbital or escape speed, it is sufficient to convert only 25-30% of this energy into heat for the entire material of a structural member to evaporate. The main problem that appears, particularly, in organizing the safe re-entry of a craft into the dense layers of the atmosphere consists in dissipating this energy so that a minimum part of it will be absorbed in the form of heat by the body. It was found that blunt-nosed bodies have such a property. This is exactly what resulted in the development of aerodynamic studies of such bodies.

An important contribution to investigating the problems of **aerodynamics of blunt-nosed bodies** was made by Soviet scientists—academicians A. Dorodnitsyn, G. Cherny, O. Belotserkovsky, and others. Similar investigations were performed by M Lighthill (Great Britain), P. Garabedian (USA), and other foreign scientists.

Blunting of the front surface must be considered in a certain sense as a way of thermal protection of a craft. The blunted nose experiences the most intensive thermal action, therefore it requires thermal protection to even a greater extent than the peripheral part of the craft. The most effective protection is associated with the use of various coatings whose material at the relevant temperatures is gradually destroyed and ablated. Here a considerable part of the energy supplied by the heated air to the craft is absorbed. The development of the theory and practical methods of calculating ablation relates to a modern branch of the aerodynamic science—**aerodynamics of ablating surfaces.**

A broad range of aerodynamic problems is associated with the determination of the interaction of a fluid with a craft having an arbitrary preset shape in the general case. The shapes of craft sur-

faces can also be chosen for special purposes ensuring a definite aerodynamic effect. The shape of blunt bodies ensures a minimum transfer of heat to the entire body. Consequently, a blunt surface can be considered optimal from the viewpoint of heat transfer. In designing craft, the problem appears of choosing a shape with the minimum force action. One of these problems is associated, particularly, with determination of the shape of a craft head ensuring the smallest drag at a given airspeed. Problems of this kind are treated in a branch of aerodynamics called **aerodynamics of optimal shapes.**

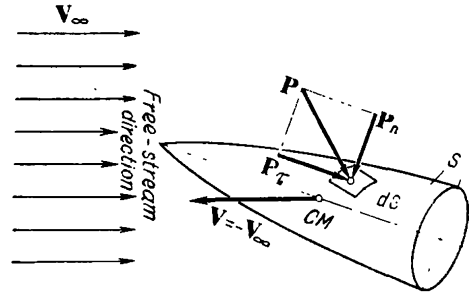

Fig. 1.1.1
Forces acting on a surface element of a moving body

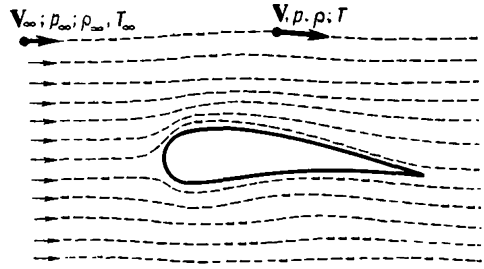

Fig. 1.1.2
Designation of parameters of disturbed and undisturbed flows

meters: the specific heats at constant pressure c_p ($c_{p\infty}$) and constant volume c_v ($c_{v\infty}$) and their ratio (the adiabatic exponent) $k = c_p/c_v$ ($k_\infty = c_{p\infty}/c_{v\infty}$).

Property of Pressures in an Ideal Fluid

To determine the property of pressures in an ideal fluid, let us take an elementary particle of the fluid having the shape of a tetrahedron $M_0M_1M_2M_3$ with edge dimensions of Δx, Δy, and Δz (Fig. 1.1.3) and compile equations of motion for the particle by equating the product of the mass of this element and its acceleration to the sum of the forces acting on it. We shall write these equations in projections onto the coordinate axes. We shall limit ourselves to the equations of motion of the tetrahedron in the projection onto the x-axis, taking into account that the other two have a similar form. The product of the mass of an element and its acceleration in the direction of the x-axis is $\rho_{av}\ \Delta W\ dV_x/dt$, where ρ_{av} is the average density of the fluid contained in the elementary volume ΔW, and dV_x/dt is the projection of the particle's acceleration onto the x-axis.

The forces acting on our particle are determined as follows. As we have already established, these forces include what we called the surface force. Here it is determined by the action of the pressure on the faces of our particle, and its projection onto the x-axis is

$$p_x\ \Delta S_x - p_n\ \Delta S_n \cos\ (\widehat{n,x}).$$

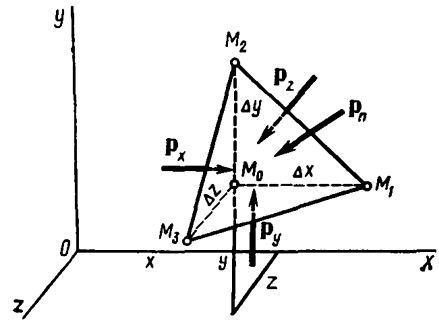

Fig. 1.1.3
Normal stresses acting on a face of an elementary fluid particle having the shape of a tetrahedron

Another force acting on the isolated fluid volume is the **mass (body) force** proportional to the mass of the particle in this volume. Mass forces include gravitational ones, and in particular the force of gravity. Another example of these forces is the mass force of an electromagnetic origin, known as a **ponderomotive force**, that appears in a gas if it is an electric conductor (ionized) and is in an electromagnetic field. Here we shall not consider the motion of a gas under the action of such forces (see a special course in magnetogasdynamics).

In the case being considered, we shall write the projection of the mass force onto the x-axis in the form of $X\rho_{av}\Delta W$, denoting by X the projection of the mass force related to a unit of mass. With account taken of these values for the projections of the surface and mass forces, we obtain an equation of motion

$$\rho_{av}\,\Delta W\,\frac{dV_x}{dt} = X\rho_{av}\,\Delta W + p_x\,\Delta S_x - p_n\,\Delta S_n\cos(\widehat{n,x})$$

where ΔS_x and ΔS_n are the areas of faces $M_0M_2M_3$ and $M_1M_2M_3$, respectively, $\cos(\widehat{n,x})$, is the cosine of the angle between a normal n to face $M_1M_2M_3$ and the x-axis, and p_x and p_n are the pressures acting on faces $M_0M_2M_3$ and $M_1M_2M_3$, respectively.

Dividing the equation obtained by ΔS_x and having in view that $\Delta S_x = \Delta S_n\cos(\widehat{n,x})$, let us pass over to the limit with Δx, Δy, and Δz tending to zero. Consequently, the terms containing $\Delta W/\Delta S_x$ will also tend to zero because ΔW is a small quantity of the third order, while ΔS_x is a small quantity of the second order in comparison with the linear dimensions of the surface element. As a result, we have $p_x - p_n = 0$, and, therefore, $p_x = p_n$.

When considering the equations of motion in projections onto the y- and z-axes, we find that $p_y = p_n$ and $p_z = p_n$.

Since our surface element with the normal n is oriented arbitrarily, we can arrive at the following conclusion from the results obtained. The pressure at any point of a flow of an ideal fluid is identical on

all surface elements passing through this point, i.e. it does not depend on the orientation of these elements. Consequently, the pressure can be treated as a scalar quantity depending only on the coordinates of a point and the time.

Influence of Viscosity on the Flow of a Fluid

Laminar and Turbulent Flow. Two modes of flow are characteristic of a viscous fluid. The first of them is **laminar** flow distinguished by the orderly arrangement of the individual filaments that do not mix with one another. Momentum, heat, and matter are transferred in a laminar flow at the expense of molecular processes of friction, heat conduction, and diffusion. Such a flow usually appears and remains stable at moderate speeds of a fluid.

If in given conditions of flow over a surface the speed of the flow exceeds a certain limiting (critical) value of it, a laminar flow stops being stable and transforms into a new kind of motion characterized by lateral mixing of the fluid and, as a result, by the vanishing of the ordered, laminar flow. Such a flow is called **turbulent.** In a turbulent flow, the mixing of macroscopic particles having velocity components perpendicular to the direction of longitudinal motion is imposed on the molecular chaotic motion characteristic of a laminar flow. This is the basic distinction of a turbulent flow from a laminar one. Another distinction is that if a laminar flow may be either steady or unsteady, a turbulent flow in its essence has an unsteady nature when the velocity and other parameters at a given point depend on the time. According to the notions of the kinetic theory of gases, random (disordered, chaotic) motion is characteristic of the particles of a fluid, as of molecules.

When studying a turbulent flow, it is convenient to deal not with the instantaneous (actual) velocity, but with its **average** (mean statistical) value during a certain time interval t_2. For example, the component of the average velocity along the x-axis is $\overline{V}_x = \\ = [1/(t_2 - t_1)] \int_{t_1}^{t_2} V_x \, dt$, where V_x is the component of the actual velocity at the given point that is a function of the time t. The components $\overline{V}_y$ and $\overline{V}_z$ along the y- and z-axes are expressed similarly. Using the concept of the average velocity, we can represent the **actual** velocity as the sum $V_x = \overline{V}_x + V'_x$ in which V'_x is a variable additional component known as the **fluctuation** velocity component (or the velocity **fluctuation**). The fluctuation components of the velocity along the y- and z-axes are denoted by V'_y and V'_z, respectively.

By placing a measuring instrument with a low inertia (for example, a hot-wire anemometer) at the required point of a flow, we can record

association", i.e. have statistically associated fluctuations. By moving together the points being considered in a turbulent flow, in the limit at $r \to 0$ we can obtain a **one-point correlation coefficient.** With this condition, (1.1.3′) acquires the form

$$R = \overline{V'_x V'_y}/(\sqrt{\overline{V'^2_x}}\sqrt{\overline{V'^2_y}}) \qquad (1.1.5)$$

This coefficient characterizes the statistical association between fluctuations at a point and, as will be shown below, directly determines the shear stress in a turbulent flow.

Turbulence will be **homogeneous** if its averaged characteristics found for a point (the level and intensity of turbulence, the one-point correlation coefficient) are the same for the entire flow (invariance of the characteristics of turbulence in transfers). Homogeneous turbulence is **isotropic** if its characteristics do not depend on the direction for which they are calculated (invariance of the characteristics of turbulence in rotation and reflection). Particularly, the following condition is satisfied for an isotropic flow:

$$\overline{V'^2_x} = \overline{V'^2_y} = \overline{V'^2_z}$$

If this condition is satisfied for all points, the turbulence is **homogeneous** and **isotropic.** For such turbulence, the constancy of the two-point correlation coefficient is retained with various directions of the line connecting the two points in the fluid volume being considered.

For an isotropic flow, the correlation coefficient (1.1.5) can be expressed in terms of the turbulence level $\varepsilon = \sqrt{\overline{V'^2_x}}/\overline{V}$:

$$R = \overline{V'_x V'_y}/\overline{V'^2_x} = \overline{V'_x V'_y}/(\overline{V}^2\varepsilon^2) \qquad (1.1.6)$$

The introduction of the concept of averaged parameters or properties appreciably facilitates the investigation of turbulent flows. Indeed, for practical purposes, there is no need to know the instantaneous values of the velocities, pressures, or shear stresses, and we can limit ourselves to their time-averaged values. The use of averaged parameters simplifies the relevant equations of motion (the Reynolds equations).

Such equations, although they are simpler, include the partial derivatives with respect to time of the averaged velocity components $\overline{V}_x$, $\overline{V}_y$, and $\overline{V}_z$ because in the general case, the turbulent motion is unsteady. In practical cases, however, averaging is performed for a sufficiently long interval of time, and now investigation of an unsteady flow can be reduced to the investigation of steady flow (quasi-steady turbulent flow).

Shear Stress. Let us consider the formula for the shear stress in a laminar flow. Here friction appears because of diffusion of the

molecules attended by transfer of the momentum from one layer to another. This leads to a change in the flow velocity, i.e. to the appearance of the relative motion of the fluid particles in the layers. In accordance with a hypothesis first advanced by I. Newton, the shear stress for given conditions is proportional to the velocity of this motion per unit distance between layers with particles moving relative to one another. If the distance between the layers is Δn and the relative speed of the particles is Δv, the ratio $\Delta v/\Delta n$ at the limit when $\Delta n \to 0$, i.e. when the layers are in contact, equals the derivative $\partial v/\partial n$ known as the **normal velocity gradient**. On the basis of this hypothesis, we can write Newton's friction law:

$$\tau = \mu \frac{\partial v}{\partial n} \tag{1.1.7}$$

where μ is a proportionality factor depending on the properties of a fluid, its temperature and pressure; it is better known as the **dynamic viscosity**.

The magnitude of μ for a gas in accordance with the formula of the kinetic theory is

$$\mu = 0.499 \rho \bar{c} l \tag{1.1.8}$$

At a given density ρ, it depends on kinetic characteristics of a gas such as the mean free path l and the mean speed $\bar{c}$ of its molecules.

Let us consider friction in a turbulent flow. We shall proceed from the simplified scheme of the appearance of additional friction forces in turbulent flow proposed by L. Prandtl for an incompressible fluid, and from the semi-empirical nature of the relations introduced for these forces. Let us take two layers in a one-dimensional flow characterized by a change in the averaged velocity only in one direction. With this in view, we shall assume that the velocity in one of the layers is such that $\bar{V}_x \neq 0$, $\bar{V}_y = \bar{V}_z = 0$. For the adjacent layer at a distance of $\Delta y = l'$ from the first one, the averaged velocity is $\bar{V}_x + (d\bar{V}_x/dy)\, l'$. According to Prandtl's hypothesis, a particle moving from the first layer into the second one retains its velocity $\bar{V}_x$ and, consequently, at the instant when this particle appears in the second layer, the fluctuation velocity $V'_x = (d\bar{V}_x/dy)\, l'$ is observed.

The momentum transferred by the fluid mass $\rho V'_y\, dS$ through the area element dS is $\rho V'_y\, (\bar{V}_x + V'_x)\, dS$. This momentum determines the additional force produced by the stress originating from the fluctuation velocities. Accordingly, the shear (friction) stress (in magnitude) in the turbulent flow due to fluctuations is

$$| \tau_t | = \rho V'_y\, (\bar{V}_x + V'_x)$$

Averaging this expression, we obtain

$$|\bar{\tau}_t| = \frac{\rho \bar{V}_x}{t_2 - t_1} \int_{t_1}^{t_2} V_y' \, dt + \frac{\rho}{t_2 - t_1} \int_{t_1}^{t_2} V_y' V_x' \, dt = \rho \bar{V}_x \bar{V}_y' + \rho \overline{V_x' V_y'}$$

where $\overline{V_x' V_y'}$ is the averaged value of the product of the fluctuation velocities, and $\bar{V}_y'$ is the averaged value of the fluctuation velocity.

We shall show that this value of the velocity equals zero. Integrating the equality $V_y = \bar{V}_y + V_y'$ termwise with respect to t within the limits from t_1 to t_2 and then dividing it by $t_2 - t_1$, we find

$$\frac{1}{t_2 - t_1} \int_{t_1}^{t_2} V_y \, dt = \frac{1}{t_2 - t_1} \int_{t_1}^{t_2} \bar{V}_y \, dt + \frac{1}{t_2 - t_1} \int_{t_1}^{t_2} V_y' \, dt$$

$$= \bar{V}_y + \frac{1}{t_2 - t_1} \int_{t_1}^{t_2} V_y' \, dt$$

But since, by definition, $\bar{V}_y = \frac{1}{t_2 - t_1} \int_{t_1}^{t_2} V_y \, dt$, it is obvious that $\bar{V}_y' = \frac{1}{t_2 - t_1} \int_{t_1}^{t_2} V_y' \, dt = 0$. Hence, the averaged value of the shear stress due to fluctuations can be expressed by the relation $|\bar{\tau}| = \rho \overline{V_x' V_y'}$ that is the generalized Reynolds formula. Its form does not depend on any specific assumptions on the structure of the turbulence.

The shear stress determined by this formula can be expressed directly in terms of the correlation coefficient. In accordance with (1.1.5), we have

$$|\tau_t| = \rho R \sqrt{\overline{V_x'^2}} \sqrt{\overline{V_y'^2}} \tag{1.1.9}$$

or for an isotropic flow for which we have $\sqrt{\overline{V_x'^2}} = \sqrt{\overline{V_y'^2}}$,

$$|\tau_t| = \rho R \overline{V_x'^2} = \rho R \varepsilon^2 \overline{V^2} \tag{1.1.9'}$$

According to this expression, an additional shear stress due to fluctuations does not necessarily appear in any flow characterized by a certain turbulence level. Its magnitude depends on the measure of the statistical mutual association of the fluctuations determined by the correlation coefficient R.

The generalized Reynolds formula for the shear stress in accordance with Prandtl's hypothesis on the proportionality of the fluctuation velocities [$V_y' = aV_x' = al' \, (d\bar{V}_x/dy)$, where a is a coefficient]

can be transformed as follows:

$$|\bar{\tau}_t| = \rho \overline{V_x' V_y'} = \frac{\rho}{t_2 - t_1} \left(\frac{d\bar{V}_x}{dy}\right)^2 \int_{t_1}^{t_2} l'^2 a \, dt = \rho l^2 \left(\frac{d\bar{V}_x}{dy}\right)^2 \qquad (1.1.10)$$

Here the proportionality coefficient a has been included in the averaged value of l', designated by l.

The quantity l is called the **mixing length** and is, as it were, an analogue of the mean free path of molecules in the kinetic theory of gases. The sign of the shear stress is determined by that of the velocity gradient. Consequently,

$$\tau_t = \rho l^2 \mid d\bar{V}_x/dy \mid d\bar{V}_x/dy \qquad (1.1.10')$$

The total value of the shear stress is obtained if to the value τ_t due to the expenditure of energy by particles on their collisions and chaotic mixing we add the shear stress occurring directly because of the viscosity and due to mixing of the molecules characteristic of a laminar flow, i.e. the value $\tau_l = \mu \, d\bar{V}_x/dy$. Hence,

$$\tau = \tau_l + \tau_t = \mu \, d\bar{V}_x/dy + \rho l^2 \mid d\bar{V}_x/dy \mid d\bar{V}_x/dy \qquad (1.1.11)$$

Prandtl's investigations show that the mixing length $l = \varkappa y$, where $\varkappa$ is a constant. Accordingly, at a wall of the body in the flow, we have

$$\tau_{y=0} = \tau_l = \mid \mu \, d\bar{V}_x/dy \mid_{y=0} \qquad (1.1.12)$$

It follows from experimental data that in a turbulent flow in direct proximity to a wall, where the intensity of mixing is very low, the shear stress remains the same as in laminar flow, and relation (1.1.12) holds for it. Beyond the limits of this flow, the stress τ_l will be very small, and we may consider that the shear stress is determined by the quantity (1.1.10').

Boundary Layer. It follows from relations (1.1.7) and (1.1.10) that for the same fluid flowing over a body, the shear stress at different sections of the flow is not the same and is determined by the magnitude of the local velocity gradient.

Investigations show that the velocity gradient is the largest near a wall because a viscous fluid experiences a retarding action owing to its adhering to the surface of the body in the fluid. The velocity of the flow is zero at the wall (see Fig. 1.1.4) and gradually increases with the distance from the surface. The shear stress changes accordingly—at the wall it is considerably greater than far from it. The thin layer of fluid adjacent to the surface of the body in a flow that is characterized by large velocity gradients along a normal to it and, consequently, by considerable shear stresses is called a **boundary layer**. In this layer, the viscous forces have a magnitude of the

same order as all the other forces (for example, the forces of inertia and pressure) governing motion and, therefore, taken into account in the equations of motion.

A physical notion of the boundary layer can be obtained if we imagine the surface in the flow to be coated with a pigment soluble in the fluid. It is obvious that the pigment diffuses into the fluid and is simultaneously carried downstream. Consequently, the coloured zone is a layer gradually thickening downstream. The coloured region of the fluid approximately coincides with the boundary layer. This region leaves the surface in the form of a coloured **wake** (see Fig. 1.1.4*a*).

As shown by observations, for a turbulent flow, the difference of the coloured region from the boundary layer is comparatively small, whereas in a laminar flow this difference may be very significant. According to theoretical and experimental investigations, with an increase, in the velocity, the thickness of the layer diminishes, and the wake becomes narrower.

The nature of the velocity distribution over the cross section of a boundary layer depends on whether it is laminar or turbulent. Owing to lateral mixing of the particles and also to their collisions, this distribution of the velocity, more exactly of its time-averaged value, will be appreciably more uniform in a turbulent flow than in a laminar one (see Fig. 1.1.4). The distribution of the velocities near the surface of a body in a flow also allows us to make the conclusion on the higher shear stress in a turbulent boundary layer determined by the increased value of the velocity gradient.

Beyond the limits of the boundary layer, there is a part of the flow where the velocity gradients and, consequently, the forces of friction are small. This part of the flow is known as the **external free flow.** In investigation of an external flow, the influence of the viscous forces is disregarded. Therefore, such a flow is also considered to be **inviscid.** The velocity in the boundary layer grows with an increasing distance from the wall and asymptotically approaches a theoretical value corresponding to the flow over the body of an inviscid fluid, i.e. to the value of the velocity in the external flow at the boundary of the layer.

We have already noted that in direct proximity to it a wall hinders mixing, and, consequently, we may assume that the part of the boundary layer adjacent to the wall is in conditions close to laminar ones. This thin section of a quasilaminar boundary layer is called a **viscous sublayer** (it is also sometimes called a **laminar sublayer**). Later investigations show that fluctuations are observed in the viscous sublayer that penetrate into it from a turbulent core, but there is no correlation between them (the correlation coefficient $R = 0$). Therefore, according to formula (1.1.9), no additional shear stresses appear.

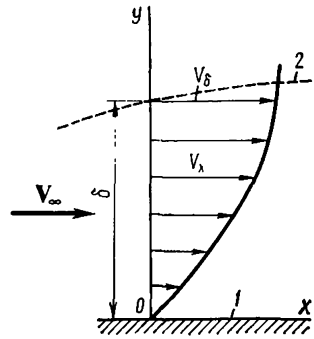

Fig. 1.1.5
Boundary layer:
1—wall of a body in the flow; *2*—outer edge of the layer

The main part of the boundary layer outside of the viscous sublayer is called the **turbulent core.** The studying of the motion in a boundary layer is associated with the simultaneous investigation of the flow of a fluid in a turbulent core and a viscous sublayer.

The change in the velocity over the cross section of the boundary layer is characterized by its gradually growing with the distance from the wall and asymptotically approaching the value of the velocity in the external flow. For practical purposes, however, it is convenient to take the part of the boundary layer in which this change occurs sufficiently rapidly, and the velocity at the boundary of this layer differs only slightly from its value in the external flow. The distance from the wall to this boundary is what is conventionally called the **thickness of the boundary layer** δ (Fig. 1.1.5). This thickness is usually defined as the distance from the contour of a body to a point in the boundary layer at which the velocity differs from its value in the external layer by not over one per cent.

The introduction of the concept of a boundary layer made possible effective research of the friction and heat transfer processes because owing to the smallness of its thickness in comparison with the dimensions of a body in a flow, it became possible to simplify the differential equations describing the motion of a gas in this region of a flow, which makes their integration easier.

1.2. Resultant Force Action

Components of Aerodynamic Forces and Moments

The forces produced by the normal and shear stresses continuously distributed over the surface of a body in a flow can be reduced to a single resultant vector $\mathbf{R}_a$ of the aerodynamic forces and a resultant vector $\mathbf{M}$ of the moment of these forces (Fig. 1.2.1) relative to a reference point called the **centre of moments**. Any point of the body

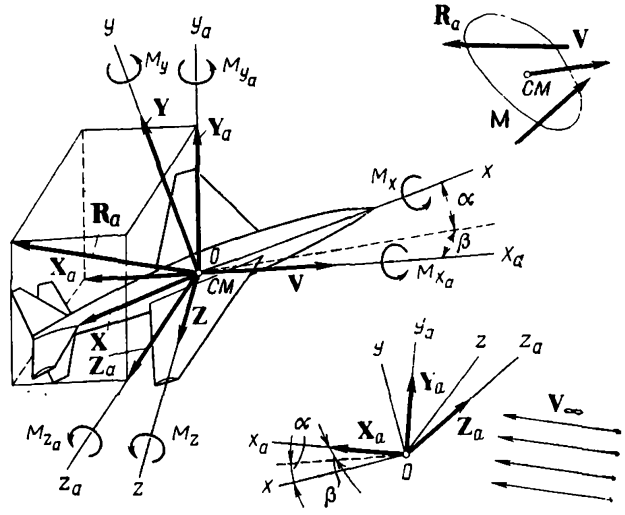

Fig. 1.2.1
Aerodynamic forces and moments acting on a craft in the flight path (x_a, y_a, and z_a) and body axis (x, y, and z) coordinate systems

can be this centre. Particularly, when testing craft in wind tunnels, the moment is found about one of the points of mounting of the model that may coincide with the nose of the body, the leading edge of a wing, etc. When studying real cases of the motion of such craft in the atmosphere, one can determine the aerodynamic moment about their centre of mass or some other point that is a centre of rotation.

In engineering practice, instead of considering the vectors $\mathbf{R}_a$ and $\mathbf{M}$, their projections onto the axes of a coordinate system are usually dealt with. Let us consider the **flight path** and **fixed** or **body axis** orthogonal coordinate systems (Fig. 1.2.1) encountered most often in aerodynamics. In the flight path system, the aerodynamic forces and moments are usually given because the investigation of many problems of flight dynamics is connected with the use of coordinate axes of exactly such a system. Particularly, it is convenient to write the equations of motion of a craft's centre of mass in projections onto these axes. The **flight path** axis Ox_a of a velocity system is always directed along the velocity vector of a craft's centre of mass. The axis Oy_a of the flight path system (the **lift axis**) is in the plane of symmetry and is directed upward (its positive direction). The axis Oz_a (the **lateral axis**) is directed along the span of the right (starboard) wing (a right-handed coordinate system). In inverted flow, the flight path axis Ox_a coincides with the direction of the flow velocity, while the axis Oz_a is directed along

the span of the left (port) wing so as to retain a right-handed coordinate system. The latter is called a **wind coordinate system.**

Aerodynamic calculations can be performed in a fixed or body axis coordinate system. In addition, rotation of a craft is usually investigated in this system because the relevant equations are written in body axes. In this system, rigidly fixed to a craft, the **longitudinal body axis** Ox is directed along the principal axis of inertia. The **normal axis** Oy is in the plane of symmetry and is oriented toward the upper part of the craft. The **lateral body axis** Oz is directed along the span of the right wing and forms a right-handed coordinate system. The positive direction of the Ox axis from the tail to the nose corresponds to non-inverted flow (Fig. 1.2.1). The origins of both coordinate systems—the flight path (wind) and the body axis systems—are at a craft's centre of mass.

The projections of the vector $\mathbf{R}_a$ onto the axes of a flight path coordinate system are called the **drag force** X_a, and **lift force** Y_a, and the **side force** Z_a, respectively. The corresponding projections of the same vector onto the axes of a body coordinate system are called the **longitudinal** X, the **normal** Y, and the **lateral** Z forces.

The projections of the vector $\mathbf{M}$ onto the axes in the two coordinate systems have the same name: the components relative to the longitudinal axis are called the **rolling moment** (the relevant symbols are M_{x_a} in a flight path system and M_x in a body one), the components relative to the vertical axis are called the **yawing moment** (M_{y_a} or M_y), and those relative to the lateral axis are called the **pitching moment** (M_{z_a} or M_z).

In accordance with the above, the vectors of the aerodynamic forces and moment in the flight path and body axis coordinate systems are:

$$\mathbf{R}_a = \mathbf{X}_a + \mathbf{Y}_a + \mathbf{Z}_a = \mathbf{X} + \mathbf{Y} + \mathbf{Z} \qquad (1.2.1)$$

$$\mathbf{M} = \mathbf{M}_{x_a} + \mathbf{M}_{y_a} + \mathbf{M}_{z_a} = \mathbf{M}_x + \mathbf{M}_y + \mathbf{M}_z \qquad (1.2.2)$$

We shall consider a moment about an axis to be positive if it tends to turn the craft counterclockwise (when watching the motion from the tip of the moment vector). In accordance with the adopted arrangement of the coordinate axes, a positive moment in Fig. 1.2.1 increases the angle of attack, and a negative moment reduces it.

The magnitude and direction of the forces and moments at a given airspeed and altitude depend on the orientation of the body relative to the velocity vector $\mathbf{V}$ (or if inverted flow is being considered, relative to the direction of the free-stream velocity $\mathbf{V}_\infty$). This orientation, in turn, underlies the relevant mutual arrangement of the coordinate systems associated with the flow and the body. This arrangement is determined by the **angle of attack** α and the **sideslip angle** β (Fig. 1.2.1). The first of them is the angle between

body axis. The angle γ is formed upon the rotation (rolling) of a craft about the longitudinal axis Ox and is measured in magnitude as the angle between the lateral body axis and the axis Oz_g displaced to a position corresponding to a zero yawing angle (or as the angle between the axis Oz and its projection onto a horizontal plane—the axis Oz_g^*). If displacement of the axis Oz_g^* with respect to the lateral axis occurs clockwise, the angle γ is positive.

The pitching angle determines the inclination of a craft to the horizon, and the yawing angle—the deviation of the direction of its flight from the initial one (for an aircraft this is the deviation from its course, for a projectile or rocket this is the deviation from the plane of launching).

Conversion of Aerodynamic Forces and Moments from One Coordinate System to Another

Knowing the angles α and β, we can convert the components of the force and moment in one coordinate system to components in another system in accordance with the rules of analytical geometry. Particularly, the components of the aerodynamic force and moment in a body axis system are converted to the drag force and the rolling moment, respectively, in a flight path system of coordinates by the formulas

$$X_a = X \cos (\widehat{xx_a}) + Y \cos (\widehat{yx_a}) + Z \cos (\widehat{zx_a}) \qquad (1.2.3)$$

$$M_{x_a} = M_x \cos (\widehat{xx_a}) + M_y \cos (\widehat{yx_a}) + M_z \cos (\widehat{zx_a}) \qquad (1.2.3')$$

where $\cos (\widehat{xx_a})$, $\cos (\widehat{yx_a})$, $\cos (\widehat{zx_a})$ are the cosines of the angles between the axis Ox_a and the axes Ox, Oy, and Oz, respectively.

The expressions for the other components of the force vector, and also for the components of the moment vector, are written in a similar way. The values of the direction cosines used for converting forces and moments from one coordinate system to another are given in Table 1.2.1.

Table 1.2.1

Body axis system	Flight path system		
	Ox_a	Oy_a	Oz_a
Ox	$\cos\alpha\cos\beta$	$\sin\alpha$	$-\cos\alpha\sin\beta$
Oy	$-\sin\alpha\cos\beta$	$\cos\alpha$	$\sin\alpha\sin\beta$
Oz	$\sin\beta$	0	$\cos\beta$

In accordance with the data of Table 1.2.1, Eqs. (1.2.3) and (1.2.3′) acquire the following form:

$$X_a = X \cos \alpha \cos \beta - Y \sin \alpha \cos \beta + Z \sin \beta \quad (1.2.4)$$

$$M_{x_a} = M_x \cos \alpha \cos \beta - M_y \sin \alpha \cos \beta + M_z \sin \beta \quad (1.2.4')$$

For example, for the motion of the aircraft shown in Fig. 1.2.1, Eq. (1.2.4) yields, with the relevant signs:

$$-X_a = -X \cos \alpha \cos \beta - Y \sin \alpha \cos \beta + Z \sin \beta$$

The force and moment components* are converted in a similar way from a flight path to a body axis coordinate system. For example, by using the data of Table 1.2.1, we obtain the following conversion formulas for the longitudinal force and the rolling moment:

$$X = X_a \cos \alpha \cos \beta + Y_a \sin \alpha - Z_a \cos \alpha \sin \beta \quad (1.2.5)$$

$$M_x = M_{x_a} \cos \alpha \cos \beta + M_{y_a} \sin \alpha - M_{z_a} \cos \alpha \sin \beta \quad (1.2.5')$$

We can go over from a local geographical coordinate system (a normal system) to a body axis or flight path one, or vice versa, if we know the cosines of the angles between the corresponding axes. Their values can be determined from Fig. 1.2.2 that shows the mutual arrangement of the axes of these coordinate systems.

1.3. Determination of Aerodynamic Forces and Moments According to the Known Distribution of the Pressure and Shear Stress. Aerodynamic Coefficients

Aerodynamic Forces and Moments and Their Coefficients

Assume that for a certain angle of attack and sideslip angle, and also for given parameters of the free stream (the speed V_∞, static pressure p_∞, density ρ_∞, and temperature T_∞), we know the distribution of the pressure p and shear stress τ over the surface of the body in the flow. We want to determine the resultant values of the aerodynamic forces and moments.

The isolated surface element dS of the body experiences a normal force produced by the excess pressure $(p - p_\infty)\, dS$ and the tangential

* We shall omit the word "components" below for brevity, but shall mean it and use formulas for scalar quantities.

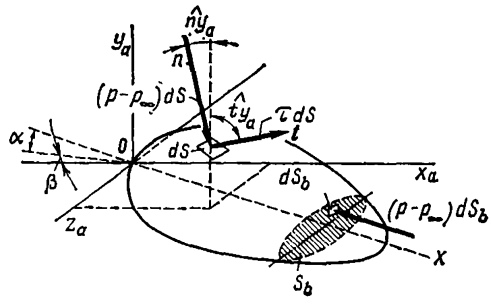

Fig. 1.3.1
Action of pressure and friction (shear) forces on an elementary area

force $\tau\, dS$. The sum of the projections of these forces onto the x-axis of a wind (flight path) coordinate system is (Fig. 1.3.1)

$$[(p - p_\infty)\cos(\widehat{n,x_a}) + \tau\cos(\widehat{t,x_a})]\, dS \qquad (1.3.1)$$

where n and t are a normal and a tangent to the element of area, respectively.

The other two projections onto the axes y_a and z_a are obtained by a similar formula with the corresponding cosines. To find the resultant forces, we have to integrate expression (1.3.1) over the entire surface S. Introducing into these equations the **pressure coefficient** $\bar{p} = (p - p_\infty)/q_\infty$ and the **local friction factor** $c_{f,x} = \tau/q_\infty$, where $q_\infty = \rho_\infty V_\infty^2/2$ is the velocity head, we obtain formulas for the drag force, the lift force, and the side force, respectively:

$$X_a = q_\infty S_r \int\limits_{(S)} [\bar{p}\cos(\widehat{n,x_a}) + c_{f,x}\cos(\widehat{t,x_a})]\, dS/S_r \qquad (1.3.2)$$

$$Y_a = q_\infty S_r \int\limits_{(S)} [-\bar{p}\cos(\widehat{n,y_a}) + c_{f,x}\cos(\widehat{t,y_a})]\, dS/S_r \qquad (1.3.3)$$

$$Z_a = -q_\infty S_r \int\limits_{(S)} [\bar{p}\cos(\widehat{n,z_a}) + c_{f,x}\cos(\widehat{t,z_a})]\, dS/S_r \qquad (1.3.4)$$

We can choose a random surface area such as that of a wing in plan view or the area of the largest cross section (the mid-section) of the fuselage as the characteristic area S_r in these formulas. The integrals in formulas (1.3.2)-(1.3.4) are dimensionless quantities taking into account how the aerodynamic forces are affected by the nature of the flow over a body of a given geometric configuration and by the distribution of the dimensionless coefficients of pressure and friction due to this flow.

In formulas (1.3.2) for the force X_a, the dimensionless quantity is usually designated by c_{x_a} and is known as the **drag coefficient.**

In the other two formulas, the corresponding symbols c_{y_a} and c_{z_a} are introduced. The relevant quantities are known as the **aerodynamic lift coefficient** and the **aerodynamic side-force coefficient.** With a view to the above, we have

$$X_a = c_{x_a} q_\infty S_r, \quad Y_a = c_{y_a} q_\infty S_r, \quad Z_a = c_{z_a} q_\infty S_r \tag{1.3.5}$$

We can obtain general relations for the moments in the same way as formulas (1.3.2)-(1.3.4) for the forces. Let us consider as an example such a relation for the pitching moment M_{z_a}. It is evident that the elementary value of this moment dM_{z_a} is determined by the sum of the moments about the axis z_a of the forces acting on an area dS in a plane at right angles to the axis z_a. If the coordinates of the area dS are y_a and x_a, the elementary value of the moment is

$$dM_{z_a} = q_\infty S_r \{[\bar{p} \cos \widehat{(n, y_a)} - c_{f,x} \cos \widehat{(t, y_a)}]\, x_a$$
$$- [\bar{p} \cos \widehat{(n, x_a)} + c_{f,x} \cos \widehat{(t, x_a)}\, y_a\}\, dS/S_r$$

Integrating this expression over the surface S and introducing the dimensionless parameter

$$m_{z_a} = \frac{M_{z_a}}{q_\infty S_r L} = \int\limits_{(S)} \{[\bar{p} \cos \widehat{(n, y_a)} - c_{f,x} \cos \widehat{(t, y_a)}]\, x_a$$
$$- [\bar{p} \cos \widehat{(n, x_a)} + c_{f,x} \cos \widehat{(t, x_a)}]\, y_a\} \frac{dS}{S_r L} \tag{1.3.6}$$

in which L is a characteristic geometric length, we obtain a formula for the pitching moment:

$$M_{z_a} = m_{z_a} q_\infty S_r L \tag{1.3.7}$$

The parameter m_{z_a} is called the **aerodynamic pitching-moment coefficient.** The formulas for the other components of the moment are written similarly:

$$M_{x_a} = m_{x_a} q_\infty S_r L \quad \text{and} \quad M_{y_a} = m_{y_a} q_\infty S_r L \tag{1.3.8}$$

The dimensionless parameters m_{x_a} and m_{y_a} are called the **aerodynamic rolling-moment** and **yawing-moment coefficients,** respectively.

The relevant coefficients of the aerodynamic forces and moments can also be introduced in a body axis coordinate system. The use of these coefficients allows the forces and moments to be written as follows:

$$\begin{aligned} X &= c_x q_\infty S_r, & M_x &= m_x q_\infty S_r L \\ Y &= c_y q_\infty S_r, & M_y &= m_y q_\infty S_r L \\ Z &= c_z q_\infty S_r, & M_z &= m_z q_\infty S_r L \end{aligned} \tag{1.3.9}$$

The quantities c_x, c_y, and c_z are called the **aerodynamic longitudinal-force, normal-force,** and **lateral-force coefficients,** and the parameters m_x, m_y, and m_z—the **aerodynamic body axis rolling-moment, yawing-moment,** and **pitching-moment coefficients,** respectively.

An analysis of the expressions for the aerodynamic forces (1.3.2)-(1.3.4) allows us to arrive at the conclusion that each of these forces can be resolved into a component due to the pressure and a component associated with the shear stresses appearing upon the motion of a viscous fluid. For example, the drag $X_a = X_{a,p} + X_{a,f}$, where $X_{a,p}$ is the **pressure drag** and $X_{a,f}$ is the **friction drag.** Accordingly, the overall coefficient of drag equals the sum of the coefficients of pressure and friction drags: $c_{x_a} = c_{x_{a,p}} + c_{x_{a,f}}$.

Similarly, the aerodynamic lift- and side-force coefficients, and also the moments, can be represented as the sum of two components. The forces, moments, and their coefficients are written in the same way in a body axes. For example, the longitudinal-force coefficient $c_x = c_{x,p} + c_{x,f}$, where $c_{x,p}$ and $x_{x,f}$ are the coefficients of the longitudinal forces due to pressure and friction, respectively.

The components of the aerodynamic forces and moments depending on friction are not always the same as those depending on the pressure as regards their order of magnitude. Investigations show that the influence of friction is more appreciable for flow over long and thin bodies. In practice, it is good to take this influence into account mainly when determining the drag or longitudinal force.

When a surface in a flow has a plane area at its tail part (a bottom cut of the fuselage or a blunt trailing edge of a wing), the pressure drag is usually divided into two more components, namely, the pressure drag on a side surface (the **nose drag**), and the drag due to the pressure on the base cut or section (the **base drag**). Hence, the overall drag and the relevant aerodynamic coefficient are

$$X_a = X_{a,n} + X_{a,b} + X_{a,f} \quad \text{and} \quad c_{x_a} = c_{x_a,n} + c_{x_a,b} + c_{x_a,f}$$

When determining the longitudinal force and its coefficient, we obtain

$$X = X_n + X_b + X_f \quad \text{and} \quad c_x = c_{x,n} + c_{x,b} + c_{x,f}$$

In accordance with Fig. 1.3.1, we have

$$X_b = -q_\infty \int_{S_b} \bar{p}_b \, dS_b \quad \text{and} \quad c_{x,b} = \frac{X_b}{q_\infty S_r}$$

where $\bar{p}_b = (p_{,b} - p_\infty)/q_\infty$ (this quantity is negative because a rarefaction appears after a bottom cut, i.e. $p_b < p_\infty$).

Characteristic Geometric Dimensions. The absolute value of an aerodynamic coefficient, which is arbitrary to a certain extent,

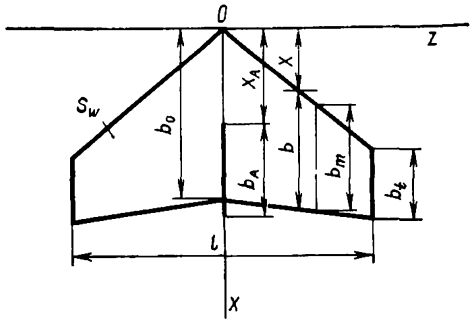

Fig. 1.3.2
Schematic view of a wing:
b_0—centre chord, b_t—tip chord, and b—local chord

depends on the choice of the characteristic geometric dimensions S_r and L. To facilitate practical calculations, however, a characteristic geometric quantity is chosen beforehand. In aerospace technology, the area of the mid-section (the largest cross section) of the body $S_r = S_{mid}$ is usually chosen as the characteristic area, and the length of the rocket is taken as the characteristic linear dimension L.

In aerodynamic calculations of aircraft, the wing plan area $S_r = S_w$, the wing span l (the distance between the wing tips) or the wing chord b are adopted as the characteristic dimensions. By the **chord of a wing** is meant a length equal to the distance between the farthest points of an airfoil (section). For a wing with a rectangular planform, the chord equals the width of the wing. In practice, a wing usually has a chord varying along its span. Either the **mean geometric chord** $b = b_m$ equal to $b_m = S_w/l$ or the mean **aerodynamic chord** $b = b_A$ is taken as the characteristic dimension for such a wing. The mean aerodynamic chord is determined as the chord of the airfoil of an equivalent rectangular wing for which with an identical wing plan area the moment aerodynamic characteristics are approximately the same as of the given wing.

The length of the mean aerodynamic chord and the coordinate of its leading edge are determined as follows (Fig. 1.3.2):

$$b_A = \frac{2}{S_w}\int_0^{l/2} b^2\,dz, \qquad x_A = \frac{2}{S_w}\int_0^{l/2} bx\,dz$$

When calculating forces and moments according to known aerodynamic coefficients, the geometric dimensions must be used for which these coefficients were evaluated. Should such calculations have to be performed for other geometric dimensions, the aerodynamic coefficients must be preliminarily converted to the relevant geometric dimension. For this purpose, one must use the relations $c_1S_1 = c_2S_2$ (for the force coefficients), and $m_1S_1L_1 = m_2S_2L_2$ (for the moment coefficients) obtained from the conditions of the constancy

1.4. Static Equilibrium and Static Stability

Concept of Equilibrium and Stability

The state of static equilibrium is determined by the flight conditions and the corresponding force action at which the overall aerodynamic moment about the centre of mass in the absence of rotation and with the angle of attack and the sideslip angle remaining constant is zero ($\mathbf{M} = 0$). Such equilibrium corresponds to conditions of steady rectilinear motion of a craft, when the parameters of this motion do not depend on the time.

It is evident that for axisymmetric configurations over which the fluid flows in a longitudinal direction, the equality $\mathbf{M} = 0$ is achieved with undeflected elevators and rudders and with zero angles of attack and sideslip. Hence, in this case, equilibrium, called the **trim equilibrium of a craft**, sets in at the **balance angle of attack** and **sideslip angle** (α_{bal}, β_{bal}) equal to zero. The need to balance flight at other angles ($\alpha \neq \alpha_{bal}$ and $\beta \neq \beta_{bal}$) requires the corresponding turning of the elevators.

Equilibrium of a craft (particularly. with the elevators fixed in place) may be stable or unstable. Equilibrium of a craft is considered to be **stable** if after the introduction of a random short-time disturbance it returns to its initial position. If these disturbances cause it to deflect still more from the initial position, equilibrium is said to be **unstable.**

The nature of the equilibrium of a craft is determined by its **static stability** or **instability.** To reveal the essence of static stability, we can consider the flow of air in a wind tunnel past a craft fixed at its centre of mass and capable of turning about it (Fig. 1.4.1). For a given elevator angle δ_e, a definite value of the aerodynamic moment M_z corresponds to each value of the angle of deflection of the craft α (the angle of attack). A possible relation between α and M_z for a certain angle δ_e is shown in Fig. 1.4.1, where points *1*, *2*, and *3* determining the balance angles α_{1bal}, α_{2bal}, and α_{3bal} at which the aerodynamic moment equals zero correspond to the equilibrium positions. The figure also shows two other moment curves for the elevator angles δ_e' and δ_e''.

Let us consider equilibrium at point *1*. If the craft is deviated through an angle smaller or larger than α_{1bal}, the induced moments, positive or negative, respectively, will result in an increase (reduction) of this angle to its previous value α_{1bal}, i.e. these moments are **stabilizing** ones. Consequently, the position of equilibrium at point *1* is stable (the craft is statically stable). It can be shown similarly that such a position of stable equilibrium also corresponds to point *3*.

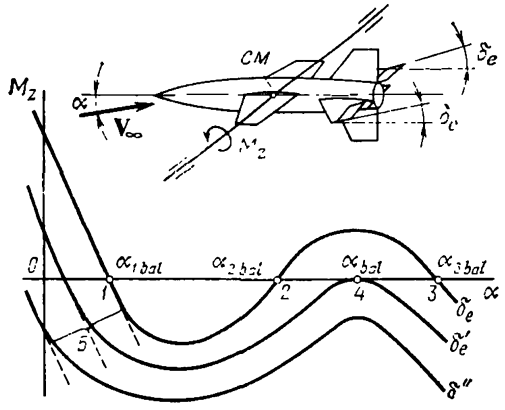

Fig. 1.4.1
Dependence of the aerodynamic moment M_z on the angle of attack α of a craft and the deflection of the elevators δ_e:
1, 2, 3, 4—points of intersection of the moment curve with the α-axis that determine the balance angles of attack; *5*—region of a linear change in the pitching moment with the angle of attack and the elevator angle

In the first case, free rotation of the craft continues until it occupies the equilibrium position at point *1*, and in the second case—at point *3*.

At point 2 (α_{2bal}) the equilibrium is unstable. Indeed, examination of Fig. 1.4.1 reveals that at values of the angle α larger or smaller than α_{2bal}, moments are induced, positive or negative, respectively, that tend to increase (or reduce) α. Hence, these moments are **destabilizing**, and the craft will be statically unstable.

Static stability is schematically divided into longitudinal and lateral stability. For static longitudinal stability, it is assumed that all the disturbing forces and moments act in the longitudinal plane of the body axes xOy. Hence, only such movements of a craft are investigated that occur in its plane of symmetry in the absence of roll and slip. When analysing static lateral stability, the disturbed movements of a craft are considered that are associated with a change in the rolling and sideslip angles at a constant angle of attack. Such movements are always mutually related. Deflection of the ailerons causes not only roll, but also slip. At the same time, turning of the rudders also leads to rolling. Therefore investigation of lateral stability is associated with an analysis of both rolling and yawing moments.

Static Longitudinal Stability

When such stability exists, an induced longitudinal moment about the centre of mass will be stabilizing. In this case, the direction of the change in the moment M_z (and accordingly of the coefficient m_z) is opposite to the change in the angle α. Consequently, the condition of static longitudinal stability can be expressed in accordance with one of the curves shown in Fig. 1.4.1 by the inequalities $\partial M_z/\partial\alpha < 0$ or $\partial m_z/\partial\alpha = m_z^\alpha < 0$ (the derivatives are evaluated for the balance angle of attack $\alpha = \alpha_{bal}$).

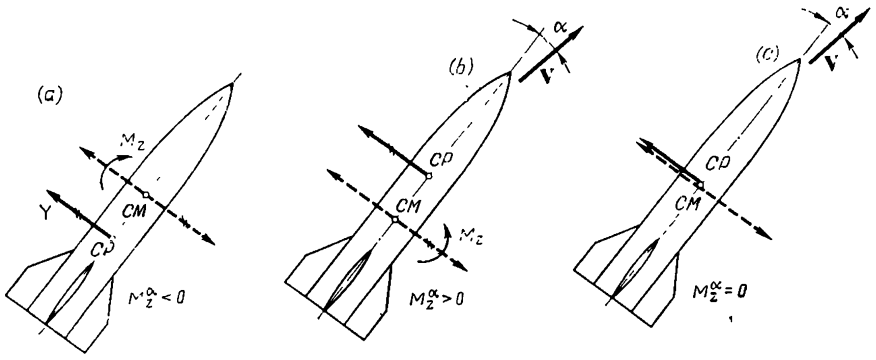

Fig. 1.4.2
Action of a force and moment in analysing the static stability of a craft: *a*—static stability; *b*—static instability; *c*—neutrality relative to static stability

With **static longitudinal instability,** a destabilizing (tilting) moment appears that tends to increase the angle of attack in comparison with its balance value. Consequently, the inequalities $\partial M_z/\partial\alpha > 0$ or $m_z^\alpha > 0$ are the condition for static longitudinal instability.

A craft will be **neutral** relative to static longitudinal stability if upon a small deflection from the balance angle of attack neither a stabilizing nor a destabilizing moment is induced. This angle of attack $\alpha = \alpha_{bal}$ in Fig. 1.4.1 corresponds to point *4* at which the moment curve is tangent to the horizontal axis. It is obvious that here the coefficient of the restoring moment $\Delta m_z = m_{z\alpha_{bal}}^\alpha \Delta\alpha = 0$.

Criteria of Static Stability. The derivative m_z^α on which the magnitude of the stabilizing or destabilizing moment depends is called the **coefficient (degree) of static longitudinal stability.** This stability criterion relates to configurations both with and without axial symmetry.

For axisymmetric craft, we can assume that the criterion of static stability equals the difference between the distances from the nose of a craft to its centre of mass and centre of pressure, i.e. the quantity $Y = x_{CM} - x_p$, or in the dimensionless form

$$\bar{Y} = x_{CM}/b - x_p/b = \bar{x}_{CM} - c_p$$

If the coefficient of the centre of pressure c_p is larger than the relative coordinate of the centre of mass $\bar{x}_{CM}$, i.e. if the centre of pressure is behind the centre of mass, the craft is statically stable; when the centre of pressure is in front (the difference $\bar{x}_{CM} - c_p$ is positive), the craft is statically unstable; when both centres coincide, the craft is neutral.

The action of the relevant pitching moments about a lateral axis passing through the centre of mass is shown in Fig. 1.4.2.

The criterion $\bar{Y} = \bar{x}_{CM} - c_p$ determines the **margin of static stability**. It may be negative (static stability), positive (static instability), and zero (neutrality relative to longitudinal stability).

The quantity $\bar{Y}$ is determined by the formula $\bar{Y} = m_z/c_y$ in which the pitching moment coefficient is evaluated about the centre of mass. For small values of α, the coefficients m_z and c_y can be written in the form $m_z = m_z^\alpha \alpha$, and $c_y = c_y^\alpha \alpha$. With this taken into account, we have

$$Y = m_z^\alpha / c_y^\alpha = \partial m_z / \partial c_y = \bar{x}_{CM} - c_p \qquad (1.4.1)$$

Hence it follows that the derivative $\partial m_z/\partial c_y = m_z^{c_y}$ may be considered as a criterion determining the qualitative and quantitative characteristics of longitudinal stability. If $m_z^{c_y} < 0$, we have static longitudinal stability, if $m_z^{c_y} > 0$, we have instability, and if $m_z^{c_y} = 0$, we have neutrality. The parameter $m_z^{c_y}$ is also called the **coefficient (degree) of static longitudinal stability**.

To appraise the static stability of asymmetric craft or of symmetric craft with deflected elevators, the concept of the aerodynamic centre is used. The dimensionless coordinate of this point with respect to the angle of attack is determined by the formula $\bar{x}_{F_\alpha} = -m_z^{c_y}$. Taking this into account and assuming in (1.3.17) that the quantity x_n equals the coordinate x_{CM} of the centre of mass, we obtain

$$m_z = m_{z0} - c_y (\bar{x}_{F_\alpha} - \bar{x}_{CM})$$

Differentiation of this expression with respect to c_y yields

$$m_z^{c_y} = -(\bar{x}_{F_\alpha} - \bar{x}_{CM}) \qquad (1.4.2)$$

Accordingly, the longitudinal stability is determined by the mutual arrangement of the aerodynamic centre and centre of mass of a craft. When the aerodynamic centre is behind the centre of mass (the difference $\bar{x}_{F_\alpha} - \bar{x}_{CM}$ is positive), the relevant craft is statically stable, and when it is in front of the centre of mass (the difference $\bar{x}_{F_\alpha} - \bar{x}_{CM}$ is negative), the craft is unstable.

By correspondingly choosing the centre of mass (or by centering), we can ensure the required margin of static stability. Centering (trimming) is **central** if the centre of mass coincides with the aerodynamic centre of the craft.

When the centering is changed, the degree of longitudinal stability is

$$m_z^{c_y} = (m_z^{c_y})' + \bar{x}_{CM} - \bar{x}'_{CM} \qquad (1.4.2')$$

where the primed parameters correspond to the previous centering of the craft.

Influence of Elevator Deflection. Investigations show (see Fig. 1.4.1) that when the moment curve $M_z = f(\alpha)$ is not linear, its slope at the points of intersection with the horizontal axis is not the same for different elevator angles. This indicates a difference in the value of the coefficients of static longitudinal stability. A glance at Fig. 1.4.1, for example, shows that upon a certain deflection of the elevator (δ_e), stability at low angles of attack ($\alpha \approx \alpha_{1bal}$) may change to instability at larger values of them ($\alpha \approx \alpha_{2bal}$) and may be restored at still larger angles ($\alpha \approx \alpha_{3bal}$). To avoid this phenomenon, it is necessary to limit the range of the angles of attack to low values at which a linear dependence of the pitching moment coefficient on the angle of attack and elevator angle is retained. In this case, the degree of stability does not change because at all possible (small) elevator angles the inclination of the moment curve to the axis of abscissas is the same.

The condition of a linear nature of the moment characteristic makes it possible to use concepts such as the aerodynamic centre or neutral centering ($x_{F_\alpha} = x_{CM}$) when studying the flying properties of craft. These concepts lose their sense when the linear nature is violated.

Longitudinal Balancing. Let us consider a flight at a uniform speed in a longitudinal plane along a curvilinear trajectory with a constant radius of curvature. Such a flight is characterized by a constant angular velocity Ω_z about a lateral axis passing through the centre of mass. This velocity can exist provided that the inclination of the trajectory changes insignificantly.

The constancy of the angular velocity is due to the equilibrium of the pitching moments about the lateral axis, i.e. to longitudinal balancing of the craft at which the equality $M_z = 0$ holds, i.e.

$$m_{z0} + m_z^{\alpha}\alpha_{bal} + m_z^{\delta_e}\delta_e + m_z^{\Omega_z}\Omega_z = 0$$

This equation allows us to find the elevator angle needed to ensure balanced flight at the given values of α_{bal} and Ω_z:

$$\delta_{e.bal} = -(1/m_z^{\delta_e})\,(m_{z0} + m_z^{\alpha}\alpha_{bal} + m_z^{\Omega_z}\Omega_z) \qquad (1.4.3)$$

For conditions of a high static stability, we have $m_z^{\Omega_z}\Omega_z \ll m_z^{\alpha}\alpha_{bal}$; consequently

$$\delta_{e.bal} = (-1/m_z^{\delta_e})\,(m_{z0} + m_z^{\alpha}\alpha_{bal}) \qquad (1.4.3')$$

For a craft with an axisymmetric configuration, $m_{z0} = 0$, therefore

$$\delta_{e.bal} = -(m_z^{\alpha}/m_z^{\delta_e})\,\alpha_{bal} \qquad (1.4.4)$$

The normal (lift) force coefficient corresponds to the balance angle of attack and elevator angle, namely,

$$c_{y.bal} = c_{y0} + (c_y^{\alpha} + c_y^{\delta_e}\delta_{e.bal}/\alpha_{bal})\,\alpha_{bal} \qquad (1.4.5)$$

The values of c_{y0} are usually very small even for asymmetric configurations (at low δ_e and α) and equal zero exactly for craft with axial symmetry. Hence, with a sufficient degree of accuracy, we can write

$$c_{y.bal} = (c_y^{\alpha} + c_y^{\delta_e}\delta_{e.bal}/\alpha_{bal})\,\alpha_{bal} \qquad (1.4.6)$$

Static Lateral Stability

To analyse the lateral stability of a craft, one must consider jointly the nature of the change in the rolling and sideslip angles upon the simultaneous action of the perturbing rolling M_x and yawing M_y moments. If after the stopping of such action these angles diminish, tending to their initial values, we have static lateral stability. Hence, when investigating lateral stability, one must consider simultaneously the change in the aerodynamic coefficients m_x and m_y. In most practical cases, however, lateral stability can be divided into two simpler kinds—rolling stability and directional stability—and can be studied separately by considering the change in the relevant moment coefficients m_x (γ) and m_y (β).

Let us consider **static rolling stability**. Assume that in steady motion at the angle of attack α_d the craft is turned about the axis Ox through a certain rolling angle γ. This turn with a constant orientation of the axis Ox relative to the velocity vector **V** causes the appearance of the angle of attack $\alpha \approx \alpha_d \cos\gamma$ and the sideslip angle $\beta \approx \alpha_d \sin\gamma$. The slip, in turn, causes a rolling moment to appear whose coefficient $m_x = m_x^{\beta}\beta \approx m_x^{\beta}\alpha_d \sin\gamma$. Differentiating with respect to γ, we obtain $m_x^{\gamma} = m_x^{\beta}\alpha$.

The derivative m_x^{γ} is a measure of the static rolling stability. If $m_x^{\gamma} < 0$ (the moment tends to eliminate rolling), the craft has static rolling stability; at $m_x^{\gamma} > 0$, a disturbing moment is formed, and **static rolling instability** sets in; when $m_x^{\gamma} = 0$, the craft is neutral with respect to rolling stability.

Since a flight usually occurs at positive angles of attack, the signs of the derivatives m_x^{γ} and m_x^{β} coincide. Hence, in analysing rolling motion, we can use the derivative m_x^{β} known as the **coefficient (degree) of static rolling stability.**

Static directional stability is characterized by a coefficient (degree) determined by the derivative $\partial M_y/\partial\beta$ (or $\partial m_y/\partial\beta = m_y^{\beta}$). If the quantity $m_y^{\beta} < 0$, the craft has static directional stability; at $m_y^{\beta} > 0$, it has static instability, and when $m_y^{\beta} = 0$, neutrality.

The concept of directional stability is associated with the property of a craft to eliminate an appearing sideslip angle β. At the same time, a craft does not maintain the stability of its own flight direction because after changing its direction of motion under the action of various disturbances, it does not return to its previous

direction, but like a weathercock, turns with its nose part in the direction of the new vleocity vector V.

Similar to the aerodynamic centre based on the angle of attack, we can introduce the concept of the **aerodynamic centre based on the sideslip angle** whose coordinate we shall designate by x_{F_β}. Using this concept, we can represent the degree of static directional stability in the form

$$m_y^{cz} = -(\bar{x}_{F_\beta} - \bar{x}_{CM}) \tag{1.4.7}$$

where $\bar{x}_{F_\beta} = x_{F_\beta}/l$ and $\bar{x}_{CM} = x_{CM}/l$ (l is a characteristic geometric dimension that can determine the wing span, fuselage length, etc.).

Hence, the static directional stability or instability depends on the mutual position of the centre of mass and the aerodynamic centre. A rear arrangement of the aerodynamic centre ($\bar{x}_{F_\beta} > \bar{x}_{CM}$) determines static directional stability ($m_y^{cz} < 0$), while its front arrangement ($\bar{x}_{F_\beta} < \bar{x}_{CM}$) determines static instability ($m_y^{cz} > 0$). When the two centres coincide ($\bar{x}_{F_\beta} = \bar{x}_{CM}$), the craft is neutral as regards static directional stability ($m_y^{cz} = 0$).

A particular case of motion of a craft in the plane of the angle of attack can be characterized by a constant angular velocity ($\Omega_y = \text{const}$) and stabilization with respect to rolling with the aid of an automatic pilot ($\Omega_x \approx 0$). The condition for such steady motion is **lateral trim** of the craft when the yawing moment vanishes, i.e.

$$m_y = m_{y0} + m_y^\beta \beta + m_y^{\delta_r} \delta_r + m_y^{\Omega_y} \Omega_y = 0$$

All craft customarily have longitudinal symmetry, therefore $m_{y_0} = 0$. When this condition holds, the equation obtained allows us to determine the balance rudder angle $\delta_r = \delta_{r.bal}$ corresponding to the given values of the balance sideslip angle β_{bal} and the angular velocity Ω_y. Most craft have a sufficiently high degree of static directional stability at which the term $m_y^{\Omega_y} \Omega_y$ is negligible. Therefore

$$\delta_{r.bal} = (-m_y^\beta / m_y^{\delta_r}) \beta_{bal} \tag{1.4.8}$$

This relation, like (1.4.4), will be accurate for conditions of rectilinear motion.

1.5. Features of Gas Flow at High Speeds

Compressibility of a Gas

One of the important properties of a gas is its compressibility—its ability to change its density under the action of a pressure. All the processes associated with the flow of a gas are characterized by

a change in the pressure and, consequently, by the influence of compressibility on these processes to some extent. Investigations show that as long as the speeds are low, the change in the density owing to insignificant changes in the pressure is not large, and the effect of compressibility may be ignored. To study low-speed flow over bodies, one may use the equations of hydrodynamics that studies the laws of motion of an incompressible fluid.

In practice, the influence of compressibility may be ignored in the range of air speeds from a few metres per second to 100-150 m/s. In real conditions, this corresponds to Mach numbers from $M_\infty = V_\infty/a_\infty = 0$ to $M_\infty = 0.3$-0.45 (here a_∞ is the speed of sound in an undisturbed flow). Idealization of the process consists in assuming the Mach number to equal zero within this region of speeds because small disturbances (sound oscillations) propagate in an incompressible fluid at an infinitely high speed and, consequently, the ratio of the flight speed to that of sound tends to zero.

Modern craft have high airspeeds at which flow over them is attended by a considerable change in the pressure and, consequently, by a substantial change in the density and temperature. In the conditions of a flight at high speeds, one must take into account the influence of compressibility, which may be very significant, on the effects of interaction of the fluid and a body. This is one of the most important features of high-speed aerodynamics.

Heating of a Gas

The appreciable increase in the speeds of craft made it necessary to take into account the features of gas streams due to the change in the physicochemical properties of the air in aerodynamic investigations. In "conventional" supersonic aerodynamics, the compressibility was taken into consideration as the most important manifestation of a feature of flow at high speeds, while the influence of the temperature on the thermodynamic parameters and kinetic coefficients of air, and also on the physicochemical processes that may proceed in it was disregarded. For very high (hypersonic) speeds, however, the features associated with the influence of high temperatures come to the forefront.

High temperatures appear owing to deceleration of the gas stream when the kinetic energy of ordered motion of the particles transforms into the internal energy of the gas.

At a temperature of the order of 1500 K, **excitation of the vibrational levels** of the internal energy of the oxygen and nitrogen molecules in the air becomes noticeable. At a temperature of about 3000 K and a pressure of 10^5 Pa, the vibrational degrees of freedom of the oxygen molecules are completely excited, and further elevation of the temperature allows the atoms to surmount the action

of the intramolecular forces. As a result, for example, a diatomic molecule breaks up into two individual atoms. This process is known as **dissociation**. The latter is attended by **recombination**—the formation of a new molecule when two atoms collide ($O_2 \rightleftarrows 2O$). This heat-producing reaction is accompanied by the collision of two atoms with a third particle that carries off part of the released energy and thus ensures the creation of a stable molecule. In addition, chemical reactions occur in the air that result in the appearance of a certain amount of nitrogen monoxide NO. The latter also dissociates upon further heating with the formation of atomic nitrogen and oxygen by the equations

$$N_2 + O_2 \rightleftarrows 2NO, \quad N_2 + O \rightleftarrows NO + N, \text{ or } N + O_2 \rightleftarrows NO + O$$

At a temperature of 5000-6000 K and a pressure of 10^5 Pa, the oxygen molecules dissociate almost completely. In addition, at such a temperature, the major part of the nitrogen molecules dissociate with simultaneous recombination of the atoms into molecules. This process follows the equation $N_2 \rightleftarrows 2N$. The intensity of dissociation is determined by the **degree of dissociation**. It equals the ratio of the number of air particles broken up in dissociation to the total number of atoms and molecules. The degree of dissociation depends on the temperature and pressure.

Elevation of the temperature is attended by an increase in the degree of dissociation because the speed and energy of the moving molecules grow, and this increases the probability of their collision and decomposition. The intensity of dissociation grows with lowering of the pressure (density) because of the lesser probability of triple collisions of the particles that lead to the formation of molecules from atoms. For example, oxygen begins to dissociate already at $T = 2000$ K if the pressure is 10^2 Pa, whereas at standard atmospheric pressure (approximately 10^5 Pa) O_2 begins to dissociate at $T = 3000$ K. The temperature at which nitrogen begins to dissociate lowers from 6000 K at a pressure of 10^5 Pa to 4000 K at 10 Pa.

At 5000-6000 K, still another process begins to develop. It consists in that because of the large influx of energy, first the electron degrees of freedom are excited, and then electrons break away from the nitrogen and oxygen atoms and also from the nitrogen monoxide molecules. This process is called **ionization**. It occurs mainly because of collision of the air particles in their thermal motion, which explains why it is also called **thermal ionization**. Ionization is more intensive with elevation of the temperature and is attended by a growth in the concentration of the free electrons. The intensity of this process is characterized by the **degree of ionization**. It equals the ratio of the number of ionized atoms (molecules) to their total number. Investigations show that nitrogen, for example, is fully ionized

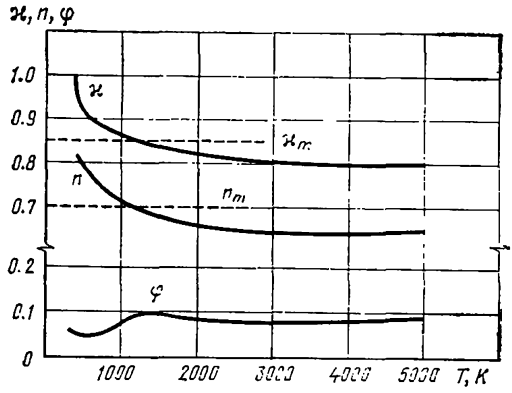

Fig. 1.5.1
Change in the exponents φ, n, and $\varkappa$ in the relevant formulas for determining the specific heat, dynamic viscosity, and thermal conductivity

thermally (the degree of ionization is unity) at a temperature of 17 000 K and a pressure of 10^5 Pa.

Change in Specific Heats. When air is heated, the heat supplied goes not only to increase the energy of the translational and rotational motion of the molecules, but also to increase the energy of vibration of the atoms in a molecule, to do the work needed to overcome the forces of interaction between atoms upon the dissociation of a molecule, and also to detach the electrons from atoms in ionization. The result is an increase in the specific heats.

Before dissociation begins, the change in the specific heat of air is determined only by the temperature. The influence of the temperature on the specific heat at a constant pressure can be estimated by the formula

$$c_p/c_{p\infty} = (T/T_\infty)^\varphi \qquad (1.5.1)$$

where the exponent φ, in turn, depends on the temperature (Fig. 1.5.1). For $T > 1000$ K, this exponent can be assumed to be constant and equal to 0.1. For $T_\infty = 288$ K, the specific heat $c_{p\infty} = 1000$ J/(kg·K) [or 1000 m^2/(s^2·K)]. Formula (1.5.1) may be used for values of T up to 2200-2500 K, at which the vibrational degrees of freedom are close to the state of complete excitation.

When dissociation sets in, the specific heat depends not only on the temperature, but also on the pressure. The specific heats and the adiabatic exponents $k = c_p/c_v$ were calculated for conditions of thermodynamic equilibrium at high temperatures on computers by a group of Soviet scientists headed by Associate member of the USSR Academy of Sciences A. Predvoditelev [6, 7]. These calculations were performed for temperatures from 1000 to 6000 K without account being taken of ionization because its influence in this temperature interval is negligible. For higher temperatures, the influence of equilibrium single ionization was taken into account. It was con-

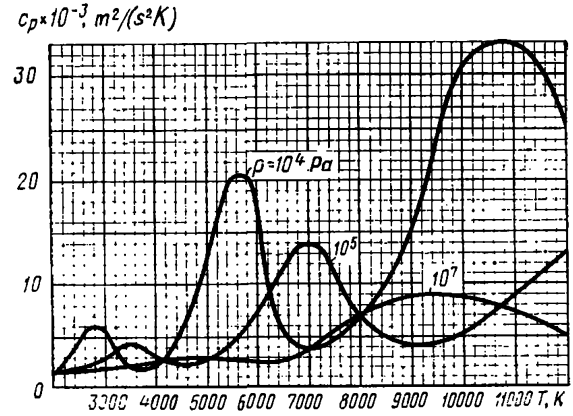

Fig. 1.5.2
Change in the specific heat c_p of air at high temperatures

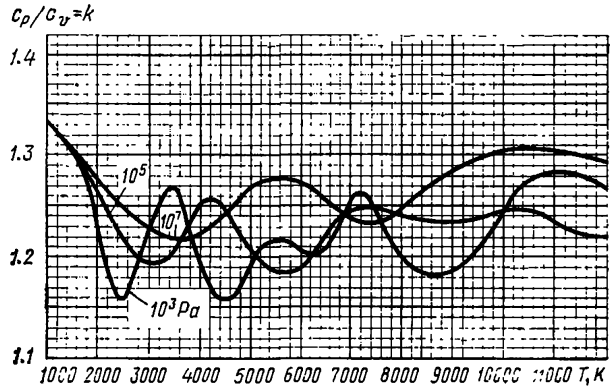

Fig. 1.5.3
Change in the ratio of the specific heats $k = c_p/c_v$ for air at high temperatures

sidered to be completed at $T = 12\,000$ K and $p = 10^2$ Pa. Curves plotted according to the data in [6, 7] and characterizing the change in c_p and k at high temperatures are given in Figs. 1.5.2. and 1.5.3 (see [8]). The data obtained indicate that at a temperature up to 2000 K and a pressure of 10^5 Pa and above, the values of c_p and $k = c_p/c_v$ are determined by the temperature and do not virtually depend on the pressure.

The general trend observed upon a change in the specific heats and their ratio is such that when the pressure drops and the degrees of dissociation and ionization, consequently, grow, the value of c_p increases, and that of the ratio $k = c_p/c_v$ diminishes, although not monotonically.

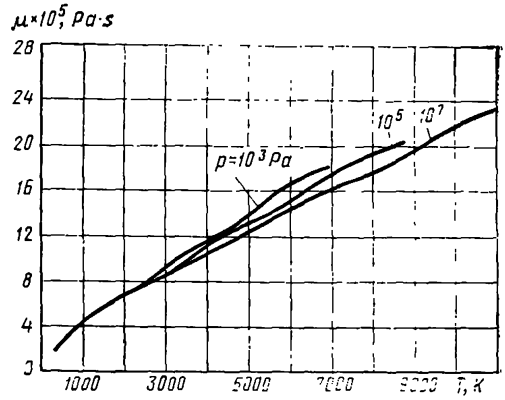

Fig. 1.5.4
Change in the dynamic viscosity of air at high temperatures

Kinetic Coefficients. The processes of friction and heat transfer occurring in a viscous heat-conducting gas depend on kinetic parameters of the gas such as the dynamic viscosity μ and the thermal conductivity λ. It was established that in the absence of dissociation, the coefficient μ depends only on the temperature and is determined by the formula

$$\mu/\mu_\infty = (T/T_\infty)^n \qquad (1.5.2)$$

in which the exponent n depends on the temperature (see Fig. 1.5.1). In approximate calculations, the mean value $n_m \approx 0.7$ may be used for a sufficiently large temperature interval; here the initial value of μ may be taken equal to $\mu_\infty = 1.79 \times 10^{-5}$ Pa·s, which corresponds to $T_\infty = 288$ K. Formula (1.5.2) is used for temperatures up to 2000-2500 K. With elevation of the temperature, this formula gives appreciable errors. Investigations show that for high temperatures up to 9000 K the dynamic viscosity of air in conditions of equilibrium dissociation can be determined with an accuracy up to 10% by Sutherland's formula

$$\mu/\mu_\infty = (T/T_\infty)^{1.2}(1 + 111/T_\infty)/(1 + 111/T) \qquad (1.5.3)$$

This formula yields better results for temperatures under 1500 K than (1.5.2). It has been established by accurate calculations that the dynamic viscosity at high temperatures also depends on the pressure. Figure 1.5.4 presents a graph (see [8]) characterizing the change in the coefficient μ at temperatures up to 12 000 K within the pressure interval from 10^3 to 10^7 Pa.

Like the viscosity, the thermal conductivity at temperatures up to about 2000 K is independent of the pressure and is determined by the power formula

$$\lambda/\lambda_\infty = (T/T_\infty)^\varkappa \qquad (1.5.4)$$

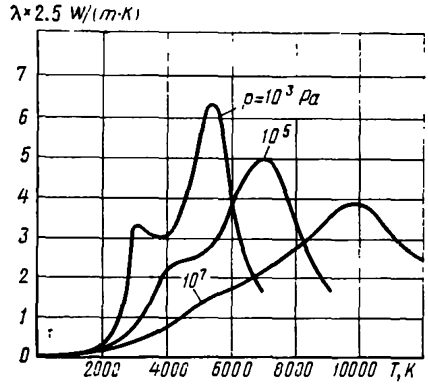

Fig. 1.5.5
Change in the thermal conductivity of air at high temperatures

in which the exponent $\varkappa$ depends, as can be seen from Fig. 1.5.1, on the temperature. For approximate calculations, one may take the mean value $\varkappa_m$ equal to 0.85, and the value of λ_∞ corresponding to $T_\infty = 261$ K equal to 23.2 W/(m·K). Dissociating air is characterized by a dependence of the thermal conductivity on the temperature and pressure. The corresponding plot is shown in Fig. 1.5.5.

The origin of viscous forces and the appearance of the process of thermal conduction in a gas are associated with the molecular structure of a substance. Gas molecules upon their proper motion transfer mass, energy, and momentum from one place to another. A result of the change in the momentum is the appearance of viscous forces, while the transfer of energy gives rise to the property of thermal conduction. Therefore, elevation of the temperature is attended by an increase in the thermal conductivity and the dynamic viscosity in a gas. When dissociation sets in, the nature of the change in λ and μ is quite involved. At a low degree of dissociation, the values of λ drop, which is caused by the expenditure of internal energy on breaking of the molecular bonds and, as a consequence, by lowering of the temperature of the gas. When the degree of dissociation grows, the more intensive breaking up of the molecules into atoms leads to a growth in the number of particles participating in the transport processes, which results in an increase in the coefficient λ.

When a gas is heated strongly, the expenditure of its internal energy on ionization substantially grows, which lowers the thermal conduction. The dynamic viscosity in a gas grows monotonically with the temperature because with the onset of dissociation and ionization more and more particles are formed that participate in the transport of momentum, and this gives rise to an increase in the viscous (friction) forces.

State of Air at High Temperatures

Equation of State. Investigation of the flow of air over bodies shows that the relations of conventional aerodynamics based on the constancy of the thermodynamic characteristics and of the physicochemical structure are sufficiently reliable as long as the air remains comparatively "cold", its specific heats change insignificantly, and, consequently, we may apply the thermal equation of state of a perfect gas

$$p = R\rho T \text{ or } p = R_0\rho T/(\mu_m)_0 \qquad (1.5.5)$$

where R and R_0 are the individual and universal (molar) gas constants, respectively [$R_0 = 8.314 \times 10^3$ J/(kmol·K)], ρ is the density, T is the temperature, and $(\mu_m)_0$ is the mean molar mass of air having a constant composition.

A gas satisfying Eq. (1.5.5) is said to be **thermally perfect.** The caloric equation of state $i = pc_p/(\rho R)$, which determines a relation for the enthalpy, corresponds to Eq. (1.5.5). If we take into account that $c_p/R = k/(k-1)$, we have

$$i = [k/(k-1)]\, p/\rho \qquad (1.5.6)$$

A gas whose state is determined by Eq. (1.5.6) corresponding to the condition at which c_p and c_v are constant and independent of the temperature is said to be **calorically perfect.**

It must be taken into account that the need to consider the change in the specific heats with the temperature sets in before the need to use an equation of state differing from that for a **perfect** gas. For example, calculations show that the change in the specific heats with the temperature when passing through a normal shock wave begins from free-stream Mach numbers of $M_\infty = 3$-4. At $M_\infty = 6$-7, the equation of state for a perfect gas retains its significance, as does the equation for the speed of sound

$$a^2 = kRT \qquad (1.5.7)$$

because the composition of the gas heated behind the shock wave does not change.

Hence, in this case a gas is not calorically perfect, but does have the properties of a thermally perfect gas.

For a gas with a varying heat capacity, the caloric equation of state (1.5.6) gives a large error. The actual relation between the enthalpy and temperature is determined by the function $f_1(T)$ that is more complicated than (1.5.6).

The following equation holds for dissociating air, for which the specific heats and molar mass are functions of its state:

$$p = (R_0/\mu_m)\,\rho T \qquad (1.5.8)$$

in which $\mu_m = f_2(p, T)$.

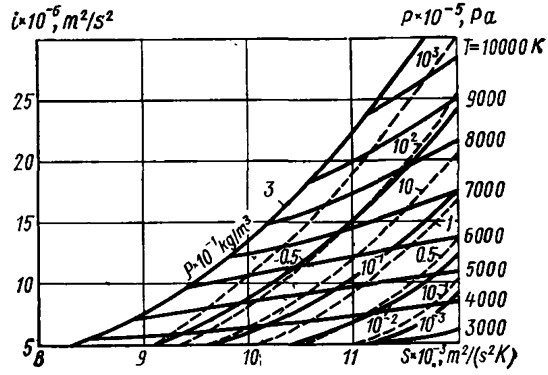

Fig. 1.5.6
An *i-S* diagram for dissociating air

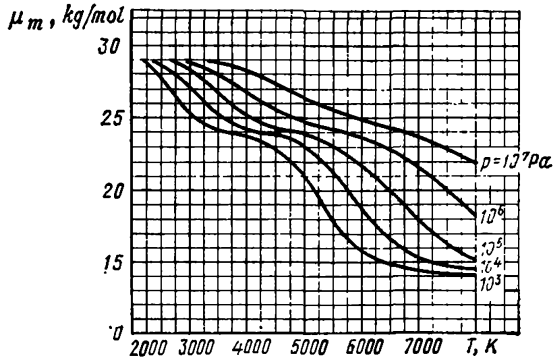

Fig. 1.5.7
Change in the mean molar mass of air at high temperatures

The caloric equation of a dissociating gaseous medium also acquires a more complicated nature, and in the general form it can be written as $i = f_3(p, T)$. Such a fluid *no longer has the properties of a perfect gas* for which the enthalpy depends only on the temperature.

The thermal and caloric equations of state of a dissociating (real) gas are still more complicated because they additionally take account of the forces of interaction between the molecules, and also the proper volume of the latter. These equations are solved by numerical methods with the aid of computers and are usually presented in the form of tables or phase diagrams.

The results of calculating the parameters of state of air in conditions of thermodynamic equilibrium for elevated temperatures at pressure intervals from 10^2 to 10^7 Pa are given in [6, 7]. These results

of calculations were used to compile an atlas of phase diagrams [8]. The most widespread use for thermal calculations in aerodynamics has been found by the i-S diagram (enthalpy-entropy diagram) of dissociating air shown in Fig. 1.5.6. This diagram, which presents the caloric equation of state in a graphic form, contains curves of $p = \text{const}$ (isobars), $T = \text{const}$ (isotherms), and $\rho = \text{const}$ (isochors—dashed lines).

Sometimes the caloric phase diagram depicting i against p with curves of $T = \text{const}$, $\rho = \text{const}$, and $S = \text{const}$ may be more convenient for calculations. Such a diagram constructed according to the data of an i-S one is given in [8]. It graphically depicts the thermal equation of state in different variants.

Graphs allowing one to determine the mean molar mass μ_m of dissociated and ionized air (Fig. 1.5.7) and also the speed of sound (Fig. 1.5.8) as a function of p and T [7] or of i and S [8] are important for practical calculations. Examination of these graphs reveals that the speed of sound changes noticeably with the temperature and to a smaller extent depends on the pressure, which is explained by the insignificant influence of the structure of air on the nature of propagation of small disturbances. At the same time, the change in the structure of air upon its dissociation appreciably affects the molar mass, which is expressed in the strong influence of the pressure on the value of μ_m. Three characteristic sections on which μ_m diminishes with increasing temperature can be noted in Fig. 1.5.7. The first of them is due to dissociation of oxygen, the second—of nitrogen, and the third—to ionization of the components of the air. The general trend of a decrease in the mean molar mass of a gas that dissociates and becomes ionized is due to the breaking up of the molecules into atoms, and also to the detachment of electrons. An increase in the pressure leads to more intensive recombinations. This results in a certain growth in μ_m.

Diatomic Model of Air. A model of the air is sometimes used in aerodynamic investigations that is a diatomic gas consisting of a mixture of oxygen and nitrogen in accordance with their mass composition. Such a mixture is treated as a single **perfect gas** if the mixture components are inert and no reactions occur between them.

At elevated temperatures, the mixture of gases *reacts chemically* because the diatomic gas dissociates and the atoms formed participate in recombination. The dissociation is assumed to be in equilibrium. This means that in the chemical reaction determined for the *pure* dissociating diatomic gas by the simplest equation of a binary process

$$A_2 \underset{r_R}{\overset{r_D}{\rightleftharpoons}} A + A \qquad (1.5.9)$$

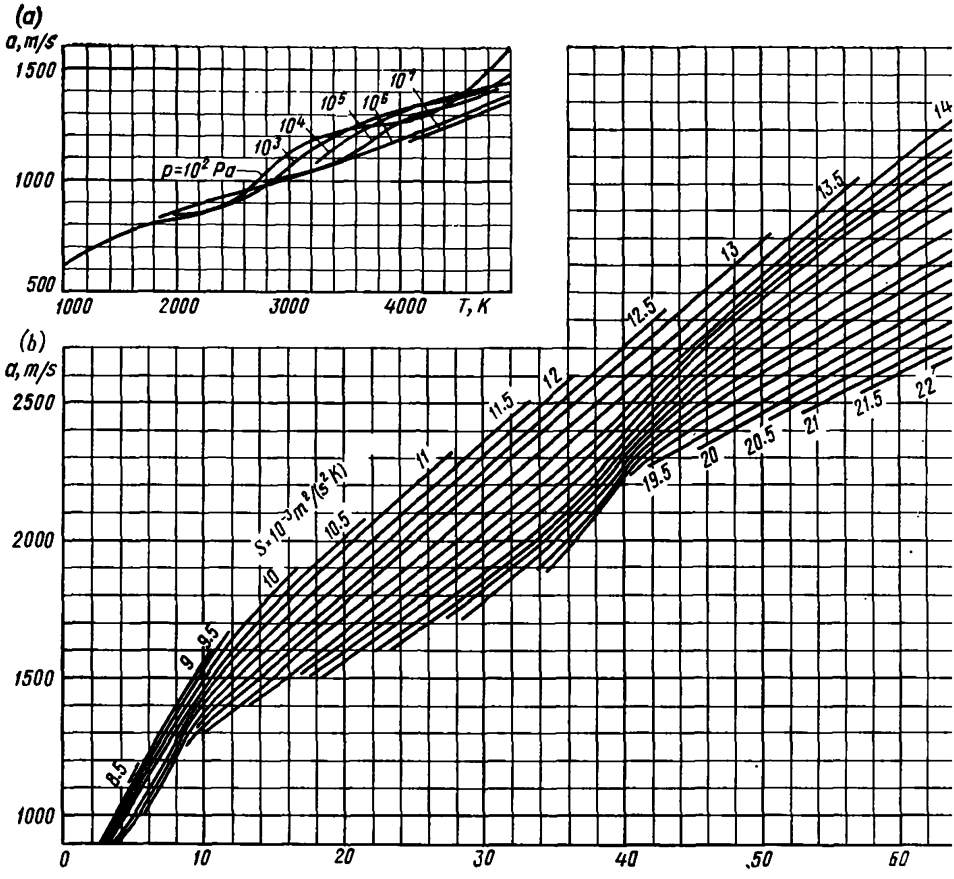

Fig. 1.5.8
Speed of sound in air at high temperatures:
a—against the temperature and pressure; *b*—against the entha py and entropy

the rates of the direct reaction r_D and of the reverse one r_R (the rates of dissociation and recombination respectively) are identical.

Investigations of a dissociating flow are connected with the determination of the degree of equilibrium dissociation α. Its value for the diatomic model of the air being considered is given in chemical thermodynamics by the expression

$$\alpha^2/(1-\alpha) = (\rho_d/\rho) \exp(-T_d/T) \tag{1.5.10}$$

where

$$\alpha = n_A/(n_A + 2n_{A_2}) \tag{1.5.11}$$

ρ_d and T_d are the **characteristic density** and **temperature** for dissociation, respectively, n_A is the number of atoms of the element A in a certain volume, and n_{A_2} is the number of molecules of the gas A_2 in the same volume.

The characteristic temperature $T_d = D/k$, where D is the dissociation energy of one molecule of A_2 and k is a gas constant related to one molecule (the Boltzmann constant). Investigations show that for the temperature interval from 1000 to 7000 K, the values of T_d and ρ_d can be assumed to be approximately constant and equal to $T_d = 50\,000$ K, $\rho_d = 150$ g/cm³ for oxygen, and to $T_d = 113\,000$ K, $\rho_d = 130$ g/cm³ for nitrogen.

To obtain an equation of state for the gas mixture appearing as a result of dissociation of diatomic molecules, we must use the expressions for determining the pressure p and molar gas constant R for the mixture of gases and the partial pressure p_i of a component:

$$\left.\begin{aligned} p = \sum_i p_i, \qquad R = \sum_i c_i R_i; \\ p_i = \rho_i T R_i = \rho_i T\,(k/m_i) = (x_i/V)\,T\,(k/m_i) \end{aligned}\right\} \tag{1.5.12}$$

where ρ_i is the density of a component, m_i is the mass of an atom or molecule, R_i is the gas constant for a component, and V is the volume of the gas mixture.

Equations (1.5.12) are known under the general name of **Dalton's law**.

We shall use the subscript A to designate an atomic component ($i = 1$) and the subscript M—a molecular one ($i = 2$). Since the concentration of a component is $c_i = \rho_i/\rho$, where ρ is the density of the mixture, then $c_1 = c_A = \alpha = \rho_A/\rho$ and $c_2 = c_M = \rho_M/\rho = 1 - \alpha$.

If $m_M = 2m_A$, and the relation between the masses x_i of the components ρ_i and the quantities ρ and α is established from the expressions $\rho_A = \rho\alpha = x_A/V$, and $\rho_M = \rho(1-\alpha) = x_M/V$, from (1.5.12) we obtain an equation of state in the following form:

$$p = \rho T k\,[\rho_A/(\rho m_A) + \rho_M/(\rho m_A)] = [k/(2m_A)]\,\rho T\,(1+\alpha) \tag{1.5.13}$$

where $k/(2m_A)$ is the gas constant for 1 g of the component A_2 in the mixture; when multiplied by $1 + \alpha$, it yields the gas constant R (the individual gas constant) for 1 g of a mixture of the components A and A_2 whose masses are in the ratio of $\alpha/(1 - \alpha)$.

It is known from thermodynamics that the mean molar mass of a mixture of gases is

$$\mu_m = (\sum_i c_i/\mu_i)^{-1} \tag{1.5.14}$$

where c_i is the mass concentration of a component, μ_i is its molar mass, and the symbol $\sum$ determines the number of moles in the mixture.

For a diatomic gas, we have $\sum_i c_i = c_1 + c_2 = c_A + c_M = 1$. Since $c_A = \alpha$, $c_M = 1 - \alpha$, and $2\mu_A = \mu_M = (\mu_m)_0$, then

$$\mu_m = (c_A/\mu_A + c_M/\mu_M)^{-1} = (\mu_m)_0/(1 + \alpha) \tag{1.5.15}$$

This expression may be used for the transformation of the equation of state (1.5.8) for a dissociating gas of an arbitrary composition:

$$p = [R_0/(\mu_m)_0]\, \rho T\, (1 + \alpha) \tag{1.5.16}$$

Kinematics of a Fluid

2.1. Approaches to the Kinematic Investigation of a Fluid

Determination of the force interaction and heat transfer between a fluid and a body about which it flows is the main task of aerodynamic investigations. The solution of this problem is associated with studying of the motion of a fluid near a body. As a result, properties are found at each point of a flow that determine this motion. Among them are the velocity, pressure, density, and temperature. With definite prerequisites, this investigation can be reduced to determination of the **velocity field**, which is a set of velocities of the fluid particles, i.e. to solution of a kinematic problem. Next the known velocity distribution is used to determine the other properties, and also the resultant forces, moments, and heat fluxes.

There are two approaches to the kinematic investigation of a fluid, known as the Lagrangian and the Eulerian approaches.

Lagrangian Approach

This approach considers the motion of individual fluid particles and for each of them determines its pathline, i.e. the coordinates of the particles as a function of time. But since there is an infinite number of particles, to set a pathline one must identify the particles which this pathline relates to. The coordinates a, b, and c at a certain instant $t = t_0$ are selected as the characteristic of a particle. This means that from among an infinite set of pathlines, the one passing through the point whose coordinates are a, b, and c will belong to the given particle. Accordingly, we shall write the equation of the pathline in the parametric form:

$$x = f_1(a, b, c, t); \quad y = f_2(a, b, c, t); \quad z = f_3(a, b, c, t) \quad (2.1.1)$$

where a, b, c, and t are the Lagrangian variables. The quantities a, b, and c are variables determining the pathline.

The components of the velocity vector at each point of the pathline equal the partial derivatives $V_x = \partial x/\partial t$, $V_y = \partial y/\partial t$, and $V_z = \partial z/\partial t$, while the components of the acceleration vector equal the relevant second partial derivatives $W_x = \partial^2 x/\partial t^2$, $W_y = \partial^2 y/\partial t^2$, and $W_z = \partial^2 z/\partial t^2$.

Eulerian Approach

The Eulerian approach is in greater favour in aerodynamic investigations. Unlike the Lagrangian approach, it fixes not a particle of a fluid, but a point of space with the coordinates x, y, and z and studies the change in the velocity at this point with time. Hence, the Eulerian approach consists in expressing the velocities of particles as a function of the time t and the coordinates x, y, and z of points in space, i.e. in setting the field of velocities determined by the vector $\mathbf{V} = V_x\mathbf{i} + V_y\mathbf{j} + V_z\mathbf{k}$, where $\mathbf{i}$, $\mathbf{j}$, and $\mathbf{k}$ are unit vectors along the coordinate axes, while $V_x = dx/dt$, $V_y = dy/dt$, and $V_z = dz/dt$ are the velocity vector components given in the form of the equations

$$V_x = f_1(x, y, z, t); \quad V_y = f_2(x, y, z, t); \quad V_z = f_3(x, y, z, t) \qquad (2.1.2)$$

The quantities x, y, z, and t are called the **Eulerian variables.** By solving the simultaneous differential equations

$$\frac{dx}{dt} = f_1(x, y, z, t); \quad \frac{dy}{dt} = f_2(x, y, z, t); \quad \frac{dz}{dt} = f_3(x, y, z, t) \qquad (2.1.3)$$

we can obtain equations of a family of pathlines in the parametric form coinciding with Eqs. (2.1.1) in which a, b, and c are integration constants.

Hence, in the Eulerian approach, we can go over from a description of the kinematics to representation of a flow by the Lagrangian approach. The reverse problem associated with the transition from the Lagrangian approach [Eq. (2.1.1)] to the Eulerian one [Eq. (2.1.3)] consists in differentiation of Eqs. (2.1.1) with respect to time and the following exclusion of the constants a, b, and c by means of Eqs. (2.1.1).

By calculating the total derivative of the velocity vector with respect to time, we obtain the acceleration vector

$$\mathbf{W} = \frac{d\mathbf{V}}{dt} = \frac{\partial \mathbf{V}}{\partial t} + V_x \frac{\partial \mathbf{V}}{\partial x} + V_y \frac{\partial \mathbf{V}}{\partial y} + V_z \frac{\partial \mathbf{V}}{\partial z} \qquad (2.1.4)$$

Projection of the vector $\mathbf{W}$ onto the axes of coordinates yields the components of the resultant acceleration. In the expanded form,

these components are as follows:

$$\left.\begin{aligned} W_x &= \frac{\partial V_x}{\partial t} + V_x \frac{\partial V_x}{\partial x} + V_y \frac{\partial V_x}{\partial y} + V_z \frac{\partial V_x}{\partial z} \\ W_y &= \frac{\partial V_y}{\partial t} + V_x \frac{\partial V_y}{\partial x} + V_y \frac{\partial V_y}{\partial y} + V_z \frac{\partial V_y}{\partial z} \\ W_z &= \frac{\partial V_z}{\partial t} + V_x \frac{\partial V_z}{\partial x} + V_y \frac{\partial V_z}{\partial y} + V_z \frac{\partial V_z}{\partial z} \end{aligned}\right\} \qquad (2.1.5)$$

Relations (2.1.5) for the accelerations correspond to a flow characterized by a change in the velocity at a given point with time and, consequently, by the inequality $\partial \mathbf{V}/\partial t \neq 0$. Such a flow of a fluid is called **unsteady**. A flow of a fluid in which the velocity and other properties at a given point are independent of the time ($\partial \mathbf{V}/\partial t = 0$) is called **steady**.

Streamlines and Pathlines

At any instant, we can imagine a curve in a flow having the property that every particle of the fluid on it has a velocity tangent to the curve. Such a curve is called a **streamline**.

To obtain a streamline, one must proceed as follows. Take a point A_1 (Fig. 2.1.1*a*) in the flow at the instant $t = t_0$ and express the velocity of the particle at this point by the vector $\mathbf{V}_1$. Next take a point A_2 adjacent to A_1 on the vector $\mathbf{V}_1$. Assume that at the instant $t = t_0$, the velocity vector at this point is $\mathbf{V}_2$. Next consider a point A_3 on the vector $\mathbf{V}_2$, the velocity at which is determined at the same instant by the vector $\mathbf{V}_3$, and so on. Such a construction yields a broken line consisting of segments of velocity vectors. By shrinking the size of these segments to zero and simultaneously increasing their number to infinity, at the limit we obtain a curve enveloping the entire family of velocity vectors. This is exactly a streamline. It is obvious that a definite streamline corresponds to each instant.

To obtain an equation of a streamline, let us take advantage of a property according to which at each point of this line the directions of the velocity vector $\mathbf{V}$ and of the vector $d\mathbf{s} = \mathbf{i}\,dx + \mathbf{j}\,dy + \mathbf{k}\,dz$, where dx, dy, and dz are the projections of the streamline arc element $d\mathbf{s}$, must coincide. Consequently, the cross product $d\mathbf{s} \times \mathbf{V} = 0$, i.e.

$$\begin{vmatrix} \mathbf{i} & \mathbf{j} & \mathbf{k} \\ dx & dy & dz \\ V_x & V_y & V_z \end{vmatrix} = \mathbf{i}\,(V_z\,dy - V_y\,dz) - \mathbf{j}\,(V_z\,dx - V_x\,dz) + \mathbf{k}\,(V_y\,dx - V_x\,dy) = 0$$

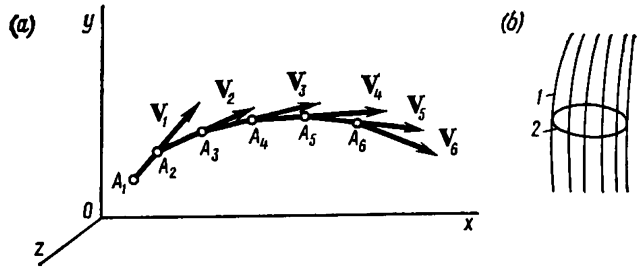

Fig. 2.1.1
Construction of a streamline (*a*) and a stream tube (*b*):
1—streamlines; *2*—contour

Hence since, for example, $V_z\,dy - V_y\,dz = 0$, and so on, we obtain a system of differential equations

$$dx/V_x = dy/V_y = dz/V_z \qquad (2.1.6)$$

The solution of the problem on determining streamlines thus consists in integration of the system of equations (2.1.6). Each of the integrals of these equations $F_1(x, y, z, C_1) = 0$ and $F_2(x, y, z, C_2) = 0$ is a family of surfaces depending on one of the parameters, C_1 or C_2, while the intersection of these surfaces forms a **family of streamlines.**

Unlike streamlines, which are constructed at a fixed instant, the concept of a pathline is associated with a certain time interval during which a particle covers a definite distance. It thus follows that a streamline and a **pathline** (or **trajectory**), which is the trace of motion of a single particle, coincide in a steady flow. If the flow is unsteady, a streamline and pathline in it do not coincide.

The concepts of a stream tube and a stream filament are considered in aerodynamics. If we draw streamlines through the points of an elementary closed contour (Fig. 2.1.1*b*), they form a surface called the surface of a stream tube. The part of the fluid confined within this surface is called a **stream tube.** If we draw pathlines through the points of an elementary closed contour, they form a surface confining a part of the fluid called a **stream filament.** A stream tube and a stream filament drawn through the points of the same closed contour in a steady flow coincide.

2.2. Analysis of Fluid Particle Motion

Unlike a solid body whose motion is determined by its translational motion together with its centre of mass and by rotation about an instantaneous axis passing through the centre, the motion of a

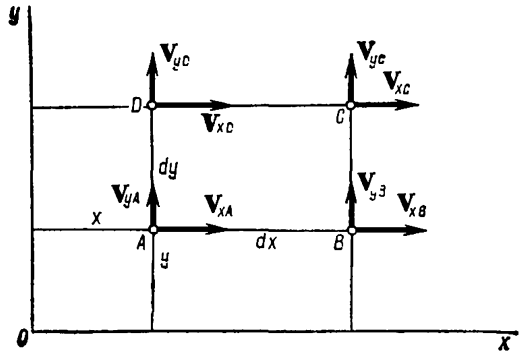

Fig. 2.2.1
Motion of a fluid particle

fluid particle is characterized, in addition, by the presence of **strain** changing the shape of the particle.

Let us consider a fluid particle in the form of an elementary parallelepiped with edges of dx, dy, and dz, and analyse the motion of face $ABCD$ (Fig. 2.2.1). Since the coordinates of the vertices of the face are different, the velocities determined at a certain instant $t = t_0$ are also different:

$$\left.\begin{aligned} V_{xA} &= V_x(x, y), \quad V_{xB} = V_x(x + dx, y) \\ V_{yA} &= V_y(x, y), \quad V_{yB} = V_y(x + dx, y) \\ V_{xC} &= V_x(x + dx, y + dy), \quad V_{xD} = V_x(x, y + dy) \\ V_{yC} &= V_y(x + dx, y + dy), \quad V_{yD} = V_y(x, y + dy) \end{aligned}\right\} \qquad (2.2.1)$$

where x and y are the coordinates of point A.

Let us expand the expressions for the velocities into a Taylor series, leaving only small quantities of the first order in them, i.e. terms containing dx, dy, and dz to a power not higher than the first one. Assuming that at point A the velocity $V_{xA} = V_x$ and $V_{yA} = V_y$, we obtain

$$\left.\begin{aligned} V_{xB} &= V_x + (\partial V_x/\partial x)\, dx + \ldots, \quad V_{xD} = V_x + (\partial V_x/\partial y) dy + \ldots \\ V_{yB} &= V_y + (\partial V_y/\partial x)\, dx + \ldots, \quad V_{yD} = V_y + (\partial V_y/\partial y)\, dy + \ldots \\ V_{xC} &= V_x + (\partial V_x/\partial x)\, dx + (\partial V_x/\partial y)\, dy + \ldots \\ V_{yC} &= V_y + (\partial V_y/\partial x)\, dx + (\partial V_y/\partial y)\, dy + \ldots \end{aligned}\right\} \qquad (2.2.2)$$

Examination of these expressions reveals that, for example, at point B the velocity component along the x-axis differs from the value of the velocity at point A by the quantity $(\partial V_x/\partial x)\, dx$. This signifies that point B, while participating in translational motion at the velocity V_x in the direction of the x-axis together with point A, simultaneously moves relative to it in the same direction at the

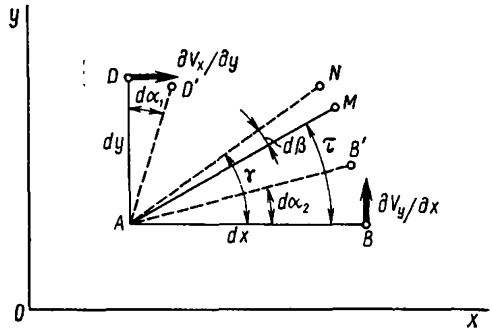

Fig. 2.2.2
Angular strain of a fluid particle

velocity $(\partial V_x/\partial x)\,dx$. The result is a linear strain of segment AB. The rate of this strain is $\theta_x = \partial V_x/\partial x$.

Point B moves in the direction of the y-axis at the velocity V_y together with point A and simultaneously moves relative to this point at the linear velocity $(\partial V_y/\partial x)\,dx$ determined by the angular velocity of segment AB.

Considering point D, we can by analogy with point B determine that the relative linear velocity of this point in the direction of the y-axis is $(\partial V_y/\partial y)\,dy$ and, consequently, the rate of linear strain of segment AD will be $\theta_y = \partial V_y/\partial y$. The angular velocity of the segment about point A is $-\partial V_x/\partial y$ (the minus sign takes into account that point D rotates about point A in a direction opposite to that of rotation of point B). Rotation of segments AD and AB causes distortion of the angle DAB (Fig. 2.2.2), i.e. angular strain of the particle is produced. Simultaneously, bisector AM of angle DAB may turn, the result being the appearance of an angle $d\beta$ between it and bisector AN of the distorted angle $D'AB'$. Hence, the particle rotates additionally.

The angle of rotation of the bisector (Fig. 2.2.2) is

$$d\beta = \gamma - \tau$$

where $\gamma = 0.5\,[\pi/2 - (d\alpha_2 + d\alpha_1)]$ and $\tau = \pi/4 - d\alpha_2$.

The angles $d\alpha_2$ and $d\alpha_1$ shown in Fig. 2.2.2 equal $(\partial V_y/\partial x)\,dt$ and $(\partial V_x/\partial y)\,dt$, respectively. Consequently

$$d\beta = 0.5\,(d\alpha_2 - d\alpha_1) = 0.5\,(\partial V_y/\partial x - \partial V_x/\partial y)\,dt$$

Hence we can find the angular velocity $d\beta/dt$ of a fluid particle about the z-axis. Denoting it by ω_z, we have

$$\omega_z = d\beta/dt = 0.5\,(\partial V_y/\partial x - \partial V_x/\partial y) \qquad (2.2.3)$$

If we consider the motion of edge AD relative to segment AB, the angular velocity of this edge will evidently be

$$2\varepsilon_z = \partial V_y/\partial x + \partial V_x/\partial y \qquad (2.2.4)$$

The quantity

$$\varepsilon_z = 0.5\ (\partial V_y/\partial x + \partial V_x/\partial y) \qquad (2.2.4')$$

is called the **semi-rate of downwash** of the right angle DAB.

Let us apply this reasoning to three-dimensional flow and consider point C belonging to a particle in the form of an elementary parallelepiped with edge lengths of dx, dy, and dz. The velocity at this point at the instant $t = t_0$ is a function of the coordinates $x + dx$, $y + dy$, and $z + dz$. Writing the velocity components in the form of a Taylor series in which only small terms of the first order are retained, we have

$$\left.\begin{aligned} V_{xC} &= V_x + (\partial V_x/\partial x)\,dx + (\partial V_x/\partial y)\,dy + (\partial V_x/\partial z)\,dz \\ V_{yC} &= V_y + (\partial V_y/\partial x)\,dx + (\partial V_y/\partial y)\,dy + (\partial V_y/\partial z)\,dz \\ V_{zC} &= V_z + (\partial V_z/\partial x)\,dx + (\partial V_z/\partial y)\,dy + (\partial V_z/\partial z)\,dz \end{aligned}\right\} \qquad (2.2.5)$$

Let us introduce a notation similar to that adopted when analysing the motion of a two-dimensional particle. We shall assume that $\theta_z = \partial V_z/\partial z$. This quantity determines the rate of linear strain of a three-dimensional particle in the direction of the z-axis. Let us also introduce the notation

$$\omega_x = 0.5\ (\partial V_z/\partial y - \partial V_y/\partial z), \quad \omega_y = 0.5\ (\partial V_x/\partial z - \partial V_z/\partial x) \qquad (2.2.6)$$

The quantities ω_x and ω_y are the components of the angular velocity of a particle along the x- and y-axes, respectively. The components of the angular velocity of a particle ω_x, ω_y, and ω_z are considered to be positive upon rotation from the x-axis to the y-axis, from the y-axis to the z-axis, and from the z-axis to the x-axis, respectively. Accordingly, the signs of the derivatives $\partial V_y/\partial x$, $\partial V_z/\partial y$, and $\partial V_x/\partial z$ coincide with those of the angular velocity, while the signs of the derivatives $\partial V_x/\partial y$, $\partial V_y/\partial z$, and $\partial V_z/\partial x$ are opposite to those of the angular velocity.

By analogy with (2.2.4'), we have the values

$$\varepsilon_x = 0.5\ (\partial V_z/\partial y + \partial V_y/\partial z), \quad \varepsilon_y = 0.5\ (\partial V_x/\partial z + \partial V_z/\partial x) \qquad (2.2.7)$$

that equal the semi-rate of downwash of the two right angles of the parallelepiped in planes yOz and xOz, respectively.

By performing simple transformations, we can see that

$$\partial V_z/\partial y = \varepsilon_x + \omega_x;\ \partial V_x/\partial z = \varepsilon_y + \omega_y;\ \partial V_y/\partial x = \varepsilon_z + \omega_z$$
$$\partial V_y/\partial z = \varepsilon_x - \omega_x;\ \partial V_z/\partial x = \varepsilon_y - \omega_y;\ \partial V_x/\partial y = \varepsilon_z - \omega_z$$

With account taken of these expressions, the velocity components at point C can be represented in the following form:

$$\left.\begin{aligned} V_{xC} &= V_x + \theta_x\,dx + \varepsilon_y\,dz + \varepsilon_z\,dy + \omega_y\,dz - \omega_z\,dy \\ V_{yC} &= V_y + \theta_y\,dy + \varepsilon_z\,dx + \varepsilon_x\,dz + \omega_z\,dx - \omega_x\,dz \\ V_{zC} &= V_z + \theta_z\,dz + \varepsilon_x\,dy + \varepsilon_y\,dx + \omega_x\,dy - \omega_y\,dx \end{aligned}\right\} \qquad (2.2.8)$$

Hence, the motion of point C can be considered as the result of addition of three kinds of motion: translational along a pathline together with point A at a velocity of $\mathbf{V}(V_x, V_y, V_z)$, rotation about it at the angular velocity

$$\boldsymbol{\omega} = \omega_x \mathbf{i} + \omega_y \mathbf{j} + \omega_z \mathbf{k} \qquad (2.2.9)$$

and pure strain. This conclusion forms the content of the **Helmholtz theorem.** Strain, in turn, consists of linear strain characterized by the coefficients θ_x, θ_y, and θ_z, and of the angular strain determined by the quantities ε_x, ε_y, and ε_z.

The linear strain of the element's edges causes a change in its volume $\tau = dx\, dy\, dz$, which is determined by the difference

$$d\tau = dx_1\, dy_1\, dz_1 - dx\, dy\, dz$$

where dx_1, dy_1, and dz_1 are the lengths of the edges at the instant $t + dt$.

Introducing the values of the lengths, we find

$$d\tau = (dx + \theta_x\, dx\, dt)(dy + \theta_y\, dy\, dt)(dz + \theta_z\, dz\, dt) - dx\, dy\, dz$$

Disregarding in this expression infinitesimal terms higher than the fourth order, we obtain

$$d\tau = (\theta_x + \theta_y + \theta_z)\, dx\, dy\, dz\, dt$$

Hence we can determine the **rate of change of the relative volume,** or the **rate of the specific volume strain** $\theta = (1/\tau)d\tau/dt$, which at each point of a flow equals the sum of the rates of linear strain along any three mutually perpendicular directions:

$$\theta = \theta_x + \theta_y + \theta_z \qquad (2.2.10)$$

The quantity θ is also known as the **divergence of the velocity vector** at a given point:

$$\operatorname{div} \mathbf{V} = \theta = \theta_x + \theta_y + \theta_z \qquad (2.2.11)$$

Hence, the motion of a fluid particle has been shown to have a complicated nature and to be the result of summation of three kinds of motion: translational and rotational motion and strain.

A flow in which the particles experience rotation is called a **vortex** one, and the angular velocity components ω_x, ω_y, and ω_z—the **vortex components.** To characterize rotation, the concept of the velocity curl is introduced. It is expressed in the form $\operatorname{curl} \mathbf{V} = 2\boldsymbol{\omega}$. The **velocity curl** is a vector

$$\operatorname{curl} \mathbf{V} = (\operatorname{curl} \mathbf{V})_x \mathbf{i} + (\operatorname{curl} \mathbf{V})_y \mathbf{j} + (\operatorname{curl} \mathbf{V})_z \mathbf{k} \qquad (2.2.12)$$

whose components equal the corresponding double values of a vortex component:

$$(\operatorname{curl} \mathbf{V})_x = 2\omega_x,\ (\operatorname{curl} \mathbf{V})_y = 2\omega_y,\ \text{and}\ (\operatorname{curl} \mathbf{V})_z = 2\omega_z$$

2.3. Vortex-Free Motion of a Fluid

When investigating the motion of a fluid, we may often take no account of rotation because of the negligibly small angular velocities of the particles. Such motion is called **vortex-free** (or **irrotational**).

For a vortex-free flow, $\omega = 0$ (or curl $\mathbf{V} = 0$), and, consequently, the vortex components ω_x, ω_y, and ω_z equal zero. Accordingly, from formulas (2.2.3) and (2.2.6) we obtain

$$\partial V_x/\partial y = \partial V_y/\partial x, \quad \partial V_z/\partial y = \partial V_y/\partial z, \quad \partial V_x/\partial z = \partial V_z/\partial x \qquad (2.3.1)$$

These equations are a necessary and sufficient condition for the differential trinomial $V_x\,dx + V_y\,dy + V_z\,dz$ to be a total differential of a function characterizing the flow of a fluid in the same way as the velocity components V_x, V_y, and V_z.

Designating this function in the form $\varphi\,(x, y, z, t)$ and considering the time t as a parameter, we can write the expression

$$d\varphi = V_x\,dx + V_y\,dy + V_z\,dz$$

On the other hand, the same differential is

$$d\varphi = (\partial\varphi/\partial x)\,dx + (\partial\varphi/\partial y)\,dy + (\partial\varphi/\partial z)\,dz$$

Comparing the last two expressions, we find

$$V_x = \partial\varphi/\partial x, \quad V_y = \partial\varphi/\partial y, \quad V_z = \partial\varphi/\partial z \qquad (2.3.2)$$

The function φ is called a **velocity potential** or a **potential function**, and the vortex-free flow characterized by this function is called a **potential flow.** Examination of relations (2.3.2) reveals that the partial derivative of the potential φ with respect to a coordinate equals the projection of the velocity onto the relevant coordinate axis. This property of the potential function also holds for an arbitrary direction. Particularly, the tangential component of the velocity at a point on an arbitrary curve s equals the partial derivative $V_s = \partial\varphi/\partial s$, while the normal component $V_n = \partial\varphi/\partial n$, where n is a normal to the arc s at the point being considered. For the polar coordinates r and θ, the projections of the velocity vector $\mathbf{V}$ of a point onto the direction of a polar position vector and onto a direction perpendicular to this vector equal, respectively, the partial derivatives

$$V_r = \partial\varphi/\partial r \text{ and } V_s = \partial\varphi/\partial s = (1/r)\,\partial\varphi/\partial\theta$$

It can be seen that the magnitude of the velocity in a certain direction is determined by the rapidity of the change in the potential φ in the same direction. If we consider the direction s, the rapidity of the change in the potential equals the partial derivative with

respect to this direction $\partial\varphi/\partial s$. The quantity $\partial\varphi/\partial s$ can be considered as the projection onto the direction s of a vector known as the **gradient of the function** φ and coinciding with the direction of the most rapid increase in this function. It is evident that this vector equals the velocity vector **V**. Denoting the gradient of a function in the form grad φ, we have

$$\mathbf{V} = \text{grad } \varphi \tag{2.3.3}$$

or

$$\mathbf{V} = \text{grad } \varphi = (\text{grad } \varphi)_x \mathbf{i} + (\text{grad } \varphi)_y \mathbf{j} + (\text{grad } \varphi)_z \mathbf{k} \tag{2.3.4}$$

where the coefficients in parentheses on the right-hand side are the projections of the vector of the velocity gradient onto the coordinate axes:

$$(\text{grad } \varphi)_x = V_x = \partial\varphi/\partial x, \quad (\text{grad } \varphi)_y = V_y = \partial\varphi/\partial y,$$
$$(\text{grad } \varphi)_z = V_z = \partial\varphi/\partial z \tag{2.3.5}$$

The use of the potential function appreciably simplifies the investigation of a fluid's motion because instead of determining three unknowns, the velocity components V_x, V_y, and V_z, it is sufficient to find one unknown function φ, which makes it possible to completely calculate the velocity field.

2.4. Continuity Equation

General Form of the Equation

The equation of continuity of motion in the mathematical form is the law of mass conservation—one of the most general laws of physics. This equation is one of the fundamental equations of aerodynamics used to find the parameters determining the motion of a gas.

To obtain the continuity equation, let us consider a moving volume of a fluid. This volume, varying with time, consists of the same particles. The mass m of this volume in accordance with the law of mass conservation remains constant, therefore $\rho_m \tau = \text{const}$, where ρ_m is the mean density within the limits of the volume τ. Consequently, the derivative $d(\rho_m \tau)/dt = 0$, or, with a view to the density and volume being variables, we have

$$(1/\rho_m)\, d\rho_m/dt + (1/\tau)\, d\tau/dt = 0$$

This volume relates to an arbitrary finite volume. To obtain a relation characterizing the motion of a fluid at each point, let us go over to the limit with $\tau \to 0$ in the last equation, which signifies contraction of this volume to an internal point. If the condition is observed that the moving fluid completely fills the space being stud-

ied and, consequently, no voids or discontinuities are formed, the density at a given point is a quite determinate quantity ρ, and we obtain the equation

$$(1/\rho)\, d\rho/dt + \operatorname{div} \mathbf{V} = 0 \qquad (2.4.1)$$

in which the value of $\lim_{\tau \to 0} [(1/\tau)\, d\tau/dt]$ has been replaced according to (2.2.10) and (2.2.11) with the divergence of the velocity.

Relation (2.4.1) is a **continuity equation**. It has been obtained in a general form and can therefore be used for any chosen coordinate system.

Cartesian Coordinate System

Let us consider the continuity equation in the Cartesian coordinate system. For this purpose, we calculate the derivative $d\rho\,(x, y, z, t)/dt$ in (2.4.1) in accordance with (2.2.11). As a result, we obtain the continuity equation

$$\partial\rho/\partial t + \partial\,(\rho V_x)/\partial x + \partial\,(\rho V_y)/\partial y + \partial\,(\rho V_z)/\partial z = 0 \qquad (2.4.2)$$

Introducing the concept of the divergence of the vector $\rho\mathbf{V}$

$$\operatorname{div}(\rho\mathbf{V}) = \partial\,(\rho V_x)/\partial x + \partial\,(\rho V_y)/\partial y + \partial\,(\rho V_z)/\partial z$$

we obtain

$$\partial\rho/\partial t + \operatorname{div}(\rho\mathbf{V}) = 0 \qquad (2.4.3)$$

instead of (2.4.2).

Continuity equation (2.4.2) describes an unsteady flow. For a steady flow, $\partial\rho/\partial t = 0$ and, consequently,

$$\partial\,(\rho V_x)/\partial x + \partial\,(\rho V_y)/\partial y + \partial\,(\rho V_z)/\partial z = 0 \qquad (2.4.4)$$

or

$$\operatorname{div}(\rho\mathbf{V}) = 0 \qquad (2.4.4')$$

For a two-dimensional flow, the continuity equation is

$$\partial(\rho V_x)/\partial x + \partial\,(\rho V_y)/\partial y = 0 \qquad (2.4.5)$$

For an incompressible flow, $\rho = \text{const}$, hence

$$\partial V_x/\partial x + \partial V_y/\partial y + \partial V_z/\partial z = 0 \qquad (2.4.6)$$

or

$$\operatorname{div}\mathbf{V} = 0 \qquad (2.4.7)$$

For potential motion, the continuity equation is transformed with account taken of (2.3.2) to the following form:

$$(1/\rho)\, d\rho/dt + \partial^2\varphi/\partial x^2 + \partial^2\varphi/\partial y^2 + \partial^2\varphi/\partial z^2 = 0 \qquad (2.4.8)$$

For an incompressible fluid, $\rho = \text{const}$, therefore

$$\partial^2\varphi/\partial x^2 + \partial^2\varphi/\partial y^2 + \partial^2\varphi/\partial z^2 = 0 \qquad (2.4.8')$$

The expression obtained is called the **Laplace equation.** The solution of this equation is known to be a harmonic function. Consequently, the velocity potential of an incompressible flow φ is such a harmonic function.

Curvilinear Coordinate System

Conversion Formulas. It is more convenient to solve some problems in aerodynamics by using a curvilinear orthogonal coordinate system. Such systems include, particularly, the cylindrical and spherical coordinate systems.

In a cylindrical coordinate system, the position of a point P in space (Fig. 2.4.1) is determined by the angle γ made by the coordinate plane and a plane passing through point P and the coordinate axis Ox, and by the rectangular coordinates x and r in this plane. The formulas for transition from a Cartesian coordinate system to a cylindrical one have the following form:

$$x = x,\ y = r\cos\gamma,\ z = r\sin\gamma \tag{2.4.9}$$

In a spherical coordinate system, the position of point P (Figure 2.4.2) is determined by the angular coordinates θ (the polar angle) and ψ (the longitude), as well as by the polar radius r. The relation between rectangular and spherical coordinates is determined as follows:

$$x = r\cos\theta,\ y = r\sin\theta\cos\psi,\ z = r\sin\theta\sin\psi \tag{2.4.10}$$

The relevant transformations of the equations of aerodynamics obtained in Cartesian coordinates to a curvilinear orthogonal system can be performed in two ways: either by direct substitution of (2.4.9) and (2.4.10) into these equations or by employing a more general approach based on the concept of generalized coordinate curves (see [9]). Let us consider this approach.

We shall represent the elementary lengths of arcs of the coordinate curves in the vicinity of point P in the general form:

$$ds_1 = h_1\,dq_1,\ ds_2 = h_2\,dq_2,\ ds_3 = h_3\,dq_3 \tag{2.4.11}$$

where q_n $(n = 1, 2, 3)$ are the curvilinear coordinates, and h_i are coefficients known as **Lamé's coefficients.**

For cylindrical and spherical coordinates, respectively, we have

$$q_1 = x,\quad q_2 = r,\quad q_3 = \gamma, \tag{2.4.12}$$

$$q_1 = r,\quad q_2 = \theta,\quad q_3 = \psi \tag{2.4.13}$$

It follows directly from Fig. 2.4.1 that for cylindrical coordinates

$$ds_1 = dx,\quad ds_2 = dr,\quad ds_3 = r\,d\gamma \tag{2.4.14}$$

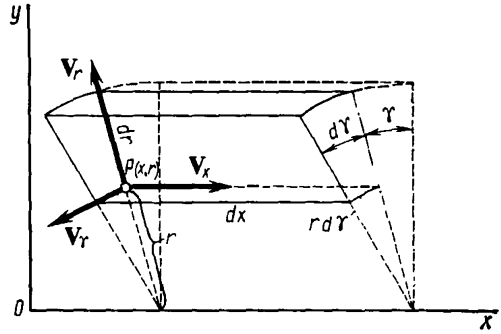

Fig. 2.4.1
An elementary fluid particle in a cylindrical coordinate system

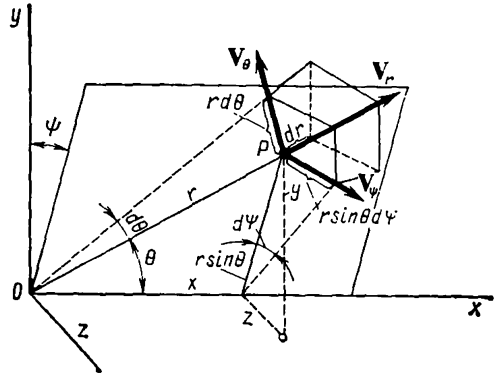

Fig. 2.4.2
An elementary fluid particle in a spherical coordinate system

Figure 2.4.2 allows us to determine the length of the arcs of the relevant coordinate lines in a spherical system:

$$ds_1 = dr, \quad ds_2 = r\,d\theta, \quad ds_3 = r \sin\theta\, d\psi \tag{2.4.15}$$

Consequently, for cylindrical coordinates, Lamé's coefficients have the form

$$h_1 = 1, \; h_2 = 1, \; h_3 = r \tag{2.4.16}$$

and for spherical ones

$$h_1 = 1, \; h_2 = r, \; h_3 = r \sin\theta \tag{2.4.17}$$

Let us consider some expressions for vector and scalar quantities in curvilinear coordinates that are needed to transform the continuity equation to these coordinates. The gradient of a scalar function Φ is

$$\text{grad}\,\Phi = (\partial\Phi/\partial s_1)\,\mathbf{i}_1 + (\partial\Phi/\partial s_2)\,\mathbf{i}_2 + (\partial\Phi/\partial s_3)\,\mathbf{i}_3$$

where $\mathbf{i}_1$, $\mathbf{i}_2$, and $\mathbf{i}_3$ are unit vectors along the relevant coordinate lines.

Having in view formulas (2.4.11), we obtain

$$\operatorname{grad}\Phi=\frac{1}{h_1}\cdot\frac{\partial\Phi}{\partial q_1}\,\mathbf{i}_1+\frac{1}{h_2}\cdot\frac{\partial\Phi}{\partial q_2}\,\mathbf{i}_2+\frac{1}{h_3}\cdot\frac{\partial\Phi}{\partial q_3}\,\mathbf{i}_3 \qquad (2.4.18)$$

For further transformations, we shall use information from the course of mathematics dealing with vector analysis. Let us find the divergence of the velocity vector, writing it as the sum of the components along the coordinate lines:

$$\mathbf{V}=V_1\mathbf{i}_1+V_2\mathbf{i}_2+V_3\mathbf{i}_3=\sum_{n=1}^{3}V_n\mathbf{i}_n \qquad (2.4.19)$$

Performing the divergence operation for both sides of this equation, we obtain

$$\operatorname{div}\mathbf{V}=\sum_{n=1}^{3}(V_n\operatorname{div}\mathbf{i}_n+\mathbf{i}_n\operatorname{grad}V_n) \qquad (2.4.20)$$

To determine div $\mathbf{i}_n$, we shall use a known relation of vector analysis

$$\operatorname{div}\mathbf{i}_n=\operatorname{div}[\mathbf{i}_m\times\mathbf{i}_j]=\mathbf{i}_j\operatorname{curl}\mathbf{i}_m-\mathbf{i}_m\operatorname{curl}\mathbf{i}_j \qquad (2.4.21)$$

where n takes on consecutively the values of $n = 1, 2, 3$ which the values of $m = 2, 3, 1$ and $j = 3, 1, 2$ correspond to. This relation includes the vectors curl $\mathbf{i}_m$ or curl $\mathbf{i}_j$ to be determined, for which we shall introduce the common symbol curl $\mathbf{i}_n$. Using (2.4.18) and the general methods of transforming vector quantities, we find

$$\operatorname{curl}\mathbf{i}_n=\frac{1}{h_n}\left(\frac{1}{h_j}\cdot\frac{\partial h_n}{\partial q_j}\,\mathbf{i}_m-\frac{1}{h_m}\cdot\frac{\partial h_n}{\partial q_m}\,\mathbf{i}_j\right) \qquad (2.4.22)$$

Let us introduce (2.4.22) into (2.4.21). For this purpose we shall first replace the subscript n in curl $\mathbf{i}_n$ with m and j, and also correspondingly arrange the subscripts on the right-hand side of (2.4.22). As a result, we have

$$\operatorname{div}\mathbf{i}_n=\frac{1}{h_n}\left(\frac{1}{h_m}\cdot\frac{\partial h_m}{\partial q_n}+\frac{1}{h_j}\cdot\frac{\partial h_j}{\partial q_n}\right) \qquad (2.4.23)$$

Let us introduce these values into (2.4.20). Having in view that in this formula, in accordance with (2.4.18), we have

$$\mathbf{i}_n\cdot\operatorname{grad}V_n=(1/h_n)\,\partial V_n/\partial q_n$$

we find the following expression for the divergence:

$$\operatorname{div}\mathbf{V}=\frac{1}{h_1h_2h_3}\cdot\left[\frac{\partial(V_1h_2h_3)}{\partial q_1}+\frac{\partial(V_2h_3h_1)}{\partial q_2}+\frac{\partial(V_3h_1h_1)}{\partial q_3}\right] \qquad (2.4.24)$$

Having this expression, we can transform the continuity equation (2.4.1) to various forms of curvilinear orthogonal coordinates.

Cylindrical Coordinates. In cylindrical coordinates, Lamé's coefficients are given by expressions (2.4.16), and the values of q_n ($n = 1, 2, 3$) by relations (2.4.12). The velocity components along the axes of cylindrical coordinates are

$$V_1 = V_x = dx/dt, \quad V_2 = V_r = dr/dt, \quad V_3 = V_\gamma = r\, d\gamma/dt \tag{2.4.25}$$

Taking this into account, the divergence of the velocity (2.4.24) becomes

$$\operatorname{div} \mathbf{V} = \frac{dV_x}{\partial x} + \frac{\partial V_r}{\partial r} + \frac{1}{r} \cdot \frac{\partial V_\gamma}{\partial \gamma} + \frac{V_r}{r} \tag{2.4.26}$$

To transform the derivative $d\rho/dt$ in the continuity equation (2.4.1) to cylindrical coordinates, we use the transformation formula

$$\frac{df}{dt} = \frac{\partial f}{\partial t} + \frac{\partial f}{\partial q_1} \cdot \frac{dq_1}{dt} + \frac{\partial f}{\partial q_2} \cdot \frac{dq_2}{dt} + \frac{\partial f}{\partial q_3} \cdot \frac{dq_3}{dt} \tag{2.4.27}$$

in which $f(x, y, z, t)$ is a function of Cartesian coordinates and time. We obtain

$$\begin{aligned} \frac{d\rho}{dt} &= \frac{\partial \rho}{\partial t} + \frac{dx}{dt} \cdot \frac{\partial \rho}{\partial x} + \frac{dr}{dt} \cdot \frac{\partial \rho}{\partial r} + \frac{d\gamma}{dt} \cdot \frac{\partial \rho}{\partial \gamma} \\ &= \frac{\partial \rho}{\partial t} + V_x \frac{\partial \rho}{\partial x} + V_r \frac{\partial \rho}{\partial r} + \frac{V_\gamma}{r} \cdot \frac{\partial \rho}{\partial \gamma}. \end{aligned} \tag{2.4.28}$$

Substituting their values for div $\mathbf{V}$ and $d\rho/dt$ in Eq. (2.4.1), we find

$$\frac{\partial \rho}{\partial t} + \frac{\partial (\rho V_x)}{\partial x} + \frac{\partial (\rho V_r)}{\partial r} + \frac{1}{r} \cdot \frac{\partial (\rho V_\gamma)}{\partial \gamma} + \frac{\rho V_r}{r} = 0 \tag{2.4.29}$$

Let us write this equation in a somewhat different form:

$$r \frac{\partial \rho}{\partial t} + \frac{\partial (\rho r V_x)}{\partial x} + \frac{\partial (\rho r V_r)}{\partial r} + \frac{1}{r} \cdot \frac{\partial (\rho r V_\gamma)}{\partial \gamma} = 0 \tag{2.4.30}$$

For the particular case of steady motion

$$\frac{\partial (\rho r V_x)}{\partial x} + \frac{\partial (\rho r V_r)}{\partial r} + \frac{1}{r} \cdot \frac{\partial (\rho r V_\gamma)}{\partial \gamma} = 0 \tag{2.4.31}$$

For potential motion, substitutions may be made in the continuity equation:

$$V_x = \partial \varphi/\partial x, \quad V_r = \partial \varphi/\partial r, \quad V_\gamma = (1/r)\, (\partial \varphi/\partial \gamma) \tag{2.4.25'}$$

If the motion of a gas is simultaneously axisymmetric as, for example, if it flows about a body of revolution at a zero angle of attack, the flow parameters do not depend on the angular coordinate γ, and the continuity equation has a simpler form:

$$\partial (\rho r V_x)/\partial x + \partial (\rho r V_r)/\partial r = 0 \tag{2.4.32}$$

Spherical Coordinates. Using relation (2.4.24), having in view formulas (2.4.13) for spherical coordinates, and also relations (2.4.17) for Lamé's coefficients and the expressions for the velocity components

$$V_1 = V_r = \frac{dr}{dt}, \quad V_2 = V_\theta = \frac{1}{r}\frac{d\theta}{dt},$$

$$V_3 = V_\psi = r \sin\theta \frac{d\psi}{dt} \tag{2.4.33}$$

we obtain the following expression for the divergence of the velocity:

$$\text{div } \mathbf{V} = \frac{1}{r^2} \cdot \frac{\partial (V_r r^2)}{\partial r} + \frac{1}{r \sin\theta} \cdot \frac{\partial (V_\theta \sin\theta)}{\partial \theta} + \frac{1}{r \sin\theta} \cdot \frac{\partial V_\psi}{\partial \psi} \tag{2.4.34}$$

We shall write the total derivative for the density $d\rho/dt$ in accordance with (2.4.27) in the following form:

$$\frac{d\rho}{dt} = \frac{\partial \rho}{\partial t} + \frac{dr}{dt} \cdot \frac{\partial \rho}{\partial r} + \frac{d\theta}{dt} \cdot \frac{\partial \rho}{\partial \theta} + \frac{d\psi}{dt} \cdot \frac{\partial \rho}{\partial \psi}$$

$$= \frac{\partial \rho}{\partial t} + V_r \frac{\partial \rho}{\partial r} + \frac{V_\theta}{r} \cdot \frac{\partial \rho}{\partial \theta} + \frac{V_\psi}{r \sin\theta} \cdot \frac{\partial \rho}{\partial \psi} \tag{2.4.35}$$

Introducing the values of div **V** from (2.4.34) and the derivative $d\rho/dt$ from (2.4.35) into (2.4.1) and grouping terms, we have

$$\frac{\partial \rho}{\partial t} + \frac{1}{r^2} \cdot \frac{\partial (\rho V_r r^2)}{\partial r} + \frac{1}{r \sin\theta} \cdot \frac{\partial (\rho V_\theta \sin\theta)}{\partial \theta} + \frac{1}{r \sin\theta} \cdot \frac{\partial (\rho V_\psi)}{\partial \psi} = 0 \tag{2.4.36}$$

For steady motion, the partial derivative $\partial\rho/\partial t = 0$, hence

$$\frac{1}{r} \cdot \frac{\partial (\rho V_r r^2)}{\partial r} + \frac{1}{\sin\theta} \cdot \frac{\partial (\rho V_\theta \sin\theta)}{\partial \theta} + \frac{1}{\sin\theta} \cdot \frac{\partial (\rho V_\psi)}{\partial \psi} = 0 \tag{2.4.37}$$

In the particular case of an incompressible fluid (ρ = const)

$$\frac{1}{r} \cdot \frac{\partial (V_r r^2)}{\partial r} + \frac{1}{\sin\theta} \cdot \frac{\partial (V_\theta \sin\theta)}{\partial \theta} + \frac{1}{\sin\theta} \cdot \frac{\partial V_\psi}{\partial \psi} = 0 \tag{2.4.38}$$

The following substitutions must be performed to transform the continuity equation for potential motion:

$$V_r = \frac{\partial \varphi}{\partial r}, \quad V_\theta = \frac{1}{r} \cdot \frac{\partial \varphi}{\partial \theta}, \quad V_\psi = \frac{1}{r \sin\theta} \cdot \frac{\partial \varphi}{\partial \psi} \tag{2.4.39}$$

Continuity Equation of Gas Flow along a Curved Surface

Let us consider a particular form of the continuity equation in curvilinear orthogonal coordinates that is used in studying flow over a curved wall. The x-axis in this system of coordinates coincides with the contour of the wall, and the y-axis with a normal to this wall at

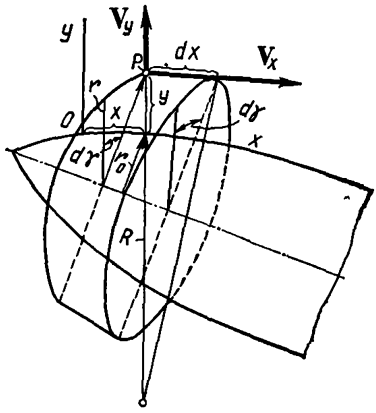

Fig. 2.4.3
To the derivation of the continuity equation in curvilinear coordinates

the point being considered. The coordinates of point P on the plane (Fig. 2.4.3) equal the length x measured along the wall and the distance y measured along a normal to it, respectively. Assume that the wall is a surface of revolution in an axisymmetric flow of a gas. The curvilinear coordinates of point P are:

$$q_1 = x,\ q_2 = y,\ q_3 = \gamma \tag{2.4.40}$$

The elementary lengths of the coordinate line arcs are

$$ds_1 = (1 + y/R)\,dx,\ ds_2 = dy,\ ds_3 = r\,d\gamma \tag{2.4.41}$$

where r is the radial coordinate of point P measured along a normal to the axis of the surface of revolution, and R is the radius of curvature of the surface in the section being considered.

Consequently, Lamé's coefficients are

$$h_1 = 1 + y/R,\ h_2 = 1,\ h_3 = r \tag{2.4.42}$$

Let us use formula (2.4.24) for div V in which the velocity components are

$$V_1 = V_x = ds_1/dt = (1 + y/R)\,dx/dt,\quad V_2 = V_y = dy/dt,\quad V_3 = 0 \tag{2.4.43}$$

Substitution yields

$$\operatorname{div} \mathbf{V} = \frac{1}{(1+y/R)\,r}\left\{\frac{\partial (V_x r)}{\partial x} + \frac{\partial [V_y r\,(1+y/R)]}{\partial y}\right\} \tag{2.4.44}$$

Let us calculate the total derivative for the density:

$$\begin{aligned}\frac{d\rho}{dt} &= \frac{\partial \rho}{\partial t} + \frac{dx}{dt}\cdot\frac{\partial \rho}{\partial x} + \frac{dy}{dt}\cdot\frac{\partial \rho}{\partial y}\\ &= \frac{\partial \rho}{\partial t} + \frac{V_x}{1+y/R}\cdot\frac{\partial \rho}{\partial x} + V_y\frac{\partial \rho}{\partial y}\end{aligned} \tag{2.4.45}$$

Introducing expressions (2.4.44) and (2.4.45) into (2.4.1), after simple transformations we obtain the continuity equation

$$\frac{\partial \rho}{\partial t} r (1 + y/R) + \frac{\partial (\rho r V_x)}{\partial x} + \frac{\partial [\rho r (1 + y/R) V_y]}{\partial y} = 0 \qquad (2.4.46)$$

When studying the motion of a gas near a wall with a small curvature or in a thin layer adjacent to a surface (for example, in a boundary layer), the coordinate $y \ll R$. Consequently

$$(\partial \rho/\partial t)\, r + \partial (\rho r V_x)/\partial x + \partial (\rho r V_y)/\partial y = 0 \qquad (2.4.47)$$

The form of the obtained equation is the same as for a surface with a straight generatrix. For steady flow

$$\partial (\rho r V_x)/\partial x + \partial (\rho r V_y)/\partial y = 0 \qquad (2.4.48)$$

For two-dimensional flow near a curved wall (a cylindrical surface), the continuity equation has the form

$$\frac{\partial \rho}{\partial t} (1 + y/R) + \frac{\partial (\rho V_x)}{\partial x} + \frac{\partial [\rho V_y (1 + y/R)]}{\partial y} = 0 \qquad (2.4.49)$$

For $y \ll R$, we approximately have

$$\partial \rho/\partial t + \partial (\rho V_x)/\partial x + \partial (\rho V_y)/\partial y = 0 \qquad (2.4.50)$$

Hence, for flow near a wall, the continuity equation in curvilinear coordinates has the same form as in Cartesian coordinates.

For steady flow, $\partial \rho/\partial t = 0$; in this case the continuity equation is

$$\partial (\rho V_x)/\partial x + \partial (\rho V_y)/\partial y = 0 \qquad (2.4.50')$$

Equations (2.4.48) and (2.4.50′) can be combined into a single one:

$$\partial/(\rho V_x r^{\varepsilon})/\partial x + \partial (\rho V_y r^{\varepsilon})/\partial y = 0 \qquad (2.4.48')$$

where $\varepsilon = 0$ for a two-dimensional plane flow and $\varepsilon = 1$ for a three-dimensional axisymmetric flow.

Flow Rate Equation

Let us consider a particular form of the continuity equation for a steady fluid flow having the shape of a stream filament. The mass of the fluid in a fixed volume confined within the surface of the filament and the end plane cross sections does not change in time because the condition that $\partial \rho/\partial t = 0$ is observed at every point. Hence the mass of the fluid entering the volume in unit time via the end cross section with an area of S_1 and equal to $\rho_1 V_1 S_1$ is the same as the mass of the fluid $\rho_2 V_2 S_2$ leaving through the opposite cross section with an area of S_2 (ρ_1 and ρ_2 are the densities, V_1 and V_2 are the speeds in the first and second cross sections of the filament, respective-

ly). We thus have $\rho_1 V_1 S_1 = \rho_2 V_2 S_2$. Since this equation can be related to any cross section, in the general form we have

$$\rho VS = \text{const} \tag{2.4.51}$$

This is the **flow rate equation.**

2.5. Stream Function

The studying of a vortex-free gas flow is simplified because it can be reduced to the finding of one unknown potential function completely determining the flow. We shall show that for certain kinds of a vortex flow there is also a function determining its kinematic characteristics.

Let us consider a two-dimensional (plane or spatial axisymmetric) steady vortex flow of a fluid. It can be established from continuity equation (2.4.32′) that there is a function ψ of the coordinates x and y determined by the relations

$$\partial\psi/\partial x = -\rho y^{\varepsilon} V_y; \quad \partial\psi/\partial y = \rho y^{\varepsilon} V_x \tag{2.5.1}$$

Indeed, introducing these relations into (2.4.32′), we obtain $\partial^2\psi/(\partial y\, \partial x) = \partial^2\psi/(\partial x\, \partial y)$, i.e. an identity. Substituting (2.5.1) into the equation of streamlines $V_y/\partial y = V_x/dx$ written in the form

$$\rho y^{\varepsilon} V_y\, dx - \rho y^{\varepsilon} V_x\, dy = 0 \tag{2.5.2}$$

we obtain the expression

$$(\partial\psi/\partial x)\, dx + (\partial\psi/\partial y)\, dy = 0$$

from which it follows that (2.5.2) is a differential of the function ψ and, consequently,

$$d\psi = 0 \tag{2.5.3}$$

Integrating (2.5.3), we find an equation of streamlines in the form

$$\psi\,(x,\ y) = \text{const} \tag{2.5.4}$$

The function ψ, called the **stream function**, completely determines the velocity of a vortex flow in accordance with the relations

$$V_x = (1/\rho y^{\varepsilon})\, \partial\psi/\partial y, \quad V_y = -\,(1/\rho y^{\varepsilon})\, \partial\psi/\partial x \tag{2.5.5}$$

We remind our reader that for a two-dimensional flow, we have to assume in these expressions that $\varepsilon = 0$, while for a three-dimensional axisymmetric flow $\varepsilon = 1$ and $y = r$.

A family of streamlines of a potential flow can also be characterized by the function $\psi = \text{const}$ that is associated with the velocity potential by the relations

$$\partial\varphi/\partial x = (1/\rho y^{\varepsilon})\, \partial\psi/\partial y, \quad \partial\varphi/\partial y = -\,(1/\rho y^{\varepsilon})\, \partial\psi/\partial x \tag{2.5.6}$$

Assuming in (2.5.5) and (2.5.6) that $\rho = \text{const}$, we obtain the relevant expressions for an incompressible flow:

$$V_x = (1/y^{\varepsilon})\,\partial\psi/\partial y, \quad V_y = -(1/y^{\varepsilon})\,\partial\psi/\partial x \tag{2.5.7}$$

$$\partial\varphi/\partial x = (1/y^{\varepsilon})\,\partial\psi/\partial y, \quad \partial\varphi/\partial y = -(1/y^{\varepsilon})\,\partial\psi/\partial x \tag{2.5.8}$$

Assuming in Eqs. (2.5.8) that $\varepsilon = 0$, we obtain the following equations for an incompressible two-dimensional flow:

$$\partial\varphi/\partial x = \partial\psi/\partial y, \quad \partial\varphi/\partial y = -\partial\psi/\partial x \tag{2.5.9}$$

Knowing the velocity potential, we can use these equations to determine the stream function with an accuracy to within an arbitrary constant, and vice versa.

In addition to streamlines, we can construct a family of equipotential curves (on a plane) or of equipotential surfaces (in an axisymmetric flow) in a potential flow that is determined by the equation $\varphi = \text{const}$.

Let us consider the vectors

$$\text{grad}\,\varphi = (\partial\varphi/\partial x)\,\mathbf{i} + (\partial\varphi/\partial y)\,\mathbf{j} \text{ and } \text{grad}\,\psi = (\partial\psi/\partial x)\,\mathbf{i} + (\partial\psi/\partial y)\mathbf{j}$$

whose directions coincide with those of normals to the curves $\varphi = \text{const}$ and $\psi = \text{const}$, respectively. The scalar (dot) product of these vectors is

$$\text{grad}\,\varphi \cdot \text{grad}\,\psi = (\partial\varphi/\partial x)\,\partial\psi/\partial x + (\partial\varphi/\partial y)\,\partial\psi/\partial y$$

With a view to formulas (2.3.2) and (2.5.5), we can establish that this product equals zero. Hence it follows that streamlines are orthogonal to equipotential lines (on a plane) or to equipotential surfaces (in an axisymmetric flow).

2.6. Vortex Lines

A **vortex line** is defined to be a curve s constructed at a definite instant in a fluid flow and having the property that at each point of it the angular velocity vector $\boldsymbol{\omega}$ coincides with the direction of a tangent.

A vortex line is constructed similarly to a streamline (see Fig. 2.1.1). The only difference is that the angular velocities of rotation of the particles $\boldsymbol{\omega}$ ($\boldsymbol{\omega}_1$, $\boldsymbol{\omega}_2$, etc.) are taken instead of the linear velocities. In accordance with this definition, the cross product $\boldsymbol{\omega} \times d\mathbf{S} = 0$, i.e.

$$\begin{vmatrix} \mathbf{i} & \mathbf{j} & \mathbf{k} \\ \omega_x & \omega_y & \omega_z \\ dx & dy & dz \end{vmatrix} = \mathbf{i}\,(\omega_y\,dz - \omega_z\,dy) - \mathbf{j}\,(\omega_x\,dz - \omega_z\,dx) + \mathbf{k}\,(\omega_x\,dy - \omega_y\,dx) = 0$$

Hence, taking into account that, for example, $\omega_y\,dz - \omega_z\,dy = 0$, and so on, we obtain an equation of a vortex line:

$$dx/\omega_x = dy/\omega_y = dz/\omega_z \qquad (2.6.1)$$

By constructing vortex lines through the points of an elementary contour with a cross-sectional area of σ, we obtain a **vortex tube.** The product $\omega\sigma$ is called the **intensity** or **strength of a vortex tube,** or simply the **vorticity.**

We shall prove that the vorticity is constant for all the sections of a vortex tube. For this purpose, we shall use the analogy with the flow of an incompressible fluid for which div $\mathbf{V} = 0$. A corollary is the flow rate equation for a stream filament $V_1S_1 = V_2S_2 = \ldots = VS = \text{const}$.

Let us consider vortex motion and the expression for the divergence of the angular velocity

$$\text{div}\,\boldsymbol{\omega} = \partial\omega_x/\partial x + \partial\omega_y/\partial y + \partial\omega_z/\partial z$$

Substituting for the components of $\boldsymbol{\omega}$ their values from (2.2.3) and (2.2.6), we obtain, provided that the second derivatives of V_x, V_y, and V_z are continuous, the expression div $\boldsymbol{\omega} = 0$. Using the analogy with the flow rate equation $VS = \text{const}$, we obtain an equation for the flow of the vector $\boldsymbol{\omega}$ along a vortex tube in the form

$$\omega_1\sigma_1 = \omega_2\sigma_2 = \ldots = \omega\sigma = \text{const} \qquad (2.6.2)$$

This equation expresses the Helmholtz theorem on the constancy of the vorticity along a vortex tube. The property of a vortex tube consisting in that *it cannot break off suddenly or terminate in a sharp point* follows from this theorem. The termination in a sharp point is impossible because at a cross-sectional area of the tube of $\sigma \to 0$, the angular velocity ω would tend to infinity according to the Helmholtz theorem, and this is not real physically.

2.7. Velocity Circulation

Concept

Velocity circulation is of major significance in aerodynamics. This concept is used when studying the flow over craft and, particularly, when determining the lift force acting on a wing.

Let us consider in a fluid flow a fixed closed contour K at each point of which the velocity $\mathbf{V}$ is known, and evaluate the integral over this contour:

$$\Gamma = \int_{(K)} \mathbf{V}\cdot d\mathbf{s} \qquad (2.7.1)$$

where $\mathbf{V} \cdot d\mathbf{s}$ is the dot product of the vectors $\mathbf{V}$ and $d\mathbf{s}$. The quantity Γ determined in this way is known as the **circulation of the velocity** around a closed contour. Since

$$\mathbf{V} = V_x\mathbf{i} + V_y\mathbf{j} + V_z\mathbf{k} \text{ and } d\mathbf{s} = dx\,\mathbf{i} + dy\,\mathbf{j} + dz\,\mathbf{k}$$

we have

$$\Gamma = \int_{(K)} V_x\,dx + V_y\,dy + V_z\,dz \tag{2.7.2}$$

Taking also into account that the dot product $\mathbf{V} \cdot d\mathbf{s} = V \cos(\widehat{\mathbf{V}\,d\mathbf{s}})\,ds = V_s\,ds$, where V_s is the projection of the velocity onto a tangent, we obtain

$$\Gamma = \int_{(K)} V_s\,ds \tag{2.7.3}$$

If the contour coincides with a streamline in the form of a circle of radius r at each point of which the velocity V_s is identical in magnitude and direction, we have

$$\Gamma = 2\pi r V_s \tag{2.7.4}$$

The circulation of the velocity in a vortex-free flow can be expressed in terms of the velocity potential. Assuming that $V_x\,dx + V_y\,dy + V_z\,dz = d\varphi$, we obtain for an open contour

$$\Gamma = \int_{(L)} d\varphi = \varphi_A - \varphi_B \tag{2.7.5}$$

where φ_A and φ_B are the values of the potential function at the ends of the contour. For a closed contour, φ_A and φ_B are the values of the velocity potential at points A and B of the contour coinciding with each other. If the potential function is unambiguous, then $\varphi_A = \varphi_B$, and the velocity circulation around the closed contour is zero; ambiguity of the velocity potential ($\varphi_A \neq \varphi_B$) determines a non-zero value of the circulation.

Stokes Theorem

Let us consider elementary contour $ABCD$ (see Fig. 2.2.1) and evaluate the circulation around this contour. We shall assume that the velocities are constant along each edge and are equal to the following values:

$$V_x\,(AB),\ V_y + \frac{\partial V_y}{\partial x}\,dx\,(BC),\ V_x + \frac{\partial V_x}{\partial y}\,dy\,(CD),\ V_y\,(AD)$$

Considering the counterclockwise direction of circumventing the contour (from the x-axis toward the y-axis) to be positive, we obtain

for the circulation

$$d\Gamma_z = V_x\,dx + \left(V_y + \frac{\partial V_y}{\partial x}\,dx\right)dy - \left(V_x + \frac{\partial V_x}{\partial y}\,dy\right)dx - V_y\,dy$$

or

$$d\Gamma_z = (\partial V_y/\partial x - \partial V_x/\partial y)\,dx\,dy$$

According to (2.2.3), the quantity in parentheses equals the double value of the angular velocity component $2\omega_z$. Consequently,

$$d\Gamma_z = 2\omega_z\,dx\,dy \tag{2.7.6}$$

We can prove similarly that

$$d\Gamma_x = 2\omega_x\,dy\,dz \text{ and } d\Gamma_y = 2\omega_y\,dx\,dz$$

In these expressions, the products of the differentials are the areas confined by the relevant elementary contours. With a view to the results obtained, for the area element $d\sigma$ oriented in space arbitrarily and confined within an elementary contour, the circulation is

$$d\Gamma_n = 2\omega_n\,d\sigma \tag{2.7.7}$$

where ω_n is the component of the angular velocity along the direction of the normal n to the surface element $d\sigma$. In accordance with (2.7.7), the velocity circulation around an elementary closed contour equals the double strength of a vortex inside the contour.

Relation (2.7.7) can be used for a contour L of finite dimensions confining a surface S at each point of which the value of ω_n is known. Here the velocity circulation around the contour is

$$\Gamma = 2\int\limits_{(S)}\int \omega_n\,d\sigma \tag{2.7.8}$$

Formula (2.7.8) expresses the Stokes theorem: the velocity circulation around the closed contour L equals the double integral of the strength of the vortices passing through the surface confined by the contour. The quantity determined by this formula is the vorticity (vortex strength) and is designated by

$$\varkappa = 2\int\limits_{(S)}\int \omega_n\,d\sigma \tag{2.7.8'}$$

Combining formulas (2.7.3) and (2.7.8) for Γ, we obtain a relation expressing the integral over the contour K in terms of the integral over the surface S confined within this contour K:

$$\int\limits_{(K)} V_s\,ds = 2\int\limits_{(S)}\int \omega_n\,d\sigma \tag{2.7.8''}$$

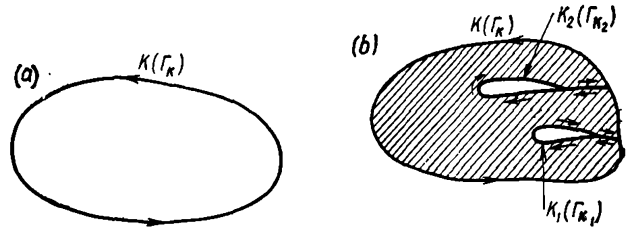

Fig. 2.7.1
Simply and triply connected regions on a plane:
a—simply connected region (Γ_K = circulation over the contour K); *b*—triply connected region (Γ_K = circulation of the external contour, Γ_{K_1} and Γ_{K_2} = circulations over the internal contours K_1 and K_2, respectively)

The above expressions relate to a simply connected contour (the region being considered is confined within a single contour, Fig. 2.7.1*a*). But the Stokes theorem can also be extended to multiply connected contours (a region confined by one external and several internal contours). Equation (2.7.8″) is used provided that the external contour is connected to the internal ones by auxiliary lines (cuts) so as to obtain a simply connected region. Now the double integral in (2.7.8″) is used for the hatched region (Fig. 2.7.1*b*), while the contour integral is taken for the obtained simply connected region, i.e. around the external contour, along all the cuts, and also around all the internal contours. In accordance with this, by formula (2.7.8″), and also with a view to Fig. 2.7.1*b* showing a triply connected region, we obtain

$$\Gamma_K - \Gamma_{K_1} - \Gamma_{K_2} = 2 \int\limits_{(S)} \int \omega_n \, d\sigma$$

whence the circulation over the contour K of the region being considered is

$$\Gamma_K = \Gamma_{K_1} + \Gamma_{K_2} + 2 \int\limits_{(S)} \int \omega_n \, d\sigma$$

Using this formula when we have n internal contours, we find

$$\Gamma_K = \sum_{i}^{i=n} \Gamma_{K_i} + 2 \int\limits_{(S)} \int \omega_n \, d\sigma$$

Vortex-Induced Velocities

Appearing vortices produce additional velocities in the fluid-filled space surrounding them. This effect is similar to the electromagnetic influence of a conductor carrying an electric current. In

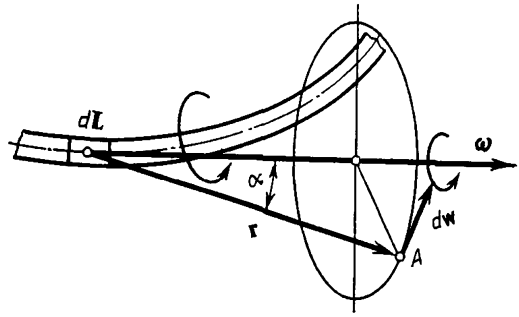

Fig. 2.7.2
Influence of a vortex

accordance with this analogy, the velocities produced by a vortex are said to be induced.

This electromagnetic analogy is expressed in that to determine the vortex-induced velocity, a **Biot-Savart relation** is used similar to the one expressing the known law of electromagnetic induction.

Let us consider a curvilinear vortex of an arbitrary shape (Fig. 2.7.2). The velocity vector $d\mathbf{w}$ induced by the vortex element $d\mathbf{L}$ at point A whose location is determined by the position vector $\mathbf{r}$ coincides in direction with the cross product $\mathbf{r} \times d\mathbf{L}$, i.e. the vector $d\mathbf{w}$ is perpendicular to the plane containing the vectors r and $d\mathbf{L}$. The value of $d\mathbf{w}$ is determined with the aid of the Biot-Savart formula, which in the vector form is as follows:

$$d\mathbf{w} = (\Gamma/4\pi)\, \mathbf{r} \times d\mathbf{L}/r^3 \qquad (2.7.9)$$

where Γ is the velocity circulation. The derivation of formula (2.7.9) is given in [10].

Since the magnitude of the cross product $|\, \mathbf{r} \times d\mathbf{L} \,| = r \sin \alpha\, dL$, where α is the angle between the direction of a vortex element and the position vector r, the magnitude of the velocity induced at point A is

$$dw = (\Gamma/4\pi) \sin \alpha\, dL/r^2 \qquad (2.7.10)$$

Let us use the Biot-Savart relation to calculate the velocity induced by a section of a line vortex (Fig. 2.7.3). Since $r = h/\sin \alpha$, $dL = r\, d\alpha/\sin \alpha = h\, d\alpha/\sin^2 \alpha$, then

$$\omega = \frac{\Gamma}{4\pi h} \int_{\alpha_1}^{\alpha_2} \sin \alpha\, d\alpha = \frac{\Gamma}{4\pi h} (\cos \alpha_1 - \cos \alpha_2) \qquad (2.7.11)$$

For a vortex both of whose ends extend to infinity (an infinite vortex), $\alpha_1 = 0$, $\alpha_2 = \pi$, and, therefore,

$$w = \Gamma/(2\pi h) \qquad (2.7.12)$$

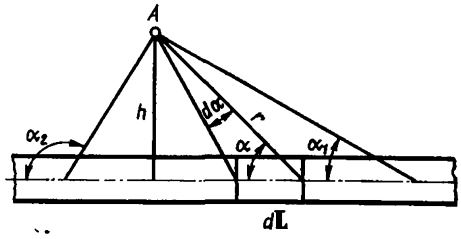

Fig. 2.7.3
Influence of a line vortex on a fluid particle at point A

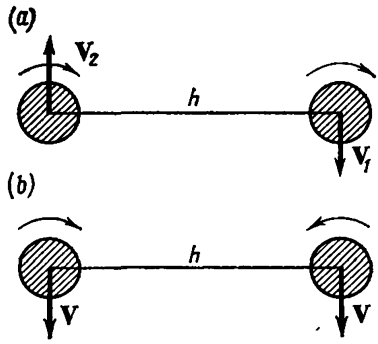

Fig. 2.7.4
Interaction of vortices:
a—vortices with an identical direction of rotation; *b*—vortices with opposite directions of motion

For a vortex, one end of which extends to infinity, and the other has its origin at point A (a semi-infinite vortex), we have $\alpha_1 = 0$ and $\alpha_2 = \pi/2$. Consequently

$$w = \Gamma/(4\pi h) \tag{2.7.13}$$

If a fluid accommodates two or more vortices, they interact with one another, and as a result the vortex system is in motion. The velocity of this motion is determined with the aid of the Biot-Savart relation. Let us take as an example two infinite vortices with the same strength and direction of rotation (Fig. 2.7.4*a*). These vortices impart to each other the velocities $V_2 = -\Gamma/(2\pi h)$ and $V_1 = \Gamma/(2\pi h)$ that are equal in magnitude and opposite in direction. As a result, both vortices rotate about an axis passing through the middle of the distance between them. If of two vortices one has a strength of the opposite sign (Fig. 2.7.4*b*), the induced velocities are of the same direction and, consequently, the system of vortices moves translationally at the velocity $V = \Gamma/(2\pi h)$ in a direction perpendicular to the straight line connecting the vortices.

2.8. Complex Potential

The motion of a vortex-free incompressible flow can be determined completely if we know the potential function φ or the stream function ψ, the relation between which is given by Eqs. (2.5.9), which

in the theory of the functions of a complex variable are known as the Cauchy-Riemann equations. They express the necessary and sufficient conditions needed for a combination of the two functions $\varphi + i\psi$ to be an analytical function of the complex variable $\sigma = x + iy$, i.e. to be differentiable at all points of a certain region.

Let us introduce a symbol for this function:

$$W(\sigma) = \varphi + i\psi \tag{2.8.1}$$

The function $W(\sigma)$ that is determined if the function of two real variables $\varphi = \varphi(x, y)$ and $\psi = \psi(x, y)$ satisfies differential equations (2.5.9) is called a **complex potential**. If we recall that the values of the functions $\varphi(x, y)$ or $\psi(x, y)$ allow one to determine the velocity field in a moving fluid unambiguously, then, consequently, any two-dimensional flow can be set by a complex potential. Hence, the problem on calculating such a flow can be reduced to finding the function $W(\sigma)$. Let us calculate the derivative of the function $W(\sigma)$ with respect to the complex variable σ:

$$dW/d\sigma = \partial\varphi/\partial x + i\partial\psi/\partial x \tag{2.8.2}$$

Since $\partial\varphi/\partial x = V_x$, $\partial\psi/\partial x = -V_y$, then

$$dW/d\sigma = V_x - iV_y \tag{2.8.3}$$

This expression is called the **complex velocity**. Its magnitude gives the value of the velocity itself, $|dW/d\sigma| = \sqrt{V_x^2 + V_y^2} = V$. It is evident that the real velocity vector $\mathbf{V} = V_x + iV_y$ is the mirror image relative to the x-axis of the vector of the complex velocity. Let us denote by θ the angle between the vector $dW/d\sigma$ and the x-axis and determine the velocities $V_x = V\cos\theta$ and $V_y = V\sin\theta$. Using the Euler formula

$$\cos\theta - i\sin\theta = e^{-i\theta}$$

we obtain

$$dW/d\sigma = Ve^{-i\theta} \tag{2.8.4}$$

2.9. Kinds of Fluid Flows

Let us consider the characteristic kinds of flows of an incompressible fluid, their geometric configuration (aerodynamic spectrum), expressions for the complex potentials, and also the relevant potential functions and stream functions.

Parallel Flow

Assume that the flow of a fluid is given by the complex potential

$$W(\sigma) = V(\cos\theta - i\sin\theta)\sigma \tag{2.9.1}$$

where V and θ are constants for the given conditions.

According to (2.8.1)

$$\varphi + i\psi = V(\cos\theta - i\sin\theta)(x + iy)$$

whence we find the velocity potential and the stream function:

$$\varphi = V(x\cos\theta + y\sin\theta) \tag{2.9.2}$$

$$\psi = V(y\cos\theta - x\sin\theta) \tag{2.9.3}$$

Examination of the expressions for φ or ψ reveals that the flow being considered is plane and steady because they do not contain the time explicitly. In such a flow, the streamlines and pathlines coincide.

From (2.9.2), we can find the components of the flow velocity:

$$\partial\varphi/\partial x = V_x = V\cos\theta,\ \partial\varphi/\partial y = V_y = V\sin\theta,\ \partial\varphi/\partial z = V_z = 0 \tag{2.9.4}$$

Here V is the resultant velocity of the flow, and θ is the angle between its direction and the x-axis. Assuming the stream function ψ in (2.9.3) to be constant and including V in it, we obtain the equation

$$y\cos\theta - x\sin\theta = \text{const} \tag{2.9.5}$$

A glance at this equation shows that the streamlines are parallel straight lines inclined to the x-axis at the angle θ (Fig. 2.9.1). Since the velocity components V_x and V_y are positive, the flow will be directed as shown in Fig. 2.9.1. This flow is called a **forward plane-parallel** one.

In the particular case when the flow is parallel to the x-axis ($\theta = 0$, $V_x = V$, $V_y = 0$), the complex potential is

$$W(\sigma) = V\sigma \tag{2.9.6}$$

Two-Dimensional Point Source and Sink

Let us consider the complex potential

$$W(\sigma) = (q/2\pi)\ln\sigma \tag{2.9.7}$$

where q is a constant. We can write this equation in the form

$$\varphi + i\psi = (q/2\pi)\ln(re^{i\theta}) = (q/2\pi)(\ln r + i\theta)$$

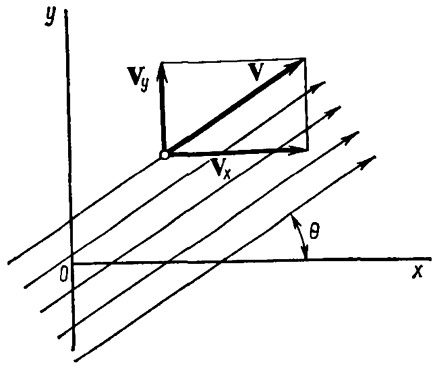

Fig. 2.9.1
General view of a forward plane-parallel flow

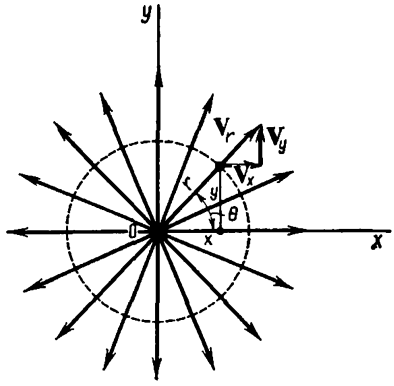

Fig. 2.9.2
A two-dimensional point source

where r is the distance to a point with the coordinates x and y (the polar radius), and θ is the polar angle.

It follows from the obtained equation that

$$\varphi = (q/2\pi) \ln r = (q/2\pi) \ln \sqrt{x^2 + y^2} \tag{2.9.8}$$

$$\psi = (q/2\pi)\,\theta \tag{2.9.9}$$

We find from (2.9.8) that the radial velocity component (in the direction of the radius r) is

$$\partial\varphi/\partial r = V_r = q/(2\pi r) \tag{2.9.10}$$

and the component along a normal to this radius is $V_s = 0$.

We thus obtain a flow whose streamlines (pathlines) are a family of straight lines passing through the origin of coordinates (this also follows from the equation of a streamline $\psi = \text{const}$). Such a radial flow issuing from the origin of coordinates is called a **two-dimensional point source** (Fig. 2.9.2).

The rate of flow of a fluid through a contour of radius r is $2\pi r V_r = Q$. Introducing into this equation the value of V_r from (2.9.10),

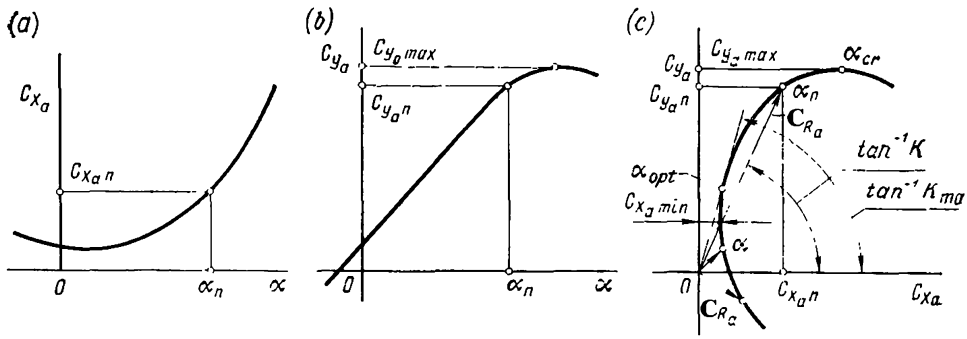

Fig. 1.3.3
Constructing a polar of the first kind of a craft:
a—c_{x_a} vs. α; *b*—c_{y_a} vs. α; *c*—polar of first kind

of the forces and moments acting on the same craft. These relations are used to find the coefficients c_2 and m_2, respectively, converted to the new characteristic dimensions S_2 and L_2:

$$c_2 = c_1 (S_1/S_2), \quad m_2 = m_1 (S_1 L_1/S_2 L_2)$$

where the previous dimensions S_1, L_1 and aerodynamic coefficients c_1, m_1, as well as the new dimensions S_2, L_2 are known.

Polar of a Craft. A very important aerodynamic characteristic that has found widespread use is what is known as the **polar** of a craft. It establishes a relation between the lift and drag forces or, which is the same, between the lift and drag coefficients in a flight path coordinate system. This curve, called a **polar of the first kind** (Fig. 1.3.3*c*) is the locus of the tips of the resultant aerodynamic force vectors $\mathbf{R}_a$ acting on a craft at various angles of attack [or of the vectors of the coefficient $\mathbf{c}_{R_a}$ of this force determined in accordance with the relation $\mathbf{c}_{R_a} = \mathbf{R}_a/(S_r q_\infty)$].

A polar of the first kind is constructed with the aid of graphs of c_{x_a} versus α and c_{y_a} versus α so that the values of c_{x_a} and c_{y_a} are laid off along the axes of abscissas and ordinates, respectively. The relevant angle of attack α, which is a parameter of the polar in the given case, is written at each point of the curve.

A polar of the first kind is convenient for practical use because it allows one to readily find for any angle of attack such a very important aerodynamic characteristic of a craft as its lift-to-drag ratio

$$K = c_{y_a}/c_{x_a} = Y_a/X_a \qquad (1.3.10)$$

If the scales of c_{y_a} (or Y_a) and c_{x_a} (or X_a) are the same, the quantity K equals the slope of a vector drawn from the origin of coordi-

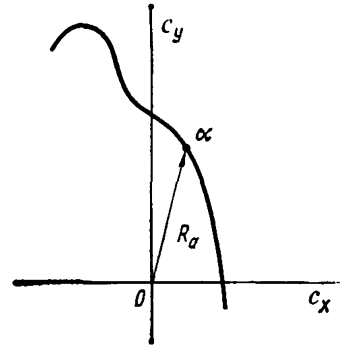

Fig. 1.3.4
Drag polar of the second kind

nates (the pole) to the point of the polar diagram corresponding to the chosen angle of attack.

We can use a polar to determine the **optimal angle of attack** α_{opt} corresponding to the **maximum lift-to-drag ratio:**

$$K_{max} = \tan \alpha_{opt} \qquad (1.3.10')$$

if we draw a tangent to the polar from the origin of coordinates.

The characteristic points of a polar include the point $c_{y_a max}$ corresponding to the **maximum lift force** that is achieved at the critical angle of attack α_{cr}. We can mark a point on the curve determining the minimum drag coefficient $c_{x_a min}$ and the corresponding values of the angle of attack and the lift coefficient.

A polar is symmetric about the axis of abscissas if a craft has horizontal symmetry. For such a craft, the value of $c_{x_a min}$ corresponds to a zero lift force, $c_{y_a} = 0$.

In addition to a polar of the first kind, a **polar of the second kind** is sometimes used. It differs in that it is plotted in a body axis coordinate system along whose axis of abscissas the values of the longitudinal-force coefficient c_x are laid off, and along the axis of ordinates—the normal-force coefficients c_y (Fig. 1.3.4). This curve is used, particularly, in the strength analysis of craft.

Theoretical and experimental investigations show that in the most general case, the aerodynamic coefficients depend for a given body configuration and angle of attack on dimensionless variables such as the Mach number $M_\infty = V_\infty/a_\infty$ and the Reynolds number $Re_\infty = V_\infty L \rho_\infty/\mu_\infty$. In these expressions, a_∞ is the speed of sound in the oncoming flow, ρ_∞ and μ_∞ are the density and dynamic viscosity of the gas, respectively, and L is the length of the body. Hence, a multitude of polar curves exists for each given craft. For example, for a definite number Re_∞, we can construct a family of such curves each of which corresponds to a definite value of the

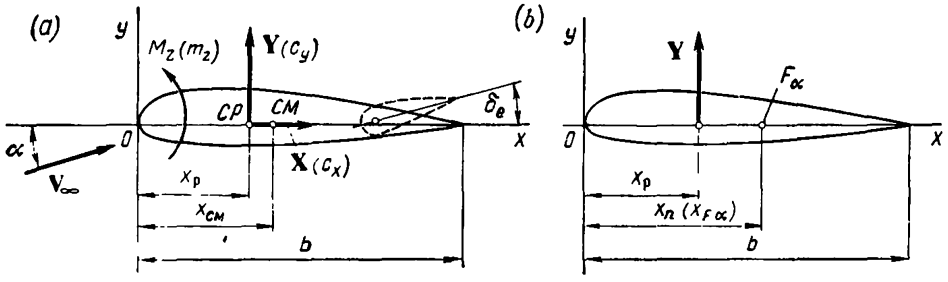

Fig. 1.3.5
Determination of the centre of pressure (*a*) and aerodynamic centre (*b*)

velocity M_∞. The curves in Figs. 1.3.3 and 1.3.4 correspond to a fixed value of Re_∞ and determine the relation between c_{y_a} and c_{x_a} for low-speed flights (of the order of 100 m/s) when the aerodynamic coefficients do not depend on M_∞.

Centre of Pressure and Aerodynamic Centre. The **centre of pressure (CP) of a craft** is the point through which the resultant of the aerodynamic forces passes. The centre of pressure is a conditional point because actually the action of fluid results not in a concentrated force, but in forces distributed over the surface of the moving body. It is customarily assumed that for symmetric bodies or ones close to them this conditional point is on one of the following axes—the longitudinal axis of the craft passing through the centre of mass, the axis of symmetry of a body of revolution, or on the chord of an airfoil.

Accordingly, the longitudinal force X is arranged along this axis, while the centre of pressure when motion occurs in the pitching plane is considered as the point of application of the normal force Y. The position of this centre of pressure is usually determined by the coordinate x_p measured from the front point on the contour of the body in a flow. If the pitching moment M_z about this point and the normal force Y are known (Fig. 1.3.5*a*), the coordinate of the centre of pressure

$$x_p = -M_z/Y \tag{1.3.11}$$

A moment M_z tending to reduce the angle of attack is considered to be negative (Fig. 1.3.5*a*); hence the coordinate x_p is positive. Taking into account that

$$M_z = m_z q_\infty S_r b \quad \text{and} \quad Y = c_y q_\infty S_r$$

we obtain

$$x_p = -m_z b/c_y$$

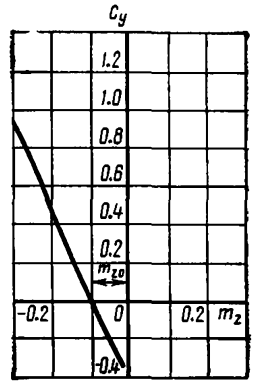

Fig. 1.3.6
Relation between the moment coefficient m_z and normal-force coefficient c_y for an asymmetric aircraft

or, since $-Yx_p = M_z$ is the moment about the front point O, we have

$$M_{zn} = Yx_n + M_z$$

Going over to aerodynamic coefficients, we obtain

$$m_{zn} = c_y (x_n/b) + m_z \tag{1.3.15}$$

For small angles of attack when there is a linear dependence of m_z on c_y of the form

$$m_z = m_{z0} + (\partial m_z/\partial c_y)\, c_y \tag{1.3.16}$$

we obtain

$$m_{zn} = c_y (x_n/b) + m_{z0} + (\partial m_z/\partial c_y)\, c_y$$

or

$$m_{zn} = m_{z0} + c_y (\partial m_z/\partial c_y + x_n/b) \tag{1.3.17}$$

where m_{z0} is the coefficient of the moment about a point on the leading edge at $c_y = 0$ (Fig. 1.3.6).

The second term in (1.3.17) determines the increment of the moment associated with a change in the normal-force coefficient. If we choose the point F_α on a chord whose coordinate $x_n = x_{F_\alpha}$ is determined by the condition (see Fig. 1.3.5*b*)

$$x_n/b = x_{F_\alpha}/b = \bar{x}_{F_\alpha} = -\partial m_z/\partial c_y \tag{1.3.18}$$

the coefficient of the moment about this point will not depend on c_y, and at all (small) angles of attack it will be a constant quantity. This point is called the aerodynamic centre (AC) of the given body. The aerodynamic centre is evidently the point of application of the additional normal force produced by the angle of attack [the coefficient of this force is $(\partial c_y/\partial\alpha)\,\alpha = c_y^\alpha \alpha$]. The pitching moment about an axis passing through this point does not depend on the

angle of attack. Such a point is called the **angle-of-attack aerodynamic centre of a craft.** The centre of pressure and the aerodynamic centre are related by the expression

$$c_p = -\frac{m_z}{c_y} = -\frac{m_{z0} + (\partial m_z/\partial c_y)\, c_y}{c_y} = c_{p0} + \bar{x}_{F_\alpha} \qquad (1.3.19)$$

where $c_{p0} = -m_{z0}/c_y$. For a symmetric configuration, $m_{z0} = 0$, and, consequently, the centre of pressure coincides with the aerodynamic centre.

Expression (1.3.19) holds, however, for a symmetric configuration provided with an elevator deflected through a certain angle δ_e (see Figs. 1.2.2 and 1.3.5). In this case, the moment coefficient is

$$m_z = m_z^\alpha \alpha + m_z^{\delta_e} \delta_e \qquad (1.3.20)$$

and the normal-force coefficient is

$$c_y = c_y^\alpha \alpha + c_y^{\delta_e} \delta_e \qquad (1.3.21)$$

where $m_z^\alpha = \partial m_z/\partial \alpha$, $c_y^\alpha = \partial c_y/\partial \alpha$, $m_z^{\delta_e} = \partial m_z/\partial \delta_e$, and $c_y^{\delta_e} = \partial c_y/\partial \delta_e$.

If a configuration is not symmetric, then

$$m_z = m_{z0} + m_z^\alpha \alpha + m_z^{\delta_e} \delta_e \qquad (1.3.22)$$

$$c_y = c_{y0} + c_y^\alpha \alpha + c_y^{\delta_e} \delta_e \qquad (1.3.23)$$

The point of application of the normal force due to the elevator deflection angle and proportional to this angle is known as the **elevator-deflection aerodynamic centre.** The moment of the forces about a lateral axis passing through this centre is evidently independent of the angle δ_e. In the general case for an asymmetric configuration, its centre of pressure coincides with none of the aerodynamic centres (based on α or δ_e). In a particular case, in a symmetric craft at $\alpha = 0$, the centre of pressure coincides with the aerodynamic centre based on δ_e.

Using the definition of the aerodynamic centres based on the angle of attack and the elevator deflection angle and introducing the corresponding coordinates x_{F_α} and x_{F_δ}, we find the coefficient of the moment about the centre of mass. This coefficient is evaluated by formula (1.3.22), in which

$$m_z^\alpha = c_y^\alpha (\bar{x}_{CM} - \bar{x}_{F_\alpha}), \quad m_z^{\delta_e} = c_y^{\delta_e} (\bar{x}_{CM} - \bar{x}_{F_\delta}) \qquad (1.3.24)$$

where $\bar{x}_{F_\alpha} = x_{F_\alpha}/b$ and $\bar{x}_{F_\delta} = x_{F_\delta}/b$ are the relative coordinates of the aerodynamic centres.

whence

$$x_p/b = c_p = -m_z/c_y \qquad (1.3.11')$$

The dimensionless quantity c_p defined as the ratio between the distance to the centre of pressure and the characteristic length of a body (in the given case the wing chord b) is called the **centre-of-pressure coefficient.** With small angles of attack, when the lift and normal-force coefficients are approximately equal ($c_{y_a} \approx c_y$), we have

$$c_p = -m_{z_a}/c_{y_a} \qquad (1.3.12)$$

In the case being considered of a two-dimensional flow past a body, the pitching-moment coefficients in wind (flight path) and body axis coordinate systems are the same, i.e. $m_{z_a} = m_z$.

For a symmetric airfoil when at $\alpha \to 0$ the quantities c_y and m_z simultaneously take on zero values in accordance with the expressions

$$c_y = (\partial c_y/\partial\alpha)\,\alpha, \quad m_z = (\partial m_z/\partial\alpha)\,\alpha$$

holding at small angles of attack (here the derivatives $\partial c_y/\partial\alpha$ and $\partial m_z/\partial\alpha$ are constant quantities that can be determined for an angle of attack of $\alpha \approx 0$), the coefficient c_p equals a constant value not depending on the angle of attack:

$$c_p = -\partial m_z/\partial c_y \qquad (1.3.13)$$

The value of the coefficient c_p and of the dimensionless coordinate of the centre of mass $\bar{x}_{CM} = x_{CM}/b$ can be used to determine the pitching-moment coefficients about this centre:

$$m_z' = c_y\,(\bar{x}_{CM} - c_p) \qquad (1.3.14)$$

Investigations show that in real conditions of flow, an appreciable displacement of the centre of pressure can be observed in craft even upon a slight change in the angles of attack. This is especially noticeable in craft with an asymmetric configuration or upon deflection of an elevator, which disturbs the existing symmetry. In these conditions, the centre of pressure is not convenient for use as a characteristic point in estimating the position of the resultant of the aerodynamic forces and the appearing pitching moment about the centre of mass. In these conditions, it is more convenient to assess the flight properties of a craft according to the aerodynamic centre location. To reveal the meaning of this concept, let us consider an asymmetric airfoil and evaluate the moment M_{zn} about an arbitrary point F_α with the coordinate x_n on the chord of the airfoil. It follows from Fig. 1.3.5*b* that

$$M_{zn} = Y\,(x_n - x_p)$$

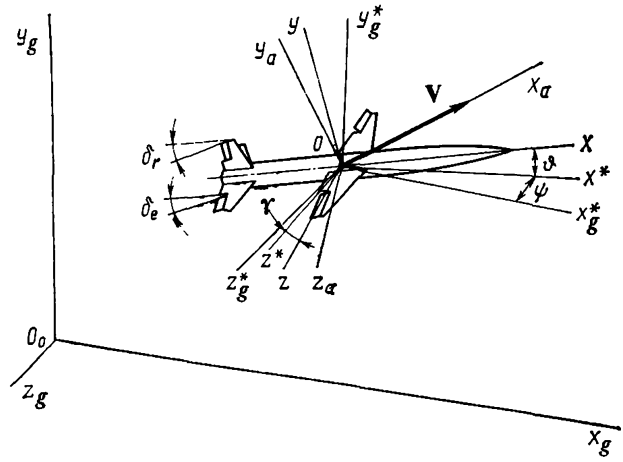

Fig. 1.2.2
Determining the position of a craft in space

the axis Ox and the projection of the vector V onto the plane xOy, and the second is the angle between the vector V and the plane xOy.

The angle of attack is considered to be positive if the projection of the air velocity onto the normal axis is negative. The sideslip angle is positive if this projection onto the lateral axis is positive.

When studying a flight, a **normal earth-fixed coordinate system** is used relative to which the position of a body moving in space is determined. The origin of coordinates of this system (Fig. 1.2.2) coincides with a point on the Earth's surface, for example with the launching point. The axis O_0y_g is directed upward along a local vertical, while the axes O_0x_g and O_0z_g coincide with a horizontal plane. The axis O_0x_g is usually oriented in the direction of flight, while the direction of the axis O_0z_g corresponds to a right-handed coordinate system.

If the origin of an earth-fixed system of coordinates is made to coincide with the centre of mass of a craft, we obtain a normal earth-fixed coordinate system also known as a local geographical coordinate system $Ox_g^*y_g^*z_g^*$ (Fig. 1.2.2). The position of a craft relative to this coordinate system is determined by three angles: the yawing (course) angle ψ, the pitching angle ϑ, and the rolling (banking) angle γ.

The angle ψ is formed by the projection of the longitudinal body axis Ox onto the horizontal plane $x_g^*Oy_g^*$ (Ox^*) and the axis Ox_g^*; this angle is positive if the axis Ox_g^* coincides with the projection of Ox^* by clockwise rotation about the axis Oy_g^*.

The angle ϑ is that between the axis Ox and the horizontal plane $x_g^*Oz_g^*$ and will be positive if this plane is below the longitudinal

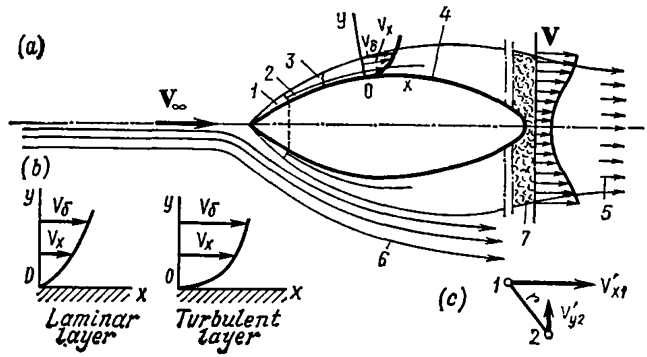

Fig. 1.1.4
Flow of a viscous fluid over a body:

a—schematic view of flow; *1*—laminar boundary layer; *2*—viscous sublayer; *3*—turbulent boundary layer; *4*—surface in the flow; *5*—wake; *6*—free flow; *7*—wake vortex; *b*—velocity profile in the boundary layer; *c*—diagram defining the concept of a two-point correlation coefficient; V_δ is the velocity component at the outer edge of the boundary layer

Turbulence is of a vortex nature, i.e. mass, momentum, and energy are transferred by fluid particles of a vortex origin. Hence it follows that fluctuations are characterized by a statistical association. The **correlation coefficient** between fluctuations at points of the region of a disturbed flow being studied is a quantitative measure of this association. In the general form, this coefficient between two random fluctuating quantities φ and ψ is written as (see [5])

$$R = \overline{\varphi\psi}/(\sqrt{\overline{\varphi^2}}\sqrt{\overline{\psi^2}}) \qquad (1.1.3)$$

If there is no statistical association between the quantities φ and ψ, then $R = 0$; if, conversely, these quantities are regularly associated, the correlation coefficient $R = 1$. This characteristic of turbulence is called a **two-point correlation coefficient.** Its expression can be written (Fig. 1.1.4*c*) for two points *1* and *2* of a fluid volume with the relevant fluctuations V'_{x1} and V'_{y2} in the form

$$R = \overline{V'_{x1}V'_{y2}}/(\sqrt{\overline{V'^2_{x1}}}\sqrt{\overline{V'^2_{y2}}}) \qquad (1.1.3')$$

When studying a three-dimensional turbulent flow, one usually considers a large number of such coefficients. The concept of the **turbulence scale** is introduced to characterize this flow. It is determined by the expression

$$L = \int_0^\infty R\,dr \qquad (1.1.4)$$

The turbulence scale is a linear dimension characterizing the length of the section of a flow on which fluid particles move "in

or measure the fluctuation speed. In a turbulent flow, the instrument registers the deviation of the speed from the mean value—the fluctuation speed.

The kinetic energy of a turbulent flow is determined by the sum of the kinetic energies calculated according to the mean and fluctuation speeds. For a point in question, the kinetic energy of a fluctuation flow can be determined as a quantity proportional to the mean value of the mean square fluctuation velocities. If we resolve the fluctuation flow along the axes of a coordinate system, the kinetic energy of each of the components of such a flow will be proportional to the relevant mean square components of the fluctuation velocities, designated by $\overline{V_x'^2}$, $\overline{V_y'^2}$, and $\overline{V_z'^2}$ and determined from the expression

$$\overline{V_{x(y,z)}'^2} = \frac{1}{t_2 - t_1} \int_{t_1}^{t_2} V_{x(y,z)}'^2 \, dt$$

The concepts of average and fluctuating quantities can be extended to the pressure and other physical parameters. The existence of fluctuation velocities leads to additional normal and shear stresses and to the more intensive transfer of heat and mass. All this has to be taken into account when running experiments in aerodynamic tunnels. The turbulence in the atmosphere was found to be relatively small and, consequently, it should be just as small in the working part of a tunnel. An increased turbulence affects the results of an experiment adversely. The nature of this influence depends on the **turbulence level** (or the **initial turbulence**), determined from the expression

$$\varepsilon = \frac{1}{\overline{V}} \sqrt{(\overline{V_x'^2} + \overline{V_y'^2} + \overline{V_z'^2})/3} \qquad (1.1.1)$$

where $\overline{V}$ is the overall average speed of the turbulent flow at the point being considered.

In modern low-turbulence aerodynamic tunnels, it is possible in practice to reach an initial turbulence close to what is observed in the atmosphere ($\varepsilon \approx 0.01$-0.02).

The important characteristics of turbulence include the root mean square (rms) fluctuations $\sqrt{\overline{V_x'^2}}$, $\sqrt{\overline{V_y'^2}}$, and $\sqrt{\overline{V_z'^2}}$. These quantities, related to the overall average speed, are known as the **turbulence intensities** in the corresponding directions and are denoted as

$$\varepsilon_x = \sqrt{\overline{V_x'^2}}/\overline{V}, \quad \varepsilon_y = \sqrt{\overline{V_y'^2}}/\overline{V}, \quad \varepsilon_z = \sqrt{\overline{V_z'^2}}/\overline{V} \qquad (1.1.2)$$

Using these characteristics, the initial turbulence (1.1.1) can be expressed as follows:

$$\varepsilon = \sqrt{(\varepsilon_x^2 + \varepsilon_y^2 + \varepsilon_z^2)/3} \qquad (1.1.1')$$

we find $Q = q$. The constant q is thus determined by the rate of flow of the fluid from the source. This quantity q is known as the **intensity or strength of the source.**

In addition to a source, there is a kind of motion of a fluid called a **two-dimensional point sink.** The complex potential of a sink is

$$W(\sigma) = -(q/2\pi) \ln \sigma \qquad (2.9.11)$$

The minus sign indicates that unlike a source, motion occurs toward the centre. A sink, like a source, is characterized by its intensity, or strength, q (the rate of flow).

Three-Dimensional Source and Sink

In addition to two-dimensional ones, there also exist **three-dimensional point sources (sinks).** The flux from them is set by the following conditions:

$$V_x = \frac{q}{4\pi} \cdot \frac{\pm x}{R^3}; \quad V_y = \frac{q}{4\pi} \cdot \frac{\pm y}{R^3}; \quad V_z = \frac{q}{4\pi} \cdot \frac{\pm z}{R^3} \qquad (2.9.12)$$

where $R = \sqrt{x^2 + y^2 + z^2}$ and q is the strength of the source (plus sign) or sink (minus sign). The strength of a source (sink) equals the quantity q defined as the flow rate (per second) through the surface of a sphere of radius R. The resultant velocity is

$$V = \sqrt{V_x^2 + V_y^2 + V_z^2} = \pm q/(4\pi R^2) \qquad (2.9.13)$$

and coincides with the direction of the position vector **R**. Consequently, the velocity potential depends only on R and, therefore,

$$\partial\varphi/\partial R = \pm q/(4\pi R^2)$$

Integration yields

$$\varphi = \mp q/(4\pi R) \qquad (2.9.14)$$

where the minus sign relates to a source, and the plus sign to a sink.

Doublet

Let us consider a flow whose complex potential is

$$W(\sigma) = (M/2\pi)(1/\sigma) \qquad (2.9.15)$$

where M is a constant. In accordance with this equation, we have

$$\varphi + i\psi = (M/2\pi)(1/re^{i\theta})$$

Let us transform the right-hand side of this equation. Taking into account that

$$\frac{1}{re^{i\theta}} = \frac{1}{r(\cos\theta + i\sin\theta)} = \frac{1}{r}(\cos\theta - i\sin\theta)$$

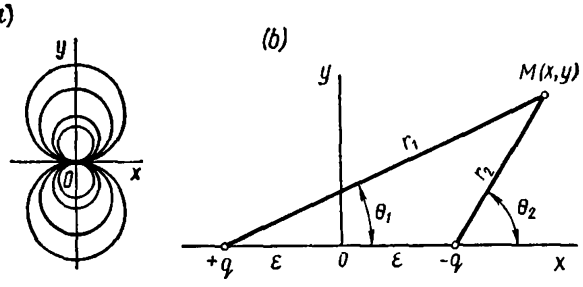

Fig. 2.9.3
To the definition of a doublet:
a—doublet streamlines; *b*—formation of a doublet

we obtain

$$\varphi + i\psi = (M/2\pi r)(\cos\theta - i\sin\theta)$$

Hence

$$\varphi = (M/2\pi)\cos\theta/r \qquad (2.9.16)$$

$$\psi = -(M/2\pi)\sin\theta/r \qquad (2.9.17)$$

Assuming that $\psi = \text{const}$ and having in view that $r = \sqrt{x^2 + y^2}$ and $\sin\theta = y/r = y/\sqrt{x^2 + y^2}$, we obtain an equation for a family of streamlines of the flow being considered:

$$y(x^2 + y^2) = \text{const} \qquad (2.9.18)$$

The family of streamlines is an infinite set of circles passing through the origin of coordinates and having centres on the y-axis (Fig. 2.9.3*a*).

To comprehend the physical essence of this flow, let us consider the flow that is obtained by summation of the flows produced by a source and a sink of the same strength located on the x-axis at a small distance ε from the origin of coordinates (Fig. 2.9.3*b*). For point M (x, y), the velocity potential due to a source at the distance of r_1 is $\varphi_s = (q/2\pi)\ln r_1$ and due to a sink at a distance of r_2 from this point is $\varphi_{sk} = (-q/2\pi)\ln r_2$.

To determine the resultant flow produced by the source and the sink, let us use the method of superposition of incompressible flows. According to this method, the velocity potential of the resultant flow is $\varphi = \varphi_s + \varphi_{sk}$. Indeed, owing to the continuity equation (the Laplace equation) obtained from (2.4.8′), we have

$$\frac{\partial^2\varphi}{\partial x^2} + \frac{\partial^2\varphi}{\partial y^2} = \frac{\partial^2(\varphi_s + \varphi_{sk})}{\partial x^2} + \frac{\partial^2(\varphi_s + \varphi_{sk})}{\partial y^2} = 0$$

Since the functions φ_s and φ_{sk} satisfy the equations

$$\partial^2\varphi_s/\partial x^2 + \partial^2\varphi_s/\partial y^2 = 0 \text{ and } \partial^2\varphi_{sk}/\partial x^2 + \partial^2\varphi_{sk}/\partial y^2 = 0$$

then $\partial^2\varphi/\partial x^2 + \partial^2\varphi/\partial y^2$ identically equals zero. Consequently, the resultant function φ satisfies the continuity equation. The resultant potential from the source and the sink is

$$\varphi = (q/2\pi) \ln (r_1/r_2)$$

Since $r_1 = \sqrt{(x+\varepsilon)^2+y^2}$, $r_2 = \sqrt{(x-\varepsilon)^2+y^2}$, then

$$\ln \frac{r_1}{r_2} = \frac{1}{2} \ln \frac{(x+\varepsilon)^2+y^2}{(x-\varepsilon)^2+y^2}, \text{ or } \ln \frac{r_1}{r_2} = \frac{1}{2} \ln \left[1 + \frac{4x\varepsilon}{(x-\varepsilon)^2+y^2}\right].$$

The value of ε can be chosen so that the second term in the brackets will be small in comparison with unity. Using the formula for expansion of a logarithm into a series and disregarding the small terms of the second and higher orders, we obtain

$$\varphi = \frac{q}{\pi} \cdot \frac{x\varepsilon}{(x-\varepsilon)^2+y^2} \tag{2.9.19}$$

Assume that the source and sink approach each other ($\varepsilon \to 0$) and simultaneously their strengths increase so that the product $q2\varepsilon$ at the limit upon coincidence of the source and sink tends to a finite value M. The complicated flow formed is called a **doublet**, the quantity M characterizing this flow is called the **moment of the doublet** and the x-axis—the **axis of the doublet**. Going over to the limit in (2.9.19) for φ at $\varepsilon \to 0$ and $2q\varepsilon \to M$, we obtain the following expression for a doublet

$$\varphi = \frac{M}{2\pi} \cdot \frac{x}{x^2+y^2} = \frac{M}{2\pi} \cdot \frac{\cos\theta}{r}$$

It coincides with (2.9.16).

Hence, the flow being considered, characterized by the complex potential (2.9.15), is a doublet. This can also be shown if we consider the stream function of such a combined flow that will coincide with (2.9.17).

Differentiation of (2.9.16) yields the doublet velocity components:

$$\frac{\partial\varphi}{\partial r} = V_r = -\frac{M}{2\pi} \cdot \frac{\cos\theta}{r^2}, \quad \frac{1}{r} \cdot \frac{\partial\varphi}{\partial\theta} = V_s = -\frac{M}{2\pi} \cdot \frac{\sin\theta}{r^2} \tag{2.9.20}$$

Let us consider the three-dimensional case. For a flow produced by a source and a sink of the identical strength q located along the axis Ox at a small distance ε from the origin of coordinates, the potential function in accordance with (2.9.14) is

$$\varphi = \frac{q}{4\pi}\left(\frac{1}{R_2} - \frac{1}{R_1}\right) = \frac{q}{4\pi}\left[\frac{1}{\sqrt{(x-\varepsilon)^2+r^2}} - \frac{1}{\sqrt{(x+\varepsilon)^2+r^2}}\right] \tag{2.9.20'}$$

where $r^2 = y^2 + z^2$.

For small values of ε, we have

$$\varphi = (q/4\pi)\, 2x\varepsilon/(x^2 + r^2)^{3/2}$$

Hence in a limit process with $\varepsilon \to 0$, considering that the product $q2\varepsilon$ tends to the finite limit M, we obtain for the flow produced by a doublet with the moment M the velocity potential

$$\varphi = (M/4\pi)\, x/(x^2 + r^2)^{3/2} \tag{2.9.21}$$

or

$$\varphi = -\frac{M}{4\pi} \cdot \frac{\partial}{\partial r}\left(\frac{1}{R}\right) \tag{2.9.21'}$$

where $R = (x^2 + r^2)^{1/2}$.

Circulation Flow (Vortex)

Let us consider a flow set by the complex potential

$$W(\sigma) = -ai \ln \sigma \tag{2.9.22}$$

where a is a constant. We can write this equation in the form

$$\varphi + i\psi = -ai \ln (re^{i\theta}) = a(\theta - i \ln r)$$

Hence

$$\varphi = a\theta \tag{2.9.23}$$

$$\psi = -a \ln r \tag{2.9.24}$$

It follows from (2.9.23) that the radial velocity component $V_r = \partial\varphi/\partial r = 0$, while the component V_s normal to the radius equals the derivative of φ with respect to the arc s of a streamline, i.e.

$$\partial\varphi/\partial s = (1/r)\, \partial\varphi/\partial\theta = V_s = a/r \tag{2.9.25}$$

We obtain the equation of streamlines (pathlines) from the condition $\psi = \text{const}$, from which in accordance with (2.9.24) we find the equation $r = \text{const}$. This equation represents a family of streamlines in the form of concentric circles. Flow along them is positive if it occurs counterclockwise (from the x-axis to the y-axis); in this case the coefficient a in (2.9.25) has the sign plus.

A flow in which the particles move (circulate) along concentric circles is said to be a **circulation flow** (Fig. 2.9.4).

The circulation of the velocity in the flow being considered is $\Gamma = 2\pi r\, \partial\varphi/\partial s$. Since $\partial\varphi/\partial s = a/r$, we have $\Gamma = 2\pi a$, whence $a = \Gamma/(2\pi)$. Hence, the physical meaning of the constant a is that its value is determined by the circulation of the flow which, as we have already established, equals the vorticity in turn. The flow produced by a vortex located at the origin of coordinates where $V_s = a/r \to \infty$ is also called a **two-dimensional vortex source** or a **vortex**.

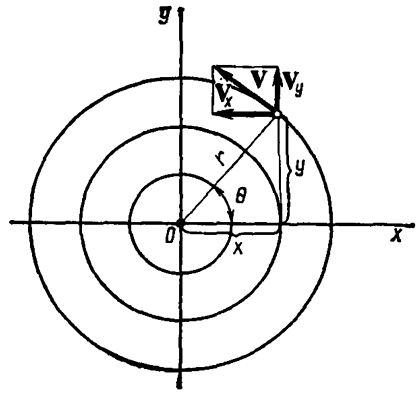

Fig. 2.9.4
A circulation flow (point vortex)

We have treated the simplest cases of flow for which we have exactly determined the velocity potentials and stream functions. By combining these flows, we can, in definite conditions, obtain more complicated potential flows equivalent to the ones that appear over bodies of a given configuration.

Let us take as an example a flow formed by the superposition of a plane-parallel flow moving in the direction of the x-axis onto the flow due to a doublet. The complex potential of the resultant two-dimensional incompressible flow is obviously

$$W(\sigma) = W_1(\sigma) + W_2(\sigma) = V\sigma + (M/2\pi)(1/\sigma) \qquad (2.9.26)$$

In accordance with this expression

$$\varphi + i\psi = V(x + iy) + (M/2\pi)/(x + iy) \qquad (2.9.27)$$

whence

$$\varphi = Vx + (M/2\pi)\, x/(x^2 + y^2),$$
$$\psi = Vy - (M/2\pi)\, y/(x^2 + y^2) \qquad (2.9.28)$$

To find the family of streamlines, we equate the stream function to a constant:

$$C = Vy - (M/2\pi)\, y/(x^2 + y^2) \qquad (2.9.29)$$

According to this equation, the streamlines are cubic curves. A value of the constant of $C = 0$ corresponds to one of the streamlines. By Eq. (2.9.29), we obtain two equations for such a **zero streamline:**

$$y = 0,\ x^2 + y^2 = M/(2\pi V) \qquad (2.9.30)$$

Hence, the obtained streamline is either a horizontal axis or a circle of radius $r_0 = [M/(2\pi V)]^{1/2}$ with its centre at the origin of coordinates. Assuming that the velocity $V = 1$, and the doublet moment $M = 2\pi$, we obtain a streamline in the form of a circle

with a unit radius. If we assume that this circle is a solid boundary surface, we can consider an incompressible flow near this surface as one flowing in a lateral direction over a cylinder of infinite length with a unit radius. The velocity potential of such an incompressible disturbed flow is determined by the first of Eqs. (2.9.28) having the form

$$\varphi = x\,[1 + 1/(x^2 + y^2)] \tag{2.9.31}$$

Introducing the polar coordinates θ and $r = x/\cos\theta = (x^2 + y^2)^{1/2}$, we obtain

$$\varphi = r\,(1 + 1/r^2)\cos\theta \tag{2.9.31'}$$

Differentiation yields the components of the velocity at a point on an arbitrary streamline along the directions of the radius r and of a normal s to it:

$$V_r = \partial\varphi/\partial r = (1 - 1/r^2)\cos\theta,$$
$$V_s = (1/r)\,\partial\varphi/\partial\theta = -(1 + 1/r^2)\sin\theta \tag{2.9.32}$$

On a cylindrical surface in a flow (a zero streamline) for which $r = 1$, we find $V_r = 0$ and $V_s = -2\sin\theta$. The above example illustrates the application of the principle of flow superposition and the concept of a complex potential to the solution of a very simple problem on the flow of an incompressible fluid over a body.

3

Fundamentals of Fluid Dynamics

3.1. Equations of Motion of a Viscous Fluid

The fundamental equations of aerodynamics include equations of motion forming its theoretical foundation. They relate quantities determining motion such as the velocity, normal, and shear stresses. The solution of the equations of motion allows one to determine these unknown quantities.

Let us consider the various kinds of equations of motion used in studying gas flows.

Cartesian Coordinates

We shall treat the motion of a fluid particle having the shape of an elementary parallelepiped with the dimensions dx, dy, and dz constructed near point A with the coordinates x, y, and z. Let the velocity components at this point be V_x, V_y, and V_z. A fluid particle of mass $\rho\tau$ (here $\tau = dx\,dy\,dz$ is the elementary volume) moves under the action of the mass (body) and surface forces. We shall denote the projections of the mass force by $X\rho\tau$, $Y\rho\tau$, and $Z\rho\tau$, and those of the surface force by $P_x\tau$, $P_y\tau$, and $P_z\tau$. The quantities P_x, P_y, and P_z are the projections of the surface force vector related to unit volume.

The equation of particle motion in the projection onto the x-axis has the form

$$\rho\tau\, dV_x/dt = X\rho\tau + P_x\tau$$

whence

$$dV_x/dt = X + (1/\rho)\, P_x \tag{3.1.1}$$

where dV_x/dt is the total acceleration in the direction of the x-axis.

We obtain similar equations in projections onto the y- and z-axes:

$$dV_y/dt = Y + (1/\rho)\, P_y \tag{3.1.2}$$

$$dV_z/dt = Z + (1/\rho)\, P_z \tag{3.1.3}$$

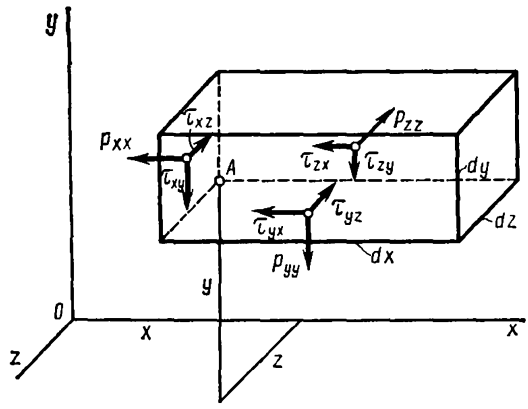

Fig. 3.1.1
Surface forces acting on a fluid particle

The surface force can be expressed in terms of the stresses acting on the faces of an elementary parallelepiped. The difference in the surface forces in comparison with an ideal (inviscid) flow consists in that not only normal, but also shear stresses act on the faces of a particle.

Every surface force acting on a face has three projections onto the coordinate axes (Fig. 3.1.1). A unit of surface area of the left-hand face experiences a surface force whose projections will be designated by p_{xx}, τ_{xz}, and τ_{xy}. The quantity p_{xx} is the normal stress, while τ_{xz} and τ_{xy} are the shear stresses. It can be seen that the first subscript indicates the axis perpendicular to the face being considered, and the second one indicates the axis onto which the given stress is projected. The rear face perpendicular to the z-axis experiences the stress components p_{zz}, τ_{zx}, and τ_{zy}; the bottom face perpendicular to the y-axis experiences the components p_{yy}, τ_{yx}, and τ_{yz}.

We shall consider normal stresses to be positive if they are directed out of the element being studied and, consequently, subject it to omnidirectional tension as shown in Fig. 3.1.1. Positive shear stresses are present if for the three faces intersecting at initial point A these stresses are oriented along directions opposite to the positive directions of the coordinate axes, and for the other three faces—in the positive direction of these axes. With this in view, let us consider the projections of the surface forces onto the x-axis. The left-hand face experiences the force due to the normal stress $-p_{xx}\,dy\,dz$, and the right-hand one—the force $[p_{xx} + (\partial p_{xx}/\partial x)\,dx]\,dy\,dz$. The resultant of these forces is therefore $(\partial p_{xx}/\partial x)\,dx\,dy\,dz$. The components of the forces produced by the shear stresses acting on these faces are zero.

Account must be taken, however, of the shear stresses τ_{zx} and τ_{yx}. The rear face experiences the force $-\tau_{zx}\,dx\,dy$, and the front one—the force $[\tau_{zx} + (\partial\tau_{zx}/\partial z)\,dz]\,dx\,dy$. The resultant of these forces is $(\partial\tau_{zx}/\partial z)\,dx\,dy\,dz$. In a similar way, we find the resultant of the forces acting on the bottom and top faces. It is $(\partial\tau_{yx}/\partial y)\,dx\,dy\,dz$.

Hence, the projection onto the x-axis of the surface force related to unit volume is

$$P_x = \partial p_{xx}/\partial x + \partial\tau_{yx}/\partial y + \partial\tau_{zx}/\partial z \qquad (3.1.4)$$

Similarly, the projections onto the other coordinate axes of the surface force related to unit volume are

$$\left.\begin{aligned} P_y &= \partial\tau_{xy}/\partial x + \partial p_{yy}/\partial y + \partial\tau_{zy}/\partial z \\ P_z &= \partial\tau_{xz}/\partial x + \partial\tau_{yz}/\partial y + \partial p_{zz}/\partial z \end{aligned}\right\} \qquad (3.1.4')$$

According to the property of reciprocity of shear stresses, the values of these stresses acting along orthogonal faces equal each other, i. e. $\tau_{zx} = \tau_{xz}$, $\tau_{zy} = \tau_{yz}$, and $\tau_{yx} = \tau_{xy}$.

Hence, of six shear stresses, three are independent.

To determine the values of the shear stresses, we shall use the hypothesis that stresses are proportional to the strains they produce. The application of this hypothesis is illustrated by Newton's formula for the shear stress appearing in the motion of a viscous fluid relative to a solid wall. By this formula, $\tau_{yx} = \mu\,(\partial V_y/\partial x)$, i.e. the stress is proportional to the half-speed $\varepsilon_z = 0.5\,(\partial V_y/\partial x)$ of angle distortion in the direction of the z-axis, whence $\tau_{yx} = 2\mu\varepsilon_z$ (here μ is the dynamic viscosity). This relation covers the general case of three-dimensional motion when the angular deformation in the direction of the z-axis is determined by the half-speed of distortion $\varepsilon_z = 0.5\,(\partial V_y/\partial x + \partial V_x/\partial y)$. We shall write the other two values of the shear stress in the form $\tau_{yz} = 2\mu\varepsilon_x$ and $\tau_{zx} = 2\mu\varepsilon_y$.

Consequently,

$$\left.\begin{aligned} \tau_{yx} &= 2\mu\varepsilon_z = \mu\,(\partial V_y/\partial x + \partial V_x/\partial y) \\ \tau_{yz} &= 2\mu\varepsilon_x = \mu\,(\partial V_y/\partial z + \partial V_z/\partial y) \\ \tau_{zx} &= 2\mu\varepsilon_y = \mu\,(\partial V_z/\partial x + \partial V_x/\partial z) \end{aligned}\right\} \qquad (3.1.5)$$

We shall use the above-mentioned proportionality hypothesis to establish relations for the normal stresses p_{xx}, p_{yy}, and p_{zz}. Under the action of the stress p_{xx}, a fluid particle experiences linear strain or deformation in the direction of the x-axis. If the relative linear deformation is $\bar{\theta}'_x$, then $p_{xx} = E\bar{\theta}'_x$, where E is a proportionality factor or the **modulus of longitudinal elasticity of the fluid**. The normal stresses p_{yy} and p_{zz} cause the particle to deform also in the directions of the y- and z-axes, which diminishes the deformation in the direction of the x-axis.

It is known from the course in the strength of materials that the decrease in the relative magnitude $\Delta\bar{\theta}_x$ of this deformation for elastic bodies is proportional to the sum of the relative deformations in the directions of y and z under the action of the indicated stresses. Accordingly,

$$\Delta\bar{\theta}_x = -(1/m)\,(p_{yy}/E + p_{zz}/E)$$

where m is a constant known as the **coefficient of lateral linear deformation.**

The total relative deformation in the direction of the x-axis is

$$\bar{\theta}_x = \bar{\theta}'_x + \Delta\bar{\theta}_x = p_{xx}/E - (1/m)\,(p_{yy}/E + p_{zz}/E) \qquad (3.1.6)$$

We can calculate the relative deformations $\bar{\theta}_y$ and $\bar{\theta}_z$ along the y- and z-axes in a similar way. The obtained expressions give us the normal stresses:

$$\left.\begin{aligned} p_{xx} &= E\bar{\theta}_x + (p_{yy} + p_{zz})/m \\ p_{yy} &= E\bar{\theta}_y + (p_{zz} + p_{xx})/m \\ p_{zz} &= E\bar{\theta}_z + (p_{xx} + p_{yy})/m \end{aligned}\right\} \qquad (3.1.7)$$

The relative linear deformations of a particle along the directions of the coordinate axes determine its relative volume deformation. Designating the magnitude of this deformation by $\bar{\theta}$, we obtain

$$\bar{\theta} = \bar{\theta}_x + \bar{\theta}_y + \bar{\theta}_z \qquad (3.1.8)$$

Summating Eqs. (3.1.7) and taking into account the expression for $\bar{\theta}$, we have

$$p_{xx} + p_{yy} + p_{zz} = mE\bar{\theta}/(m - 2) \qquad (3.1.9)$$

Determining the sum $p_{yy} + p_{zz}$ from this expression and introducing it into (3.1.6), we find

$$p_{xx} = \frac{m}{m+1} E\bar{\theta}_x + \frac{m}{m+1} \cdot \frac{E}{m-2} \bar{\theta} \qquad (3.1.10)$$

For our following transformations, we shall use the known relation between the shear modulus G, the modulus of longitudinal elasticity E, and the coefficient of lateral deformation m that is valid for elastic media including a compressible fluid:

$$G = mE/[2(m + 1)] \qquad (3.1.11)$$

Substituting this relation into (3.1.10), we obtain

$$p_{xx} = 2G\bar{\theta}_x + \frac{2G}{m-2} \bar{\theta} \qquad (3.1.12)$$

Let us introduce the symbol

$$\bar{\sigma} = (p_{xx} + p_{yy} + p_{zz})/3 \qquad (3.1.13)$$

Adding and subtracting $\bar{\sigma}$ on the right-hand side of (3.1.12), we have

$$p_{xx} = \bar{\sigma} + 2G\bar{\theta}_x + \frac{2G}{m-2}\bar{\theta} - (p_{xx} + p_{yy} + p_{zz})/3$$

Transformations involving Eqs. (3.1.9) and (3.1.11) yield

$$p_{xx} = \bar{\sigma} + G(2\bar{\theta}_x - 2\bar{\theta}/3) \qquad (3.1.14)$$

Similarly,

$$p_{yy} = \bar{\sigma} + G(2\bar{\theta}_y - 2\bar{\theta}/3); \quad p_{zz} = \bar{\sigma} + G(2\bar{\theta}_z - 2\bar{\theta}/3) \qquad (3.1.14')$$

It has been established for an inviscid fluid that the pressure p at any point of the flow is identical for all the areas including this point, i.e. with a view to the adopted notation, in the case being considered we have $p_{xx} = p_{yy} = p_{zz} = -p$; consequently, $p = -(p_{xx} + p_{yy} + p_{zz})/3$.

Hence, when studying the motion of a viscous fluid, the pressure can be determined as the arithmetical mean, taken with the minus sign, of the three normal stresses corresponding to three mutually perpendicular areas. Accordingly, $\bar{\sigma} = -p$.

The theory of elasticity establishes the following relations for the shear stresses acting in a solid body:

$$\tau_{yx} = G\gamma_{yx}, \quad \tau_{yz} = G\gamma_{yz}, \quad \tau_{zx} = G\gamma_{zx} \qquad (3.1.15)$$

where γ_{yx}, γ_{yz}, and γ_{zx} are the angles of shear in the directions of the axes z, x, and y, respectively.

A comparison of formulas (3.1.15) with the corresponding relations (3.1.5) for a viscous fluid reveals that these formulas can be obtained from one another if the shear modulus G is replaced by the dynamic viscosity μ, and the angles of shear γ by the relevant values of the speeds of distortion ε of the angles. In accordance with this analogy, when substituting μ for G in formulas (3.1.14) and (3.1.14'), the strains (relative elongations) $\bar{\theta}_x$, $\bar{\theta}_y$, and $\bar{\theta}_z$ have to be replaced with the relevant values of the rates of strain $\theta_x = \partial V_x/\partial x$, $\theta_y = \partial V_y/\partial y$, $\theta_z = \partial V_z/\partial z$, and the volume strain $\bar{\theta}$ by the rate of the volume strain $\theta = \partial V_x/\partial x + \partial V_y/\partial y + \partial V_z/\partial z = \operatorname{div} \mathbf{V}$.

The relevant substitutions in (3.1.14) and (3.1.14') yield:

$$\left.\begin{aligned} p_{xx} &= -p + \mu\left(2\frac{\partial V_x}{\partial x} - \frac{2}{3}\operatorname{div}\mathbf{V}\right) \\ p_{yy} &= -p + \mu\left(2\frac{\partial V_y}{\partial y} - \frac{2}{3}\operatorname{div}\mathbf{V}\right) \\ p_{zz} &= -p + \mu\left(2\frac{\partial V_z}{\partial z} - \frac{2}{3}\operatorname{div}\mathbf{V}\right) \end{aligned}\right\} \qquad (3.1.16)$$

The second terms on the right-hand sides of expressions (3.1.16) determine the additional stresses due to viscosity.

By using relations (3.1.4), (3.1.4′), (3.1.5), and (3.1.16), we can evaluate the quantities P_x, P_y, and P_z. For example, for P_x from (3.1.4) we obtain

$$P_x = -\frac{\partial p}{\partial x} + \frac{\partial}{\partial x}\left[\mu\left(2\frac{\partial V_x}{\partial x} - \frac{2}{3}\operatorname{div}\mathbf{V}\right)\right] + \frac{\partial}{\partial y}\left[\mu\left(\frac{\partial V_y}{\partial x} + \frac{\partial V_x}{\partial y}\right)\right]$$
$$+ \frac{\partial}{\partial z}\left[\mu\left(\frac{\partial V_z}{\partial x} + \frac{\partial V_x}{\partial z}\right)\right] = -\frac{\partial p}{\partial x} + \mu\Delta V_x + \frac{\mu}{3}\frac{\partial}{\partial x}\operatorname{div}\mathbf{V}$$
$$+ \frac{\partial \mu}{\partial x}\left(2\frac{\partial V_x}{\partial x} - \frac{2}{3}\operatorname{div}\mathbf{V}\right) + \frac{\partial \mu}{\partial y}\left(\frac{\partial V_x}{\partial y} + \frac{\partial V_y}{\partial x}\right) + \frac{\partial \mu}{\partial z}\left(\frac{\partial V_x}{\partial z} + \frac{\partial V_z}{\partial x}\right)$$

where Δ is the Laplacian operator:

$$\Delta = \partial^2/\partial x^2 + \partial^2/\partial y^2 + \partial^2/\partial z^2$$

Particularly,

$$\Delta V_x = \partial^2 V_x/\partial x^2 + \partial^2 V_x/\partial y^2 + \partial^2 V_x/\partial z^2$$

In a similar way, we can find the expressions for P_y and P_z.

The relations for the stresses due to the surface forces in a fluid have been obtained here by generalizing the laws relating stresses and strains in solids for a fluid having the property of elasticity and viscosity. We shall obtain the same relations proceeding from a number of hypothetic notions on the molecular forces acting in a fluid (see [9, 11]).

By compiling projections of the total acceleration in an expanded form according to the rule of calculating the derivative of a composite function $f(x, y, z, t)$ in which, in turn, x, y, and z are functions of the time t. and taking into consideration the expressions found for P_x, P_y, and P_z, we can obtain the equations of motion (3.1.1)–(3.1.3) in the following form:

$$\left.\begin{aligned}
&\frac{\partial V_x}{\partial t} + V_x\frac{\partial V_x}{\partial x} + V_y\frac{\partial V_x}{\partial y} + V_z\frac{\partial V_x}{\partial z} = X - \frac{1}{\rho}\cdot\frac{\partial p}{\partial x}\\
&+ \nu\Delta V_x + \frac{\nu}{3}\cdot\frac{\partial}{\partial x}\operatorname{div}\mathbf{V} + \frac{1}{\rho}\left[\frac{\partial \mu}{\partial x}\left(2\frac{\partial V_x}{\partial x} - \frac{2}{3}\operatorname{div}\mathbf{V}\right)\right.\\
&\left.+ \frac{\partial \mu}{\partial y}\left(\frac{\partial V_x}{\partial y} + \frac{\partial V_y}{\partial x}\right) + \frac{\partial \mu}{\partial z}\left(\frac{\partial V_x}{\partial z} + \frac{\partial V_z}{\partial x}\right)\right]\\
&\frac{\partial V_y}{\partial t} + V_x\frac{\partial V_y}{\partial x} + V_y\frac{\partial V_y}{\partial y} + V_z\frac{\partial V_y}{\partial z} = Y - \frac{1}{\rho}\cdot\frac{\partial p}{\partial y}\\
&+ \nu\Delta V_y + \frac{\nu}{3}\cdot\frac{\partial}{\partial y}\operatorname{div}\mathbf{V} + \frac{1}{\rho}\left[\frac{\partial \mu}{\partial y}\left(2\frac{\partial V_y}{\partial y} - \frac{2}{3}\operatorname{div}\mathbf{V}\right)\right.\\
&\left.+ \frac{\partial \mu}{\partial z}\left(\frac{\partial V_y}{\partial z} + \frac{\partial V_z}{\partial y}\right) + \frac{\partial \mu}{\partial x}\left(\frac{\partial V_y}{\partial x} + \frac{\partial V_x}{\partial y}\right)\right]
\end{aligned}\right\} \quad (3.1.17)$$

$$\left.\begin{aligned}\frac{\partial V_z}{\partial t}+V_x\frac{\partial V_z}{\partial x}+V_y\frac{\partial V_z}{\partial y}+V_z\frac{\partial V_z}{\partial z}=Z-\frac{1}{\rho}\cdot\frac{\partial p}{\partial z}\\ +\nu\Delta V_z+\frac{\nu}{3}\cdot\frac{\partial}{\partial z}\operatorname{div}\mathbf{V}+\frac{1}{\rho}\left[\frac{\partial\mu}{\partial z}\left(2\frac{\partial V_z}{\partial z}-\frac{2}{3}\operatorname{div}\mathbf{V}\right)\right.\\ \left.+\frac{\partial\mu}{\partial x}\left(\frac{\partial V_z}{\partial x}+\frac{\partial V_x}{\partial z}\right)+\frac{\partial\mu}{\partial y}\left(\frac{\partial V_z}{\partial y}+\frac{\partial V_y}{\partial z}\right)\right]\end{aligned}\right\}$$

where $\nu = \mu/\rho$ is the kinematic viscosity.

The differential equations (3.1.17) form the theoretical foundation of the gas dynamics of a viscous compressible fluid and are known as the **Navier-Stokes equations**. It is assumed in the equations that the dynamic viscosity μ is a function of the coordinates x, y, and z, i.e. $\mu = f(x, y, z)$. Presuming that $\mu = \text{const}$, the Navier-Stokes equations acquire the following form:

$$\left.\begin{aligned}\frac{dV_x}{dt}&=X-\frac{1}{\rho}\cdot\frac{\partial p}{\partial x}+\nu\Delta V_x+\frac{\nu}{3}\cdot\frac{\partial}{\partial x}\operatorname{div}\mathbf{V}\\ \frac{dV_y}{dt}&=Y-\frac{1}{\rho}\cdot\frac{\partial p}{\partial y}+\nu\Delta V_y+\frac{\nu}{3}\cdot\frac{\partial}{\partial y}\operatorname{div}\mathbf{V}\\ \frac{dV_z}{dt}&=Z-\frac{1}{\rho}\cdot\frac{\partial p}{\partial z}+\nu\Delta V_z+\frac{\nu}{3}\cdot\frac{\partial}{\partial z}\operatorname{div}\mathbf{V}\end{aligned}\right\}\qquad(3.1.18)$$

When studying gas flows, the mass forces may be left out of account, and, therefore, we assume that $X = Y = Z = 0$. In this case, we have

$$\left.\begin{aligned}\frac{dV_x}{dt}&=-\frac{1}{\rho}\cdot\frac{\partial p}{\partial x}+\nu\Delta V_x+\frac{\nu}{3}\cdot\frac{\partial}{\partial x}\operatorname{div}\mathbf{V}\\ \frac{dV_y}{dt}&=-\frac{1}{\rho}\cdot\frac{\partial p}{\partial y}+\nu\Delta V_y+\frac{\nu}{3}\cdot\frac{\partial}{\partial y}\operatorname{div}\mathbf{V}\\ \frac{dV_z}{dt}&=-\frac{1}{\rho}\cdot\frac{\partial p}{\partial z}+\nu\Delta V_z+\frac{\nu}{3}\cdot\frac{\partial}{\partial z}\operatorname{div}\mathbf{V}\end{aligned}\right\}\qquad(3.1.19)$$

For two-dimensional plane motion characterized by a varying dynamic viscosity $\mu \neq \text{const}$, equations are obtained from (3.1.17) as a result of simple transformations:

$$\left.\begin{aligned}\frac{\partial V_x}{\partial t}&=-\frac{1}{\rho}\cdot\frac{\partial p}{\partial x}+\frac{1}{\rho}\cdot\frac{\partial}{\partial x}\left[\mu\left(2\frac{\partial V_x}{\partial x}-\frac{2}{3}\operatorname{div}\mathbf{V}\right)\right]\\ &\quad+\frac{2}{\rho}\cdot\frac{\partial}{\partial y}(\mu\varepsilon_z)\\ \frac{\partial V_y}{\partial t}&=-\frac{1}{\rho}\cdot\frac{\partial p}{\partial y}+\frac{1}{\rho}\cdot\frac{\partial}{\partial y}\left[\mu\left(2\frac{\partial V_y}{\partial y}-\frac{2}{3}\operatorname{div}\mathbf{V}\right)\right]\\ &\quad+\frac{2}{\rho}\cdot\frac{\partial}{\partial x}(\mu\varepsilon_z)\end{aligned}\right\}\qquad(3.1.20)$$

When div $\mathbf{V} = 0$, and $\mu = \text{const}$, these equations are reduced to equations of motion of a viscous incompressible fluid.

Let us consider the equation of motion of an ideal (inviscid) compressible fluid. Assuming the coefficients μ and ν in (3.1.17) to be zero, we obtain:

$$\left.\begin{aligned}
\frac{\partial V_x}{\partial t} + V_x\frac{\partial V_x}{\partial x} + V_y\frac{\partial V_x}{\partial y} + V_z\frac{\partial V_x}{\partial z} &= X - \frac{1}{\rho}\cdot\frac{\partial p}{\partial x}\\
\frac{\partial V_y}{\partial t} + V_x\frac{\partial V_y}{\partial x} + V_y\frac{\partial V_y}{\partial y} + V_z\frac{\partial V_y}{\partial z} &= Y - \frac{1}{\rho}\cdot\frac{\partial p}{\partial y}\\
\frac{\partial V_z}{\partial t} + V_x\frac{\partial V_z}{\partial x} + V_y\frac{\partial V_z}{\partial y} + V_z\frac{\partial V_z}{\partial z} &= Z - \frac{1}{\rho}\cdot\frac{\partial p}{\partial z}
\end{aligned}\right\} \quad (3.1.17')$$

These equations were first obtained by Leonard Euler, which is why they are called **Euler equations**. They are the theoretical cornerstone of the science dealing with the motion of an ideal gas whose hypothetic properties are determined by the absence or negligibly small influence of viscosity.

Vector Form of the Equations of Motion

By multiplying Eqs. (3.1.18) by the unit vectors **i**, **j**, and **k**, respectively, and then summating them, we obtain an equation of motion in the vector form:

$$d\mathbf{V}/dt = \mathbf{G} - (1/\rho)\,\text{grad}\,p + \nu\,\Delta\mathbf{V} + (\nu/3)\,\text{grad div}\,\mathbf{V} \quad (3.1.21)$$

where the vector of the mass forces in Cartesian coordinates is

$$\mathbf{G} = X\mathbf{i} + Y\mathbf{j} + Z\mathbf{k}$$

the pressure gradient is

$$\text{grad}\,p = (\partial p/\partial x)\,\mathbf{i} + (\partial p/\partial y)\,\mathbf{j} + (\partial p/\partial z)\,\mathbf{k}$$

the vectors

$$\Delta\mathbf{V} = \Delta V_x\mathbf{i} + \Delta V_y\mathbf{j} + \Delta V_z\mathbf{k}$$

$$\text{grad div}\,\mathbf{V} = (\partial\,\text{div}\,\mathbf{V}/\partial x)\,\mathbf{i} + (\partial\,\text{div}\,\mathbf{V}/\partial y)\mathbf{j} + (\partial\,\text{div}\,\mathbf{V}/\partial z)\mathbf{k}$$

If a fluid is incompressible, div $\mathbf{V} = 0$, and, consequently,

$$d\mathbf{V}/dt = \mathbf{G} - (1/\rho)\,\text{grad}\,p + \nu\,\Delta\mathbf{V} \quad (3.1.21')$$

In the absence of mass forces, $\mathbf{G} = 0$, therefore

$$d\mathbf{V}/dt = -(1/\rho)\,\text{grad}\,p + \nu\Delta\mathbf{V} + (\nu/3)\,\text{grad div}\,\mathbf{V} \quad (3.1.21'')$$

The vector of the total acceleration can also be expressed as

$$d\mathbf{V}/dt = \partial\mathbf{V}/\partial t + \text{grad}\,(V^2/2) + \text{curl}\,\mathbf{V}\times\mathbf{V} \quad (3.1.22)$$

With account taken of (3.1.21″) and (3.1.22), we can write the equation of motion as

$$\frac{\partial \mathbf{V}}{\partial t} + \operatorname{grad} \frac{V^2}{2} + \operatorname{curl} \mathbf{V} \times \mathbf{V} = -\frac{1}{\rho} \operatorname{grad} p + \nu \Delta \mathbf{V} + \frac{\nu}{3} \operatorname{grad} \operatorname{div} \mathbf{V} \tag{3.1.22'}$$

For an inviscid compressible fluid, the equation of motion is

$$\frac{\partial \mathbf{V}}{\partial t} + \operatorname{grad} \frac{V^2}{2} + \operatorname{curl} \mathbf{V} \times \mathbf{V} = -\frac{1}{\rho} \operatorname{grad} p \tag{3.1.22″}$$

Curvilinear Coordinates

Let us transform Eq. (3.1.22′) using the concept of generalized curvilinear coordinates q_n. This allows us to go over comparatively simply to equations of motion containing a specific form of curvilinear orthogonal coordinates, as was done with respect to the continuity equation.

Let us consider the transformation of separate terms in (3.1.22′). For the second term on the left-hand side, and also for the first and third terms on the right-hand sides, with a view to (2.4.18), we have the following expressions:

$$\operatorname{grad} \frac{V^2}{2} = \sum_{n=1}^{3} \left(\operatorname{grad} \frac{V^2}{2} \right)_n \mathbf{i}_n = \sum_{n=1}^{3} \frac{1}{h_n} \cdot \frac{\partial (V^2/2)}{\partial q_n} \mathbf{i}_n \tag{3.1.23}$$

$$\operatorname{grad} p = \sum_{n=1}^{3} (\operatorname{grad} p)_n \mathbf{i}_n = \sum_{n=1}^{3} \frac{1}{h_n} \cdot \frac{\partial p}{\partial q_n} \mathbf{i}_n \tag{3.1.24}$$

$$\operatorname{grad} \operatorname{div} \mathbf{V} = \sum_{n=1}^{3} (\operatorname{grad} \operatorname{div} \mathbf{V})_n \mathbf{i}_n = \sum_{n=1}^{3} \frac{1}{h_n} \cdot \frac{\partial \operatorname{div} \mathbf{V}}{\partial q_n} \mathbf{i}_n \tag{3.1.25}$$

For transformation of the vector product curl $\mathbf{V} \times \mathbf{V}$, it is necessary to find the form of the expression of the vector curl $\mathbf{V}$ in generalized coordinates. For this purpose, let us calculate the curl of both sides of Eq. (2.4.19):

$$\operatorname{curl} \mathbf{V} = \sum_{n=1}^{3} (V_n \operatorname{curl} \mathbf{i}_n + \operatorname{grad} V_n \times \mathbf{i}_n) \tag{3.1.26}$$

where

$$\operatorname{grad} V_n \times \mathbf{i}_n = (\operatorname{grad} V_n)_j \mathbf{i}_m - (\operatorname{grad} V_n)_m \mathbf{i}_j \tag{3.1.27}$$

Here the projections of the vector grad V_n onto the relevant coordinate directions are determined from expression (2.4.18) with V_n substituted for Φ. Introducing (3.1.27), and also the expressions for curl $\mathbf{i}_n$ from (2.4.22) into (3.1.26), we obtain the following expres-

sion for the curl of the velocity:

$$\operatorname{curl} \mathbf{V} = \frac{1}{h_2 h_3}\left[\frac{\partial (h_3 V_3)}{\partial q_2} - \frac{\partial (h_2 V_2)}{\partial q_2}\right]\mathbf{i}_1 + \frac{1}{h_3 h_1} \times \left[\frac{\partial (h_1 V_1)}{\partial q_3} - \frac{\partial (h_3 V_3)}{\partial q_1}\right]\mathbf{i}_2 + \frac{1}{h_1 h_2}\left[\frac{\partial (h_2 V_2)}{\partial q_1} - \frac{\partial (h_1 V_1)}{\partial q_2}\right]\mathbf{i}_3 \quad (3.1.28)$$

Consequently, the cross product

$$\operatorname{curl} \mathbf{V} \times \mathbf{V} = \sum_{n=1}^{3} (\operatorname{curl} \mathbf{V} \times \mathbf{V})_n \mathbf{i}_n \quad (3.1.29)$$

where the projection of this vector onto a tangent to the corresponding coordinate curve is

$$(\operatorname{curl} \mathbf{V} \times \mathbf{V})_n = \frac{V_j}{h_j h_n}\left[\frac{\partial (h_n V_n)}{\partial q_j} - \frac{\partial (h_j V_j)}{\partial q_n}\right] - \frac{V_m}{h_n h_m}\left[\frac{\partial (h_m V_m)}{\partial q_n} - \frac{\partial (h_n V_n)}{\partial q_m}\right] \quad (3.1.30)$$

Recall that the relation between the subscripts m, j, and n is as follows:

n . . .	1	2	3
m . . .	2	3	1
j . . .	3	1	2

The left-hand side of Eq. (3.1.22) is the vector of the total acceleration $\mathbf{W} = d\mathbf{V}/dt$ that has the form

$$\mathbf{W} = \sum_{n=1}^{3} W_n \mathbf{i}_n \quad (3.1.31)$$

where W_n is the projection of the acceleration vector onto the direction of a tangent to the coordinate line q_n.

Each quantity W_n can be considered as the sum of the relevant projections of the vectors $\partial \mathbf{V}/\partial t$, and also of the vectors (3.1.23) and (3.1.29) onto the indicated directions. Accordingly,

$$W_n = \frac{\partial V_n}{\partial t} + \frac{V_n}{h_n} \cdot \frac{\partial V_n}{\partial q_n} + \frac{V_m}{h_n h_m} \cdot \frac{\partial (h_n V_n)}{\partial q_m} + \frac{V_j}{h_j h_n} \cdot \frac{\partial (h_n V_n)}{\partial q_j} - \frac{V_m^2}{h_n h_m} \cdot \frac{\partial h_m}{\partial q_n} - \frac{V_j^2}{h_j h_n} \cdot \frac{\partial h_j}{\partial q_n} \quad (3.1.32)$$

Let us apply the Laplacian operator to the vector $\mathbf{V}$, and use the expression

$$\Delta \mathbf{V} = \sum_{n=1}^{3} \Delta V_n \mathbf{i}_n = \operatorname{grad} \operatorname{div} \mathbf{V} - \operatorname{curl} \operatorname{curl} \mathbf{V} \quad (3.1.33)$$

where ΔV_n are the projections of the vector along the coordinate lines q_n.

The first vector on the right-hand side of (3.1.33) has been determined in the form of (3.1.25), while for calculating the second one Eq. (3.1.28) should be used. Taking the curl of both sides of this equation, we obtain

$$\operatorname{curl}\operatorname{curl}\mathbf{V}=\sum_{n=1}^{3}(\operatorname{curl}\operatorname{curl}\mathbf{V})_n\mathbf{i}_n$$

$$=\sum_{n=1}^{3}\frac{1}{h_m h_j}\left\{\frac{\partial\left[h_j(\operatorname{curl}\mathbf{V})_j\right]}{\partial q_m}-\frac{\partial\left[h_m(\operatorname{curl}\mathbf{V})_m\right]}{\partial q_j}\right\}\mathbf{i}_n \qquad (3.1.34)$$

where the corresponding projections of the vector curl V are found from (3.1.28).

Having these data at hand, we can consider the transformation of the equations of motion as applied to specific forms of curvilinear orthogonal coordinates.

Cylindrical Coordinates

In accordance with (2.4.12), (2.4.16), and (2.4.25), we have

$$q_1=x,\ q_2=r,\ q_3=\gamma,\ h_1=1,\ h_2=1,\ h_3=r,$$
$$V_1=V_x,\ V_2=V_r,\ V_3=V_\gamma$$

Consequently,

$$W_1=\frac{\partial V_x}{\partial t}+V_x\frac{\partial V_x}{\partial x}+V_r\frac{\partial V_x}{\partial r}+\frac{V_\gamma}{r}\cdot\frac{\partial V_x}{\partial\gamma}\ ;\qquad (\operatorname{grad}p)_1=\partial p/\partial x$$

Next we find

$$(\operatorname{grad}\operatorname{div}\mathbf{V})_1=\partial\operatorname{div}\mathbf{V}/\partial x$$

Since div V is determined by formula (2.4.26), we have

$$\frac{\partial\operatorname{div}\mathbf{V}}{\partial x}=\frac{\partial}{\partial x}\left(\frac{\partial V_x}{\partial x}+\frac{\partial V_r}{\partial r}+\frac{1}{r}\cdot\frac{\partial V_\gamma}{\partial\gamma}+\frac{V_r}{r}\right)$$

From (3.1.28), we have

$$(\operatorname{curl}\mathbf{V})_3=\frac{\partial V_r}{\partial x}-\frac{\partial V_x}{\partial r}\qquad (\operatorname{curl}\mathbf{V})_2=\frac{1}{r}\left(\frac{\partial V_x}{\partial\gamma}-r\frac{\partial V_\gamma}{\partial x}\right)$$

Introducing these expressions into (3.1.34), we obtain

$$(\operatorname{curl}\operatorname{curl}\mathbf{V})_1=\frac{1}{r}\left\{\frac{\partial\left[r\left(\frac{\partial V_r}{\partial x}-\frac{\partial V_x}{\partial r}\right)\right]}{\partial r}-\frac{\partial\left[\frac{1}{r}\left(\frac{\partial V_x}{\partial\gamma}-r\frac{\partial V_\gamma}{\partial x}\right)\right]}{\partial\gamma}\right\}$$

$$=\frac{\partial^2 V_r}{\partial x\,\partial r}-\frac{\partial^2 V_x}{\partial r^2}+\frac{1}{r}\left(\frac{\partial V_r}{\partial x}-\frac{\partial V_x}{\partial r}\right)-\frac{1}{r^2}\left(\frac{\partial^2 V_x}{\partial\gamma^2}-r\frac{\partial^2 V_\gamma}{\partial x\,\partial\gamma}\right)$$

Since $(\text{grad div } \mathbf{V})_1 = \partial \text{ div } \mathbf{V}/\partial x$, in accordance with (3.1.33) we have

$$(\Delta \mathbf{V})_1 = (\text{grad div } \mathbf{V})_1 - (\text{curl curl } \mathbf{V})_1$$
$$= \frac{\partial^2 V_x}{\partial x^2} + \frac{\partial^2 V_x}{\partial r^2} + \frac{1}{r^2} \cdot \frac{\partial^2 V_x}{\partial \gamma^2} + \frac{1}{r} \cdot \frac{\partial V_x}{\partial r}$$

We thus compile an equation of motion in a projection onto the x-axis of a cylindrical coordinate system:

$$\frac{\partial V_x}{\partial t} + V_x \frac{\partial V_x}{\partial x} + V_r \frac{\partial V_x}{\partial r} + \frac{V_\gamma}{r} \cdot \frac{\partial V_x}{\partial \gamma} = -\frac{1}{\rho} \cdot \frac{\partial p}{\partial x}$$
$$+ \nu \Delta V_x + \frac{\nu}{3} \cdot \frac{\partial \text{ div } \mathbf{V}}{\partial x} \qquad (3.1.35)$$

We obtain the other two equations in projections onto the coordinate lines r and γ in a similar way:

$$\left.\begin{aligned} &\frac{\partial V_r}{\partial t} + V_x \frac{\partial V_r}{\partial x} + V_r \frac{\partial V_r}{\partial r} + \frac{V_\gamma}{r} \cdot \frac{\partial V_r}{\partial \gamma} - \frac{V_\gamma^2}{r} \\ &= -\frac{1}{\rho} \frac{\partial p}{\partial r} + \nu \left(\Delta V_r - \frac{2}{r^2} \cdot \frac{\partial V_\gamma}{\partial \gamma} - \frac{V_r}{r^2} \right) + \frac{\nu}{3} \cdot \frac{\partial \text{ div } \mathbf{V}}{\partial r} \\ &\frac{\partial V_\gamma}{\partial t} + V_x \frac{\partial V_\gamma}{\partial x} + V_r \frac{\partial V_\gamma}{\partial r} + \frac{V_\gamma}{r} \cdot \frac{\partial V_\gamma}{\partial \gamma} + \frac{V_r V_\gamma}{r} \\ &= -\frac{1}{\rho r} \cdot \frac{\partial p}{\partial \gamma} + \nu \left(\Delta V_\gamma + \frac{2}{r^2} \cdot \frac{\partial V_r}{\partial \gamma} - \frac{V_\gamma}{r^2} \right) + \frac{\nu}{3r} \cdot \frac{\partial \text{ div } \mathbf{V}}{\partial \gamma} \end{aligned}\right\} \qquad (3.1.35')$$

In these equations, we have introduced a symbol for the Laplacian operator in cylindrical coordinates:

$$\Delta = \frac{\partial^2}{\partial x^2} + \frac{\partial^2}{\partial r^2} + \frac{1}{r^2} \cdot \frac{\partial^2}{\partial \gamma^2} + \frac{1}{r} \cdot \frac{\partial}{\partial r}$$

We determine the divergence of the velocity by formula (2.4.26). For an axisymmetric flow, the equations of motion are simplified:

$$\left.\begin{aligned} &\frac{\partial V_x}{\partial t} + V_x \frac{\partial V_x}{\partial x} + V_r \frac{\partial V_x}{\partial r} = -\frac{1}{\rho} \cdot \frac{\partial p}{\partial x} + \nu \Delta V_x \\ &\qquad + \frac{\nu}{3} \cdot \frac{\partial \text{ div } \mathbf{V}}{\partial x} \\ &\frac{\partial V_r}{\partial t} + V_x \frac{\partial V_r}{\partial x} + V_r \frac{\partial V_r}{\partial r} = -\frac{1}{\rho} \cdot \frac{\partial p}{\partial r} + \nu \Delta V_r \\ &\qquad + \frac{\nu}{3} \cdot \frac{\partial \text{ div } \mathbf{V}}{\partial r} \end{aligned}\right\} \qquad (3.1.36)$$

where $\text{div } \mathbf{V} = \partial V_x/\partial x + \partial V_r/\partial r + V_r/r$; $\Delta = \partial^2/\partial x^2 + \partial^2/\partial r^2 + (1/r)\,\partial/\partial r$.

For a steady flow, one must assume in the equations that

$$\partial V_x/\partial t = \partial V_r/\partial t = \partial V_\gamma/\partial t = 0$$

Spherical Coordinates

The spherical coordinates, Lamé coefficients, and the projections of the velocity vector onto the directions of the coordinate lines are related by formulas (2.4.13), (2.4.17), and (2.4.33):

$$q_1 = r,\ q_2 = \theta,\ q_3 = \psi,\ h_1 = 1,\ h_2 = r,\ h_3 = r\sin\theta,$$
$$V_1 = V_r,\ V_2 = V_\theta,\ V_3 = V_\psi$$

According to these data, from (3.1.32) we find the projection of the acceleration onto the direction of the coordinate line r:

$$W_1 = \frac{\partial V_r}{\partial t} + V_r\frac{\partial V_r}{\partial r} + \frac{V_\theta}{r}\cdot\frac{\partial V_r}{\partial\theta} + \frac{V_\psi}{r\sin\theta}\cdot\frac{\partial V_r}{\partial\psi} - \frac{V_\theta^2 + V_\psi^2}{r} \quad (3.1.37)$$

The projection of the pressure gradient is

$$(\operatorname{grad} p)_1 = \partial p/\partial r \quad (3.1.38)$$

With a view to the expression for div V (2.4.34), we find the relation

$$(\operatorname{grad}\operatorname{div}\mathbf{V})_1 = \frac{\partial \operatorname{div}\mathbf{V}}{\partial r}$$
$$= \frac{\partial}{\partial r}\left[\frac{1}{r^2}\cdot\frac{\partial(V_r r^2)}{\partial r} + \frac{1}{r\sin\theta}\cdot\frac{\partial(V_\theta\sin\theta)}{\partial\theta} + \frac{1}{r\sin\theta}\cdot\frac{\partial V_\psi}{\partial\psi}\right] \quad (3.1.39)$$

We shall use this relation for determining the projections $(\Delta V)_1$ of the vector $\Delta\mathbf{V}$. To do this, we shall calculate the value of (curl curl V)$_1$ in (3.1.33). From (3.1.28), we have

$$(\operatorname{curl}\mathbf{V})_3 = \frac{1}{r}\left[\frac{\partial(V_\theta r)}{\partial r} - \frac{\partial V_r}{\partial\theta}\right],\quad (\operatorname{curl}\mathbf{V})_2 = \frac{1}{r\sin\theta}\left[\frac{\partial V_r}{\partial\psi} - \frac{\partial(V_\psi r\sin\theta)}{\partial r}\right]$$

Introducing these relations into (3.1.34), we obtain

$$(\operatorname{curl}\operatorname{curl}\mathbf{V})_1 \frac{1}{r^2\sin\theta}\left\{\frac{\partial\left\{\sin\theta\left[\frac{\partial(V_\theta r)}{\partial r} - \frac{\partial V_r}{\partial\theta}\right]\right\}}{\partial\theta}\right.$$
$$\left. - \frac{\partial\left\{\frac{1}{\sin\theta}\left[\frac{\partial V_r}{\partial\psi} - \frac{\partial(V_\psi r\sin\theta)}{\partial r}\right]\right\}}{\partial\psi}\right\} \quad (3.1.40)$$

With a view to expressions (3.1.39) and (3.1.40), we find

$$(\Delta V)_1 = (\operatorname{grad}\operatorname{div}\mathbf{V})_1 - (\operatorname{curl}\operatorname{curl}\mathbf{V})_1 = \Delta V_r - \frac{2V_r}{r^2}$$
$$- \frac{2}{r^2}\cdot\frac{\partial V_\theta}{\partial\theta} - \frac{2V_\theta\cot\theta}{r^2} - \frac{2}{r^2\sin\theta}\cdot\frac{\partial V_\psi}{\partial\psi} \quad (3.1.41)$$

where

$$\Delta V_r = \frac{1}{r^2}\cdot\frac{\partial}{\partial r}\left(r^2\frac{\partial V_r}{\partial r}\right) + \frac{1}{r^2\sin\theta}\cdot\frac{\partial}{\partial\theta}\left(\sin\theta\frac{\partial V_r}{\partial\theta}\right)$$
$$+ \frac{1}{r^2\sin^2\theta}\cdot\frac{\partial^2 V_r}{\partial\psi^2} \quad (3.1.42)$$

Taking into account (3.1.37)-(3.1.39) and (3.1.41), we find the equation of motion in a projection onto the coordinate line r:

$$\frac{\partial V_r}{\partial t}+V_r\frac{\partial V_r}{\partial r}+\frac{V_\theta}{r}\cdot\frac{\partial V_r}{\partial\theta}+\frac{V_\psi}{r\sin\theta}\cdot\frac{\partial V_r}{\partial\psi}-\frac{V_\theta^2+V_\psi^2}{r}=-\frac{1}{\rho}\cdot\frac{\partial p}{\partial r}+\nu\left(\Delta V_r-\frac{2}{r^2}\cdot\frac{\partial V_\theta}{\partial\theta}-\frac{2}{r^2\sin\theta}\cdot\frac{\partial V_\psi}{\partial\psi}-\frac{2V_r}{r^2}-\frac{2V_\theta\cot\theta}{r^2}\right)+\frac{\nu}{3}\cdot\frac{\partial\,\mathrm{div}\,\mathbf{V}}{\partial r} \quad (3.1.43)$$

We obtain the other two equations in a similar way:

$$\left.\begin{aligned}&\frac{\partial V_\theta}{\partial t}+V_r\frac{\partial V_\theta}{\partial r}+\frac{V_\theta}{r}\cdot\frac{\partial V_\theta}{\partial\theta}+\frac{V_\psi}{r\sin\theta}\cdot\frac{\partial V_\theta}{\partial\psi}\\&\frac{V_rV_\theta-V_\psi^2\cot\theta}{r}=-\frac{1}{r\rho}\cdot\frac{\partial p}{\partial\theta}+\nu\left(\Delta V_\theta+\frac{2}{r^2}\cdot\frac{\partial V_r}{\partial\theta}-\frac{V_\theta}{r^2\sin^2\theta}-\frac{2\cos\theta}{r^2\sin^2\theta}\cdot\frac{\partial V_\psi}{\partial\psi}\right)+\frac{\nu}{3}\cdot\frac{1}{r}\cdot\frac{\partial\,\mathrm{div}\,\mathbf{V}}{\partial\theta}\\&\frac{\partial V_\psi}{\partial t}+V_r\frac{\partial V_\psi}{\partial r}+\frac{V_\theta}{r}\cdot\frac{\partial V_\psi}{\partial\theta}+\frac{V_\psi}{r\sin\theta}\cdot\frac{\partial V_\psi}{\partial\psi}\\&+\frac{V_\psi(V_r+V_\theta\cot\theta)}{r}=-\frac{1}{\rho r\sin\theta}\cdot\frac{\partial p}{\partial\psi}\\&+\nu\left(\Delta V_\psi-\frac{V_\psi}{r^2\sin^2\theta}+\frac{2}{r^2\sin\theta}\cdot\frac{\partial V_r}{\partial\psi}+\frac{2\cos\theta}{r^2\sin^2\theta}\cdot\frac{\partial V_\theta}{\partial\psi}\right)\\&+\frac{\nu}{3r\sin\theta}\cdot\frac{\partial\,\mathrm{div}\,\mathbf{V}}{\partial\psi}\end{aligned}\right\}\quad(3.1.43')$$

where the Laplacian operator in spherical coordinates is

$$\Delta=\frac{1}{r^2}\cdot\frac{\partial}{\partial r}\left(r^2\frac{\partial}{\partial r}\right)+\frac{1}{r^2\sin\theta}\cdot\frac{\partial}{\partial\theta}\left(\sin\theta\frac{\partial}{\partial\theta}\right)+\frac{1}{r^2\sin^2\theta}\cdot\frac{\partial^2}{\partial\psi^2} \quad (3.1.44)$$

For two-dimensional spatial gas flows characterized by a change in the parameters (velocity, pressure, density, etc.) in the direction of only two coordinate lines, let us write the equation of motion in a simpler form:

$$\left.\begin{aligned}&\frac{\partial V_r}{\partial t}+V_r\frac{\partial V_r}{\partial r}+\frac{V_\theta}{r}\cdot\frac{\partial V_r}{\partial\theta}-\frac{V_\theta^2}{r}=-\frac{1}{\rho}\cdot\frac{\partial p}{\partial r}\\&+\nu\left(\Delta V_r-\frac{2}{r^2}\cdot\frac{\partial V_\theta}{\partial\theta}-\frac{2V_r}{r^2}-\frac{2V_\theta\cot\theta}{r^2}\right)+\frac{\nu}{3}\cdot\frac{\partial\,\mathrm{div}\,\mathbf{V}}{\partial r}\\&\times\frac{\partial V_\theta}{\partial t}+V_r\frac{\partial V_\theta}{\partial r}+\frac{V_\theta}{r}\cdot\frac{\partial V_\theta}{\partial\theta}+\frac{V_rV_\theta}{r}=-\frac{1}{r\rho}\cdot\frac{\partial p}{\partial\theta}\\&+\nu\left(\Delta V_\theta+\frac{2}{r^2}\cdot\frac{\partial V_r}{\partial\theta}-\frac{V_\theta}{r^2\sin^2\theta}\right)+\frac{\nu}{3r}\cdot\frac{\partial\,\mathrm{div}\,\mathbf{V}}{2\theta}\end{aligned}\right\}\quad(3.1.45)$$

where

$$\Delta = \frac{1}{r^2} \cdot \frac{\partial}{\partial r}\left(r^2 \frac{\partial}{\partial r}\right) + \frac{1}{r^2 \sin\theta} \cdot \frac{\partial}{\partial \theta}\left(\sin\theta \frac{\partial}{\partial \theta}\right) \quad (3.1.46)$$

$$\operatorname{div} \mathbf{V} = \frac{1}{r^2} \cdot \frac{\partial (V_r r^2)}{\partial r} + \frac{1}{r \sin\theta} \cdot \frac{\partial (V_\theta \sin\theta)}{\partial \theta} \quad (3.1.47)$$

Equations of Two-Dimensional Flow of a Gas Near a Curved Surface

For the case being considered, the curvilinear coordinates, Lamé coefficients, and velocity components are determined by formulas (2.4.40), (2.4.42), and (2.4.43), respectively. We shall adopt the further condition that motion occurs near a wall, and, consequently, $y \ll R$. Accordingly,

$$q_1 = x,\ q_2 = y,\ q_3 = \gamma,\ h_1 = 1,\ h_2 = 1,\ h_3 = r$$
$$V_1 = dx/dt = V_x,\ V_2 = V_y,\ V_3 = 0$$

With a view to these data, the acceleration component is

$$W_1 = \partial V_x/\partial t + V_x\, \partial V_x/\partial x + V_y\, \partial V_x/\partial y \quad (3.1.48)$$

and the projection of the pressure gradient is

$$(\operatorname{grad} p)_1 = \partial p/\partial x \quad (3.1.49)$$

In addition,

$$(\operatorname{grad} \operatorname{div} \mathbf{V})_1 = \partial \operatorname{div} \mathbf{V}/\partial x \quad (3.1.50)$$

where the divergence of the velocity has been determined by relation (2.4.44).

Consequently,

$$(\operatorname{grad} \operatorname{div} \mathbf{V})_1 = \frac{\partial}{\partial x}\left\{\frac{1}{r}\left[\frac{\partial (V_x r)}{\partial x} + \frac{\partial (V_y r)}{\partial y}\right]\right\} \quad (3.1.51)$$

We use (3.1.28) to calculate the projections of the velocity curl vector:

$$(\operatorname{curl} \mathbf{V})_3 = \partial V_y/\partial x - \partial V_x/\partial y,\ (\operatorname{curl} \mathbf{V})_2 = 0 \quad (3.1.52)$$

Introducing these expressions into (3.1.34), we obtain

$$(\operatorname{curl} \operatorname{curl} \mathbf{V})_1 = \frac{1}{r} \cdot \frac{\partial}{\partial y}\left[r\left(\frac{\partial V_y}{\partial x} - \frac{\partial V_x}{\partial y}\right)\right] \quad (3.1.53)$$

With a view to relations (3.1.51) and $(3.1.53)_1$ we have

$$(\Delta V)_1 = (\operatorname{grad} \operatorname{div} \mathbf{V})_1 - (\operatorname{curl} \operatorname{curl} \mathbf{V})_1 = \frac{\partial}{\partial x}\left\{\frac{1}{r}\left[\frac{\partial (V_x r)}{\partial x} + \frac{\partial (V_y r)}{\partial y}\right]\right\} - \frac{1}{r} \cdot \frac{\partial}{\partial y}\left[r\left(\frac{\partial V_y}{\partial x} - \frac{\partial V_x}{\partial y}\right)\right] \quad (3.1.54)$$

Similarly, when considering the coordinate line q_2, we have

$$W_2 = \partial V_y/\partial t + V_x\,\partial Vy/\partial x + V_y\,\partial V_y/\partial y \qquad (3.1.55)$$

$$(\text{grad } p)_2 = \partial p/\partial y \qquad (3.1.56)$$

$$(\text{grad div } \mathbf{V})_2 = \partial \text{ div } \mathbf{V}/\partial y \qquad (3.1.57)$$

$$(\Delta V)_2 = (\text{grad div } \mathbf{V})_2 - (\text{curl curl } \mathbf{V})_2$$

$$= -\frac{\partial}{\partial y}\left\{\frac{1}{r}\left[\frac{\partial (V_x r)}{\partial x} + \frac{\partial (V_y r)}{\partial y}\right]\right\} - \frac{1}{r}\cdot\frac{\partial}{\partial x}\left[r\left(\frac{\partial V_y}{\partial x} - \frac{\partial V_x}{\partial y}\right)\right] \qquad (3.1.58)$$

Using the obtained relations, we have:

$$\left.\begin{aligned} \frac{\partial V_x}{\partial t} + V_x\frac{\partial V_x}{\partial x} + V_y\frac{\partial V_x}{\partial y} &= -\frac{1}{\rho}\cdot\frac{\partial p}{\partial x} + \nu(\Delta V)_1 \\ &\quad + \frac{\nu}{3}\cdot\frac{\partial \text{ div } \mathbf{V}}{\partial x} \\ \frac{\partial V_y}{\partial t} + V_x\frac{\partial V_y}{\partial x} + V_y\frac{\partial V_y}{\partial y} &= -\frac{1}{\rho}\cdot\frac{\partial p}{\partial y} + \nu(\Delta V)_2 \\ &\quad + \frac{\nu}{3}\cdot\frac{\partial \text{ d v } \mathbf{V}}{\partial y} \end{aligned}\right\} \qquad (3.1.59)$$

where $(\Delta V)_1$ and $(\Delta V)_2$ are determined by formulas (3.1.54) and (3.1.58), respectively.

We have thus obtained various forms of the equations of motion for a viscous liquid. Experience shows that this is needed because in some cases, when studying the laws of interaction of gas flows with bodies in them, it is convenient to use one form of the equation, and in others, a different form.

3.2. Equations of Energy and Diffusion of a Gas

Diffusion Equation

The motion of a dissociating viscous fluid can be investigated with account taken of the influence of gas diffusion on this motion. This is expressed, particularly, in that diffusion is taken into consideration when deriving the equation of energy—one of the fundamental equations of gas dynamics.

By **diffusion** is meant the levelling out of the concentration because of the molecular transfer of a substance. This is a thermodynamically irreversible process, and it is one of the reasons why a gas in motion loses mechanical energy.

The diffusion equation is an equation of the transfer of the i-th component in a gas mixture (it is a continuity equation for the same component).

To simplify our investigation, we can assume that the intensity of thermal and pressure diffusion is negligibly small and determine the diffusion flux of the i-th component in a direction n by the equation

$$Q_{i,\mathrm{d},n} = -\rho D_i \, \partial c_i/\partial n \qquad (3.2.1)$$

where c_i is the concentration of the i-th component, and D_i is the diffusivity that determines the diffusion flux when a concentration gradient is present.

For a mixture of gas components, we must take into consideration the binary diffusivities corresponding to each pair of components, for example, to oxygen atoms and molecules, or to nitrogen atoms and molecules in the air. In approximate calculations, we can proceed from a certain value of the binary diffusivity $\bar{D}$ that is the same for all the pairs of components. Taking this into account, we have $Q_{i,\mathrm{d},n} = -\rho\bar{D} \, \partial c_i/\partial n$. Considering the directions x, y, and z along which diffusion occurs, we have

$$Q_{i,\mathrm{d},x} = -\rho\bar{D} \, \partial c_i/\partial x, \; Q_{i,\mathrm{d},y} = -\rho\bar{D} \, \partial c_i/\partial y, \; Q_{i,\mathrm{d},z} = -\rho\bar{D} \, \partial c_i/\partial z \qquad (3.2.2)$$

or in the vector form

$$\mathbf{Q}_{i,\mathrm{d}} = -\rho\bar{D} \operatorname{grad} c_i \qquad (3.2.3)$$

The diffusion of a substance is directed into a region with a reduced concentration, therefore $\partial c_i/\partial n$ has a negative sign. Since the right-hand side of (3.2.3) contains a minus sign, the quantity $\mathbf{Q}_{i,\mathrm{d}}$ is positive.

Let us consider the derivation of the diffusion equation in a cylindrical coordinate system assuming the motion to be steady. We shall assume the flow to be three-dimensional and symmetric about the x-axis, i.e. such in which the velocity component $V_y = 0$. Let us separate an elementary volume of the gas in the form of a ring with dimensions of dr and dx (Fig. 3.2.1) constructed near point P whose coordinates are x and r and whose velocity components are V_x and V_r. We shall assume that the substance diffuses only in a radial direction. Consequently, the flux of the i-th component through the internal surface of the element is $m_r = 2\pi r\rho V_r c_i \, dx + Q_{i,\mathrm{d}} 2\pi r \, dx$, where c_i and $Q_{i,\mathrm{d}}$ are the concentration and the diffusion flux of the i-th component, respectively, evaluated per unit area.

The flux of the i-th component through the outer surface is

$$m_r + \frac{\partial m_r}{\partial r} dr = m_r + \frac{\partial (\rho V_r r c_i)}{\partial r} 2\pi \, dr \, dx + \frac{\partial (Q_{i,\mathrm{d}} r)}{\partial r} 2\pi \, dr \, dx$$

Consequently, the flow of the component into the volume being considered is

$$[\partial (\rho V_r r c_i)/\partial r] \, 2\pi \, dr \, dx + [\partial (Q_{i,\mathrm{d}} r)/\partial r] \, 2\pi \, dr \, dx$$

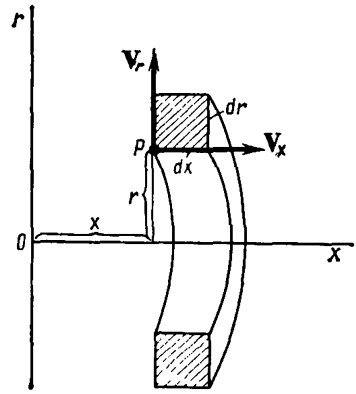

Fig. 3.2.1
An elementary gas particle in an axisymmetric three-dimensional flow

Disregarding the diffusion flux of the substance along the x-axis, we find the rate of flow of the gas through the left-hand face of the element normal to this axis:

$$m_x = 2\pi\rho V_x c_i r\, dr$$

and through the right-hand one

$$m_x + (\partial m_x/\partial x)\, dx = m_x + [\partial\, (\rho V_x r c_i)/\partial x]\, 2\pi\, dr\, dx$$

Hence, the flow of the component into the volume is

$$2\pi\, [\partial\, (\rho V_x r c_i)/\partial x]\, dr\, dx$$

Since the amount of gas in the volume does not change, the total flow of the component into the volume equals its outflow because of chemical reactions. If the rate of formation of the i-th component in a unit volume caused by chemical reactions is $(W_{ch})_i$, the consumption of the component in the elementary volume is $2\pi\, (W_{ch})_i r \times$ $\times\, r\, dr\, dx$. Therefore, the balance of mass of the i-th component in the volume being considered is

$$\partial\, (\rho V_x r c_i)/\partial x + \partial\, (\rho V_r r c_i)/\partial r = -\partial\, (Q_{i,d}\, r)/\partial r + (W_{ch})_i r \quad (3.2.4)$$

This equation is known as the diffusion equation in a cylindrical coordinate system. In a similar way, we can obtain a diffusion equation in the Cartesian coordinates x and y for a plane flow:

$$\partial\, (\rho V_x c_i)/\partial x + \partial\, (\rho V_y c_i)/\partial y = -\partial Q_{i,d}/\partial y + (W_{ch})_i \quad (3.2.5)$$

where $Q_{i,d}$ is found from (3.2.3).

If we consider a binary mixture of atoms and molecules, then $\sum c_i = c_A + c_M = 1$ and, consequently, $Q_{A,d} = -Q_{M,d}$. We determine the value of $(W_{ch})_i$ for a given reaction in a dissociating gas by the formulas of chemical kinetics.

Energy Equation

Together with the equations of state, motion, and continuity, the energy equation belongs to the system of fundamental differential equations as a result of whose solution we completely determine the motion of a gas.

Let us consider a system of rectangular Cartesian coordinates and compile an energy equation for a fluid particle in the form of an elementary parallelepiped. This equation expresses the law of energy conservation, according to which the change in the total energy of a particle, consisting of its kinetic and internal energy, during the time dt equals the work of the external forces applied to the particle plus the influx of heat from the surroundings.

The kinetic energy of a particle of volume $\tau = dx\,dy\,dz$ is $(\rho V^2/2)\,\tau$, and its internal energy is $u\rho\tau$ (u is the internal energy of a unit mass of the gas). Consequently, the change in the total energy during the time dt is

$$\frac{d}{dt}\left[\left(\frac{\rho V^2}{2}+\rho u\right)\tau\right]dt=\rho\tau\,\frac{d}{dt}\left(\frac{V^2}{2}+u\right)dt$$

The work of the external mass (volume) forces in the displacement of the particle during the time dt can be represented in the form of the dot product $\mathbf{G}\cdot\mathbf{V}$ multiplied by the mass of the particle $\rho\tau$ and the time dt. The mass force vector is $\mathbf{G} = X\mathbf{i} + Y\mathbf{j} + Z\mathbf{k}$, consequently,

$$(\mathbf{G}\cdot\mathbf{V})\,\rho\tau\,dt = (XV_x - YV_y + ZV_z)\,\rho\tau\,dt$$

Let us calculate the work of the surface forces. First we shall consider the work done during the time dt by the forces induced by the stresses acting on the right-hand and left-hand faces. The work done by the forces acting on the left-hand face equals the dot product $\boldsymbol{\sigma}_x\cdot\mathbf{V}$ multiplied by the area $dy\,dz$ and the time dt. In the dot product, the vector of the surface forces is

$$\boldsymbol{\sigma}_x = p_{xx}\mathbf{i} + \tau_{xy}\mathbf{j} + \tau_{xz}\mathbf{k}$$

The work done by the surface forces acting on the right-hand face is

$$\left[\boldsymbol{\sigma}_x\mathbf{V}+\frac{\partial(\boldsymbol{\sigma}_x\mathbf{V})}{\partial x}\,dx\right]dy\,dz\,dt$$

Having in view that the forces for the left-hand and right-hand faces are directed oppositely, we must assume that the work done by these forces is opposite in sign, for example, positive for the right-hand and negative for the left-hand face. Accordingly, the work of all the surface forces applied to the left-hand and right-hand faces is

$$\frac{\partial(\boldsymbol{\sigma}_x\mathbf{V})}{\partial x}\,\tau\,dt=\left[\frac{\partial}{\partial x}(p_{xx}V_x+\tau_{xy}V_y+\tau_{xz}V_z\right]\tau\,dt \qquad (3.2.6)$$

We obtain expressions for the work done by the surface forces acting on the lower and upper, and also on the front and rear faces, in a similar way:

$$[\partial (\sigma_y \mathbf{V})/\partial y]\, \tau\, dt \text{ and } [\partial (\sigma_z \mathbf{V})/\partial z]\, \tau\, dt$$

Considering that the vectors of the surface forces acting on the lower and rear faces are, respectively,

$$\sigma_y = \tau_{yx}\mathbf{i} + p_{yy}\mathbf{j} + \tau_{yz}\mathbf{k},\ \sigma_z = \tau_{zx}\mathbf{i} + \tau_{zy}\mathbf{j} + p_{zz}\mathbf{k}$$

we obtain the following expressions for the work:

$$\frac{\partial (\sigma_y \mathbf{V})}{\partial y}\, \tau\, dt = \left[\frac{\partial}{\partial y}(\tau_{yx}V_x + p_{yy}V_y + \tau_{yz}V_z)\right] \tau\, dt \qquad (3.2.6')$$

$$\frac{\partial (\sigma_z \mathbf{V})}{\partial z}\, \tau\, dt = \left[\frac{\partial}{\partial z}(\tau_{xx}V_x + \tau_{zy}V_y + p_{zz}V_z)\right] \tau\, dt \qquad (3.2.6'')$$

In expressions (3.2.6), (3.2.6′), and (3.2.6″), the stresses are determined by relations (3.1.5) and (3.1.16), respectively.

The influx of heat to the particle occurs owing to heat conduction, diffusion, and radiation. Let $q_x\, dy\, dz$ (where q_x is the specific heat flow) be the amount of heat due to heat conduction or diffusion transferred to the particle through the left-hand face in unit time. During the time dt, the heat flux $q_x\, dy\, dz\, dt$ is supplied to the particle. The heat flux through the right-hand face is $-[q_x + (\partial q_x/\partial x)\, dx]\, dy\, dz\, dt$. The amount of heat transferred to the particle through both faces is $-(\partial q_x/\partial x)\, \tau\, dt$. We obtain similar expressions for the faces perpendicular to the y- and z-axes. Hence, the total heat flux transferred to the particle is $-(\partial q_x/\partial x + \partial q_y/\partial y + \partial q_z/\partial z)\, \tau\, dt$.

If we consider the supply of heat caused by conduction, the specific heat flows, equal to the heat fluxes along the relevant coordinate directions through a unit area, are expressed by the Fourier law

$$q_{T,x} = -\lambda\, \partial T/\partial x,\ q_{T,y} = -\lambda\, \partial T/\partial y,\ q_{T,z} = -\lambda\, \partial T/\partial z \qquad (3.2.7)$$

With this taken into account, we have

$$-(\partial q_{T,x}/\partial x + \partial q_{T,y}/\partial y + \partial q_{T,z}/\partial z)\, \tau\, dt = \operatorname{div}(\lambda \operatorname{grad} T)\, \tau\, dt \qquad (3.2.8)$$

where $\operatorname{grad} T = (\partial T/\partial x)\mathbf{i} + (\partial T/\partial y)\mathbf{j} + (\partial T/\partial z)\mathbf{k}$.

The energy supplied to a gas particle at the expense of diffusion is

$$q_{\mathrm{d},x} = \sum_i Q_{i,\mathrm{d},x} i_i,\ q_{\mathrm{d},y} = \sum_i Q_{i,\mathrm{d},y} i_i,\ q_{\mathrm{d},z} = \sum_i Q_{i,\mathrm{d},z} i_i$$

where i_i is the generalized enthalpy component of the gas mixture.

Hence,

$$-\left(\frac{\partial q_{\mathrm{d},x}}{\partial x}+\frac{\partial q_{\mathrm{d},y}}{\partial y}+\frac{\partial q_{\mathrm{d},z}}{\partial z}\right)\tau\,dt=-\left(\sum_i i_i\frac{\partial Q_{i,\mathrm{d},x}}{\partial x}\right.$$

$$\left.+\sum_i i_i\frac{\partial Q_{i,\mathrm{d},y}}{\partial y}+\sum_i i_i\frac{\partial Q_{i,\mathrm{d},z}}{\partial z}\right)\tau\,dt=\left(-\sum_i i_i\,\mathrm{div}\,\mathbf{Q}_{i,\mathrm{d}}\right)\tau\,dt$$

Introducing into this equation the value of $\mathbf{Q}_{i,\mathrm{d}}$ from (3.2.3), we obtain

$$-(\partial q_{\mathrm{d},x}/\partial x+\partial q_{\mathrm{d},y}/\partial y+\partial q_{\mathrm{d},z}/\partial z)\,\tau\,dt$$
$$=\sum_i i_i\,\mathrm{div}\,(\rho D\,\mathrm{grad}\,c_i)\,\tau\,dt \qquad (3.2.9)$$

In addition to the energy transferred to a particle by conduction and diffusion, it also receives heat owing to radiation, equal to $\varepsilon\tau\,dt$ (ε is the heat flux due to radiation absorbed by unit volume).

By equating the change in the energy of a particle during the time dt to the sum of the work done by the mass and surface forces and the influx of heat because of conduction, diffusion, and radiation, we obtain the energy equation:

$$\rho\frac{d}{dt}\left(\frac{V^2}{2}+u\right)=\rho\,(XV_x+YV_y+ZV_z)+\frac{\partial}{\partial x}(p_{xx}V_x$$
$$+\tau_{xy}V_y+\tau_{xz}V_z)+\frac{\partial}{\partial y}(\tau_{yx}V_x+p_{yy}V_y+\tau_{yz}V_z)$$
$$+\frac{\partial}{\partial z}(\tau_{zx}V_x+\tau_{zy}V_y+p_{zz}V_z)+\mathrm{div}\,(\lambda\,\mathrm{grad}\,T)$$
$$+\sum_i i_i\,\mathrm{div}\,(\rho\overline{D}\,\mathrm{grad}\,c_i)+\varepsilon \qquad (3.2.10)$$

Upon the motion of a chemically reacting mixture of gases, the energy equation expresses the condition of the heat balance including the heat that may appear as a result of chemical reactions. If we take into account, however, that upon the proceeding of reactions the generalized enthalpy of the gas mixture $\sum c_i i_i$ does not change, then upon introducing the generalized enthalpy into Eq. (3.2.10), we can no longer take into account separately the release or absorption of heat because of chemical reactions.

Introducing into (3.2.10) the expressions for the stresses (3.1.5) and (3.1.16) and excluding the term taking into account the work done by the mass forces, after transformations we obtain an energy equation for a gas:

$$\rho\frac{d}{dt}\left(\frac{V^2}{2}+u\right)=-\,\mathrm{div}\,(p\mathbf{V})-\frac{2}{3}\,\mathrm{div}\,(\mu\mathbf{V}\,\mathrm{div}\,\mathbf{V})$$
$$+\frac{\partial}{\partial x}\left(\mu\frac{\partial V_x^2}{\partial x}\right)+\frac{\partial}{\partial y}\left(\mu\frac{\partial V_y^2}{\partial y}\right)+\frac{\partial}{\partial z}\left(\mu\frac{\partial V_z^2}{\partial z}\right)$$

$$+2\frac{\partial}{\partial x}[\mu(V_y\varepsilon_z+V_z\varepsilon_y)]+2\frac{\partial}{\partial y}[\mu(V_x\varepsilon_z+V_z\varepsilon_x)]$$
$$+2\frac{\partial}{\partial z}[\mu(V_x\varepsilon_y+V_y\varepsilon_x)]+\operatorname{div}(\lambda\operatorname{grad}T)$$
$$+\sum_i i_i\operatorname{div}(\rho\overline{D}\operatorname{grad}c_i)+\varepsilon \qquad (3.2.11)$$

Equation (3.2.11) shows what causes the kinetic energy of a fluid to change. In addition to conduction, diffusion, and radiation, this energy changes at the expense of the work of compression div $(p\mathbf{V})$ and the work of the friction forces (the terms of the equation containing the dynamic viscosity μ). The dissipation of energy is associated with the losses of mechanical energy for overcoming the friction forces. Energy dissipation consists in that the mechanical energy in part transforms irreversibly into heat. Accordingly, the friction forces are called **dissipative**. The terms on the right-hand side of (3.2.11) containing μ form the **dissipative function.**

For two-dimensional plane motion of a viscous fluid, the energy equation is

$$\rho\frac{\partial}{\partial t}\left(\frac{V^2}{2}+u\right)=-\operatorname{div}(p\mathbf{V})-\frac{2}{3}\operatorname{div}(\mu\mathbf{V}\operatorname{div}\mathbf{V})$$
$$+\frac{\partial}{\partial x}\left(\mu\frac{\partial V_x^2}{\partial r}\right)+\frac{\partial}{\partial y}\left(\mu\frac{\partial V_y^2}{\partial y}\right)$$
$$+2\frac{\partial}{\partial x}(\mu V_y\varepsilon_z)+2\frac{\partial}{\partial y}(\mu V_x\varepsilon_z)+\operatorname{div}(\lambda\operatorname{grad}T)$$
$$+\sum_i i_i\operatorname{div}(\rho\overline{D}\operatorname{grad}c_i)+\varepsilon \qquad (3.2.12)$$

where

$$\mathbf{V}=V_x\mathbf{i}+V_y\mathbf{j},\quad \operatorname{div}\mathbf{V}=\partial V_x/\partial x+\partial V_y/\partial y,$$
$$\operatorname{grad}T=(\partial T/\partial x)\,\mathbf{i}+(\partial T/\partial y)\mathbf{j},\quad \operatorname{grad}c_i=(\partial c_i/\partial x)\mathbf{i}+(\partial c_i/\partial y)\mathbf{j}$$

Let us transform the energy equation (3.2.12). To do this, we multiply the first equation (3.1.20) by V_x, the second one by V_y, and sum up the results. We obtain

$$\rho\frac{d}{dt}\left(\frac{V^2}{2}\right)=-\left(V_x\frac{\partial p}{\partial x}+V_y\frac{\partial p}{\partial y}\right)$$
$$+V_x\frac{\partial}{\partial x}\left[\mu\left(2\frac{\partial V_x}{\partial x}-\frac{2}{3}\operatorname{div}\mathbf{V}\right)\right]+V_y\frac{\partial}{\partial y}\left[\mu\left(2\frac{\partial V_y}{\partial y}-\frac{2}{3}\operatorname{div}\mathbf{V}\right)\right]$$
$$+2\left[V_x\frac{\partial}{\partial y}(\mu\varepsilon_z)+V_y\frac{\partial}{\partial x}(\mu\varepsilon_z)\right] \qquad (3.2.13)$$

We can show by simple transformations that

$$V_x\,\partial p/\partial x+V_y\,\partial p/\partial y=\operatorname{div}(p\mathbf{V})-p\operatorname{div}\mathbf{V}$$

where we find p div V by using the continuity equation

$$p \operatorname{div} \mathbf{V} = -(p/\rho)\, d\rho/dt, \text{ or } p \operatorname{div} \mathbf{V} = \rho\, (d/dt)\, (p/\rho) - dp/dt$$

We transform the sum of the other two terms on the right-hand side of the equation to the form

$$V_x \frac{\partial}{\partial x}\left[\mu\left(2\frac{\partial V_x}{\partial x} - \frac{2}{3}\operatorname{div}\mathbf{V}\right)\right] + V_y \frac{\partial}{\partial y}\left[\mu\left(2\frac{\partial V_y}{\partial y} - \frac{2}{3}\operatorname{div}\mathbf{V}\right)\right]$$
$$= \frac{\partial}{\partial x}\left(\mu\frac{\partial V_x^2}{\partial x}\right) + \frac{\partial}{\partial y}\left(\mu\frac{\partial V_y^2}{\partial y}\right) - 2\mu\left[\left(\frac{\partial V_x}{\partial x}\right)^2 + \left(\frac{\partial V_y}{\partial y}\right)^2\right]$$
$$- \frac{2}{3}\operatorname{div}(\mu\mathbf{V}\operatorname{div}\mathbf{V}) + \frac{2}{3}\mu(\operatorname{div}\mathbf{V})^2$$

For the last term in (3.2.13), we have the expression

$$2\left[V_x \frac{\partial}{\partial y}(\mu\varepsilon_z) + V_y \frac{\partial}{\partial x}(\mu\varepsilon_z)\right] = 2\frac{\partial}{\partial x}(\mu V_y \varepsilon_z) + 2\frac{\partial}{\partial y}(\mu V_x \varepsilon_z) - 4\mu\varepsilon_z^2$$

Let us make the relevant substitution in (3.2.13) and subtract the obtained equation from (3.2.12). Having in view that $i = u + p/\rho$, we obtain

$$\rho\frac{di}{dt} = \frac{dp}{dt} + 2\mu\left\{\left[\left(\frac{\partial V_x}{\partial x}\right)^2 + \left(\frac{\partial V_y}{\partial y}\right)^2\right] - \frac{2}{3}(\operatorname{div}\mathbf{V})^2 + 4\varepsilon_z^2\right\}$$
$$+ \operatorname{div}(\lambda \operatorname{grad} T) + \sum_i i_i \operatorname{div}(\rho\overline{D}\operatorname{grad} c_i) + \varepsilon \qquad (3.2.14)$$

In the absence of heat transfer by diffusion and radiation, we can write the energy equation in the form

$$\rho\frac{di}{dt} = \frac{dp}{dt} + 2\mu\left\{\left[\left(\frac{\partial V_x}{\partial x}\right)^2 + \left(\frac{\partial V_y}{\partial y}\right)^2\right] - \frac{2}{3}(\operatorname{div}\mathbf{V})^2 + 4\varepsilon_z^2\right\}$$
$$+ \operatorname{div}(\lambda \operatorname{grad} T) \qquad (3.2.15)$$

At low gas velocities, when the work of the friction forces is not great, we may disregard the dissipative terms. In addition, the work done by the pressure forces is also insignificant ($dp/dt \approx$ ≈ 0). In the given case, instead of (3.2.15), we have

$$dT/dt = (\lambda/\rho c_p) \operatorname{div}(\operatorname{grad} T) \qquad (3.2.16)$$

The quantity $\lambda/(\rho c_p) = a$, called the **thermal diffusivity**, characterizes the intensity of molecular heat transfer.

3.3. System of Equations of Gas Dynamics. Initial and Boundary Conditions

The investigation of the motion of a gas, i.e. the determination of the parameters characterizing this motion for each point of space, consists in solving the relevant equations that relate these parameters to one another. All these equations are independent and form a **system of equations of gas dynamics**. We determine the number of independent equations by the number of unknown parameters of the gas being sought.

Let us consider the motion of an ideal compressible gas. If the velocities of the flow are not high, we may ignore the change in the specific heats with the temperature and take no account of radiation. In this case, the gas flow is a thermodynamically isolated system and is adiabatic. The unknown quantities for the flow being considered are the three velocity components V_x, V_y, and V_z. and also the pressure p, density ρ, and temperature T. Consequently, the system of equations of gas dynamics must include six independent ones. Among them are the equations of motion, continuity, state, and energy, which are customarily called the **fundamental equations of gas dynamics**.

Before compiling this system of equations, let us consider separately the energy equation. In accordance with our assumption on the adiabatic nature of the flow, we transform the energy equation (3.2.14) as follows:

$$di = dp/\rho \tag{3.3.1}$$

If we take into consideration the equation $di = c_p\, dT$, and also the expressions $c_p - c_v = R$ and $p = R\rho T$, from which we can find

$$c_p = \frac{(c_p/c_v)\, R}{c_p/c_v - 1} = \frac{k}{k-1} R, \quad dT = \frac{1}{R} d\left(\frac{p}{\rho}\right)$$

then (3.3.1) is reduced to the form $dp/p = k\, d\rho/\rho$.

Hence

$$p = A\rho^k \tag{3.3.2}$$

where A is a constant characteristic of the given conditions of gas flow.

Equation (3.3.2) is known as the equation of an adiabat (isentrope). Hence, in the case being considered, the energy equation coincides with that of an adiabat. Having the energy equation in this

form, we shall write all the equations of the system:

$$\left.\begin{aligned} &\frac{dV_x}{dt} = -\frac{1}{\rho}\cdot\frac{\partial p}{\partial x}, \quad \frac{dV_y}{dt} = -\frac{1}{\rho}\cdot\frac{\partial y}{\partial y} \\ &\frac{dV_z}{dt} = -\frac{1}{\rho}\cdot\frac{\partial p}{\partial z}, \quad \frac{d\rho}{dt} + \rho \operatorname{div} \mathbf{V} = 0 \\ &p = R\rho T, \quad A\rho^{k-1} = RT \end{aligned}\right\} \qquad (3.3.3)$$

Let us consider the system of equations for the more general case of the motion of an inviscid gas at high speeds when the specific heats change with the temperature, and dissociation and ionization may occur in the gas. For generality, we shall retain the possibility of the heated gas radiating energy. Now the thermodynamic process in the gas flow will not be adiabatic. Accordingly, the quantity ε determining the radiation heat flux remains on the right-hand side of energy equation (3.2.14). We shall note that the equation of state must be adopted in the form of (1.5.8) taking into account the change in the mean molar mass μ_m with the temperature and pressure. In accordance with the above, and also taking into account that the equations of motion and continuity do not change in form, we shall give the fundamental equations of the system:

$$\left.\begin{aligned} &\frac{dV_x}{dt} = -\frac{1}{\rho}\cdot\frac{\partial p}{\partial x}, \quad \frac{\partial V_y}{dt} = -\frac{1}{\rho}\cdot\frac{\partial p}{\partial y} \\ &\frac{dV_z}{dt} = -\frac{1}{\rho}\cdot\frac{\partial p}{\partial z}, \quad \frac{d\rho}{dt} + \rho \operatorname{div} \mathbf{V} = 0 \\ &p = \frac{R_0}{\mu_m}\rho T, \quad \rho\frac{di}{dt} = \frac{dp}{dt} + \varepsilon \end{aligned}\right\} \qquad (3.3.4)$$

We can see that in the given system in addition to the six unknown quantities indicated above (V_x, V_y, V_z, p, ρ, and T) three more have appeared: the enthalpy i, mean molar mass of the gas μ_m, and the heat flux ε produced by radiation. Besides these quantities, when studying the flow of a gas, we must also determine the entropy S and the speed of sound a. Hence, the total number of unknown parameters characterizing a gas flow and being additionally sought is five. Therefore, we must add this number of independent relations for the additional unknowns to the system of fundamental equations. These expressions can be written in the form of general relations determining the unknown quantities as functions of the pressure and temperature:

$$i = f_1(p, T) \qquad (3.3.5)$$

$$S = f_2(p, T) \qquad (3.3.6)$$

$$\mu_m = f_3(p, T) \qquad (3.3.7)$$

$$a = f_4(p, T) \qquad (3.3.8)$$

$$\varepsilon = f_5(p, T) \qquad (3.3.9)$$

The finding of these functions is the subject of special branches of physics and thermodynamics.

The solution of Eqs. (3.3.4)-(3.3.9) determines the parameters of flow of an inviscid dissociating and ionizing gas with account taken of the radiation effect. Such flow is studied by the aerodynamics of a radiating gas.

Let us consider a more general case of flow characterized by the action of friction forces and heat transfer. We shall assume that chemical reactions occur in the gas. Therefore, the fundamental equations of the system (for simplification we shall consider two-dimensional plane flow) will include two differential equations (3.1.20) of motion of a viscous compressible fluid with a varying dynamic viscosity ($\mu \neq \text{const}$), and also continuity equation (2.4.1). These equations must be supplemented with equation of state (1.5.8) relating to the general case of a dissociated and ionized gas, and with expression (3.2.14) that is the energy equation for a two-dimensional compressible gas flow in which heat transfer by diffusion and radiation occur. These equations describe the general case of unsteady motion and characterize the unsteady thermal processes occurring in a gas flow. Hence, we have

$$\left.\begin{aligned}
\frac{dV_x}{dt} &= -\frac{1}{\rho}\cdot\frac{\partial p}{\partial x}+\frac{1}{\rho}\cdot\frac{\partial}{\partial x}\left[\mu\left(2\frac{\partial V_x}{\partial x}-\frac{2}{3}\operatorname{div}\mathbf{V}\right)\right] \\
&\quad +\frac{2}{\rho}\frac{\partial}{\partial y}(\mu\varepsilon_z) \\
\frac{dV_y}{dt} &= -\frac{1}{\rho}\cdot\frac{\partial p}{\partial y}+\frac{1}{\rho}\cdot\frac{\partial}{\partial y}\left[\mu\left(2\frac{\partial V_y}{\partial y}-\frac{2}{3}\operatorname{div}\mathbf{V}\right)\right] \\
&\quad +\frac{2}{\rho}\cdot\frac{\partial}{\partial x}(\mu\varepsilon_z) \\
\frac{d\rho}{dt}&+\rho\operatorname{div}\mathbf{V}=0; \qquad p=\frac{R_0}{\mu_m}\rho T \\
\rho\frac{di}{dt}&=\frac{dp}{dt}+2\mu\left\{\left[\left(\frac{\partial V_x}{\partial x}\right)^2+\left(\frac{\partial V_y}{\partial y}\right)^2\right]-\frac{2}{3}(\operatorname{div}\mathbf{V})^2+4\varepsilon_z^2\right\} \\
&\quad +\operatorname{div}(\lambda\operatorname{grad}T)+\sum_i i_i\operatorname{div}(\rho\overline{D}\operatorname{grad}c_i)+\varepsilon
\end{aligned}\right\} \quad (3.3.10)$$

This system must be supplemented with relations (3.3.5)-(3.3.9), and also with the general relations for the thermal conductivity

$$\lambda = f_6(p, T) \qquad (3.3.11)$$

the dynamic viscosity

$$\mu = f_7(p, T) \qquad (3.3.12)$$

and the specific heats

$$c_p = f_8(p, T),\ c_v = f_9(p, T) \qquad (3.3.13)$$

The last two quantities are not contained explicitly in Eqs. (3.3.10), but they are nevertheless used in solving them because when studying the flow of a gas its thermodynamic characteristics are determined. Since the energy equation also takes into account heat transfer by diffusion, equation (3.2.5) has to be included additionally. It must be taken into account simultaneously that the concentration c_i in the energy and diffusion equations is a function of the pressure and temperature, and it can be written in the form of the general relation

$$c_i = f_{10}(p, T) \tag{3.3.14}$$

The above system of equations including the fundamental equations of gas dynamics and the corresponding number (according to the number of unknowns being sought) of additional relations is considered in the aerodynamics of a viscous gas and allows one to find the distribution of the normal and shear stresses, and also the aerodynamic heat fluxes from the heated gas to the wall over which it flows. In specific cases, for which a definite schematization of the flow process is possible, the above system is simplified, and this facilitates the solution of the differential equations.

When solving the equations, it becomes necessary to involve additional relations used for determining the characteristic parameters of motion. Among them are, for example, relations for determining the specific heats and the degree of dissociation depending on the pressure and temperature, and formulas for calculating the shear stress depending on the velocity.

The solution of a system of gas-dynamic equations describing the flow over a given surface must satisfy definite initial and boundary conditions of this flow.

The initial conditions are determined by the values of the gas parameters *for a certain instant* and have sense, evidently, for unsteady motion.

The **boundary conditions** are superposed on the solution of the problem both for steady and for unsteady motion and must be observed *at every instant* of this motion. According to one of them, the solution must be such that the parameters determined by it equal the values of the parameters for the undisturbed flow at the boundary separating the disturbed and undisturbed flow regions.

The second boundary condition is determined by the nature of gas flow over the relevant surface. If the gas is inviscid and does not penetrate through such a surface, the flow is said to be **without separation** (a **free streamline flow**). In accordance with this condition, the normal velocity component at each point of the surface is zero, while the vector of the total velocity coincides with the direction of a tangent to the surface.

It is general knowledge that the vector grad F [here $F(q_1, q_2, q_3) = 0$ is the equation of the surface in the flow, and q_1, q_2, q_3 are the generalized curvilinear coordinates] coincides in direction with a normal to the surface. Hence, for conditions of flow without separation, the dot product of this vector and the velocity vector **V** is zero.

Consequently, the condition of flow without separation can be written in a mathematical form as follows:

$$\mathbf{V}\ \mathrm{grad}\ F = 0$$

Taking into account that

$$\mathrm{grad}\ F = \frac{1}{h_1}\cdot\frac{\partial F}{\partial q_1}\mathbf{i}_1 + \frac{1}{h_2}\cdot\frac{\partial F}{\partial q_2}\mathbf{i}_2 + \frac{1}{h_3}\cdot\frac{\partial F}{\partial q_2}\mathbf{i}_3 \qquad (3.3.15)$$

the condition of flow without separation can be written as

$$\frac{1}{h_1}\cdot\frac{\partial F}{\partial q_1}V_1 + \frac{1}{h_2}\cdot\frac{\partial F}{\partial q_2}V_2 + \frac{1}{h_3}\cdot\frac{\partial F}{\partial q_3}V_3 = 0 \qquad (3.3.16)$$

For Cartesian coordinates, we have

$$\mathrm{grad}\ F = (\partial F/\partial x)\,\mathbf{i}_1 + (\partial F/\partial y)\,\mathbf{i}_2 + (\partial F/\partial z)\,\mathbf{i}_3$$

Consequently, for (3.3.16)

$$V_x\,\partial F/\partial x + V_y\,\partial F/\partial y + V_z\,\partial F/\partial z = 0 \qquad (3.3.17)$$

For two-dimensional plane flow

$$\frac{V_y}{V_x} = -\frac{\partial F/\partial x}{\partial F/\partial y} \qquad (3.3.17')$$

If the equation of the surface is given in cylindrical coordinates, we have

$$\mathrm{grad}\ F = \frac{\partial F}{\partial x}\mathbf{i}_1 + \frac{\partial F}{\partial r}\mathbf{i}_2 + \frac{1}{r}\cdot\frac{\partial F}{\partial \gamma}\mathbf{i}_3$$

therefore, the condition of flow without separation has the form

$$\frac{\partial F}{\partial x}V_x + \frac{\partial F}{\partial r}V_r + \frac{1}{r}\cdot\frac{\partial F}{\partial \gamma}V_\gamma = 0 \qquad (3.3.18)$$

In a particular case, when a surface of revolution is in the flow, we obtain the equation

$$V_x\,\partial F/\partial x + V_r\,\partial F/\partial r = 0 \qquad (3.3.18')$$

from which we find the condition for the velocity ratio:

$$\frac{V_r}{V_x} = -\frac{\partial F/\partial x}{\partial F/\partial r} \qquad (3.3.19)$$

Other boundary conditions can also be formulated. They are determined for each specific problem, the boundary conditions for

a viscous gas differing from the conditions for an ideal fluid. Particularly, when studying the flow of a viscous gas in a boundary layer, the solutions of the pertinent equations must satisfy the conditions on the surface of the body and at the edge of the boundary layer. According to experimental data, the gas particles adhere, as it were, to the surface, and therefore the velocity on it is zero. At the boundary layer edge, the velocity becomes the same as in free (inviscid) flow, and the shear stress equals zero.

3.4. Integrals of Motion for an Ideal Fluid

The differential equations derived for the general case of motion of a gas are non-integrable in the finite form. Integrals of these equations can be obtained only for the particular case of an ideal (inviscid) gas flow.

The equation of motion of an ideal gas in the vector form is

$$\partial \mathbf{V}/\partial t + \text{grad}\,(V^2/2) + \text{curl}\,\mathbf{V} \times \mathbf{V} = -(1/\rho)\,\text{grad}\,p \qquad (3.4.1)$$

This equation can be obtained from vector relation (3.1.22′) in which the terms on the right-hand side taking into account the influence of the viscosity should be taken equal to zero.

In its form (3.4.1), the equation of motion was first obtained by the Russian scientist prof. I. Gromeka. With a view to the mass forces, Gromeka's equation becomes

$$\partial \mathbf{V}/\partial t + \text{grad}\,(V^2/2) + \text{curl}\,\mathbf{V} \times \mathbf{V} = \mathbf{G} - (1/\rho)\,\text{grad}\,p \qquad (3.4.2)$$

Let us assume that the unsteady flow will be potential, hence curl $\mathbf{V} = 0$ and $\mathbf{V} = \text{grad}\,\varphi$. In addition, let us assume that the mass forces have the potential U, therefore the vector

$$\mathbf{G} = -\text{grad}\,U$$

where $\text{grad}\,U = (\partial U/\partial x)\mathbf{i} + (\partial U/\partial y)\mathbf{j} + (\partial U/\partial z)\mathbf{k}$.

If a fluid has the property of barotropy characterized by an unambiguous relation between the pressure and density (this occurs, for example, in an adiabatic flow, for which $p = A\rho^k$), then the ratio dp/ρ equals the differential of a certain function P and, therefore,

$$(1/\rho)\,\text{grad}\,p = \text{grad}\,P$$

With a view to this equation, expression (3.4.2) becomes

$$\partial\,(\text{grad}\,\varphi)/\partial t + \text{grad}\,(V^2/2) = -\text{grad}\,U - \text{grad}\,P$$

Substituting the quantity $\text{grad}\,(\partial\varphi/\partial t)$ for the derivative $\partial\,(\text{grad}\,\varphi)/\partial t$, we obtain

$$\text{grad}\,(\partial\varphi/\partial t) + \text{grad}\,(V^2/2) = -\text{grad}\,U - \text{grad}\,P \qquad (3.4.3)$$

Going over from the relation for the gradients to one between the corresponding scalar functions, we find

$$\partial\varphi/\partial t + V^2/2 + P + U = C(t) \qquad (3.4.4)$$

where

$$P = \int dp/\rho \qquad (3.4.5)$$

Expression (3.4.4) is known as the **Lagrange equation** or **integral.** The right-hand side of (3.4.4) is a function that *depends on the time*, but does not depend on the coordinates, i.e. *is identical for any point of a potential flow.* The terms on the left-hand side of (3.4.4) have a simple physical meaning: $V^2/2$ is the kinetic energy, $P = \int dp/\rho$ is the potential energy due to the pressure for a unit mass, and U is the potential energy due to the position of the fluid particles and related to their mass.

To reveal the physical meaning of the first term, let us use the expression for the potential function $\partial\varphi/\partial s = V_s$, where V_s is the projection of the velocity vector onto a certain direction s. We can determine the function φ from the condition $\varphi = \int_{s_0}^{s} V_s\, ds$ (where s_0 and s are the coordinates of a fixed and an arbitrary point, respectively). The derivative $\partial\varphi/\partial t = \int_{s_0}^{s} (\partial V_s/\partial t)\, ds$.

The local acceleration $\partial V_s/\partial t$ can be considered as the projection of the inertia force due to the presence of local acceleration and related to unit mass, and the product $(\partial V_s/\partial t)\, ds$ as the work done by this force on the section ds. Accordingly, the derivative $\partial\varphi/\partial t$ equals the work done by the inertia force on the section between points s_0 and s and can be considered as the energy of unit mass due to the change in time of the velocity and the pressure associated with it at the given point.

With a view to the above, the expression on the left-hand side of (3.4.4) is the total energy of a unit mass of the gas. Hence, the Lagrange equation establishes the fact that the total energy of unit mass at a given instant is a quantity identical for all points of the potential flow.

For an incompressible fluid whose motion occurs under the action of mass and pressure forces, integral (3.4.4) has the form

$$\partial\varphi/\partial t + V^2/2 + p/\rho + U = C(t) \qquad (3.4.6)$$

If, particularly, the y-axis is directed vertically upward, then $U = gy$, and

$$\partial\varphi/\partial t + V^2/2 + p/\rho + gy = C(t) \qquad (3.4.6')$$

Of major practical significance is the particular case of a steady potential flow for which $\partial\varphi/\partial t = 0$ and the function $C(t) = \text{const}$, i.e. is independent of the time. In this case, Eq. (3.4.4) is reduced to the form

$$V^2/2 + \int dp/\rho + U = \text{const} \qquad (3.4.7)$$

This partial form of the Lagrange equation is called the **Euler equation.** It expresses the law according to which *the total energy of a unit mass is a constant quantity for all points of the steady potential flow.* Hence, the constant in the Euler equation is the same not only for the entire region of a flow, but also, unlike the function $C(t)$ of the Lagrange integral, *is independent of the time.*

The Euler equation for an incompressible fluid ($\rho = \text{const}$) has the same form as (3.4.7), the only difference being that instead of $\int dp/\rho$ it includes the ratio p/ρ.

Let us consider the more general case of a non-potential steady flow of a gas. The equation of this motion has the form

$$\text{grad}\,(V^2/2) + \text{curl}\,\mathbf{V} \times \mathbf{V} = -\text{grad}\,P - \text{grad}\,U \qquad (3.4.8)$$

or

$$\text{grad}\,(V^2/2 + \int dp/\rho + U) = -\text{curl}\,\mathbf{V} \times \mathbf{V} \qquad (3.4.8')$$

The right-hand side of (3.4.8′) equals zero if the vectors curl **V** and **V** are parallel, i.e. provided that a vortex line and streamline coincide. In this case, we have

$$V^2/2 + \int dp/\rho + U = C_1 \qquad (3.4.9)$$

This equation was first obtained by I. Gromeka. The constant C_1 *is the same for the entire region where the condition of the coincidence of the vortex lines and streamlines is observed.* Such regions, to study which the Gromeka equation is used, appear, for example, in a flow past a finite-span wing. This flow is characterized by the formation of vortices virtually coinciding in direction near the wing with the streamlines. A flow does not always contain such regions, however. A flow is customarily characterized by the presence of vortex lines and streamlines *not coinciding* with one another. The family of vortex lines is given by Eq. (2.6.1), and that of the streamlines (pathlines), by Eq. (2.1.6). The flow being considered is described by Eq. (3.4.8′).

Let us take the vector of the arc in the form $d\mathbf{s} = dx\mathbf{i} + dy\mathbf{j} + dz\mathbf{k}$ belonging to a streamline or vortex line, and determine the dot product

$$d\mathbf{s} \cdot \text{grad}\,(V^2/2 + \int dp/\rho + U) = -d\mathbf{s} \cdot (\text{curl}\,\mathbf{V} \times \mathbf{V})$$

The left-hand side in this equation is the total differential of the trinomial in parentheses, consequently,

$$d\,(V^2/2 + \int dp/\rho + U) = -d\mathbf{s}\cdot(\text{curl } \mathbf{V} \times \mathbf{V}) \qquad (3.4.10)$$

The product curl $\mathbf{V} \times \mathbf{V}$ is a vector perpendicular to the vectors curl $\mathbf{V}$ and $\mathbf{V}$. The dot product of this vector and the vector $d\mathbf{s}$ is zero in two cases: *when the vector* $d\mathbf{s}$ *coincides with the direction of a streamline* (*pathline*) or *when this vector coincides with the direction of a vortex*. In these two cases, the following solution of the equation of motion is valid:

$$V^2/2 + \int dp/\rho + U = C_2 \qquad (3.4.11)$$

where the value of the constant C_2 depends on what pathline or vortex line is being considered.

Relation (3.4.11) is known as the **Bernoulli equation.** It is obvious that for various vortex lines passing through points on a given streamline, the constant is the same as for the streamline. In exactly the same way, the constants are identical for a family of streamlines (pathlines) and the vortex through whose points a streamline passes.

One must clearly understand the distinction between the Gromeka and Bernoulli equations considered above. They are both derived for a vortex (non-potential) flow, however the first of them reflects the fact that the total energy of a unit mass of the gas is constant *in the entire region* where the vortex lines and streamlines coincide, while the second equation establishes the law according to which this energy is constant along a given *streamline* or *vortex line*. Accordingly, in the Gromeka equation, the constant is the same for the entire flow region being considered, whereas in the Bernoulli equation it relates to a given streamline or vortex line. Naturally, in the general case, the two constants C_1 and C_2 are not the same. From the above, there also follows a distinction, on the one hand, between these equations, and, on the other, between the Lagrange and Euler equations relating to an *unsteady* and *steady vortex-free* (*potential*) *flow*, respectively, and also between each of the considered equations.

When studying the flow of a fluid, investigators give the greatest favour to the Bernoulli equation related to the conditions on the streamlines (pathlines). It is known that the constant C_2 in this equation (3.4.11) is determined for every streamline being considered. If, however, a steady flow is also vortex-free (potential), the Bernoulli equation coincides with the Euler equation, and, therefore, the constant is identical for all the streamlines, i.e. for the entire flow region.

Let us consider some specific forms of the Bernoulli equation. For an incompressible fluid and provided that the function $U = gy$,

we shall write this equation in the form

$$V^2/2 + p/\rho + yg = C_2 \qquad (3.4.12)$$

When studying the motion of a gas, we may disregard the influence of the mass forces. Consequently, we must assume that $U = 0$ in Eq. (3.4.11) and the other integrals. Particularly, instead of (3.4.12), we have

$$V^2/2 + p/\rho = C_2 \qquad (3.4.13)$$

Let us consider the motion of an ideal compressible gas. In such a gas, heat transfer processes due to viscosity (heat conduction, diffusion) are absent. Assuming also that the gas does not radiate energy, we shall consider its adiabatic (isentropic) motion. Examination of energy equation (3.2.14) reveals that Eq. (3.3.1) holds for such an inviscid gas in the absence of radiation ($\varepsilon = 0$). Consequently, the Bernoulli integral is

$$V^2/2 + i = C \qquad (3.4.14)$$

In this form, the Bernoulli integral is an energy equation for an isentropic flow. According to this equation, the sum of the kinetic energy and enthalpy of a gas particle is constant. Assuming that $i = c_p T = c_p p/(\rho R)$, $c_p - c_v = R$, and $k = c_p/c_v$, we find

$$i = [k/(k-1)]\, p/\rho \qquad (3.4.15)$$

Consequently,

$$V^2/2 + [k/(k-1)]\, p/\rho = C \qquad (3.4.16)$$

or

$$V^2/2 + kRT/(k-1) = C \qquad (3.4.16')$$

The Bernoulli equation for an ideal compressible gas is the theoretical foundation for investigating the laws of isentropic flows of a gas.

3.5. Aerodynamic Similarity

Concept of Similarity

The aerodynamic characteristics of craft or their individual elements can be determined both theoretically and experimentally. The theoretical approaches are based on the use of a system of equations of gas dynamics that is solved as applied to a body in a flow, the body having a given configuration and arbitrary absolute dimensions.

When running experiments intended for obtaining aerodynamic parameters that can be used directly for further ballistic calculations or for verifying the results of theoretical investigations, it is not always possible to use a full-scale body because of its large size, and a smaller-size model of the body has to be used. In this con-

nection, the question appears on the possibility of transferring the experimental results obtained to full-scale bodies. The answer to this question is given by the **dimensional analysis and similarity method.** The latter establishes the conditions that must be observed in scale-model experiments and indicates characteristic and convenient parameters determining the basic effects and flow conditions.

Let us assume that measurements in a wind tunnel yielded a drag force which in accordance with (1.3.5) is $X_{\text{mod}} = c_{x,\text{mod}} q_{\text{mod}} S_{\text{mod}}$. Now let us see when we can use the result obtained to determine the drag force of a full-scale body in accordance with the formula $X_{\text{fs}} = c_{x,\text{fs}} q_{\text{fs}} S_{\text{fs}}$ in which the drag coefficient $c_{x,\text{fs}}$ for this body is an unknown quantity, while the velocity head q_{fs} and the reference or characteristic area S_{fs} are given. From the two formulas for X_{fs} and X_{mod}, we obtain

$$X_{\text{fs}} = X_{\text{mod}} (c_{x,\text{fs}}/c_{x,\text{mod}}) (q_{\text{fs}} S_{\text{fs}}/q_{\text{mod}} S_{\text{mod}}) \qquad (3.5.1)$$

A glance at this expression reveals that the experimental value X_{mod} can be used to evaluate the full-scale force X_{fs} only upon the equality of the aerodynamic coefficients $c_{x,\text{mod}}$ and $c_{x,\text{fs}}$ because the quantities $q_{\text{mod}} S_{\text{mod}}$ and $q_{\text{fs}} S_{\text{fs}}$ are determined unambiguously by the given values of the velocity heads and the reference areas.

Here both flows—the model and full-scale ones—have the property of **dynamic similarity.** It consists in this case in that the preset force characteristic of one flow (the drag X_{mod}) is used to find the characteristic of the other flow (the force X_{fs}) by simple conversion, similar to the transition from one system of units of measurement to another.

The requirements whose satisfaction in the given case ensures the equality $c_{x,\text{mod}} = c_{x,\text{fs}}$, and in the general case of other dimensionless aerodynamic coefficients too, are established in the dimensional analysis and similarity method proceeding either from the physical nature of the phenomenon being studied or from the corresponding differential equations of aerodynamics.

Considering the expression for the aerodynamic coefficient

$$c_{x_a} = \int_{(S)} [\bar{p} \cos (\widehat{nx_a}) + c_{f,x} \cos (\widehat{tx_a})] \frac{dS}{S_r} \qquad (3.5.2)$$

obtained from (1.3.2), we can see that this coefficient depends on dimensionless geometric parameters, and also on dimensionless quantities such as the pressure coefficient and local friction factor. Hence it follows that the aerodynamic coefficients for a full-scale object and an experimental one with different absolute dimensions remain constant if these bodies are geometrically similar and an identical distribution of the coefficients $\bar{p}$ and $c_{f,x}$ over their surface is ensured.

If we consider a steady uniform flow over a body in the absence of heat transfer, the coefficients $\bar{p}$ and $c_{f,x}$ with a given configuration

of the body in the flow and known values of the angle of attack and the sideslip angle, as well as of the rudder and elevator angles, will be functions of the free stream velocity V_∞, the pressure p_∞, the density ρ_∞, the dynamic viscosity μ_∞, the specific heats $c_{p\infty}$ and $c_{v\infty}$ of the gas, as well as of a certain characteristic (reference) linear dimension of the body L. Consequently, the drag coefficient will also depend on these parameters, and we can compile a functional relation for it in the form $c_x = f(V_\infty, p_\infty, \rho_\infty, \mu_\infty, c_{p\infty}, c_{v\infty}, L)$. Since this coefficient is a dimensionless quantity, it must also be a function of dimensionless parameters. From the general considerations of the dimensional method, it follows that the seven different arguments of the function c_x can be reduced to three. The latter are dimensionless combinations compiled from V_∞, p_∞, ρ_∞, μ_∞, $c_{p\infty}$, $c_{v\infty}$, and L because there are four independent units of measurement, namely, mass, length, time, and temperature. These dimensionless combinations have the following form: $V_\infty/\sqrt{k_\infty p_\infty/\rho_\infty} = V_\infty/a_\infty = M_\infty$—the Mach number for an undisturbed flow; $V_\infty \rho_\infty L/\mu_\infty = Re_\infty$—the Reynolds number based on the parameters of an undisturbed flow and the characteristic linear dimension L; $c_{p\infty}/c_{v\infty} = k_\infty$—the adiabatic exponent.

In the expression for M_∞, it is assumed that $\sqrt{k_\infty p_\infty/\rho_\infty} = a_\infty$ is the speed of sound in the undisturbed flow. Indeed, in accordance with the general expression for the speed of sound $a^2 = dp/d\rho$, and also with a view to the adiabatic nature of propagation of sonic disturbances in a gas, according to which $p = A\rho^k$, we have $a^2 = d(A\rho^k)/d\rho = kp/\rho$. Accordingly, the square of the speed of sound in an undisturbed flow is $a_\infty^2 = k_\infty p_\infty/\rho_\infty$. Hence, the ratio $V_\infty/\sqrt{k_\infty p_\infty/\rho_\infty} = V_\infty/a_\infty$. All other dimensionless combinations except for M_∞, Re_∞, and k_∞ formed from the seven parameters indicated above or in general from any quantities that can be determined by them are functions of the combinations M_∞, Re_∞, and k_∞. Consequently, the drag coefficient is

$$c_x = f(M_\infty, Re_\infty, k_\infty) \qquad (3.5.3)$$

Similar expressions can be obtained for the other aerodynamic coefficients. It follows from these expressions that when the numbers M_∞, Re_∞ and the parameter k_∞ for a model and a full-scale flows are equal, the aerodynamic coefficients for geometrically similar bodies are the same. Hence, an important conclusion can be made in the dimensional analysis and similarity method in accordance with which the necessary and sufficient condition for aerodynamic similarity is the constancy of the numerical values of the dimensionless combinations forming what is called a base, i.e. a system of dimensionless quantities determining all the other parameters of a flow. These dimensionless combinations are called **similarity criteria.**

The similarity criteria given above have a definite physical meaning. In accordance with the expression $a^2 = dp/d\rho$, the speed of sound can be considered as a criterion depending on the property of compressibility, i.e. on the ability of a gas to change its density with a change in the pressure. Consequently, the Mach number is the similarity criterion that is used to characterize the *influence of compressibility on the flow of a gas.* The Reynolds number is a parameter used to appraise the *influence of viscosity on a gas in motion,* while the parameter $k_\infty = c_{p\infty}/c_{v\infty}$ determines the features of a flow due to the *thermodynamic properties of a gas.*

Similarity Criteria Taking Account of the Viscosity and Heat Conduction

In the more general conditions of flow characterized by the influence of a number of other physical and thermodynamic parameters on the aerodynamic properties of craft, the dynamic similarity criteria are more complicated and diverse. To establish these criteria, we can use a different approach of the dimensional analysis and similarity method based on the use of the equation of motion of a viscous heat-conducting gas.

Let us write these equations in the dimensionless form, i.e. in a form such that the parameters (velocity, pressure, temperature, etc.) in the equations are related to reference parameters. The latter are constants for a given flow and determine its scale. We shall take as references the parameters of the free stream: its velocity V_∞, pressure p_∞, density ρ_∞, temperature T_∞. dynamic viscosity μ_∞ (or, respectively, the kinematic viscosity ν_∞), and so on. It must be remembered that of the three parameters p_∞, ρ_∞, and T_∞, two may be set arbitrarily, while the third one is determined from the first two with the aid of an equation of state. The quantity t_∞ is the reference time characterizing unsteady flow conditions, while a characteristic linear dimension L (for example, the length of the body in the flow) is the reference length. The acceleration of free fall g can be chosen as the reference acceleration of the mass forces. The dimensionless variables for the length and time have the form

$$\bar{x} = x/L,\ \bar{y} = y/L,\ \bar{z} = z/L,\ \bar{t} = t/t_\infty \tag{3.5.4}$$

while those for the velocity, pressure, density, viscosity, and mass forces have the following form:

$$\left.\begin{aligned} &\bar{V}_x = V_x/V_\infty,\quad \bar{V}_y = V_y/V_\infty,\quad \bar{V}_z = V_z/V_\infty,\quad \bar{p} = p/p_\infty,\\ &\qquad\qquad \bar{\rho} = \rho/\rho_\infty\\ &\bar{\mu} = \mu/\mu_\infty,\quad \bar{\nu} = \nu/\nu_\infty,\quad \bar{X} = X/g,\quad \bar{Y} = Y/g,\quad \bar{Z} = Z/g \end{aligned}\right\} \tag{3.5.5}$$

Let us introduce dimensionless variables into the equation of motion (3.1.17) and the continuity equation (2.4.2). We shall use only the first equation of system (3.1.17) for transformation because the other two equations are compiled in a similar way. Let us write the indicated equations using dimensionless variables:

$$\frac{V_\infty}{t_\infty}\cdot\frac{\partial \bar{V}_x}{\partial \bar{t}}+\frac{V_\infty^2}{L}\left(\bar{V}_x\frac{\partial \bar{V}_x}{\partial \bar{x}}+\bar{V}_y\frac{\partial \bar{V}_x}{\partial \bar{y}}+\bar{V}_z\frac{\partial \bar{V}_x}{\partial \bar{z}}\right)=g\bar{X}$$

$$-\frac{p_\infty}{\rho_\infty L}\cdot\frac{1}{\bar{\rho}}\cdot\frac{\partial \bar{p}}{\partial \bar{x}}+\frac{\nu_\infty V_\infty}{L^2}\left\{\bar{\nu}\Delta\bar{V}_x+\frac{\bar{\nu}}{3}\cdot\frac{\partial}{\partial \bar{x}}\operatorname{div}\mathbf{V}\right.$$

$$+\frac{1}{\rho}\left[\frac{\partial \bar{\mu}}{\partial \bar{x}}\left(2\frac{\partial \bar{V}_x}{\partial \bar{x}}-\frac{2}{3}\operatorname{div}\mathbf{V}\right)+\frac{\partial \bar{\mu}}{\partial \bar{y}}\left(\frac{\partial \bar{V}_x}{\partial \bar{y}}+\frac{\partial \bar{V}_y}{\partial \bar{x}}\right)\right.$$

$$\left.\left.+\frac{\partial \bar{\mu}}{\partial \bar{z}}\left(\frac{\partial \bar{V}_x}{\partial \bar{z}}+\frac{\partial \bar{V}_z}{\partial \bar{x}}\right)\right]\right\}$$

$$\frac{\rho_\infty}{t_\infty}\cdot\frac{\partial \bar{\rho}}{\partial \bar{t}}+\frac{\rho_\infty V_\infty}{L}\left[\frac{\partial(\bar{\rho}\bar{V}_x)}{\partial \bar{x}}+\frac{\partial(\bar{\rho}\bar{V}_y)}{\partial \bar{y}}+\frac{\partial(\bar{\rho}\bar{V}_z)}{\partial \bar{z}}\right]=0$$

where $\operatorname{div}\mathbf{V}=\partial\bar{V}_x/\partial\bar{x}+\partial V_y/\partial\bar{y}+\partial V_z/\partial\bar{z}$.

From the reference quantities in these equations, we can form dimensionless numbers characterizing the similarity of gas flows. These numbers, named after the scientists who were the first to obtain them, are given in the following form:

$$\left.\begin{array}{l}\boldsymbol{Sh}=V_\infty t_\infty/L\text{ — the Strouhal number;}\\ \boldsymbol{Fr}=V_\infty^2/(gL)\text{ — the Froude number;}\\ \boldsymbol{M}=V_\infty/a_\infty\text{ — the Mach number;}\\ \boldsymbol{Re}=V_\infty\rho_\infty L/\mu_\infty=V_\infty L/\nu_\infty\text{ — the Reynolds number}\\ \text{(the subscript "}\infty\text{" on }\boldsymbol{M}\text{ and }\boldsymbol{Re}\text{ has been omitted).}\end{array}\right\}\quad(3.5.6)$$

Here $a_\infty=\sqrt{k_\infty RT_\infty}$ is the speed of sound in an undisturbed flow (k_∞ and T_∞ are the adiabatic exponent and the temperature of a gas in the undisturbed flow, respectively). Introducing these numbers into the equation of motion and the continuity equation, we obtain:

$$\boldsymbol{Sh}^{-1}\frac{\partial \bar{V}_x}{\partial \bar{t}}+\bar{V}_x\frac{\partial \bar{V}_x}{\partial \bar{x}}+\bar{V}_y\frac{\partial \bar{V}_x}{\partial \bar{y}}+\bar{V}_z\frac{\partial \bar{V}_x}{\partial \bar{z}}=\frac{1}{\boldsymbol{Fr}}\bar{X}$$

$$-\frac{1}{k_\infty \boldsymbol{M}}\cdot\frac{1}{\bar{\rho}}\cdot\frac{\partial \bar{p}}{\partial \bar{x}}+\frac{1}{\boldsymbol{Re}}\left\{\bar{\nu}\Delta\bar{V}_x+\frac{\bar{\nu}}{3}\cdot\frac{\partial}{\partial \bar{x}}\operatorname{div}\mathbf{V}\right.$$

$$+\frac{1}{\rho}\left[\frac{\partial\bar{\mu}}{\partial\bar{x}}\left(2\frac{\partial\bar{V}_x}{\partial\bar{x}}-\frac{2}{3}\operatorname{div}\mathbf{V}\right)+\frac{\partial\bar{\mu}}{\partial\bar{y}}\left(\frac{\partial\bar{V}_x}{\partial\bar{y}}+\frac{\partial\bar{V}_y}{\partial\bar{x}}\right)\right.$$
$$\left.+\frac{\partial\bar{\mu}}{\partial\bar{z}}\left(\frac{\partial\bar{V}_x}{\partial\bar{z}}+\frac{\partial\bar{V}_z}{\partial\bar{x}}\right)\right]\Bigg\} \qquad (3.5.7)$$

$$Sh\frac{\partial\bar{\rho}}{\partial\bar{t}}+\frac{\partial(\bar{\rho}\bar{V}_x)}{\partial\bar{x}}+\frac{\partial(\bar{\rho}\bar{V}_y)}{\partial\bar{y}}+\frac{\partial(\bar{\rho}\bar{V}_z)}{\partial\bar{z}}=0 \qquad (3.5.8)$$

Let us transform the energy equation (3.2.14) in which we shall exclude terms taking into account radiation and diffusion. We introduce the dimensionless variables

$$\bar{T}=T/T_\infty,\ \bar{c}_p/=c_p/c_{p\infty},\ \bar{\lambda}=\lambda/\lambda_\infty \qquad (3.5.9)$$

where $c_{p\infty}$ and λ_∞ are the specific heat and the heat conductivity of a gas in the undisturbed flow, respectively.

Having in view that $di=c_p\,dT$ and expanding the total derivative dT/dt, we obtain after the corresponding substitutions:

$$\frac{\rho_\infty c_{p\infty}T_\infty}{t_\infty}\bar{\rho}\bar{c}_p\frac{\partial\bar{T}}{\partial\bar{t}}+\frac{\rho_\infty c_{p\infty}V_\infty T_\infty}{L}\bar{\rho}\bar{c}_p\left(\bar{V}_x\frac{\partial\bar{T}}{\partial\bar{x}}\right.$$
$$\left.+\bar{V}_y\frac{\partial\bar{T}}{\partial\bar{y}}+\bar{V}_z\frac{\partial\bar{T}}{\partial\bar{z}}\right)=\frac{p_\infty}{t_\infty}\cdot\frac{d\bar{p}}{d\bar{t}}+\frac{\mu_\infty V_\infty^2}{L^2}\bar{\mu}$$
$$\times\left\{\left[\left(\frac{\partial\bar{V}_x}{\partial\bar{x}}\right)^2+\left(\frac{\partial\bar{V}_y}{\partial\bar{y}}\right)^2\right]-\frac{2}{3}\bar{\mu}(\operatorname{div}\mathbf{V})^2+4\bar{\mu}\bar{\varepsilon}_z^2\right\}$$
$$+\frac{\lambda_\infty T_\infty}{L^2}\operatorname{div}(\bar{\lambda}\operatorname{grad}\bar{T}) \qquad (3.5.10)$$

Let us introduce the dimensionless Prandtl number

$$Pr=\mu_\infty c_{p\infty}/\lambda_\infty \qquad (3.5.11)$$

by means of which *we shall compare the relative effect of the viscosity and heat conduction*, or, in other words, appraise the relation between the heat flux due to skin friction and the molecular transfer of heat. Hence, taking into account that $p_\infty/\rho_\infty=RT_\infty=c_{p\infty}(1-1/k_\infty)\times$ $\times T_\infty$, we have:

$$\bar{\rho}\bar{c}_p\left(Sh^{-1}\frac{\partial\bar{T}}{\partial\bar{t}}+\bar{V}_x\frac{\partial\bar{T}}{\partial\bar{x}}+\bar{V}_y\frac{\partial\bar{T}}{\partial\bar{y}}+\bar{V}_z\frac{\partial\bar{T}}{\partial\bar{z}}\right)$$
$$=Sh^{-1}\frac{k_\infty-1}{k_\infty}\cdot\frac{d\bar{p}}{d\bar{t}}+\frac{M^2(k_\infty-1)}{Re}\left\{\left[\left(\frac{\partial\bar{V}_x}{\partial\bar{x}}\right)^2+\left(\frac{\partial\bar{V}_y}{\partial\bar{y}}\right)^2\right]\right.$$
$$\left.-\frac{2}{3}\bar{\mu}(\operatorname{div}\mathbf{V})^2+4\bar{\mu}\bar{\varepsilon}_z^2\right\}+\frac{1}{RePr}\operatorname{div}(\bar{\lambda}\operatorname{grad}\bar{T}) \qquad (3.5.10')$$

Let us convert several additional relations of the system of equations of gas dynamics (see Sec. 3.3) to the dimensionless form:

$$\bar{p} = \bar{\rho}\bar{T} \tag{3.5.12}$$

$$\bar{\mu}_m = f_3(p_\infty \bar{p},\ T_\infty \bar{T})\ (1/\mu_{m\infty}) \tag{3.5.13}$$

$$\bar{\lambda} = f_6(p_\infty \bar{p},\ T_\infty \bar{T})\ (1/\lambda_\infty) \tag{3.5.14}$$

$$\bar{\mu} = f_7(p_\infty \bar{p},\ T_\infty \bar{T})\ (1/\mu_\infty) \tag{3.5.15}$$

$$\bar{c}_p = f_8(p_\infty \bar{p},\ T_\infty \bar{T})\ (1/c_{p\infty}) \tag{3.5.16}$$

Assume that we are investigating two flows over geometrically similar surfaces. For such surfaces, the dimensionless coordinates of analogous points are identical, which is a necessary condition for the aerodynamic similarity of flows. To observe the sufficient condition for such similarity, we must ensure equality of the dimensionless values of the gas-dynamic parameters (velocity, pressure, density, etc.) at analogous points. Since the dimensionless variables are simultaneously solutions of the system of equations (3.5.7), (3.5.8), (3.5.10′), and (3.5.12)-(3.5.16), the indicated equality is evidently observed provided that the systems of dimensionless equations, and also the dimensionless boundary and initial conditions for each flow are the same.

When considering systems of dimensionless equations for two flows, we see that both these systems are identical if:

(1) the similarity criteria are equal:

$$\boldsymbol{Fr}_1 = \boldsymbol{Fr}_2,\ \boldsymbol{Re}_1 = \boldsymbol{Re}_2,\ \boldsymbol{M}_1 = \boldsymbol{M}_2,\ \boldsymbol{Sh}_1 = \boldsymbol{Sh}_2 \tag{3.5.17}$$

(2) the equality of the Prandtl numbers $\boldsymbol{Pr}_1 = \boldsymbol{Pr}_2$ is observed, i.e.

$$(c_{p\infty}\mu_\infty/\lambda_\infty)_1 = (c_{p\infty}\mu_\infty/\lambda_\infty)_2 \tag{3.5.18}$$

and also the equality of the specific heat ratios for the two gas flows

$$k_{\infty 1} = k_{\infty 2} \tag{3.5.19}$$

(3) each of the equations (3.5.13)-(3.5.16) determines the dependences for the dimensionless variables $\bar{\mu}_m$, $\bar{\lambda}$, $\bar{\mu}$, or $\bar{c}_p$ on the relative quantities $\bar{p}$ and $\bar{T}$, and also on the variables (3.5.17)-(3.5.19). Such relations do not exist for a dissociated gas because similarity criteria of the form of (3.5.17)-(3.5.19) or of some other form cannot be found. This is why the corresponding dimensionless equations (3.5.13)-(3.5.16) are not the same for a full-scale and a model flows, and complete dynamic similarity cannot be ensured.

Two particular cases can be indicated when this similarity is ensured. The first is the flow of an undissociated gas for which the mean molar mass remains constant ($\mu_{m1} = \mu_{m2}$), while the specific

heats, heat conductivity, and viscosity vary depending on the temperature according to a power law of the kind $y = aT^x$. In this case, Eqs. (3.5.14)-(3.5.16) for the quantities $\bar{\lambda}$, $\bar{\mu}$, and $\bar{c}_p$ are replaced by the corresponding dependences only on the dimensionless temperature $\bar{T} = T/T_\infty$. The second case is the flow of a gas at low speeds when the parameters λ, μ, and c_p do not depend on the temperature. The corresponding values of these parameters are identical for the full-scale and model flows. For this case, the system of equations includes the dimensionless equations of Navier-Stokes, continuity, energy, and also an equation of state.

The boundary conditions imposed on the solutions of the dimensionless equations give rise to additional similarity criteria. This does not relate to the condition of flow without separation, which does not introduce new similarity criteria. Indeed, this condition in the dimensionless form is

$$\bar{V}_x \, \partial\bar{F}/\partial\bar{x} + \bar{V}_y \, \partial\bar{F}/\partial\bar{y} + \bar{V}_z \, \partial\bar{F}/\partial\bar{z} = 0$$

and is the same both for a full-scale and for a model flow because of the geometrical similarity of the surfaces. But the temperature boundary condition according to which the solution for the temperature must satisfy the equality $T = T_w$ (here T_w is the temperature of the wall) introduces an additional similarity criterion. In reality, it follows from the boundary conditions for a full-scale and model surfaces having the form $T_1 = (T_w)_1$ and $T_2 = (T_w)_2$, respectively, that the dimensionless temperatures are $\bar{T}_1 = (\bar{T}_w)_1$ and $\bar{T}_2 = (\bar{T}_w)_2$. From the condition of similarity, $\bar{T}_1 = \bar{T}_2$. therefore the equality $(\bar{T}_w)_1 = (\bar{T}_w)_2$ must be observed. Hence, the boundary condition for the wall temperature leads to an additional similarity criterion:

$$(T_w/T_\infty)_1 = (T_w/T_\infty)_2 \qquad (3.5.20)$$

The dimensionless gas-dynamic variables on the surface of a body in a flow, as can be seen from the system of dimensionless equations [provided that Eqs. (3.5.13)-(3.5.16) determine $\bar{\mu}_m$, $\bar{\lambda}$, $\bar{\mu}$, and $\bar{c}_p$ as a function of $\bar{T}$] depend on the dimensionless coordinates and the time, and also on the similarity criteria (3.5.17)-(3.5.19). Particularly, the dimensionless pressure can be represented as the function

$$p/p_\infty = \varphi_1 (\boldsymbol{Fr}, \boldsymbol{Re}, \boldsymbol{M}, \boldsymbol{Sh}, \boldsymbol{Pr}, k_\infty, \bar{T}_w, \bar{x}, \bar{y}, \bar{z}, \bar{t}) \qquad (3.5.21)$$

We can use the known pressure distribution to determine the dimensionless drag force coefficient for a given instant:

$$c_{x_a} = X_a/(q_\infty S) = \varphi_2 (\boldsymbol{Fr}, \boldsymbol{Re}, \boldsymbol{M}, \boldsymbol{Sh}, \boldsymbol{Pr}, k_\infty, \bar{T}_w) \qquad (3.5.22)$$

This expression determines the dependence of the aerodynamic drag coefficient on the dimensionless similarity criterion more completely than (3.5.3). But relation (3.5.22) does not reflect all the features of flow of a dissociated gas because it was obtained from the simplified equations (3.5.13)-(3.5.16). Consequently, formula (3.5.22) is less accurate for such a flow than for that of an undissociated gas, and determines only partial similarity.

The similarity criteria on which a dimensionless aerodynamic variable depends have a definite physical meaning and characterize the real factors affecting the aerodynamic force.

The Froude number ***Fr*** is a similarity criterion taking into account the influence of the mass force (force of gravity) on the drag. It can be seen from the equation of motion given in the dimensionless form that the number ***Fr*** equals the ratio of the quantity V_∞^2/L due to the influence of the inertia forces to the scaling of the mass forces g. The equality of the Froude numbers ***Fr*** for a full-scale body and its geometrically similar model signifies that they have identical drag coefficients due to the influence of the force of gravity of the fluid. This similarity criterion is of no significance when studying gas flows because the influence of the force of gravity of a gas on motion is negligibly small. But the importance of this criterion may be appreciable in hydrodynamics, particularly in the experimental investigation of the wave resistance of various navigable vessels.

When a body moves in a real fluid, the aerodynamic forces depend on the viscosity. The viscous force is characterized by the Reynolds number ***Re*** that can be obtained as the ratio of the quantity V_∞^2/L describing the influence of inertia forces to the parameter $\nu_\infty V_\infty/L^2$ determining the influence of the viscosity. If the equality of the Reynolds numbers for two geometrically similar flows is observed, the condition of partial aerodynamic similarity with account taken of the influence of viscosity is satisfied. In this condition, the friction factors for a full-scale and a model bodies are equal.

The similarity with respect to the Mach number is obtained from the ratio of the quantity V_∞^2/L to the parameter $p_\infty/(\rho_\infty L)$ that takes into account the influence of the pressure forces depending on the compressibility of the gas. The partial similarity of two flows of a compressible gas flowing over geometrically similar bodies is observed when the Mach numbers are equal.

When investigating unsteady flow, similarity with respect to the Strouhal number is significant. It is obtained by comparing the inertia forces and the forces due to the influence of the unsteadiness, i.e. from the ratio of the quantities V_∞^2/L and V_∞/t_∞. Two unsteady flows around a full-scale body and a model have partial aerodynamic similarity with identical values of the Strouhal number.

The similarity criteria with respect to the Prandtl number ***Pr***

and the ratio of the specific heats are due to definite requirements to the physical properties of the gases in the full-scale and model flows. The gases may differ, but their physical properties must observe the equalities $\boldsymbol{Pr}_1 = \boldsymbol{Pr}_2$ and $k_{\infty 1} = k_{\infty 2}$. The Prandtl number depends on the dynamic viscosity and the heat conductivity. The dynamic viscosity reflects the properties of a gas which the molecular transfer of the momentum depends on, while the heat conductivity characterizes the intensity of the molecular transfer of heat. Consequently, the Prandtl number $\boldsymbol{Pr} = \mu c_{p\infty}/\lambda_\infty$ is the measure of the transformation of the energy of molecular transfer into heat. For a gas, $\boldsymbol{Pr} < 1$.

A dimensionless variable of the aerodynamic force or heat transfer is a composite function of a number of similarity criteria, each of which reflects the influence of a definite physical process. Complete similarity of a full-scale and a model flows can be ensured only when equality of all the similarity criteria is observed. In practice, this cannot be done because some of these criteria are contradictory.

Let us consider, for example, the Reynolds, Froude, and Mach numbers. For the observance of similarity with respect to the skin friction forces, it is essential that $V_1 L_1/\nu_1 = V_2 L_2/\nu_2$. If we assume that for a full-scale and model flows the coefficients $\nu_1 = \nu_2$, then the speed of the model flow $V_2 = V_1 (L_1/L_2)$, i.e. it is greater than the speed of the full-scale flow the same number of times that the model of the body in the flow is less than the full-scale one.

To ensure similarity with respect to the forces of gravity, it is necessary to ensure equality of the Froude numbers, i.e. $V_1^2/(L_1 g_1) = V_2^2/(L_2 g_2)$, whence it follows that if experiments were run at identical values of g, then the speed of the model flow is $V_2 = V_1 \sqrt{L_2/L_1}$. We can see that in the given case the speed V_2 for the small-size model must be smaller than V_1 instead of greater as in the previous example.

Upon equality of the Mach numbers, we have $V_1/a_1 = V_2/a_2$. Assuming for simplification that $a_2 = a_1$, we obtain the condition for equality of the speeds of the model and full-scale flows.

It is natural that all these conditions for the speed cannot be observed simultaneously, therefore we can consider only incomplete similarity. We must note, however, that in practice there is no need to satisfy all the similarity criteria because their influence in a specific case of motion is not the same. For example, the forces of skin friction and pressure have a more significant influence on the flow of a gas over a body than the forces of gravity, and accordingly the numbers $\boldsymbol{Re}$ and $\boldsymbol{M}$ are more significant than $\boldsymbol{Fr}$. In this connection, the Froude number is not taken into consideration as a similarity criterion in such cases.

If at the same time the speeds are not great, then the influence of the pressure forces due to compressibility of the gas is negligibly small, and, consequently, no account may be taken of the similarity criterion with respect to the Mach number, assuming that the aerodynamic coefficient depends on the Reynolds number.

The aerodynamic force, moment, or heat flux from a gas to a surface is the result of the action of a moving gas on a body. Various processes occur simultaneously in the gas: skin friction, compression (or expansion), heating, a change in the physical properties, etc. Therefore, one must try to satisfy the maximum number of similarity criteria. For example, it is expedient that the equality of the Reynolds and Mach numbers for a full-scale and model flows be retained simultaneously, i.e. $\boldsymbol{Re}_1 = \boldsymbol{Re}_2$ and $\boldsymbol{M}_1 = \boldsymbol{M}_2$. This is especially important when studying aerodynamic forces, which for bodies with a large surface may consist of equivalent components depending on the friction and pressure due to compressibility. This condition can be ensured when running experiments in variable density wind tunnels.

If tests are being performed in a gas flow in which the speed of sound is the same as in the full-scale flow ($a_2 = a_1$), it follows from the equality of the Mach numbers that $V_2 = V_1$. Having this in view and using the equality $\boldsymbol{Re}_1 = \boldsymbol{Re}_2$ or, which is the same, $V_2\rho_2 L_2/\mu_2 = V_1\rho_1 L_1/\mu_1$, we obtain $L_2\rho_2/\mu_2 = L_1\rho_1/\mu_1$. Assuming that $\mu_2 = \mu_1$, we find that the density of the gas in the wind tunnel flow is $\rho_2 = \rho_1(L_1/L_2)$. Assuming that the temperature of the full-scale and model flows is the same ($T_2 = T_1$) and using an equation of state, we obtain the condition $p_2 = p_1\,(L_1/L_2)$. Hence, to simultaneously ensure similarity with respect to the forces of skin friction and of pressure with account taken of compressibility, i.e. to observe the equalities $\boldsymbol{Re}_1 = \boldsymbol{Re}_2$ and $\boldsymbol{M}_1 = \boldsymbol{M}_2$, it is essential that the static pressure in the flow of a gas produced by a wind tunnel be greater than the pressure in the full-scale flow by the same number of times by which the model is smaller than the full-scale body. The design of a wind tunnel makes it possible within known limits to control the static pressure in the model flow of a gas depending on the size of the model.

With a known approximation, the influence of heat transfer may not be taken into account when determining the force interaction. Here the aerodynamic coefficients will depend on the numbers $\boldsymbol{Re}$, $\boldsymbol{M}$, and $\boldsymbol{Sh}$. If in addition the tests are conducted in a gas for which $k_{\infty 2} = k_{\infty 1}$, we have

$$c_x = f\,(\boldsymbol{Re},\ \boldsymbol{M},\ \boldsymbol{Sh}) \tag{3.5.23}$$

For a steady flow

$$c_x = f\,(\boldsymbol{Re},\ \boldsymbol{M}) \tag{3.5.24}$$

3.6. Isentropic Gas Flows

Configuration of Gas Jet

Let us consider the steady motion of an ideal (inviscid) gas in a stream or jet with a small expansion and a slight curvature. Motion in such a jet can be studied as one-dimensional, characterized by the change in the parameters depending on one linear coordinate measured along the axis of the jet. For a steady flow, the parameters determining this flow are identical in each cross section at any instant. If the width of the jet is small in comparison with the radius of curvature of the centre line, the lateral pressure gradient may be disregarded, and one may consider that the pressure at each point of the jet cross section is the same.

The consideration of such a one-dimensional steady flow of a compressible gas leads to the simplest approximate solution of the equations of gas dynamics. Condition (2.4.51) of a constant mass flow is retained along the jet, i.e. $\rho_1 V_1 S_1 = \rho_2 V_2 S_2 = \rho_3 V_3 S_3 = \ldots$, or $\rho VS = \text{const}$, where the subscripts 1, 2, 3 signify the corresponding parameters of the gas at the control surfaces. Cross sections of the channel with an area of S_1, S_2, and S_3 have been chosen as these surfaces. Taking logarithms, we obtain $\ln \rho + \ln V + \ln S = \text{const}$. Differentiation of this expression yields

$$d\rho/\rho + dV/V + dS/S = 0$$

whence

$$\frac{dS}{dV} = -S\left(\frac{1}{V} + \frac{1}{\rho} \cdot \frac{d\rho}{dV}\right) \tag{3.6.1}$$

Let us use relation (3.4.14), by differentiation of which we have

$$V\,dV = -di \tag{3.6.2}$$

Substituting dp/ρ for di, we find

$$V\,dV = -dp/\rho \tag{3.6.3}$$

Taking the speed of sound $a = \sqrt{dp/d\rho}$ into account and using relation (3.6.3), we transform (3.6.1) to the form

$$dS/dV = (S/V)\,(M^2 - 1) \tag{3.6.4}$$

where $M = V/a$ is the Mach number in the given cross section of the jet.

Let us assume that the velocity along the jet grows ($dV > 0$), but remains subsonic and, consequently, $M < 1$. A glance at (3.6.4) reveals that for this case the derivative $dS/dV < 0$. This indicates that the jet converges downstream. Conversely, for a subsonic

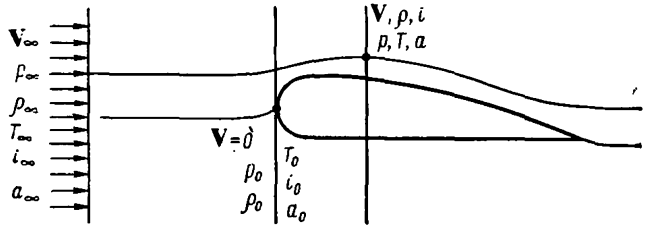

Fig. 3.6.1
Parameters of a gas flowing over a body

flow with a diminishing velocity ($M < 1$, $dV < 0$), the cross section increases, which is indicated by the inequality $dS > 0$ following from (3.6.4).

Let us consider a supersonic flow ($M > 1$). If the velocity decreases, then, as can be seen from (3.6.4), the differential $dS < 0$, and, consequently, the jet converges. Conversely, when the velocity grows, the value of $dS > 0$, i.e. the jet diverges.

Let us take a nozzle that first has the shape of a converging, and then of a diverging channel. In definite conditions in the converging part of the nozzle, a subsonic flow is accelerated, reaching the speed of sound in the narrowest cross section [here $dS = 0$ and, as follows from (3.6.4), $M = 1$], and then becomes supersonic. This is how nozzles are designed in rocket engines, gas turbines, and wind tunnels intended for obtaining supersonic flows.

Flow Velocity

Let us consider a gas jet flowing over a surface (Fig. 3.6.1). We shall denote the free-stream parameters by V_∞, p_∞, ρ_∞, T_∞, i_∞, and a_∞, and the parameters for the part of the jet in the disturbed region by the same symbols without subscripts. To find the velocity in an arbitrary cross section of the jet, we shall use Eq. (3.4.14) in which we shall determine the constant C according to the preset parameters of the free stream:

$$C = V_\infty^2/2 + i_\infty \tag{3.6.5}$$

With this in view, we have

$$V^2/2 + i = V_\infty^2/2 + i_\infty$$

whence

$$V = \sqrt{V_\infty^2 + 2(i_\infty - i)} \tag{3.6.6}$$

At the stagnation point, $V = 0$, consequently the enthalpy is

$$i = i_0 = V_\infty^2/2 + i_\infty \tag{3.6.7}$$

Hence, the constant C as regards its physical meaning can be considered as the stagnation enthalpy. With a view to this value of C, the velocity in the jet is

$$V=\sqrt{2(i_0-i)} \tag{3.6.8}$$

The stagnation pressure p_0 and density ρ_0 correspond to the enthalpy i_0. They are determined from the condition

$$i_0=\frac{k}{k-1}\cdot\frac{p_0}{\rho_0}=\frac{V_\infty^2}{2}+i_\infty=\frac{V_\infty^2}{2}+\frac{k}{k-1}\cdot\frac{p_\infty}{\rho_\infty} \tag{3.6.9}$$

We can rewrite Eq. (3.6.9) as follows:

$$\frac{V^2}{2}+\frac{k}{k-1}\cdot\frac{p}{\rho}=\frac{k}{k-1}\cdot\frac{p_0}{\rho_0} \tag{3.6.10}$$

Since the flow is isentropic, we have

$$p/\rho^k=p_0/\rho_0^k \tag{3.6.11}$$

consequently

$$V=\sqrt{\frac{2k}{k-1}\cdot\frac{p_0}{\rho_0}\left[1-\left(\frac{p}{p_0}\right)^{(k-1)/k}\right]} \tag{3.6.12}$$

Seeing that for conditions of stagnation the speed of sound is $a_0=\sqrt{kp_0/\rho_0}$, we find

$$V=a_0\sqrt{\frac{2}{k-1}\left[1-\left(\frac{p}{p_0}\right)^{(k-1)/k}\right]} \tag{3.6.13}$$

Examination of (3.6.8) reveals that the velocity along the jet grows with diminishing of the enthalpy, and therefore more and more of the heat is converted into kinetic energy. The maximum velocity is reached provided that the enthalpy $i=0$, i.e. all the heat is spent to accelerate the gas. The value of this velocity is

$$V_{\max}=\sqrt{2i_0} \tag{3.6.14}$$

or with a view to (3.6.9):

$$V_{\max}=\sqrt{\frac{2k}{k-1}\cdot\frac{p_0}{\rho_0}}=a_0\sqrt{\frac{2}{k-1}} \tag{3.6.15}$$

Accordingly, the velocity in an arbitrary section is

$$V=V_{\max}\sqrt{1-i/i_0} \tag{3.6.16}$$

or

$$V=V_{\max}\sqrt{1-(p/p_0)^{(k-1)/k}} \tag{3.6.17}$$

In the narrowest, critical, cross section of the jet, the velocity equals the local speed of sound. The latter is called critical and is

designated by a^*. The critical pressure p^* and density ρ^* correspond to the critical speed. It follows from the Bernoulli equation that for the critical section we have

$$\frac{a^{*2}}{2}+\frac{k}{k-1}\cdot\frac{p^*}{\rho^*}=\frac{k}{k-1}\cdot\frac{p_0}{\rho_0}$$

Having in view that $kp^*/\rho^* = a^{*2}$, the critical speed is

$$a^*=\sqrt{\frac{2k}{k+1}\cdot\frac{p_0}{\rho_0}}=a_0\sqrt{\frac{2}{k+1}} \tag{3.6.18}$$

or, taking into account (3.6.15),

$$a^*=V_{\max}\sqrt{(k-1)/(k+1)} \tag{3.6.19}$$

To determine the **local sound speed** a, we shall use Eq. (3.6.10). Performing the substitutions $a^2 = kp/\rho$ and $a_0^2 = kp_0/\rho_0$ in it, we obtain

$$a^2=a_0^2-\frac{k-1}{2}V^2 \tag{3.6.20}$$

or

$$a^2=\frac{k+1}{2}a^{*2}-\frac{k-1}{2}V^2 \tag{3.6.21}$$

$$a^2=\frac{k-1}{2}(V_{\max}^2-V^2) \tag{3.6.22}$$

Let us introduce the **velocity ratio (relative velocity)** $\lambda = V/a^*$. Dividing Eq. (3.6.21) by V^2 and having in view that the ratio $V/a = M$, we can establish the relation between λ and M:

$$\lambda^2=[(k+1)/2]M^2/\{1+[(k-1)/2]M^2\} \tag{3.6.23}$$

Hence it follows that in the cross section of the jet where $V_{\max}$ is reached, the number $M = \infty$. We find the corresponding value of $\lambda = \lambda_{\max}$ from (3.6.23) provided that $M \to \infty$:

$$\lambda_{\max}=\sqrt{(k+1)/(k-1)} \tag{3.6.24}$$

Evidently, in the critical section where $M = 1$, we also have $\lambda = 1$. In an arbitrary section characterized by the values $1 \leqslant M \leqslant \infty$, the velocity ratio is

$$1\leqslant\lambda\leqslant\sqrt{(k+1)/(k-1)} \tag{3.6.25}$$

Pressure, Density, and Temperature

It follows from (3.6.17) that the pressure in an arbitrary cross section of the jet is

$$p=p_0\,(1-V^2/V_{\max}^2)^{k/(k-1)} \tag{3.6.26}$$

By (3.6.22), the difference

$$1-\frac{V^2}{V_{\max}^2}=\left(1+\frac{k-1}{2}M^2\right)^{-1} \tag{3.6.27}$$

consequently,

$$p=p_0\left(1+\frac{k-1}{2}M^2\right)^{-k/(k-1)}=p_0\pi(M) \tag{3.6.28}$$

where the function π of the argument M is determined by the pressure ratio p/p_0.

For the conditions of the free-stream flow, formula (3.6.28) yields:

$$p_0=p_\infty\left(1+\frac{k-1}{2}M_\infty^2\right)^{k/(k-1)}=\frac{p_\infty}{\pi M_\infty} \tag{3.6.29}$$

Consequently,

$$p=p_\infty\left\{\frac{1+[(k-1)/2]M_\infty^2}{1+[(k-1)/2]M^2}\right\}^{k/(k-1)}=p_\infty\frac{\pi(M)}{\pi(M_\infty)} \tag{3.6.30}$$

From the equation of an adiabat $p\rho^k=p_0/\rho_0^k$, in which p is replaced in accordance with formulas (3.6.26) and (3.6.28), we find a relation for the density

$$\rho=\rho_0\left(1-\frac{V^2}{V_{\max}^2}\right)^{1/(k-1)}=\rho_0\left(1+\frac{k-1}{2}M^2\right)^{-1/(k-1)}=\rho_0\varepsilon(M) \tag{3.6.31}$$

where the function ε of the argument M is determined by the ratio of the densities ρ/ρ_0.

Using the equation of state

$$p/p_0=(\rho/\rho_0)\,T/T_0 \tag{3.6.32}$$

and also Eqs. (3.6.26) and (3.6.28) for the pressure and (3.6.31) for the density, we have

$$T=T_0\left(1-\frac{V^2}{V_{\max}^2}\right)=T_0\left(1+\frac{k-1}{2}M\right)^{-1}=T_0\tau(M) \tag{3.6.33}$$

where the function τ of the argument M is determined by the ratio of the temperatures T/T_0.

Tables of the gas-dynamic functions $\pi(M)$, $\varepsilon(M)$, and $\tau(M)$ for values of the exponent k from 1.1 to 1.67 are given in [12].

We shall determine the corresponding relations for the density ρ_0 and temperature T_0 by means of expressions (3.6.31) and (3.6.33). For the conditions of a free-stream flow, these expressions yield:

$$\rho_0=\rho_\infty\left(1+\frac{k-1}{2}M_\infty^2\right)^{1/(k-1)}=\frac{\rho_\infty}{\varepsilon(M_\infty)} \tag{3.6.34}$$

$$T_0=T_\infty\left(1+\frac{k-1}{2}M_\infty^2\right)=\frac{T_\infty}{\tau(M_\infty)} \tag{3.6.35}$$

In the critical cross section of the stream, $M = 1$. Consequently, from (3.6.28), (3.6.31), and (3.6.33), we obtain the following formulas for the critical values of the pressure p^*, density ρ^*, and temperature T^*:

$$p^* = p_0 \left(\frac{2}{k+1}\right)^{k/(k-1)} = p_0 \pi(1) \tag{3.6 36}$$

$$\rho^* = \rho_0 \left(\frac{2}{k+1}\right)^{1/(k-1)} = \rho_0 \varepsilon(1) \tag{3.6.37}$$

$$T^* = T_0 \left(\frac{2}{k+1}\right) = T_0 \tau(1) \tag{3.6.38}$$

where $\pi(1)$, $\varepsilon(1)$, and $\tau(1)$ are the values of the gas-dynamic functions at $M = 1$.

The above formulas, suitable for any speeds, can give us approximate relations for cases when the numbers M are very large. A glance at (3.6.30) reveals that when $M \gg 1$ and $M_\infty \gg 1$, we have

$$p/p_\infty = (M_\infty/M)^{2k/(k-1)} \tag{3.6.39}$$

Similar relations for the density and temperature have the form

$$\rho/\rho_\infty = (M_\infty/M)^{2/(k-1)} \tag{3.6.40}$$

$$T/T_\infty = (M_\infty/M)^2 \tag{3.6.41}$$

Using relation (3.6.27) for the velocity of the free-stream flow,

$$1 - \frac{V_\infty^2}{V_{\max}^2} = \left(1 + \frac{k-1}{2} M_\infty^2\right)^{-1} \tag{3.6.27'}$$

for the conditions $M_\infty \gg 1$ and $M \gg 1$, we obtain the following approximate formula for the local velocity:

$$\frac{V}{V_\infty} = 1 + \frac{1}{k-1}\left(\frac{1}{M_\infty^2} - \frac{1}{M^2}\right) \tag{3.6.42}$$

Flow of a Gas from a Reservoir

Formula (3.6.12) allows us to determine the velocity of a gas flowing out through a nozzle from a reservoir (Fig. 3.6.2) in which the parameters are determined by the conditions of stagnation corresponding to a velocity of the gas in the reservoir of $V \approx 0$. Such conditions are ensured in practice if the critical cross section of the nozzle is sufficiently small in comparison with the cross-sectional dimension of the reservoir. In the critical section of the nozzle, which the value of the derivative $dS/dV = 0$ corresponds

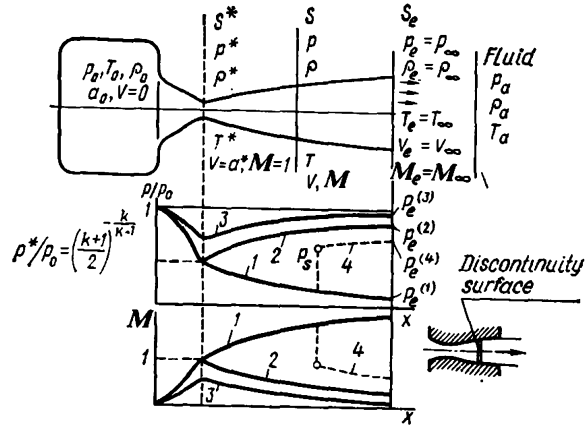

Fig. 3.6.2
Parameters of a gas flowing from a reservoir

to, the Mach number, as can be seen from (3.6.4), equals unity, i.e. the velocity in this section equals the local speed of sound:

$$V = a^* = \sqrt{\frac{2k}{k+1} \cdot \frac{p_0}{\rho_0}} = a_0 \sqrt{\frac{2}{k+1}} = \sqrt{\frac{2kRT_0}{k+1}}$$

Such a speed is ensured provided that the pressure in the reservoir according to (3.6.36) is not lower than the value

$$p_0 = p^* \left(\frac{k+1}{2}\right)^{k/(k-1)} \qquad (3.6.43)$$

If the nozzle communicates with the atmospheric air whose pressure is $p_a = 10^5$ Pa (this pressure is called the backpressure), flow through the nozzle is possible when $p^* \geqslant 10^5$ Pa. Assuming that $p^* = 10^5$ Pa and $k = 1.4$, we obtain the pressure needed to ensure the speed of sound at the outlet of a converging nozzle:

$$p_0 = 10^5 \left(\frac{1.4+1}{2}\right)^{1.4/(1.4-1)} \approx 1.9 \times 10^5 \text{ Pa}$$

When the critical parameters are reached in the throat of a nozzle, a further reduction of the backpressure ($p_a < p^*$) no longer affects the values of a^* and p^*, which depend on the state of the gas in the reservoir. But here conditions are created for the appearance of a supersonic speed of the gas in the diverging part of the nozzle. In Fig. 3.6.2, these conditions of isentropic motion are characterized by curves *1* determining the change in the ratio p/p_0 and in the number M along the nozzle. Such conditions are realized when the backpressure p_a equals the pressure $p_e^{(1)}$ at the exit of the expanding nozzle or is less than it. A change in the backpressure does not affect the parameters of the gas in the outlet cross section.

Let us consider another set of possible conditions of isentropic flow along a nozzle. Let us assume that the backpressure grows to the value $p_a^{(2)} > p_e^{(1)}$ at which the pressure $p_e^{(2)}$ at the exit reaches the same value as $p_a^{(2)}$. The subsonic flow formed in this case is characterized by curves *2* shown in Fig. 3.6.2. We find the velocity ratio λ (M) of this flow by Eq. (3.6.23), choosing from the two solutions for λ the one that is less than unity.

Upon a further increase in the backpressure to the value $p_a^{(3)}$, conditions appear in which the pressure $p_e^{(3)}$ at the exit will equal the backpressure, i.e. $p_e^{(3)} = p_a^{(3)}$, while the pressure in the throat will exceed the critical pressure p^*; the relevant speed in this cross section is subsonic ($V < a^*$). Consequently, in the diverging part of the nozzle, the speed lowers, remaining subsonic (curve *3* in Fig. 3.6.2).

At pressures at the exit smaller than $p_e^{(2)}$ and larger then $p_e^{(1)}$, the isentropic nature of the flow is disturbed. At a certain cross section of the nozzle, a jump (discontinuity of the parameters) occurs, the transition through which is attended by sharp deceleration of the flow. As a result of this deceleration, having an *irreversible adiabatic nature*, the supersonic flow *transforms abruptly* into a subsonic one. The change in the pressure and in the number M along the nozzle in these flow conditions is characterized by curves *4* (Fig. 3.6.2). The surface of discontinuity of the parameters (shock) must be in a cross section with a Mach number M such that would correspond to the pressure p_s past this surface ensuring a gas pressure of $p_e^{(4)}$ ($p_e^{(1)} < p_e^{(4)} < p_e^{(2)}$) at the exit as a result of further expansion of the gas. Hence, in the given case, the flow of the gas must be analysed with the aid of the shock-wave theory whose fundamentals are treated in Chap. 4.

In an arbitrary cross section of the nozzle, including its outlet section, we determine the supersonic speed by (3.6.12). At $M_e = M_\infty$ and a pressure of $p_e = p_\infty$ in the outlet section, the required pressure p_0 in the reservoir is determined by (3.6.29).

The mass flow rate equation has the form

$$\rho S V = \rho^* S^* a^* \tag{3.6.44}$$

from which we find that the ratio of the mass velocity (the specific mass flow rate) $q = \rho V$ through the cross section S being considered to the mass velocity $q^* = \rho^* a^*$ through the critical section S^* is

$$\bar{q} = q/q^* = \rho V/(\rho^* a^*) = S^*/S \tag{3.6.45}$$

With a view to relations (3.6.19) and (3.6.31), we find

$$\rho = \rho_0 \left(1 - \frac{V^2}{V_{max}^2}\right)^{1/(k-1)} = \rho_0 \left(1 - \frac{k-1}{k+1} \cdot \frac{V^2}{a^{*2}}\right)^{1/(k-1)}$$

$$= \rho_0 \left(1 - \frac{k-1}{k+1} \lambda^2\right)^{1/(k-1)}$$

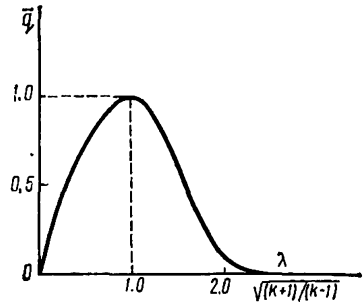

Fig. 3.6.3
Change in the mass velocity ratio when a gas flows out from a reservoir

After now determining the ratio ρ_0/ρ^* from (3.6.37), **we obtain** relation (3.6.45) in the following form:

$$\bar{q}(\lambda) = \lambda\left(1 - \frac{k-1}{k+1}\lambda^2\right)^{1/(k-1)}\left(\frac{k+1}{2}\right)^{1/(k-1)} = \frac{S^*}{S} \quad (3.6.46)$$

The function $\bar{q}(\lambda)$ is called the **reduced mass density.** Taking formula (3.6.23) into account, we can determine this function **of** the argument M:

$$\bar{q}(M) = M\left[\frac{2}{k+1}\left(1 + \frac{k-1}{2}M^2\right)\right]^{-(k+1)/[2(k-1)]} = \frac{S^*}{S} \quad (3.6.46')$$

Tabulated values of the function $\bar{q}$ within the range of values of k from 1.1 to 1.67 are given in [12]. It follows from these relations that the number λ (or M) in a certain section S of a nozzle is a function of only the ratio of the areas S^*/S and does not depend on the parameters of the gas in the reservoir.

The dependence of the mass velocity ratio $\bar{q}$ (or of the ratio S^*/S of the areas) on λ is shown in Fig. 3.6.3. At a given critical nozzle section in the subsonic region ($\lambda < 1$), the speed grows at the expense of the reduction in the area S, while in the supersonic region, conversely, it grows at the expense of the increase in the area. In accordance with the above, a decrease in the pressure in the reservoir does not affect the value of λ or M at the nozzle exit. In the case being considered, as follows from (3.6.29), a change in the pressure p_0 is attended by a proportional change in the pressure at the exit $p_e = p_\infty$.

The mass flow rate of a gas from a reservoir can be determined by the formula

$$G_{sec} = \rho^* a^* S^*$$

Evaluation of ρ^* and a^* by formulas (3.6.37) and (3.6.18), respectively, yields

$$G_{sec} = S^*\left(\frac{2}{k+1}\right)^{1/(k-1)}\sqrt{\frac{2k}{k+1}p_0\rho_0} \quad (3.6.47)$$

where ρ_0 is the density of the gas in the reservoir.

Upon the motion of an incompressible fluid, the mass flow rate equation in accordance with (2.4.51) and provided that $\rho = \text{const}$ becomes

$$VS = \text{const} \tag{3.6.48}$$

Kinematic equation (3.6.48) completely characterizes the one-dimensional flow of an incompressible fluid. It shows that the flow velocity is inversely proportional to the cross-sectional area of the channel. The pressure in steady flow is calculated by the Bernoulli equation (3.4.12) or (3.4.13).

Shock Wave Theory

4.1. Physical Nature of Shock Wave Formation

A feature of supersonic gas flows is that deceleration is attended by the formation of discontinuity surfaces in them. When a gas passes through these surfaces, its parameters change abruptly: the velocity sharply diminishes, and the pressure, temperature, and density grow. Such continuity surfaces moving relative to a gas are often referred to as **shock waves**, while the immovable discontinuity surfaces are called **stationary shock waves** or simply **shocks.** Below we consider the conditions of gas flow after stationary shock waves, and we shall use the term "shock", as a rule.

In the most general case, a shock has a curved shape. Figure 4.1.1*a* shows schematically an **attached curved shock** formed in a flow past a sharp-nosed body, and Fig. 4.1.1*b*—a **detached curved shock** appearing in front of a blunt surface in a supersonic flow. Upon the supersonic flow past a sharp-nosed body with straight walls, an **attached straight shock** may appear (Fig. 4.4.1*c*).

A glance at Fig. 4.1.1*b* reveals that the surfaces of shocks may be oriented along a normal to the free-stream velocity (the shock angle $\theta_s = \pi/2$) or inclined at an angle other than a right one ($\theta_s < \pi/2$). In the first case, the shock is said to be **normal**, in the second—**oblique**. An attached curved shock can evidently be considered as a set of oblique shocks, and a detached shock as consisting of a normal shock and a system of oblique shocks.

The formation of shocks is due to the specific nature of propagation of disturbances in a supersonic gas flow. By a disturbance is meant a local compression causing a pressure increase. The latter appears in a flow passing around an obstacle called a **source of disturbances.**

Let us consider a source of infinitely small disturbances at point O (Fig. 4.1.2). Such disturbances propagate in a gas at rest ($V = 0$) in all directions at the speed of sound a in the form of spherical waves in space or circular waves in a plane (Fig. 4.1.2*a*). At the instant t, the radius of a wave is $r = at$. If a subsonic gas flow is

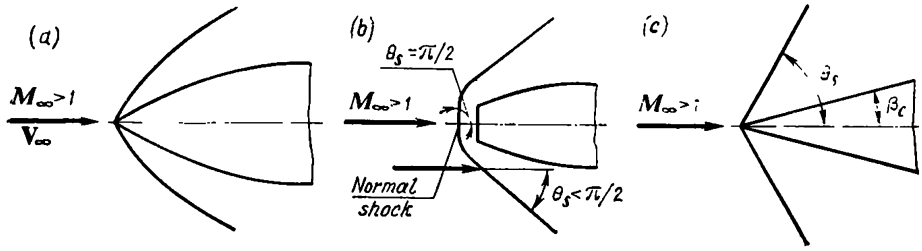

Fig. 4.1.1
Shocks:
a—attached curved shock; *b*—detached curved shock; *c*—attached straight shock

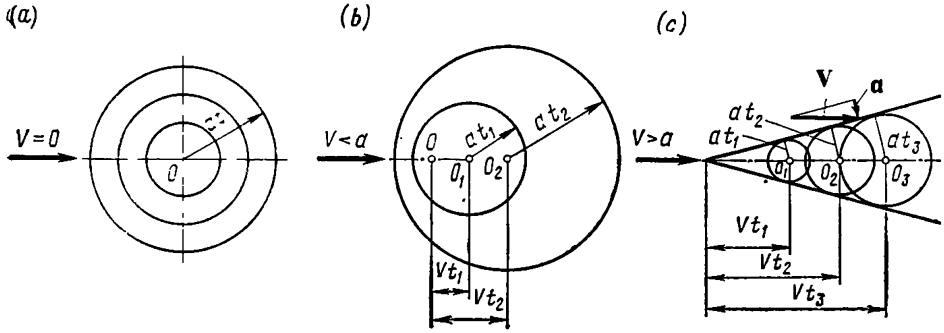

Fig. 4.1.2
Propagation of disturbances in a gas:
a—gas at rest; *b*—subsonic flow; *c*—supersonic flow

incident on a source ($V < a$, Fig. 4.1.2*b*), the waves are carried downstream: the centre of a wave travels at a speed of $V < a$, while the wave propagates at the speed of sound. During a certain time t, the centre of the wave travels the distance Vt, while the radius of the wave $r = at$, here $at > Vt$. Hence, in a subsonic flow, disturbances also propagate upstream.

In the particular case of a sonic velocity ($V = a$), the front of spherical or circular disturbance waves is limited by a flat vertical surface or straight line tangent to a sphere or circle, respectively, and passing through point O because in this case the distance over which the centre of the wave travels during the time t equals its radius at the same instant t.

Let us assume that the free-stream velocity is supersonic ($V > a$). During the time t, the centre of the wave travels the distance Vt, while a sound wave covers the distance at. Since $at < Vt$, for all the spherical sound waves we can draw an enveloping conical surface (Fig. 4.1.2*c*), i.e. a **disturbance cone** (or **Mach cone**). On a plane, **disturbance lines** (or **Mach lines**) are envelopes of the family of circular waves. The disturbances are the densest on the disturbance

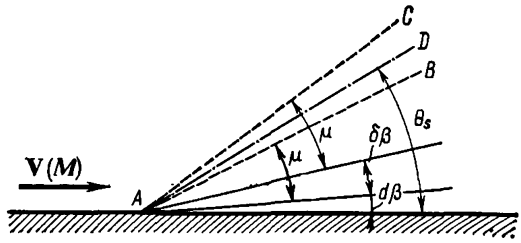

Fig. 4.1.3
Origination of a shock

cone or lines that are boundaries of a disturbed and undisturbed region because all the sound waves on this cone are in the same phase of oscillation—the compression phase. Such disturbed regions—conical or plane waves confined within straight Mach lines, are called **simple pressure waves** or **Mach waves.**

The angle μ formed by the generatrix of a conical wave or line of disturbances is determined from the condition (Fig. 4.1.2*c*) that $\sin \mu = at/(Vt)$, whence

$$\sin \mu = 1/M \qquad (4.1.1)$$

The angle μ is called the **Mach angle.** A supersonic flow carries all the sound disturbances downstream, limiting their propagation by the Mach cone or lines inclined at the angle μ. The front of a pressure wave propagates at the same speed of sound as the front of a spherical (or circular) wave. This is why the projection of the free-stream velocity onto a normal to the wave front equals the speed of sound (Fig. 4.1.2*c*).

In a simple pressure wave, as in a sound one, the gas parameters (pressure, density, etc.) change by an infinitely small magnitude, which is indicated, particularly, by the relation for the speed of sound $a = \sqrt{dp/d\rho}$ known from physics. In the disturbed region, the velocity remains virtually the same as in the undisturbed flow. Therefore, a simple pressure wave can be considered as a shock (or shock wave) of an infinitely small strength, and we can assume for practical purposes that the parameters do not change when traversing it. This is why such a simple pressure wave is also called a **weak shock wave**, while its front (Mach line) is called a **line of weak disturbances** or a **wavelet.**

It is natural to assume that the formation of a shock of a finite strength is associated with the superposition of simple pressure waves and, as a result, with their mutual amplification. Let us consider the process of formation of such a shock taking an oblique shock as an example. Let us assume that a supersonic flow initially travels along a level and smooth surface (Fig. 4.1.3). We create artificially a local pressure increment at point A by turning the flow through the infinitely small angle $d\beta$. This produces a simple press-

ure wave AB emerging from point A as from the source of disturbance and inclined to the surface at the angle μ. If we again turn the flow slightly through the angle $\delta\beta$, a new simple wave AC is formed that emerges from the same point A, but is higher than the first wave. But in a supersonic flow, as shown above, waves cannot propagate upstream, therefore the wave AC will drift downstream until it coincides with the first one. A more intensive wave is formed that is considerably amplified upon a further turning of the flow. The shock of a finite strength formed in this way has a speed of propagation higher than the speed of sound at which the simple pressure wave travels. Therefore, the shock of finite strength must deviate from the simple wave AB to the left and occupy the new position AD. Here it is kept in equilibrium because the speed of its propagation equals the component of the free-stream velocity along a normal to the shock front $V \sin \theta_s$, where θ_s is the angle of inclination of the shock. It follows that the angle of inclination of a shock of finite strength is larger than that of the Mach line (cone), i.e. $\theta_s > \mu$.

4.2. General Equations for a Shock

We shall consider the more general case when the gas behind a shock, owing to substantial heating, experiences physicochemical transformations and *changes its specific heat.* Of major significance when studying shocks behind which oscillations are generated and dissociation, ionization, and chemical reactions occur are the rates of the physicochemical transformations.

Processes behind shock waves are characterized by a fraction of the kinetic energy of the moving gas virtually instantaneously transforming into the internal energy of the gas. In these conditions, we cannot ignore the fact that thermodynamic equilibrium is achieved after a certain time elapses only in conditions of such equilibrium do *all the parameters experiencing discontinuities* (the pressure, density, temperature) *become time-independent.* The analysis of these phenomena is a more involved problem and is associated primarily with studying of the mechanism of non-equilibrium processes, and with a knowledge, particularly, of the rates of chemical reactions in the air.

The simplest case is characterized by an infinitely high rate of the physicochemical transformations and, consequently, by the instantaneous setting in of thermodynamic equilibrium. Such processes behind shock waves are possible physically, which is confirmed by experimental studies.

Let us consider the basic theoretical relations allowing one to evaluate the equilibrium parameters behind a shock wave.

Oblique Shock

A shock formed in real conditions is characterized by a certain thickness. The parameters of the gas in such a shock change not instantaneously, but during a certain time interval. As shown by theoretical and experimental investigations, however, the thickness of a shock is very small and is of the order of the mean free path of the molecules.

For atmospheric conditions, calculations yielded the following values of the thickness of a shock measured in the direction of the free-stream velocity:

Mach number M_∞	1.5	2	3	10
Thickness, mm	4.5×10^{-4}	1.2×10^{-4}	0.7×10^{-4}	0.2×10^{-4}

For $M_\infty = 2$, the thickness of a shock equals about four molecular free paths, and for $M_\infty = 3$—about three. Therefore, when studying a shock in an ideal fluid, this thickness may be disregarded and the shock represented in the form of a geometric discontinuity surface for the gas parameters, assuming these parameters to change instantaneously.

Our task consists in determining the unknown parameters of a gas behind a shock according to the preset parameters characterizing the flow of the gas ahead of the shock.

For an oblique shock formed in a dissociating and ionizing gas, there are nine unknown parameters: the pressure p_2, density ρ_2, temperature T_2, velocity V_2, enthalpy i_2, entropy S_2, speed of sound a_2, the mean molar mass μ_{m2}, and the shock angle θ_s (or the flow deviation angle β_s). Consequently, it is necessary to compile nine simultaneous equations. The parameters ahead of a shock will be the known ones in these equations, namely, the pressure p_1, density ρ_1, velocity V_1, etc. Instead of the velocity V_2 behind a shock, we can determine its components along a normal V_{n2} and a tangent $V_{\tau 2}$ to the shock. This will increase the number of equations needed to ten. These equations include the fundamental equations of gas dynamics (of motion, continuity, energy, and state), a number of kinematic relations for the velocities, and also thermodynamic relations characterizing the properties of a gas. Let us consider each equation of this system.

Figure 4.2.1 shows triangles of the flow velocities ahead of a shock (the parameters with the subscript 1) and behind it (the subscript 2). We shall use the figure to determine the following relations for these components:

$$V_{\tau 2} = V_2 \cos(\theta_s - \beta_s), \quad V_{n2} = V_2 \sin(\theta_s - \beta_s) \tag{4.2.1}$$

This yields the first equation of the system of simultaneous ones:

$$V_{n2}/V_{\tau 2} = \tan(\theta_s - \beta_s) \tag{4.2.2}$$

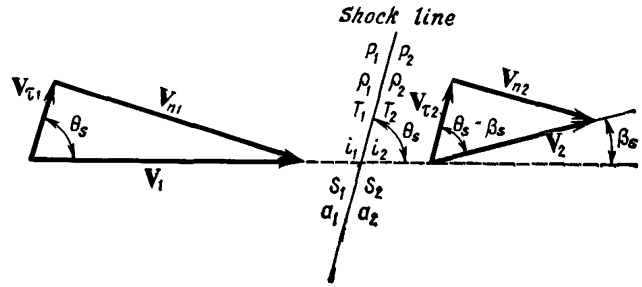

Fig. 4.2.1
Oblique shock

The continuity equation (or the mass flow equation) is the second one. It determines the amount of fluid passing through unit surface of a shock in unit time:

$$\rho_1 V_{1n} = \rho_2 V_{n2} \tag{4.2.3}$$

here $V_{n1} = V_1 \sin \theta_s$ is the normal component of the velocity ahead of the shock (Fig. 4.2.1).

Let us use the equation of motion reduced to the form of an equation of momentum for the conditions of the passage through a shock. This is the third equation of the system. We shall obtain it by assuming that the change in the momentum of the fluid passing in unit time through unit surface area of the shock in the direction of a normal to this surface equals the impulse of the pressure forces:

$$\rho_1 V_{n1}^2 - \rho_2 V_{n2}^2 = p_2 - p_1 \tag{4.2.4}$$

With a view to Eq. (4.2.3), we can write this equation in the form

$$\rho_1 V_{n1} (V_{n1} - V_{n2}) = p_2 - p_1 \tag{4.2.4'}$$

Equation (4.2.4) can also be written as

$$p_1 + \rho_1 V_{n1}^2 = p_2 + \rho_2 V_{n2}^2 \tag{4.2.4''}$$

In this form, the equation expresses the law of momentum conservation when passing through a shock. If we consider the change in the momentum in a direction tangent to the shock surface, then, taking into account that the pressure gradient in this direction is zero, we obtain the following relation:

$$\rho_1 V_{n1} V_{\tau 1} - \rho_2 V_{n2} V_{\tau 2} = 0$$

whence, when $\rho_1 V_{n1} = \rho_2 V_{n2}$, we have

$$V_{\tau 1} = V_{\tau 2} \tag{4.2.5}$$

Equation (4.2.5) is the fourth one of the system. It indicates that the tangential components of the velocity when passing through

a shock do not change. A glance at Fig. 4.2.1 reveals that $V_{\tau 1} = V_1 \cos \theta_s$, therefore we can write (4.2.5) in the form

$$V_{\tau 2} = V_1 \cos \theta_s = V_{n1}/\tan \theta_s \qquad (4.2.5')$$

We can write the equation of energy conservation in the form

$$i_1 + V_1^2/2 = i_2 + V_2^2/2$$

Provided that

$$V_1^2 = V_{n1}^2 + V_{\tau 1}^2, \quad V_2^2 = V_{n2}^2 + V_{\tau 2}^2, \text{ and } V_{\tau 1} = V_{\tau 2}$$

the equation of energy conservation can be transformed:

$$i_1 + V_{n1}^2/2 = i_2 + V_{n2}^2/2 \qquad (4.2.6)$$

By combining the equations of state for the conditions ahead of the shock and behind it, we obtain the relation

$$p_2 - p_1 = R_2 \rho_2 T_2 - R_1 \rho_1 T_1$$

or, taking into account that $R = R_0/\mu_m$, we have

$$p_2 - p_1 = R_0 (\rho_2 T_2/\mu_{m2} - \rho_1 T_1/\mu_{m1}) \qquad (4.2.7)$$

We can write four equations of the system being considered that allow us to determine the enthalpy, entropy, mean molar mass, and speed of sound in a dissociating gas in the form of general dependences of these parameters on the pressure and temperature:

$$i_2 = f_1 (p_2, T_2) \qquad (4.2.8)$$

$$S_2 = f_2 (p_2, T_2) \qquad (4.2.9)$$

$$\mu_{m2} = f_3 (p_2, T_2) \qquad (4.2.10)$$

$$a_2 = f_4 (p_2, T_2) \qquad (4.2.11)$$

These functions are not expressed analytically in the explicit form and are determined by means of experimental investigations or with the aid of rather involved calculations based on the solution of the relevant thermodynamic equations. The relations for these functions are usually constructed in the form of graphs, and their values are tabulated in special tables of thermodynamic functions for air at high temperatures (see [6, 7, 13]).

Let us express the basic parameters behind a shock wave in terms of the relative change in the normal components of the velocity, i.e. in terms of the quantity

$$\Delta \bar{V}_n = \Delta V_n/V_{n1} = (V_{n1} - V_{n2})/V_{n1} \qquad (4.2.12)$$

From (4.2.3), we find the ratio of the densities:

$$\rho_2/\rho_1 = 1/(1 - \Delta \bar{V}_n) \qquad (4.2.13)$$

and from (4.2.4'), the ratio of the pressures:

$$p_2/p_1 = 1 + (\rho_1 V_{n1}^2/p_1)\,\Delta\bar{V}_n \qquad (4.2.14)$$

Introducing the concept of the "normal component" of the number M_1 as the ratio $M_{n1} = V_{n1}/a_1$ or $M_{n1} = M_1 \sin\theta_s$, and assuming that ahead of a shock the gas is not dissociated and the speed of sound for it is $a_1 = \sqrt{k_1 p_1/\rho_1}$, we obtain

$$p_2/p_1 = 1 + k_1 M_{n1}^2\,\Delta\bar{V}_n \qquad (4.2.15)$$

instead of (4.2.14).

We find the ratio of the enthalpies i_2/i_1 from (4.2.6):

$$i_2/i_1 = 1 + (1/2i_1)\,(V_{n1}^2 - V_{n2}^2)$$

Let us write the difference of the velocity squares in the form

$$V_{n1}^2 - V_{n2}^2 = V_{n1}^2\,(1 - V_{n2}/V_{n1})\,(1 + V_{n2}/V_{n1}) = V_{n1}^2 \Delta\bar{V}_n\,(2 - \Delta\bar{V}_n)$$

Hence

$$i_2/i_1 = 1 + (V_{n1}^2/2)\,(\Delta\bar{V}_n/i_1)\,(2 - \Delta\bar{V}_n) \qquad (4.2.16)$$

To determine the ratio of the temperatures T_2/T_1, we shall use the equations of state for the conditions ahead of a shock and behind it, from which

$$T_2/T_1 = (p_2/p_1)\,(\mu_{m2}/\mu_{m1})\,\rho_1/\rho_2 \qquad (4.2.17)$$

Substituting for the ratio of the densities and pressures in this equation their values from Eqs. (4.2.13) and (4.2.15), respectively, we obtain

$$T_2/T_1 = (1 + k_1 M_{n1}^2 \Delta\bar{V}_n)\,(1 - \Delta\bar{V}_n)\,\mu_{m2}\mu_{m1} \qquad (4.2.17')$$

To determine the velocity behind a shock, we shall use the relations

$$V_2^2 = V_\tau^2 + V_{n2}^2 \text{ and } V_1^2 = V_\tau^2 + V_{n1}^2$$

from which we find

$$V_2^2/V_1^2 = 1 - (V_{n1}^2/V_1^2)\,\Delta\bar{V}_n\,(2 - \Delta\bar{V}_n) \qquad (4.2.18)$$

Since

$$V_{n1}/V_1 = \sin\theta_s$$

then

$$V_2^2/V_1^2 = 1 - \sin^2\theta_s \Delta\bar{V}_n\,(2 - \Delta\bar{V}_n) \qquad (4.2.18')$$

Let us find a relation for the flow deviation angle behind a shock. By (4.2.2) and (4.2.5'), we have

$$\Delta\bar{V}_n = 1 - \tan(\theta_s - \beta_s)/\tan\theta_s \qquad (4.2.19)$$

Hence, having in view that

$$\tan(\theta_s - \beta_s) = (\tan\theta_s - \tan\beta_s)/(1 + \tan\theta_s \tan\beta_s)$$

we obtain

$$\tan\beta_s = \tan\theta_s \frac{\Delta\bar{V}_n}{1-\Delta\bar{V}_n}\left(\frac{1}{1-\bar{V}_n} + \tan^2\theta_s\right)^{-1} \qquad (4.2.20)$$

The relative change in the velocity $\Delta\bar{V}_n$ is determined in accordance with (4.2.13) by the dimensionless density

$$\Delta\bar{V}_n = 1 - \rho_1/\rho_2 \qquad (4.2.21)$$

This shows that the ratios of the pressures, temperatures, and enthalpies, and also the flow deviation angle β_s can be written as functions of the relative density ρ_2/ρ_1. In addition, we can introduce the values $V_{n1} = V_1 \sin\theta_s$ and $M_{n1} = M_1 \sin\theta_s$ into the formulas instead of the quantities V_{n1} and M_{n1}, respectively.

Hence, the solution of the problem on an oblique shock when its angle of inclination θ_s is known consists in finding the ratio of the densities ρ_2/ρ_1, or, which is the same, in determining the function $\Delta\bar{V}_n$. This function is determined with the aid of expressions (4.2.16) and (4.2.17′), each of which can be written in the form of a quadratic equation in $\Delta\bar{V}_n$. From the first quadratic equation, we have

$$\Delta\bar{V}_n = 1 - \sqrt{1 - 2(i_2 - i_1)/V_{n1}^2} \qquad (4.2.22)$$

and from the second

$$\Delta\bar{V}_n = A + \sqrt{A^2 - B} \qquad (4.2.23)$$

where

$$A = \frac{k_1 M_{n1}^2 - 1}{2k_1 M_{n1}^2}, \quad B = \frac{1}{k_1 M_{n1}^2}\left(\frac{T_2}{T_1}\cdot\frac{\mu_{m1}}{\mu_{m2}} - 1\right) \qquad (4.2.24)$$

The signs of the square roots—minus in (4.2.22) and plus in (4.2.23)—were chosen with a view to the fact that the velocity behind a shock is always lower than ahead of it, and, consequently, $\Delta\bar{V}_n < 1$. The plus sign in (4.2.23) also indicates that physically the larger of the two values of $\Delta\bar{V}_n < 1$ is real.

Equations (4.2.22) and (4.2.23) are solved by the method of successive approximations. The problem of an oblique shock can be solved if the angle β_s is given. Here the angle θ_s is calculated with the aid of relation (4.2.20), in accordance with which

$$\tan^2\theta_s - \frac{\tan\theta_s}{\tan\beta_s}\frac{\Delta\bar{V}_n}{1-\Delta\bar{V}_n} + \frac{1}{1-\Delta\bar{V}_n} = 0$$

The solution of this equation yields

$$\tan\theta_s = \cot\beta_s\left[\frac{1}{2}\cdot\frac{\Delta\bar{V}_n}{1-\Delta\bar{V}_n} \pm \sqrt{\frac{1}{4}\cdot\frac{\Delta\bar{V}_n^2}{(1-\Delta\bar{V}_n)^2} - \frac{\tan^2\beta_s}{1-\Delta\bar{V}_n}}\right] \quad (4.2.25)$$

One of the solutions (the plus sign before the root) determines the larger value of the angle θ_s realized in a detached curved shock, and the other (the minus sign) determines the smaller value realized in an attached shock with a lower strength.

To facilitate calculations, we can evaluate the angles θ_s beforehand from the given values of β_s, and compile a corresponding table or plot a graph. With their aid, for a value of $\Delta\bar{V}_n$ which previously calculated values of the ratios p_2/p_1, ρ_2/ρ_1, etc. correspond to, we can find one of the angles θ_s or β_s from the other known one.

The velocity V_1 and the number M_1 of the free stream at which the parameters are realized in a shock with the given values of the angle θ_s (or β_s), and also V_{n1} (or M_{n1}) are calculated by the formulas

$$V_1 = V_{n1}/\sin\theta_s, \quad M_1 = M_{n1}/\sin\theta_s \quad (4.2.26)$$

Normal Shock

The formulas for calculating a normal shock can be obtained from the above relations for an oblique one if we assume that $\theta_s = \pi/2$ and $\beta_s = 0$. Accordingly, the velocity $V_{n1} = V_1$, and the number $M_{n1} = M_1$. Now the basic relations acquire the following form:

$$p_2/p_1 = 1 + k_1 M_1^2 \Delta\bar{V} \quad (4.2.27)$$

$$i_2/i_1 = 1 + (V_1^2/2)\,(\Delta\bar{V}/i_1)\,(2 - \Delta\bar{V}) \quad (4.2.28)$$

$$T_2/T_1 = (1 + k_1 M_1^2 \Delta\bar{V})\,(1 - \Delta\bar{V})\,\mu_{m2}\mu_{m1} \quad (4.2.29)$$

$$V_2^2/V_1^2 = 1 - \Delta\bar{V}\,(2 - \Delta\bar{V}) \quad (4.2.30)$$

where the change in the relative velocity

$$\Delta\bar{V} = \Delta V/V_1 = (V_1 - V_2)/V_1 \quad (4.2.31)$$

is determined with the aid of expressions (4.2.22)-(4.2.24):

$$\Delta\bar{V} = 1 - \sqrt{1 - 2\,(i_2 - i_1)/V_1^2} \quad (4.2.32)$$

$$\Delta\bar{V} = A + \sqrt{A^2 - B} \quad (4.2.33)$$

in which

$$A = \frac{k_1 M_1^2 - 1}{2k_1 M_1^2}, \quad B = \frac{1}{k_1 M_1^2}\left(\frac{T_2}{T_1}\cdot\frac{\mu_{m1}}{\mu_{m2}} - 1\right) \quad (4.2.34)$$

The relation between $\Delta\bar{V}$ and the relative density is determined by the formula

$$\Delta\bar{V} = 1 - \rho_1/\rho_2 \quad (4.2.35)$$

We have given the general relations for shocks. Now let us use them to analyse the nature of flow and the ways of calculating the parameters of a gas behind shocks for *constant specific heats* and then consider in greater detail practical ways of calculating similar parameters for a dissociating fluid, i.e. for the more general case of *varying specific heats.*

4.3. Shock in the Flow of a Gas with Constant Specific Heats

Of major theoretical and practical interest is the problem on the flow of a gas behind a shock when the specific heats c_p and c_v are constant. Although such a flow is considered to be a particular (idealized) case of the flow of a gas whose physicochemical properties change to a greater or smaller extent when passing through a shock, nevertheless the results obtained in solving this problem make it possible to comprehend the general *qualitative* nature of a shock transition. The relations characterizing the change in the parameters of a gas when passing through a shock are obtained here in the explicit form. They can also be used for an approximate *quantitative* estimation of these parameters when the more general case of varying specific heats is being treated. The problem being considered also has an independent significance because its solution can be used directly for determining the parameters of a gas behind a shock in a flow at comparatively low supersonic velocities at which the change in the specific heats in the compressed gas is negligibly small. These velocities, which are determined for the most intensive (normal) shock, correspond approximately to Mach numbers $M_\infty < 3\text{-}4$.

System of Equations

The method of calculating an oblique shock treated below is based on the use of a system of equations that is a particular case of the system (4.2.2)-(4.2.11).

If in a shock transition the specific heats do not change, it should also be assumed that the mean molar mass remains constant, and the speed of sound and the enthalpy depend only on the temperature. Equations (4.2.8), (4.2.10), and (4.2.11) accordingly acquire the following form:

$$i_2 = c_p T_2 \tag{4.3.1}$$

$$\mu_{m2} = \mu_{m1} = \mu_m = \text{const} \tag{4.3.2}$$

$$a_2^2 = kRT_2 \tag{4.3.3}$$

Instead of Eq. (4.2.9), it is necessary to use the thermodynamic equation for the entropy of a non-dissociating perfect gas:

$$dS = di/T - dp/(\rho T)$$

Having in view the equations $di = c_p\, dT$ and $dp = d\,(R\rho T) = R\rho\, dT + RT\, d\rho$, we obtain

$$dS = c_p\, d \ln T = R\, d \ln T - R\, d \ln \rho$$

But

$$c_p - R = c_v \text{ and } R/c_v = (c_p - c_v)/c_v = k - 1$$

Consequently,

$$dS = c_v\, [d \ln T - (k - 1)\, d \ln \rho]$$

Integrating this equation at $k = \text{const}$, we find

$$S = c_v \ln (T/\rho^{k-1}) + \text{const} \qquad (4.3.4)$$

It follows from the equation of state $p = R\rho T$ that

$$T/\rho^{k-1} = p/(\rho^k R), \text{ and } \ln [p/(\rho^k R)] = \ln (p/\rho^k) - \ln R$$

Introducing the quantity $\ln R$ into the constant on the right-hand side of (4.3.4), we obtain a relation for the entropy in the form

$$S = c_v \ln (p/\rho^k) + \text{const} \qquad (4.3.5)$$

By applying this equation to the conditions ahead of a shock and behind it, and then determining the difference between the entropies, we obtain instead of (4.2.9) the equation for the entropy used in the theory of an oblique shock:

$$S_2 - S_1 = c_v \ln [(p_2/p_1)\, (\rho_1^k/\rho_2^k)] \qquad (4.3.6)$$

Equation of state (4.2.7) for the case of constant specific heats being considered is simplified:

$$p_2 - p_1 = R\, (\rho_2 T_2 - \rho_1 T_1) \qquad (4.3.7)$$

Equations (4.2.2)-(4.2.6) of the system are retained with no alterations.

Formulas for Calculating the Parameters of a Gas Behind a Shock

To calculate the density, pressure, and enthalpy, the formulas needed are (4.2.13), (4.2.15) and (4.2.16), respectively. To determine the temperature, the formula needed is (4.2.17′) with the assumption made that $\mu_{m2} = \mu_{m1}$:

$$T_2/T_1 = (1 + kM_{n1}^2 \Delta \bar{V}_n)\, (1 - \Delta \bar{V}_n) \qquad (4.3.8)$$

The unknown quantity in all these expressions is the change in the relative velocity $\Delta\bar{V}_n$. Let us determine it by assuming that the shock angle θ_s and the free-stream Mach number M_1 are known. We shall use Eq. (4.2.4′) for this purpose. After dividing it by $\rho_1 V_{n1} = \rho_2 V_{n2}$, we obtain

$$p_2/(\rho_2 V_{n2}) - p_1/(\rho_1/V_{n1}) = V_{n1} - V_{n2} \qquad (4.3.9)$$

Inserting a_2^2/k and a_1^2/k here instead of p_2/ρ_2 and p_1/ρ_1, respectively, and using Eq. (3.6.21) for the speed of sound, we find

$$\frac{1}{kV_{n2}}\left(\frac{k+1}{2}a^{*2} - \frac{k-1}{2}V_2^2\right) - \frac{1}{kV_{n1}}\left(\frac{k+1}{2}a^{*2} - \frac{k-1}{2}V_1^2\right) = V_{n1} - V_{n2}$$

Introducing the values of $V_2^2 = V_{n2}^2 + V_\tau^2$ and $V_1^2 = V_{n1}^2 + V_\tau^2$ and multiplying both sides of the equation by $V_{n1}V_{n2}$, we obtain after simple transformations

$$\frac{k+1}{2k}a^{*2}(V_{n1} - V_{n2}) - \frac{k-1}{2k}V_\tau^2(V_{n1} - V_{n2}) + \frac{k-1}{2k}V_{n1}V_{n2}(V_{n1} - V_{n2}) = V_{n1}V_{n2}(V_{n1} - V_{n2})$$

Excluding the trivial solution $V_{n1} = V_{n2} = 0$ corresponding to the absence of a shock, we obtain

$$V_{n1}V_{n2} = a^{*2} - \frac{k-1}{k+1}V_\tau^2 \qquad (4.3.10)$$

This equation is used to determine the velocity behind a shock. It is called the **basic equation of an oblique shock**, and allows us to find the relative change in the velocity $\Delta\bar{V}_n = (V_{n1} - V_{n2})/V_{n1}$. For this purpose, let us write $V_{n1}V_{n2} = V_{n1}^2(V_{n2}/V_{n1})$ and use the relations $V_{n1} = V_1 \sin\theta_s$ and $V_\tau = V_1 \cos\theta_s$. After the relevant substitutions in (4.3.10), we obtain

$$\sin^2\theta_s(1 - \Delta\bar{V}_n) = \frac{1}{\lambda_1^2} - \frac{k-1}{k+1}(1 - \sin^2\theta_s)$$

where $\lambda_1 = V_1/a^*$.

Substituting Eq. (3.6.23) for λ_1 and performing transformations, we find

$$\Delta\bar{V}_n = \frac{2}{k+1}\left(1 - \frac{1}{M_1^2\sin^2\theta_s}\right) \qquad (4.3.11)$$

Let us introduce the symbol

$$\delta = (k-1)/(k+1) \qquad (4.3.12)$$

with a view to which formula (4.3.11) becomes

$$\Delta\bar{V}_n = (1-\delta)[1 - 1/(M_1^2\sin^2\theta_s)] \qquad (4.3.11')$$

By inserting this quantity into (4.2.13), we can determine the density ratio:

$$\rho_2/\rho_1 = M_1^2 \sin^2 \theta_s/(1 - \delta + \delta M_1^2 \sin^2 \theta_s) \qquad (4.3.13)$$

To determine the pressure ratio p_2/p_1, we shall use formula (4.2.15). We shall assume in it that $M_{n1} = M_1 \sin \theta_s$, substitute expression (4.3.11′) for $\Delta \bar{V}_n$, and replace the quantity k in accordance with (4.3.12) by the value

$$k = (1 + \delta)/(1 - \delta) \qquad (4.3.14)$$

The result is the parameter

$$p_2/p_1 = (1 + \delta) M_1^2 \sin^2 \theta_s - \delta \qquad (4.3.15)$$

that characterizes the **shock strength.** We may also use the following relation for this purpose:

$$(p_2 - p_1)/p_1 = \Delta p/p_1 = (1 + \delta)(M_1^2 \sin^2 \theta_s - 1) \qquad (4.3.15')$$

Formula (4.3.15′) can be used to obtain another parameter characterizing the shock strength, namely, the pressure coefficient $\bar{p}_2 = (p_2 - p_1)/q_1$, where $q_1 = [(1 + \delta)/(1 - \delta)] p_1 M_1^2/2$. By subtracting unity from both the left-hand and right-hand sides of (4.3.15′) and relating the expression obtained to q_1, we have

$$\bar{p}_2 = [2 (1 - \delta)/M_1^2] (M_1^2 \sin^2 \theta_s - 1) \qquad (4.3.15'')$$

Eliminating the quantity $M_1^2 \sin^2 \theta_s$ from Eqs. (4.3.15) and (4.3.13), we find the relation for the pressure-to-density ratios—the **Hugoniot equation:**

$$p_2/p_1 = (\rho_2/\rho_1 - \delta)/(1 - \delta\rho_2/\rho_1) \qquad (4.3.13')$$

This relation is also known as the **shock adiabat**. Unlike the conventional equation of an adiabat (isentrope) of the form $p = A\rho^k$, it shows how the parameters change in a transition through a shock wave. This transition process is attended by a growth in the entropy determined from Eq. (4.3.6).

Hence, the process of the transition through a shock is **non-isentropic.** In accordance with the change in the indicated parameters, the temperature behind a shock grows. Its value is calculated by the equation of state

$$\frac{T_2}{T_1} = \frac{p_2}{p_1} \cdot \frac{\rho_1}{\rho_2} = \frac{[(1+\delta) M_1^2 \sin^2 \theta_s - \delta]\,(1 - \delta + \delta M_1^2 \sin^2 \theta_s)}{M_1^2 \sin^2 \theta_s} \qquad (4.3.16)$$

The dependences of the ratios of the gas parameters behind a shock and ahead of it (ρ_2/ρ_1, p_2/p_1, T_2/T_1) on the quantity $M_{n1} = M_\infty \sin \theta_s$ for $k = 1.4$ ($\delta = 1/6$) are shown graphically in Fig. 4.3.1, and the Hugoniot equation (4.3.13′), in Fig. 4.3.2.

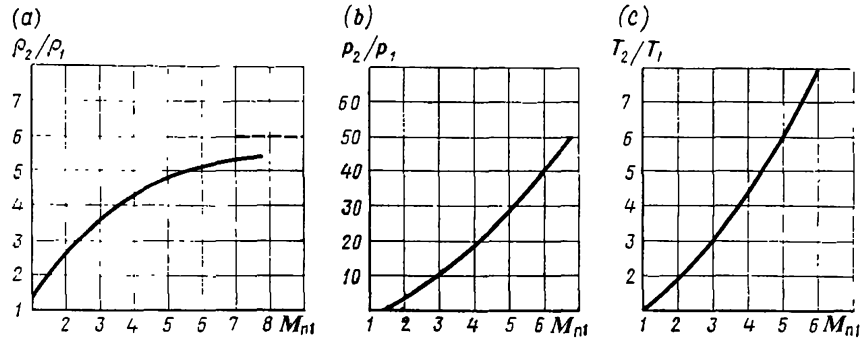

Fig. 4.3.1
Dependences of the ratios of the gas parameters behind a shock and ahead of it on the value of $M_{n1} = M_\infty \sin \theta_s$ for $k = 1.4$ ($\delta = 1/6$):
a—density ratio ρ_2/ρ_1; *b*—pressure ratio p_2/p_1; c—temperature ratio T_2/T_1

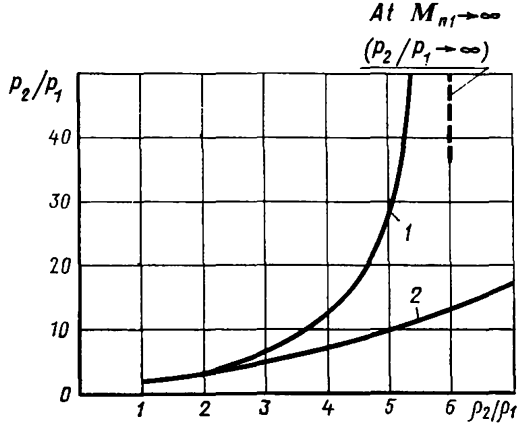

Fig. 4.3.2
Shock adiabat (1) and isentrope (2)
($k = 1.4$, $\delta = 1/6$)

The special form of the transition through a shock, differing from an isentropic process, manifests itself in the different nature of the change in the gas parameters. It follows from (4.3.15) and (4.3.16) that at $M_1 \to \infty$, the pressure and temperature grow without a limit. It also follows from (4.3.13) that for the same condition $M_1 \to \infty$ the density tends to a certain definite value equal to $(\rho_2/\rho_1)_{M_1 \to \infty} = 1/\delta$. When $k = 1.4$, this yields the value of $1/\delta = 6$. It follows from the formula $p = A\rho^k$ or $T = B\rho^{k-1}$ (A and B are constants) that in an isentropic process an infinite increase in the density and temperature corresponds to an infinite pressure increase. A comparison allows us to arrive at the conclusion that with an identical change in the pressure in both a shock and isentropic processes, the former is attended by greater heating of the gas, and this is just what facilitates a certain drop in the density.

Formula (4.3.16) determines the ratio of the squares of the sound speed in accordance with the relation

$$a_2^2/a_1^2 = T_2/T_1 \qquad (4.3.17)$$

Using this relation, and also Eq. (4.2.18′), we can determine the number M_2 behind a shock. Inserting expression (4.2.21) for $\Delta\bar{V}_n$ into (4.2.18′), we find

$$V_2^2/V_1^2 = \cos^2\theta_s + (\rho_1/\rho_2)^2 \sin^2\theta_s \qquad (4.3.18)$$

Dividing Eq. (4.3.18) by (4.3.17), we obtain an expression for the ratio of the squares of the Mach numbers:

$$M_2^2/M_1^2 = (T_1/T_2)\,[\cos^2\theta_s + (\rho_1/\rho_2)^2 \sin^2\theta_s] \qquad (4.3.19)$$

where T_1/T_2 and ρ_1/ρ_2 are found from formulas (4.3.16) and (4.3.13), respectively.

The formula for calculating M_2 can be obtained in a somewhat different form with the aid of momentum equation (4.2.4″). Let us write it in the form

$$\frac{p_1}{p_2}\left(1 + \frac{\rho_1}{\rho_2} V_1^2 \sin^2\theta_s\right) = 1 + \frac{\rho_2}{p_2} V_2^2 \sin^2(\theta_s + \beta_s)$$

Taking into account that $kp/\rho = [(1 + \delta)/(1 - \delta)]\, p/\rho$, and determining p_2/p_1 by the Hugoniot equation (4.3.13′), we obtain

$$\frac{1-\delta(\rho_2/\rho_1)}{\rho_2/\rho_1 - \delta}\left(1 + \frac{1+\delta}{1-\delta} M_1^2 \sin^2\theta_s\right) = 1 + \frac{1+\delta}{1-\delta} M_2^2 \sin^2(\theta_s - \beta_s)$$

After substituting for $M_1^2 \sin^2\theta_s$ its value found from (4.3.13), we obtain the relation

$$M_2^2 \sin^2(\theta_s - \beta_s) = (1 - \delta)(\rho_2/\rho_1 - \delta)^{-1} \qquad (4.3.19')$$

Let us determine the stagnation pressure for the conditions of a flow behind a shock. Considering the flow of a gas behind a shock and ahead of it to be isentropic, we can compile the thermodynamic relations:

$$p_2/\rho_2^k = p_0'/\rho_0'^k, \quad p_1/\rho_1^k = p_0/\rho_0^k$$

where p_0 and p_0', ρ_0 and ρ_0' are the stagnation pressure and density in the regions of the flow ahead of the shock and behind it, respectively. These relations yield the **pressure recovery ratio across a shock wave:**

$$\nu_0 = p_0'/p_0 = (p_2/p_1)\,(\rho_1/\rho_2)^k\,(\rho_0'/\rho_0)^k$$

Multiplying both sides of this equation by the ratio $(p_0/p_0')^k$, we obtain

$$\nu_0^{1-k} = \left(\frac{p_0'}{p_0}\right)^{1-k} = \frac{p_2}{p_1}\left(\frac{\rho_1}{\rho_2}\right)^k \left(\frac{\rho_0'}{p_0'} \cdot \frac{p_0}{\rho_0}\right)$$

Let us use the energy equation $V^2/2 + c_pT = \text{const}$ and write it for the conditions ahead of and behind a shock:

$$V_1^2/2 + c_pT_1 = V_2^2/2 + c_pT_2$$

At points of stagnation, $V_1 = V_2 = 0$. It follows from the energy equation that the temperatures at these points are identical, i.e. $T_0 = T_0'$ or, which is the same, $p_0/\rho_0 = p_0'/\rho_0'$.

Consequently,

$$\nu_0 = p_0'/p_0 = (p_1/p_2)^{1/(k-1)} (\rho_2/\rho_1)^{k/(k-1)} \tag{4.3.20}$$

or

$$\nu_0 = p_0'/p_0 = (p_1/p_2)^{(1-\delta)/2\delta} (\rho_2/\rho_1)^{(1-\delta)/2\delta} \tag{4.3.20'}$$

where p_1/p_2 and ρ_2/ρ_1 are found by (4.3.15) and (4.3.13), respectively.

By (3.6.28), the stagnation pressure is

$$p_0 = p_1 \left(1 + \frac{\delta}{1-\delta} M_1^2\right)^{(1+\delta)/2\delta} \tag{4.3.21}$$

Consequently,

$$\frac{p_0'}{p_1} [(1+\delta) M_1^2 \sin^2\theta_s - \delta]^{(\delta-1)/2\delta} (M_1 \sin\theta_s)^{(1+\delta)/\delta} \times (1-\delta)^{-(1+\delta)/2\delta} \frac{\left(1+\frac{\delta}{1-\delta} M_1^2\right)^{(1+\delta)/2\delta}}{\left(1+\frac{\delta}{1-\delta} M_1^2 \sin^2\theta_s\right)^{(1+\delta)/2\delta}} \tag{4.3.22}$$

Let us determine the stagnation pressure coefficient behind an oblique shock

$$\bar{p}_0 = \frac{p_0' - p_1}{q_1} = \frac{2(1-\delta)}{(1+\delta) M_1^2} \left\{ [(1+\delta) M_1^2 \sin^2\theta_s - \delta]^{(\delta-1)/2\delta} \times (M_1 \sin\theta_s)^{(1+\delta)/\delta} (1-\delta)^{-(1+\delta)/2\delta} \times \frac{\left(1+\frac{\delta}{1-\delta} M_1^2\right)^{(1+\delta)/2\delta}}{\left(1+\frac{\delta}{1-\delta} M_1^2 \sin^2\theta_s\right)^{(1+\delta)/2\delta}} - 1 \right\} \tag{4.3.23}$$

An analysis of relation (4.3.20) shows that behind a shock of finite strength the pressure ratio p_0'/p_0 is always less than unity. The stronger the shock, the larger are the stagnation pressure losses and, consequently, the smaller is the ratio p_0'/p_0.

When establishing the physical nature of these losses, we cannot consider a shock as a discontinuity surface; we must take into account that a real compression process occurs in a layer with a small thickness of the order of the molecular free path. It is exactly such a process

of transition through a shock in a layer that is possible because the existence of two contacting regions with a finite difference of their temperatures, pressures, and densities cannot be visualized. It is only a mathematical abstraction.

The transition through a shock having a small thickness is characterized by so great velocity and temperature gradients that in the compression regions the *influence of skin friction and heat conduction* becomes quite substantial. It thus follows that the irreversible losses of the kinetic energy of gas in a transition through a shock are associated with the work done by the friction forces, and also with the heat conduction. The action of these dissipative forces and also heat transfer within the compression zone cause an *increase in the entropy* and a resulting *reduction in the pressure* in the flow behind the shock in comparison with an isentropic compression process.

Oblique Shock Angle

The parameters behind an oblique shock are determined by the number M_1 and the shock angle θ_s. Its magnitude, determined by the same number M_1 and the flow deflection angle β_s, can be calculated by using Eq. (4.2.19). Substituting for $\Delta\overline{V}_n$ in it its value from (4.2.21), we obtain a working relation:

$$\tan\theta_s/\tan(\theta_s - \beta_s) = \rho_2/\rho_1 \qquad (4.3.24)$$

Determining ρ_1/ρ_2 from (4.3.13), we find

$$\tan\theta_s/\tan(\theta_s - \beta_s) = M_1^2\sin^2\theta_s/(1 - \delta + \delta M_1^2\sin^2\theta_s) \qquad (4.3.25)$$

On the other hand, this relation allows us to find the flow deflection angle β_s behind a shock according to the known shock angle. Figure 4.3.3 presents graphically the relation between the angles θ_s and β_s for various values of the number M_1. In the region to the left of the dashed line, which corresponds to the maximum values of the angle β_s (i.e., $\beta_{s,\max}$), the value of the angle θ_s diminishes with decreasing β_s, and to the right, conversely, it grows with decreasing β_s. This nature of the relation is due to the different form of a shock. In the first case, the change in the angle θ_s corresponds to an attached curved shock ahead of a sharp-nosed body. As the body becomes blunter (the nose angle increases), the flow deflection angle grows, and, consequently, the shock angle increases. The maximum flow deflection angle $\beta_s = \beta_{s,\max}$ is determined only by the given value of M_1. This angle is also called the **critical flow deflection (deviation) angle** β_{cr}. The points corresponding to its values are connected in Fig. 4.3.3 by a dashed line. Investigations show that a flow behind an attached shock is stable as long as in the entire region behind it the flow deflection angle is smaller than the critical one. This flow is accordingly referred to as a **subcritical** one.

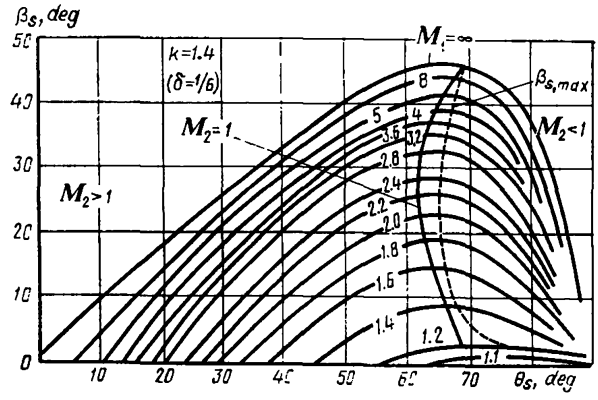

Fig. 4.3.3
Change in the flow deflection angle β_s depending on the shock angle θ_s for various numbers M_1

Upon a further growth of the nose angle, the angle β_s may become critical. According to Fig. 4.3.3, its value grows with an increase in the number M_1. From the physical viewpoint, this is explained by an increase in the strength of a shock, a greater density behind it, and, as a result, by the shock coming close to the surface of the body, which leads to deflection of the flow through a larger angle.

At a still larger nose angle, the flow behind an attached shock becomes unstable, as a result of which the shock moves away from the nose. Behind such a detached shock, a new stable flow region appears. It is characterized by deflection through an angle also less than the critical one. But unlike a subcritical flow, this one is called **supercritical.** This definition corresponds to the fact that the nose angle of the body in the flow exceeds the value at which a shock is still attached.

A detached shock changes its shape absolutely, which can be seen especially clearly in the example of a flow over a sharp-nosed cone or wedge (Fig. 4.3.4). As long as the flow is subcritical, the shock is attached to the nose and the generatrix of its surface is straight. The flow around thick wedges or cones may become supercritical, upon which the shock detaches and acquires a curved shape. At the point of intersection of the shock surface with the flow axis, the shock angle $\theta_s = \pi/2$ and, consequently, the parameters change according to the law of a normal shock. In practice, there is a section of such a normal shock near the axis.

With an increase in the distance from the axis, the shock angle θ_s in accordance with Fig. 4.3.4 diminishes, remaining on a certain section larger than the value that a subcritical flow corresponds to. The change in the flow deflection angle is of the opposite nature.

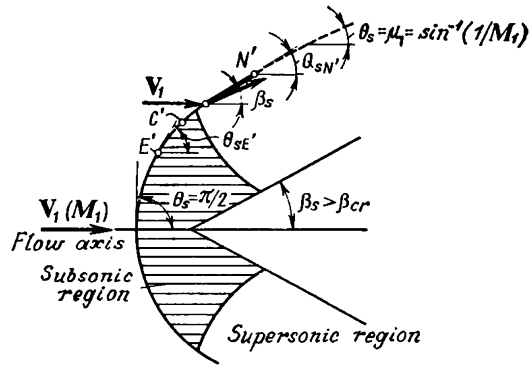

Fig. 4.3.4
Detached shock ahead of a sharp-nosed body

At the apex of the detached wave behind its straight part, $\beta_s = 0$, and then it grows. At a certain point on the surface, the angle β_s becomes critical, and then it again diminishes together with the shock angle. As follows from (4.3.25), at the limit when $\beta_s \to 0$, the angle θ_s tends to the value $\mu_1 = \sin^{-1}(1/M_1)$. Hence, the shock angles at a preset number M_1 vary within the interval $\mu_1 \leqslant \theta_s \leqslant \pi/2$. A shock of an infinitely small strength that is a simple pressure wave corresponds to the value $\theta_s = \mu_1$.

On a curved shock (see Fig. 4.3.3), we can find two points corresponding to two different angles θ_s that at a given M_1 determine the same value of the angle β_s. This angle is calculated by formula (4.2.20), which after introducing into it the value of $\Delta\bar{V}_n$ from (4.3.11) acquires the form

$$\tan\beta_s = \cot\theta_s\,(M_1^2\sin^2\theta_s - 1)\left[1 + \left(\frac{1}{1-\delta} - \sin^2\theta_s\right)M_1^2\right]^{-1} \quad (4.3.26)$$

A strong shock with a subsonic flow behind it corresponds to a larger value of the angle θ_s, and a weak shock with a supersonic flow behind it (if we exclude the vicinity of the shock with angles β_s close to the critical ones, where the flow may be subsonic) corresponds to a smaller value of the angle θ_s.

An oblique shock angle can be evaluated by using formula (4.2.25). Substituting the relative density from (4.2.21) for $\Delta\bar{V}_n$, we obtain

$$\tan\theta_s = \cot\beta_s\left[\frac{1}{2}\left(\frac{\rho_2}{\rho_1} - 1\right) \pm \sqrt{\frac{1}{4}\left(\frac{\rho_2}{\rho_1} - 1\right)^2 - \tan^2\beta_s\,\frac{\rho_2}{\rho_1}}\right] \quad (4.3.27)$$

On each curve shown in Fig. 4.3.3, we can indicate a point corresponding to the value of $M_2 = 1$ behind a curved shock. By connecting these points with a solid curve, we obtain the boundary of

two flow conditions behind such a shock: to the left of the curve the flow will be supersonic ($M_2 > 1$), and to the right of it—subsonic ($M_2 < 1$).

4.4. Hodograph

In addition to an analytical solution of the problem of determining the flow parameters behind an oblique shock, there is a graphical method based on the concept of a hodograph.

A **hodograph** is a curve forming the locus of the tips of the velocity vectors in the plane behind a shock. Let us consider the equation of a hodograph. Let point A (Fig. 4.4.1) be the tip of the velocity vector $\mathbf{V}_2$ and be located, consequently, on a hodograph constructed in a coordinate system whose horizontal axis coincides with the direction of the velocity $\mathbf{V}_1$ ahead of a shock. Hence, the inclination of the velocity vector $\mathbf{V}_2$ is determined by the angle β_s. Let us designate the vertical and horizontal components of this velocity by w and u, respectively. A glance at Fig. 4.4.1 reveals that u and w can be expressed in terms of the normal V_{n2} and tangential V_τ components of the velocity $\mathbf{V}_2$ to the plane of the shock as follows:

$$u = V_\tau \cos\theta_s + V_{n2}\sin\theta_s, \quad w = V_\tau \sin\theta_s - V_{n2}\cos\theta_s \quad (4.4.1)$$

We determine the component V_{n2} from formula (4.3.10) in which we assume that $V_{n1} = V_1 \sin\theta_s$ and $V_\tau = V_1 \cos\theta_s$. Accordingly,

$$u = V_1\cos^2\theta_s + \left(a^{*2} - \frac{k-1}{k+1}V_1^2\cos^2\theta_s\right)\Big/ V_1 \quad (4.4.2)$$

Let us eliminate the angle θ_s from this equation. For this purpose, we shall use Eqs. (4.4.1). Multiplying the first of them by $\cos\theta_s$, the second by $\sin\theta_s$ and summating them, we obtain

$$u\cos\theta_s + w\sin\theta_s = V_\tau$$

Having in view that $V_\tau = V_1\cos\theta_s$, we find

$$\tan\theta_s = (V_1 - u)/w \quad (4.4.3)$$

Substituting for $\tan\theta_s$ its value from (4.4.3) into the trigonometric relation $\cos^2\theta_s = (1 + \tan^2\theta_s)^{-1}$, we obtain

$$\cos^2\theta_s = [1 + (V_1 - u)^2/w^2]^{-1}$$

Introduction of this value into (4.4.2) yields

$$u = \frac{V_1}{1 + [(V_1 - u)/w]^2} + \left\{a^{*2} - \frac{k-1}{k+1}V_1^2\left[1 + \left(\frac{V_1 - u}{w}\right)^2\right]^{-1}\right\}\Big/ V_1$$

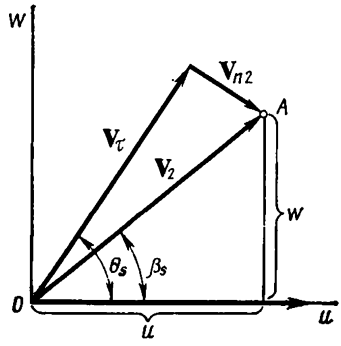

Fig. 4.4.1
To the derivation of the hodograph equation

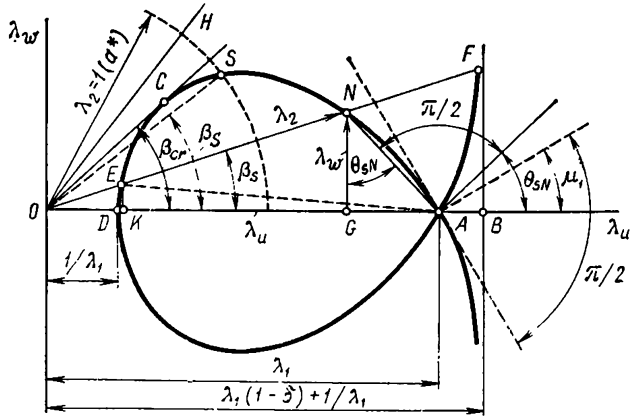

Fig. 4.4.2
Strophoid (shock polar)

This expression, relating the variables w and u, is an **equation of a hodograph**. It is usually written in the form

$$\frac{w^2}{(V_1-u)^2} = (u-a^{*2}/V_1)\Big/\left(\frac{2}{k+1}V_1+\frac{a^{*2}}{V_1}-u\right) \qquad (4.4.4)$$

Let us introduce the dimensionless quantities $\lambda_u = u/a^*$, $\lambda_w = w/a^*$, $\lambda_1 = V_1/a^*$, and the parameter $\delta = (k-1)/(k+1)$. The hodograph equation now becomes

$$\lambda_w^2/(\lambda_1-\lambda_u)^2 = (\lambda_u\lambda_1-1)/[(1-\delta)\lambda_1^2+1-\lambda_1\lambda_u] \qquad (4.4.4')$$

Equation (4.4.4') graphically depicts on the plane λ_w, λ_u a curve known as a **strophoid** (Fig. 4.4.2). Let us determine certain characteristic points of a strophoid. Particularly, let us calculate the coordinates of points A and D of intersection of the strophoid with the axis λ_u. Examination of (4.4.4') reveals that the condition λ_w is

satisfied if $\lambda_u = \lambda_1$ or $\lambda_u = 1/\lambda_1$. The value $\lambda_u = \lambda_1$ determines the coordinate of point A and makes it possible to obtain a solution corresponding to a shock of an infinitely small strength behind which the velocity does not change. The value $\lambda_u = 1/\lambda_1$ determines the coordinate of intersection point D closest to the origin of coordinates and is the solution for a normal shock.

It follows from the construction of a strophoid that its two branches to the right of point A extend to infinity, asymptotically approaching the straight line passing through point B and parallel to the vertical axis. The coordinate of this point can be obtained from (4.4.4′) by a limit transition at $\lambda_w \to \infty$. The result is the condition $(1 - \delta)\lambda_1^2 + 1 - \lambda_1\lambda_u = 0$. from which we find the coordinate of point B, i.e. $\lambda_u = \lambda_1(1 - \delta) + 1/\lambda_1$.

Any point on a strophoid branch extending to infinity formally yields a solution for a shock. Considering, for example, point F in Fig. 4.2.2, we may assume that for a shock behind which the direction of the velocity changes by a preset value of the angle β_s, the velocity increases abruptly to the value λ_2 determined by the length of segment OF. The pressure and density would also decrease abruptly. In other words, in the given case there would be not a compression shock, but an expansion one. But the formation of such shocks is impossible physically. To prove this, let us use formula (4.3.6) for the change in the entropy. Applying the ratios $p_2\rho_2^k = p_0'(\rho_0')^k$. $p_1/\rho_1^k = p_0/\rho_0^k$, and taking into account that $p_0'/p_0 = \rho_0'/\rho_0$, from formula (4.3.6) we obtain

$$S_2 - S_1 = R \ln (p_0/p_0') \tag{4.4.5}$$

When there is a compression shock, $p_0 > p_0'$ and, consequently, $S_2 - S_1 > 0$. This conclusion corresponds to the second law of thermodynamics, according to which the entropy of an isolated system with compression shocks increases.

Let us now consider the reverse situation when a gas passes from a state characterized by the stagnation pressure p_0' (the parameters with the subscript 2) into a state with the stagnation pressure p_0 (the parameters with the subscript 1) through an expansion shock. In this case, by analogy with (4.4.5), the change in the entropy is

$$S_1 - S_2 = R \ln (p_0'/p_0)$$

Hence, when the condition $p_0' < p_0$ is retained, the entropy should diminish, but this contradicts the second law of thermodynamics. It thus follows that expansion shocks cannot appear.

In accordance with the above, the passage of a gas through a shock, which is adiabatic in its nature because it occurs in a thermally insulated system, is an **irreversible adiabatic non-isentropic process.**

Equation (4.3.6) can be used to verify that a real process of an increase in the entropy ($S_2 - S_1 > 0$) corresponds to a supersonic

flow [$M_1 > 1$ (a normal shock), $M_1 \sin \theta_s > 1$ (an oblique shock)], while the physically impossible phenomenon of a decrease in the entropy ($S_2 - S_1 < 0$), to a subsonic flow ($M_1 < 1$ and $M_1 \sin \theta_s < 1$). Hence, *shocks can appear only in a supersonic flow.* We must note that the relations obtained for the change in the entropy are valid when an irreversible process of transition through a shock is attended by an isentropic flow of the gas both ahead of a shock and behind it.

It follows from the above that the branches of a strophoid extending to infinity have no physical meaning. The part of a strophoid (to the left of point A, Fig. 4.4.2) having a physical meaning is called a **shock polar.** Such a curve is constructed for a given number λ_1 (or M_1). Several curves constructed for various values of λ_1 form a family of shock polars allowing one to calculate graphically the velocity of a flow behind a shock and the flow deflection angle.

Let us consider an attached shock ahead of a wedge-shaped surface with the half-angle β_s (see Fig. 4.1.1*c*). To determine the velocity behind such a shock, we construct a shock polar corresponding to the given number λ_1 (or M_1) and draw a straight line from point O (Fig. 4.4.2) at the angle β. Point of intersection N with the shock polar determines the vector $\overrightarrow{ON}$ whose magnitude shows the value of the velocity ratio λ_2 behind the shock. By formula (4.4.3), which we shall write in the form

$$\tan \theta_s = (\lambda_1 - \lambda_u)/\lambda_w \qquad (4.4.3')$$

the angle ANG on the shock polar equals the shock angle θ_{sN}. We must note that this angle can also be determined as the angle between the horizontal axis and a normal to the straight line connecting the tips of the velocity vectors ahead of a shock and behind it (points A and N, respectively, in Fig. 4.4.2).

When considering the shock polar, we can arrive at the conclusion that a decrease in the angle β_s (point N moves along the curve toward point A) is attended by a decrease in the shock angle θ_{sN}. At the limit, when $\beta_s \to 0$, point N merges with point A, which physically corresponds to the transformation of the shock wave into an **infinitesimal shock wave,** i.e. into a **line of weak disturbances.** The shock angle for such a shock $\theta_s = \mu_1$ is determined as the angle between the horizontal axis and the straight line perpendicular to a tangent to the shock polar at point A (Fig. 4.4.2).

A growth in the flow deflection angle (in Fig. 4.4.2 this corresponds to point N moving away from A) leads to an increase in the shock angle and to a higher strength of the shock. A glance at the shock polar shows that at a certain angle β_s a straight line drawn from point O will be tangent to the curve at point C. The angle of inclination of this tangent determines the maximum flow deflection angle, called the critical one above ($\beta_s = \beta_{cr}$). Assume that the wedge

angle $\beta_s > \beta_{cr}$. In the graph, solid line OH drawn from point O and not intersecting the shock polar corresponds to this angle.

Therefore, when $\beta_s > \beta_{cr}$, we cannot find a graphical solution for a shock with the aid of a shock polar. This is due to the fact that the inequality $\beta_s > \beta_{cr}$ does not correspond to the assumptions (on the basis of which we obtained equations for a shock) consisting in that a shock is straight and should be attached to a nose. Physically—in the given case of the wedge angle β_s exceeding the critical deflection angle β_{cr}—the compression shock detaches and becomes curved.

The determination of the shape of such a curved shock and of its distance to the body is the task of a special problem of aerodynamics associated, particularly, with the conditions of supercritical flow past a wedge. If such a problem is not solved, then with the aid of a polar in the field of definition from point D to A we can give only a qualitative appraisal of the change in the parameters in a region ahead of the surface in the flow. If, on the other hand, the shape of the shock is determined for preset flow conditions (in addition to calculations, this can also be done with the aid of blowing in a wind tunnel), it is possible to establish quantitative correspondence between the points of a shock polar and the shock surface.

Assume, for example, that we have set the angle β_s and points E and N on a shock polar (Fig. 4.4.2). The shock angle $\theta_{sN} = \angle ANG$ corresponds to point N, and the angle $\theta_{sE} = \angle AEK$ ($EK \perp OB$) to point E. If the configuration of the shock wave front is known, then by direct measurement we can find on it a point N' with the wave angle $\theta_{sN'}$ and a point E' with the angle $\theta_{sE'}$ (see Fig. 4.3.4). In the same way, we can find a point C' on the shock that corresponds to the critical (maximum) deflection angle β_{cr}.

On a preset surface of a detached shock, point D on the shock polar corresponds to the shock apex (a normal shock), and terminal point A of the polar corresponds to the remotest part of the shock that has transformed into a line of weak disturbances.

For an attached shock ($\beta_s < \beta_{cr}$), we can indicate two solutions, as can be seen on the shock polar. One of them (point E) corresponds to a lower velocity behind the shock, and the other (point N), to a higher one. Observations show that attached shocks with a higher velocity behind them, i.e. shocks with a lower strength are possible physically.

If we draw on the graph the arc of a circle whose radius is unity (in the dimensional axes w and u this corresponds to a radius equal to the critical speed of sound a^*), we can determine the regions of the flow—subsonic and supersonic—which points on the shock polar to the left and right of the arc correspond to. In Fig. 4.3.4, the section of the flow corresponding to a subsonic velocity is hatched. A close look at the shock polar reveals that the velocity is always

subsonic behind a normal shock. On the other hand, behind an oblique (curved) shock, the velocity may be either supersonic (the relevant points on the shock polar are to the right of point S) or subsonic (the points on the polar are to the left of point S). Points on the polar between S and C correspond to an attached shock behind which the velocities are subsonic. Experimental investigations show that for wedge angles β_s less than the critical one β_{cr} or larger than $\angle SOB$, a shock remains attached, but it becomes curved. The theoretical values for the angle θ_s and the gas velocity λ_2 on the entire section behind such a curved shock found on the polar according to the wedge angle β_s do not correspond to the actual values.

4.5. A Normal Shock in the Flow of a Gas with Constant Specific Heats

We shall obtain the corresponding relations for a normal shock from the condition that $\theta_s = \pi/2$ and, consequently, $V_{n1} = V_1$ and $V_{n2} = V_2$. Basic equation (4.3.10) becomes

$$V_1 V_2 = a^{*2} \tag{4.5.1}$$

or

$$\lambda_1 \lambda_2 = 1 \tag{4.5.1'}$$

where $\lambda_1 = V_1/a^*$ and $\lambda_2 = V_2/a^*$.

We find the relative change in the velocity from (4.3.11'):

$$\Delta\overline{V} = (V_1 - V_2)/V_1 = (1 - \delta)(1 - 1/M_1^2) \tag{4.5.2}$$

We obtain the corresponding relations for the ratios of the densities, pressures, and temperatures from (4.3.13), (4.3.15), and (4.3.16):

$$\rho_2/\rho_1 = M_1^2/(1 - \delta + \delta M_1^2) \tag{4.5.3}$$

$$p_2/p_1 = (1 + \delta) M_1^2 - \delta \tag{4.5.4}$$

$$T_2/T_1 = [(1 + \delta) M_1^2 - \delta](1 - \delta + \delta M_1^2)/M_1^2 \tag{4.5.5}$$

By eliminating M_1^2 from (4.5.3) and (4.5.4), we obtain an equation of a shock adiabat for a normal shock that in its appearance differs in no way from the similar equation for an oblique shock [see (4.3.13')].

Assuming in (4.3.19) that $\theta_s = \pi/2$, we find the relation for the Mach number behind a normal shock:

$$M_2^2/M_1^2 = (T_1/T_2)(\rho_1/\rho_2)^2 \tag{4.5.6}$$

Let us consider the parameters of a gas at the point of stagnation (at the critical point) of a blunt surface behind a normal shock (Fig. 4.5.1). The pressure p_0' at this point is determined by formula

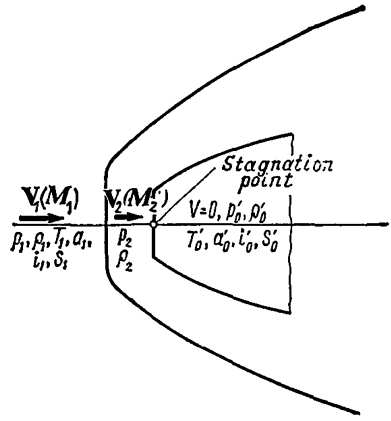

Fig. 4.5.1
Parameters of a gas at the stagnation point behind a normal shock

(4.3.20′) in which the ratios ρ_2/ρ_1 and p_2/p_1 are found from (4.5.3) and (4.5.4), respectively. With this in view, we have

$$p_0'/p_0 = [(1+\delta)M_1^2 - \delta]^{(\delta-1)/2\delta}\,[M_1^2/(1-\delta+\delta M_1^2)]^{(1+\delta)/2\delta} \qquad (4.5.7)$$

Determining p_0 by (4.3.21), we find

$$p_0'/p_1 = [(1+\delta)M_1^2 - \delta]^{(\delta-1)/2\delta}\,M_1^{(1+\delta)/\delta}\,(1-\delta)^{-(1+\delta)/2\delta} \qquad (4.5.8)$$

Knowing the absolute pressure p_0', we can determine the dimensionless quantity $\bar{p}_0 = (p_0' - p_1)/q_1$—the pressure coefficient at the stagnation point. Taking into account that the velocity head is

$$q_1 = \frac{kp_1M_1^2}{2} = \frac{1+\delta}{2(1-\delta)}\,p_1M_1^2$$

we obtain

$$\bar{p}_0 = \frac{2(1-\delta)}{(1+\delta)M_1^2}\{[(1+\delta)M_1^2-\delta]^{(\delta-1)/2\delta}M_1^{(1+\delta)/\delta} \times (1-\delta)^{-(1+\delta)/2\delta} - 1\} \qquad (4.5.9)$$

It is proved in Sec. 4.3 that the stagnation temperature behind a shock does not change, i.e. $T_0' = T_0$. Consequently, at the stagnation point, we have

$$T_0' = T_1\left(1 + \frac{\delta}{1-\delta}M_1^2\right) \qquad (4.5.10)$$

Let us use the expression $i_0' = c_pT_0'$ and $i_1 = c_pT_1$ to determine the enthalpy. Accordingly, at the stagnation point, we have

$$i_0' = i_1\left(1 + \frac{\delta}{1-\delta}M_1^2\right) \qquad (4.5.11)$$

4.6. A Shock at Hypersonic Velocities and Constant Specific Heats of a Gas

At hypersonic (very high) velocities, which values of $M_1 \sin \theta_s \gg \gg 1$ correspond to, the dimensionless parameters of a gas behind a shock are very close to their limiting values obtained at $M_1 \sin \theta_s \to \to \infty$. It follows from (4.3.11′) that for this condition, we have

$$\Delta \bar{V}_n = 1 - \delta \tag{4.6.1}$$

Consequently, the limiting ratio of the densities by (4.2.13) is

$$\rho_1/\rho_2 = 1 - \Delta \bar{V}_n = \delta \tag{4.6.2}$$

Introducing this value into (4.3.27), we obtain the following expression at the limit when $M_1 \sin \theta_s \to \infty$:

$$\tan \theta_s = (\cot \beta_s/2\delta)\,[1 - \delta \pm \sqrt{(1-\delta)^2 - 4\delta \tan^2 \beta_s}\,] \tag{4.6.3}$$

Let us find the limiting value of the pressure coefficient. For the conditions directly behind a shock, as follows from (4.3.15″), when $M_1 \sin \theta_s \to \infty$ and $M_1 \to \infty$, we have

$$\bar{p}_2 = 2\,(1 - \delta) \sin^2 \theta_s \tag{4.6.4}$$

We obtain the corresponding quantity for the point of stagnation from (4.3.23):

$$\bar{p}_0 = 2\,(1 - \delta)^{(\delta-1)/2\delta}\ (1 + \delta)^{-(1+\delta)/2\delta} \sin^2 \theta_s \tag{4.6.5}$$

The ratio of the pressure coefficients is

$$\bar{p}_0/\bar{p}_2 = (1 - \delta^2)^{-(1+\delta)/2\delta} \tag{4.6.6}$$

In the particular case when $\delta = 1/6$ ($k = 1.4$), the ratio $\bar{p}_0/\bar{p}_2 = 1.09$. The limiting value of the number M_2 can be found from (4.3.19), using relation (4.3.16) for T_2/T_1. A passage to the limit when $M_1 \sin \theta_s \to \infty$ and $M_1 \to \infty$ yields

$$M_2^2 = \{1/[\delta\,(1 + \delta)]\}\,(\cot^2 \theta_s + \delta^2) \tag{4.6.7}$$

To find the limiting parameters behind a normal shock, we must assume that $\theta_s = \pi/2$ in the above relations. As a result, from (4.6.4) and (4.6.5) we have:

$$\bar{p}_2 = 2\,(1 - \delta) \tag{4.6.4′}$$

$$\bar{p}_0 = 2\,(1 - \delta)^{(\delta-1)/2\delta}\,(1 + \delta)^{-(1+\delta)/2\delta} \tag{4.6.5′}$$

We can see that the ratio $\bar{p}_0/\bar{p}_2$ is the same as for an oblique shock. The limiting Mach number behind a normal shock is

$$M_2 = \sqrt{\delta/(1-\delta)} \qquad (4.6.7')$$

For $\delta = 1/6$ ($k = 1.4$), the number $M_2 = \sqrt{1/7} \approx 0.38$. The actual values of the dimensionless parameters behind a shock at finite, although very large, Mach numbers depend on M_1.

Let us consider the corresponding working relations for the case when attached shocks originate ahead of slender wedges, and the shock angles are therefore low. Assuming in (4.3.25) that $\tan\theta_s \approx \approx \theta_s$ and $\tan(\theta_s - \beta_s) \approx \theta_s - \beta_s$. we obtain

$$(\theta_s - \beta_s)\,\theta_s = (1 - \delta + \delta M_1^2\theta_s^2)/(M_1^2\theta_s^2)$$

Introducing the symbol $K = M_1\beta_s$, after transformations, we find

$$\frac{\theta_s^2}{\beta_s^2} - \frac{1}{1-\delta}\cdot\frac{\theta_s}{\beta_s} - \frac{1}{K^2} = 0 \qquad (4.6.8)$$

Solving this equation for θ_s/β_s and taking into account that the condition $\theta_s/\beta_s > 1$ is physically possible. we find

$$\frac{\theta_s}{\beta_s} = \frac{1}{2(1-\delta)} + \sqrt{\frac{1}{4(1-\delta)^2} + \frac{1}{K^2}} \qquad (4.6.9)$$

Inspection of Eq. (4.6.9) reveals that the parameters determining the flow in a shock at very high velocities are combined into functional groups such that they are *a solution of the problem of a shock for a broad range of numbers* M_∞ *and values of the angle* β_s *in the form of a single curve*. Equation (4.6.9) is an example of a similarity relation. In accordance with this equation for the ratio θ_s/β_s, the quantity $K = M_1\beta_s$ is a **similarity criterion**. This similarity must be understood in the sense that regardless of the absolute value of the quantities characterizing hypersonic flows, when such flows have identical parameters K, the ratios of the angles θ_s/β_s are also identical. When $K \to \infty$, the ratio θ_s/β_s tends to a limit equal to

$$\theta_s/\beta_s = 1/(1-\delta) \qquad (4.6.10)$$

Let us consider the relation for the pressure coefficient. At low values of θ_s, formula (4.3.15″) acquires the form

$$\bar{p}_2 = 2(1-\delta)(\theta_s^2 - 1/M_1^2)$$

or

$$\bar{p}_2 = 2(1-\delta)\beta_s^2(\theta_s^2/\beta_s^2 - 1/K^2) \qquad (4.6.11)$$

Introducing the value of $1/K^2$ from (4.6.8). we obtain

$$\bar{p}_2 = 2\beta_s\theta_s \qquad (4.6.11)$$

Substituting for the angle θ_s the value determined from (4.6.9), we find

$$\frac{\bar{p}^2}{\beta_s^2} = \frac{1}{1-\delta}\left[1 + \sqrt{1 + \frac{4(1-\delta)^2}{K^2}}\right] \qquad (4.6.12)$$

This formula shows that K is also a similarity criterion for the ratio $\bar{p}_2/\beta_s^2$. At the limit when $K \to \infty$, this ratio becomes

$$\bar{p}_2/\beta_s^2 = 2/(1-\delta) \qquad (4.6.13)$$

In accordance with (4.3.13), at small value of θ_s, the density ratio is

$$\rho_2/\rho_1 = K_s^2/(1 - \delta + \delta K_s^2) \qquad (4.6.14)$$

where the parameter $K_s = M_1\theta_s$ is determined with the aid of (4.6.9) in the following form:

$$K_s = \frac{K}{2(1-\delta)}\left[1 + \sqrt{1 + \frac{4(1-\delta)^2}{K^2}}\right] \qquad (4.6.15)$$

We can see from (4.3.18) that at low values of θ_s the second term on the right-hand side may be ignored, and we can thus consider that $V_2 \approx V_1$. With this in view, the ratio of the squares of the Mach numbers in accordance with (4.3.19) is $M_2^2/M_1^2 = T_1/T_2$. Substituting for the ratio T_1/T_2 here its value from formula (4.3.16) in which we assume that $\sin\theta_s \approx \theta_s$, we obtain

$$\theta_s^2 M_2^2 = K_s^4/\{[(1+\delta)K_s^2 - \delta](1 - \delta + \delta K_s^2)\} \qquad (4.6.16)$$

When $K_s \to \infty$, we have

$$\theta_s^2 M_2^2 \to 1/[\delta(1+\delta)] \qquad (4.6.16')$$

4.7. A Shock in a Flow of a Gas with Varying Specific Heats and with Dissociation and Ionization

When solving a problem on a shock in a dissociated and ionized gas, the parameters of the air at an altitude H (the pressure p_1, temperature T_1, density ρ_1, speed of sound a_1, etc.), and also the value of the normal velocity component V_{n1} (or the number $M_{n1} = V_{n1}/a_1$) are taken as the initial data. Hence, an oblique shock in the given case is treated as a normal one. Assuming in a first approximation that the value of $\Delta\bar{V}_n \approx 0.9\text{-}0.95$, which corresponds to setting a relative density for a shock of $\rho_2/\rho_1 = (1 - \Delta\bar{V}_n)^{-1} \approx$ $\approx$ 10-20, from (4.2.15) we find the pressure p_2, and from (4.2.16), the enthalpy i_2 that is evidently close to the stagnation enthalpy i_0'.

By next using an i-S diagram (see [6, 8]), we determine the temperature T_2, and then from Fig. 1.5.7, the mean molar mass μ_{m2}. Instead of the diagram, one may use suitable tables of the thermodynamic functions of air (see [7]), which will increase the accuracy of the calculations.

By inserting the found values of p_2, T_2, and μ_{m2} into the equation of state (1.5.8), we can determine the density ρ_2 and define the value of $\Delta\bar{V}_n$ more precisely by (4.2.21). We next use this value in a second approximation to find the pressure and enthalpy, respectively, by formulas (4.2.15) and (4.2.16). According to these values and with the aid of tables and graphs, we define the temperature and mean molar mass more exactly. We use the refined values of p_2, T_2, and μ_{m2} to find the density in the second approximation by the equation of state. The approximations are terminated when the preset accuracy is achieved.

We can evaluate the shock angle corresponding to a given velocity V_1 by the formula $\sin\theta_s = V_{n1}/V_1$. By introducing the value of θ_s and also the number $M_1 = V_1/a_1$ into (4.3.26), we determine the flow deviation angle β_s behind the shock.

An oblique shock can also be calculated when the values of the free-stream parameters (including the number M_1) and the angle β_s are known. In a first approximation, we determine the shock angle θ_s for an undissociating gas [see (4.3.27)], and then find the corresponding values of $\Delta\bar{V}_n$, p_2, and i_2 by formulas (4.2.19), (4.2.15), and (4.2.16). Using these values, we determine the temperature T_2 and the mean molar mass μ_{m2} from tables [7] or graphs [6, 8]. Next by formulas (4.2.23) and (4.2.24), we define $\Delta\bar{V}_n$ more precisely, and by expression (4.2.25), $\tan\theta_s$ and the angle θ_s. We refine the other parameters according to the relevant formulas.

We calculate the parameters of a gas behind a normal shock in a similar way with the use of tables or graphs of the thermodynamic functions for high temperatures. We assume that $\theta_s = \pi/2$ and $\beta_s = 0$ and, therefore, use (4.2.27)-(4.2.35).

When dissociation and ionization occur, the relative values of the parameters of a gas behind a shock wave depend not only on the temperature, which is characteristic of varying specific heats, but also on the pressure. These relations are shown graphically in Figs. 4.7.1-4.7.3. The ratios of the temperatures and densities are calculated for averaged values of the temperature T_1 of 220 and 350 K. These values equal, respectively, the probable minimum and maximum that are chosen depending on the change in the air temperature with altitude for decreased and increased annual average values. Available data show that dissociation and ionization give rise to a substantial change in the equilibrium temperature and density in comparison with constant specific heats ($k = 1.4 = = \text{const}$). The pressure depends to a considerably smaller extent

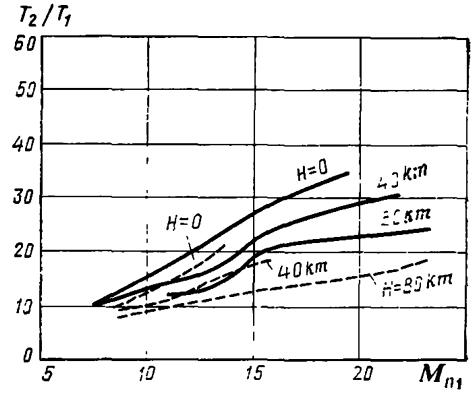

Fig. 4.7.1
Ratio of the air temperatures behind and ahead of a shock with account taken of dissociation and ionization:
solid lines—$T_1 = 220$ K, dashed lines—$T_1 = 350$ K

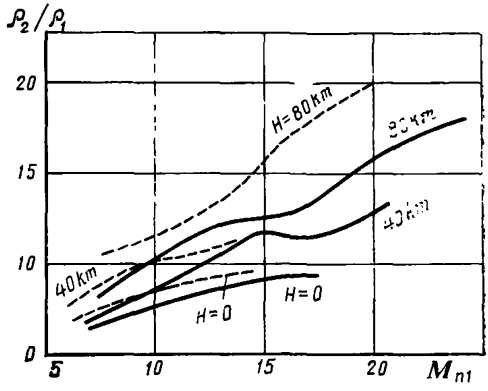

Fig. 4.7.2
Ratio of the air densities behind and ahead of a shock with account taken of dissociation and ionization:
solid lines—$T_1 = 220$ K, dashed lines—$T_1 1 = 350$ K

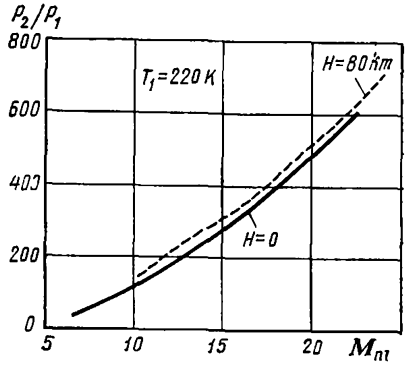

Fig. 4.7.3
Ratio of the air pressures behind and ahead of a shock with account taken of dissociation and ionization

on the physicochemical transformations of the air. The ratio p_2/p_1 differs only slightly from the maximum value of $p_2/p_1 = 1 + k_1 M_{n1}^2$ determined only by the conditions of the oncoming flow, but not by the change in the structure and physicochemical properties of the air behind a shock wave.

The temperature behind a shock in a dissociated gas is lower than that with constant specific heats (Fig. 4.7.1). The explanation is the loss of energy on the thermal dissociation of the molecules.

The lowering of the temperature due to this phenomenon causes the density to grow (Fig. 4.7.2). This greater "yielding" of the gas to compression reduces the space between a shock and a surface in the flow, thus diminishing the shock angle. And conversely, at the same angle θ_s in a real heated gas, the flow deflection (the angle β_s) is greater than in a perfect gas (k = const). The result is that in a heated gas a detached shock forms with a certain delay in comparison with a cold gas. Particularly, the wedge angle (critical angle) at which detachment of a shock begins is larger in a heated gas than in a cold one.

Account of the influence of dissociation leads to a certain increase in the pressure behind a shock in comparison with a gas having constant specific heats (Fig. 4.7.3). This is explained by the increase in the number of particles in the gas owing to dissociation and by the increase in the losses of kinetic energy when they collide. But the drop in the temperature in a dissociated gas causes an opposite effect, but smaller in magnitude. As a result, the pressure increases, although only slightly.

The theory of a normal shock has an important practical application when determining the parameters of a gas at the **point of stagnation**. The procedure is as follows. According to the found values i_2 and p_2 with account taken of dissociation and ionization, we find the entropy S_2 from an i-S diagram or tables of thermodynamic functions for air. Considering the flow behind a shock to be isentropic, we assume that the entropy S_0' at the stagnation point equals the value S_2 behind the shock wave. In addition, for this point we can find the enthalpy $i_0' = i_1 + 0.5V_1^2$. Now knowing S_0' and i_0', we can use an i-S diagram or thermodynamic tables to find the other parameters, namely, p_0', T_0', ρ_0', etc.

The results of the calculations correspond to the preset flight altitude. A change in the altitude is attended by a change in the conditions of flow past a body and, consequently, in the parameters at the point of stagnation. This relation is shown graphically in Fig. 4.7.4. The curves allow us to determine the temperature T_0' and pressure p_0' as a function of the velocity V_1 and the flight altitude H.

The value of p_0', in turn, can be used to calculate the pressure coefficient at the point of stagnation: $\bar{p}_0 = 0.5kM_\infty^2 (p_0'/p_\infty - 1)$. Its value grows somewhat in a dissociating flow. For example, at an altitude of 10 km at $M_\infty = 16.7$, its value is $\bar{p}_0 = 2.08$, whereas without account taken of dissociation $\bar{p}_0 = 1.83$ (for $k = c_p/c_v = 1.4$). The pressure coefficient can be seen to grow by about 13%.

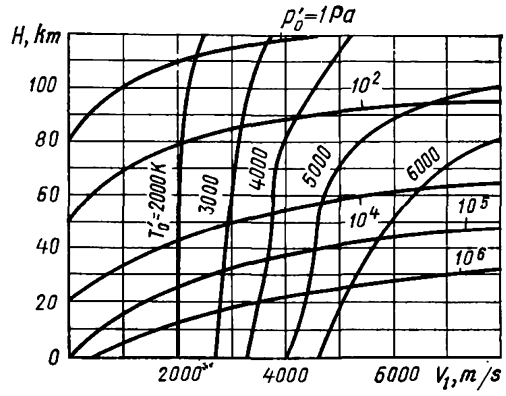

Fig. 4.7.4
Pressure and temperature at the point of stagnation

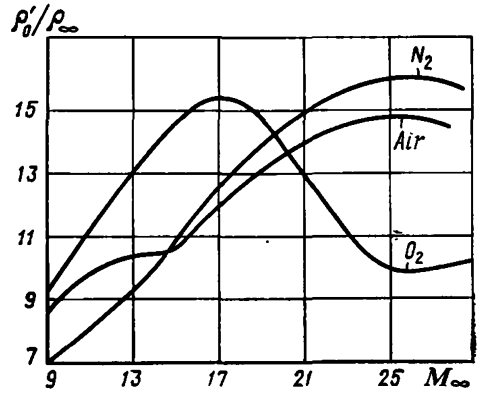

Fig. 4.7.5
Density at the point of stagnation on the surface of a sphere for nitrogen, oxygen, and air ($p_\infty = 10^3$ Pa, $T_\infty = 290$ K)

The results of calculating the density at the point of stagnation with account taken of dissociation and ionization for air, and also for pure oxygen and nitrogen, are given in Fig. 4.7.5. An analysis of these results allows us to arrive at the following conclusion. At $M_\infty = 18$, when oxygen is already noticeably dissociated, the quantity ρ_0'/ρ_∞ reaches its maximum value. Upon a further increase in M_∞, the gas completely dissociates, and the density drops. Next a growth in M_∞ is attended by primary ionization of the oxygen. This leads to an increase in the specific heat and, consequently, to a certain growth in the density.

The influence of the varying nature of the specific heat on the change in the density of nitrogen is observed only at very large numbers M_∞ when dissociation and ionization take place. These processes run not consecutively, as in oxygen, but virtually simultaneously, which is due to the smaller difference between the energies of dissociation and ionization of nitrogen. This is why the curve ρ_0'/ρ_∞ for nitrogen is more monotonic than for oxygen.

At $M_\infty < 13$, what mainly occurs in the air is dissociation of oxygen, and the density curve for air is closer to the relevant curve for oxygen. At $M_\infty > 13$, when the dissociation of the nitrogen becomes appreciable, the dependence of ρ_0'/ρ_∞ on M_∞ for air reminds one of the similar relation for gaseous nitrogen because the latter is the predominating component in the air.

The calculation of the parameters of a gas behind a shock with a view to the varying nature of the specific heats is described in greater detail in [14].

4.8. Relaxation Phenomena

Section 4.7 deals with ways of calculating the parameters of a gas behind a shock with account taken of the physicochemical transformations for conditions of **equilibrium** of the thermodynamic processes. In a more general case, however, these processes are characterized by **non-equilibrium**, which has a definite influence on the gas flow behind shocks.

Non-Equilibrium Flows

It is known from thermodynamics that the assumption of thermodynamic equilibrium consists in agreement between the levels of the internal degrees of freedom and the parameters characterizing the state of a gas. For example, at comparatively low temperatures (low velocities), equilibrium sets in between the temperature and the vibrational degree of freedom, which corresponds to equilibrium between the temperature and the specific heat. At high temperatures (high velocities), when a gas dissociates, the equilibrium state is reached as follows. As dissociation develops, the probability of triple collisions grows (for a binary mixture of diatomic gases) because the number of gas particles increases. This leads to the acceleration of recombination and the retardation of the rate of dissociation. At a certain instant and temperature, the rates of the direct and reverse reactions become equal, and the gas arrives at an equilibrium state. The latter is characterized by a constant composition and agreement between the degree of dissociation, on the one hand, and the temperature and pressure, on the other. At still higher temperatures (very high velocities), equilibrium processes of excitation of the electron levels and ionization can be considered.

Upon a sudden change in the temperature in an equilibrium flow, the corresponding internal degrees of freedom also set in instantaneously; dissociation and ionization can be considered as the manifestation of new degrees of freedom. Consequently, in these cases, there is no delay in establishing the degrees of freedom, i.e. the time needed for achieving equilibrium is zero.

In practice, an equilibrium flow is observed under supersonic flows past bodies at Mach numbers of $M_\infty = 4\text{-}5$ in conditions corresponding to altitudes of 10-15 km and less. The explanation is that at the maximum temperatures of the order of 1000-1500 K appearing in these conditions, the main part of the internal energy falls to the share of the translational and rotational degrees of freedom, which upon sudden changes in the temperature are established virtually instantaneously because only a few molecular collisions are needed to achieve equilibrium. This is why the translational and rotational degrees of freedom are usually called "active" degrees. With an increase in the velocities and, consequently, in the temperatures, a substantial part of the internal energy is spent on vibrations, then on dissociation, excitation of the electron levels, and ionization.

Actual processes are such that these energy levels set in more slowly than the translational and rotational ones because a much greater number of collisions is needed. For this reason, the vibrational and dissociative degrees of freedom are sometimes called **"inert" degrees.** Hence, the inert degrees are featured by a delay in the achievement of equilibrium called **relaxation.** The time in which equilibrium sets in, i.e. correspondence between the temperature and the energy level is established, is called the **relaxation time.**

The relaxation time characterizes the rate of attenuation of departures of a gas state from an equilibrium one, which in a general case manifests itself in the form of a change in the energy distribution among the different degrees of freedom.

Relaxation processes are determined by what degree of freedom is excited. If upon a sudden change in the temperature, vibrations appear, the corresponding non-equilibrium process is called **vibrational relaxation.** It is characterized by a lag in the specific heat when the temperature changes. If the temperature rises, the specific heat grows because of the appearance of vibrations of the atoms in the molecules. The time during which vibrational motion reaches equilibrium is called the **vibrational relaxation time.**

In a non-equilibrium dissociating gas upon a sudden change in the temperature, a delay occurs in the change in the degree of dissociation. This phenomenon is called **dissociative relaxation.** Owing to the difference between the rates of formation of the atoms and their vanishing (the rate of dissociation is higher than that of recombination), a gradual increase in the degree of dissociation occurs. The equilibrium value of the degree of dissociation is achieved at the instant when the rates of the direct and reverse reactions become equal. The time needed to obtain an equilibrium degree of dissociation is called the **dissociative relaxation time.**

Experimental data on the relaxation time for oxygen and nitrogen are given in Fig. 4.8.1.

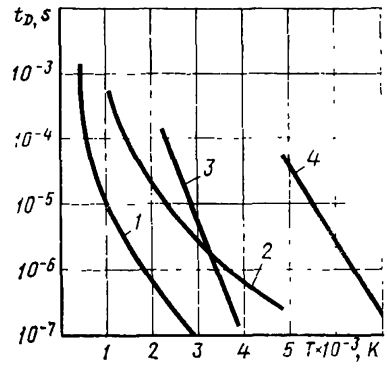

Fig. 4.8.1
Experimental (*1*, *2*) curves of the vibrational relaxation time and calculated (*3*, *4*) curves of the relaxation time for the dissociation of oxygen and nitrogen, respectively, at atmospheric pressure

At temperatures approximately up to 10 000 K, the vibrational and dissociative relaxation processes are the main ones. The relaxation phenomena associated with the excitation of the electron levels of the molecules and atoms, and also with ionization, may be disregarded because a small fraction of the internal energy falls to the share of these degrees of freedom at the indicated temperatures.

A non-equilibrium state has a substantial influence on the various processes attending the flow of a gas at very high velocities. Particularly, vibrational and dissociative relaxations change the parameters of a gas in a transition through shock waves and in the flow past bodies. This, in turn, affects the processes of friction, heat exchange, and also the redistribution of the pressure.

The studying of non-equilibrium flows consists in the joint investigation of the motion of the fluid and of the chemical processes occurring at finite velocities. This is expressed formally in that an equation for the rate of chemical reactions is added to the usual system of equations of gas dynamics.

Equilibrium Processes

Equilibrium flows have been studied better than non-equilibrium ones both from the qualitative and the quantitative standpoints. The regions of a flow in which equilibrium sets in are different because of the different relaxation times for the excitation levels. The duration of the establishment of equilibrium relative to the vibrational degrees of freedom is longer by several orders than relative to the translational and rotational ones. Equilibrium sets in even more slowly relative to the composition of a gas mixture when dissociation and ionization occur. Accordingly, the scheme of a non-equilibrium process is such that the attainment of equilibrium of one degree of freedom may be attended by the beginning of a relax-

ation phenomenon of another one. In more general case, overlapping of the regions of establishing equilibrium is observed.

An approximate model of the process can be conceived on the basis of the "freezing" principle. It is considered that a region of achievement of equilibrium relates to one or several degrees of freedom, while the others are not excited. The sequence of these regions of equilibrium can be represented by degrees of freedom with elevation of the temperature in the following order: translational, rotational, and vibrational degrees, dissociation, excitation of electron levels, and ionization. When considering, for example, the process of establishing equilibrium of vibrations, the first two degrees of freedom can be considered to be completely excited. This process occurs in conditions of "frozen" dissociation and ionization.

Such a scheme is not suitable for certain gases, particularly nitrogen at high temperatures, because ionization begins before dissociation is completed. This is explained by the fact that the energies of dissociation and ionization of nitrogen differ from each other only one-and-a-half times. In this case, the regions of attainment of equilibrium overlap. A similar phenomenon is observed in the air at comparatively low temperatures. At temperatures exceeding 3200 K, the relaxation time for the dissociation of oxygen is lower than the duration of setting in of nitrogen vibrations. Consequently, equilibrium in the dissociation of oxygen is established before the vibrations of the nitrogen are in equilibrium.

Investigation of the flow of a non-equilibrium gas over bodies is facilitated if the characteristic time of this process is considerably lower than the relaxation time of one of the inert processes and conditions of a frozen flow occurring without the participation of this inert process appear. Particularly, if the duration of flow over a section of a surface is small in comparison with the time needed for chemical equilibrium to set in, but is commensurable with the vibrational relaxation time, a process with frozen dissociation and ionization may be considered on this section.

Relaxation Effects In Shock Waves

In the transition of a gas through a shock wave, a portion of the kinetic energy is converted into the energy of active and inert degrees of freedom. For the active degrees (superscript "A")—translational and rotational—equilibrium sets in during the relaxation time t_D^A commensurable with the time taken by the gas to pass through the thickness of the shock. Since this time is very small, we can consider in practice that the active degrees are excited instantaneously. At the same time, dissociation does not yet begin because during a small time interval the number of collisions of the molecules is not

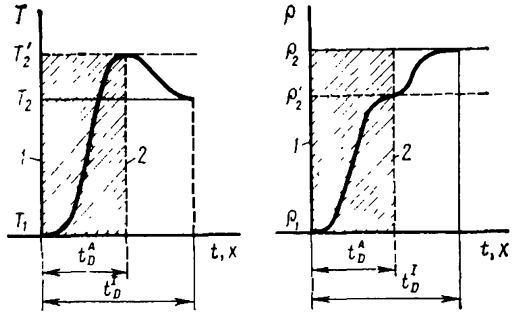

Fig. 4.8.2
Relaxation process in a shock wave:
(the hatched region determines the thickness of the shock wave):
1 and *2*—front and rear surfaces of the shock wave, respectively

large. Hence, directly behind a shock wave, the temperature T_2' is the same as in a gas with constant specific heats.

In accordance with this scheme, no inert degrees of freedom (superscript "I") are excited directly after a shock. Since these degrees have a finite relaxation time t_D^I considerably greater than the time t_D^A and the duration of transition through the thickness of a real shock, then *the temperature lowers* until the inert degrees of freedom (first vibrations, then dissociation, excitation of the electron levels, and ionization) reach equilibrium.

In Fig. 4.8.2, schematically illustrating a relaxation process, the relaxation time t_D^A measured from the instant of the beginning of motion on the front surface of the shock wave ahead of which the temperature of the undisturbed gas is T_1 corresponds to the temperature T_2'. The figure also shows the density ρ_2' corresponding to the temperature T_2', while the equilibrium state is established at a temperature of $T_2 < T_2'$. A non-equilibrium process of gas flow behind a shock is attended by an *increase in the density* to the equilibrium value $\rho_2 > \rho_2'$. Here a small *growth in the pressure* is observed in comparison with an ideal gas. Simultaneously *the degree of dissociation* (and at very high temperatures, the degree of ionization) *grows from zero to its equilibrium value.*

The investigation of the non-equilibrium flow behind a shock consists in determining the length of the non-equilibrium zone, or the relaxation length, and also in estimating the non-equilibrium parameters. The system of equations describing such motion includes equations of the momentum, energy, state, and an equation for the rate of chemical reactions.

The initial conditions upon its integration are determined by the parameters directly behind the shock wave, which are found with the assumption that dissociation is absent. At the end of the

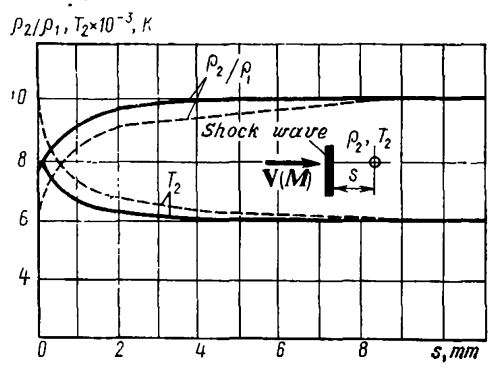

Fig. 4.8.3
Influence of non-equilibrium dissociation on the density and temperature behind a shock wave
($M_1 = 14.2$, $T_1 = 300$ K, $p_1 = 120$ Pa)

relaxation length, these parameters reach equilibrium values corresponding to the equilibrium degree of dissociation.

The results of such investigations of a non-equilibrium flow of a gaseous mixture of oxygen and nitrogen behind a shock wave are given in Fig. 4.8.3. The solid curves were obtained on the assumption of instantaneous vibrational excitation, and the dashed ones in the absence of excitation. These results reveal that vibrations have an appreciable significance in direct proximity to a shock. For example, without account of excitations, the temperature behind a shock is 12 000 K, while for a completely excited state it is about 9800 K, i.e. considerably lower. At the end of the relaxation zone, vibrational excitation is of virtually no importance. Therefore in calculations of equilibrium dissociation, we can assume that the rates of vibrational excitation are infinitely high, thus considering a gas before the beginning of dissociation to be completely excited. It is shown in Fig. 4.8.3 that the length of the non-equilibrium zone is comparatively small and is approximately 8-10 mm.

The data of investigations of the relaxation in shock waves can be used to determine the nature of non-equilibrium flow in the vicinity of a blunt nose in a hypersonic flow. Here we find the length of the relaxation (non-equilibrium) zone and determine whether such a zone reaches the vicinity of the point of stagnation. In accordance with this, the stagnation parameters are calculated, and with a view to their values, similar parameters are evaluated for the peripheral sections of the surface in the flow.

The length of the non-equilibrium zone is found as the relaxation length calculated by means of the expression

$$x_D = 0.5 V_C t_D \qquad (4.8.1)$$

where V_C is the velocity directly behind the normal part of the shock wave, and t_D is the relaxation time.

The relaxation time can be found by the formula

$$t_D \approx 2.8 \times 10^{-7} (1 - \alpha_e) \{[f(H)\,\bar{\rho}]^2\, \alpha_e (3 - \alpha_e)\}^{-1} \quad (4.8.2)$$

in which $f(H) = \rho_{\infty H}/\rho_{\infty E}$ is a function of the altitude ($\rho_{\infty H}$ and $\rho_{\infty E}$ are the densities of the atmosphere at the altitude H and at the Earth's surface, respectively), $\bar{\rho} = \rho/\rho_{\infty H}$ [the density $\rho = 0.5 (\rho_C + \rho_e)$, where ρ_C and ρ_e are the densities behind the shock in the undissociated gas and for equilibrium dissociation, respectively].

If the length x_D is smaller than the distance s_0 between a shock wave and the point of stagnation, the non-equilibrium zone is near the wave and does not include the body in the flow. Consequently, the condition for equilibrium in the vicinity of a blunted surface will be $x_D < s_0$, or $0.5 V_0 t_D < s_0$. Hence we can also find the inequality $t_D < s_0/(0.5 V_C)$ in which the term on the right-hand side is the characteristic time t_{s_0} spent by a particle in the compression zone. If $t_{s_0} > t_D$, a particle of the gas will have time to reach the state of equilibrium before it reaches the surface.

It is not difficult to see from formula (4.8.2) that the relaxation time grows with increasing flight altitude H and, consequently, the length of the non-equilibrium zone increases. At the same time, t_D diminishes with an increase in the intensity of a compression shock for very high supersonic velocities of the flow (here the relative density behind a shock $\bar{\rho} = \rho/\rho_{\infty H}$ becomes larger).

A non-equilibrium state substantially affects the distance between a shock wave and a body. With a completely non-equilibrium flow behind a shock (the degree of dissociation $\alpha = 0$), this distance can be appreciably larger than in equilibrium dissociation ($\alpha = \alpha_e > 0$). It decreases in the real conditions of a gradual transition from a non-equilibrium state to an equilibrium flow behind a shock wave, i.e. when the degree of dissociation changes from 0 behind the wave to the equilibrium value $\alpha = \alpha_e$ at the end of the relaxation zone.

5

Method of Characteristics

5.1. Equations for the Velocity Potential and Stream Function

An important place in aerodynamics is occupied by the **method of characteristics**, which allows one to calculate the disturbed flow of an ideal (inviscid) gas. This method makes it possible to design correctly the contours of nozzles for supersonic wind tunnels, determine the parameters of supersonic flow over airfoils and craft bodies.

The method of characteristics has been developed comprehensively for solving the system of equations of steady supersonic two-dimensional (plane or spatial axisymmetric) vortex and vortex-free gas flows. Investigations associated with the use of the method of characteristics for calculating the three-dimensional flow over bodies are being performed on a broad scale. Below we consider the method of characteristics and its application to problems on supersonic two-dimensional flows.

Equations for a two-dimensional plane steady flow of an inviscid gas are obtained from (3.1.20) provided that $\mu = 0$, $\partial V_x/\partial t = \partial V_y/\partial t = 0$ and have the following form:

$$\left.\begin{aligned} V_x \frac{\partial V_x}{\partial x} + V_y \frac{\partial V_x}{\partial y} &= -\frac{1}{\rho} \cdot \frac{\partial p}{\partial x} \\ V_x \frac{\partial V_y}{\partial x} + V_y \frac{\partial V_y}{\partial y} &= -\frac{1}{\rho} \cdot \frac{\partial p}{\partial y} \end{aligned}\right\} \qquad (5.1.1)$$

For a two-dimensional axisymmetric flow, the equations of motion obtained from (3.1.36) for similar conditions ($\nu = 0$, $\partial V_x/\partial t = \partial V_y/\partial t = 0$) can be written in the form

$$\left.\begin{aligned} V_x \frac{\partial V_x}{\partial x} + V_r \frac{\partial V_x}{\partial r} &= -\frac{1}{\rho} \cdot \frac{\partial p}{\partial x} \\ V_x \frac{\partial V_r}{\partial x} + V_r \frac{\partial V_r}{\partial r} &= -\frac{1}{\rho} \cdot \frac{\partial p}{\partial r} \end{aligned}\right\} \qquad (5.1.2)$$

The continuity equations for plane and axisymmetric flows having respectively the form of (2.4.5) and (2.4.32) can be generalized as

follows:

$$\partial (\rho V_x y^\varepsilon)/\partial x + \partial (\rho V_y y^\varepsilon)/\partial y = 0 \qquad (5.1.3)$$

When $\varepsilon = 0$, this equation coincides with the continuity equation for a two-dimensional plane flow in the Cartesian coordinates x and y. If $\varepsilon = 1$, we have a continuity equation for a two-dimensional axisymmetric flow in the cylindrical coordinates y (r), x. Accordingly, for both kinds of flow, we may consider that the equations of motion (5.1.1) are written in a generalized form.

Having determined the partial derivatives in continuity equation (5.1.3), we obtain

$$\left(V_x \frac{\partial \rho}{\partial x} + V_y \frac{\partial \rho}{\partial y}\right) y^\varepsilon + \rho y^\varepsilon \left(\frac{\partial V_x}{\partial x} + \frac{\partial V_y}{\partial y}\right) + \rho V_y \varepsilon y^{\varepsilon - 1} = 0 \qquad (5.1.4)$$

We can replace the partial derivative $\partial\rho/\partial x$ with the expression $\partial\rho/\partial x = (\partial\rho/\partial p)\,\partial p/\partial x$, in which $\partial\rho/\partial p = 1/a^2$, while the derivative $\partial p/\partial x$ is found from (5.1.1) in the form

$$\frac{\partial p}{\partial x} = -\rho \left(V_x \frac{\partial V_x}{\partial x} + V_y \frac{\partial V_x}{\partial y}\right)$$

With this in view, we have

$$\frac{\partial \rho}{\partial x} = -\frac{\rho}{a^2} \left(V_x \frac{\partial V_x}{\partial x} + V_y \frac{\partial V_x}{\partial y}\right) \qquad (5.1.5)$$

An expression for the derivative $\partial\rho/\partial y$ is found in a similar way:

$$\frac{\partial \rho}{\partial y} = -\frac{\rho}{a^2} \left(V_x \frac{\partial V_y}{\partial x} + V_y \frac{\partial V_y}{\partial y}\right) \qquad (5.1.6)$$

Substitution of the values of these derivatives into (5.1.4) yields

$$(V_x^2 - a^2) \frac{\partial V_x}{\partial x} + V_x V_y \left(\frac{\partial V_x}{\partial y} + \frac{\partial V_y}{\partial x}\right) + (V_y^2 - a^2) \frac{\partial V_y}{\partial y} - \frac{a^2 V_y \varepsilon}{y} = 0 \qquad (5.1.7)$$

This equation is the **fundamental differential equation of gas dynamics for a two-dimensional (plane or spatial axisymmetric) steady flow** which the velocity components V_x and V_y must satisfy. Since this equation relates the velocities, it is also referred to as the **fundamental kinematic equation.**

If a flow is potential, then

$$V_x = \partial\varphi/\partial x, \quad V_y = \partial\varphi/\partial y, \quad \partial V_x/\partial y = \partial V_y/\partial x = \partial^2\varphi/\partial x\,\partial y$$

therefore, Eq. (5.1.7) can be transformed as follows:

$$(V_x^2 - a^2) \frac{\partial^2 \varphi}{\partial x^2} + 2 V_x V_y \frac{\partial^2 \varphi}{\partial x\,\partial y} + (V_y^2 - a^2) \frac{\partial^2 \varphi}{\partial y^2} - \frac{a^2 V_y \varepsilon}{y} = 0 \qquad (5.1.8)$$

where

$$a^2 = \frac{k-1}{2}\left[V_{\max}^2 - \left(\frac{\partial\varphi}{\partial x}\right)^2 - \left(\frac{\partial\varphi}{\partial y}\right)^2\right]$$

Equation (5.1.8) is the **fundamental differential equation of gas dynamics for a two-dimensional potential steady flow** and is called an **equation for the velocity potential.** Hence, unlike (5.1.7), Eq. (5.1.8) is used only for studying vortex-free gas flows.

If a two-dimensional gas flow is a *vortex* one, the **stream function** ψ has to be used for studying it. The velocity components expressed in terms of the function ψ have the form of (2.5.5). Replacing ρ in accordance with formula (3.6.31) in which the stagnation density ρ_0 along a given streamline is assumed to be constant, expressions (2.5.5) can be written as follows:

$$V_x = y^{-\varepsilon}(1 - \bar{V}^2)^{-1/(k-1)}\,\partial\psi/\partial y, \quad V_y = -y^{-\varepsilon}(1 - \bar{V}^2)^{-1/(k-1)}\,\partial\psi/\partial x \tag{5.1.9}$$

where $\bar{V} = V/V_{\max}$.

The calculation of a vortex gas flow consists in solving a differential equation for the stream function ψ. To obtain this equation, let us differentiate (5.1.9) with respect to y and to x:

$$\frac{\partial V_x}{\partial y} = -\varepsilon y^{-\varepsilon-1}(1-\bar{V}^2)^{-1/(k-1)}\frac{\partial\psi}{\partial y} + y^{-\varepsilon}\frac{1}{k-1}$$

$$\times (1-\bar{V}^2)^{-1/(k-1)-1}\frac{\partial\bar{V}^2}{\partial y}\cdot\frac{\partial\psi}{\partial y} + y^{-\varepsilon}(1-\bar{V}^2)^{-1/(k-1)}\frac{\partial^2\psi}{\partial y^2}$$

$$\frac{\partial V_y}{\partial x} = -y^{-\varepsilon}\frac{1}{k-1}(1-\bar{V}^2)^{-1/(k-1)-1}\frac{\partial\bar{V}^2}{\partial x}\cdot\frac{\partial\psi}{\partial x} - y^{-\varepsilon}(1-\bar{V}^2)^{-1(k-1)}\frac{\partial^2\psi}{\partial x^2}$$

Taking into account expression (3.6.22) for the square of the speed of sound, and also relations (5.1.9), we can write the expressions obtained for the derivatives $\partial V_x/\partial y$ and $\partial V_y/\partial x$ as follows:

$$\frac{\partial V_x}{\partial y} = -\frac{\varepsilon}{y}V_x + \frac{V_x}{2a^2}\cdot\frac{\partial V^2}{\partial y} + y^{-\varepsilon}(1-\bar{V}^2)^{-1/(k-1)}\frac{\partial^2\psi}{\partial x^2} \tag{5.1.10}$$

$$\frac{\partial V_y}{\partial x} = \frac{V_y}{2a^2}\cdot\frac{\partial V^2}{\partial x} - y^{-\varepsilon}(1-\bar{V}^2)^{-1/(k-1)}\frac{\partial^2\psi}{\partial x^2} \tag{5.1.11}$$

We shall determine the derivatives $\partial V^2/\partial y$ and $\partial V^2/\partial x$ in Eqs. (5.1.10) and (5.1.11) with the aid of relations (5.1.9). Combining these relations, we obtain

$$(\partial\psi/\partial x)^2 + (\partial\psi/\partial y)^2 = V^2 y^{2\varepsilon}(1 - \bar{V}^2)^{2/(k-1)} \tag{5.1.12}$$

By differentiating (5.1.12) with respect to x and y, we find the relevant relations:

$$2\frac{\partial\psi}{\partial x}\cdot\frac{\partial^2\psi}{\partial x^2}+2\frac{\partial\psi}{\partial y}\cdot\frac{\partial^2\psi}{\partial x\,\partial y}=\frac{\partial V^2}{\partial x}y^{2\varepsilon}(1-\overline{V}^2)^{2/(k-1)}$$

$$-V^2y^{2\varepsilon}\frac{2}{k-1}(1-\overline{V}^2)^{2/(k-1)-1}\frac{\partial\overline{V}^2}{\partial x}$$

$$2\frac{\partial\psi}{\partial x}\cdot\frac{\partial^2\psi}{\partial x\,\partial y}+2\frac{\partial\psi}{\partial y}\cdot\frac{\partial^2\psi}{\partial y^2}=\frac{\partial V^2}{\partial y}y^{2\varepsilon}(1-\overline{V}^2)^{2/(k-1)}$$

$$+2\varepsilon V^2y^{2\varepsilon-1}(1-\overline{V}^2)^{2/(k-1)}-V^2y^{2\varepsilon}\frac{2}{k-1}(1-\overline{V}^2)^{2/(k-1)-1}\frac{\partial\overline{V}^2}{\partial y}$$

We transform these relations with a view to Eq. (3.6.22) for the square of the speed of sound and to relations (5.1.9):

$$-V_y\frac{\partial^2\psi}{\partial x^2}+V_x\frac{\partial^2\psi}{\partial x\,\partial y}=\frac{y^\varepsilon}{2}\cdot\frac{\partial V^2}{\partial x}(1-\overline{V}^2)^{1/(k-1)}\left(1-\frac{V^2}{a^2}\right) \quad (5.1.13)$$

$$-V_y\frac{\partial^2\psi}{\partial x\,\partial y}+V_x\frac{\partial^2\psi}{\partial y^2}=\frac{y^\varepsilon}{2}\cdot\frac{\partial V^2}{\partial y}(1-\overline{V}^2)^{1/(k-1)}$$

$$\times\left(1-\frac{V^2}{a^2}\right)+\frac{\varepsilon}{y^{1-\varepsilon}}V^2(1-\overline{V}^2)^{1/(k-1)} \quad (5.1.14)$$

Determining the derivatives $\partial V^2/\partial y$ and $\partial V^2/\partial x$ from these expressions and inserting them into (5.1.10) and (5.1.11), respectively, we obtain

$$\frac{y^\varepsilon}{2}(1-\overline{V}^2)^{1/(k-1)}\left(1-\frac{V^2}{a^2}\right)\frac{\partial V_x}{\partial y}=-\frac{\varepsilon}{2y^{1-\varepsilon}}V_x(1-\overline{V}^2)^{1/(k-1)}$$

$$\times\left(1-\frac{V^2}{a^2}\right)+\frac{V_x}{2a^2}\left[-V_y\frac{\partial^2\psi}{\partial x\,\partial y}+V_x\frac{\partial^2\psi}{\partial y^2}\right.$$

$$\left.-\frac{\varepsilon}{y^{1-\varepsilon}}V^2(1-\overline{V}^2)^{1/(k-1)}\right]+\frac{1}{2}\left(1-\frac{V^2}{a^2}\right)\frac{\partial^2\psi}{\partial y^2}$$

$$\frac{y^\varepsilon}{2}(1-\overline{V}^2)^{1/(k-1)}\left(1-\frac{V^2}{a^2}\right)\frac{\partial V_y}{\partial x}$$

$$=\frac{V_y}{2a^2}\left(-V_y\frac{\partial^2\psi}{\partial x^2}+V_x\frac{\partial^2\psi}{\partial x\,\partial y}\right)-\frac{1}{2}\left(1-\frac{V^2}{a^2}\right)\frac{\partial^2\psi}{\partial x^2}$$

Subtraction of the first equation from the second one yields a relation for a *vortex*:

$$\frac{\partial V_y}{\partial x}-\frac{\partial V_x}{\partial y}=\frac{V_y}{a^2-V^2}\cdot\frac{1}{y^\varepsilon}\left(-V_y\frac{\partial^2\psi}{\partial x^2}\right.$$

$$\left.+V_x\frac{\partial^2\psi}{\partial x\,\partial y}\right)(1-\overline{V}^2)^{-1/(k-1)}-\frac{1}{y^\varepsilon}(1-\overline{V}^2)^{-1/(k-1)}\frac{\partial^2\psi}{\partial x^2}$$

$$-\frac{V_x}{a^2-V^2}\cdot\frac{1}{y^\varepsilon}\left(-V_y\frac{\partial^2\psi}{\partial x\,\partial y}+V_x\frac{\partial^2\psi}{\partial y^2}\right)(1-\overline{V}^2)^{-1/(k-1)}$$

$$-\frac{1}{y^\varepsilon}(1-\overline{V}^2)^{-1/(k-1)}\frac{\partial^2\psi}{\partial y^2}+\frac{\varepsilon}{y}\cdot\frac{a^2}{a^2-V^2}V_x \qquad (5.1.15)$$

A vortex can also be determined with the aid of Eq. (3.1.22′) transformed for the conditions of the steady flow of an ideal gas and having the form

$$\text{grad}\,(V^2/2)+\text{curl}\,\mathbf{V}\times\mathbf{V}=-(1/\rho)\,\text{grad}\,p \qquad (5.1.16)$$

By applying the grad operation to the energy equation (3.4.14), we have:

$$\text{grad}\,(V^2/2)=-\text{grad}\,i \qquad (5.1.17)$$

Consequently, Eq. (5.1.16) can be written in the form

$$\text{curl}\,\mathbf{V}\times\mathbf{V}=\text{grad}\,i-(1/\rho)\,\text{grad}\,p \qquad (5.1.18)$$

Vortex supersonic gas flows can be characterized thermodynamically *by the change in the entropy* when going over from one streamline to another. This is why it is convenient to introduce into the calculations a parameter that reflects this change in the entropy as a feature of vortex flows.

In accordance with the second law of thermodynamics

$$T\,dS=di-dp/\rho$$

or in the vector form,

$$T\,\text{grad}\,S=\text{grad}\,i-(1/\rho)\,\text{grad}\,p \qquad (5.1.19)$$

Combining (5.1.18) and (5.1.19), we obtain

$$\text{curl}\,\mathbf{V}\times\mathbf{V}=T\,\text{grad}\,S \qquad (5.1.20)$$

Let us calculate the cross product curl $\mathbf{V}\times\mathbf{V}$, having in view that by (2.2.12) the vector

$$\text{curl}\,\mathbf{V}=(\partial V_y/\partial x-\partial V_x/\partial y)\,\mathbf{i}_3$$

(here $\mathbf{i}_3$ is a unit vector), and, therefore, the projections $(\text{curl}\,\mathbf{V})_x=(\text{curl}\,\mathbf{V})_y=0$. Let us use a third-order determinant:

$$\text{curl}\,\mathbf{V}\times\mathbf{V}=\begin{vmatrix}\mathbf{i}_1 & \mathbf{i}_2 & \mathbf{i}_3\\ 0 & 0 & (\text{curl}\,\mathbf{V})_3\\ V_x & V_y & 0\end{vmatrix}$$

in which the projection

$$(\text{curl}\,\mathbf{V})_3=\partial V_y/\partial x-\partial V_x/\partial y$$

Calculations yield

$$\text{curl } \mathbf{V} \times \mathbf{V} = -V_y \left(\frac{\partial V_y}{\partial x} - \frac{\partial V_x}{\partial y} \right) \mathbf{i}_1 + V_x \left(\frac{\partial V_y}{\partial x} - \frac{\partial V_x}{\partial y} \right) \mathbf{i}_2 \tag{5.1.21}$$

Accordingly, for the projection of the vector curl $\mathbf{V} \times \mathbf{V}$ onto a normal n to a streamline, we obtain the relation

$$(\text{curl } \mathbf{V} \times \mathbf{V})_n^2 = (\text{curl } \mathbf{V} \times \mathbf{V})_x^2 + (\text{curl } \mathbf{V} \times \mathbf{V})_y^2 = V^2 (\partial V_y/\partial x - \partial V_x/\partial y)^2 \tag{5.1.22}$$

Examination of (5.1.20) reveals that this projection can also be written in the form

$$(\text{curl } \mathbf{V} \times \mathbf{V})_n = T \, dS/dn$$

or, with a view to (5.1.22)

$$V (\partial V_y/\partial x - \partial V_x/\partial y) = T \, \partial S/dn \tag{5.1.23}$$

Since $a^2 = kRT$, then, taking (3.6.22) into account, we find an expression for the temperature:

$$T = \frac{a^2}{kR} = \frac{k-1}{2k} \cdot \frac{1}{R} (V_{\max}^2 - V^2) = \frac{k-1}{2k} \cdot \frac{V_{\max}^2}{R} (1 - \overline{V}^2)$$

Introducing this relation into (5.1.23), we obtain

$$\frac{\partial V_y}{\partial x} - \frac{\partial V_x}{\partial y} = \frac{k-1}{2k} \cdot \frac{V_{\max}^2}{RV} (1 - \overline{V}^2) \frac{dS}{dn} \tag{5.1.24}$$

By introducing the vortex according to this expression into (5.1.15), we find a differential equation for the stream function:

$$(V_x^2 - a^2) \frac{\partial^2 \psi}{\partial x^2} + 2V_x V_y \frac{\partial^2 \psi}{\partial x \, \partial y} + (V_y^2 - a^2) \frac{\partial^2 \psi}{\partial y^2} + \frac{\varepsilon}{y^{1-\varepsilon}} a^2 V_x (1 - \overline{V}^2)^{1/(k-1)} = \frac{k-1}{2k} \cdot \frac{V_{\max}^2}{RV} (1 - \overline{V}^2)^{k/(k-1)} y^{\varepsilon} (a^2 - V^2) \frac{dS}{dn} \tag{5.1.25}$$

5.2. The Cauchy Problem

Equations (5.1.8) for the velocity potential and (5.1.25) for the stream function are inhomogeneous non-linear second-order partial differential equations. The solutions of these equations $\varphi = \varphi(x, y)$ and $\psi = \psi(x, y)$ are depicted geometrically by integral surfaces in a space determined by the coordinate systems x, y, φ or x, y, ψ. In these systems, the plane x, y is considered as the basic one and is called the **physical plane** or the **plane of independent variables.**

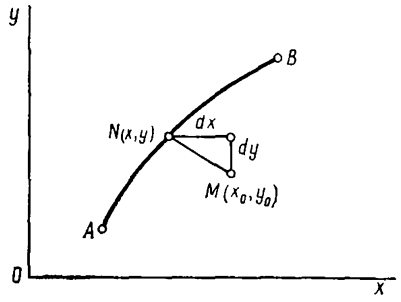

Fig. 5.2.1
Initial curve AB; the required function and its first derivatives with respect to x and y are known on it

The Cauchy problem consists in finding such solutions in the vicinity of an initial curve $y = y(x)$ satisfying the additional conditions set on this curve. The values of the required function $\varphi(x, y)$ or $\psi(x, y)$ and the first derivatives φ_x (ψ_x) or φ_y (ψ_y) are such additional conditions. They are known as Cauchy's initial conditions.

From the geometric viewpoint, the Cauchy problem consists in finding an integral surface in the space x, y, φ (or x, y, ψ) that passes through a preset spatial curve. It is just the projection of this curve onto the plane y, x that is the initial curve $y = y(x)$ on this plane. The solution of the Cauchy problem as applied to the investigation of supersonic gas flows and the development of the corresponding method of characteristics are the results of work performed by the Soviet scientist, prof. F. Frankl.

To consider the Cauchy problem, let us write Eqs. (5.1.8) and (5.1.25) in the general form

$$Au + 2Bs + Ct + H = 0 \tag{5.2.1}$$

where $u = \varphi_{xx}$ (or ψ_{xx}), $s = \varphi_{xy}$ (or ψ_{xy}), and $t = \varphi_{yy}$ (or ψ_{yy}) are second partial derivatives, the values of A, B, and C equal the coefficients of the corresponding second partial derivatives, and the quantity H is determined by the free terms in Eqs. (5.1.8) and (5.1.25).

We shall find a solution of Eq. (5.2.1) in the vicinity of the initial curve AB (Fig. 5.2.1) in the form of a series. At a point $M(x_0, y_0)$, the required function is

$$\varphi(x_0, y_0) = \varphi(x, y) + \sum_{n=1}^{\infty} \frac{1}{n!} \left[(\Delta x)^n \frac{\partial^n \varphi}{\partial x^n} + \frac{n}{1} (\Delta x)^{n-1} \Delta y \frac{\partial^n \varphi}{\partial x^{n-1} \partial y} + \frac{n(n-1)}{1 \cdot 2} (\Delta x)^{n-2} (\Delta y^2) \times \frac{\partial^n \varphi}{\partial x^{n-2} \partial y^2} + \ldots + (\Delta y)^n \frac{\partial^n \varphi}{\partial y^n} \right] \tag{5.2.2}$$

where $\varphi(x, y)$ is the value of this function at the given point $N(x, y)$ on the initial curve, $\Delta x = x_0 - x$, and $\Delta y = y_0 - y$. The function ψ may be used in (5.2.2) instead of φ.

Series (5.2.2) yields the required solution if values of the functions φ (or ψ) and also their derivatives of any order exist on a given curve and are known. Since the first derivatives on this curve [we shall denote them by $p = \varphi_x$ (or ψ_x) and $q = \varphi_y$ (or ψ_y)] are given, our task consists in finding the second derivatives on it, and also derivatives of a higher order. Hence, the solution of the Cauchy problem is associated with finding of the conditions in which the higher derivatives on the given curve can be determined. We shall limit ourselves to determination of the second derivatives. Since these derivatives are three in number (u, s, and t), we have to compile the same number of independent equations to find them. Equation (5.2.2), which is satisfied on the initial curve AB, is the first of them. The other two are obtained from the following known relations for the total differentials of the functions of two independent variables on this curve:

$$dp = (\partial p/\partial x)\,dx + (\partial p/\partial y)\,dy = u\,dx + s\,dy$$
$$dq = (\partial q/\partial x)\,dx + (\partial q/\partial y)\,dy = s\,dx + t\,dy$$

Hence, we can write the system of equations for determining the second derivatives in the form

$$\left.\begin{aligned} Au + 2Bs + Ct + H &= 0 \\ dx\,u + dy\,s + 0\cdot t - dp &= 0 \\ 0\cdot u + dx\,s + dy\,t - dq &= 0 \end{aligned}\right\} \qquad (5.2.3)$$

This system of equations is solved for the unknowns u, s, and t with the aid of determinants. If we introduce the symbols Δ and Δ_u, Δ_s, Δ_t for the principal and partial determinants, respectively, we have

$$u = \Delta_u/\Delta,\quad s = \Delta_s/\Delta,\quad t = \Delta_t/\Delta \qquad (5.2.4)$$

where

$$\left.\begin{aligned} \Delta &= \begin{vmatrix} A & 2B & C \\ dx & dy & 0 \\ 0 & dx & dy \end{vmatrix};\quad \Delta_u = \begin{vmatrix} -H & 2B & C \\ dp & dy & 0 \\ dq & dx & dy \end{vmatrix} \\ \Delta_s &= \begin{vmatrix} A & -H & C \\ dx & dp & 0 \\ 0 & dq & dy \end{vmatrix};\quad \Delta_t = \begin{vmatrix} A & 2B & -H \\ dx & dy & dp \\ 0 & dx & dq \end{vmatrix} \end{aligned}\right\} \qquad (5.2.4')$$

It follows from these relations that if the principal determinant Δ does not equal zero on the initial curve AB, the second derivatives u, s, and t are calculated *unambiguously*.

Let us assume that the curve has been chosen so that the principal determinant on it is zero, i.e. $\Delta = 0$. Hence

$$A\,(dy/dx)^2 - 2B\,(dy/dx) + C = 0 \qquad (5.2.5)$$

It is known from mathematics that when the principal determinant Δ of the system of equations (5.2.3) is zero on the curve given by Eq. (5.2.5), the second derivatives u, s, and t (5.2.4) are either determined *ambiguously*, or in general *cannot be determined* in terms of φ, p, and q.

Let us consider quadratic equation (5.2.5). Solving it for the derivative dy/dx, we obtain

$$(dy/dx)_{1,2} = y'_{1,2} = (1/A)\,(B \pm \sqrt{B^2 - AC}) \qquad (5.2.6)$$

This equation determines the slope of a tangent at each point of the initial curve on which the principal determinant $\Delta = 0$. It is not difficult to see that (5.2.6) is a differential equation of two families of real curves if $B^2 - AC > 0$. Such curves, at each point of which the principal determinant of system (5.2.3) is zero, are called **characteristics**, and Eq. (5.2.5) is called a **characteristic one.**

From the above, there follows a condition in which the unambiguous determination of the second derivatives on the initial curve is possible: no arc element of this curve should coincide with the characteristics. The same condition $\Delta \neq 0$ holds for the unambiguous determination of the higher derivatives in series (5.2.2). Consequently, if $\Delta \neq 0$, all the coefficients of series (5.2.2) are determined unambiguously according to the data on the initial curve.

Consequently, the condition $\Delta \neq 0$ is necessary and sufficient to solve the Cauchy problem. This problem has a fundamental significance in the theory of partial differential equations, and formula (5.2.2) can be used to calculate the flow of a gas. But from the viewpoint of the physical applications, particularly of the calculation of supersonic gas flows, of greater interest is the problem of determining the solution according to the characteristics, i.e. the **method of characteristics**. This method can be obtained from an analysis of the Cauchy problem and consists in the following. Let us assume that the initial curve AB coincides with one of the characteristics, and not only the principal determinant of the system (5.2.3) equals zero along it, but also the partial determinants $\Delta_u = \Delta_s = \Delta_t = 0$. It can be proved here that if, for example, the determinants Δ and Δ_t equal zero, i.e.

$$Ay'^2 - 2By' + C = 0 \qquad (5.2.5')$$

$$A\,(y'q' - p') - 2Bq' - H = 0 \qquad (5.2.7)$$

where $p' = dp/dx$, $q' = dq/dx$, then the equality to zero of the other determinants is satisfied automatically.

According to the theory of systems of algebraic equations, the equality to zero of the principal and all the partial determinants signifies that solutions of system (5.2.3), although they are *ambiguous, can exist.* If one of the solutions, for example, that for u, is finite, then the solutions for s and t are also finite.

5.3. Characteristics

Compatibility Conditions

Equations (5.2.5) and (5.2.7) determining the conditions in which solutions, although ambiguous, exist for u, s, and t are known as the **compatibility conditions.** Geometrically, the first of these equations represents two families of curves that are characteristics in the physical plane x, y, and the second equation two families of curves that are characteristics in the plane p, q.

Any solution of the problem on the supersonic flow of a gas found by solving equations of characteristics (or compatibility conditions) is a *solution of the fundamental equation of gas dynamics* (5.1.8) or (5.1.25). The proof follows from what is known as the **equivalence theorem,** according to which the equations of characteristics (5.2.5) and (5.2.7) are equivalent to the fundamental equation (5.1.8) or (5.1.25) (a proof of this theorem is given in [15]).

From the geometric viewpoint, the proved equivalence signifies that the solution of the equations of the characteristics also gives the image of a plane x, y on the plane p, q when points of the curves determined by differential equation (5.1.8) correspond to points of the curves determined by differential equation (5.1.25).

Hence, a definite point on a characteristic in the plane p, q corresponds to each point on a characteristic in the plane x, y. This correspondence can evidently be established in different ways depending on the preset boundary conditions, and, as will be shown below, it is just this correspondence that makes it possible to use characteristics for calculating gas flows.

Accordingly, a feature of characteristics is that the initial conditions cannot be set arbitrarily along them, while they can along a curve that is not a characteristic.

Determination of Characteristics

Kind of Characteristics. A close look at (5.2.6) reveals that the roots of quadratic characteristic equation (5.2.5) may be real (equal or not equal in magnitude) and also complex conjugate. The difference between the roots is determined by the expression $B^2 - AC = \delta$. When $\delta > 0$, Eq. (5.2.5) gives two different families of real

characteristics; the value of $\delta = 0$ determines two identical roots, which corresponds to two coinciding families of characteristics, i.e. actually to one characteristic; when $\delta < 0$, the roots of the equation are a pair of imaginary characteristics.

Since the roots of a characteristic equation depend on the coefficients A, B, and C of differential equation (5.2.1), it is customary practice to establish the type of these equations depending on the kind of characteristics. When $\delta > 0$, Eq. (5.2.1) is a **hyperbolic** one, when $\delta = 0$, a **parabolic**, and when $\delta < 0$, an **elliptic** one.

The coefficients A, B, and C in Eqs. (5.1.8) for the velocity potential and (5.1.25) for the stream function are determined identically:

$$A = V_x^2 - a^2, \quad B = V_x V_y, \quad C = V_y^2 - a^2 \tag{5.3.1}$$

Consequently,

$$\delta = B^2 - AC = a^2 (V^2 - a^2) \tag{5.3.2}$$

where $V = \sqrt{V_x^2 + V_y^2}$ is the total velocity.

Therefore, for the regions of a gas flow with supersonic velocities ($V > a$), hyperbolic equations are employed, and for regions of a flow with subsonic velocities ($V < a$), elliptic ones. At the boundary of these regions, the velocity equals that of sound ($V = a$), and the equations will be parabolic.

Characteristics in a Physical Plane. Characteristics in the plane x, y are determined from the solution of the differential equation (5.2.6) in which the plus sign corresponds to the characteristics of the first family, and the minus sign to those of the second one.

The quantity $\lambda_1 = dy/dx$ directly calculated by expression (5.2.6) and the plus sign in this expression determine the angular coefficient of the **characteristic of the first family,** and $\lambda_2 = dy/dx$ and the minus sign—that of the **characteristic of the second family.** Both these characteristics are customarily referred to as **conjugate.** With a view to expressions (5.3.1) and (5.3.2), we obtain the following expression for the characteristics in the plane x, y:

$$\lambda_{1,2} = dy/dx = [1/(V_x^2 - a^2)] (V_x V_y \pm a\sqrt{V^2 - a^2}) \tag{5.3.3}$$

The characteristics in the plane x, y have a definite physical meaning that can be determined if we find the angle μ between the velocity vector $\mathbf{V}$ at a point A of the flow (Fig. 5.3.1) and the direction of the characteristic at this point. The angle is determined with the aid of Eq. (5.3.3) if we use the local system of coordinates x_1, y_1 with its origin at point A and with the x_1-axis coinciding with the direction of the vector $\mathbf{V}$. With such a choice of the coordinate axes, $V_x = V$, $V_y = 0$, and, consequently,

$$\lambda_{1,2} = \tan \mu_{1,2} = \pm (M^2 - 1)^{-1/2}$$

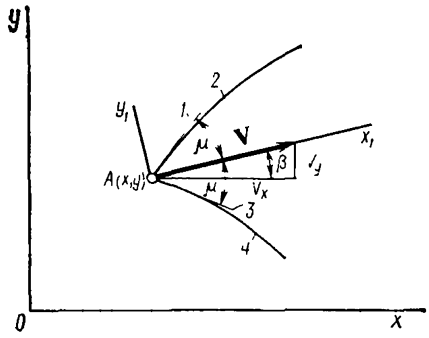

Fig. 5.3.1
To the explanation of the physical meaning of a characteristic:
1—direction of a characteristic of the first family at point *A*; *2*—characteristic of the first family with the angular coefficient λ_1; *3*—direction of a characteristic of the second family at point *A*; *4*—characteristic of the second family with the angular coefficient λ_2

It thus follows that μ is the Mach angle. We have therefore established an important property of characteristics consisting in that at every point belonging to a characteristic, the angle between a tangent to it and the velocity vector at this point *equals the Mach angle.* Consequently, a characteristic is a **line of weak disturbances** (or a **Mach line**) having the shape of a curve in the general case.

The definition of a characteristic as a Mach line has a direct application to a two-dimensional plane supersonic flow. If we have to do with a two-dimensional spatial (axisymmetric) supersonic flow, the Mach lines (characteristics) should be considered as the **generatrices of a surface of revolution enveloping the Mach cones** issuing from vertices at the points of disturbance (on the characteristics). A surface confining a certain region of disturbance is called a **wave surface** or **three-dimensional Mach wave.**

We already know that pressure waves appear in a gas whose supersonic flow is characterized by a *growth in the pressure.* But such a flow may be attended by *lowering of* the pressure, i.e. there will be a supersonic expanding flow, and the Mach lines will characterize expansion waves. The relevant characteristics, which in the general case are curved lines (for a plane flow) or surfaces formed by the rotation of these lines (for a spatial axisymmetric flow) coincide with these Mach lines. If a flow contains Mach lines (characteristics) in the form of straight lines, then **simple expansion waves** whose velocity of propagation has one direction correspond to them. When Mach lines correspond to expansion waves, we call them lines of weak disturbances, using the terminology adopted for weak pressure waves. It must be remembered here that no other expansion waves except weak ones appear in an expanding supersonic flow, because otherwise we would have to assume the possibility of the formation of "strong" expansion waves (expansion shocks) which in real flow conditions cannot exist.

If at a point of a physical plane the flow velocity and speed of sound are known, the above property of characteristics makes it possible

to determine their directions at this point by calculating the Mach angle by the formula $\mu = \pm\sin^{-1}(1/M)$. We determine the angular coefficients of the characteristics in the coordinates x, y (Fig. 5.3.1) from the equation

$$\lambda_{1,2} = dy/dx = \tan(\beta \pm \mu) \tag{5.3.4}$$

where β is the angle of inclination of the velocity vector to the x-axis; the plus sign relates to the characteristic of the first family, and the minus sign to that of the second family.

Equation (5.3.4) is a differential equation for the characteristics in a physical plane.

Characteristics in the Plane p,q. If we substitute for y' in Eq. (5.2.7) the first root of the characteristic equation (5.2.5) equal to $y' = \lambda_1$, the equation obtained, namely,

$$A(\lambda_1 q' - p') - 2Bq' - H = 0 \tag{5.3.5}$$

is the first family of characteristics in the plane p, q. A similar substitution for y' of the second root $y' = \lambda_2$ yields an equation for the second family of characteristics in the same plane:

$$A(\lambda_2 q' - p') - 2Bq' - H = 0 \tag{5.3.6}$$

Equations (5.3.5) and (5.3.6) for the characteristics can be transformed by using the property of the roots of quadratic equation (5.2.5) according to which

$$\lambda_1 + \lambda_2 = 2B/A \tag{5.3.7}$$

By considering the first family of characteristics and by introducing the relation $A\lambda_1 - 2B = -\lambda_2 A$ obtained from (5.3.7) into (5.3.5), we compile the equation

$$A(\lambda_2 q' + p') + H = 0 \tag{5.3.8}$$

Similarly, for a characteristic of the second family, we have

$$A(\lambda_1 q' + p') + H = 0 \tag{5.3.9}$$

With a view to expression (5.3.4), Eqs. (5.3.8) and (5.3.9) can be written in the form

$$\frac{dp}{dx} + \tan(\beta \mp \mu)\frac{dq}{dx} + \frac{H}{A} = 0 \tag{5.3.10}$$

where the minus sign relates to characteristics of the first family, and the plus sign to those of the second one. Equation (5.3.10) determines the **conjugated characteristics** in the plane p, q.

Orthogonality of Characteristics

If we replace the differentials in the equations for the characteristics with finite differences, the equations obtained will be ones of straight lines in the corresponding planes x, y and p, q.

Let us consider the equations, particularly, for the characteristics of the first family in the plane x, y and of the second family in the plane p, q. It follows from (5.3.4) that for an element of a characteristic—a straight line in the plane x, y—the equation has the form

$$y - y_0 = (x - x_0)\,\lambda_1 \qquad (5.3.4')$$

where x_0, y_0 are the coordinates of a fixed point, λ_1 is an angular coefficient calculated from the parameters of the gas at this point, and x, y are the running coordinates.

Let us compile an equation for an element of a characteristic of the second family in the plane p, q in accordance with (5.3.9):

$$A\lambda_1 (q - q_0) + A (p - p_0) + H (x - x_0) = 0 \qquad (5.3.9')$$

where p_0, q_0 are the values of the functions p and q at point x_0, y_0 of the physical plane, the angular coefficient λ_1 and also the values of A and H are calculated according to the parameters of the gas at this point, and p and q are running coordinates.

Examination of Eqs. (5.3.4′) and (5.3.9′) reveals that the inclination of a straight line in the plane x, y is determined by the angular coefficient λ_1, and in the plane p, q by the angular coefficient $-1/\lambda_1$. It can be proved similarly that an element of a characteristic of the second family in the plane x, y has the angular coefficient λ_2, and an element of a characteristic of the first family in the plane p, q—the angular coefficient $-1/\lambda_2$. It thus follows that *the characteristics of different families in the two planes are perpendicular to each other.*

This property makes it possible to determine the direction of the characteristics in the plane p, q if the direction of the conjugate characteristics in the physical plane is known. Assume that for a point P (x_0, y_0) of the plane x, y we know the velocity components V_{x0}, V_{y0} and the values of the functions p_0, q_0. We can determine the directions of the Mach lines at this point (Fig. 5.3.2) by (5.3.4′). To an element of characteristic PN of the first family in the plane x, y there corresponds an element of a characteristic of the second family—a straight line in the plane p, q set by Eq. (5.3.9′). This line is perpendicular to line PN, but does not pass through point P' with the coordinates p_0, q_0, which is indicated by the presence of a free term in Eq. (5.3.9′). Consequently, to construct an element of a characteristic according to the rules of analytic geometry, we must first determine the distance δ_1 to it from point P'. A characteristic

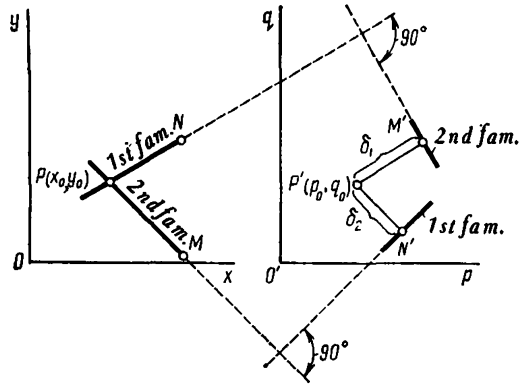

Fig. 5.3.2
Property of orthogonality of characteristics

of the first family is constructed in a similar way in the plane p, q perpendicular to straight line PM and at a distance of δ_2 from point P' (Fig. 5.3.2).

The property of orthogonality of characteristics belonging to different families manifests itself in the case of a potential flow for the planes x, y and V_x, V_y (the hodograph plane), and also in the case of a vortex flow, for which the plane p, q is replaced with the same hodograph plane V_x, V_y.

Transformation of the Equations for Characteristics in a Hodograph

Let us transform Eq. (5.3.10) to a form such that it will determine the characteristics in a hodograph where the velocity components V_x, V_y are the coordinates or independent variables. For this purpose, by differentiating expressions (5.1.9) with respect to x, we calculate the derivatives dp/dx and dq/dx:

$$\frac{dp}{dx} = \frac{d}{dx}\left(\frac{\partial \psi}{\partial x}\right) = -V_y \varepsilon y^{\varepsilon-1} \frac{dy}{dx}(1-\bar{V}^2)^{1/(k-1)} - y^{\varepsilon}\frac{dV_y}{dx}(1-\bar{V}^2)^{1/(k-1)} + \frac{2y^{\varepsilon}}{k-1} V_y (1-\bar{V}^2)^{1/(k-1)-1}\bar{V}\frac{d\bar{V}}{dy} \tag{5.3.11}$$

$$\frac{dq}{dx} = \frac{d}{dx}\left(\frac{\partial \psi}{\partial y}\right) = V_x \varepsilon y^{\varepsilon-1}\frac{dy}{dx}(1-\bar{V}^2)^{1/(k-1)} + y^{\varepsilon}\frac{dV_x}{dx} \times (1-\bar{V}^2)^{1/(k-1)} - \frac{2y^{\varepsilon}}{k-1} V_x (1-\bar{V}^2)^{1/(k-1)-1}\bar{V}\frac{d\bar{V}}{dx} \tag{5.3.12}$$

A glance at Eq. (5.1.25) reveals that

$$\left.\begin{aligned} H &= \varepsilon y^{\varepsilon-1} a^2 V_x (1-\bar{V}^2)^{1/(k-1)} - \frac{k-1}{2k} \\ &\times \frac{V_{\max}^2}{RV} (1-\bar{V}^2)^{k/(k-1)} y^{\varepsilon} (a^2 - V^2) \frac{dS}{dn}; \quad A = V_x^2 - a^2 \end{aligned}\right\} \quad (5.3.13)$$

After introducing (5.3.11)-(5.3.13) into (5.3.10) and replacing the quantities dy/dx with the angular coefficients $\lambda_{1,2}$ of the characteristics, and the functions $\tan(\beta \mp \mu)$ with the corresponding values of $\lambda_{2,1}$, we obtain

$$\begin{aligned} &\varepsilon y^{\varepsilon-1} \lambda_{1,2} (1-\bar{V}^2)^{1/(k-1)} (V_x \lambda_{2,1} - V_y) + y^{\varepsilon} (1-\bar{V}^2)^{1/(k-1)} \\ &\times \left(\frac{dV_x}{dx} \lambda_{2,1} - \frac{dV_y}{dx} \right) + \frac{2y^{\varepsilon}}{k-1} (1-\bar{V}^2)^{1/(k-1)-1} \bar{V} \frac{d\bar{V}}{dx} (V_y - V_x \lambda_{2,1}) \\ &+ \frac{1}{V_x^2 - a^2} \left[\varepsilon y^{\varepsilon-1} a^2 V_x (1-\bar{V}^2)^{1/(k-1)} - \frac{k-1}{2k} \right. \\ &\left. \times \frac{V_{\max}^2}{RV} (1-\bar{V}^2)^{k/(k-1)} y^{\varepsilon} (a^2 - V^2) \frac{dS}{dn} \right] = 0 \end{aligned}$$

After cancelling quantities where possible and introducing the dimensionless variables

$$\bar{V}_x = V_x/V_{\max}, \quad \bar{V}_y = V_y/V_{\max}, \quad \bar{V} = V/V_{\max}, \quad V/a = M$$

we can write this equation in the form

$$\begin{aligned} &\frac{\varepsilon}{y} \lambda_{1,2} (\bar{V}_x \lambda_{2,1} - \bar{V}_y) + \left(\frac{d\bar{V}_x}{dx} \lambda_{2,1} - \frac{d\bar{V}_y}{dx} \right) \\ &+ \frac{2\bar{V}}{k-1} \cdot \frac{\bar{V}_y - \bar{V}_x \lambda_{2,1}}{1-\bar{V}^2} \cdot \frac{d\bar{V}}{dx} - \frac{\varepsilon}{y} \cdot \frac{\bar{V}_x}{1 - V_x^2/a^2} \\ &- \frac{k-1}{2k} \cdot \frac{1}{R\bar{V}} \cdot (1-\bar{V}^2) \frac{M^2-1}{1-V_x^2/a^2} \cdot \frac{dS}{dn} = 0 \end{aligned} \quad (5.3.14)$$

By introducing the polar angle β, we obtain the following expressions for the projections of the velocity vector:

$$\bar{V}_x = \bar{V} \cos\beta, \quad \bar{V}_y = \bar{V} \sin\beta \quad (5.3.15)$$

Let us differentiate these expressions with respect to x:

$$\left.\begin{aligned} d\bar{V}_x/dx &= (d\bar{V}/dx) \cos\beta - \bar{V} \sin\beta \, d\beta/dx \\ d\bar{V}_y/dx &= (d\bar{V}/dx) \sin\beta + \bar{V} \cos\beta \, d\beta/dx \end{aligned}\right\} \quad (5.3.16)$$

Introducing (5.3.15) and (5.3.16) into (5.3.14) and taking into account that $\tan^2\mu = (M^2 - 1)^{-1}$ and $\sin^2\mu = M^{-2}$, we have

$$\frac{d\bar{V}}{dx} \left(\frac{2\bar{V}^2}{k-1} \cdot \frac{\sin\beta - \lambda_{1,2}\cos\beta}{1-\bar{V}^2} + \lambda_{2,1}\cos\beta - \sin\beta \right)$$

$$-\bar{V}\frac{d\beta}{dx}(\lambda_{2,1}\sin\beta+\cos\beta)+\frac{\varepsilon}{y}\bar{V}\left[\lambda_{1,2}(\lambda_{2,1}\cos\beta-\sin\beta)\right.$$
$$\left.-\frac{\cos\beta}{1-\cos^2\beta/\sin^2\mu}\right]-\frac{k-1}{2k}\cdot\frac{1}{R\bar{V}}(1-\bar{V}^2)\frac{\cot^2\mu}{1-\cos^2\beta/\sin^2\mu}\cdot\frac{dS}{dn}=0$$

Having in view that $[(k-1)/2](1-V^2/V_{\max}^2)=a^2/V_{\max}^2=\bar{V}^2\sin^2\mu$, we find

$$\frac{dV}{V}+d\beta\frac{(\lambda_{2,1}\sin\beta+\cos\beta)\tan^2\mu}{\lambda_{2,1}\cos\beta-\sin\beta}-\varepsilon\frac{dx}{y}$$
$$\times\left[\lambda_{1,2}-\frac{\sin^2\mu\cos\beta}{(\lambda_{2,1}\cos\beta-\sin\beta)(\sin^2\mu-\cos^2\beta)}\right]\tan^2\mu$$
$$+\frac{dx}{kR}\cdot\frac{\sin^4\mu}{(\sin^2\mu-\cos^2\beta)(\lambda_{2,1}\cos\beta-\sin\beta)}\frac{dS}{dn}=0 \qquad (5.3.17)$$

Performing the substitutions $\lambda_{2,1}=\tan(\beta\mp\mu)$ and $\lambda_{1,2}=\tan(\beta\pm\mu)$, we transform the individual expressions contained in (5.3.17) to the following form:

$$\frac{\lambda_{2,1}\sin\beta+\cos\beta}{\lambda_{2,1}\cos\beta-\sin\beta}=\frac{1}{\mp\tan\mu} \qquad (5.3.18)$$

$$\lambda_{1,2}-\frac{\sin^2\mu\cos\beta}{(\lambda_{2,1}\cos\beta-\sin\beta)(\sin^2\mu-\cos^2\beta)}=\frac{\sin\beta\cos\mu}{\cos(\beta\pm\mu)} \qquad (5.3.19)$$

$$\frac{\sin^4\mu}{(\sin^2\mu-\cos^2\beta)(\lambda_{2,1}\cos\beta-\sin\beta)}=\pm\frac{\sin^3\mu}{\cos(\beta\pm\mu)} \qquad (5.3.20)$$

With a view to (5.3.18)-(5.3.20), Eq. (5.3.17) for the characteristics of the first and second families, respectively, acquire the form

$$\frac{dV}{V}-\tan\mu\,d\beta-\varepsilon\frac{dx}{y}\cdot\frac{\sin\mu\sin\beta\tan\mu}{\cos(\beta+\mu)}$$
$$+\frac{dx}{kR}\cdot\frac{\sin^3\mu}{\cos(\beta+\mu)}\cdot\frac{dS}{dn}=0 \qquad (5.3.21)$$

$$\frac{dV}{V}+\tan\mu\,d\beta-\varepsilon\frac{dx}{y}\cdot\frac{\sin\mu\sin\beta\tan\mu}{\cos(\beta-\mu)}$$
$$-\frac{dx}{kR}\cdot\frac{\sin^3\mu}{\cos(\beta-\mu)}\cdot\frac{dS}{dn}=0 \qquad (5.3.22)$$

The entropy gradient dS/dn can be calculated according to the value of the derivative of the stagnation pressure dp_0'/dn. For this purpose, we shall use relations (4.3.6) and (4.3.20) from which we obtain the following formula for the difference of the entropies:

$$S_2-S_1=-c_v(k-1)\ln(p_0'/p_0) \qquad (5.3.23)$$

Since $c_v(k-1)=R$, then by calculating the derivative with respect to n and designating dS_2/dn by dS/dn, we find

$$\frac{1}{R}\cdot\frac{dS}{dn}=-\frac{1}{p_0'}\cdot\frac{dp_0'}{dn} \qquad (5.3.24)$$

For our further transformations, we shall introduce the new variable

$$\omega = \int_{a^*}^{V} \cot \mu \frac{dV}{V} \tag{5.3.25}$$

that is an angle. We shall express the ratio dV/V in the form $d\lambda/\lambda$. ($\lambda = V/a^*$), and cot μ with the aid of (3.6.23) in the form

$$\cot \mu = \sqrt{M^2 - 1} = \sqrt{(\lambda^2 - 1) \Big/ \left(1 - \frac{k-1}{k+1} \lambda^2\right)} \tag{5.3.26}$$

Consequently,

$$\omega = \int_{1}^{\lambda} \sqrt{(\lambda^2 - 1) \Big/ \left(1 - \frac{k-1}{k+2} \lambda^2\right)} \frac{d\lambda}{\lambda} \tag{5.3.27}$$

Integration of (5.3.27) yields

$$\omega = \sqrt{\frac{k+1}{k-1}} \tan^{-1} \sqrt{\frac{k-1}{k+1} \cdot \frac{\lambda^2 - 1}{1 - \frac{k-1}{k+1} \lambda^2}} - \tan^{-1} \sqrt{\frac{\lambda^2 - 1}{1 - \frac{k-1}{k+1} \lambda^2}} \tag{5.3.28}$$

Having in view that $\lambda_{max} = V_{max}/a^* = \sqrt{(k+1)/(k-1)}$, we obtain

$$\omega = \sqrt{\frac{k+1}{k-1}} \tan^{-1} \sqrt{\frac{\lambda^2 - 1}{\lambda_{max}^2 - \lambda^2}} - \tan^{-1} \sqrt{\frac{k+1}{k-1} \cdot \frac{\lambda^2 - 1}{\lambda_{max}^2 - \lambda^2}} \tag{5.3.29}$$

Substituting M for λ in (5.3.28) in accordance with (5.3.26), we have

$$\omega = \sqrt{\frac{k+1}{k-1}} \tan^{-1} \sqrt{\frac{k-1}{k+1} (M^2 - 1)} - \tan^{-1} \sqrt{M^2 - 1} \tag{5.3.30}$$

Examination of Eqs. (5.3.29) and (5.3.30) reveals that the angle ω is a function only of the number λ (or M), and, consequently, it can be evaluated beforehand, which facilitates calculations of supersonic gas flows by the method of characteristics.

The values of ω for various numbers M at $k = 1.4$ are contained in Table 5.3.1, which also gives the angles of inclination of the disturbance line calculated by the formula $\mu = \sin^{-1}(1/M)$.

Table 5.3.1

M	ω, deg	μ, deg	M	ω, deg	μ, deg	M	ω, deg	μ, deg
1.00	0.000	90.000	4.00	65.785	14.478	7.00	90.973	8.213
1.10	1.336	65.38[illegible]	4.10	67.082	14.117	7.10	91.491	8.097
1.20	3.558	56.443	4.20	68.333	13.774	7.20	91.997	7.984
1.30	6.170	50.285	4.30	69.541	13.448	7.30	92.490	7.873
1.40	8.987	45.585	4.40	70.706	13.137	7.40	92.970	7.776
1.50	11.905	41.810	4.50	71.832	12.814	7.50	93.440	7.662
1.60	14.861	38.682	4.60	72.919	12.556	7.60	93.898	7.561
1.70	17.810	36.032	4.70	73.970	12.284	7.70	94.345	7.462
1.80	20.725	33.749	4.80	74.986	12.025	7.80	94.781	7.366
1.90	23.586	31.757	4.90	75.969	11.776	7.90	95.208	7.272
2.00	26.380	30.000	5.00	76.920	11.537	8.00	95.625	7.181
2.10	29.097	28.437	5.10	77.841	11.308	8.20	96.430	7.005
2.20	31.732	27.036	5.20	78.732	11.087	8.40	97.200	6.837
2.30	34.283	25.771	5.30	79.596	10.876	8.60	97.936	6.677
2.40	36.746	24.624	5.40	80.433	10.672	8.80	98.642	6.525
2.50	39.124	23.578	5.50	81.245	10.476	9.00	99.318	6.379
2.60	41.415	22.620	5.60	82.032	10.287	9.20	99.967	6.240
2.70	43.621	21.738	5.70	82.796	10.104	9.40	100.589	6.107
2.80	45.746	20.925	5.80	83.537	9.928	9.60	101.188	5.979
2.90	47.790	20.171	5.90	84.256	9.758	9.80	101.763	5.857
3.00	49.757	19.471	6.00	84.955	9.594	10.00	102.316	5.739
3.10	51.650	18.819	6.10	85.635	9.435	10.20	102.849	5.626
3.20	53.470	18.210	6.20	86.296	9.282	10.40	103.362	5.518
3.30	55.222	17.640	6.30	86.937	9.133	10.60	103.857	5.413
3.40	56.907	17.105	6.40	87.561	8.989	10.80	104.335	5.313
3.50	58.530	16.602	6.50	88.168	8.850	11.00	104.796	5.216
3.60	60.091	16.128	6.60	88.759	8.715	11.20	105.241	5.133
3.70	61.595	15.680	6.70	89.335	8.584	11.40	105.671	5.032
3.80	63.044	15.258	6.80	89.895	8.457	11.60	106.087	4.945
3.90	64.440	14.857	6.90	90.441	8.333	11.80	106.489	4.861
						12.00	106.879	4.780

Introducing the angle ω into (5.3.21) and (5.3.22), we obtain the following equation for the characteristics:

$$d(\omega \mp \beta) - \varepsilon \frac{dx}{y} \cdot \frac{\sin\beta \sin\mu}{\cos(\beta \pm \mu)} \pm \frac{dx}{kR} \cdot \frac{\sin^2\mu \cos\mu}{\cos(\beta \pm \mu)} \cdot \frac{dS}{dn} = 0 \tag{5.3.31}$$

Equation (5.3.31) corresponds to the most general case of supersonic two-dimensional (plane or spatial) vortex (non-isentropic) flow of a gas.

Equations for Characteristics in a Hodograph for Particular Cases of Gas Flow

The form of Eq. (5.2.5) for characteristics in a physical plane is the same for all cases of gas flow if the latter is supersonic and two-dimensional. But in a hodograph, the equations for the characteristics differ and depend on the kind of flow.

If a two-dimensional flow is vortex-free, then according to (5.1.23) at all points of space occupied by the gas, the entropy is constant ($dS/dn = 0$), and, therefore, the equation for the characteristics acquires a simpler form:

$$d(\omega \mp \beta) - \varepsilon \frac{dx}{y} \cdot \frac{\sin\beta \sin\mu}{\cos(\beta \pm \mu)} = 0 \tag{5.3.32}$$

For a plane non-isentropic flow ($\varepsilon = 0$), we have

$$d(\omega \mp \beta) \pm \frac{dx}{kR} \cdot \frac{\sin^2\mu \cos\mu}{\cos(\beta \pm \mu)} \cdot \frac{dS}{dn} = 0 \tag{5.3.33}$$

In the simplest case of a plane vortex-free flow ($dS/dn = 0$), we have

$$d(\omega \mp \beta) = 0 \tag{5.3.34}$$

Integration of (5.3.34) yields $\beta = \pm \omega + \text{const}$. Introducing fixed values of the angles β_1 and β_2 instead of the constant, where β_1 corresponds to the plus sign of ω, and β_2 to the minus sign, we find an equation for the characteristics in the form

$$\beta = \pm \omega + \beta_{1,2} \tag{5.3.35}$$

Introducing instead of ω relation (5.3.29), we obtain

$$\beta = \pm \left(\sqrt{\frac{k+1}{k-1}} \tan^{-1} \sqrt{\frac{\lambda^2-1}{\lambda_{\max}^2-\lambda^2}} - \tan^{-1} \sqrt{\frac{k+1}{k-1} \cdot \frac{\lambda^2-1}{\lambda_{\max}^2-\lambda^2}} \right) + \beta_{1,2} \tag{5.3.36}$$

Hence, unlike Eq. (5.2.5) for characteristics in a physical plane and Eqs. (5.3.31), (5.3.32) or (5.3.33) for characteristics in a hodograph in a differential form, the corresponding equation (5.3.36) for the characteristics of a plane isentropic flow has an explicit form. Geometrically, this equation defines two families of curves—characteristics in a ring whose inner radius is $\lambda = 1$ and whose outer one is $\lambda_{\max} = [(k+1)/(k-1)]^{1/2}$ (Fig. 5.3.3). The integration constant β_1 and the plus sign in front of the function $\omega(\lambda)$ correspond to a characteristic of the first family, while the constant β_2 and the minus sign, to the second one. These curves are **epicycloids**

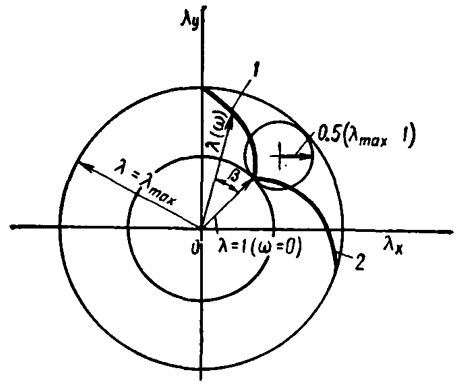

Fig. 5.3.3
Epicycloids—characteristics of a plane supersonic flow:
1—characteristic of the first family;
2—characteristic of the second family

and can be obtained as the path of a point on a circle of radius 0.5 ($\lambda_{max} - 1$) travelling along the inner (or outer) circle of the ring (Fig. 5.3.3). The angle β of inclination of the velocity vector and the speed ratio λ are the polar coordinates of points on an epicycloid.

By analysing a graph depicting a network of epicycloids, we can conclude that angles β larger in their magnitude, i.e. a more considerable deflection of the flow from its initial direction, correspond to an increase in the velocity due to expansion of the flow. A smaller deflection of the flow is observed at lower velocities.

The angle of inclination of the velocity vector is determined directly by the angle ω whose physical meaning can be established from (5.3.35). Assume that the integration constants $\beta_{1,2} = 0$. This signifies that expansion of the flow begins when $\beta = 0$ and $M = 1$. In accordance with this, the quantity $\beta = \pm\omega\,(M)$ is the angle of deflection of the flow upon its isentropic expansion from the point where $M = 1$ to a state characterized by an arbitrary number $M > 1$ equal to the upper limit when evaluating integral (5.3.27).

Hence, there is a difference between the angle of deflection of a flow with the number $M > 1$ from a certain initial direction and the angle $\beta = \pm\omega$ determining the complete turning of the flow upon its expansion from a state characterized by the number $M = 1$.

The angle of flow deflection in an arbitrary cross section can be determined as follows. Let us assume that we know the initial number $M_1 > 1$ which as a result of expansion of the flow increases and reaches the value $M_2 > M_1$. The angles ω_1 and ω_2 of deflection of the flow from its direction at a point with the number $M = 1$ correspond to the numbers M_1 and M_2. The angles ω_1 and ω_2 can be determined graphically with the aid of an epicycloid from expression (5.3.30) or Table 5.3.1. We use their values to find the angle of inclination of the velocity vectors. Considering, particularly, a characteristic of the first family, we obtain $\beta_1 = \omega_1\,(M_1)$ and $\beta_2 = \omega_2\,(M_2)$. Conse-

quently, the angle of deflection from the initial direction is

$$\Delta\beta = \beta_2 - \beta_1 = \omega_2(M_2) - \omega_1(M_1) \qquad (5.3.37)$$

The calculations can be performed in the opposite sequence, determining the local number M_2 according to the known angle $\Delta\beta$ of deflection of the flow and the initial number M_1. For this purpose, from (5.3.37) (in the given example we also consider a characteristic of the first family), we find

$$\omega_2(M_2) = \Delta\beta + \omega_1(M_1) \qquad (5.3.38)$$

We find the corresponding values of λ_2 or M_2 from Fig. 5.3.3 or Table 5.3.1 according to the value of ω_2.

Of interest is the calculation of the **ultimate flow angle** or the angle of deflection of the flow needed to obtain the maximum velocity V_{max}. Assume that deviation begins from the initial number $M = 1$. In this case, we find the ultimate flow angle by formula (5.3.30) in which we must adopt a value of M corresponding to V_{max} equal to infinity:

$$\omega_{max} = (\pi/2)\left[\sqrt{(k+1)/(k-1)} - 1\right] \qquad (5.3.39)$$

for $k = 1.4$, the value of $\omega_{max} = 0.726\pi = 130.46°$.

Consequently, a supersonic flow cannot turn through an angle larger than ω_{max}, and theoretically part of space remains unfilled with the gas.

If the initial number M from which the deflection begins is larger than unity, the angle of this deflection measured from the direction at $M = 1$ will be $\omega(M)$, while the ultimate flow angle corresponding to this number is

$$\beta_{max} = \omega_{max} - \omega(M) = (\pi/2)\left[\sqrt{(k+1)/(k-1)} - 1\right] - \omega(M) \qquad (5.3.40)$$

for $k = 1.4$, the angle $\beta_{max} = 130.46° - \omega(M)$.

For hypersonic velocities, the calculation of the function ω and, consequently, of the angles of deflection is simplified. Indeed, for $M \gg 1$, the terms in (5.3.30) can be represented in the following form with an accuracy within quantities of a higher order of infinitesimal:

$$\sqrt{\frac{k+1}{k-1}}\tan^{-1}\sqrt{\frac{k-1}{k+1}(M^2-1)} \approx \sqrt{\frac{k+1}{k-1}}\left(\frac{\pi}{2} - \frac{1}{M}\sqrt{\frac{k+1}{k-1}}\right)$$

$$\tan^{-1}\sqrt{M^2-1} \approx \pi/2 - 1/M.$$

Accordingly,

$$\omega = \frac{\pi}{2}\left(\sqrt{\frac{k+1}{k-1}} - 1\right) - \frac{2}{k-1}\cdot\frac{1}{M} \qquad (5.3.41)$$

The formula corresponding to (5.3.37) acquires the form

$$\Delta\beta = \beta_2 - \beta_1 = -\frac{2}{k-1}\left(\frac{1}{M_2} - \frac{1}{M_1}\right) \qquad (5.3.37')$$

All the above relations have been found for a perfect gas. At very low pressures, however, a gas is no longer perfect. This is why the calculated ultimate flow angles are not realized and have only a theoretical significance.

5.4. Outline of Solution of Gas-Dynamic Problems According to the Method of Characteristics

The determination of the parameters of a disturbed supersonic flow is associated with the solution of a system of equations for the characteristics in a physical plane and in a hodograph if the initial conditions in some way or other are set in the form of Cauchy's conditions. In the general case of a two-dimensional non-isentropic flow, this system has the form:

for characteristics of the first family

$$dy = dx \tan (\beta + \mu) \tag{5.4.1}$$

$$d(\omega - \beta) - \varepsilon (dx/y)\, l + (dx/kR)(dS/dn)\, c = 0 \tag{5.4.2}$$

for characteristics of the second family

$$dy = dx \tan (\beta - \mu) \tag{5.4.3}$$

$$d(\omega + \beta) - \varepsilon (dx/y)\, m - (dx/kR)(dS/dn)\, t = 0 \tag{5.4.4}$$

where the coefficients are

$$l = \sin\beta \sin\mu/\cos(\beta + \mu),\quad c = \sin^2\mu \cos\mu/\cos(\beta + \mu) \tag{5.4.5}$$

$$m = \sin\beta \sin\mu/\cos(\beta - \mu),\quad t = \sin^2\mu \cos\mu/\cos(\beta - \mu) \tag{5.4.6}$$

For a two-dimensional isentropic flow, we have

$$dS/dn = 0 \tag{5.4.7}$$

therefore the system of equations is simplified:

for characteristics of the first family

$$dy = dx \tan(\beta + \mu);\ d(\omega - \beta) - \varepsilon (dx/y)\, l = 0 \tag{5.4.8}$$

for characteristics of the second family

$$dy = dx \tan(\beta - \mu);\ d(\omega + \beta) - \varepsilon (dx/y)\, m = 0 \tag{5.4.9}$$

For a plane flow, we assume that $\varepsilon = 0$ in the equations, for a spatial axisymmetric flow, $\varepsilon = 1$, and we introduce r instead of y.

A solution according to the method of characteristics of any problem on the flow over a body consists of the solution of three particular problems.

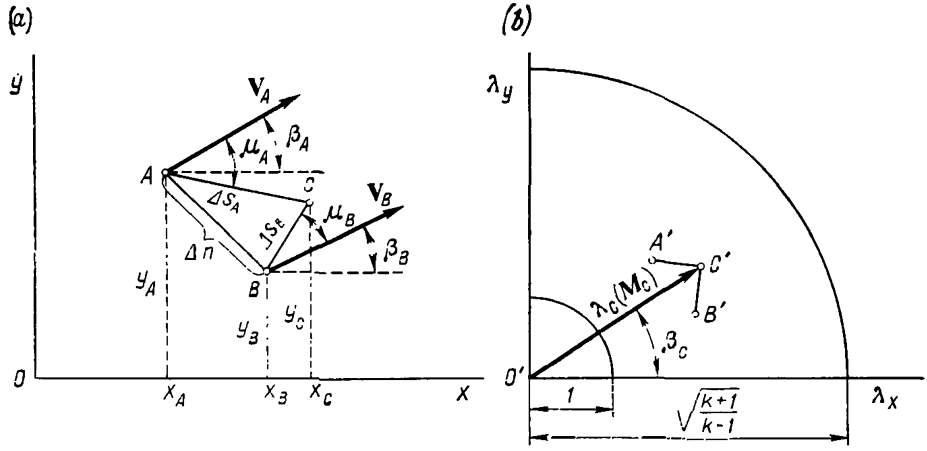

Fig. 5.4.1
Calculation of the velocity at the intersection point of two characteristics of different families:
a—physical plane; *b*—plane of hodograph

The **first problem** is associated with the determination of the velocity and other parameters at the point of intersection of characteristics of different families issuing from two close points.

Assume that we are determining the parameters at point C (velocity $\mathbf{V}_C$, number M_C, flow deflection angle β_C, entropy S_C, etc.) at the intersection of elements of characteristics of the first and second families drawn from points A and B (Fig. 5.4.1*a*). At these points, which are on different streamlines, we know the velocities $\mathbf{V}_A$, $\mathbf{V}_B$, and other parameters, including the entropies S_A and S_B.

All the calculations are based on the use of Eqs. (5.4.1)-(5.4.4) for the characteristics, which in finite differences have the form:

for the first family

$$\Delta y_B = \Delta x_B \tan(\beta_B + \mu_B) \tag{5.4.10}$$

$$\Delta\omega_B - \Delta\beta_B - \varepsilon(\Delta x_B/y_B) l_B + (\Delta x_B/kR)(\Delta S/\Delta n) c_B = 0 \tag{5.4.11}$$

for the second family

$$\Delta y_A = \Delta x_A \tan(\beta_A - \mu_A) \tag{5.4.12}$$

$$\Delta\omega_A + \Delta\beta_A - \varepsilon(\Delta x_A/y_A) m_A - (\Delta x_A/kR)(\Delta S/\Delta n) t_A = 0 \tag{5.4.13}$$

where

$$\left.\begin{aligned} &\Delta y_B = y_C - y_B, \quad \Delta x_B = x_C - x_B, \quad \Delta\omega_B = \omega_C - \omega_B, \\ &\qquad\qquad \Delta\beta_B = \beta_C - \beta_B \\ &\Delta y_A = y_C - y_A, \quad \Delta x_A = x_C - x_A. \quad \Delta\omega_A = \omega_C - \omega_A, \\ &\qquad\qquad \Delta\beta_A = \beta_C - \beta_A \end{aligned}\right\} \tag{5.4.14}$$

$$\left.\begin{aligned} l_B &= \sin\beta_B \sin\mu_B/\cos(\beta_B + \mu_B) \\ c_B &= \sin^2\mu_B \cos\mu_B/\cos(\beta_B + \mu_B) \\ m_A &= \sin\beta_A \sin\mu_A/\cos(\beta_A - \mu_A) \\ t_A &= \sin^2\mu_A \cos\mu_A/\cos(\beta_A - \mu_A) \end{aligned}\right\} \quad (5.4.15)$$

Equations (5.4.10)-(5.4.13) were derived assuming that the coefficients l, m, c, and t remain *constant* upon motion along characteristic elements BC and AC and equal their values at the initial points B and A.

The change in the entropy per unit length of a normal $\Delta S/\Delta n$ is calculated as follows. It is shown in Fig. 5.4.1*a* that the distance between points B and A is

$$\Delta n \approx (AC) \sin\mu_A + (BC) \sin\mu_B$$

where

$$AC = (x_C - x_A)/\cos(\beta_A - \mu_A), \quad BC = (x_C - x_B)/\cos(\beta_B - \mu_B)$$

Introducing the notation

$$e = (x_C - x_A) \sin\mu_A \cos(\beta_B + \mu_B), \quad f = (x_C - x_B) \sin\mu_B \cos \times (\beta_A - \mu_A)$$

we obtain

$$\Delta S/\Delta n = (S_A - S_B) \cos(\beta_B + \mu_B) \cos(\beta_A - \mu_A)/(f + e) \quad (5.4.16)$$

The entropy at point C is determined from the relation

$$S_C = \Delta S_B + S_B = \frac{\Delta S}{\Delta n}(BC) \sin\mu_B + S_B = \frac{(S_A - S_B) f}{f + e} + S_B \quad (5.4.17)$$

The entropy gradient may be replaced with the stagnation pressure gradient in accordance with (5.3.24):

$$\frac{1}{R} \cdot \frac{\Delta S}{\Delta n} = -\frac{1}{p_0'} \cdot \frac{\Delta p_0'}{\Delta n} = -\frac{(p_{0,A}' - p_{0,B}') \cos(\beta_B + \mu_B) \cos(\beta_A - \mu_A)}{(f + e)\, p_{0,B}'} \quad (5.4.18)$$

The stagnation pressure at point C is

$$p_{0,C}' = (p_{0,A}' - p_{0,B}')\, f/(f + e) + p_{0,B}' \quad (5.4.19)$$

To find the coordinates x_C and y_C of point C, we have to solve the simultaneous equations (5.4.10) and (5.4.12) for the elements of the characteristics in a physical plane:

$$y_C - y_B = (x_C - x_B) \tan(\beta_B + \mu_B);$$
$$y_C - y_A = (x_C - x_A) \tan(\beta_A - \mu_A)$$

A graphical solution of these equations is shown in Fig. 5.4.1*a*. We use the found value of x_C to determine the differences $\Delta x_B =$

$= x_C - x_B$ and $\Delta x_A = x_C - x_A$ in Eqs. (5.4.11) and (5.4.13). The increments $\Delta\omega_B$, $\Delta\omega_A$, $\Delta\beta_B$, and $\Delta\beta_A$ are the unknowns in these equations, but the latter are only two in number. The number of unknowns can be reduced to two in accordance with the number of equations in the system. For this purpose, we compile the obvious relations

$$\left.\begin{aligned}\Delta\omega_A &= \omega_C - \omega_A = \Delta\omega_B + \omega_B - \omega_A\\ \Delta\beta_A &= \beta_B - \beta_A = \Delta\beta_B + \beta_B - \beta_A\end{aligned}\right\} \qquad (5.4.20)$$

With account taken of these relations, Eq. (5.4.13) is transformed as follows:

$$\Delta\omega_B + \omega_B - \omega_A + \Delta\beta_B + \beta_B - \beta_A - \varepsilon\frac{\Delta x_A}{y_A} m_A - \frac{\Delta x_A}{kR}\cdot\frac{\Delta S}{\Delta n} t_A = 0 \qquad (5.4.21)$$

By solving this equation simultaneously with (5.4.11) for the variable $\Delta\beta_B$, we obtain

$$\Delta\beta_B = \frac{1}{2}\left[\frac{1}{kR}\cdot\frac{\Delta S}{\Delta n}(\Delta x_A t_A + \Delta x_B c_B) + \varepsilon\left(\frac{\Delta x_A}{y_A} m_A - \frac{\Delta x_B}{y_B} l_B\right) - (\omega_B - \omega_A) - (\beta_B - \beta_A)\right] \qquad (5.4.22)$$

We use the found value of $\Delta\beta_B$ to evaluate the increment of the function ω by (5.4.11):

$$\Delta\omega_B = \Delta\beta_B + \varepsilon\frac{\Delta x_B}{y_B} l_B - \frac{\Delta x_B}{kR}\cdot\frac{\Delta S}{\Delta n} c_B \qquad (5.4.23)$$

Now we can calculate the angles for point C:

$$\beta_C = \Delta\beta_B + \beta_B;\ \omega_C = \Delta\omega_B + \omega_B \qquad (5.4.24)$$

According to the found value of ω_C, we determine the number M_C and the Mach angle μ_C at point C from Table 5.3.1.

A graphical solution of the system of equations for characteristics in a hodograph as a result of which the angle β_C and the number λ_C (M_C) are determined is shown in Fig. 5.4.1*b*, where $B'C'$ and $A'C'$ are elements of the characteristics of the first and second families corresponding to elements of the conjugate characteristics BC and AC in a physical plane. The found number M_C (or λ_C) when necessary can be used to determine parameters such as the pressure, density, and temperature.

The calculated parameters can be determined more precisely if we substitute for l_B, m_A, c_B, and t_A in Eqs. (5.4.10)-(5.4.13) the quantities obtained from the values of the angles β and μ that are the average between the ones set at points A and B, and those found

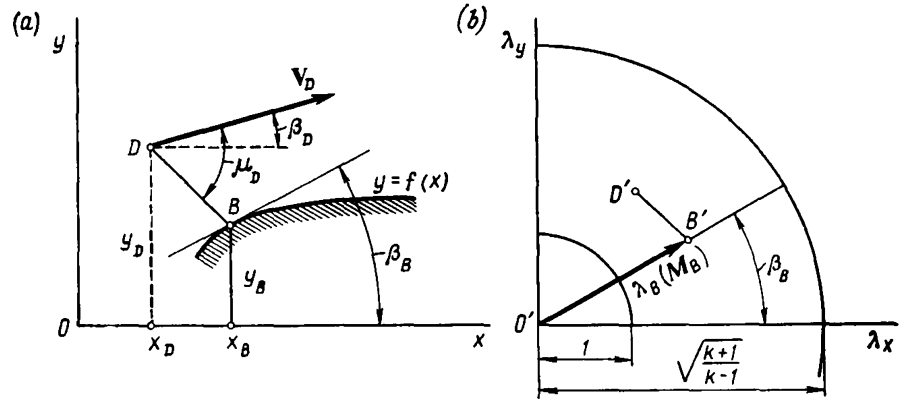

Fig. 5.4.2
Calculation of the velocity at the intersection point of a characteristic with a surface in a flow:
a—physical plane; *b*—plane of hodograph

at point C in the first approximation, i.e. from the values:

$$\left.\begin{aligned} \mu_A^{(2)} &= (\mu_A + \mu_C)/2,\ \mu_B^{(2)} = (\mu_B + \mu_C)/2 \\ \beta_A^{(2)} &= (\beta_A + \beta_C)/2,\ \beta_B^{(2)} = (\beta_B + \beta_C)/2 \end{aligned}\right\} \quad (5.4.25)$$

We find the more precise coordinates x_C and y_C of point C from the equations

$$\begin{aligned} \Delta y_B &= \Delta x_B \tan (\beta_B^{(2)} + \mu_B^{(2)}); \\ \Delta y_A &= \Delta x_A \tan (\beta_A^{(2)} - \mu_A^{(2)}) \end{aligned} \quad (5.4.26)$$

The **second problem** consists in calculating the velocity at the point of intersection of a characteristic with a surface in a flow. Assume that point B is located at the intersection with linear element DB of a characteristic of the second family drawn from point D near a surface (Fig. 5.4.2). The velocity at this point (both its magnitude and direction), the entropy, and the coordinates of the point are known.

The velocity at point B is determined directly with the aid of Eq. (5.4.4) for a characteristic of the second family. If we relate this equation to the conditions along characteristic element DB and express it in finite differences, we have

$$\Delta\omega_D = -\Delta\beta_D + \varepsilon\,(\Delta x_D/y_D)\,m_D - (\Delta x_D/kR)\,(\Delta S/\Delta n)\,t_D \quad (5.4.27)$$

where

$$\left.\begin{aligned} &\Delta\omega_D = \omega_B - \omega_D,\ \Delta\beta_D = \beta_B - \beta_D,\ \Delta x_D = x_B - x_D \\ &m_D = \sin\beta_D \sin\mu_D/\cos(\beta_D - \mu_D) \\ &t_D = \sin^2\mu_D \cos\mu_D/\cos(\beta_D - \mu_D) \end{aligned}\right\} \quad (5.4.28)$$

$$\Delta S/\Delta n = (S_B - S_D) \cos(\beta_D - \mu_D)/(x_D - x_B) \sin \mu_D$$

or

$$\frac{\Delta S}{\Delta n} = -\frac{R}{p'_{0,D}} \cdot \frac{\Delta p'_0}{\Delta n} = -\frac{R}{p'_{0,D}} \frac{(p'_{0,B} - p'_{0,D}) \cos(\beta_D - \mu_D)}{(x_D - x_B) \sin \mu_D} \tag{5.4.29}$$

The coordinates x_B and y_B of point B are determined by the simultaneous solution of the equation for a characteristic of the second family and the equation of the wall contour:

$$y_B - y_D = (x_B - x_D) \tan(\beta_D - \mu_D); \quad y_B = f(x_D) \tag{5.4.30}$$

A graphical solution of these equations is shown in Fig. 5.4.2*a*.

We use the found coordinates x_B and y_B to evaluate the angle β_B from the equation

$$\tan \beta_B = (dy/dx)_B \tag{5.4.31}$$

The entropy S_B (or the stagnation pressure $p'_{0,B}$) at point B is considered to be a known quantity and equal to its value on the streamline coinciding with a tangent to the surface. The entropy is considered to be constant along an element of the tangent.

Upon calculating the increment $\Delta\omega_D$ by (5.4.27), we can find the angle $\omega_B = \Delta\omega_D + \omega_D$, and then determine the number M_B from Table 5.3.1. How the velocity at point B is determined is shown graphically in Fig. 5.4.2*b*, where element $D'B'$ of a characteristic of the second family in a hodograph corresponds to an element of a characteristic of the same family in a physical plane.

The **third problem** consists in calculating the velocity at the intersection of the characteristics with a shock and in determining the change in the inclination of the shock at this point. Since a characteristic in its nature is a line of weak disturbances, this intersection physically corresponds to the interaction of a weak wave with a compression shock. Assume that closely arranged expansion waves, which characteristics of the first family correspond to, fall at points J and H on compression shock N of a preset shape $y = f(x)$ (Fig. 5.4.3*a*). As a result, the strength diminishes, as does the inclination angle of the shock. Since points J and H are sources of disturbances, expansion waves appear, and characteristics of the second family can be drawn through these points. One of such characteristics, passing through point J, intersects the neighbouring conjugate characteristic at point F called the **nodal point of the characteristics**.

To determine the change in the inclination of the shock and in the velocity behind it, one must use the properties of the characteristics JF and FH passing through nodal point F, and also the relations for calculating a compression shock. Since length JH of the shock is small, this section may be assumed to be linear. The angle of inclination of the shock on this section and the corresponding pa-

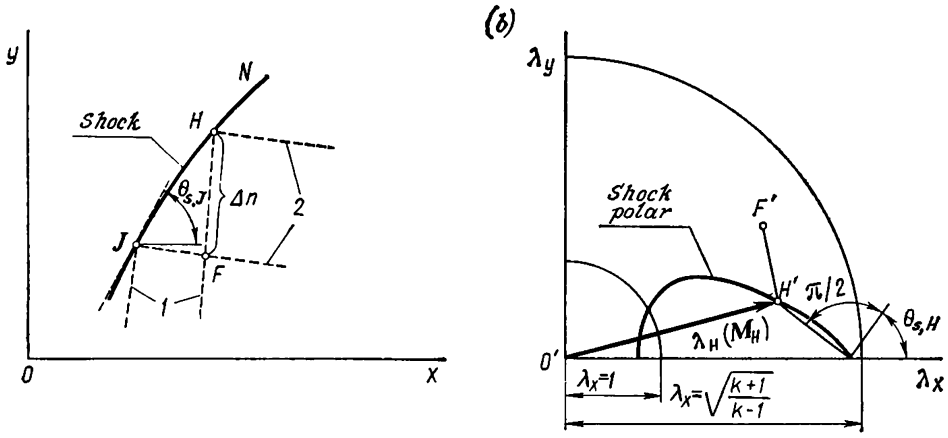

Fig. 5.4.3
Calculation of the velocity at the intersection of characteristics with a shock: *a*—physical plane; *b*—plane of hodograph; *1*—characteristics of the first family; *2*—characteristics of the second family

rameters of the gas are approximately equal to their values at intersection point H of element FH of a first family characteristic with the shock.

One of the unknown parameters is the angle of inclination β_H of the velocity vector at this point, which can be written as $\beta_H = \Delta\beta_F + \beta_F$, where $\Delta\beta_F = \beta_H - \beta_F$, and β_F is the known angle of inclination of the velocity vector at point F. To evaluate the second unknown (the number M_H at the same point) we shall use the formula

$$M_H = M_J + (dM/d\beta)_J \Delta\beta_{JH} \qquad (5.4.32)$$

in which $(dM/d\beta)_J$ is a derivative calculated with the aid of the relevant expressions for a compression shock according to the known parameters at point J, and the quantity $\Delta\beta_{JH}$ determined by the change in the angle β along a shock element equals the difference $\beta_H - \beta_J$. We may assume that this quantity approximately equals the change in the angle β along the element FH of a characteristic of the first family $\Delta\beta_{FH} = \Delta\beta_F = \beta_H - \beta_F$.

The derivative $dM/d\beta$ is evaluated as a result of differentiation of (4.3.19'):

$$\frac{dM}{d\beta} = \frac{dM_2}{d\beta_s} = -M_2\left[\cot(\theta_s - \beta_s)\left(\frac{d\theta_s}{d\beta_s} - 1\right) + \frac{M_2^2}{2(1-\delta)}\sin^2(\theta_s - \beta_s)\frac{d}{d\beta_s}\left(\frac{\rho_2}{\rho_1}\right)\right] \qquad (5.4.33)$$

We shall calculate the derivative $d(\rho_2/\rho_1)/d\beta_s$ on the right-hand side by differentiating (4.3.13):

$$\frac{d}{d\beta_s}\left(\frac{\rho_2}{\rho_1}\right) = 2\cot\theta_s\left(1 - \delta\frac{\rho_2}{\rho_1}\right)\frac{\rho_2}{\rho_1}\cdot\frac{d\theta_s}{d\beta_s} \qquad (5.4.34)$$

We determine the derivative $d\theta_s/d\beta_s$ as follows. We differentiate (4.3.24):

$$\frac{d}{d\beta_s}\left(\frac{\rho_2}{\rho_1}\right)=\frac{\rho_2}{\rho_1}\left\{\frac{d\theta_s}{d\beta_s}\left[\frac{1}{\sin\theta_s\cos\theta_s}-\frac{1}{\sin(\theta_s-\beta_s)\cos(\theta_s-\beta_s)}\right.\right.$$
$$\left.\left.+\frac{1}{\sin(\theta_s-\beta_s)\cos(\theta_s-\beta_s)}\right\}\right.$$

This relation can be transformed somewhat by using (4.3.24):

$$\frac{d}{d\beta_s}\left(\frac{\rho_2}{\rho_1}\right)=\frac{\rho_2}{\rho_1}\cdot\frac{1}{\tan\theta_s\cos^2(\theta_s-\beta_s)}$$
$$\times\left\{\frac{d\theta_s}{d\beta_s}\left[\frac{\cos^2(\theta_s-\beta_s)}{\cos^2\theta_s}-\frac{\rho_2}{\rho_1}\right]+\frac{\rho_2}{\rho_1}\right\} \qquad (5.4.35)$$

Equating the right-hand sides of (5.4.34) and (5.4.35) and solving the equation obtained for the derivative $d\theta_s/d\beta_s$, we obtain:

$$\frac{d\theta_s}{d\beta_s}=\frac{\rho_2}{\rho_1}\left[2\cos^2(\theta_s-\beta_s)\left(1-\delta\frac{\rho_2}{\rho_1}\right)\right.$$
$$\left.-\frac{\cos^2(\theta_s-\beta_s)}{\cos^2\theta_s}+\frac{\rho_2}{\rho_1}\right]^{-1} \qquad (5.4.36)$$

Let us derive an expression for the change in the number M when travelling along the characteristics from point F to point H, i.e. for the quantity $\Delta M_F = M_H - M_F$. To do this, we shall substitute expression (5.4.32) here for M_H:

$$\Delta M_F = M_J + (dM/d\beta)_J\,\Delta\beta_F - M_F \qquad (5.4.37)$$

We can go over from the number M to the function ω determined by relation (5.3.30):

$$\Delta\omega_F = \omega_J + (d\omega/d\beta)_J\,\Delta\beta_F - \omega_F \qquad (5.4.38)$$

where

$$(d\omega/d\beta)_J = (dM/d\beta)_J\,(d\omega/dM)_J \qquad (5.4.39)$$

The derivative $d\omega/dM$ is determined as a result of differentiating (5.3.30):

$$\frac{d\omega}{dM}=\sqrt{M^2-1}\left[M\left(1+\frac{k-1}{1}M^2\right)\right]^{-1} \qquad (5.4.40)$$

Equation (5.4.11) for a characteristic of the first family applied along element FH yields

$$\Delta\omega_F-\Delta\beta_F-\varepsilon\,(\Delta x_F/y_F)\,l_F+(\Delta x_F/kR)\,(\Delta S/\Delta n)\,c_F=0 \qquad (5.4.41)$$

where

$$\left.\begin{aligned}&\Delta\omega_F=\omega_H-\omega_F,\quad \Delta\beta_F=\beta_H-\beta_F,\quad \Delta x_F=x_H-x_F\\ &l_F=\sin\beta_F\sin\mu_F/\cos(\beta_F+\mu_F)\\ &c_F=\sin^2\mu_F\cos\mu_F/\cos(\beta_F+\mu_F)\end{aligned}\right\} \qquad (5.4.42)$$

The distance along a normal to a streamline between points F and H is

$$\Delta n = (FH)\sin\mu_F = \frac{x_H - x_F}{\cos\beta_F + \mu_F}\sin\mu_F \qquad (5.4.43)$$

Consequently, the entropy gradient in (5.4.41) is

$$\Delta S/\Delta n = (S_H - S_F)\cos(\beta_F + \mu_F)/(x_H - x_F)\sin\mu_F \qquad (5.4.44)$$

or

$$\frac{\Delta S}{\Delta n} = -\frac{R}{p'_{0,F}}\cdot\frac{(p'_{0,H} - p'_{0,F})\cos(\beta_F + \mu_F)}{(x_H - x_F)\sin\mu_F} \qquad (5.4.45)$$

where $p'_{0,H}$ is found according to the number M_H from the shock theory.

The entropy S_F or the stagnation pressure $p'_{0,F}$ at point F can be adopted approximately equal to the corresponding values at point J on the shock, i.e. $S_F \approx S_J$ and $p'_{0,F} \approx p'_{0,J}$.

Solving Eqs. (5.4.38) and (5.4.41) for $\Delta\beta_F$, we obtain

$$\Delta\beta_F = \left[\left(\frac{d\omega}{d\beta}\right)_J - 1\right]^{-1}\left(\omega_F - \omega_J + \varepsilon\frac{\Delta x_F}{y_F}l_F - \frac{\Delta x_F}{kR}\cdot\frac{\Delta S}{\Delta n}c_F\right) \qquad (5.4.46)$$

Inserting the value of $\Delta\beta_F$ into (5.4.38), we can find $\Delta\omega_F$, calculate the angle $\omega_H = \Delta\omega_F + \omega_F$, and determine more precisely the number M_H. By calculating the angle $\beta_H = \Delta\beta_F + \beta_F$, we use the values of this angle, and also of the preset number M_∞ to find the shock angle $\theta_{s,H}$ at point H and, consequently, to determine the shape of the shock more accurately on section JH. If necessary, the calculations can be performed in a second approximation, adopting instead of the parameters at point J their average values between points J and H. Particularly, instead of the angles ω_J and β_J, we take the relevant average values of $0.5(\omega_J + \omega_H)$ and $0.5(\beta_J + \beta_H)$.

Figure 5.4.3*b* shows how the problem is solved graphically. Point H' on a hodograph, corresponding to point H on a physical plane, is determined as a result of the intersection of element $F'H'$ of a first family characteristic with a shock polar constructed for the given free-stream number M_∞. The vector $O'H'$ determines the velocity λ_H at point H.

5.5. Applications of the Method of Characteristics to the Solution of the Problem on Shaping the Nozzles of Supersonic Wind Tunnels

The method of characteristics allows us to solve one of the most important problems of gas dynamics associated with the determination of the shape of a wind tunnel nozzle intended for producing a two-dimensional plane parallel supersonic flow at a preset velocity.

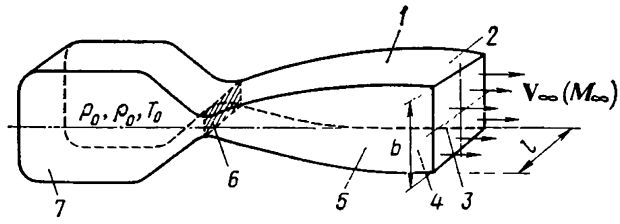

Fig. 5.5.1
Nozzle of supersonic tunnel:
1—top wall; *2* and *5*—side walls; *3*—exit section; *4*—bottom wall; *6*—critical section; *7*—receiver

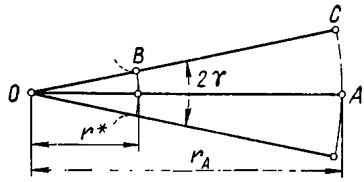

Fig. 5.5.2
Unshaped two-dimensional supersonic nozzle with a radial flow

The nozzle ensuring such a flow is a mouthpiece whose side walls are flat, while its top and bottom walls have a specially **shaped contour** (Fig. 5.5.1).

In addition to determining the shape of its curved contour, the design of a nozzle includes calculation of the parameters of the gas in the receiver (the parameters of stagnation) and in the critical section, and also its area S^*. The parameters of the gas at the nozzle exit are usually preset, namely, the number M_∞, the pressure p_∞, the area of the exit section $S = lb$, and the temperature of the gas in the receiver T_0. The area of the critical nozzle section is found from flow rate equation (3.6.44) which we shall write in the form $\rho_\infty V_\infty S = \rho^* a^* S^*$. Hence $S^* = (\rho_\infty V_\infty / \rho^* a^*) S = \bar{q} S$.

It follows from (3.6.46′) that the parameter $\bar{q}$ is determined by the preset number M_∞ at the nozzle exit. According to this value of M_∞ and the pressure p_∞ at the exit, and by using formula (3.6.29), we can find the pressure p_0 in the receiver needed to ensure the preset number M_∞ at the exit.

Next the angle 2γ of an unshaped nozzle is set (Fig. 5.5.2). Experimental investigations show that this angle is generally chosen equal to 30-35°.

If the section of the inlet part of a nozzle changes sufficiently gradually, the flow downstream of the critical section can be considered as an **expanding radial flow** from a source at point O. Such a flow has the property that its direction coincides with that of radial lines emerging from point O. The change in the parameters of the gas in magnitude along each of these lines is of the same nature. The length of the subsonic portion of the nozzle of unit width is de-

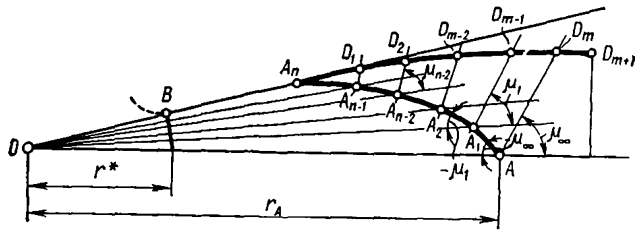

Fig. 5.5.3
Construction of a shaped supersonic two-dimensional nozzle

termined by the quantity $r^* = S^* [360/(2\pi \cdot 2\gamma \cdot 1)]$, while the distance to the exit section $r_A = S [360/(2\pi \cdot 2\gamma \cdot 1)]$.

In the region of the nozzle confined by two circles of radii r^* and r_A, i.e. beyond the limits of the critical section, the gas flow is supersonic. Shaping of the nozzle consists in replacing straight wall BC in this region with a curved contour ensuring the gradual transition of the radial flow into a *plane parallel flow at the exit at a preset velocity*. For this purpose, let us draw through point O a number of closely arranged lines and determine the velocities (the numbers M) on these lines at their intersection points $A_1, \ldots, A_n$ with a characteristic of one of the families AA_n (let us consider it to be a characteristic of the second family) emerging from point A on an arc of radius r_A (Fig. 5.5.3). Point A_1 is at the intersection of ray $r_1 = OA_1$ with the element of characteristic AA_1 drawn at an angle of $\mu_\infty = -\sin^{-1}(1/M_\infty)$.

We find the number M_1 at point A_1 with the aid of the expression $\bar{q}_1 = S^*/S_1$. Since $S_1 = 2\pi r_1 \cdot 1\ (2\gamma/360)$, and $S^* = 2\pi r^* \cdot 1\ (2\gamma/360)$, we have $\bar{q}_1 = r^*/r_1$. Employing (3.6.46), we can find λ_1 and the corresponding number M_1.

We determine in a similar way the coordinates of intersection point A_2 of the adjacent ray $r_2 = OA_2$ with the element of characteristic A_1A_2 inclined to straight line OA_1 at the angle $\mu_1 = -\sin^{-1}(1/M_1)$, the number M_2 at point A_2, and so on. As a result, we can construct a characteristic of the second family in the form of broken line $AA_1 \ldots A_{n-1}A_n$ intersecting straight wall BA_n of the nozzle at point A_n. For this point, as for the other points A_{n-2}, A_{n-1}, and A_n of intersection of the characteristic with the straight lines emerging from source O, we can calculate the relevant Mach numbers and the angles $\mu = -\sin^{-1}(1/M)$.

The flow region OAA_n with a known velocity field confined by the characteristic AA_n and the straight walls of the nozzle is called a **triangle of definiteness**. The shape of this flow is preserved if we change the wall behind point A_n so that the radial flow on the Mach line gradually transforms into a plane parallel flow at the exit.

With a view to this condition, we can construct a characteristic of the first family emerging from point A and having the form of a straight line. If we now determine the field of velocities between the characteristics AA_n and AD_m, we can find the relevant streamlines. It is exactly the streamline passing through point A_n that coincides with the shaped contour of the nozzle.

To determine the velocity field, we shall assume that in the two-dimensional flow being considered all the characteristics of the first family emerging from points A_{n-2}, A_{n-1}, as well as the characteristic AD_m are straight lines (Fig. 5.5.3). The inclination of each characteristic to a radial line is determined by the corresponding Mach angle $\mu_1 = \sin^{-1}(1/M_1)$, $\mu_2 = \sin^{-1}(1/M_2)$, etc., while the velocity along a characteristic is determined by its relevant value at the initial points A_1, A_2, . . .

Let us consider the streamline emerging from point A_n. The initial part of this line coincides with the direction of the velocity at point A_n and is a straight line that is an extension of contour BA_n up to its intersection point D_1 with the characteristic of the first family $A_{n-1}A_n$. Behind point D_1, the streamline element coincides with the direction of the velocity at point D_1 equal to the velocity at point A_{n-1}. Drawing through point D_1 a straight line parallel to ray OA_{n-1} up to its intersection point D_2 with the characteristic $A_{n-2}D_2$, we obtain the next part of the streamline. Behind point D_2, part D_2D_{m-2} of the streamline (point D_{m-2} is on the characteristic of the first family A_2D_{m-2}) is parallel to straight line OA_{n-2}. The remaining parts of the streamline are constructed similarly. Behind point D_m, which is on the characteristic AD_m, the part of the streamline is parallel to the axis of the nozzle. The contour of the nozzle coinciding with the streamline A_nD_{m+1} and constructed in the form of a smooth curve ensures a parallel supersonic flow with the preset number M_∞ at the nozzle exit.

6

Airfoil and Finite-Span Wing in an Incompressible Flow

Let us consider the problems associated with the application of the aerodynamic theory to calculating the flow past an airfoil. A feature of this flow is the formation of a two-dimensional disturbed flow over the airfoil. We shall use simpler equations of aerodynamics than for three-dimensional flows to investigate it.

The flow over an airfoil treated as a two-dimensional one is idealized. Actually, the flow past an airfoil belonging to a real finite-span wing is three-dimensional. This is why the aerodynamic characteristics of an airfoil cannot be transferred directly to a wing. But these characteristics can be among the basic parameters used in calculating similar characteristics of real wings. At the same time, the solution of the problem on an airfoil has an independent significance because cases are possible when on individual parts of wings the flow past airfoils is practically of a two-dimensional nature.

We shall investigate the flow of an incompressible fluid past an airfoil. We shall simultaneously consider the problem of a finite-span wing in a similar flow. The results obtained, which have an independent significance in low-speed aerodynamics, can be used for aerodynamic investigations at high speeds.

6.1. Thin Airfoil in an Incompressible Flow

Let us consider the method of calculating the steady flow of an incompressible fluid past a thin slightly bent airfoil at a small angle of attack (Fig. 6.1.1). The aerodynamic characteristics of the airfoil obtained as a result of these calculations can be used directly for flight at low subsonic speeds ($M_\infty < 0.3$-0.4) when the air may be considered as an incompressible fluid. They can also be used as

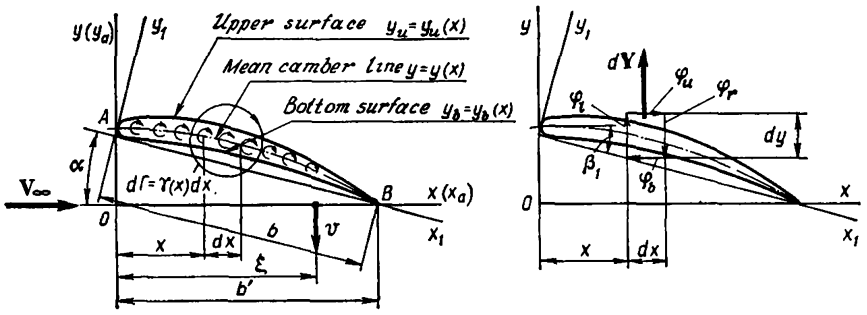

Fig. 6.1.1
Thin airfoil in an incompressible flow

the initial data when performing aerodynamic calculations of airfoils having a given configuration in a subsonic compressible flow.

Since the airfoil is thin, and the angle of attack is not large, the velocity of the flow near it differs only slightly from that of the undisturbed flow. Such a flow is called **nearly uniform**.

We can write the following condition for the velocity of a nearly uniform flow:

$$V_x = V_\infty + u \ (u \ll V_\infty), \ V_y = v \ (v \ll V_\infty) \qquad (6.1.1)$$

where u and v are the components of the **velocity of small disturbances**.

In accordance with this condition,

$$V^2 = V_x^2 + V_y^2 = (V_\infty + u)^2 + v^2 \approx V_\infty^2 + 2V_\infty u \qquad (6.1.2)$$

Let us now determine the pressure in a nearly uniform flow. From the Bernoulli equation (3.4.13), in which we assume that the constant C_2 equals $p_\infty/\rho_\infty + V_\infty^2/2$ and $\rho = \text{const}$, we obtain the excess pressure

$$p - p_\infty = \rho_\infty (V_\infty^2/2 - V^2/2) = -\rho_\infty V_\infty u \qquad (6.1.3)$$

We define u in terms of the velocity potential, $u = \partial\varphi/\partial x$:

$$p - p_\infty = -\rho_\infty V_\infty \partial\varphi/\partial x \qquad (6.1.4)$$

The corresponding pressure coefficient is

$$\bar{p} = (p - p_\infty)/q_\infty = -2u/V_\infty = -(2/V_\infty)\ \partial\varphi/\partial x \qquad (6.1.5)$$

By (6.1.4), the excess pressure on the bottom surface of the airfoil is

$$p_b - p_\infty = -(\partial\varphi_b/\partial x)\ V_\infty\rho_\infty$$

and on its upper surface is

$$p_u - p_\infty = -(\partial\varphi_u/\partial x)\ V_\infty\rho_\infty$$

where φ_b and φ_u are the velocity potentials on the bottom and upper surfaces, respectively. Consequently, the lift force produced by the pressure acting on an element of area is

$$dY_{a,ic} = (p_b - p_u)\,dx = -V_\infty \rho_\infty (\partial\varphi_b/\partial x - \partial\varphi_u/\partial x)\,dx$$

while the lift force for the entire airfoil with the chord b is

$$Y_{a,ic} = -V_\infty \rho_\infty \int_0^{b'} \left(\frac{\partial\varphi_b}{\partial x} - \frac{\partial\varphi_u}{\partial x}\right) dx$$

Assuming the upper limit b' of the integral to be approximately equal to the chord b (because of the smallness of the angle of attack), we find the corresponding lift coefficient:

$$c_{y_a,ic} = \frac{Y_{a,ic}}{q_\infty b} = -\frac{2}{V_\infty b} \int_0^b \left(\frac{\partial\varphi_b}{\partial x} - \frac{\partial\varphi_u}{\partial x}\right) dx \qquad (6.1.6)$$

Let us consider the circulation of the velocity over a contour that is a rectangle with the dimensions dx and dy and encloses an element of the airfoil. In accordance with Fig. 6.1.1, the circulation is

$$d\Gamma = \left(V_\infty + \frac{\partial\varphi_u}{\partial x}\right) dx - \left(V_\infty + \frac{\partial\varphi_b}{\partial x}\right) dx + \left(\frac{\partial\varphi_l}{\partial y} - \frac{\partial\varphi_r}{\partial y}\right) dy$$

where φ_l and φ_r are the velocity potentials on the left and right surfaces, respectively.

Let us introduce the concept of the **intensity of circulation (of a vortex)** determined by the derivative $d\Gamma/dx = \gamma(x)$. The magnitude of this intensity is

$$\gamma(x) = \frac{\partial\varphi_u}{\partial x} - \frac{\partial\varphi_b}{\partial x} + \frac{dy}{dx}\left(\frac{\partial\varphi_l}{\partial y} - \frac{\partial\varphi_r}{\partial y}\right)$$

Since for a thin airfoil, the angular coefficient dy/dx is small, the product of this coefficient and the difference of the vertical component of the velocities is a second-order infinitesimal and, consequently,

$$\gamma(x) = \partial\varphi_u/\partial x - \partial\varphi_b/\partial x \qquad (6.1.7)$$

Hence, (6.1.6) can be written in the form

$$c_{y_a,\,ic} = \frac{2}{V_\infty b} \int_0^b \gamma(x)\,dx \qquad (6.1.8)$$

We calculate the moment coefficient in a similar way:

$$m_{z_a,\,ic} = -\frac{2}{V_\infty b^2} \int_0^b \gamma(x)\,x\,dx \qquad (6.1.9)$$

In accordance with formulas (6.1.8) and (6.1.9), the coefficients of the lift force and the moment produced by the pressure depend on the distribution of the intensity of the circulation along the airfoil. This signifies that the flow over an airfoil can be calculated by replacing it with a system of continuously distributed vortices.

According to the Biot-Savart formula (2.7.12), an element of a distributed vortex with the circulation $d\Gamma = \gamma(x)\,dx$ induces the vertical velocity at a point with the abscissa ξ (Fig. 6.1.1)

$$dv = d\Gamma/[2\pi(x-\xi)] = \gamma(x)\,dx/[2\pi(x-\xi)]$$

The velocity induced at this point by all the vortices is

$$v = \frac{1}{2\pi}\int_0^b \frac{\gamma(x)\,dx}{x-\xi} \tag{6.1.10}$$

According to the boundary condition, $v/(V_\infty + \partial\varphi/\partial x) = dy/dx$. Taking into account that the airfoil is thin, we can assume that $V_\infty + \partial\varphi/\partial x \approx V_\infty$, and calculate the derivative dy/dx from the equation of the mean camber line

$$y = y(x) = 0.5\,(y_u + y_b) \tag{6.1.11}$$

where $y_u = y_u(x)$ and $y_b = y_b(x)$ are the equations of the upper and bottom contours of the airfoil, respectively.

Hence, the intensity of vortex circulation $\gamma(x)$ is determined by the integral equation

$$\frac{1}{2\pi V_\infty}\int_0^b \frac{\gamma(x)\,dx}{x-\xi} = \left(\frac{dy}{dx}\right)_\xi \tag{6.1.12}$$

Let us introduce instead of x a new independent variable θ determined by the equation

$$x = (b/2)(1-\cos\theta) \tag{6.1.13}$$

We find the solution of Eq. (6.1.12) in the form of a trigonometric Fourier series:

$$\gamma(\theta_0) = 2V_\infty\left[A_0\cot\frac{\theta_0}{2} + \sum_{n=1}^{\infty} A_n \sin(n\theta_0)\right] \tag{6.1.14}$$

in which the variable θ_0 in accordance with (6.1.13) is related to the coordinate $x = \xi$ by the equation

$$\xi = (b/2)(1-\cos\theta_0) \tag{6.1.15}$$

We change the variables in (6.1.12). By differentiation of (6.1.13), we find

$$dx = (b/2)\sin\theta\,d\theta \tag{6.1.16}$$

Substitutions yield

$$\frac{A_0}{\pi}\int_0^{\pi}\frac{\cot(\theta/2)\sin\theta\,d\theta}{\cos\theta_0-\cos\theta}+\frac{1}{\pi}\sum_{n=1}^{\infty}A_n\int_0^{\pi}\frac{\sin(n\theta)\sin\theta\,d\theta}{\cos\theta_0-\cos\theta}=\beta(\theta_0)\quad(6.1.17)$$

where $\beta(\theta_0)=(dy/dx)_{\xi}$.

After introducing the values of the integrals in (6.1.17) calculated in [16], we find

$$-A_0+\sum_{n=1}^{\infty}A_n\cos(n\theta_0)=\beta(\theta_0).\quad(6.1.18)$$

By integrating both sides of Eq. (6.1.18) from 0 to π, we obtain a relation for the coefficient A_0 of the Fourier series:

$$A_0=-\frac{1}{\pi}\int_0^{\pi}\beta(\theta)\,d\theta\quad(6.1.19)$$

By multiplying (6.1.19) in turn by $\cos\theta$, $\cos 2\theta$, . . ., $\cos(n\theta)$, we find expressions for the coefficients A_1, A_2, . . ., A_n, respectively. Hence,

$$A_n=\frac{2}{\pi}\int_0^{\pi}\beta(\theta)\cos(n\theta)\,d\theta\quad(6.1.20)$$

Let us consider relation (6.1.8) for the lift coefficient. Going over to the variable θ and introducing (6.1.16), we obtain

$$c_{y_a,\mathrm{ic}}=\frac{1}{V_\infty}\int_0^{\pi}\gamma(\theta)\sin\theta\,d\theta\quad(6.1.21)$$

With a view to (6.1.14)

$$c_{y_a,\mathrm{ic}}=2A_0\int_0^{\pi}\cot\frac{\theta}{2}\sin\theta\,d\theta+2\sum_{n=1}^{\infty}A_n\int_0^{\pi}\sin(n\theta)\sin\theta\,d\theta$$

Integration yields

$$c_{y_a,\mathrm{ic}}=2\pi(A_0+A_1/2)\quad(6.1.22)$$

Hence, the lift coefficient depends on the first two coefficients of the series. Introducing into (6.1.22) expression (6.1.19) and formula (6.1.20) in which $n=1$, we have

$$c_{y_a,\mathrm{ic}}=-2\int_0^{\pi}\beta(\theta)(1-\cos\theta)\,d\theta\quad(6.1.23)$$

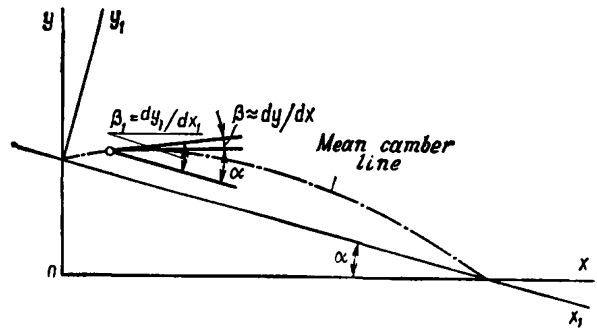

Fig. 6.1.2
Mean camber line of an airfoil

We change the variables in (6.1.9) for the moment coefficient:

$$m_{z_a,\,ic} = \frac{-1}{2V_\infty} \int_0^\pi \gamma(\theta)\,(1-\cos\theta)\sin\theta\,d\theta \qquad (6.1.24)$$

With a view to expression (6.1.14) for $\gamma(\theta)$, we have

$$m_{z_a,\,ic} = -A_0 \int_0^\pi (1-\cos\theta)^2\,d\theta - \sum_{n=1}^{\infty} A_n \int_0^\pi \sin(n\theta)\,(1-\cos\theta)\sin\theta\,d\theta$$

Integration yields

$$m_{z_a,ic} = -(\pi/2)\,(A_0 + A_1 - A_2/2) \qquad (6.1.25)$$

With a view to (6.1.22), we have

$$m_{z_a,ic} = -(\pi/4)\,(A_1 - A_2) - (1/4)\,c_{y_a ic} \qquad (6.1.26)$$

By determining A_1 and A_2 from (6.1.20) and introducing their values into (6.1.26), we obtain

$$m_{z_a,\,ic} = -\frac{1}{2}\int_0^\pi \beta(\theta)\,(\cos\theta - \cos 2\theta)\,d\theta - \frac{1}{4}\,c_{y_a,\,ic} \qquad (6.1.27)$$

Let us consider the body axis coordinates x_1 and y_1 in which the equation of the mean camber line is $y_1 = y_1(x_1)$, and the slope of a tangent is determined by the derivative dy_1/dx_1. This angle (Fig. 6.1.2) is $\beta_1 = \beta + \alpha$, where $\beta \approx dy/dx$. Hence we determine the angle $\beta = \beta_1 - \alpha$ and introduce its value into (6.1.23) and (6.1.27):

$$c_{y_a,ic} = 2\pi\,(\alpha + \varepsilon_0) \qquad (6.1.28)$$

$$m_{z_a,\,ic} = -2\left(\frac{\pi}{4}\,\varepsilon_0 - \mu_0\right) - \frac{1}{4}\,c_{y_a,\,ic} \qquad (6.1.29)$$

where

$$\varepsilon_0 = \frac{1}{\pi}\int_0^{\pi} \beta_1 (1-\cos\theta)\, d\theta; \quad \mu_0 = -\frac{1}{4}\int_0^{\pi} \beta_1 (1-\cos 2\theta)\, d\theta \qquad (6.1.30)$$

A glance at (6.1.28) reveals that when $\alpha = -\varepsilon_0$, the lift coefficient equals zero. The angle $\alpha = -\varepsilon_0$ is called the **angle of zero lift**. The coefficients ε_0 and μ_0 are evaluated according to the given equation of the mean camber line of the airfoil provided that in the expression for the function $\beta_1 (\bar{x}_1)$ the variable $\bar{x}_1 = x_1/b$ is replaced according to (6.1.13) with the relation $\bar{x}_1 = (1/2)(1-\cos\theta)$.

We can use the found values of m_{z_a} and c_{y_a} to approximately determine the coefficient of the centre of pressure $c_p = x_p/b$ and the relative coordinate of the aerodynamic centre $\bar{x}_{AC} = x_{AC}/b$:

$$c_p = -\frac{m_{z_a}}{c_{y_a}} = \frac{1}{4} + \frac{(\pi/4)\varepsilon_0 - \mu_0}{\pi(\alpha+\varepsilon_0)}, \quad \bar{x}_{AC} = -\frac{\partial m_{z_a}}{\partial c_{y_a}} = \frac{1}{4} \qquad (6.1.31)$$

It follows from these relations that the coordinate of the centre of pressure depends on the angle of attack and the shape of the airfoil, whereas the aerodynamic centre is at a fixed point at a distance of one-fourth of the chord length from the leading edge. For a symmetric airfoil $\varepsilon_0 = \mu_0 = 0$ [which follows from formulas (6.1.30) in which $\beta_1 = dy_1/dx_1 = 0$], therefore the value of c_p, like that of the relative coordinate of the aerodynamic centre, is 1/4.

6.2. Transverse Flow over a Thin Plate

Let us consider the flow of an incompressible fluid over a very simple airfoil in the form of a thin plate arranged at right angles to the direction of the free-stream velocity. We can solve this problem by means of the **conformal transformation** (or **mapping**) **method**. We shall use the results of the solution in real cases to determine the aerodynamic characteristics of finite-span wings.

Let us arrange the plate in the plane of the complex variable $\sigma = x + iy$ along the real axis x (Fig. 6.2.1*b*). Now the free-stream velocity vector **V** will coincide with the direction of the imaginary axis y. In this case, the flow over such a plate can be obtained by conformal transformation of the flow over a circular cylinder on the plane $\zeta = \xi + i\eta$ (Fig. 6.2.1*a*). If we know the function $W = f(\zeta)$ that is a complex potential for the flow over a circular cylinder and the analytical function $\zeta = F(\sigma)$ of the complex variable $\sigma = x + iy$ (known as the **conformal function**) that transforms the contour of a circle on the plane ζ into a segment of a straight line placed across

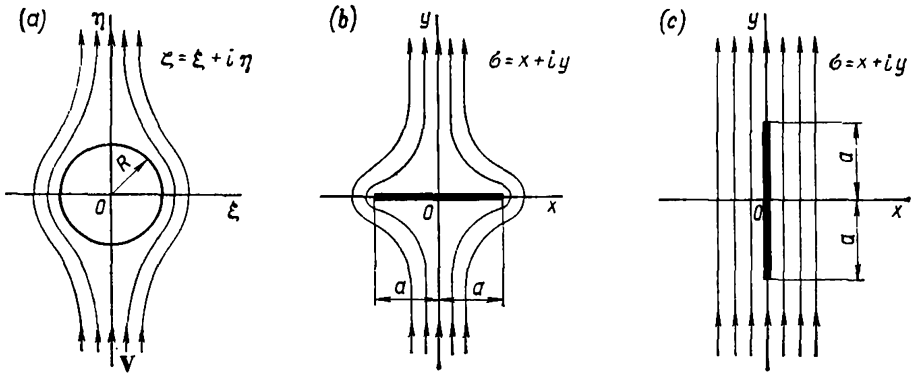

Fig. 6.2.1
Conformal transformation of the flow past a round cylinder (*a*) into a flow past a flat plate arranged (*b*) at right angles to the direction of the free-stream velocity, or (*c*) along the flow

the flow on the plane σ, then the function $W = f[F(\sigma)]$ is the complex potential for the flow over the plate.

Let us see how we can determine the complex potential for the flow over a circular cylinder. For this purpose, we shall again revert to the method of conformal transformation, using the known function of the complex potential for the flow over a plate arranged along it. This function has the form

$$W = \varphi + i\psi = -iV(x + iy) = iV\sigma \tag{6.2.1}$$

We shall show that the conformal function

$$\sigma = \zeta - R^2/\zeta \tag{6.2.2}$$

transforms a segment of a straight line arranged along the flow on the plane σ into a circle on the plane ζ (Fig. 6.2.1*c*, *a*). Indeed, examination of (6.2.2) reveals that since for points satisfying the conditions $-a \leqslant y \leqslant a$, $x = 0$, and $a = 2R$, we have $\sigma = iy$, then from the solution of the quadratic equation $\zeta^2 - \sigma\zeta - R^2 = 0$, we obtain

$$\zeta = iy/2 \pm \sqrt{R^2 - y^2/4} = \xi + i\eta \tag{6.2.3}$$

Separating the real and imaginary parts, we obtain

$$\eta = y/2, \quad \xi = \pm\sqrt{R^2 - y^2/4}$$

whence $\xi^2 + \eta^2 = R^2$.

Consequently, points on the circle in the plane ζ correspond to points in the plane σ on the vertical segment. Substituting for σ in (6.2.1) its value from (6.2.2), we obtain the complex potential of the flow over a circular cylinder of radius R in a plane parallel flow

at the velocity V:

$$W = iV(\zeta - R^2/\zeta) \tag{6.2.4}$$

To obtain the complex potential for the flow over a plate arranged across the flow (Fig. 6.2.1*b*), let us substitute for ζ in (6.2.4) the following value obtained from the conformal formula $\sigma = \zeta + R^2/\zeta$ transforming a circle of radius R (plane ζ) into a segment of a straight line across the flow (plane σ):

$$\zeta = \sigma/2 \pm \sqrt{\sigma^2/4 - R^2} \tag{6.2.5}$$

Therefore,

$$W = -iV\left(\frac{\sigma}{2} \pm \sqrt{\frac{\sigma^2}{4} - R^2} - \frac{R^2}{\sigma/2 \pm \sqrt{\sigma^2/4 - R^2}}\right) \tag{6.2.6}$$

Since for points on the plate we have $\sigma = x$, where $-a \leqslant x \leqslant a$ and $a = 2R$, then

$$W = \varphi + i\psi = -iV\left(\frac{x}{2} \pm i\sqrt{R^2 - \frac{x^2}{4}} - \frac{R^2}{x/2 \pm i\sqrt{R^2 - x^2/4}}\right)$$

whence the potential function is

$$\varphi = \pm V\sqrt{4R^2 - x^2} = \pm V\sqrt{a^2 - x^2} \tag{6.2.7}$$

where the plus sign corresponds to the upper surface, and the minus sign to the bottom one.

By evaluating the derivatives $\partial\varphi/\partial x$, we can find the velocity on the plate and calculate the pressure. It follows from the data obtained that the pressure on the upper and bottom sides of the plate is the same. Consequently, in the case being considered of the transverse free streamline flow of an ideal (inviscid) fluid over a plate, drag of the plate is absent. This interesting aerodynamic effect is considered below in Sec. 6.3 using the example of flow over a flat plate arranged at a certain finite angle of attack.

A flow characterized by the potential function (6.2.7) is shown in Fig. 6.2.1*b*. It is a **non-circulatory flow** past the plate obtained upon the superposition onto an undisturbed flow with the potential

$$W_\infty = -iV\zeta \tag{6.2.8}$$

of the flow from a doublet with the potential

$$W_d = iVR^2/\zeta \tag{6.2.9}$$

where ζ is determined by the conformal function (6.2.5).

6.3. Thin Plate at an Angle of Attack

Let us calculate the potential function for the disturbed flow of an incompressible fluid over a thin plate at the angle of attack α using, as in the preceding problem, the method of conformal transformation. We arrange the plate in the plane of the complex variable $\sigma = x + iy$ along the real axis x.

If we assume that the flow being considered is a non-circulatory one, the complex potential of such a flow can be written as the sum of the potentials of the longitudinal $W_1 = V_\infty \sigma$ and transverse W_2 flows at the velocity of the undisturbed flow $V = \alpha V_\infty$ (Fig. 6.3.1). The total complex potential is

$$W = W_1 + W_2 = V_\infty \sigma - i\alpha V_\infty \left[\frac{\sigma}{2} \pm \sqrt{\frac{\sigma^2}{4} - R^2}\right.$$

$$\left. - R^2 \left(\frac{\sigma}{2} \pm \sqrt{\frac{\sigma^2}{4} - R^2}\right)^{-1}\right] = V_\infty \sigma \pm i\alpha V_\infty \sqrt{\sigma^2 - 4R^2} \qquad (6.3.1)$$

With account taken of formula (6.2.7), the total velocity potential on the plate is

$$\varphi = V_\infty x \pm \alpha V_\infty \sqrt{a^2 - x^2} \qquad (6.3.2)$$

We use this value of the potential to find the velocity component

$$V_x = V_\infty \mp \alpha V_\infty x / \sqrt{a^2 - x^2} \qquad (6.3.3)$$

The second velocity component on the thin plate $V_y = 0$.

A close look at (6.3.3) reveals that at the leading ($x = -a$) and trailing ($x = a$) edges, the velocity V_x is infinite. Physically, such a flow is impossible. The velocity at one of the edges, for example, the trailing one, can be restricted by superposition of a **circulatory flow** onto the flow being considered. In the plane ζ, the potential of the circulatory flow is determined in accordance with (2.9.22) by the expression

$$W_3 = -(i\Gamma/2\pi) \ln \zeta \qquad (6.3.4)$$

Let us substitute for ζ its value from (6.2.5):

$$W_3 = -\frac{\Gamma i}{2\pi} \ln \left(\frac{\sigma}{2} \pm \sqrt{\frac{\sigma^2}{4} - R^2}\right) \qquad (6.3.5)$$

Summation of (6.3.1) and (6.3.5) yields the complex potential of a **circulatory-forward flow** over an inclined plate:

$$W = W_1 + W_2 + W_3 = V_\infty \sigma \pm i\alpha V_\infty \sqrt{\sigma^2 - 4R^2}$$

$$- \frac{\Gamma i}{2\pi} \ln \left(\frac{\sigma}{2} \pm \sqrt{\frac{\sigma^2}{4} - R^2}\right) \qquad (6.3.6)$$

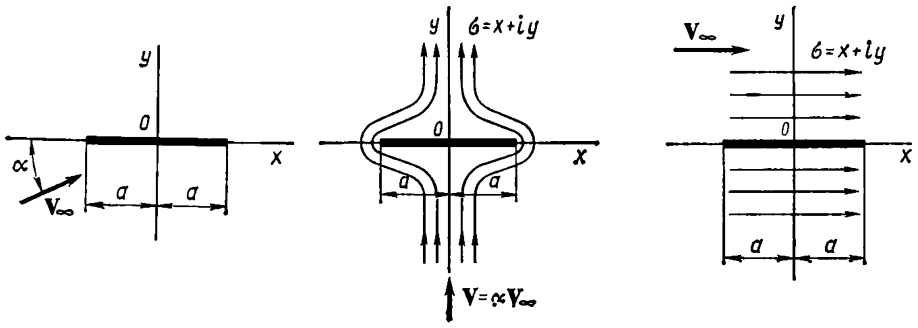

Fig. 6.3.1
Flow over a flat plate at an angle of attack

We determine the circulation Γ on the basis of the **Zhukovsky-Chaplygin hypothesis,** according to which the velocity at the trailing edge of the plate *is finite.* This value of the velocity can be obtained, as we already know from the theory of conformal transformation, in the form of the derivative $d\overline{W}/d\sigma$ of the complex potential $\overline{W}$ for a cylinder. This potential, in turn, makes it possible to find the complex velocity at the relevant point on the cylinder as the derivative $d\overline{W}/d\zeta$, which according to the rules of differentiation of a complex function is

$$d\overline{W}/d\zeta = (dW/d\sigma)\, d\sigma/d\zeta \qquad (6.3.7)$$

where $\overline{W}$ and W are the complex potentials for the cylinder and plate, respectively.

According to the Zhukovsky-Chaplygin hypothesis, the quantity $dW/d\sigma$ is limited in magnitude. Since the derivative $d\sigma/d\zeta$ calculated by the formula

$$d\sigma/d\zeta = 1 - R^2/\zeta^2$$

equals zero on the cylinder at the point $\zeta = R$ corresponding to a point on the trailing edge of the plate, the derivative $d\overline{W}/d\zeta = 0$.

The complex potential for a cylinder is

$$\overline{W} = \overline{W_1} + \overline{W_2} + \overline{W_3}$$

The potential $\overline{W_1}$ characterizes the flow in an axial direction corresponding to the flow over the plate in the same direction at the velocity V_∞. It is obtained by substituting the value $\sigma = \zeta + R^2/\zeta$ for σ in the formula $W_1 = V_\infty \sigma$:

$$\overline{W_1} = V_\infty (\zeta + R^2/\zeta)$$

The complex potentials $\overline{W}_2$ and $\overline{W}_3$ are determined by Eqs. (6.2.4) and (6.3.4), respectively. We shall substitute αV_∞ for V in the first of them and find the total complex potential:

$$\overline{W} = V_\infty (\zeta + R^2/\zeta) - i\alpha V_\infty (\zeta - R^2/\zeta) - (i\Gamma/2\pi) \ln \zeta \quad (6.3.8)$$

We calculate the derivative:

$$d\overline{W}/d\zeta = V_\infty (1 - R^2/\zeta^2) - i\alpha V_\infty (1 + R^2/\zeta^2) - i\Gamma/(2\pi\zeta) \quad (6.3.8')$$

For the coordinate $\zeta = R$ corresponding to a point on the trailing edge of the plate, the derivative $d\overline{W}/d\zeta$ is zero, i.e.

$$2i\alpha V_\infty - i\Gamma/(2\pi R) = 0$$

Hence

$$\Gamma = -4\pi\alpha R V_\infty \quad (6.3.9)$$

or, since $2R = a$,

$$\Gamma = -2\pi\alpha a V_\infty \quad (6.3.9')$$

After inserting this result into (6.3.6) and differentiating with respect to σ, we find the complex velocity:

$$\frac{dW}{d\sigma} = V_x - iV_y = V_\infty \pm \frac{i\alpha V_\infty \sigma}{\sqrt{\sigma^2 - 4R^2}}$$
$$+ \frac{2\pi i\alpha a V_\infty}{2\pi} \cdot \frac{2}{\sigma \pm \sqrt{\sigma^2 - 4R^2}} \left(\frac{1}{2} \pm \frac{\sigma}{\sqrt{\sigma^2 - 4R^2}} \right)$$

Simple transformations and the substitution $2R = a$ yield

$$dW/d\sigma = V_x - iV_y = V_\infty (1 \mp i\alpha \sqrt{(\sigma - a)/(\sigma + a)}) \quad (6.3.10)$$

On the surface of the plate ($\sigma = x$)

$$dW/d\sigma = V_x - iV_y = V_\infty (1 \mp i\alpha \sqrt{(x - a)/(x + a)}) \quad (6.3.11)$$

Since $|x| \leqslant a$, we have

$$dW/d\sigma = V_x - iV_y = V_\infty (1 \pm \alpha \sqrt{(a - x)/(a + x)}) \quad (6.3.11')$$

whence it follows that the total velocity on the plate is

$$V = V_x = V_\infty (1 \pm \alpha \sqrt{(a - x)/(a + x)}) \quad (6.3.12)$$

The plus sign relates to the upper surface, and the minus sign to the bottom one.

The velocity on the trailing edge ($x = a = 2R$) is V_∞, and on the leading edge ($x = -a$) it is found to be infinite. In real conditions, the thickness of the leading edge is not zero; particularly, the nose may have a *finite*, although small, radius of curvature. Therefore the velocities on such an edge have high, but finite values.

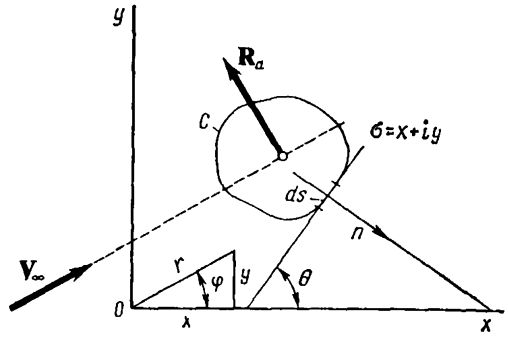

Fig. 6.3.2
Contour in the flow of an incompressible fluid

To determine the force acting on the plate, we shall use the general expression for the principal vector of the hydrodynamic pressure forces applied to a stationary cylindrical body of an arbitrary shape in the steady flow of an incompressible fluid. By analogy with the complex velocity, let us introduce the concept of the complex force $\overline{R_a} = X - iY$, determining this force as the mirror reflection of the principal vector $\overline{R_a}$ of the pressure forces with respect to the real axis.

The vector $\overline{R_a}$ being considered is determined by formulas (1.3.2) and (1.3.3) in which the friction coefficient $c_{f.x}$ is taken equal to zero:

$$\overline{R_a} = X - iY = -\oint_C p\,[\cos(\widehat{n,\ x}) - i\cos(\widehat{n,\ y})]\,ds$$

$$= -\oint_C p\,(\sin\theta + i\cos\theta)\,ds = -i\oint_C pe^{-i\theta}\,ds \qquad (6.3.13)$$

where n is the direction of an outward normal to contour C of the body in the flow, and θ is the angle between the element ds of the contour and the x-axis (Fig. 6.3.2).

Since

$$\left.\begin{aligned} d\sigma &= dx + i\,dy = ds\,(\cos\theta + i\sin\theta) = e^{i\theta}\,ds \\ d\bar{\sigma} &= dx - i\,dy = ds\,(\cos\theta - i\sin\theta) = e^{-i\theta}\,ds \end{aligned}\right\} \qquad (6.3.14)$$

and the pressure is determined by the Bernoulli equation

$$p = p_\infty + \rho V_\infty^2/2 - \rho V^2/2 = C_2 - \rho V^2/2 \qquad (6.3.15)$$

then

$$\overline{R_a} = -iC_2\oint_C d\bar{\sigma} + \frac{i\rho}{2}\oint_C V^2\,d\bar{\sigma} = \frac{i\rho}{2}\oint_C V^2\,d\bar{\sigma}$$

Taking into account that by (6.3.14) we have $d\bar{\sigma} = e^{-2i\theta}\,d\sigma$, and also that in accordance with the condition of flow without separa-

tion the complex velocity at the point of the contour being considered is

$$\overline{V} = V_x - iV_y = V\cos\theta - iV\sin\theta = Ve^{-i\theta} \qquad (6.3.16)$$

we find

$$\overline{R}_a = X - iY = \frac{i\rho}{2}\oint_C \overline{V}^2\, d\sigma \qquad (6.3.17)$$

Since for a potential flow, the complex velocity is $\overline{V} = dW/d\sigma$, we have

$$\overline{R}_a = X - iY = \frac{i\rho}{2}\oint_C \left(\frac{dW}{d\sigma}\right)^2 d\sigma \qquad (6.3.18)$$

Expression (6.3.18) is called the **Zhukovsky-Chaplygin formula.**

Integration in (6.3.18) can be performed over another contour enveloping the given contour C of the body in the flow, for example, over a circle K whose complex velocity in the plane σ is written as follows:

$$dW/d\sigma = \overline{V}_\infty - i\Gamma/(2\pi\sigma) + A/\sigma^2 \qquad (6.3.19)$$

where $\overline{V}_\infty = V_{x\infty} - iV_{y\infty} = V_\infty e^{-i\theta_\infty}$, and A is a coefficient determined with the aid of an equation similar to (6.3.8).

The square of the complex velocity is

$$\left(\frac{dW}{d\sigma}\right)^2 = \overline{V}_\infty^2 - \frac{i\Gamma\overline{V}_\infty}{\pi\sigma} + \frac{2A\overline{V}_\infty - \Gamma^2/(4\pi^2)}{\sigma^2} + \ldots$$

Introducing this value into (6.3.18), we find

$$\overline{R}_a = X - iY = \frac{i\rho}{2}\left[\overline{V}_\infty^2\oint_K d\sigma - \frac{i\Gamma\overline{V}_\infty}{\pi}\oint_K \frac{d\sigma}{\sigma} + \left(2A\overline{V}_\infty - \frac{\Gamma^2}{4\pi^2}\right)\oint_K \frac{d\sigma}{\sigma^2} + \ldots\right]$$

Here the first and third integrals equal zero. The integral $\oint_K d\sigma/\sigma$ is evaluated with a view to the formula $\sigma = x + iy = re^{i\varphi}$ (Fig. 6.3.2) and equals

$$\oint_K \frac{d\sigma}{\sigma} = \ln\sigma\,|_K = \ln(re^{i\varphi})\,|_K = 2\pi i$$

Hence,

$$\overline{R}_a = X - iY = i\rho\overline{V}_\infty\Gamma \quad \text{or} \quad X - iY = i\rho V_\infty\Gamma e^{-i\theta_\infty} \qquad (6.3.20)$$

where V_∞ is the magnitude of the free-stream velocity.

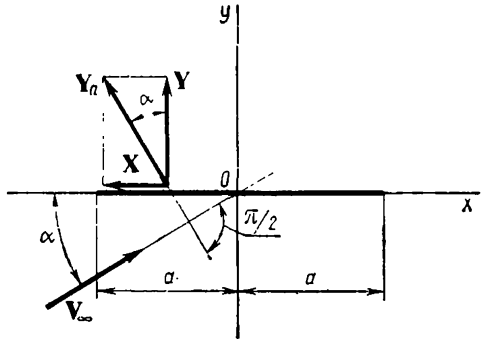

Fig. 6.3.3
Diagram of the forces acting on a plate (X is the suction force)

If its direction coincides with the horizontal axis ($\theta_\infty = \pi$), we have

$$\overline{R}_a = X - iY = -i\rho V_\infty \Gamma \tag{6.3.21}$$

whence it follows that

$$|\overline{R}_a| = Y = Y_a = \rho V_\infty \Gamma \tag{6.3.22}$$

Expression (6.3.22) is known as the **Zhukovsky formula.**

It follows from (6.3.21) that the force is a vector perpendicular to the free-stream velocity vector, and, therefore, is a lift force. Its direction coincides with that of the vector obtained by turning the velocity vector $\mathbf{V}_\infty$ through the angle $\pi/2$ against the circulation.

A glance at (6.3.21) reveals that $X = X_a = 0$. Hence, when an inviscid incompressible fluid flows over a surface without separation, the resistance associated with the distribution of the pressure is zero. This aerodynamic effect is known as the **Euler-D'Alembert paradox.** This name corresponds to the fact that actually resistance is present because there always occurs a relevant redistribution of the pressure caused by separation of the flow and the action of skin friction (viscosity).

Let us use formula (6.3.22) to evaluate the lift force of a flat plate. Taking into account the value of the circulation (6.3.9′), we obtain (Fig. 6.3.3)

$$Y_a = 2\pi\alpha a \rho V_\infty^2 \tag{6.3.23}$$

Let us determine the normal Y and longitudinal X components of the force Y_a:

$$Y = Y_a \cos\alpha \approx Y_a = 2\pi\alpha a \rho V_\infty^2 \tag{6.3.24}$$

$$X = -Y_a \sin\alpha \approx -Y_a\alpha = -2\pi\alpha^2 a \rho V_\infty^2 \tag{6.3.25}$$

The arising of the force X acting along the plate opposite to the flow seems to be paradoxical because all the elementary forces produced by the pressure are directed along a normal to the surface.

This component is called the **suction force**. The physical nature of its appearance consists in the following. Assume that the leading edge is slightly rounded. Now the velocities near it will be considerable, but not infinitely high as at the leading edge of a plate. In accordance with the Bernoulli equation, the difference between the pressure at the edge and that at infinity will be negative. The resulting rarefaction is exactly what causes the suction force. Its limiting value is given by expression (6.3.25) relating to the case of flow over a plate when the velocity near its leading edge is determined by formula (6.3.12). In accordance with this formula, the longitudinal component of the disturbed velocity at the indicated point of the plate is

$$V'_x = \pm\alpha V_\infty \sqrt{(a-x)/(a+x)} \tag{6.3.26}$$

The expression for the suction force can be generalized for an arbitrary velocity near the leading edge. For this purpose, we shall transform (6.3.25) to the form

$$T = -X = \pi\rho c^2 \tag{6.3.27}$$

where

$$c^2 = 2a\alpha^2 V_\infty^2 \tag{6.3.28}$$

We shall write the quantity c^2 in the form of the limit

$$c^2 = \lim_{x \to x_{l.e}} [V_x'^2 (x - x_{l.e})] \tag{6.3.28'}$$

where $x_{l.e}$ is the abscissa of the leading edge ($x_{l.e} = -a$), x is the running abscissa of points of the plate, and V'_x is the longitudinal component of the disturbed velocity on the upper surface of a wing.

Formula (6.3.28') can be shown to be correct. For this purpose, we shall insert expression (6.3.26) into (6.3.28'):

$$c^2 = \lim_{x \to -a} \left[V_\infty^2 \alpha^2 \left(\frac{a-x}{a+x} \right) (x+a) \right] = 2a\alpha^2 V_\infty^2$$

By introducing this value into (6.3.27), we obtain formula (6.3.25).

The conclusions on an incompressible circulatory-forward flow over an airfoil in the form of a thin plate are used in studying the aerodynamic characteristics of airfoils encountered in practice, and also of finite-span wings in flows of an incompressible fluid or of a compressible gas.

6.4. Finite-Span Wing in an Incompressible Flow

Up to now, we considered an airfoil in an incompressible flow. We can presume that such an airfoil relates to an elementary part of a lifting surface belonging to an **infinite-span wing** in a plane parallel

Basic Information from Aerodynamics

1.1. Forces Acting on a Moving Body

Surface Force

Let us consider the forces exerted by a gaseous viscous continuum on a moving body. This action consists in the uniform distribution over the body's surface of the forces $\mathbf{P}_n$ produced by the normal and the forces $\mathbf{P}_\tau$ produced by the shear stresses (Fig. 1.1.1). The surface element dS being considered is acted upon by a resultant force called a surface one. This force $\mathbf{P}$ is determined according to the rule of addition of two vectors: $\mathbf{P}_n$ and $\mathbf{P}_\tau$. The force $\mathbf{P}_n$ in addition to the force produced by the pressure, which does not depend on the viscosity, includes a component due to friction (Maxwell's hypothesis).

In an ideal fluid in which viscosity is assumed to be absent, the action of a force on an area consists only in that of the forces produced by the normal stress (pressure). This is obvious, because if the force deviated from a normal to the area, its projection onto this area would appear, i.e. a shear stress would exist. The latter, however, is absent in an ideal fluid.

In accordance with the principle of inverted flow, the effect of the forces will be the same if we consider a body at rest and a uniform flow over it having a velocity at infinity equal to the speed of the body before inversion. We shall call this velocity the **velocity at infinity** or the **free-stream velocity** (the velocity of the undisturbed flow) and shall designate it by $-\mathbf{V}_\infty$, in contrast to $\mathbf{V}$ (the velocity of the body relative to the undisturbed flow), i.e. $|\mathbf{V}| = |\mathbf{V}_\infty|$.

A free stream is characterized by the undisturbed parameters—the pressure p_∞, density ρ_∞, and temperature T_∞ differing from their counterparts p, ρ, and T of the flow disturbed by the body (Fig. 1.1.2). The physical properties of a gas (air) are also characterized by the following kinetic parameters: the dynamic viscosity μ and the coefficient of heat conductivity λ (the undisturbed parameters are μ_∞ and λ_∞, respectively), as well as by thermodynamic para-

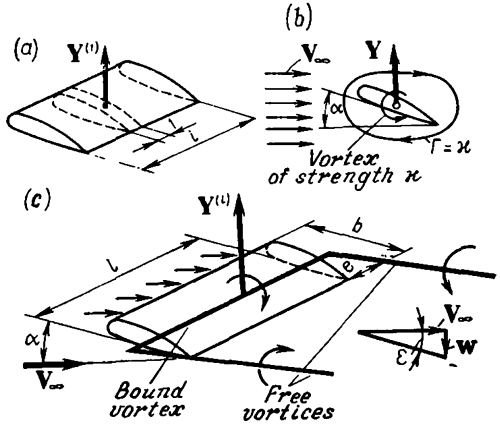

Fig. 6.4.1
System of equivalent vortices for a rectangular wing

flow. Hence, the theory of this flow is also a foundation of the aerodynamics of an infinite-span wing.

By formula (6.3.22), the lift force of a unit-span wing part is $Y^{(1)} = \rho_\infty V_\infty \Gamma$ (Fig. 6.4.1*a*). Consequently, there is a circulation flow around the airfoil with the velocity circulation Γ. If the circulation is clockwise, the velocities on the upper surface of the airfoil are higher (a circulation flow having the same direction as the oncoming one is superposed on it), while on the bottom surface they are lower (the circulation flow does not coincide with the direction of the oncoming flow). Therefore, in accordance with the Bernoulli equation, the pressure from above is lower than from below, and the lift force is directed upward as shown in Fig. 6.4.1*b*.

Since by (2.7.8) and (2.7.8′), the circulation equals the vorticity (vortex strength) $\varkappa$, the part of the wing can be replaced with an equivalent vortex of the indicated strength passing along its span. N. Zhukovsky used the term **bound** to designate this vortex. Hence, in the hydrodynamic sense, an infinite-span wing is equivalent to a bound vortex.

Let us now consider an *approximate scheme of the flow past a finite-span wing* with a rectangular planform. As established by S. Chaplygin, a bound vortex near the side edges turns and is cast off the wing in the form of a pair of vortex cores approximately coinciding with the direction of the free-stream velocity. The distance e (Fig. 6.4.1*c*) from a vortex core to the relevant side edge depends on the geometry of the wing. Consequently, the hydrodynamic effect of a finite-span wing can be obtained by replacing it with a bound vortex and a pair of free horseshoe vortices. This wing pattern is called **Chaplygin's horseshoe one.**

A vortex system equivalent to a finite-span wing induces **additional velocities** in the flow and thus causes downwash, which is a fea-

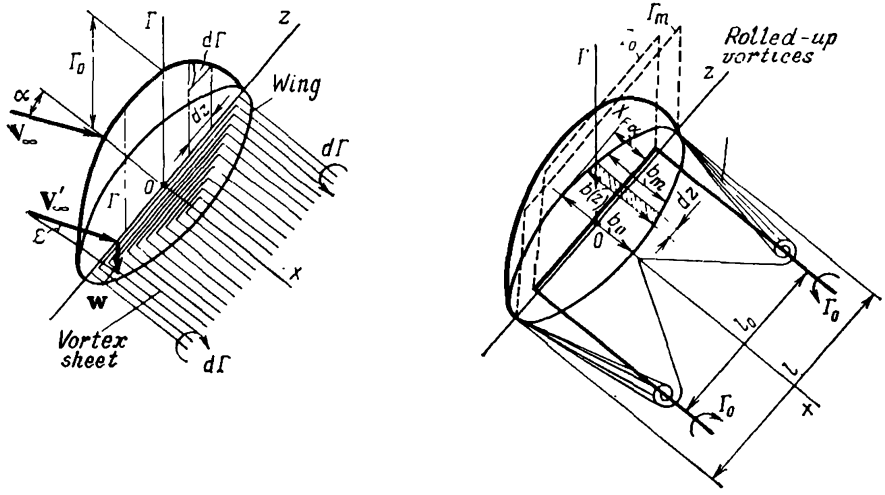

Fig. 6.4.2
Vortex sheet and rolled-up vortices behind a wing

ture of flow past a finite-span wing. The calculations of the induced velocities and the downwash angle caused by the free vortices are based on the following theorems formulated by H. Helmholtz:

(1) the strength along a vortex does not change in magnitude, and as a result, a vortex cannot end somewhere in a fluid. It must either be closed or reach the boundary of the fluid;

(2) the strength of a vortex does not depend on the time;

(3) a vortex is not disrupted in an ideal fluid.

In the considered scheme of a rectangular wing, the circulation along the span was presumed to be constant in accordance with the assumption that the lift force of each elementary part of the wing is identical. Actually, the lift force along the span of a wing having such a rectangular planform varies. This change is not great in the middle part of the wing and is more noticeable at the side edges. For a wing with an arbitrary planform, the change in the circulation is clearly expressed and is due to the different dimensions of the elementary parts and, consequently, to different values of the lift force. We can obtain the vortex pattern of flow over a wing with a system of horseshoe vortices forming a **vortex sheet** (Fig. 6.4.2). The circulation along each vortex will be constant, but changes when going over from one vortex to another. For the section at the middle of the wing, the lift force is maximum, therefore the strength of the relevant vortex and the circulation will be maximum.

Now let us see what changes the downwash introduces into the flow over a wing arranged at the geometric angle of attack α (the angle between the chord of a wing section and the vector V_∞ is also

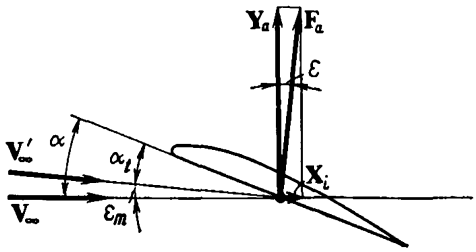

Fig. 6.4.3
Flow downwash at a wing and the appearance of induced drag

called the **setting angle**). The appearance of downwash of the flow behind the wing at the angle ε leads to the fact that the flow over the wing in the section being considered is characterized by values of the velocity V'_∞ and the angle of attack α_t differing from the corresponding values of V_∞ and α that determine the flow over an infinite-span wing. *The true angle of attack* α_t of a section of a finite-span wing *is smaller than the setting angle by the magnitude of the downwash angle* ε (Fig. 6.4.3), i.e. $\alpha_t = \alpha - \varepsilon$. The downwash angle $\varepsilon = -w/V_\infty$ varies along the span of the wing, increasing toward its tips. For convenience, the concept of the span-averaged downwash angle is introduced, determined by the formula $\varepsilon_m = \frac{1}{l}\int_{-l/2}^{l/2} \varepsilon\, dz$. Accordingly, the true angle of attack of the wing is

$$\alpha_t = \alpha - \varepsilon_m \tag{6.4.1}$$

The existence of a downwash angle leads to a change in the forces acting on a body in the flow. If flow downwash is absent, the vector of the aerodynamic force by (6.3.21) is normal to the direction of the velocity of the **undisturbed flow** V_∞. If downwash is present, the vector of the resultant aerodynamic force is oriented along a normal to the direction of the **true velocity** V'_∞ (Fig. 6.4.3). Such deviation of the resultant force through the angle ε_m causes the component X_i to appear in the direction of the undisturbed flow. This additional force X_i appearing as a result of flow downwash is called the **induced resistance** or **induced drag.** From the physical viewpoint, an induced drag is due to losses of a portion of the kinetic energy of a moving wing spent on the formation of vortices cast off its trailing edge. The magnitude of this drag is determined in accordance with Fig. 6.4.3 from the expression

$$X_i = Y_a \varepsilon_m \tag{6.4.2}$$

The lift force Y_a, owing to the smallness of the downwash, is determined in the same way as for an infinite-span wing. If we divide X_i by the quantity $(\rho_\infty V_\infty^2/2)\, S_w$, we obtain the **induced drag coefficient**

$$c_{x,i} = 2X_i/(\rho_\infty V_\infty^2 S_w) = c_{y_a} \varepsilon_m \tag{6.4.3}$$

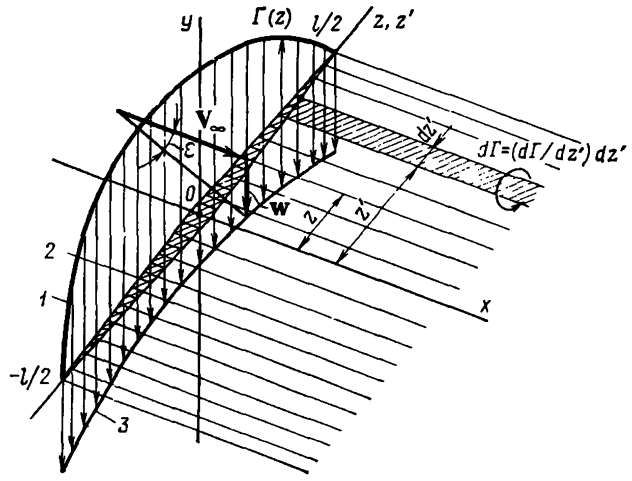

Fig. 6.4.4
Replacement of a finite-span wing with a loaded line:
1—distribution of circulation; *2*—loaded line; *3*—distribution of induced velocities or downwash angles

We shall determine this coefficient on the basis of the theory of a "loaded line". According to this theory, a finite-span wing is replaced with a single bound vortex (a loaded line). The circulation $\Gamma(z)$ for the loaded line is the same as for the corresponding sections of the wing itself (Fig. 6.4.4). Upon such a replacement, a plane vortex sheet begins directly on the loaded line and has a strength $d\Gamma(z)/dz$ that varies along the span. The flow downwash in a given section is determined for a semi-infinite vortex core having the strength $[d\Gamma(z)/dz]\,dz$. Accordingly, the total downwash angle for a section, as can be seen from Fig. 6.4.4, is

$$\varepsilon = -\frac{w}{V_\infty} = -\frac{1}{4\pi V_\infty}\int\limits_{-l/2}^{l/2}\frac{d\Gamma(z')}{dz'}\cdot\frac{dz'}{z'-z} \qquad (6.4.4)$$

Here the improper integral must be considered in the sense of its principal value.

By (6.4.4), the mean downwash angle over a span is

$$\varepsilon_m = -\frac{1}{4\pi V_\infty l}\int\limits_{-l/2}^{l/2}\left[\int\limits_{-l/2}^{l/2}\frac{d\Gamma(z')}{dz'}\cdot\frac{dz'}{z'-z}\right]dz \qquad (6.4.5)$$

The lift force coefficient c_{y_a} can be determined according to the known law of circulation distribution along the span. With such a determination, we can proceed from the hypothesis of plane sections according to which the flow over a wing element being considered is

the same as over the corresponding airfoil belonging to a cylindrical infinite-span wing. Calculations on the basis of this hypothesis give a satisfactory accuracy for wings with a low sweep and an aspect ratio of $\lambda_w > 3$-4.

According to the Zhukovsky formula, the lift force of an airfoil is

$$dY_a = \rho_\infty V_\infty \Gamma(z)\, dz \tag{6.4.6}$$

its total value for a wing is

$$Y_a = \rho_\infty V_\infty \int_{-l/2}^{l/2} \Gamma(z)\, dz \tag{6.4.6'}$$

and the corresponding aerodynamic coefficient is

$$c_{y_a} = \frac{Y}{q_\infty S_w} = \frac{2}{V_\infty S_w} \int_{-l/2}^{l/2} \Gamma(z)\, dz \tag{6.4.6''}$$

To find the law of circulation distribution $\Gamma(z)$, let us consider an airfoil in an arbitrary section of a wing for which the lift force can be written in the form

$$dY_a = c_y(z)\, q_\infty b(z)\, dz \tag{6.4.7}$$

where $b(z)$ is the chord of the airfoil in the section being considered.

With a view to the Zhukovsky formula (6.4.6), we find a **coupling equation** determining the relation for the velocity circulation in a given section:

$$\Gamma(z) = 0.5 c_{y_a}(z)\, b(z)\, V_\infty \tag{6.4.8}$$

According to the hypothesis of plane sections, the lift coefficient $c_{y_a}(z)$ of a section being considered is the same as for the corresponding infinite-span cylindrical wing. Its magnitude can be determined with account taken of the downwash angle by the formula

$$c_{y_a}(z) = c_{y_a}^{\alpha}(z)\,(\alpha - \varepsilon) \tag{6.4.9}$$

where the derivative $c_{y_a}^{\alpha}(z) = \partial c_{y_a}(z)/\partial\alpha$ is determined for an infinite-span wing and a range of angles of attack corresponding to the linear section of the curve $c_{y_a}(\alpha)$. After inserting into (6.4.8) the values from (6.4.4) and (6.4.9), we obtain

$$\Gamma(z) = (1/2)\; c_{y_a}^{\alpha}(z)\, b(z)\, V_\infty \left(\alpha + \frac{1}{4\pi V_\infty} \int_{-l/2}^{l/2} \frac{d\Gamma(z')}{dz'} \cdot \frac{dz'}{z'-z}\right) \tag{6.4.10}$$

This equation is called the **fundamental integro-differential equation** of a finite-span wing. It allows one to find the law of circulation distribution $\Gamma(z)$ for a given wing shape according to the known conditions of its flight. The angle of attack α in (6.4.10) may be fixed

(i.e. the same for all sections) or may vary along the span if geometric warp of the wing is present.

One of the most favoured ways of solving Eq. (6.4.10) is based on expanding the required function $\Gamma(z)$ into a trigonometric series (the Glauert-Trefftz method)

$$\Gamma(z) = 2lV_\infty \sum_{n=1}^{\infty} A_n \sin(n\theta) \tag{6.4.11}$$

where the new variable θ is related to the variable z by the expression $z = -(l/2)\cos\theta$ (see Fig. 6.5.1), and A_n are constant coefficients determined with the aid of Eq. (6.4.10).

Since the series (6.4.11) is a rapidly descending one, a small number m of terms is usually sufficient. To determine the unknown coefficients A_m, we compile m algebraic equations (according to the number of selected sections). Each of these equations is obtained by introducing into (6.4.10) the value of the circulation $\Gamma(z) = 2lV_\infty \sum_{n=1}^{m} A_n \sin(n\theta)$ for the corresponding section.

For conventional wings that are symmetric about the central (root) chord, the distribution of the circulation over the span is also symmetric, i.e. the equality $\Gamma(\theta) = \Gamma(\pi - \theta)$ holds (see Fig. 6.5.1). Accordingly, the terms of the series with even indices equal zero, and the circulation can be written in the approximate form

$$\Gamma = 2lV_\infty [A_1 \sin\theta + A_3 \sin(3\theta) + \ldots + A_m \sin(m\theta)]$$

Consequently, the number of algebraic equations needed to determine the coefficients A_m diminishes. The procedure followed to determine these coefficients is set out in detail in [16].

Using the found law of distribution of the circulation in the form of a series, we can determine the flow downwash and the corresponding aerodynamic coefficients (see [13]). By going over in (6.4.6″) from the variable z to the variable θ in accordance with the expression $dz = (l/2)\sin\theta\, d\theta$, introducing the formula for the circulation in the form of a series, and taking into account that $l^2/S_w = \lambda_w$, we find a relation for the lift coefficient:

$$c_{y_a} = \pi\lambda_w A_1 \tag{6.4.12}$$

Using (6.4.5), we determine the mean downwash angle:

$$\varepsilon_m = (c_{y_a}/\pi\lambda_w)(1 + \tau) \tag{6.4.13}$$

where τ is a coefficient taking into account the influence of the aspect ratio:

$$\tau = \sum_{n=2}^{m} A_n/A_1 \tag{6.4.14}$$

From (6.4.3), we obtain the relevant induced drag coefficient. Its value can be determined more precisely, however, by going over from the mean downwash angle to its local value in accordance with the expression $dX_1 = \varepsilon\, dY_a$. By introducing into this expression instead of ε and dY_a their values from (6.4.4) and (6.4.6), integrating, and determining the induced drag coefficient, we obtain

$$c_{x.\,i} = \frac{-1}{2\pi V_\infty^2 S_w} \int_{-l/2}^{l/2} \Gamma(z) \left[\int_{-l/2}^{l/2} \frac{d\Gamma(z')}{dz'} \cdot \frac{dz'}{z'-z} \right] dz \qquad (6.4.15)$$

Introducing the value of $\Gamma(z)$ and substituting λ_w for l^2/S_w, we have

$$c_{x,i} = (c_{y_a}^2/\pi\lambda_w)\,(1 + \delta) \qquad (6.4.16)$$

where the coefficient δ taking into account the influence of the aspect ratio on the drag depending on the lift is

$$\delta = \sum_{n=2}^{m} n A_n^2/A_1^2 \qquad (6.4.17)$$

The coefficients τ and δ for wings of various planforms can be determined according to the data given in [13, 16].

The results of the general theory of a loaded line obtained can be seen to be characterized by a comparative simplicity of the aerodynamic relations, provide a clear notion of the physical phenomena attending flow past finite-span wings, and allow one to reveal the mechanism of formation of the lift force and induced drag. The application of this theory, however, is limited to wings with a sufficiently small sweep and a relatively large aspect ratio. In modern aerodynamics, more accurate and more general solutions are worked out. They are described in special literature.

At the same time, the development of ways of evaluating the aerodynamic properties of wings by constructing approximate models of the flow over finite-span wings is of practical significance. Let us consider one of them based on the representation of the aerodynamic scheme of a wing in the form of a bound and a pair of free vortex cores. This representation is based on experimental data according to which a vortex sheet is not stable and at a comparatively short distance from the wing rolls up into two parallel vortex cores (see Fig. 6.4.2).

The basic element of this problem is the finding of the distance l_0 between the free (rolled up) vortices. We proceed here from the fact that for a wing with a span of l, the vortex pattern of the wing may be replaced with a single horseshoe vortex with the constant circulation Γ_0 corresponding to the root section. We also assume that the bound vortex (the loaded line) passes through the aerodynamic cen-

tre of the wing with the coordinate $x_{F\alpha}$. The magnitude of this circulation can be determined by a coupling equation according to which

$$\Gamma_0 = 0.5 c_{y_{a0}} b_0 V_\infty \tag{6.4.18}$$

where $c_{y_{a0}}$ and b_0 are the lift coefficient and the section chord, respectively.

A similar expression can be compiled for the mean circulation over the span, the same as in the section with the chord b_m:

$$\Gamma_m = 0.5 c_{y_a} b_m V_\infty \tag{6.4.19}$$

where c_{y_a} is the lift coefficient of the wing.

From Eqs. (6.4.18) and (6.4.19), we find the relation between the circulations:

$$\Gamma_0 = \Gamma_m c_{y_{a0}} b_0 / (c_{y_a} b_m) \tag{6.4.20}$$

As stipulated, the adopted vortex systems Γ_m and Γ_0 correspond to the same lift force ($Y_a = \rho_\infty V_\infty \Gamma_m l = \rho_\infty V_\infty \Gamma_0 l_0$), hence $\Gamma_m l = \Gamma_0 l_0$. Therefore, by Eq. (6.4.20), we have

$$l_0 = l b_m c_{y_a} / (b_0 c_{y_{a0}}) \tag{6.4.21}$$

Now, according to the known arrangement of the horseshoe vortex system, we can use formula (2.7.13) to determine the downwash angle at each point behind a wing, also taking into account the induction of the bound vortex.

To find the induced drag coefficient by formula (6.4.3), we must find the mean downwash angle $\varepsilon_m = (1/l) \int_{-l/2}^{l/2} \varepsilon \, dz$ on the loaded line, taking account only of a pair of free vortices with the aid of formula (2.7.13). According to calculations (see [13]), this angle is

$$\varepsilon_m = \frac{-\Gamma_0}{2\pi l V_\infty} \ln \frac{l_0 + l}{l_0 - l} \tag{6 4.22}$$

where Γ_0 is determined by (6.4.18). Having in view that $l/b_0 = \lambda_w (b_m/b_0)$, we finally obtain

$$\varepsilon_m = -\frac{c_{y_a} b_0}{4\pi \lambda_w b_m} \ln \frac{l_0 + l}{l_0 - l} = -\frac{c_{y_a}}{\pi \lambda_w} \cdot \frac{l}{4 l_0} \ln \frac{l_0 + l}{l_0 - l} \tag{6.4.23}$$

We can use this downwash angle to estimate the value of the induced drag coefficient with the aid of (6.4.3). In a particular case for an infinite-span wing ($\lambda_w \to \infty$), the downwash angle is absent and, consequently, the induced drag vanishes.

6.5. Wing with Optimal Planform

Conversion of Coefficients c_y and $c_{x,1}$ from One Wing Aspect Ratio to Another

A finite-span lifting plane having the minimum induced drag is called a **wing with the optimal planform.** A glance at formula (6.4.16) reveals that at the given values of c_{y_a} and λ_w, the value of $c_{x,1}$ will be minimum when the coefficient $\delta = 0$, or $\sum_{n=2}^{m} nA_n^2/A_1^2 = 0$. It follows from this equality that all the coefficients of the expansion of the circulation Γ into a series (6.4.11), except for A_1, equal zero ($A_3 = A_5 = \ldots = 0$). Hence, the circulation in an arbitrary section is

$$\Gamma(\theta) = 2lV_\infty A_1 \sin\theta \tag{6.5.1}$$

For the central section ($\theta = \pi/2$), the circulation is maximum and equals $\Gamma_0 = 2lV_\infty A_1$. Hence, $\Gamma(\theta) = \Gamma_0 \sin\theta$. Inserting into this formula $\sin\theta = \sqrt{1-(2z/l)^2}$, we obtain

$$\Gamma^2(z)/\Gamma_0^2 + z^2/(0.5l)^2 = 1 \tag{6.5.2}$$

This equation determines the **elliptic** law of distribution of the circulation over the span of a wing having the optimal planform (Fig. 6.5.1). For such a wing, the induced drag coefficient $c_{x,1} = c_{y_a}^2/(\pi\lambda_w)$, while the mean flow downwash angle $\varepsilon_m = c_{y_a}/(\pi\lambda_w)$; by analysing (6.4.4), we can convince ourselves that the quantity ε_m exactly equals the downwash angle in an arbitrary section. In other words, the downwash angle does not change along the span in a wing with the minimum induced drag.

In accordance with the coupling equation, for an arbitrary wing section, we have $\Gamma(z) = 0.5c_{y_a} b(z) V_\infty$, and for a central one, we have $\Gamma_0 = 0.5c_{y_a 0} b_0 V_\infty$. Now we can use Eq. (6.5.2) to find the following expression for the chord in a wing section with the optimal planform:

$$b(z) = b_0 (c_{y_a 0}/c_{y_a}) \sqrt{1-(z/0.5l)^2} \tag{6.5.3}$$

Let us consider a wing at the angle of attack α having section profiles that are identical along the span. We shall assume that the sections of the wing are arranged at the same local geometric angle of attack determined by the given value of α. Since the downwash angle does not change from one section to another for a wing with an elliptical distribution of the circulation, the true angles of attack

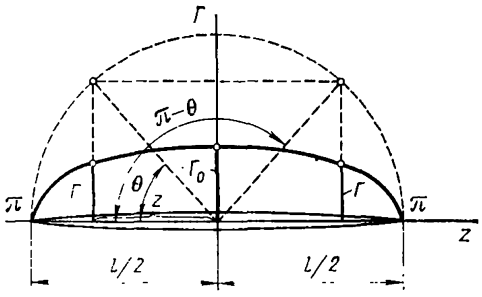

Fig. 6.5.1
Elliptical distribution of the circulation and a geometric interpretation of the constants z and θ

are the same: $\alpha_t = \alpha - \varepsilon$, and, therefore, the lift coefficients of the profiles are the same, i.e. the ratio $c_{y_a}/c_{y_{a0}} = 1$. Hence, the local chord of the wing is determined by the relation

$$b(z) = b_0 \sqrt{1-(z/0.5l)^2} \qquad (6.5.4)$$

In accordance with the result obtained, a wing with the minimum induced drag has an elliptical planform. In the case being considered, a constant coefficient $c_{y_a} = c^{\alpha}_{y_a}\alpha_t$ is ensured as a result of the constancy along the span of the quantity α_t and the derivative $c^{\alpha}_{y_a}$ identical for the same profiles. For a wing with an elliptical planform, the same effect can be achieved by varying the parameters $c^{\alpha}_{y_a}$ and α_t, i.e. by selecting the corresponding profiles in combination with geometric warp (upon which the sections are set at different geometric angles of attack).

It must be noted that just such a method of varying the geometric and aerodynamic parameters is used to achieve an elliptical (or close to it) distribution of the circulation on modern wings. Here three factors change in the corresponding way simultaneously. These factors, namely, $c^{\alpha}_{y_a}(z)$, $\alpha_t(z)$, and $b(z)$ characterize the circulation $\Gamma(z) = 0.5c^{\alpha}_{y_a}\alpha_t b V_\infty$ that is distributed according to the elliptical law (6.5.2).

In the simplest case of a wing with a rectangular planform, $b = \text{const}$, this law of circulation distribution is ensured by only varying the values of $c^{\alpha}_{y_a}$ and α_t (by selecting the profiles and warping, respectively). It must be borne in mind that for wings of a non-elliptical planform, including rectangular ones, an elliptical distribution of the circulation can be achieved only at a definite angle of attack, and the distribution will be different if the value of the angle is changed.

It is interesting to appraise by how much wings with a different planform differ from their elliptical counterparts in their aerodynamic properties. Table 6.5.1 gives the results of evaluating the coeffi-

Table 6.5.1

Planform of wing	δ	τ
Elliptical	0	0
Trapezoidal ($\eta_w = 2$-3)	0	0
Rectangular ($\lambda_w = 5$-8)	0.053	0.179
Rectangular with rounded tips	0	0.147

cients δ and τ, called corrections for wings of a non-elliptical planform. These coefficients depend mainly on the planform of a wing and its aspect ratio. A glance at the table reveals that trapezoidal wings do not virtually differ from elliptical ones. A slight deviation in the values of δ and τ is observed in rectangular wings with straight tips. Rounding of these tips leads to complete analogy with an elliptical wing as regards the value of δ and to a smaller difference in the coefficients τ.

The relations obtained for determining the aerodynamic coefficients of finite-span wings make it possible to solve an important problem associated with the finding of these coefficients when going over from one wing aspect ratio λ_{w1} to another one λ_{w2}. This solution appreciably facilitates aerodynamic calculations because it makes it possible to use the data obtained when testing serial models of wings with the adopted (standard) value of the aspect ratio in wind tunnels.

Let us assume that for a wing with the aspect ratio λ_{w1} we know the coefficients c_{y_a} and $c_{x,1}$ and we have to convert these coefficients to another aspect ratio λ_{w2} of a wing having the same set of sections, but differing in its planform. If both of these wings have the same lift coefficient c_{y_a}, the mean downwash angles behind them are

$$\varepsilon_{m1} = (c_{y_a}/\pi\lambda_{w1})(1 + \tau_1), \quad \varepsilon_{m2} = (c_{y_a}/\pi\lambda_{w2})(1 + \tau_2)$$

Identical values of c_{y_a} for wings are determined by identical true angles of attack, i.e. $\alpha_{t1} = \alpha_{t2}$, where

$$\alpha_{t1} = \alpha_1 - \varepsilon_{m1}, \quad \alpha_{t2} = \alpha_2 - \varepsilon_{m2}$$

Consequently, for the setting angle of the second wing, we obtain the expression

$$\alpha_2 = \alpha_1 - (c_{y_a}/\pi)[(1 + \tau_1)/\lambda_{w1} - (1 + \tau_2)/\lambda_{w2}] \qquad (6.5.5)$$

According to this formula for converting the lift coefficient, a wing with a smaller aspect ratio ($\lambda_{w2} < \lambda_{w1}$) having a larger down-

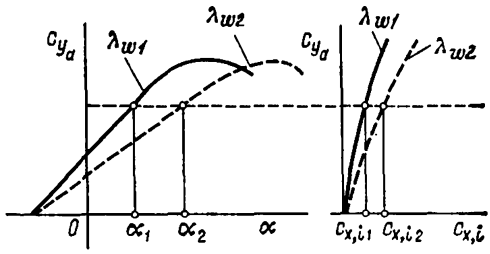

Fig. 6.5.2
Conversion of aerodynamic coefficients of a wing from one aspect ratio to another

wash angle ($\varepsilon_{w2} > \varepsilon_{w1}$) must have an increased setting angle ($\alpha_2 > \alpha_1$) to obtain the same coefficient c_{y_a}.

The induced drag coefficients for two wings with the aspect ratios λ_{w1} and λ_{w2} and with identical coefficients c_{y_a} are determined by the following formulas, respectively:

$$c_{x,i1} = (c_{y_a}/\pi\lambda_{w1})\ (1 + \delta_1),\quad c_{x,i2} = (c_{y_a}/\pi\lambda_{w2})\ (1 + \delta_2)$$

Accordingly, for a wing with the aspect ratio λ_{w2}, the induced drag coefficient is

$$c_{x,i2} = c_{x,i1} - (c_{y_a}/\pi)\ [(1 + \delta_1)/\lambda_{w1} - (1 + \delta_2)/\lambda_{w2}] \qquad (6.5.6)$$

This formula is used to convert the value of $c_{x,i}$ for a wing with the aspect ratio λ_{w1} to its value for the aspect ratio λ_{w2}. If this new ratio is smaller than the given one ($\lambda_{w2} < \lambda_{w1}$), a large downwash appears ($\varepsilon_{m2} > \varepsilon_{m1}$), and, consequently, the induced drag coefficient grows ($c_{x,i2} > c_{x,i1}$).

Figure 6.5.2 shows graphically how the coefficients c_{y_a} and $c_{x,i}$ are converted from the aspect ratio λ_{w1} to λ_{w2} in accordance with formulas (6.5.5) and (6.5.6). First the curves $c_{y_a} = f_1(\alpha_1)$ and $c_{y_a} = \varphi_1(c_{x,i1})$ are plotted for a wing with the given aspect ratio λ_{w1}. Next, setting a number of values of c_{y_a}, we use the plot to determine the corresponding values of α_1 and $c_{x,i1}$, and then calculate the angles of attack α_2 and the coefficients $c_{x,i2}$ for the second wing by formulas (6.5.5) and (6.5.6). The corresponding points are laid off, and the curves $c_{y_a} = f_2(\alpha_2)$ and $c_{y_a} = \varphi_2(c_{x,i2})$ are plotted.

For wings with smaller aspect ratios ($\lambda_{w2} < \lambda_{w1}$), these curves will be to the right of those of the ratio λ_{w1} because with the same true angle of attack, the increase in the downwash angle ε_{w2} for the second wing with a smaller λ_{w2} is compensated by the growth in the setting angle of attack ($\alpha_2 > \alpha_1$); in turn, an increased coefficient $c_{x,i2}$ corresponds to the greater downwash angle ε_{w2}, and this is exactly what is shown in Fig. 6.5.2.

The plots in Fig. 6.5.2 can be used to convert c_{y_a} and $c_{x,i}$ to a wing with an infinitely large aspect ratio (airfoil). For this purpose,

the second terms in the brackets in formulas (6.5.5) and (6.5.6) must be taken equal to zero. The converted curves $c_{y_a} = f_2(\alpha_2)$ and $c_{y_a} = \varphi_2(c_{x,12})$ will occupy a position at the extreme left of the corresponding curves $c_{y_a} = f_1(\alpha_1)$ and $c_{y_a} = \varphi_1(c_{x,11})$.

Mean Aerodynamic Chord. When performing aerodynamic calculations of finite-span wings, the **mean aerodynamic chord** is selected as the characteristic geometric dimension of the span. Such a chord belongs to a conditional wing having a rectangular planform for which the planform area, the aerodynamic force, and the pitching moment are the same as for a wing of the given planform. The mean aerodynamic chord allows us to compare the moment characteristics of various wings with a varying chord along their span. One of such characteristics is the pitching moment coefficient determined as $m_{zA} = M_z/(b_A q S_w)$, where b_A is the mean aerodynamic chord. The quantity m_{zA} is sufficiently stable when the planform of a wing and its dimensions change.

The value of the chord b_A, and those of the coordinates of its leading point x_A, y_A (relative to coordinate axes passing through the apex of the given wing), are usually determined approximately assuming equality of the aerodynamic coefficients (of the moment, drag, and lift) of a wing as a whole and its individual section (profile). Accordingly, we have

$$\left.\begin{aligned} b_A &= \frac{2}{S_w}\int_0^{l/2} b^2(z)\,dz, \qquad x_A = \frac{2}{S_w}\int_0^{l/2} xb(z)\,dz \\ y_A &= \frac{2}{S_w}\int_0^{l/2} yb(z)\,dz \end{aligned}\right\} \tag{6.5.7}$$

where x, y are the longitudinal and vertical coordinates of the leading point of a section with the varying chord $b(z)$. Evidently, knowing x_A and the equation of the leading edge of a given wing, we can determine the lateral coordinate z_A of the mean aerodynamic chord.

Formulas (6.5.7) make it possible to calculate the magnitude of the chord b_A by numerical or graphical integration and determine its position. The middle of b_A coincides with the centre of gravity of the wing area.

For a broad range of wings having a trapezoidal planform, we can find analytical relations for b_A, x_A, y_A, and z_A. For such wings

$$\left.\begin{aligned} b(z) &= b_0[1-(\eta_w-1)\bar{z}/\eta_w] \\ S_w &= b_0 l(\eta_w+1)/(2\eta_w) \\ x &= z\tan\varkappa_0; \quad y = z\tan\psi \end{aligned}\right\} \tag{6.5.8}$$

where $\eta_w = b_0/b_A$ is the taper ratio of the wing, $\varkappa_0$ is the sweep angle of the leading edge, ψ is the dihedral angle, and $\bar{z} = 2z/l$.

Introduction of (6.5.8) into (6.5.7) yields

$$\left.\begin{aligned} b_A &= 4S_w\,[1-\eta_w/(\eta_w+1)^2]/(3l)\\ x_A &= l\,(\eta_w+2)\tan\varkappa_0/[6\,(\eta_w+1)]\\ y_A &= l\,(\eta_w+2)\tan\psi/[6\,(\eta_w+1)] \end{aligned}\right\} \qquad (6.5.9)$$

The lateral coordinate of the chord b_A is found from the formula $z_A = x_A/\tan\varkappa_0$. If a wing has no dihedral, the coordinate y_A is evidently zero.

7

An Airfoil in a Compressible Flow

7.1. Subsonic Flow over a Thin Airfoil

Linearization of the Equation for the Velocity Potential

The calculation of a subsonic flow over an airfoil is associated with solution of the equation for the velocity potential of a plane two-dimensional flow that is obtained from (5.1.8) provided that $\varepsilon = 0$ and has the form

$$(V_x^2 - a^2)\frac{\partial^2\varphi}{\partial x^2} + 2V_xV_y\frac{\partial^2\varphi}{\partial x\,\partial y} + (V_y^2 - a^2)\frac{\partial^2\varphi}{\partial y^2} = 0. \qquad (7.1.1)$$

This partial differential equation of the second order is **non-linear** in the unknown function φ and describes the flow past sufficiently thick airfoils. The latter cause large disturbances of the gas upon which the flow velocities V and the speeds of sound a differ appreciably from the relevant free-stream flow parameters.

If an airfoil is thin and the disturbances it produces are small, Eq. (7.1.1) can be simplified by reducing it to a linear equation with constant coefficients of the second partial derivatives. Such a simplification is called **linearization**, while the obtained equation and the nearly uniform flow it describes are called **linearized.**

For a linearized flow, conditions (6.1.1) for the velocities are satisfied, and equation (6.1.2) holds. Since the disturbance velocities u and v (6.1.1) are infinitesimal, the equation for the speed of sound obtained from (3.6.20) can be transformed as follows:

$$a^2 = a_\infty^2 + [(k-1)/2]\,(V_\infty^2 - V^2) \qquad (7.1.2)$$

Substituting for V^2 its value from (6.1.2), we obtain

$$a^2 = a_\infty^2 - (k-1)\,V_\infty u \qquad (7.1.2')$$

Inserting into (7.1.1) the value of a^2 from (7.1.2'), and also $V_x = V_\infty + u$, $V_y = v$, $V_x^2 = V_\infty^2 + 2V_\infty u$, $V_y^2 \approx v^2$, and taking into account that the total velocity potential of a linearized flow can be written in the form $\varphi = \varphi_\infty + \varphi'$, where φ_∞ is the velocity potential of the oncoming flow, while the additional potential according to

condition (6.1.1) is $\varphi' \ll \varphi_\infty$, we obtain

$$[V_\infty^2 - a_\infty^2 + (k+1) V_\infty u] \frac{\partial^2 \varphi'}{\partial x^2} + 2(V_\infty + u) v \frac{\partial^2 \varphi'}{\partial x \partial y}$$
$$+ [v^2 - a_\infty^2 + (k-1) V_\infty u] \frac{\partial^2 \varphi'}{\partial y^2} = 0 \qquad (7.1.3)$$

The second partial derivatives of the potential φ' with respect to the coordinates x and y are first-order infinitesimals:

$$\frac{\partial^2 \varphi'}{\partial x^2} = \frac{\partial u}{\partial x}, \quad \frac{\partial^2 \varphi'}{\partial x \partial y} = \frac{\partial u}{\partial y} = \frac{\partial v}{\partial x}, \quad \frac{\partial^2 \varphi'}{\partial y^2} = \frac{\partial v}{\partial y}$$

With this in view, in (7.1.3), we can determine the group of terms that are second- and third-order infinitesimals; disregarding them, we obtain a linearized equation in the following form:

$$(a_\infty^2 - V_\infty^2) \frac{\partial^2 \varphi'}{\partial x^2} + a_\infty^2 \frac{\partial^2 \varphi'}{\partial y^2} = 0 \qquad (7.1.4)$$

or

$$(1 - M_\infty^2) \frac{\partial^2 \varphi'}{\partial x^2} + \frac{\partial^2 \varphi'}{\partial y^2} = 0 \qquad (7.1.4')$$

where $M_\infty = V_\infty / a_\infty$.

Let us consider the expression for the pressure in a linearized flow. To do this, we shall use formula (3.6.26), which we shall write in the form

$$p/p_\infty = (1 - V^2/V_{max}^2)^{k/(k-1)} (1 - V_\infty^2/V_{max}^2)^{-k/(k-1)}$$

Inserting the value of V^2 from (6.1.2), we have

$$p/p_\infty = [1 - 2V_\infty u/(V_{max}^2 - V_\infty^2)]^{k/(k-1)}$$

Taking into account that by formula (3.6.22)

$$V_{max}^2 - V_\infty^2 = \frac{2}{k-1} a_\infty^2 = \frac{2k}{k-1} \cdot \frac{p_\infty}{\rho_\infty}$$

we find

$$\frac{p}{p_\infty} = \left(1 - \frac{k-1}{k} \cdot \frac{\rho_\infty V_\infty u}{p_\infty}\right)^{k/(k-1)} \qquad (7.1.5)$$

Let us expand the expression on the right-hand side into a binomial series and retain the second term in the expansion:

$$p/p_\infty = 1 - \rho_\infty V_\infty u / p_\infty \qquad (7.1.5')$$

Hence we find the excess pressure $p - p_\infty = -\rho_\infty V_\infty u$ and the pressure coefficient $\bar{p} = -2u/V_\infty$, i.e. we obtain the same relations (6.1.3) and (6.1.5) as for an incompressible fluid. But when using these relations for high subsonic velocities, one must take into account that the disturbance velocity $u = \partial \varphi' / \partial x$ is determined with a view to compressibility.

Relation Between the Parameters of a Compressible and Incompressible Fluid Flow over a Thin Airfoil

The flow over a thin airfoil at a small angle of attack in a compressible subsonic flow is investigated with the aid of Eq. (7.1.4′) in which $M_\infty < 1$. Let us change the variables in this equation in accordance with the relations

$$x_0 = x, \quad y_0 = y\sqrt{1-M_\infty^2}, \quad \varphi_0' = \varphi'\gamma V_{\infty 0}/V_\infty \tag{7.1.6}$$

where γ is an arbitrary parameter, and $V_{\infty 0}$ is the velocity of a conditional flow (fictitious velocity) that in the general case differs from the velocity V_∞ of a given flow.

By introducing (7.1.6) into (7.1.4′), we obtain the Laplace equation for determining the velocity potential φ_0' of an incompressible flow in the plane x_0, y_0:

$$\partial^2\varphi_0'/\partial x_0^2 + \partial^2\varphi_0'/\partial y_0^2 = 0 \tag{7.1.4″}$$

Hence, the problem of a compressible flow over a given airfoil can be solved by using the results of solving the problem on an incompressible flow at the fictitious velocity $V_{\infty 0}$ over a modified airfoil. Let us find the relation between the corresponding parameters of flow over the airfoils and between their geometric characteristics. The relation between the disturbance velocities u_0 in the incompressible and u in the compressible flows is established in accordance with (7.1.6) as follows:

$$u_0 = \frac{\partial\varphi_0'}{\partial x_0} = \frac{\partial\varphi'}{\partial x}\gamma\frac{V_{\infty 0}}{V_\infty} = u\gamma\frac{V_{\infty 0}}{V_\infty} \tag{7.1.7}$$

Using (6.1.5), we find the pressure coefficients in an incompressible fluid $\bar{p}_{1c} = -2u_0/V_{\infty 0}$ and in a compressible gas $\bar{p} = -2u/V_\infty$. Consequently, with a view to (7.1.7), we obtain

$$\bar{p}_{1c} = \gamma\bar{p} \tag{7.1.8}$$

From the formulas $c_{y,1c} = \oint \bar{p}_{1c}\, d\bar{x}_0$, $m_{z,1c} = \oint \bar{p}_{1c}\bar{x}_0\, d\bar{x}_0$, in which $\bar{x}_0 = x/b$, and expression (7.1.8), we find the relation between the corresponding lift and moment coefficients:

$$c_{y_a 1c} = \gamma\oint \bar{p}\, d\bar{x} = \gamma c_{y_a}; \quad m_{z_a 1c} = \gamma\oint \bar{p}\bar{x}\, d\bar{x} = \gamma m_{z_a} \tag{7.1.9}$$

where $\bar{x} = x/b$.

Let us establish the relation between the configurations of airfoils and the angles of attack. For this purpose, we shall first determine

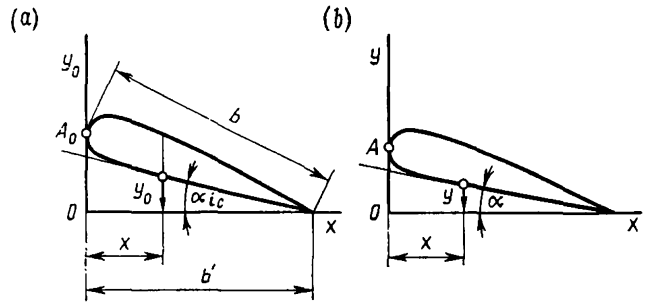

Fig. 7.1.1
Airfoils in a nearly uniform incompressible (a) and compressible (b) flows: A and A_0—stagnation points

the relation between the vertical velocity components. In accordance with (7.1.6), we have

$$v_0 = \frac{\partial \varphi_0'}{\partial y_0} = \frac{\partial \varphi'}{\partial y} \cdot \frac{1}{\sqrt{1-M_\infty^2}} \cdot \frac{V_{\infty 0}}{V_\infty} = v \frac{\gamma}{\sqrt{1-M_\infty^2}} \cdot \frac{V_{\infty 0}}{V_\infty} \quad (7.1.10)$$

In an incompressible fluid by Eq. (3.3.17'), in which the function F is taken equal to $y_0 - f_0(x_0)$ if $y_0 = f_0(x_0)$, we may consider for an airfoil that $v_0/(V_{\infty 0} + u_0) = dy_0/dx_0$ or, taking into account that $u_0 \ll V_{\infty 0}$, assume that $v_0/V_{\infty 0} = dy_0/dx_0$. Similarly, we find for an airfoil in a compressible gas that $v/V_\infty = dy/dx$. Consequently, $(v_0/v)(V_\infty/V_{\infty 0}) = (dy_0/dy)\, dx/dx_0$. Taking (7.1.6) and (7.1.10) into account, we find $dy_0/dy = \gamma/\sqrt{1-M_\infty^2}$. Integration for the condition that for $y = 0$ the quantity $y_0 = 0$ yields an equation relating the vertical coordinates of the fictitious and given airfoils:

$$y_0 = y\gamma/\sqrt{1-M_\infty^2} \quad (7.1.11)$$

At the same time, as follows from (7.1.6), the horizontal coordinates of the airfoils do not change. With this in view, the angles of attack can be written in the form

$$\alpha_{1c} = y_0/(b'-x) \text{ and } \alpha = y/(b'-x)$$

where b' is the distance to the trailing edge of the airfoil, and x is the horizontal coordinate (Fig. 7.1.1).

Hence, by (7.1.11), we have

$$\alpha_{1c} = \alpha\gamma/\sqrt{1-M_\infty^2} \quad (7.1.12)$$

Let us assume that the arbitrary parameter $\gamma = 1$. Therefore,

$$\left.\begin{aligned} &\bar{p} = \bar{p}_{1c}, \quad y = y_0\sqrt{1-M_\infty^2}, \quad \alpha = \alpha_{1c}\sqrt{1-M_\infty^2} \\ &c_{y_a} = c_{y_a 1c}, \quad m_{z_a} = m_{z_a 1c} \end{aligned}\right\} \quad (7.1.13)$$

Consequently, if the pressure coefficients are the same at corresponding points of thin airfoils in compressible and incompressible flows, then in the compressible flow the airfoil is thinner than in the incompressible one $\sqrt{1-M_\infty^2}$ times. The angle of attack decreases to the same extent.

Let us consider the case when $\gamma = \sqrt{1-M_\infty^2}$ and, therefore,

$$\left.\begin{aligned} \bar{p} &= \bar{p}_{1c}/\sqrt{1-M_\infty^2}, \quad y = y_0, \quad \alpha = \alpha_{1c} \\ c_{y_a} &= c_{y_a 1c}/\sqrt{1-M_\infty^2}, \quad m_{z_a} = m_{z_a 1c}/\sqrt{1-M_\infty^2} \end{aligned}\right\} \qquad (7.1.14)$$

According to the results obtained, for two identical airfoils at the same angle of attack, the pressure coefficients at corresponding points of the airfoils, and also their overall lift and moment coefficients in a compressible flow are *larger* than those in an incompressible one $1/\sqrt{1-M_\infty^2}$ times. Hence follows the conclusion that compressibility leads *to an increase* in the pressure and lift force. The coefficient $1/\sqrt{1-M_\infty^2}$ is known as the **Prandtl-Glauert correction** (for the compressibility effect). The corresponding relation (7.1.14) for $\bar{p}$ is known as the Prandtl-Glauert formula. It can be considered as a first approximation when calculating the pressure coefficient in a compressible flow according to the relevant value of $\bar{p}_{1c}$. More accurate results relating to thickened airfoils and increased angles of attack are obtained by the **Kármán-Tsien formula**

$$\bar{p} = \bar{p}_{1c}\left(\sqrt{1-M_\infty^2} + \frac{M_\infty^2}{1+\sqrt{1-M_\infty^2}}\,\frac{\bar{p}_{1c}}{2}\right)^{-1} \qquad (7.1.15)$$

The use of formulas (7.1.14) and (7.1.15) for $\bar{p}$ leads to quite a large error when determining the pressure coefficient at the stagnation point where the velocities and, consequently, the local Mach number, equal zero. For example, for this point, at which $\bar{p}_{0\,1c} = 1$, formula (7.1.14) when $M_\infty = 0.8$ yields a coefficient $\bar{p}_0 = 1.67$, and formula (7.1.15), $\bar{p}_0 = 1.26$ instead of the actual value of 1.17.

At the stagnation point, the pressure coefficient $\bar{p}_0 = 2(p_0 - p_\infty)/(kp_\infty M_\infty^2)$ for arbitrary numbers $M_\infty < 1$ is evaluated with the aid of an expression obtained from (3.6.30) provided that $M = 1$:

$$\bar{p}_0 = \frac{2}{kM_\infty^2}\left[\left(1+\frac{k-1}{2}M_\infty^2\right)^{k/(k-1)} - 1\right] \qquad (7.1.16)$$

When $M_\infty < 1$, the quantity in parentheses can be written in the form of a series in which the first three terms are retained:

$$\bar{p}_0 = 1 + \frac{M_\infty^2}{4} + \frac{2-k}{24}M_\infty^2 \qquad (7.1.17)$$

This relation is suitable for quite a broad range of values of $0 \leqslant M_\infty \leqslant 1$.

7.2. Khristianovich Method

Content of the Method

If an airfoil or another body in a flow introduces finite disturbances into it, the linearized equations are not suitable. Non-linear equations of gas dynamics must be used when studying such a flow.

Many problems on supersonic flow can be solved by employing, particularly, the method of characteristics. The number of solvable problems of supersonic aerodynamics increases still more owing to the numerical methods of integrating the equations of motion. It is much more difficult to analyse subsonic flow. This is explained mathematically by the different nature of the equations: for supersonic flows they are hyperbolic, and for subsonic ones, elliptic.

The use of imaginary characteristics in the elliptic equations does not yield appreciable simplifications. The more complicated nature of studying subsonic flows is explained physically by the fact that disturbances in them propagate into all the regions of motion, whereas the disturbances in supersonic flows are confined within conical surfaces issuing from the point of disturbance and propagating only downstream. Owing to the linearized nature of the equations, the investigation of nearly uniform subsonic flows is somewhat simpler than of subsonic flows with finite disturbances over, for example, thick airfoils.

A method of studying such flows is described by Academician S. Chaplygin [17]. He gives equations forming the mathematical basis of the theory of potential subsonic flows. They are known in gas dynamics as the **Chaplygin equations**. Their feature is that they describe the flow of a gas not in the plane y, x, but in that of the special coordinates τ and β ($\tau = V^2$ is the square of the total velocity at a given point in the flow, and β is the polar angle determined from the condition $V_x = V \cos \beta$). Unlike the conventional equations, they are *linear* because the coefficients of the equations are functions of the independent variables τ and β. These equations were solved by Chaplygin for a number of cases of flow at high subsonic velocities.

The Chaplygin equations underlie many other methods in the field of high-speed aerodynamics. Academician S. Khristianovich, using these equations, developed a method making it possible to take into account the influence of compressibility on the subsonic flow over airfoils of an arbitrary configuration. The theoretical tenets of this method are described in detail in [3]. We shall consider the basic content of the method and its application to the solution of various problems of a compressible subsonic flow over airfoils.

When considering a compressible flow over an airfoil of a given configuration, Khristianovich showed that the flow equations can be

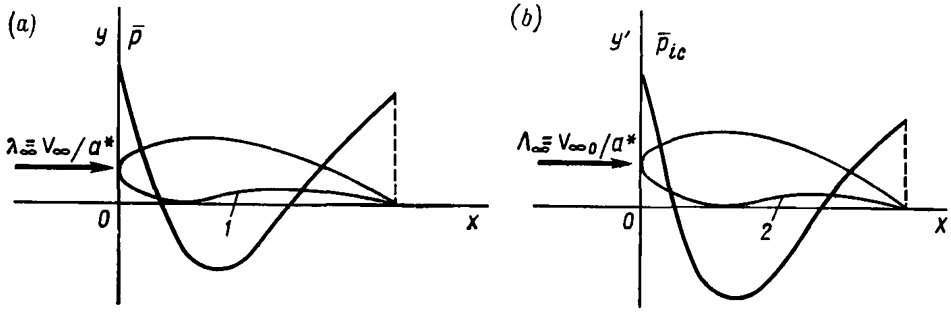

Fig. 7.2.1

Calculation of the pressure on an airfoil in a compressible flow:
***a*—true flow; *b*—fictitious flow; *1*—given airfoil; *2*—fictitious airfoil**

reduced to *equations of an incompressible flow over an airfoil with a modified configuration* (Fig. 7.2.1). Hence, according to Khristianovich's approach, first the relatively simple problem of a *conditional (fictitious) incompressible flow over a fictitious airfoil is solved, and then the parameters obtained are converted to the conditions of a compressible flow over the given airfoil.*

Table 7.2.1

λ	0	0.05	0.10	0.15	0.20	0.25	0.30	0.35
Λ	0	0.0500	0.0998	0.1493	0.1983	0.2467	0.2943	0.3410
λ	0.40	0.45	0.50	0.55	0.60	0.625	0.650	0.675
Λ	0.3862	0.4307	0.4734	0.5144	0.5535	0.5722	0.5904	0.6080
λ	0.700	0.725	0.750	0.775	0.800	0.825	0.850	0.875
Λ	0.6251	0.6413	0.6568	0.6717	0.6857	0.6988	0.7110	0.7223
λ	0.900		0.925	0.950		0.975	1	
Λ	0.7324		0.7413	0.7483		0.7546	0.7577	

This conversion is based on the use of a **functional relation** between the true speed ratio $\lambda = V/a^*$ of a compressible flow and the fictitious speed ratio $\Lambda = V_0/a^*$ at the corresponding points of the given and fictitious airfoils (Table 7.2.1). The method being considered makes it possible to *reconstruct* the given airfoil to the fictitious one.

As shown by Khristianovich, for prolate airfoils, the difference between the configurations of the given and fictitious airfoils may be disregarded. In this case, the **Khristianovich method** allows one to convert the parameters of the flow over an airfoil (pressure, velocity) to any number $M_\infty > 0$, i.e. to take account of compressibility, if the distribution of these parameters over the same airfoil is known for a low-speed flow when the influence of compressibility is absent ($M_\infty \approx 0$). In addition, this method allows us to convert the flow parameters from one number $M_{\infty 1} > 0$ to another one $M_{\infty 2} > 0$.

The Khristianovich method is suitable provided that the velocity is subsonic over the entire airfoil. This condition is satisfied if the Mach number of the oncoming flow is less than the **critical value** $M_{\infty, cr}$. Consequently, before performing calculations, one must find this critical value and determine the number $M_\infty < M_{\infty, cr}$ for which calculations are possible. The critical number $M_{\infty, cr}$ can also be found by the Khristianovich method.

Conversion of the Pressure Coefficient for an Incompressible Fluid to the Number $M_\infty > 0$

Assume that we know the distribution of the pressure coefficient over an airfoil in an incompressible flow, i.e. we know the form of the function $\bar{p}_{ic} = \bar{p}_{ic}(x)$ (Fig. 7.2.2). This function is converted to the number $M_{\infty, cr} > M_\infty > 0$ as follows.

We determine the speed ratio according to the given number $M_\infty > 0$:

$$\lambda_\infty = \left[\frac{k+1}{2} M_\infty^2 \left(1 + \frac{k-1}{2} M_\infty^2\right)^{-1}\right]^{1,2} \qquad (7.2.1)$$

From Table 7.2.1, we find the fictitious speed ratio Λ_∞ of an incompressible flow corresponding to the value λ_∞, and for the chosen value of $\bar{p}_{ic}$ from the Bernoulli equation

$$\bar{p}_{ic} = 1 - (\Lambda/\Lambda_\infty)^2 \qquad (7.2.2)$$

we determine the local fictitious speed ratio

$$\Lambda = \Lambda_\infty \sqrt{1 - \bar{p}_{ic}} \qquad (7.2.2')$$

Knowing Λ, we use Table 7.2.1 to find the local true speed ratio λ of the compressible flow, and we calculate the pressure p by formula (3.6.26) in which it is necessary to assume that $V^2/V_{max}^2 = [(k-1)/(k+1)]\,\lambda^2$. We determine the pressure coefficient by the

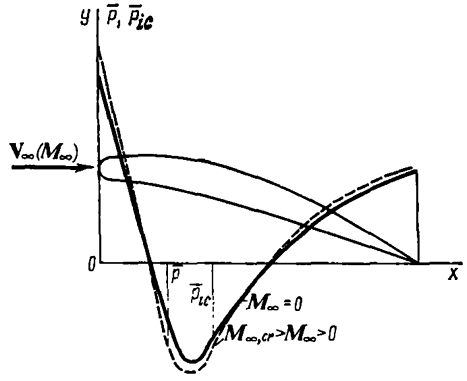

Fig. 7.2.2
Nature of the pressure distribution on one side of an airfoil at different values of M_∞

formula $\bar{p} = 2\,(p/p_\infty - 1)/(kM_\infty^2)$. The curve $\bar{p} = \bar{p}\,(x)$ converted to the given number M_∞ is shown by a dashed line in Fig. 7.2.2.

Conversion of the Pressure Coefficient from $M_{\infty 1} > 0$ to $M_{\infty 2} > 0$

Assume that we know the distribution of the pressure coefficient of a compressible fluid $\bar{p}_1 = \bar{p}_1\,(x)$ at a certain number $M_{\infty 1}$ (where $M_{\infty,cr} > M_{\infty 1} > 0$). To convert this distribution to the number $M_{\infty 2} > 0$, it is necessary to first calculate the speed ratios $\lambda_{\infty 1}$ and $\lambda_{\infty 2}$ corresponding to the numbers $M_{\infty 1}$ and $M_{\infty 2}$ by formula (7.2.1) and use Table 7.2.1 to find the speed ratios $\Lambda_{\infty 1}$ and $\Lambda_{\infty 2}$ of the fictitious incompressible flow.

After assigning a value to the pressure coefficient $\bar{p}_1$, from the formula $\bar{p}_1 = 2\,(p_1 - p_\infty)/(kM_{\infty 1}p_{\infty 1})$ we find the absolute pressure:

$$p_1 = p_{\infty 1}\,[\bar{p}_1\,(kM_{\infty 1}^2/2) + 1] \tag{7.2.3}$$

and evaluate the local speed ratio of the given flow:

$$\lambda_1 = \left\{\frac{k+1}{k-1}\left[1 - \left(\frac{p_1}{p_0}\right)^{(k-1)/k}\right]\right\}^{1/2} \tag{7.2.4}$$

From Table 7.2.1 according to the value of λ_1, we find the local speed ratio of the fictitious incompressible flow, and from the Bernoulli equation (7.2.2), we calculate the corresponding pressure coefficient:

$$\bar{p}_{ic} = 1 - (\Lambda_1/\Lambda_{\infty 1})^2$$

The pressure coefficient $\bar{p}_2$ for the number $M_{\infty 2}$ is determined according to this value of $\bar{p}_{ic}$ in the same way as the pressure coefficient of an incompressible flow is converted to the number $M_\infty > 0$ according to the procedure set out previously.

Determination of the Critical Number M

According to Khristianovich's hypothesis, *a local sonic velocity, which the critical Mach number $M_{\infty, cr}$ of the oncoming flow corresponds to, appears near an airfoil where the maximum rarefaction is observed in an incompressible flow.* Khristianovich established the relation between the minimum coefficient $\bar{p}_{ic, min}$ corresponding to this maximum rarefaction and the number $M_{\infty, cr}$.

Hence, to find the critical Mach number, it is necessary in some way or other, for example, by blowing air over a model in a low-speed wind tunnel, to determine the magnitude of the maximum rarefaction $\bar{p}_{ic, min}$. If as a result we find the distribution of the pressure with account taken of the compressibility for $M_{\infty, cr} > M_{\infty} > 0$, we can determine the value of $\bar{p}_{ic, min}$ by the conversion of $\bar{p}_{ic, min}$ to the number $M_{\infty} = 0$.

Assume that we know the value of the maximum rarefaction $\bar{p}_{ic, min}$. Since $\lambda = 1$ where a sonic velocity appears, from Table 7.2.1 we can find the corresponding value of the local speed ratio of the fictitious incompressible flow, i.e. $\Lambda = 0.7577$. Using the Bernoulli equation $\bar{p}_{ic, min} = 1 - (\Lambda/\Lambda_{\infty})^2$ we can find the speed ratio for the fictitious oncoming flow:

$$\Lambda_{\infty} = \Lambda \Big/ \sqrt{1 - \bar{p}_{ic, min}} = 0.7577 \Big/ \sqrt{1 - \bar{p}_{ic, min}} \qquad (7.2.5)$$

while using Table 7.2.1 and the value of Λ_{∞}, we can determine the critical speed ratio $\lambda_{\infty, cr}$ of the compressible flow. The corresponding critical Mach number is

$$M_{\infty, cr} = \lambda_{\infty, cr} \left(\frac{k+1}{2} - \frac{k-1}{2} \lambda^2_{\infty, cr} \right)^{-1/2} \qquad (7.2.6)$$

A plot of the critical Mach number versus $\bar{p}_{ic, min}$ constructed according to the results of the above calculation is shown in Fig. 7.2.3.

An increase in the airfoil thickness is attended by a decrease in the number $M_{\infty, cr}$. The explanation is that such an increase leads to contraction of the stream filament and to an increase in the local flow velocity. Consequently, sonic velocity on a thickened airfoil is achieved at a lower free-stream velocity, i.e. at a lower value of $M_{\infty} = M_{\infty, cr}$. This conclusion follows directly from Fig. 7.2.3 in accordance with which at an increased local velocity lower values of $M_{\infty, cr}$ correspond to a lower value of the coefficient $\bar{p}_{ic, min}$. Upon an increase in the angle of attack, the number $M_{\infty, cr}$ diminishes, which is also explained by the greater contraction of the stream filaments and by the associated increase in the local subsonic velocity.

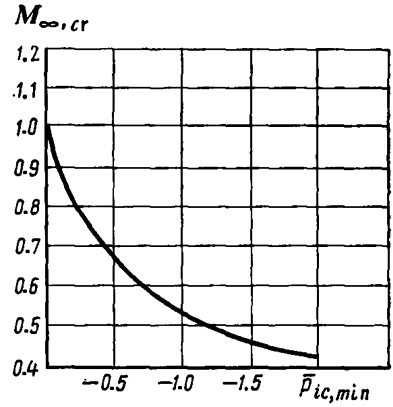

Fig. 7.2.3
A Khristianovich curve for determining the critical Mach number

Aerodynamic Coefficients

Khristianovich's investigations made it possible to obtain more accurate relations for the lift and moment coefficients than relations (7.1.14) found on the basis of the Prandtl-Glauert formula for the pressure coefficient. These relations are as follows:

$$c_{y_a} = c_{y,\,ic} L / \sqrt{1 - M_\infty^2}; \quad m_{z_a} = m_{z_a ic} L^2 / \sqrt{1 - M_\infty^2} \qquad (7.2.7)$$

where

$$L = 1 + 0.05 M_\infty^2 / M_{\infty,\,cr}^2$$

Compressibility changes the position of the centre of pressure of an airfoil (the coordinate x_p of this centre is measured from the leading edge along the chord). It follows from (7.2.7) that in a compressible flow, the coefficient of the centre of pressure is

$$c_p = c_{p,\,ic} L \qquad (7.2.8)$$

where

$$c_p = x_p / b = -m_{z_a} / c_{y_a}, \quad c_{p,\,ic} = -m_{z_a ic} / c_{y_a ic}$$

Examination of (7.2.8) reveals that the centre of pressure in a compressible flow in comparison with an incompressible one is displaced toward the trailing edge. This is explained by the increase in the aerodynamic load on the tail sections of an airfoil at increased flow speeds and, as a consequence, by the appearance of an additional stabilizing effect.

7.3. Flow at Supercritical Velocity over an Airfoil ($M_\infty > M_{\infty,\,cr}$)

Subsonic flow over an airfoil can be characterized by two cases. In the first one, the local velocity of the flow on a surface does not exceed the speed of sound anywhere. This case is **purely subsonic**

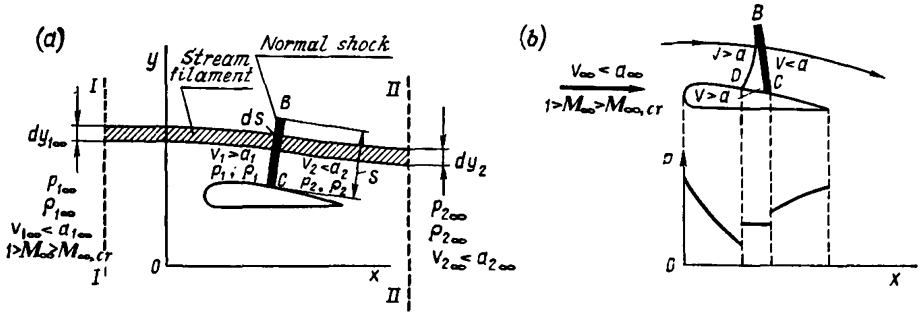

Fig. 7.3.1
Subsonic flow over an airfoil at a supercritical velocity:
a—diagram of the flow used for calculations when a local normal shock is present; *b*—distribution of the pressure over the airfoil when a local λ-shaped shock forms

flow. It is general knowledge that at such a velocity, no shocks can form at any point on an airfoil, while the lift force and drag are determined with a view to the compressibility and in the general case depend on the normal pressure and skin friction forces. Such a drag, including that produced by the normal stress (pressure) and the friction drag is called the **profile drag.**

In the second case, called **supercritical flow**, at which the number M of the oncoming flow is larger than the critical one, i.e. $M_\infty > M_{\infty, cr}$, the local velocity at some points in the vicinity of an airfoil becomes higher than the speed of sound, and a zone of local **supersonic velocities** appears. Here the flow over an airfoil is characterized by the fact that both behind it and ahead of the leading edge the local velocity is lower than the speed of sound. Hence, local compression shocks form in the transition from supersonic velocities to subsonic ones in the vicinity of the wing (Fig. 7.3.1). Such λ-shaped shocks consist, as it were, of two shocks: a front curved (oblique) one *DB* and a rear almost straight one *CB* (Fig. 7.3.1*b*).

Local shocks that may form on both the upper and bottom sides of an airfoil substantially change the distribution of the pressure and lead to the appearance of an additional wave drag X_w. Hence. the total drag of an airfoil X_a consists of the profile X_{pr} and the wave X_w drags, i.e. $X_a = X_{pr} + X_w$, or $c_{x_a} = c_{x, pr} + c_{x, w}$, where c_{x_a} is the total drag coefficient of the airfoil, $c_{x, pr}$ and $c_{x, w}$ are the profile and wave drag coefficients, respectively.

Let us consider a simple method of calculating wave drag proposed by Prof. G. Burago [16]. Let us assume that a local supersonic zone closed by nearly normal shock *BC* is formed on the upper side of an airfoil (Fig. 7.3.1*a*). Let us separate a stream filament passing through this shock in the flow. The parameters of the gas in the filament directly ahead of the shock are V_1, p_1, ρ_1, and M_1, and behind it are

V_2, p_2, ρ_2, and M_2. Let us introduce two control surfaces *I-I* and *II-II* to the left and right of the airfoil at a sufficiently large distance from it; let the parameters of the gas along the left plane be $V_{1\infty}$, $p_{1\infty}$, and $\rho_{1\infty}$, and along the right plane be $V_{2\infty}$, $p_{2\infty}$, and $\rho_{2\infty}$.

Using the theorem of the change in the momentum of the mass of a gas when flowing through the control surfaces, we obtain

$$\int_{-\infty}^{\infty} V_{2\infty}\, dm_{2\infty} - \int_{-\infty}^{\infty} V_{1\infty}\, dm_{1\infty} = \int_{-\infty}^{\infty} (p_{1\infty} - p_{2\infty})\, dy - X_w \qquad (7.3.1)$$

where $p_{1\infty}$ and $p_{2\infty}$ are the forces acting on the left and right surfaces, X_w is the force of the wave drag with which the airfoil acts on the flow, and $dm_{1\infty} = \rho_{1\infty} V_{1\infty}\, dy_{1\infty}$, $dm_{2\infty} = \rho_{2\infty} V_{2\infty}\, dy_{2\infty}$ are the rates of flow of the gas along the stream filaments that according to the condition of the constancy of the flow rate are equal, i.e.

$$\rho_{1\infty} V_{1\infty}\, dy_{1\infty} = \rho_{2\infty} V_{2\infty}\, dy_{2\infty} \qquad (7.3.2)$$

Let us assume (see [16]) that levelling out of the velocities occurs behind the wing at a large distance from it, i.e. $V_{2\infty} \to V_{1\infty}$. Accordingly, and by (7.3.2), we have

$$\int_{-\infty}^{\infty} V_{2\infty}\, dm_{2\infty} - \int_{-\infty}^{\infty} V_{1\infty}\, dm_{1\infty} = \int_{-\infty}^{\infty} \rho_{1\infty} V_{1\infty} (V_{2\infty} - V_{1\infty})\, dy_{1\infty} = 0$$

Consequently,

$$X_w = \int_{-\infty}^{\infty} (p_{1\infty} - p_{2\infty})\, dy \qquad (7.3.3)$$

We can assume that for stream filaments not intersecting the shock, $p_{2\infty} = p_{1\infty}$ i.e. the pressure at a large distance from the airfoil behind it is restored to the value of the free-stream pressure. For the filaments that pass through the shock, $p_{2\infty} < p_{1\infty}$. Indeed, since

$$\left.\begin{aligned} p_{1\infty} &= p_0 (1 - V_{1\infty}^2/V_{\max}^2)^{k/(k-1)} \\ p_{2\infty} &= p_0' (1 - V_{2\infty}^2/V_{\max}^2)^{k/(k-1)} = p_0' (1 - V_{1\infty}^2/V_{\max}^2)^{k/(k-1)} \end{aligned}\right\} \qquad (7.3.4)$$

where $p_0' < p_0$, we have

$$p_{2\infty}/p_{1\infty} = p_0'/p_0 = \nu_0 < 1 \qquad (7.3.5)$$

According to (7.3.5), formula (7.3.3) can be transformed by taking into account the flow rate equation $\rho_{1\infty} V_{1\infty}\, dy_{1\infty} = \rho_1 V_1\, ds$, in accordance with which

$$dy_{1\infty} = dy = (\rho_1 V_1/\rho_{1\infty} V_{1\infty})\, ds$$

where s is the length of the shock.

As a result of transformations, the wave drag force is

$$X_w = p_{1\infty} \int_0^S \frac{\rho_1 V_1}{\rho_{1\infty} V_{1\infty}} (1 - v_0)\, ds \qquad (7.3.6)$$

and the coefficient of this force is

$$c_{x,w} = \frac{2X_w}{kp_\infty M_\infty^2 b} = \frac{2}{kM_\infty^2 b} \int_0^s \frac{\rho_1 V_1}{\rho_{1\infty} V_{1\infty}} (1 - v_0)\, ds \qquad (7.3.6')$$

Let us expand the function v_0 in (4.3.20) into a series in powers of $n = M_1 - 1$:

$$v_0(n) = v_0(0) + \left(\frac{dv_0}{dn}\right)_{n=0} n + \frac{1}{2}\left(\frac{d^2v_0}{dn^2}\right)_{n=0} n^2 + \frac{1}{6}\left(\frac{d^3v_0}{dn^3}\right)_{n=0} n^3 + \ldots \qquad (7.3.7)$$

In expression (7.3.7), the quantity $v_0(0) = 1$ because at $M_1 = 1$ ($n = 0$), the shock transforms into a wave of an infinitesimal strength, and the pressure $p_0' = p_0$.

Using (4.3.13), (4.3.15), and (4.3.20), we can also show that

$$\left(\frac{dv_0}{dn}\right)_{n=0} = \left(\frac{dv_0}{DM_1}\right)_{M_1=1} = 0 \text{ and } \left(\frac{d^2v_0}{dn^2}\right)_{n=0} = \left(\frac{d^2v_0}{dM_1^2}\right)_{M_1=1} = 0$$

Having in view that for thin airfoils at small angles of attack, the difference $M_1 - 1$ is small, we can limit ourselves to the fourth term in expansion (7.3.7):

$$v_0(n) = 1 + \frac{1}{6}\left(\frac{d^3v_0}{dM_1^3}\right)_{M_1=1} (M_1 - 1)^2 \qquad (7.3.7')$$

Investigations have shown that for a given airfoil, the quantity $M_1 - 1$ can be considered approximately proportional to the difference $M_\infty - M_{\infty,cr}$. Designating the relevant proportionality factor by A_1 and including it in the overall coefficient A determined in the form

$$A = -\frac{A_1}{3kM_\infty^2 b}\left(\frac{d^3v_0}{dM_1^3}\right)_{M_1=1} \int_0^s \frac{\rho_1 V_1}{\rho_{1\infty} V_{1\infty}}\, ds \qquad (7.3.8)$$

we obtain an expression from (7.3.6') and (7.3.7') for the wave drag coefficient:

$$c_{x,w} = A\,(M_\infty - M_{\infty,cr})^3 \qquad (7.3.9)$$

The coefficient A in the general case depends on the configuration of the airfoil, the angle of attack, and the number M_∞. It may be considered as approximately constant, however. Tests of modern airfoils installed at small angles of attack in wind tunnels show that

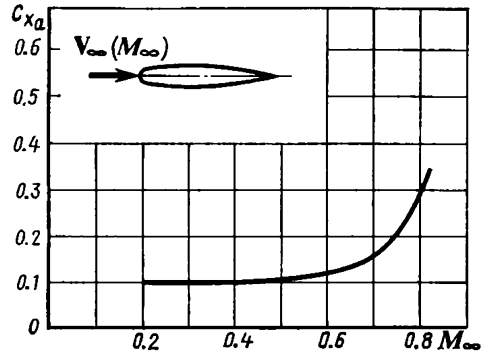

Fig. 7.3.2
Drag of an airfoil in a nearly sonic flow

the coefficient $A \approx 11$. At this value, satisfactory results of calculations by formula (7.3.9) are obtained if the difference $M_\infty - M_{\infty, cr}$ does not exceed 0.15.

It follows from formula (7.3.9) that the wave drag coefficient increases with increasing M_∞. This is due to the fact that upon a growth in the airspeed, the shocks formed on an airfoil become more and more intensive and extended. To lower $c_{x, w}$ at a given M_∞, one must ensure an increase in the number $M_{\infty, cr}$, which is achieved mainly by reducing the thickness of the airfoil. A similar result can be obtained when the angle of attack is made smaller.

Figure 7.3.2 shows an experimental curve characterizing the change in the drag coefficient $c_{x_a} = c_{x, pr} + c_{x, w}$ in nearly sonic flow. For values of $M_\infty < 0.45$ -0.5, only profile drag is observed, while at $M_\infty > 0.5$-0.55 (supercritical flow velocities) a wave drag also appears that is due to local shocks.

7.4. Supersonic Flow of a Gas with Constant Specific Heats over a Thin Plate

Let us consider a very simple airfoil in the form of an infinitely thin plate placed in a supersonic flow at the angle of attack α. The flow over such a plate is shown schematically in Fig. 7.4.1. At its leading edge, the supersonic flow divides into two parts—an upper one (above the plate) and a bottom one (under it) that do not influence each other. This is why the supersonic flow over each side can be investigated independently.

Let us consider the upper side of the plate. The flow here is a plane supersonic flow over a surface forming an angle larger than 180° with the direction of the undisturbed flow. Such a flow is shown schematically in Fig. 7.4.2, where plane OC corresponds to the upper

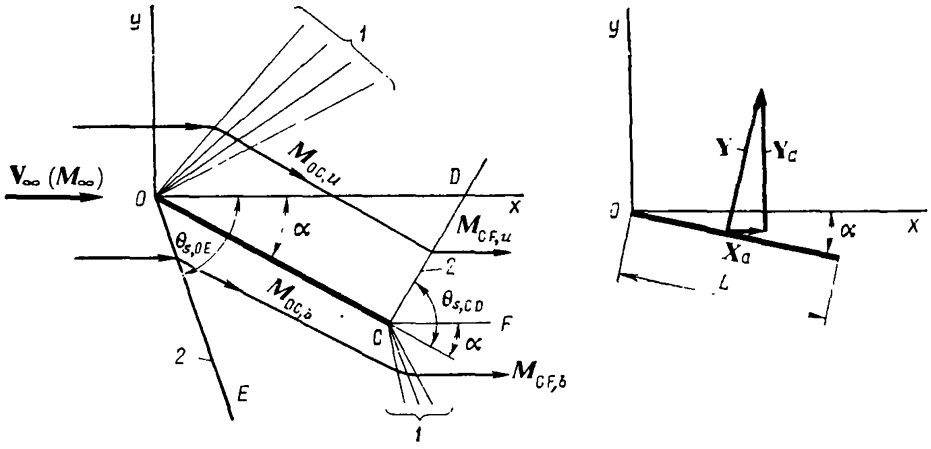

Fig. 7.4.1
Supersonic flow over a thin plate:
1—expansion fan; *2*—shock

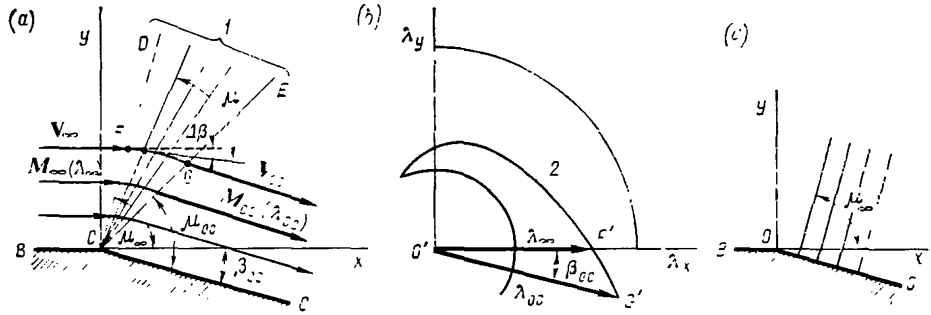

Fig. 7.4.2
Prandtl-Meyer flow:
a—physical plane; *b*—hodograph plane; *c*—diagram of a nearly uniform flow; *1*—expansion fan; *2*—epicycloid

side of the plate. It was first investigated by L. Prandtl and T. Meyer and is called a **Prandtl-Meyer flow.**

In accordance with the flow diagram in Fig. 7.4.2*a*, the flow parallel to plane *OB* when passing around angle *O* gradually turns, expands, and acquires a new direction parallel to plane *OC*. The angle β_{OC} of inclination of this plane to the vector $\mathbf{V}_\infty$ corresponds to the angle of attack α of the plate (see Fig. 7.4.1). The disturbed region of the expanding flow is limited at the left-hand side by Mach line *OD* inclined to the free-stream velocity vector $\mathbf{V}_\infty$ at the angle $\mu_\infty = \sin^{-1}(1/M_\infty)$, where M_∞ is the Mach number of the undisturbed flow. The expansion process terminates on Mach line *OE* inclined to

the disturbed velocity vector V_{OC} at the angle $\mu_{OC} = \sin^{-1}(1/M_{OC})$ determined from the Mach number o the disturbed flow along plane OC. The change in the direction of the flow between Mach lines OD and OE can be represented as a consecutive set of deflections of the streamlines through the small angles $\Delta\beta$. A straight Mach line issuing from point O corresponds to each of these deflections indicating the formation of an additional disturbance.

Hence, the turning flow is filled with an infinite multitude of Mach lines forming a "fan" of disturbance lines that characterizes a **centered expansion wave**. This centered wave, sometimes called a **Prandtl-Meyer fan**, is defined by straight Mach lines along each of which the flow parameters are constant, and this is why it belongs to the class of simple expansion waves.

The problem on the disturbed motion of a gas near an obtuse angle, which is associated with the formation of a centered expansion wave, can be solved according to the method of characteristics. Point F' on an epicycloid—a characteristic in a hodograph of the same family—corresponds to point F of intersection of a streamline belonging to the plane parallel oncoming flow (the inclination of a streamline at this point is $\beta = 0$) with characteristic OD in a physical plane. To be specific, we can relate each of these characteristics to those of the first family. The equation $\beta = \omega + \beta_1$ is used for a characteristic of this family in the hodograph. Since we have assumed that $\beta = 0$, the constant $\beta_1 = -\omega_\infty (M_\infty)$, where the angle ω_∞ is found from (5.3.30) according to the known number M_∞. Consequently, the equation for the characteristic has the form $\beta = \omega - \omega_\infty$, whence

$$\omega = \beta + \omega_\infty \tag{7.4.1}$$

By setting the inclination of a streamline on the small angle $\beta = \Delta\beta$, we can calculate the corresponding angle $\omega = \Delta\beta + \omega_\infty$ and find the number M on the neighbouring Mach line inclined to the new direction of a streamline at the angle $\mu = \sin^{-1}(1/M)$. The Mach number on plane OC with an inclination of $\beta = \beta_{OC} = \alpha$, i.e. *on the upper* side of the plate, is determined according to the angle

$$\omega_{OC} = \beta_{OC} + \omega_\infty \tag{7.4.2}$$

The found value of the local number M_{OC} makes it possible to determine the Mach angle $\mu_{OC} = \sin^{-1}(1/M_{OC})$. A graphical solution of the problem on the Prandtl-Meyer flow is shown in Fig. 7.4.2*b*. The coordinate of point G' of intersection of the epicycloid with straight line $O'G'$ parallel to plane OC determines the speed ratio λ_{OC} of the disturbed flow near plane OC. The point G of intersection of a streamline with characteristic OE corresponds to point G' in a physical plane.

According to the known number M_{OC} (λ_{OC}), by using formula (3.6.30), we can determine the pressure on the upper side of the plate:

$$p_u = p_{OC,\,u} = p_\infty \left[\left(1 + \frac{k-1}{2} M_\infty^2\right) \Big/ \left(1 + \frac{k-1}{2} M_{OC}^2\right) \right]^{k/(k-1)} \qquad (7.4.3)$$

and the corresponding value of the pressure coefficient:

$$\bar{p}_u = \bar{p}_{OC,\,u} = 2\,(p_{OC,\,u} - p_\infty)/(kM_\infty^2 p_\infty)$$

At hypersonic velocities ($M_\infty \gg 1$), the calculation of the Prandtl-Meyer flow is simplified, because to determine the function ω we can use formula (5.3.41). This allows us to determine the local number M directly. Substituting for the angles ω_{OC} and ω_∞ in (7.4.2) their values in accordance with (5.3.41), we obtain

$$M_u = M_{OC} = \left(\frac{1}{M_\infty} - \frac{k-1}{2}\beta_{OC}\right)^{-1} \qquad (7.4.4)$$

The corresponding pressure can be determined by formula (3.6.39).

Let us consider the Prandtl-Meyer flow appearing at hypersonic velocities with small flow deflections $\beta_{OC} = \alpha$. At very large numbers M_∞, the beam of Mach lines issuing from point O will be very narrow. We can consider to a sufficiently good approximation that the beam is compressed into a single line on which the flow immediately turns, with expansion. This line can therefore be conditionally considered as an "expansion shock" behind which the velocities (Mach numbers) grow and the pressures lower. The angle μ'_{OC} of inclination of this line to the vector V_∞ is obtained if we take advantage of the analogy with a compression shock and calculate this angle by formula (4.6.9) provided that the angle $\beta_s = \beta_{OC} = \alpha$ in this formula is negative. Assuming that $\theta_s = \mu'_{OC}$, we find

$$\frac{\mu'_{OC}}{|\beta_{OC}|} = \frac{1}{2(1-\delta)} + \sqrt{\frac{1}{4(1-\delta)^2} + \frac{1}{K^2}} \qquad (7.4.5)$$

where $|\beta_{OC}| = |\alpha|$ is the magnitude of the turning angle of the flow (the angle of attack), and $K^2 = (M_\infty \beta_{OC})^2$.

By using formula (4.6.11′) to evaluate the pressure coefficient with a view to the sign of the angle $\beta_{OC} = \alpha$, we obtain

$$\frac{\bar{p}_u}{\alpha^2} = \frac{\bar{p}_{OC,\,u}}{\alpha^2} = \frac{1}{1-\delta} - \sqrt{\frac{1}{(1-\delta)^2} + \frac{4}{K^2}} \qquad (7.4.6)$$

At low numbers M_∞ and small angles $\beta_{OC} = \alpha$, a nearly uniform Prandtl-Meyer flow appears near the deflected surface. For such a flow, relation (7.1.2′) for the speed of sound holds. If we now find a formula for the Mach number from (7.1.2), namely,

$$M^2 = \frac{V^2}{a^2} = \frac{2}{k-1}\left(\frac{a_\infty^2}{a^2} - 1\right) + \frac{V_\infty^2}{a^2}$$

and introduce the value of a^2 from (7.1.2′) into this formula, we obtain

$$\frac{V^2}{a^2} = M^2 = M_\infty^2 \left(1 + \frac{2u}{V_\infty}\right) \left[1 - (k-1)\frac{uV_\infty}{a_\infty^2}\right]^{-1} \qquad (7.4.7)$$

In accordance with this expression, we can assume in a first approximation that in a nearly uniform flow $M \approx M_\infty$ and, consequently, the equation $dy/dx = \tan(\beta \pm \mu_\infty)$ is used for the characteristics in a physical plane. Since the flow deflection angle β is small and $\beta \ll \mu_\infty$, then $dy/dx \approx \pm \tan \mu_\infty$. Consequently, the characteristics are Mach lines inclined to the x-axis at angles of $\pm\mu_\infty$. For a Prandtl-Meyer flow, we have a family of characteristics in the form of parallel lines inclined to the horizontal axis at the angle μ_∞ (Fig. 7.4.2c).

We obtain difference equations for the characteristics in the hodograph of a supersonic flow from (5.3.21) and (5.3.22):

$$\Delta V/V \mp \tan \mu \Delta\beta = 0 \qquad (7.4.8)$$

For a nearly uniform flow, we have

$$\Delta V = u, \quad V = V_\infty, \quad \Delta\beta = \beta, \quad \tan \mu = \tan \mu_\infty = (M_\infty^2 - 1)^{-1/2}$$

Consequently,

$$u/V_\infty = \pm\beta/\sqrt{M_\infty^2 - 1} \qquad (7.4.8')$$

Inserting the value of u from (7.4.8′) into (6.1.5), we obtain the pressure coefficient

$$\bar{p} = \mp 2\beta/\sqrt{M_\infty^2 - 1} \qquad (7.4.9)$$

Since we are considering an expanding flow for which $\bar{p} < 0$ and are having in view that the magnitude of the angle β is being found, we must take the minus sign in formula (7.4.9). Accordingly, *on the upper* side of the plate inclined at a small angle of attack $\beta = \alpha$, the pressure coefficient is

$$\bar{p}_u = \bar{p}_{OC,u} = -2\alpha/\sqrt{M_\infty^2 - 1} \qquad (7.4.10)$$

Let us consider the *bottom* side of the plate. The flow over this side (see Fig. 7.4.1) is attended by the formation of shock OE issuing from a point on the leading edge and, consequently, by compression of the flow. To determine the angle $\theta_{s,OE}$ of inclination of the shock, we should use formula (4.3.25) in which we must assume that $M_1 = M_\infty$ and $\beta_s = \alpha$. According to the found value of $\theta_{s,OE}$, we find the Mach number $M_2 = M_{OC,b}$ on the bottom side by (4.3.19) or (4.3.19′).

When determining the nature of the flow in the region behind point C on the trailing edge, we can proceed from the following considerations. On the upper side of the plate, the number $M_{OC,u}$ ahead of shock CD is larger than the number M_∞ ahead of shock OE

formed on the leading edge from below. If we assume that behind point C the flow does not deflect from the direction of the undisturbed flow (streamline CF is parallel to the vector $\mathbf{V}_\infty$), the losses in the upper shock will evidently be greater, and therefore $M_{CF,u} < M_{CF,b}$. The pressure in the region above line CF will be greater than in that below it.

A pressure jump cannot be retained on a boundary surface in a gas flow, although the velocities may remain different. Therefore, in real conditions, the direction of streamline CF differs from that of the free-stream velocity, i.e. a downwash of the flow forms behind the plate. It is clear from physical notions that line CF deviates in the direction of the bottom region. Here turning of the flow behind shock CD through a smaller angle is ensured, which is just what leads to lowering of the pressure.

Investigations show that the downwash angle is small, hence to a sufficiently good approximation we can proceed from the assumption that at point C the direction of the flow coincides with that of the free stream. Accordingly, the shock angle $\theta_{s,CD}$ on the upper side is determined by formula (4.3.25) in which we assume that $M_1 = M_{OC,u}$ and $\beta_s = \alpha$. The corresponding Mach number behind the shock $M_2 = M_{CF,u}$ is determined from (4.3.19) or (4.3.19′) according to the values of $\theta_s = \theta_{s,CD}$, $M_1 = M_{OC,u}$, and $\beta_s = \alpha$.

Below line CF in the region behind the trailing edge, a Prandtl-Meyer flow appears with the Mach number $M_{CF,b}$ determined with the aid of the formula $\omega_{CF,b} = \omega_{OC,b} + \alpha$.

The pressure $p_u = p_{OC,u}$ on the upper side of the plate is determined by formula (7.4.3), while the corresponding pressure $p_b = p_{OC,b}$ on the bottom side is calculated by expression (4.3.15) in which it is assumed that $p_2 = p_b$, $p_1 = p_\infty$, $\theta_s = \theta_{s,OE}$, and $p_u < p_\infty < p_b$.

If the length of the plate is L, and its width is taken equal to unity, the force produced by the normal pressure applied to the plate is $Y = L(p_b - p_u)$. Consequently, the lift force is $Y_a = Y \cos \alpha$, while the drag is $X_a = Y \sin \alpha$. The corresponding values of the lift and drag coefficients are $c_{y_a} = Y/(q_\infty L)$ and $c_{x_a} = X_a/(q_\infty L)$. Introducing the pressure coefficients $\bar{p}_u = (p_u - p_\infty)/q_\infty$ for the upper and $\bar{p}_b = (p_b - p_\infty)/q_\infty$ for the lower sides, respectively, we obtain the following expressions for the aerodynamic coefficients:

$$c_{y_a} = (\bar{p}_b - \bar{p}_u)\cos\alpha, \quad c_{x_a} = (\bar{p}_b - \bar{p}_u)\sin\alpha \qquad (7.4.11)$$

The force X_a appearing upon supersonic flow over the plate and caused by the formation of shock waves and ordinary disturbance waves is called the **wave drag**, and the corresponding quantity $c_{x_a} = c_{xw}$ is called the **wave drag coefficient**. This drag does not equal zero even in an ideal (inviscid) fluid.

The fineness of the plate $K = c_{y_a}/c_{x_a} = \cot \alpha$ can be seen to be a function of only the angle of attack. Owing to the uniform distribution of the pressure over the surface of the plate, the centre of pressure is at its middle. Consequently, the moment of the pressure forces about the leading edge is $M_z = -YL/2$, and the corresponding moment coefficient is

$$m_z = m_{z_a} = M_z/(q_\infty L^2) = -(\bar{p}_b - \bar{p}_u)/2 \qquad (7.4.12)$$

At hypersonic velocities, the pressure coefficient for the upper side of the plate is determined approximately by (7.4.6), and for its lower side, by (4.6.12). With this in view and assuming in (4.6.12) that $\beta_s = \alpha$, we obtain for the difference of the pressure coefficients $\bar{p}_b - \bar{p}_u$, also known as the **pressure-drop coefficient**, the expression

$$(\bar{p}_b - \bar{p}_u)/\alpha^2 = 4\sqrt{1/[4(1-\delta)^2] + 1/K^2} \qquad (7.4.13)$$

Consequently,

$$c_{y_a}/\alpha^2 = 4\sqrt{1/[4(1-\delta)^2] + 1/K^2} \qquad (7.4.14)$$

$$c_{x_a}/\alpha^3 = 4\sqrt{1/[4(1-\delta)^2] + 1/K^2} \qquad (7.4.15)$$

$$m_{z_a}/\alpha^2 = -2\sqrt{1/[4(1-\delta)^2] + 1/K^2} \qquad (7.4.16)$$

Formulas (7.4.13)-(7.4.16) express the law of hypersonic similarity as applied to the flow over a thin plate. This law consists in that regardless of the values of M_∞ and α, but at identical values of $K = M_\infty \alpha$, the corresponding quantities $\bar{p}/\alpha^2$, c_{y_a}/α^2, c_{x_a}/α^3, and m_{z_a}/α^2 for plates are identical. The parameter $K = M_\infty \alpha$ is called the **hypersonic similarity criterion.**

Examination of formulas (7.4.13)-(7.4.16) reveals that the relations for the pressure, lift, and moment coefficients are quadratic, and for the drag coefficients—cubic functions of the angle of attack α. At the limit, when $K \to \infty$, we have

$$(\bar{p}_b - \bar{p}_u)/\alpha^2 = c_{y_a}/\alpha^2 = c_{x_a}/\alpha^3 = 2/(1-\delta) \qquad (7.4.17)$$

$$m_{z_a}/\alpha^2 = -1/(1-\delta) \qquad (7.4.18)$$

For a plate in a nearly uniform (linearized) flow, the pressure coefficients are calculated by formula (7.4.9) in which we should assume that $\beta = \alpha$. The minus sign in this formula determines the pressure coefficient for the upper side, and the plus sign—for the bottom side. Accordingly, the difference between the pressure coefficients related to the angle of attack is

$$(\bar{p}_b - \bar{p}_u)/\alpha = 4/\sqrt{M_\infty^2 - 1} \qquad (7.4.19)$$

Introducing (7.4.19) into formulas (7.4.11) and (7.4.12), we obtain

$$c_{y_a}/\alpha = 4/\sqrt{M_\infty^2 - 1} \tag{7.4.20}$$

$$c_{x_a}/\alpha^2 = 4/\sqrt{M_\infty^2 - 1} \tag{7.4.21}$$

$$m_{z_a}/\alpha = -2/\sqrt{M_\infty^2 - 1} \tag{7.4.22}$$

In the given case, the number M_∞ is the similarity criterion. When its value is retained, and regardless of the value of the angle of attack, the corresponding values of $\bar{p}/\alpha$, c_{y_a}/α, c_{x_a}/α^2, and m_{z_a}/α are identical. If we consider a nearly uniform flow at very large numbers $M_\infty \gg 1$, formulas similar to (7.4.19)-(7.4.22) can be written in the form

$$(\bar{p}_b - \bar{p}_u)/\alpha^2 = c_{y_a}/\alpha^2 = c_{x_a}/\alpha^3 = 4/K \tag{7.4.23}$$

$$m_{z_a}/\alpha^2 = -2/K \tag{7.4.24}$$

Hence, the hypersonic similarity criterion $K = M_\infty \alpha$ is also valid for a nearly uniform (linearized) flow with large Mach numbers. It is evident that such a flow can appear only at very small angles of attack.

7.5. Parameters of a Supersonic Flow over an Airfoil with an Arbitrary Configuration

Use of the Method of Characteristics

Let us consider a supersonic flow over a sharp-nosed airfoil with an arbitrary configuration (Fig. 7.5.1). The upper contour of the airfoil is given by the equation $y_u = f_u(x)$, and the bottom one by the equation $y_b = f_b(x)$. Assume that the angle of attack is larger than the angle $\beta_{0,u}$ formed by a tangent to the airfoil contour on its upper side at point O on the leading edge. Consequently, a Prandtl-Meyer flow develops at this point. The flow passes through an *expansion fan* issuing from point O as from a source of disturbances, and acquires a direction tangent to the contour at this point. Further expansion of the flow occurs behind point O along the contour. Consequently, the flow near the airfoil can be considered as a *consecutive set of Prandtl-Meyer flows.* Since the turning angle at the points on the contour is infinitely small, individual Mach lines issue from them instead of a fan of expansion lines (Fig. 7.5.1).

We find the velocity at point O by formula (7.4.2), which we shall write in the form

$$\omega_0 = \omega_\infty + \alpha - \beta_{0,u} \tag{7.5.1}$$

where $\beta_{0,u} = \tan^{-1}(dy_u/dx)_0$.

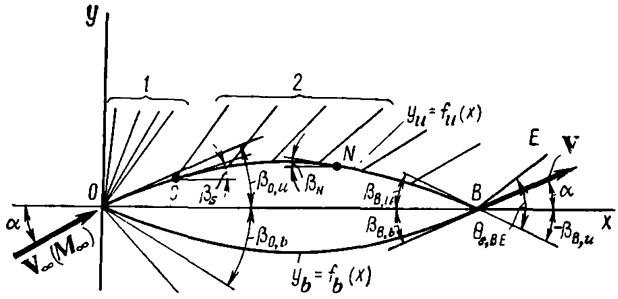

Fig. 7.5.1
Supersonic flow over a sharp-nosed airfoil:
1—expansion fan; *2*—Mach lines

Using the value of ω_O, we determine the corresponding number M_0 from Table 5.3.1. At point C, which is at a small distance from the nose, the velocity of the gas is calculated as for a Prandtl-Meyer flow by the formula

$$\omega_C = \omega_O + \beta_{O,u} - \beta_C \tag{7.5.2}$$

where $\beta_C = \tan^{-1}(dy_u/dx)_C$.

Inserting Eq. (7.5.1) into (7.5.2), we obtain

$$\omega_C = \omega_\infty + \alpha - \beta_C \tag{7.5.3}$$

Hence, by (7.5.3) for any arbitrary point N on the contour, we have

$$\omega_N = \omega_\infty + \alpha - \beta_N \tag{7.5.4}$$

where $\beta_N = \tan^{-1}(dy_u/dx)_N$ is the angle calculated with a view to the sign (for the leading part of the contour the signs of the angles are positive, and for the trailing part, negative).

Let us assume, as for flow over a flat plate, that the flow behind point B approximately retains the direction of the free stream. Therefore, at point B, the flow moving near the contour at a velocity corresponding to the number $M_{B,u}$ turns, and a shock BE appears issuing from point B. The angle $\theta_{s,BE}$ of inclination of the shock and the parameters behind it are calculated with the aid of the relevant formulas of the shock theory according to the known values of the angle of attack α, the number $M_{B,u}$, and the contour nose angle at point B on the upper side. The parameters on the upper side of the airfoil (pressure, velocity, etc.) are determined from the known value of the local Mach number with the aid of the relations for an isentropic flow of a gas.

If the angle of attack equals the angle $\beta_{O,u}$, we have the *limiting case* of a Prandtl-Meyer flow at point O where the Mach number is $M_{O,b} = M_\infty$. Formula (7.5.4) can be written as

$$\omega_N = \omega_\infty + \beta_{O,u} - \beta_N \tag{7.5.4'}$$

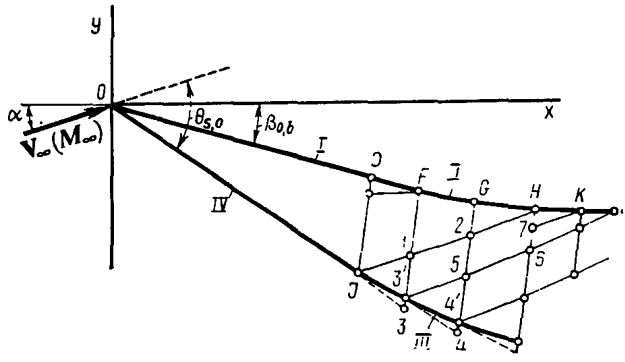

Fig. 7.5.2

Supersonic flow over the bottom side of an airfoil with the formation of a shock: *I*—straight part of the contour of the airfoil in the flow; *II*—curved part of the airfoil contour; *III*—curved part of the shock; *IV*—straight part of the shock

Calculation of the flow over the bottom side of the airfoil (Fig. 7.5.2) begins with determination of the gas parameters at point O—directly behind the shock. For this purpose, using formula (4.3.25) and the values $M_1 = M_\infty$ and $\beta_C = \alpha + \beta_{O,b}$, we calculate the shock angle $\theta_{s.O}$. We find the number $M_{O,b} = M_2$ at point O from (4.3.19) or (4.3.19'). We may assume that this number remains constant within a very small neighbourhood of point O on straight line element OD of the contour. Straight element OJ of an oblique shock corresponds to OD. Its length is determined as the distance from point O to point J that is on the intersection of the shock with a first family characteristic issuing from point D.

The flow behind a straight shock is *vortex-free*, consequently there is an isentropic flow over part of the contour behind point D. To determine the velocity of such a flow at point F, we shall use Eq. (7.4.1), from which we find $\omega_F = \omega_D - (\beta_D - \beta_F)$, where ω_D is the value of the angle ω calculated by formula (5.3.30) for the number M on part OD of the contour. The values of the angles β_D and β_F are determined with a view to the sign (in the given case the angles β_D and β_F are negative on the leading part of the contour).

The flow near part DF of the contour can be considered as a Prandtl-Meyer flow, therefore disturbance line *F-1-3* issues from point F as from a perturbation source. It intersects the continuation of the normal shock at point *3* and curves it, as a result of which the actual direction of the shock is determined by point *3* of intersection of the shock and the characteristic.

Downstream, curving of the shock is due to its interaction with the characteristics issuing from points G, H, K, etc. Curving of the shock causes a *vortex flow* to form for whose calculation we must use relations on the characteristics for a non-isentropic plane flow. The

second family characteristic JH is the boundary of this vortex flow. The characteristic is gradually constructed in the form of a broken line according to the known values of the number M and the angles β along the straight second family characteristics issuing from contour points F, G, etc. At point H of the contour, which is simultaneously on characteristic JH, the velocity is found from the expression $\omega_H = \omega_D - (\beta_D - \beta_H)$. At point K adjacent to H, the parameters are calculated according to the equations for the characteristics taking into account the vortex nature of the flow behind a shock. To determine the velocity at this point, it is sufficient to know the velocity and its direction (the angle β) at point *7* near point K on element *7-K* of the second family characteristic. To find this velocity, it is necessary to calculate the curving of the shock behind point J on element *J-3'* and find the parameters on the shock at point *3'*. To do this, we have the following data at our disposal: the number $M = M_1 = M_F$ and the angle $\beta = \beta_F$ of deflection of the flow at point *1*, and also the parameters $M_2 = M_J$ and $\beta_s = \beta_{s,J}$ on the shock at point J. By using formula (5.4.46) and assuming that $\varepsilon = 0$, we obtain the following expression for the change in the angle β along characteristic *1-3*:

$$\Delta\beta_1 = \left[\left(\frac{d\omega}{d\beta}\right)_J - 1\right]^{-1}\left(\omega_1 - \omega_J - \frac{\Delta x_1}{kR}\cdot\frac{\Delta S}{\Delta n}c_1\right) \qquad (7.5.5)$$

where $\Delta\beta_1 = \beta_3 - \beta_1$, $\Delta x_1 = x_3 - x_1$;

$$\frac{\Delta S}{\Delta n} = \frac{(S_3 - S_1)\cos(\beta_1 + \mu_1)}{(x_3 - x_1)\sin\mu_1}, \quad c_1 = \frac{\sin^2\mu_1\cos\mu_1}{\cos(\beta_1 + \mu_1)}$$

The derivative $(d\omega/d\beta)_J$ is evaluated by (5.4.39) for the values of the relevant parameters at point *1*; the angles ω_1 and ω_J are determined from (5.3.30) according to the numbers M at points *1* and J, respectively.

Point *3* in Fig. 7.5.2 is at the intersection of the normal shock and characteristic *1-3*. Consequently, its coordinates are found as a result of the simultaneous solution of the equations

$$y_3 - y_1 = (x_3 - x_1)\tan(\beta_1 + \mu_1), \quad y_3 = x_3\tan(\theta_{s,O} - \alpha) \qquad (7.5.6)$$

The intersection of the characteristic with the shock at point *3'* is different because of *curving* of the shock. We shall find the new shock angle $\theta_{s,J3'}$ on *J-3'* according to the flow deflection angle behind the shock $\beta_s = \beta_{3'} = \Delta\beta_1 + \beta_1$ and the number M_3' calculated by means of the expression $\omega_3' = \Delta\omega_1 + \omega_1$ in which $\Delta\omega_1$ is found from (5.4.38):

$$\Delta\omega_1 = \omega_J + (d\omega/d\beta)_J\,\Delta\beta_1 - \omega_1 \qquad (7.5.7)$$

Consequently, the equation of the shock element *J-3'* has the form

$$y_{3'} - y_J = (x_{3'} - x_J)\tan(\theta_{s,J3'} - \alpha)$$

Owing to deflection of the flow at point 3′, the characteristic on element 1-3′ changes its direction. The equation of the characteristic on this element has the form

$$y_{3'} - y_1 = (x_{3'} - x_1) \tan (\beta_{3'} + \mu_{3'})$$

By solving these two equations simultaneously, we find the coordinates $x_{3'}$ and $y_{3'}$ of point *3′*.

Let us consider point *5* at the intersection of characteristic elements *2-5* of the first and *3′-5* of the second family. We determine the coordinates y_5 and x_5 of this point from the solution of the equations for the elements of the corresponding characteristics:

$$\left.\begin{aligned} y_5 - y_2 &= (x_5 - x_2) \tan (\beta_2 + \mu_2) \\ y_5 - y_{3'} &= (x_5 - x_{3'}) \tan (\beta_{3'} - \mu_{3'}) \end{aligned}\right\} \qquad (7.5.8)$$

We determine the change in the direction of the flow when passing from point *2* to point *5* along characteristic element *2-5* from Eq. (5.4.22) in which we assume that $\varepsilon = 0$:

$$\Delta\beta_2 = \frac{1}{2}\left[\frac{1}{kR} \cdot \frac{\Delta S}{\Delta n} (\Delta x_{3'} t_{3'} + \Delta x_2 c_2) - (\omega_2 - \omega_{3'}) - (\beta_2 - \beta_{3'})\right] \qquad (7.5.9)$$

where $\Delta\beta_2 = \beta_5 - \beta_2$; $\Delta x_{3'} = x_5 - x_{3'}$;

$$\frac{\Delta S}{\Delta n} = \frac{(S_{3'} - S_2) \cos (\beta_2 + \mu_2) \cos (\beta_{3'} - \mu_{3'})}{f + e}$$

we assume that

$$f = (x_5 - x_2) \sin \mu_{3'} \cos (\beta_2 + \mu_2);$$

$$e = (x_5 - x_{3'}) \sin \mu_2 \cos (\beta_{3'} - \mu_{3'})$$

We determine the values of c_2 and $t_{3'}$ by (5.4.15). We find the number M at point *5* from (5.4.23) using $\Delta\beta_2$. Similarly, according to the known values of the gas parameters at point *5* and at point *H* on the wall, we determine the velocity at point *6* at the intersection of the characteristic elements *H-6* of the first family and *5-6* of the second one. We find the coordinates x_H and y_H of point *H* by solving the equations of the contour $y_H = f_H(x_H)$ and of element *2-H* of the characteristic $y_H - y_2 = (x_H - x_2) \tan (\beta_2 - \mu_2)$.

Let us now choose arbitrary point *7* with the coordinates x_7 and y_7 on characteristic element *H-6*. We shall determine the parameters at this point by interpolation. For example, the angle $\beta_7 = \beta_6 - (\beta_6 - \beta_H)\, l_{6-7}/l_{6-H}$, where l_{6-7} and l_{6-H} are the distances from point 6 to point 7 and to point *H*, respectively. Similarly, we can find the number M_7 and the corresponding Mach angle μ_7. We choose point *7* so that characteristic element *7-K* drawn from this point at the angle β_7-μ_7 will intersect the contour at point *K* at a small distance from point *H*. We determine the coordinates x_K, y_K of this

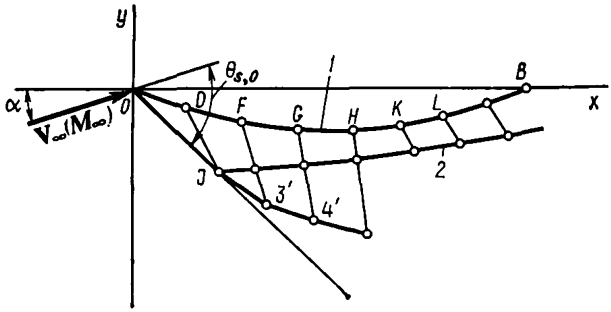

Fig. 7.5.3
Supersonic isentropic flow over a curved sharp-nosed airfoil:
1—contour of the body in the flow; *2*—second family characteristic

point as a result of solving the equation $y_K - y_7 = (x_K - x_7) \times \times \tan(\beta_7 - \mu_7)$ for the characteristic element 7-K and the equation $y_K = f_H(x_K)$ of the contour. Since the flow at point K is a vortex one, Eq. (5.4.27) must be used to calculate the velocity at this point. Assuming in the equation that $\varepsilon = 0$, we obtain

$$\Delta\omega_7 = -\Delta\beta_7 - \frac{\Delta x_7}{kR} \cdot \frac{\Delta S}{\Delta n} t_7 \qquad (7.5.10)$$

where $\Delta\omega_7 = \omega_K - \omega_7$ and $\Delta\beta_7 = \beta_K - \beta_7$, the angle $\beta_K = \tan^{-1}(dy_H/dx)_K$. We determine the parameter t_7 from (5.4.28) for the values μ_7 and β_7 and evaluate the entropy gradient by the formula (5.4.29):

$$\Delta S/\Delta n = (S_7 - S_K)\cos(\beta_7 - \mu_7)/[(x_K - x_7)\sin\mu_7]$$

We find the entropy S_K at point K as a result of calculating its value at point O directly behind the shock, and the entropy S_7 at point 7 by interpolation between its values at points H and 6.

Similarly, by consecutively solving each of the three problems considered in Sec. 5.4, we determine the velocity field in the region between characteristic DJ, the contour, and curved shock J-3'-4'. We find the shape of this shock gradually in the form of a broken line, and fill the indicated region of the flow with a **network of characteristic curves (characteristics).**

We can determine the pressure at the nodes of the network of characteristics according to the Mach number with the aid of formula (3.6.28). We calculate the corresponding stagnation pressure $p_O = p_0'$ needed in this formula by interpolation, using formula (5.4.19). We find the pressure at points on the contour using the corresponding Mach numbers and the stagnation pressure $p_O = p_0'$ evaluated by (4.3.22) for the angle $\theta_{s,O}$ and the number M_∞.

Calculation of the flow on the bottom side of an airfoil is simplified when a second family characteristic drawn from point J *does not intersect the contour*, and, consequently, this flow can be considered as an isentropic one (Fig. 7.5.3). We use Eq. (5.3.38) to calculate the Mach number at arbitrary point L of the contour:

$$\omega_{\text{L}} = \omega_{\text{D}} - (\beta_{\text{D}} - \beta_{\text{L}}) \qquad (7.5.11)$$

Here we determine the angle β_{L} by the formula $\beta_{\text{L}} = \tan^{-1}(dy_{\text{H}}/dx)_{\text{L}}$ with a view to the sign: at the leading edge of the contour it is negative, at the trailing edge, positive, the angle β_{D} is negative. We determine the shape of the shock by its angles θ_{s} at points 3′ and 4′ at the intersection of the straight characteristics drawn from points F and G. We find the shock angle θ_{s} at point 3′ approximately by formula (4.3.25), using the values of $\beta_{3'} = \beta_{\text{F}}$ and M_∞. We calculate the shock angle at point 4′ in a similar way.

We have considered the calculation of the flow at such angles of attack $\alpha \geqslant \beta_{\text{O, u}}$ when there is an expanding flow all over the upper side. If this condition is not observed ($\alpha < \beta_{\text{O, u}}$), the flow over the upper contour occurs with compression of the gas at the leading edge and the *formation of a compression shock*. Hence, such a flow should be calculated in the same way as for the bottom surface.

Hypersonic Flow over a Thin Airfoil

If a thin sharp-nosed airfoil (see Fig. 7.5.1) is in a hypersonic flow at such small angles of attack that the local Mach numbers on its upper and bottom surfaces at all points considerably exceed unity and, in addition, the conditions of isentropic flow over the bottom contour (Fig. 7.5.3) are retained, we can use simplified relations for the characteristics to calculate the disturbance velocity.

If the angle of attack $\alpha \geqslant \beta_{\text{O, u}}$, to determine the number M at an arbitrary point N on the upper contour, we must use the formula

$$M_{\text{N}} = \left[\frac{1}{M_\infty} - \frac{k-1}{2}(\alpha - \beta_N)\right]^{-1} \qquad (7.5.12)$$

obtained from (7.4.4).

Since everywhere on the upper contour there is an *expanding flow*, the number $M_{\text{N}} > M_\infty$.

Flow over the bottom surface is attended by the formation of a shock and, therefore, by *compression of the gas*. We calculate the pressure coefficient at point O directly behind the shock with the aid of formula (4.6.12) as follows:

$$\bar{p}_{\text{b}}/(\alpha - \beta_{\text{O, b}})^2 = 1/(1-\delta) + \sqrt{1/(1-\delta)^2 + 4/K^2} \qquad (7.5.13)$$

where $K = M_\infty(\alpha - \beta_{\text{O,b}})$; we take the angle $\beta_{\text{O,b}}$ with a minus sign.

From the formula $\bar{p}_b = 2\theta_{s,O}(\alpha - \beta_{O,b})$, we can calculate the shock angle $\theta_{s,O}$, and then using the value of $K_s = M_\infty\theta_{s,O}$ we can find the Mach number at point O, using formula (4.6.16):

$$M^2_{O,b}/M^2_\infty = K_s^2/\{[(1+\delta)K_s^2 - \delta](1 - \delta + \delta K_s^2)\} \quad (7.5.14)$$

Behind point O, expansion of the flow occurs, therefore to determine the velocity at an arbitrary point L, we can use the relation

$$M_L = \left[\frac{1}{M_{O,b}} + \frac{k-1}{2}(\beta_{O,b} - \beta_L)\right]^{-1} \quad (7.5.15)$$

Hypersonic flow over a thin airfoil can be calculated approximately by using the **method of tangent wedges**. According to this method, we calculate the flow at an arbitrary point of a contour by the relevant formulas for a flat plate assuming that the latter is in a flow with the number M_∞ at an angle of attack equal to the angle between the vector V_∞ and a tangent to the contour at the point being considered. Hence, for a point N on the upper side, the pressure coefficient by (7.4.6) is

$$\bar{p}_N/(\alpha - \beta_N)^2 = 1/(1-\delta) - \sqrt{1/(1-\delta)^2 + 4/K_N^2} \quad (7.5.16)$$

where $K_N = M_\infty(\alpha - \beta_N)$.

For an arbitrary point L on the bottom side, with a view to (7.5.13), we have

$$\bar{p}_L/(\alpha - \beta_L)^2 = 1/(1-\delta) + \sqrt{1/(1-\delta)^2 + 4/K_L^2} \quad (7.5.17)$$

where $K_L = M_\infty(\alpha - \beta_L)$.

In formula (7.5.16), the angle β_N has a plus sign at the leading edge of the contour and a minus sign at the trailing edge, whereas in formula (7.5.17) the angle β_L has a minus sign at the leading edge and a plus sign at the trailing one.

At the limit, when $K \to \infty$, we have

$$\bar{p}_N = 0 \quad (7.5.18)$$

$$\bar{p}_L = 2(\alpha - \beta_L)^2/(1-\delta) \quad (7.5.19)$$

With a zero angle of attack, formulas (7.5.16), (7.5.17), and (7.5.19) acquire the following form:

$$\bar{p}_N/\beta_N^2 = 1/(1-\delta) - \sqrt{1/(1-\delta)^2 + 4/K_N^2} \quad (7.5.16')$$

$$\bar{p}_L/\beta_L^2 = 1/(1-\delta) + \sqrt{1/(1-\delta)^2 + 4K_L^2} \quad (7.5.17')$$

$$\bar{p}_L = 2\beta_L^2/(1-\delta) \quad (7.5.19')$$

In formulas (7.5.16') and (7.5.17'), $K_N = M_\infty\beta_N$ and $K_L = M_\infty\beta_L$

Nearly Uniform Flow over a Thin Airfoil

At this case, we consider a flow over a thin airfoil at small angles of attack. This flow is featured by shocks of a finite intensity being absent and by the characteristics on the upper and bottom sides being *straight lines* with an angle of inclination of $\mu_\infty = \sin^{-1}(1/M_\infty)$.

To determine the pressure coefficient for the airfoil, we shall use Eq. (7.4.9). According to this equation, for an arbitrary point N *on the upper* side of the airfoil

$$\bar{p}_N = -2(\alpha - \beta_N)/\sqrt{M_\infty^2 - 1} \qquad (7.5.20)$$

and for a point L *on the bottom* side

$$\bar{p}_L = 2(\alpha - \beta_L)/\sqrt{M_\infty^2 - 1} \qquad (7.5.20')$$

For a zero angle of attack

$$\bar{p}_N = 2\beta_N/\sqrt{M_\infty^2 - 1}, \quad \bar{p}_L = -2\beta_L/\sqrt{M_\infty^2 - 1} \qquad (7.5.20'')$$

An increase in the small angles of attack leads to a growth in the error when calculating the pressure on a thin airfoil in a nearly uniform flow. The accuracy of these calculations can be increased by using the *second-order aerodynamic theory*. According to the latter, the pressure coefficient is

$$\bar{p} = \pm c_1\theta + c_2\theta^2 \qquad (7.5.21)$$

where

$$c_1 = 2(M_\infty^2 - 1)^{-1/2}, \quad c_2 = 0.5\,(M_\infty^2 - 1)^{-2}\,[(M_\infty^2 - 2)^2 + kM_\infty^4] \qquad (7.5.22)$$

The plus sign in (7.5.21) relates to the bottom side of the plate ($\bar{p}_L$; $\theta = \alpha - \beta_L$), and the minus sign, to the upper one ($\bar{p}_N$; $\theta = \alpha - \beta_N$).

Aerodynamic Forces and Their Coefficients

To determine the aerodynamic pressure forces, we shall use formulas (1.3.2) and (1.3.3), relating them to the body axes x, y (see Fig. 7.5.1) and assuming that $c_{f,x} = 0$. In this condition, formula (1.3.2) determines the longitudinal force X for an airfoil, and (1.3.3), the normal force Y produced by the pressure:

$$X = q_\infty S_r \int_{(S)} \bar{p} \cos(\widehat{n, x}) \frac{dS}{S_r}, \quad Y = -q_\infty S_r \int_{(S)} \bar{p} \cos(\widehat{n, y}) \frac{dS}{S_r}$$

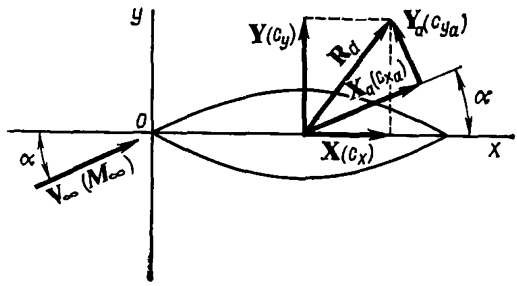

Fig. 7.5.4
Aerodynamic forces for an airfoil in a body axis and flight path coordinate systems

Adopting the quantity $S_r = b \times 1$ as the characteristic area and taking into account that $dS = dl \times 1$ (b is the chord of the airfoil, and dl is an arc element of the contour), we obtain the following expressions for the aerodynamic coefficients:

$$c_x = X/(q_\infty S_r) = \oint \bar{p} \cos(\widehat{n, x})\, d\bar{l},$$

$$c_y = Y/(q_\infty S_r) = -\oint \bar{p} \cos(\widehat{n, y})\, d\bar{l}$$

where $d\bar{l} = dl/b$, while the curvilinear integrals are taken along the contour of the airfoil (counterclockwise circumvention of the contour is usually taken as positive).

Let us introduce into this expression $d\bar{l} = d\bar{x}/\sin(\widehat{n, x})$, $\cos(\widehat{n, y})\, d\bar{l} = d\bar{x}$, where $d\bar{x} = dx/b$.

Next passing over from curvilinear integrals to ordinary ones, we obtain

$$c_x = -\int_0^1 \bar{p}_b \left(\frac{dy}{dx}\right)_b d\bar{x} + \int_0^1 \bar{p}_u \left(\frac{dy}{dx}\right)_u d\bar{x} \qquad (7.5.23)$$

$$c_y = \int_0^1 (\bar{p}_b - \bar{p}_u)\, d\bar{x} \qquad (7.5.24)$$

where $\bar{p}_b$ and $\bar{p}_u$ are the pressure coefficients for the bottom and upper sides of the airfoil, respectively.

Using the formula for conversion [see formula (1.2.3) and Table 1.2.1], we obtain the aerodynamic coefficients in a wind (flight path) coordinate system (Fig. 7.5.4):

$$c_{x_a} = c_x \cos\alpha + c_y \sin\alpha, \quad c_{y_a} = c_y \cos\alpha - c_x \sin\alpha \qquad (7.5.25)$$

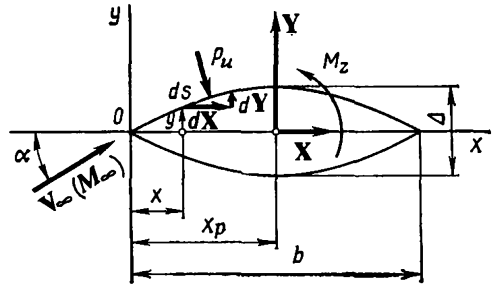

Fig. 7.5.5
Determination of the moment of the forces for an airfoil

With flight angles of attack not exceeding the values of $\alpha \approx 10\text{-}12$, we have

$$c_{x_a} = c_x + c_y\alpha, \quad c_{y_a} \approx c_y \tag{7.5.25'}$$

For the coefficient of the moment about the leading edge of the airfoil due to the pressure force (Fig. 7.5.5), by analogy with (1.3.6), we derive the formula

$$m_z = \frac{M_z}{q_\infty S_r b} = \frac{1}{q_\infty S_r b}\left(\int x\,dY - \int y\,dX\right)$$

$$= \frac{1}{b}\left\{\int_{(S)} \bar{p}x\cos(\widehat{n, y})\frac{dS}{S_r} - \int_{(S)} \bar{p}y\cos(\widehat{n, x})\frac{dS}{S_r}\right\}$$

or

$$m_z = \frac{M_z}{q_\infty b^2} = -\int_0^1 (\bar{p}_b - \bar{p}_u)\,\bar{x}\,d\bar{x} - \int_0^1 \left[\bar{p}_b\bar{y}_b\left(\frac{dy}{dx}\right)_b - \bar{p}_u\bar{y}_u\left(\frac{dy}{dx}\right)_u\right] d\bar{x} \tag{7.5.26}$$

where $\bar{y}_b = y_b/b$ and $\bar{y}_u = y_u/b$.

We determine the coefficient of the centre of pressure for the condition that the point of application of the resultant of the aerodynamic forces is on the chord of the airfoil. If its coordinate is x_p, we have

$$c_p = \frac{x_p}{b} = -\frac{m_z}{c_y} = \frac{\int_0^1 (\bar{p}_b - \bar{p}_u)\,\bar{x}\,d\bar{x} + \int_0^1 \left[\bar{p}_b\bar{y}_b\left(\frac{dy}{dx}\right)_b - \bar{p}_u\bar{y}_u\left(\frac{dy}{dx}\right)_u\right] d\bar{x}}{\int_0^1 (\bar{p}_b - \bar{p}_u)\,d\bar{x}} \tag{7.5.27}$$

For thin airfoils, we may disregard the second integral on the right-hand side of (7.5.26) and in the numerator of (7.5.27). Accord-

ingly,

$$m_z = -\int_0^1 (\bar{p}_b - \bar{p}_u)\,\bar{x}\,d\bar{x} \qquad (7.5.26')$$

$$c_p = \int_0^1 (\bar{p}_b - \bar{p}_u)\,\bar{x}\,d\bar{x}\left[\int_0^1 (\bar{p}_b - \bar{p}_u)\,d\bar{x}\right]^{-1} \qquad (7.5.27')$$

By comparing the first and second terms on the right-hand side of (7.5.26), we can estimate the order of the discarded infinitesimals. It is determined by the value of $\int_0^1 \bar{y}\,(d\bar{y}/d\bar{x})\,d\bar{x} \approx \bar{\Delta}^2$, where $\bar{\Delta} = \Delta/b$ is the relative thickness of the airfoil.

Using relation (7.5.21), we obtain the longitudinal-force coefficient (7.5.23) corresponding to the second-order aerodynamic theory:

$$c_x = c_1 K_1 + 2c_2 K_2 \alpha \qquad (7.5.28)$$

where

$$K_1 = \int_0^1 (\beta_b^2 + \beta_u^2)\,d\bar{x}, \quad K_2 = \int_0^1 (\beta_b^2 - \beta_u^2)\,d\bar{x} \qquad (7.5.29)$$

The normal force coefficient in accordance with (7.5.24) is

$$c_y = 2c_1\alpha + c_2 K_2 \qquad (7.5.30)$$

According to the results obtained, the drag and lift coefficients are

$$c_{x_a} = 2c_1\alpha^2 + 3c_2 K_2 \alpha + c_1 K_1, \quad c_{y_a} = 2c_1\alpha + c_2 K_2 \qquad (7.5.31)$$

In the particular case of a symmetric airfoil, $\beta_b^2 = \beta_u^2 = \beta^2 = (dy/dx)^2$ and, consequently, $K_1 = 2\int_0^1 \beta^2\,dx$ and $K_2 = 0$. Accordingly,

$$c_{x_a} = 2c_1\alpha^2 + 2c_1 \int_0^1 \beta^2\,d\bar{x}, \quad c_{y_a} = 2c_1\alpha \qquad (7.5.31')$$

From these two relations, we find

$$c_{x_a} = \frac{c_y^2}{2c_1} + 2c_1 \int_0^1 \beta^2\,d\bar{x} \qquad (7.5.32)$$

Equation (7.5.32) determines the relation between the drag and lift coefficients—what is called the polar of an airfoil.

We find the coefficient of the longitudinal moment about the leading edge by inserting (7.5.21) into (7.5.26′):

$$m_z = c_1 A_1 - c_2 B_2 + (2c_2 A_2 - c_1)\,\alpha \qquad (7.5.33)$$

where

$$A_1 = \int_0^1 (\beta_b + \beta_u)\,\bar{x}\,d\bar{x}; \quad A_2 = \int_0^1 (\beta_b - \beta_u)\,\bar{x}\,d\bar{x} \qquad (7.5.34)$$

$$B_2 = \int_0^1 (\beta_b^2 - \beta_u^2)\,\bar{x}\,d\bar{x} \qquad (7.5.35)$$

For a symmetric airfoil, $\beta_u = -\beta_u = \beta$, therefore $A_1 = B_2 = 0$; $A_2 = 2\int_0^1 \beta\bar{x}\,d\bar{x}$. Accordingly,

$$m_z = \left(4c_2 \int_0^1 \beta\bar{x}\,d\bar{x} - c_1\right)\alpha \qquad (7.5.33')$$

The coefficient of the centre of pressure, by (7.5.27′), is

$$c_p = -[c_1 A_1 - c_2 B_2 + (2c_2 A_2 - c_1)\,\alpha]/(2c_1\alpha + c_2 K_2) \qquad (7.5.36)$$

For a symmetric airfoil

$$c_p = 0.5\left(1 - 4\,\frac{c_2}{c_1}\int_0^1 \beta\bar{x}\,d\bar{x}\right) \qquad (7.5.36')$$

For a linearized flow (low supersonic velocities), the coefficient c_2 should be taken equal to zero in the above relations.

With *hypersonic velocities* of a thin airfoil, formulas (7.4.6) and (4.6.12) can be used to calculate the pressure coefficients in (7.5.23), (7.5.24), (7.5.26′)and(7.5.27′). The pressure coefficient for the bottom side in accordance with (4.6.12) is

$$\bar{p}_b = (\alpha - \beta_b)^2\,[1/(1-\delta) + \sqrt{1/(1-\delta)^2 + 4/K_b^2}] \qquad (7.5.37)$$

while for the upper side, the value of this coefficient by (7.4.6) is

$$\bar{p}_u = (\alpha - \beta_u)^2\,[1/(1-\delta) - \sqrt{1/(1-\delta)^2 + 4/K_u^2}] \qquad (7.5.38)$$

where $K_b = M_\infty(\alpha - \beta_b)$ and $K_u = M_\infty(\alpha - \beta_u)$.

Let us find the relations for the aerodynamic coefficients of a wedge-shaped airfoil (Fig. 7.5.6). Since for the bottom contour we have $(dy/dx)_b = \tan\beta_b$, and for the upper one $(dy/dx)_u = \tan\beta_u$, and taking into account that the pressure coefficients $\bar{p}_b$ and $\bar{p}_u$

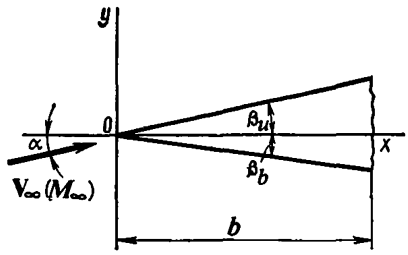

Fig. 7.5.6
Wedge-shaped airfoil

are constant, we obtain from (7.5.23) and (7.5.24):

$$c_x = -\bar{p}_b \tan \beta_b + \bar{p}_u \tan \beta_u \tag{7.5.39}$$

$$c_y = \bar{p}_b - \bar{p}_u \tag{7.5.40}$$

The angle β_b should be considered negative in formula (7.5.39). We find the moment coefficient from (7.5.26):

$$m_z = -0.5\,(\bar{p}_b - \bar{p}_u) - 0.5\,(\bar{p}_b \tan^2 \beta_b - \bar{p}_u \tan^2 \beta_u) \tag{7.5.41}$$

while the coefficient of the centre of pressure by (7.5.27) is

$$c_p = 0.5\,[1 + (\bar{p}_b \tan^2 \beta_b - \bar{p}_u \tan^2 \beta_u)/(\bar{p}_b - \bar{p}_u)] \tag{7.5.42}$$

For a symmetric airfoil, we have

$$\left.\begin{aligned} c_x = (\bar{p}_b + \bar{p}_u) \tan \beta, \quad c_y = \bar{p}_b - \bar{p}_u \\ m_z = -0.5\,(\bar{p}_b - \bar{p}_u)(1 + \tan^2 \beta), \quad c_p = 0.5\,(1 + \tan^2 \beta) \end{aligned}\right\} \tag{7.5.43}$$

In the above relations, the pressure coefficient $\bar{p}_b$ is determined by accurate relations obtained in the theory of an oblique shock. We also use this theory to find the pressure coefficient $\bar{p}_u$ for $\alpha < \beta_u$. For $\alpha > \beta_u$, the finding of $\bar{p}_u$ is associated with calculation of the Prandtl-Meyer flow on the upper side of the airfoil.

The relations obtained for the aerodynamic coefficients of the airfoil relate to arbitrary values of the nose angle (β_b, β_u) and the angle of attack. If these values are not large, the second-order theory can be used to calculate the coefficients. According to this theory, in formulas (7.5.31) for c_{x_a} and c_{y_a}, we must assume that

$$K_1 = \beta_b^2 + \beta_u^2, \quad K_2 = \beta_b^2 - \beta_u^2$$

When calculating the moment coefficients (7.5.33) and (7.5.36), we must proceed from the fact that

$$A_1 = 0.5\,(\beta_b + \beta_u), \quad A_2 = 0.5\,(\beta_b - \beta_u), \quad B_2 = 0.5\,(\beta_b^2 - \beta_u^2)$$

For a symmetric airfoil, we have

$$\left.\begin{aligned} c_{x_a} &= 2c_1(\alpha^2+\beta^2), \quad c_{y_a} = 2c_1\alpha \\ m_z &= (2c_2\beta - c_1)\alpha, \quad c_p = 0.5\left(1-2\frac{c_2}{c_1}\beta\right) \end{aligned}\right\} \qquad (7.5.44)$$

where the angle β is chosen with a minus sign (for the bottom side).

The use of formulas (7.5.37), (7.5.38) allows us to determine the aerodynamic coefficients (7.5.39)-(7.5.43) corresponding to hypersonic velocities of a thin airfoil at a small angle of attack.

7.6. Sideslipping Wing Airfoil

Definition of a Sideslipping Wing

Let us assume that an infinite-span rectangular wing performs longitudinal motion at the velocity $\mathbf{V}_1$ (normal to the leading edge) and lateral motion along the span at the velocity $\mathbf{V}_2$. The resultant velocity $\mathbf{V} = \mathbf{V}_1 + \mathbf{V}_2$ is directed toward the plane of symmetry of the wing at the sideslip angle β. A rectangular wing performing such motion is said to be a sideslipping one.

The flow over a sideslipping wing does not change if we consider inverted flow in which a rectangular wing encounters a stream of air at the velocity $-\mathbf{V}_1$ perpendicular to the leading edge, and a stream at the velocity $-\mathbf{V}_2$ in the direction of the wing span (Fig. 7.6.1).

The nature of the flow is the same if the resultant velocity $\mathbf{V}_\infty$ is parallel to the initial velocity $-\mathbf{V}_1$ (see Fig. 7.6.1) and the rectangular wing is turned through the angle $\varkappa = \beta$ (Fig. 7.6.2). Such a wing, which is also a sideslipping one, is usually called an **infinite-span swept wing**. The angle $\varkappa$ is determined as the sweep angle relative to the leading edge.

Let us consider some features of the flow over sideslipping wings. The flow about such wings can be divided into two flows: a **longitudinal** one (along the span of the wing) characterized by the velocity $V_{\tau\infty} = V_\infty \sin\varkappa$ parallel to the leading edge, and a **lateral** one depending on the magnitude of the normal velocity component to this edge $V_{n\infty} = V_\infty \cos\varkappa$.

The distribution of the velocities and pressures along the wing does not depend on the longitudinal flow, and is due only to the lateral flow at the velocity $V_{n\infty} = V_\infty \cos\varkappa$. The nature of this flow and, therefore, the pressure distribution change depending on the configuration of the airfoil in a plane normal to the leading edge, and on the angle of attack measured in this plane. Accordingly, the aerodynamic characteristics of the airfoil are the same as of a rectangular (unswept) wing airfoil in a flow with a free-stream velocity of $V_{n\infty}$ at the indicated angle of attack.

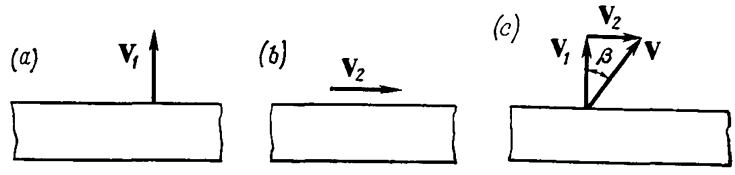

Fig. 7.6.1
Motion of a wing with sideslipping:
a—longitudinal motion of an infinite-span rectangular wing; *b*—lateral motion; *c*—resultant motion at the sideslip angle

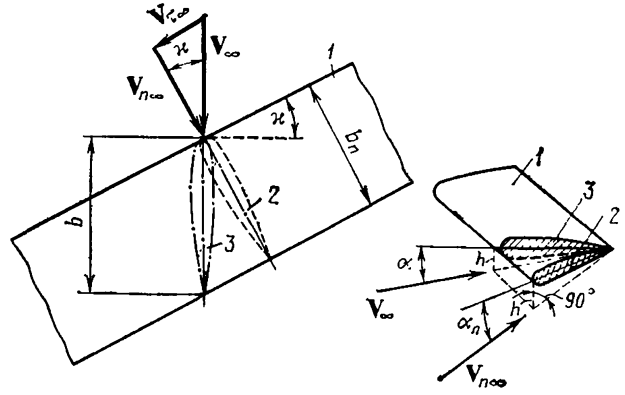

Fig. 7.6.2
Sideslipping wing:
1—wing surface; *2*—airfoil in a section along a normal; *3*—airfoil in a section along the flow

This is exactly the content of the **sideslip effect** which to a considerable extent determines the aerodynamic properties of finite-span swept wings. The term swept is conventionally applied to a wing in which the line connecting the aerodynamic centres (foci) of the airfoils (the aerodynamic centre line) makes with a normal to the longitudinal plane of symmetry the angle χ (the sweep angle).

In aerodynamic investigations, the sweep angle is often measured from another characteristic line, for example, from the leading or trailing edge (χ_1, χ_3), from lines connecting the ends of selected elements of a chord ($\chi_{1/4}$, $\chi_{1/2}$, . . .), from the lines of the maximum thickness of the airfoils, etc. (Fig. 7.6.3a).

If the leading edges are curved or have sharp bends, the sweep angle will be variable along the span.

The flow over swept wings in real conditions is distinguished by its very intricate nature, due primarily to the partial realization of the sideslip effect. Figure 7.6.3b shows a possible scheme of such flow over a swept finite-span wing with a sufficiently large aspect ratio.

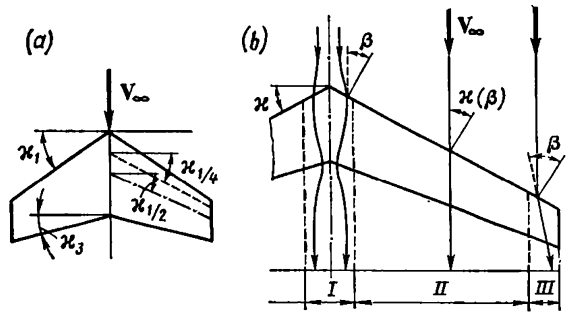

Fig. 7.6.3
Finite-span swept wing:
a—designation of the sweep angles; *b*—subsonic flow over a swept wing

The middle region of the wing (region *I*) is characterized by the mutual influence of neighbouring airfoils reducing the sweep (sideslip) angle. Here the **mid-span effect** appears that detracts from the aerodynamic properties because of the decrease in the sideslip effect. In region *III*, the **tip effect** acts. It is due to an appreciable deflection of the streamlines in comparison with a sideslipping wing. And only in region *II*, distinguished by a more uniform flow, is the curvature of the streamlines relatively small, and the sideslip angles β are close to the sweep angle χ. In aerodynamic investigations, this region of the wing can be represented in the "pure" form as a region of a swept (sideslipping) infinite-span wing arranged in the flow at the sweep angle. It will be shown in Chap. 8 that the conclusions relating to such wings of a small thickness can be used to calculate the flow over separate parts of swept finite-span wings at supersonic velocities.

Aerodynamic Characteristics of a Sideslipping Wing Airfoil

When determining such characteristics, a sideslipping wing is considered as a straight one turned through the sideslip angle χ. In this case, the airfoil of a sideslipping wing in a normal section will evidently be the same as that of a straight one.

The airfoil and the angle of attack in a plane normal to the leading edge differ from the airfoil and angle of attack in the section along the flow (see Fig. 7.6.2). The chord in a normal section b_n and the chord b along the flow are related by the expression $b_n = b \cos \chi$.

The angle of attack α_n in a normal section is determined from the expression

$$\sin \alpha_n = h/b_n = h/(b \cos \chi) = \sin \alpha/\cos \chi \qquad (7.6.1)$$

where α is the angle of attack in the plane of the flow. It is evident that at small angles of attack we have

$$\alpha_n = \alpha/\cos \varkappa \qquad (7.6.1')$$

If at a point on a wing airfoil in flow without sideslipping at the velocity V_∞ the pressure coefficient is $\bar{p}$, then when the wing is turned through the angle $\varkappa$ the pressure coefficient $\bar{p}_n$ at the corresponding point is the same, i.e.

$$2(p_n - p_\infty)/(\rho_\infty V_\infty^2 \cos^2 \varkappa) = 2(p - p_\infty)/(\rho_\infty V_\infty^2)$$

Accordingly, for the airfoil of a sideslipping wing, the pressure coefficient calculated from the velocity head $q_\infty = 0.5\rho_\infty V_\infty^2$ is

$$\bar{p}_\varkappa = 2(p_n - p_\infty)/(\rho_\infty V_\infty^2) = \bar{p} \cos^2 \varkappa \qquad (7.6.2)$$

With a view to (7.6.2) and in accordance with (7.5.23), (7.5.24), and (7.5.26), the aerodynamic coefficients for the airfoil of a thin sideslipping wing are

$$c_{x,\varkappa} = c_x \cos^2 \varkappa, \qquad c_{y,\varkappa} = c_y \cos^2 \varkappa, \quad m_{z,\varkappa} = m_z \cos^2 \varkappa \qquad (7.6.3)$$

Evidently, by (7.5.25'), we have

$$c'_{x_a \varkappa} = (c_x + c_y \alpha) \cos^2 \varkappa = c_{x_a} \cos^2 \varkappa$$

Since the drag force is determined not in the direction of the velocity component $V_\infty \cos \varkappa$, but in the direction of the free-stream velocity V_∞, the coefficient of this drag is

$$c_{x_a \varkappa} = c'_{x_a \varkappa} \cos \varkappa = c_{x_a} \cos^3 \varkappa \qquad (7.6.4)$$

All these coefficients are determined for a velocity head of $q_\infty = 0.5\rho_\infty V_\infty^2$. Inspection of formulas (7.6.3) for $c_{y,\varkappa}$ and $m_{z,\varkappa}$ reveals that the coefficient of the centre of pressure $c_p = -m_{z,\varkappa}/c_{y,\varkappa}$ corresponding to small angles of attack does not depend on the angle of attack, i.e. $c_p = -m_z/c_y$.

Compressible Flow. According to the linearized theory, the pressure coefficient for the airfoil of a sideslipping wing in a *subsonic compressible flow* can be obtained from the corresponding coefficient for the same wing in an incompressible fluid by the Prandtl-Glauert formula (7.1.14), substituting the number $M_\infty \cos \varkappa$ for M_∞ in it:

$$\bar{p}_\varkappa = \bar{p}_{\varkappa, ic}/\sqrt{1 - M_\infty^2 \cos^2 \varkappa} \qquad (7.6.5)$$

or, with a view to (7.6.2)

$$\bar{p}_\varkappa = \bar{p}_{ic} \cos^2 \varkappa/\sqrt{1 - M_\infty^2 \cos^2 \varkappa} \qquad (7.6.5')$$

The relevant aerodynamic coefficients are obtained from (7.5.23), (7.5.24), and (7.5.26), and are found with the aid of formulas (7.6.3)

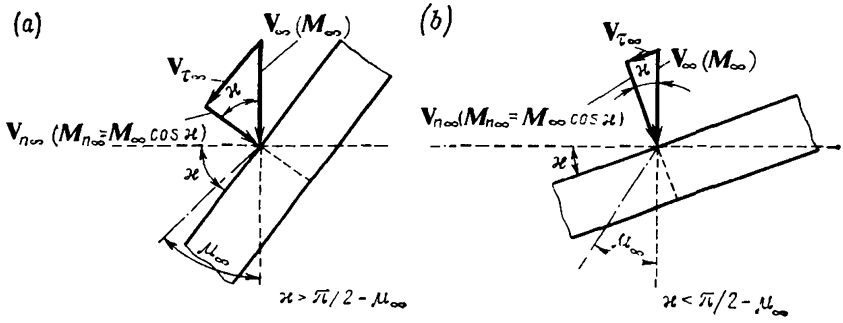

Fig. 7.6.4
Sideslipping wing with subsonic (a) and supersonic (b) leading edges

and (7.6.4) whose right-hand sides contain the quantity $\sqrt{1 - M_\infty^2 \cos^2 \varkappa}$ in the denominator. Particularly, the coefficients of the normal force and the longitudinal moment are

$$c_{y,\varkappa} = c_y \cos^2 \varkappa / \sqrt{1 - M_\infty^2 \cos^2 \varkappa}; \quad m_{z,\varkappa} = m_z \cos^2 \varkappa / \sqrt{1 - M_\infty^2 \cos^2 \varkappa} \tag{7.6.6}$$

It follows from these relations that for thin airfoils, the coefficient of the centre of pressure $c_p = -m_{z,\varkappa}/c_{y,\varkappa}$ depends neither on the sideslip (sweep) angle nor on the compressibility (the number M_∞).

The use of a sideslipping wing produces the same flow effect that appears when the free-stream velocity is lowered from V_∞ to $V_\infty \cos \varkappa$ (or the Mach number from M_∞ to $M_\infty \cos \varkappa$). Here, naturally, the local velocities on an airfoil of the sideslipping wing also decrease, and this, in turn, leads to diminishing of the rarefaction and, as a result, to an increase in the critical Mach number. The latter can be determined from its known value $M_{\infty\,cr}$ for a straight wing of the same shape and angle of attack as the airfoil of the sideslipping wing in a normal section:

$$M_{\infty\,cr,\varkappa} = M_{\infty\,cr}/\cos^2 \varkappa \tag{7.6.7}$$

Supersonic Velocities. Let us assume that at a supersonic free-stream velocity ($V_\infty > a_\infty$, $M_\infty > 1$), the sweep angle satisfies the inequality $\varkappa > \pi/2 - \mu_\infty$, according to which $\cos \varkappa < \sin \mu_\infty$ and, consequently, $V_{n\infty} < a_\infty = V_\infty \sin \mu_\infty$, i.e. the normal component to the leading edge is subsonic. Hence, the flow over the sections of a sideslipping wing is subsonic in its nature. In the case being considered, the swept edge is called subsonic (Fig. 7.6.4*a*).

At increased flow velocities, the normal velocity component may become higher than the speed of sound ($V_{n\infty} > a_\infty = V_\infty \sin \mu_\infty$), so that $\varkappa < \pi/2 - \mu_\infty$ and $\cos \varkappa > \sin \mu_\infty$. In this case, the flow

over the airfoils of a sideslipping wing is supersonic. Accordingly, the leading edge of such a wing is called **supersonic** (Fig. 7.6.4*b*).

Let us consider the calculation of the supersonic flow over a sideslipping wing in each of these cases.

Supersonic Leading Edge. The flow over such a wing can be calculated by the formulas obtained for an infinite-span thin plate provided that the free-stream velocity is $V_{n\infty} = V_\infty \cos \varkappa > a_\infty$, and the corresponding number $M_{n\infty} = M_\infty \cos \varkappa > 1$. The angle of attack of the plate α_n is related to the given angle of attack α of the sideslipping wing by expression (7.6.1), or at small angles of attack by (7.6.1′).

Using formula (7.4.9) and substituting $\alpha_n = \alpha/\cos \varkappa$ for β and $M_{n\infty} = M_\infty \cos \varkappa$ for M_∞ in it, we obtain a relation for the pressure coefficient in a plane perpendicular to the leading edge:

$$\bar{p} = \pm 2\alpha/(\cos \varkappa \sqrt{M_\infty^2 \cos^2 \varkappa - 1})$$

In this formula, the pressure coefficient $\bar{p}$ is related to the velocity head $q_n = 0.5 k p_\infty M_{n\infty}^2$. To obtain the value of the pressure coefficient related to the free-stream velocity head $q_\infty = 0.5 k p_\infty M_\infty^2$, we must use formula (7.6.2) according to which

$$\bar{p}_\varkappa = \pm 2\alpha \cos \varkappa / \sqrt{M_\infty^2 \cos^2 \varkappa - 1} \qquad (7.6.8)$$

In (7.6.8), the plus sign determines the pressure coefficient for the bottom side of a wing, and the minus sign for the upper side.

In accordance with formulas (7.4.20)-(7.4.22) (replacing α with α_n and M_∞ with $M_\infty \cos \varkappa$ in them), and also with a view to relations (7.6.3) and (7.6.4), we find a relation for the aerodynamic coefficients of a sideslipping wing airfoil

$$\left.\begin{aligned} c_{y_a \varkappa} &= 4\alpha_n \cos^2 \varkappa / \sqrt{M_\infty^2 \cos^2 \varkappa - 1} \\ c_{x_a \varkappa} &= 4\alpha_n^2 \cos^3 \varkappa / \sqrt{M_\infty^2 \cos^2 \varkappa - 1} \\ m_{z_a \varkappa} &= -2\alpha_n \cos^2 \varkappa / \sqrt{M_\infty^2 \cos^2 \varkappa - 1} \end{aligned}\right\} \qquad (7.6.9)$$

Upon analysing these relations, we can establish a feature of swept wings consisting in that in comparison with straight ones ($\varkappa = 0$), the lift force and drag coefficients, and also the coefficient of the longitudinal moment of airfoils (in their magnitude) are smaller at identical angles of attack α_n along a normal to the leading edge. The physical explanation is that in flow over a sideslipping wing not the total velocity head $q_\infty = 0.5 \rho_\infty V_\infty^2$ is realized, but only a part of it, $q_n = q_\infty \cos^2 \varkappa$, and flow in the direction of the oncoming stream occurs at a smaller angle of attack than in the absence of sideslip ($\alpha < \alpha_n$, $\alpha_n = \alpha/\cos \varkappa$).

Subsonic Leading Edge. The flow over sections corresponding to the motion of a straight wing with the number $M_{n\infty} < 1$ is investi-

gated with the aid of the subsonic or transonic (combined) theory of flow over an airfoil. The drag and lift forces are determined by the laws of subsonic flows characterized by interaction of the flows on the upper and bottom sides of a wing that manifests itself in the gas flowing over from a region of high pressure into a zone with reduced pressure values. Wave losses may appear only in supercritical flow ($M_{n\infty} > M_{\infty\,cr}$) when shocks form on the surface. If $M_{n\infty} < M_{\infty\,cr}$, then shocks and, therefore, wave drag are absent. This conclusion relates to an infinite-span wing. For finite-span wings, wave losses are always present because flow over their tips is affected by the velocity component $V_\infty \sin \varkappa$. A result is the appearance of supersonic flow properties and of a wave drag. The three-dimensional theory of supersonic flow has to be used to study this drag.

Suction Force

As we have established in Sec. 6.3, a suction force appears on the leading edge of an airfoil over which an incompressible fluid is flowing. The same effect occurs when an airfoil is in a subsonic flow of a compressible gas. The magnitude of the suction force is affected by the sweep of the leading edge of the wing.

To calculate this force, we shall use expression (6.3.25), which by means of the corresponding transformations can be made to cover the more general case of the flow over an airfoil of a wing with a swept leading edge (Fig. 7.6.5). Let us consider this transformation. In an inviscid flow, the free-stream velocity component tangent to the leading edge of a sideslipping wing does not change the field of the disturbed velocities, and it remains the same as for a straight wing in a flow at the velocity $V_{n\infty} = V_\infty \cos \varkappa$. The forces acting on the wing also remain unchanged.

Therefore, the following suction force acts on a wing element dz_0 with a straight edge (in the coordinates x_0, z_0):

$$dT_0 = \pi\rho c_0^2\, dz_0 \tag{7.6.10}$$

where in accordance with (6.3.28′)

$$c_0^2 = \lim_{x_0 \to x_{s.e0}} [u_0^2 (x_0 - x_{s.e0})]$$

A glance at Fig. 7.6.3 reveals that $dT_0 = dT/\cos \varkappa$, $dz_0 = dz/\cos \varkappa$, $u_0 = u/\cos \varkappa$, and $x_0 - x_{s.e0} = (x - x_{s.e}) \cos \varkappa$.

Insertion of these values into (7.6.10) yields

$$dT/dz = \pi\rho c^2 \sqrt{1 + \tan^2 \varkappa} \tag{7.6.11}$$

where

$$c^2 = \lim_{x \to x_{s.e}} [u^2 (x - x_{s.e})] \tag{7.6.12}$$

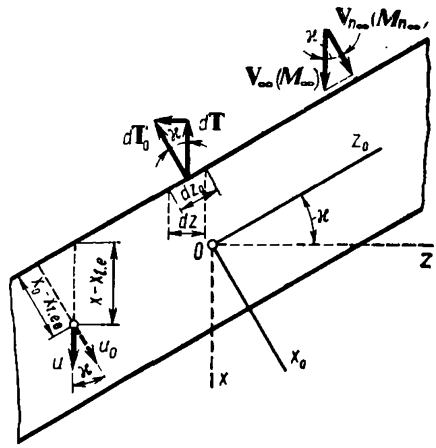

Fig. 7.6.5
Suction force of a sideslipping wing

Expressions (7.6.11) and (7.6.12) can be generalized for compressible flows. For this purpose, we shall use expressions (8.2.4) relating the geometric characteristics of wings in a compressible and an incompressible flows. It follows from these relations that all the linear dimensions in the direction of the x-axis for a wing in a compressible flow are $\sqrt{1-M_\infty^2}$ times smaller than the relevant dimensions for a wing in an incompressible flow, whereas the thickness of the wing and its lateral dimensions (in the direction of the z-axis) do not change. Accordingly, we have

$$x = x_{1c}\sqrt{1-M_\infty^2}, \quad b\,dz = b_{1c}\,dz_{1c}\sqrt{1-M_\infty^2}$$
$$\tan\varkappa = \tan\varkappa_{1c}\sqrt{1-M_\infty^2} \tag{7.6.13}$$

From the conditions that $x = x_{1c}\sqrt{1-M_\infty^2}$ and $\varphi' = \varphi'_{1c}$, we find

$$\frac{\partial\varphi'}{\partial x} = \frac{\partial\varphi'_{1c}}{\partial x_{1c}} \cdot \frac{1}{\sqrt{1-M_\infty^2}}$$

i.e.

$$u = u_{1c}/\sqrt{1-M_\infty^2} \tag{7.6.14}$$

Therefore, the pressure coefficient for a compressible flow is determined by the Prandtl-Glauert formula:

$$\bar{p} = \bar{p}_{1c}/\sqrt{1-M_\infty^2} \tag{7.6.15}$$

The suction force T in its physical nature is a force produced by the action of the normal stress (pressure) and at low angles of attack is determined from the condition $T \approx \alpha Y_a$. The corresponding suction

force coefficient is $c_{x,T} = T/(q_\infty S_w) = \alpha c_{y_a}$. Since the dimensions of a wing in the direction of the y-axis do not change in a compressible and an incompressible flows, the angles of attack for both flows also do not change, i.e. $\alpha = \alpha_{ic}$. Consequently, $c_{x.T}/c_{x.T,ic} = c_{y_a}/c_{y_a ic}$, or by (7.1.14)

$$c_{x,T} = c_{x,T,ic}/\sqrt{1 - M_\infty^2} \tag{7.6.16}$$

With a view to the relations for an airfoil of a sideslipping wing, we have

$$c_{x.\,T}\frac{\rho_\infty V_\infty^2}{2} b\,dz = \frac{c_{x.\,T}}{\sqrt{1-M_\infty^2}} \cdot \frac{\rho_\infty V_\infty^2}{2} b_{ic}\sqrt{1-M_\infty^2}\,dz_{ic}$$

or

$$dT = dT_{ic}$$

But since $dz = dz_{ic}$, then

$$dT/dz = dT_{ic}/dz_{ic} \tag{7.6.17}$$

The right-hand side of Eq. (7.6.17) corresponding to an incompressible flow is determined by formulas (7.6.11) and (7.6.12):

$$dT_{ic}/dz_{ic} = \pi\rho_\infty c_{ic}^2\sqrt{1 + \tan^2\varkappa_{ic}}$$

where

$$c_{ic}^2 = \lim_{x_{ic}\to x_{s.e.\,ic}} [u_{ic}^2 (x_{ic} - x_{s.e.\,ic})]$$

In accordance with (7.6.17), (7.6.13), and (7.6.14), we obtain

$$c_{ic}^2 = \lim_{x\to x_{s.e}} [u^2 (x - x_{s.e})]\sqrt{1-M_\infty^2};\quad \sqrt{1+\tan^2\varkappa_{ic}}$$

$$= \sqrt{1 + \frac{\tan^2\varkappa}{1-M_\infty^2}}$$

Consequently,

$$dT/dz = \pi\rho_\infty c^2\sqrt{1 + \tan^2\varkappa - M_\infty^2} \tag{7.6.18}$$

where

$$c^2 = \lim_{x\to x_{s.e}} [u^2 (x - x_{s.e})] \tag{7.6.19}$$

It follows from the above formulas that at a given value of the number M_∞, the suction force depends on the sideslip angle and on the nature of the change in the velocity u within a very small vicinity of the leading edge. We can assume that a finite-span swept wing is also characterized by a similar relation for the suction force.

8

A Wing in a Supersonic Flow

8.1. Linearized Theory of Supersonic Flow over a Finite-Span Wing

Linearization of the Equation for the Potential Function

Let us consider a thin slightly bent finite-span wing of an arbitrary planform in a supersonic flow at a small angle of attack. The disturbances introduced by such a wing into the flow are small, and for investigation of the flow we can use the linearized theory as when studying a nearly uniform flow near a thin airfoil (see Sec. 6.2). The conditions for such a flow are given for the velocities in the form of (6.1.1). If we are considering a linearized three-dimensional gas flow, these conditions are supplemented with a given velocity component along the z-axis. Accordingly, the following relations hold for a linearized three-dimensional disturbed flow:

$$V_x = V_\infty + u, \quad V_y = v, \quad V_z = w \tag{8.1.1}$$

where u, v, and w are the disturbance velocity components along the x, y, and z axes, respectively.

In accordance with the property of a linearized flow, we have

$$u \ll V_\infty, \quad v \ll V_\infty, \quad w \ll V_\infty \tag{8.1.2}$$

These conditions make it possible to linearize the equations of motion and continuity and thus simplify the solution of the problem on a thin wing in an inviscid steady flow. In the general form, the equations of motion of such a flow are obtained from system (3.1.17) in which $\mu = 0$, $\partial V_x/\partial t = \partial V_y/\partial t = \partial V_z/\partial t = 0$:

$$\left.\begin{aligned} V_x\frac{\partial V_x}{\partial x} + V_y\frac{\partial V_x}{\partial y} + V_z\frac{\partial V_x}{\partial z} &= -\frac{1}{\rho}\cdot\frac{\partial p}{\partial x} \\ V_x\frac{\partial V_y}{\partial x} + V_y\frac{\partial V_y}{\partial y} + V_z\frac{\partial V_y}{\partial z} &= -\frac{1}{\rho}\cdot\frac{\partial p}{\partial y} \\ V_x\frac{\partial V_z}{\partial x} + V_y\frac{\partial V_z}{\partial y} + V_z\frac{\partial V_z}{\partial z} &= -\frac{1}{\rho}\cdot\frac{\partial p}{\partial z} \end{aligned}\right\} \tag{8.1.3}$$

We shall adopt the continuity equation in the form of (2.4.4). Calculation of the partial derivatives yields

$$\rho\left(\frac{\partial V_x}{\partial x}+\frac{\partial V_y}{\partial y}+\frac{\partial V_z}{\partial z}\right)+V_x\frac{\partial \rho}{\partial x}+V_y\frac{\partial \rho}{\partial y}+V_z\frac{\partial \rho}{\partial z}=0 \qquad (8.1.4)$$

It was shown in Sec. 5.1 that the equations of continuity and motion can be combined into a single equation relating the velocity components to one another. By performing transformations similar to those made in Sec. 5.1, we can write this equation in the form

$$\begin{aligned}(V_x^2-a^2)\frac{\partial V_x}{\partial x}+(V_y^2-a^2)\frac{\partial V_y}{\partial y}+(V_z^2-a^2)\frac{\partial V_z}{\partial z}\\ +V_xV_y\left(\frac{\partial V_x}{\partial y}+\frac{\partial V_y}{\partial x}\right)+V_xV_z\left(\frac{\partial V_x}{\partial z}+\frac{\partial V_z}{\partial x}\right)\\ +V_yV_z\left(\frac{\partial V_y}{\partial z}+\frac{\partial V_z}{\partial y}\right)=0 \qquad (8.1.5)\end{aligned}$$

Taking into account relations (2.3.2) for the potential function, and also the condition of equality of the cross partial derivatives ($\partial^2\varphi/\partial x\,\partial y=\partial^2\varphi/\partial y\,\partial x$, etc.), from (8.1.5) we derive an equation for the velocity potential:

$$\begin{aligned}(V_x^2-a^2)\frac{\partial^2\varphi}{\partial x^2}+(V_y^2-a^2)\frac{\partial^2\varphi}{\partial y^2}+(V_z^2-a^2)\frac{\partial^2\varphi}{\partial z}\\ +2V_xV_y\frac{\partial^2\varphi}{\partial x\,\partial y}+2V_xV_z\frac{\partial^2\varphi}{\partial x\,\partial z}+2V_yV_z\frac{\partial^2\varphi}{\partial y\,\partial z}=0 \qquad (8.1.6)\end{aligned}$$

Equations (8.1.5) and (8.1.6) are the *fundamental differential equations of gas dynamics for three-dimensional steady gas flows.* The first of them relates to the more general case of a *vortex* (*non-potential*) flow of a gas, while the second is used to investigate *only vortex-free* (*potential*) flows.

Since the flow over thin wings at small angles of attack is potential, we can use Eq. (8.1.6) for the velocity potential to investigate this flow. To linearize Eq. (8.1.6), which is a non-linear differential equation, we shall introduce into it expression (7.1.2′) for the speed of sound, and also the values

$$\begin{gathered}V_x=V_\infty+u,\quad V_y=v,\quad V_z=w\\ V_x^2=V_\infty^2+2V_\infty u,\quad V_y^2\approx v^2,\quad V_z^2=w^2;\\ \varphi=\varphi_\infty+\varphi'\end{gathered}$$

After analysing the order of magnitude of the terms in the obtained equation in the same way as we did in Sec. 7.1 when considering a

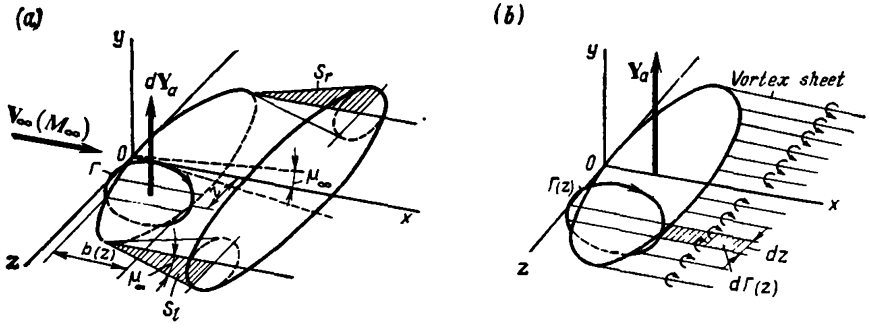

Fig. 8.1.1
Thin wing in a linearized flow

nearly uniform plane flow, we obtain a linearized equation for the velocity potential of a three-dimensional disturbed flow in the following form:

$$(M_\infty^2 - 1)\frac{\partial^2\varphi'}{\partial x^2} - \frac{\partial^2\varphi'}{\partial y^2} - \frac{\partial^2\varphi'}{\partial z^2} = 0 \qquad (8.1.7)$$

Boundary Conditions

Investigation of the flow over a thin finite-span wing consists in solving the linearized partial differential equation (8.1.7) of the second order for the velocity potential φ' at the given boundary conditions. Let us consider these boundary conditions.

1. A wing in a linearized flow (Fig. 8.1.1*a*, *b*) causes disturbances that are concentrated inside the wave zone. This zone is limited by a surface that is the envelope of Mach cones issuing from points on the leading edge and having an apex (cone) angle of $\mu_\infty = \sin^{-1}(1/M_\infty)$. The boundary condition satisfied by the solution of Eq. (8.1.7) for the function φ' has the form

$$[\varphi'(x, y, z)]_\Sigma = 0 \qquad (8.1.8)$$

According to this condition, on the wave surface (we shall designate this surface by Σ) or outside of it, the disturbance velocities are zero.

2. The solution for the additional potential φ' also satisfies the boundary condition of flow over the wing surface S without separation, in accordance with which the normal velocity component at each point is zero, i.e.

$$(V_n)_S = \left(\frac{\partial\varphi}{\partial n}\right)_S = \frac{\partial\varphi}{\partial x}\cos\widehat{(n, x)} + \frac{\partial\varphi}{\partial y}\cos\widehat{(n, y)} + \frac{\partial\varphi}{\partial z}\cos\widehat{(n, z)} = 0 \qquad (8.1.9)$$

Here

$$\frac{\partial \varphi}{\partial x} = V_\infty + u = V_\infty + \frac{\partial \varphi'}{\partial x}, \quad \frac{\partial \varphi}{\partial y} = v = \frac{\partial \varphi'}{\partial y}, \quad \frac{\partial \varphi}{\partial z} = w = \frac{\partial \varphi'}{\partial}$$

The direction cosines of an outward normal to the surface are found by formulas of analytical geometry:

$$\cos\widehat{(n, x)} = -A\,\partial f/\partial x, \quad \cos\widehat{(n, y)} = A; \quad \cos\widehat{(n, z)} = -A\,\partial f/\partial z \tag{8.1.10}$$

in which

$$A = [1 + (\partial f/\partial x)^2 + (\partial f/\partial z)^2]^{-1/2} \tag{8.1.11}$$

while the function f is determined by the shape of the wing surface [the function $y = f_u(x, z)$ for the upper surface, and $y = f_b(x, z)$ for the bottom one].

A linearized (nearly uniform) flow is realized provided that the wing is thin and, consequently, $\partial f/\partial x \ll 1$ and $\partial f/\partial z \ll 1$. Accordingly, $\cos\widehat{(n, x)} = -\partial f/\partial x$, $\cos\widehat{(n, y)} = 1$, and $\cos\widehat{(n, z)} = -\partial f/\partial z$. The conditions $(\partial \varphi'/\partial x)\,\partial f/\partial x \ll 1$ and $(\partial \varphi'/\partial z)\,\partial f/\partial z \ll 1$ are also observed in the flow over a thin wing. With this in view, (8.1.9) can be written as

$$-V_\infty\,\partial f/\partial x + \partial \varphi'/\partial y = 0$$

whence the boundary condition is

$$\partial \varphi'/\partial y = V_\infty\,\partial f/\partial x \tag{8.1.12}$$

3. The flow over a wing may be attended by the developing of a lift force whose total magnitude is determined by integration over the surface of the values of the lift force acting on an elementary surface [a part of the wing having a width of dz and a chord length of $b(z)$ (Fig. 8.1.1)]. In accordance with (6.1.8), and with the fact that $\int_0^b \gamma(x)\,dx$ equals the circulation Γ in the section z being considered, the lift coefficient for an elementary surface equals the value $c'_{y_a} = (2/V_\infty b)\,\Gamma(z)$, whence the circulation in the given section is

$$\Gamma(z) = 0.5 c'_{y_a} V_\infty b \tag{8.1.13}$$

According to the coupling equation (8.1.13) [see (6.4.8)], upon moving to a neighbouring section with a different lift coefficient, the velocity circulation also changes. This change is

$$d\Gamma(z) = (d\Gamma/dz)\,dz = 0.5 V_\infty [d(c'_{y_a} b)/dz]\,dz \tag{8.1.14}$$

In accordance with the vortex model of a wing treated in Sec. 6.4, an *elementary bound vortex* belonging only to the section being con-

sidered passes within the contour enclosing the adjacent section. This vortex turns and is cast off the trailing edge in the form of a *pair of elementary free vortices* forming a **vortex sheet** behind the wing (Fig. 8.1.1). For a thin wing in a flow at a small angle of attack, we may assume that the width of this sheet equals the span of the wing, and that the direction of the free vortices coincides with the free-stream velocity.

Physical notions allow us to establish the following boundary conditions on a vortex sheet. The normal component of a particle's velocity $v_n = \partial\varphi'/\partial n$ remains continuous on the sheet. Since the direction of a normal on the vortex sheet differs only slightly from the direction of the axis Oy, the derivative $\partial\varphi'/\partial n$ equals the quantity $\partial\varphi'/\partial y$. Consequently, we can write the condition

$$(\partial\varphi'/\partial y)_{y=+0} = (\partial\varphi'/\partial y)_{y=-0} \tag{8.1.15}$$

in which the left-hand side corresponds to the *velocity* V_n directly *above the vortex sheet* ($y = +0$), and the right-hand side, to the velocity *under it* ($y = -0$). Hence, condition (8.1.15) expresses the continuity of the function $\partial\varphi'/\partial y$ when passing through a vortex sheet.

In addition, the condition of the continuity of the pressure is satisfied on a vortex sheet. According to (7.1.5′), we obtain the relation

$$(\partial\varphi'/\partial x)_{y=+0} = (\partial\varphi'/\partial x)_{y=-0} \tag{8.1.16}$$

that also expresses the continuity of the partial derivative $\partial\varphi'/\partial x$ when passing through a vortex sheet.

Let us consider the flow over a wing with a symmetric airfoil ($y_u = -y_b$) at a zero angle of attack. In this case, there is no lift force and, consequently, no vortex sheet. Owing to the wing being symmetric, the vertical components of the velocity on its upper and bottom sides are equal in magnitude and opposite in sign, i.e. $v(x, +y, z) = -v(x, -y, z)$. On plane xOz outside the wing, the component $v = 0$, therefore

$$\partial\varphi'/\partial y = 0 \tag{8.1.17}$$

Let us assume further that we have a zero-thickness wing of the same planform in a flow at a small angle of attack. The equation of the wing's surface is $y = f(x, z)$. A glance at (8.1.12) reveals that the vertical velocity components $V_n = \partial\varphi'/\partial y$ on the upper and bottom sides of the wing are identical at corresponding points. Since we are dealing with a sufficiently small angle of attack of the wing, the same condition can be related to the plane $y = 0$. At the same time, such a condition can be extended to the vortex sheet behind the wing, which is considered as a continuation of the vortices in the plane $y = 0$. Therefore, at points symmetric about this plane, the

components V_n are the same, i.e. $\partial\varphi'(x, -y, z)/\partial y = \partial\varphi'(x, +y, z)/\partial y$. Consequently, the additional potential φ' is an odd function relative to the coordinate y, i.e.

$$\varphi'(x, -y, z) = -\varphi'(x, +y, z) \tag{8.1.18}$$

Accordingly, the partial derivative $\partial\varphi'/\partial x$ on the bottom side of the vortex sheet equals the value $-\partial\varphi'/\partial x$ on the upper side. But the equality of the derivatives $\partial\varphi'/\partial x$ was established from the condition of pressure continuity. This equality can be observed only when

$$\partial\varphi'/\partial x = 0 \tag{8.1.19}$$

on the vortex sheet.

4. To establish the last boundary condition, let us consider the disturbed regions S_r and S_l (Fig. 8.1.1) that are cut off from the plane $y = 0$ by the Mach wave surface and located outside the wing and the vortex sheet. Over these regions of the plane $y = 0$ and within the limits of the wave zone, the flow is continuous, therefore the potential φ' here is also a continuous function. At the same time, taking into account that by (8.1.18) the function φ' is odd, we should adopt the following equation for the plane $y = 0$:

$$\varphi'(x, 0, z) = 0 \tag{8.1.20}$$

Components of the Total Values of the Velocity Potentials and Aerodynamic Coefficients

The solution of Eq. (8.1.7) for the additional potential φ' must correspond to the considered boundary conditions. This solution can be obtained for a wing with a given planform by summation of two potentials: the first, φ_1', is found for an idealized flat wing *1* (Fig. 8.1.2) of the same planform as the given one, but with a *symmetric airfoil*, and at a zero angle of attack ($\alpha = 0$). The second potential, φ_2', is evaluated for a different idealized *cambered* wing *2 of zero thickness*, but for the given angle of attack α.

The surface of an idealized symmetric airfoil wing can be given by the equation

$$y = \pm 0.5 (f_u - f_b) \tag{8.1.21}$$

and of a zero-thickness airfoil wing, by the equation of the surface of the mean camber lines of the airfoil

$$y = 0.5 (f_u + f_b) \tag{8.1.22}$$

Hence, the total potential of the given wing is

$$\varphi' = \varphi_1' + \varphi_2' \tag{8.1.23}$$

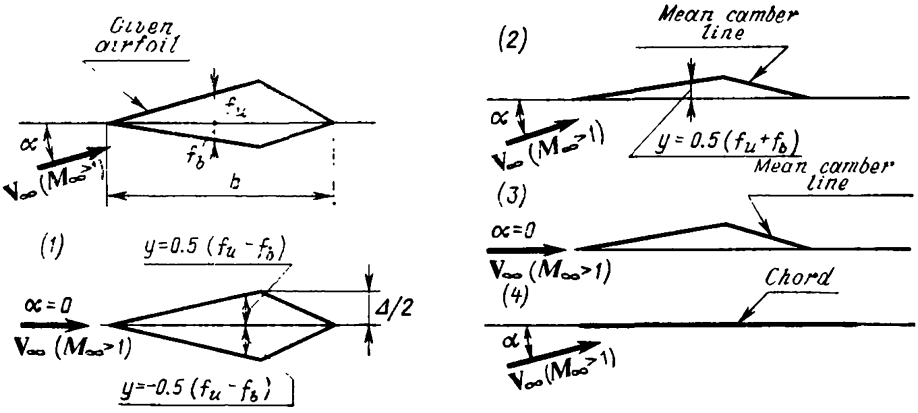

Fig. 8.1.2
Linearized supersonic flow over a finite thickness airfoil at an angle of attack α: *1*—$\alpha = 0$, symmetric airfoil, and given thickness distribution; *2*—$\alpha \neq 0$, zero thickness (the airfoil coincides with the mean camber line); *3*—$\alpha = 0$, zero thickness (the airfoil coincides with the mean camber line); *4*—$\alpha \neq 0$, zero thickness (the plate airfoil coincides with the chord)

The flow past wing *2*, in turn, at $\alpha \neq 0$ can be represented as a flow past wing *3 with a zero angle of attack* and a surface equation $y = 0.5\,(f_u + f_b)$ and an additional flow superposed onto this one. The additional flow is formed near wing *4* in the form of a zero thickness plate coinciding with the chord of the initial wing having an angle of attack α (Fig. 8.1.2). In accordance with this flow scheme, the total potential for the given wing is

$$\varphi' = \varphi_1' + \varphi_3' + \varphi_4' \tag{8.1.24}$$

We can use this value of the velocity potential to calculate the distribution of the pressure coefficient

$$\overline{p} = \overline{p_1} + \overline{p_3} + \overline{p_4} \tag{8.1.25}$$

and then find the drag and lift forces. By (8.1.24) and (8.1.25), the total drag of the given wing is composed of the drags produced by wings *1*, *3*, and *4*, i.e.

$$X_a = X_1 + X_3 + X_4 \tag{8.1.26}$$

Introducing the notation $X_3 + X_4 = X_i$ and going over from the forces to the corresponding aerodynamic coefficients, we have

$$\frac{X_a}{q_\infty S_w} = \frac{X_1}{q_\infty S_w} + \frac{X_3 + X_4}{q_\infty S_w} = \frac{X_1}{q_\infty S_w} + \frac{X_i}{q_\infty S_w}$$

or

$$c_{x_a} = c_{x0} + c_{x3} + c_{x4} = c_{x0} + c_{x,\,i} \tag{8.1.27}$$

In accordance with (8.1.27), the wing drag coefficient c_{x_a} consists of the drag coefficient c_{x0} of a symmetric wing at $c_{y_a} = 0$ and the additional drag coefficient $c_{x.i}$ due to the lift force and calculated for a zero-thickness wing at $c_{y_a} \neq 0$. The coefficient $c_{x,i}$, in turn, consists of the **induced wave drag coefficient** calculated for the case when the influence of vortices is absent and an additional **induced vortex drag coefficient** due to the span being finite and to the formation in this connection of a vortex sheet behind the trailing edge.

By analogy with expression (8.1.26) for the drag, let us give in the general form a relation determining the total magnitude of the lift force of a wing $Y_a = Y_1 + Y_3 + Y_4$. A glance at Fig. 8.1.2 reveals that wing *1* having a symmetric airfoil and arranged at a zero angle of attack does not create a lift force ($Y_1 = 0$). Consequently, the total lift force of the wing is

$$Y_a = Y_3 + Y_4 \tag{8.1.28}$$

and the corresponding coefficient of this force is

$$c_{y_a} = c_{y3} + c_{y4} \tag{8.1.29}$$

Hence, according to the approximate linearized theory of flow, the thickness of a wing does not affect the lift force. Wing *3* produces a constant lift force that does not depend on the angle of attack. It corresponds to the value of this force at a zero angle of attack and a given concavity of a wing. A lift force due to the angle of attack is produced by wing *4* and, therefore, depends on the planform of the wing.

The finding of the pressure distribution, the resultant forces, and the relevant aerodynamic coefficients with a view to their possible resolution into components according to formulas (8.1.27) and (8.1.29) is the basic problem of the aerodynamics of a finite-span wing in a nearly uniform supersonic flow.

Features of Supersonic Flow over Wings

When determining the aerodynamic characteristics of wings, we must take account of the features of the supersonic flow over them. These features are due to the specific property of supersonic flows in which the disturbances propagate only downstream and within the confines of a disturbance (Mach) cone with an apex angle of $\mu_\infty = \sin^{-1}(1/M_\infty)$.

Let us consider a supersonic flow over a thin wing having an arbitrary planform (Fig. 8.1.3). Point *O* on the leading edge is a source of disturbances propagating downstream within the confines of a Mach cone. The Mach lines *OF* and *OG* are both ahead of the leading edges

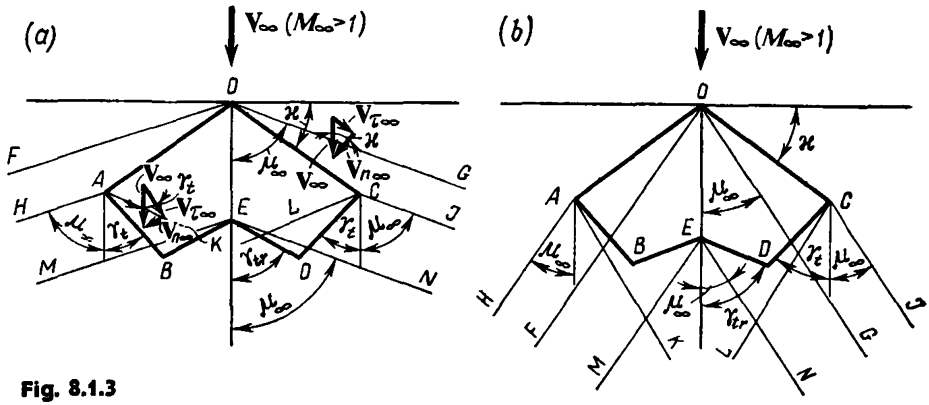

Fig. 8.1.3

Supersonic flow over a wing:
a—wing with subsonic edges; *b*—wing with supersonic edges

(Fig. 8.1.3*a*) and behind them (Fig. 8.1.3*b*). The arrangement of the Mach lines at a given wing planform depends on the number M_∞. In the first case, the number M_∞ is smaller than in the second one, and the angle of inclination of the Mach line $\mu_\infty > \pi/2 - \varkappa$ ($\varkappa$ is the sweep angle). The normal velocity component to the leading edge is $V_{n\infty} = V_\infty \cos \varkappa$. Since $\cos \varkappa < \sin \mu_\infty = 1/M_\infty$ and $V_\infty/a_\infty = M_\infty$, the normal component $V_{n\infty}$ is evidently smaller than the speed of sound. The flow of a gas in the region of the leading edge of a swept wing for this case was considered in Sec. 7.6. This flow corresponds to the subsonic flow over an airfoil that is characterized by interaction between the upper and bottom surfaces occurring through the leading edge. *Such a leading edge is called* ***subsonic*** (Fig. 8.1.3a).

Upon an increase in the flow velocity, when the zone of disturbance propagation narrows and the Mach lines are behind the leading edges as shown in Fig. 8.1.3*b*, the normal velocity component becomes supersonic. Indeed, examination of Fig. 8.1.3*b* reveals that the angle of inclination of the Mach line $\mu_\infty < \pi/2 - \varkappa$, hence $\sin \mu_\infty = 1/M_\infty < \cos \varkappa$, and therefore $V_{n\infty} = V_\infty \cos \varkappa > a_\infty$. *Such a leading edge is called* ***supersonic.*** The flow over airfoils in the region of the leading edge is of a supersonic nature whose feature is the absence of interaction between the bottom and the upper surfaces.

If the Mach line coincides with the leading edge ($\varkappa = \pi/2 - \mu_\infty$), *such an edge is* ***sonic.*** It is quite evident that in this case the magnitude of the normal velocity component to the edge equals the speed of sound.

Let us introduce the leading edge sweep parameter $n = \tan \varkappa / \cot \mu_\infty$. For a supersonic leading edge, $\cot \mu_\infty > \tan \varkappa$, therefore

$n < 1$. For subsonic and sonic leading edges, we have $n > 1$ and $n = 1$, respectively, because in the first case $\cot \mu_\infty < \tan \varkappa$ and in the second one $\cot \mu_\infty = \tan \varkappa$.

By analogy with the leading edges, we can introduce the concept of subsonic, sonic, and supersonic tips (side edges) and trailing edges of a wing. *Tip CD with an angle of inclinaion γ_t to the direction of the free-stream velocity smaller than the Mach angle* (Fig. 8.1.3*a*) *is called* ***subsonic.*** The velocity component normal to a tip and equal to $V_{n\infty} = V_\infty \sin \gamma_t$ is lower than the speed of sound in the given case. Indeed, since $a_\infty = V_\infty \sin \mu_\infty$ and $\mu_\infty > \gamma_t$, we have $V_{n\infty} < a_\infty$. It is obvious that the leading edge sweep parameter $n > 1$. The part of the wing surface with a subsonic tip is inside the region cut off by the Mach cones issuing from corners A and C of the contour. Owing to a subsonic normal velocity component determining the flow over this part of the wing, air is observed to overflow the tips, the result being a change in the pressure distribution. Such an influence of the wing tips on the flow over the wing as a whole is not observed if the tips are supersonic, as when $\gamma_t > \mu_\infty$ (Fig. 8.1.3*b*). In this case, the normal component $V_{n\infty} = V_\infty \sin \gamma_t$ is higher than the speed of sound $a_\infty = V_\infty \sin \mu_\infty$.

Similar reasoning can be related to the trailing edge of the wing. Fig. 8.1.3*a* shows a subsonic trailing edge ($\gamma_{tr} < \mu_\infty$; $V_{n\infty} < a_\infty$), and Fig. 8.1.3*b*—a supersonic one ($\gamma_{tr} > \mu_\infty$; $V_{n\infty} > a_\infty$).

The above analysis allows one to establish the qualitative difference between supersonic and subsonic flow over wings. This difference manifests itself in the different influence of the tips and trailing edges on the flow over the entire wing surface. If in a supersonic flow, the tips and trailing edges do not affect the flow over the wing (Fig. 8.1.3*b*), or this influence is limited to the part of the surface adjoining these tips and edges (Fig. 8.1.3*a*), in a subsonic flow the action of the tips and trailing edges manifests itself on the entire surface because the disturbances can propagate both downstream and upstream.

8.2. Method of Sources

To solve the problem on determining the aerodynamic characteristics ($\bar{p}_1$, c_{x0}) of a thin symmetric airfoil wing of an arbitrary planform in a nearly uniform supersonic flow at a zero angle of attack ($c_y = 0$), we shall use the **method of sources.**

Sources in an incompressible fluid are treated in Sec. 2.9. The velocity potential of the incompressible flow from a point source at the origin of coordinates of the system x_{1c}, y_{1c}, z_{1c}, according to (2.9.14), is

$$\varphi_{1c} = -q_{1c}/(4\pi \sqrt{x_{1c}^2 + y_{1c}^2 + z_{1c}^2}) \qquad (8.2.1)$$

where q_{1c} is the flow rate of the source, i.e. the volume of fluid flowing out of the source in unit time.

The method of sources deals not with individual point sources, but with sources continuously distributed over a part of a plane, usually the coordinate plane xOz.

Let dq_{1c} be the elementary volume flow rate of the fluid produced by the sources on the small area $d\sigma_{1c} = d\xi_{1c}\, d\zeta_{1c}$ in the plane xOz. Hence the derivative $dq_{1c}/d\sigma_{1c} = Q_{1c}$, known as the **density (or intensity) of source distribution**, determines the strength of the sources per unit area.

If $\pm v$ is the vertical component of the velocity on the area $d\sigma_{1c}$ (the plus sign signifies that the fluid is discharged upward from the sources, and the minus sign—downward), the elementary volume flow rate is evidently $dq_{1c} = 2v\, d\sigma_{1c}$ and, therefore,

$$Q_{1c} = 2v \tag{8.2.2}$$

The following potential corresponds to an elementary source:

$$d\varphi'_{1c} = -Q_{1c}\, d\sigma_{1c}/(4\pi \sqrt{x_{1c}^2 + y_{1c}^2 + z_{1c}^2}) \tag{8.2.3}$$

Using this expression, we can obtain a relation for the elementary potential of a source in a subsonic compressible flow. To do this, let us consider Eq. (8.1.7) and introduce the new variables

$$x_{1c} = x/\sqrt{1 - M_\infty^2}, \quad y_{1c} = y, \quad z_{1c} = z \tag{8.2.4}$$

With the aid of these variables, Eq. (8.1.7) is transformed as follows

$$\partial^2\varphi'/\partial x_{1c}^2 + \partial^2\varphi'/\partial y_{1c}^2 + \partial^2\varphi'/\partial z_{1c}^2 = 0 \tag{8.2.5}$$

This expression coincides with the continuity equation (2.4.8′) for an incompressible flow. Consequently, the problem on the compressible disturbed flow in the coordinates x, y, and z can be reduced to the problem on an incompressible disturbed flow in the coordinates x_{1c}, y_{1c}, and z_{1c}, both systems of coordinates being related by conditions (8.2.4).

Accordingly, we can go over from potential (8.2.3) for an elementary source of an incompressible fluid to the relevant potential for a subsonic source of a compressible fluid. To do this, we shall find the relation between the small area $d\sigma_{1c}$ on the plane $x_{1c}Oz_{1c}$ in the incompressible flow and the area $d\sigma$ on a corresponding plane in the compressible flow. Using (8.2.4) (with the substitution of ξ for x_{1c} and ζ for z_{1c}) and the expression $d\sigma_{1c} = d\xi_{1c}\, d\zeta_{1c}$, we find that $d\sigma_{1c} = d\xi\, d\zeta\, (1/\sqrt{1 - M_\infty^2})$, whence, taking into account that $d\xi\, d\zeta = d\sigma$, we find

$$d\sigma_{1c} = d\sigma/\sqrt{1 - M_\infty^2} \tag{8.2.6}$$

Let us transform the expression for Q_{1c} in (8.2.3). The component $v_{1c} = \partial\varphi'/\partial y_{1c}$, or with a view to (8.2.4), $v_{1c} = \partial\varphi'/\partial y$. It thus follows

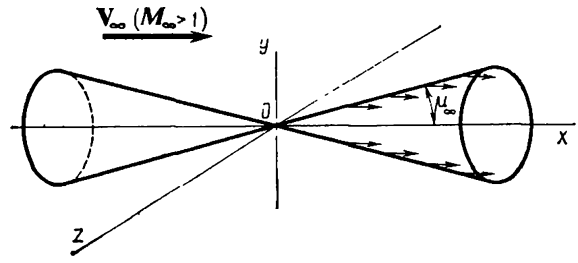

Fig. 8.2.1
Disturbed flow due to a supersonic source:
at the right—a Mach (disturbance) cone in a real supersonic flow, at the left—an "inverted Mach cone"

that in a compressible flow, the velocity component v equals the component v_{ic} in an incompressible flow. Hence, the density of source distribution in a compressible and incompressible flows is the same, i.e.

$$Q_{ic} = Q = 2v_{ic} = 2v \tag{8.2.7}$$

With account taken of the relations obtained for a compressible flow, (8.2.3) is transformed to the following expression:

$$d\varphi' = Q\, d\sigma/[4\pi \sqrt{x^2 + (1 - M_\infty^2)(y^2 + z^2)}] \tag{8.2.8}$$

We can convince ourselves by direct substitution that the function φ' is an integral of Eq. (8.2.5). It does not matter whether the velocity is subsonic ($M_\infty < 1$) or supersonic ($M_\infty > 1$). In the latter case, it is convenient to write the expression for the elementary potential as

$$d\varphi' = -Q\, d\sigma/[4\pi \sqrt{x^2 - \alpha'^2 (y^2 + z^2)}] \tag{8.2.9}$$

where $\alpha'^2 = M_\infty^2 - 1$.

Examination of expression (8.2.9) reveals that when $M_\infty > 1$ it has real values in the region of space where $x^2 \geqslant \alpha'^2 (y^2 + z^2)$. This signifies that the region of source influence, i.e. the region of disturbed flow experiencing the action of these sources, is inside the conical surface represented by the equation $x^2 = \alpha'^2 (y^2 + z^2)$. If a point is outside this surface, the sources have no influence on it. Here there is no disturbed flow from a given source.

Formally, the equation $x^2 = \alpha'^2 (y^2 + z^2)$ determines the surfaces of two aligned cones (Fig. 8.2.1) with their vertices at the origin of coordinates, and, consequently, the strength of a source $Q\, d\sigma$ is used to produce disturbed flows inside these cones. In a real case, supersonic disturbances propagate only downstream and only inside one cone (the right-hand one in Fig. 8.2.1).

The disturbed flow in such a cone is determined by a potential double that given by (8.2.9) because the entire strength of the source,

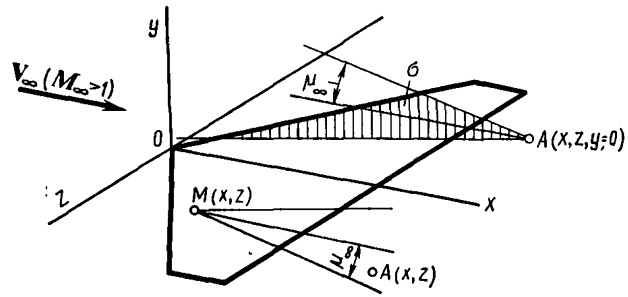

Fig. 8.2.2
Region of influence of supersonic sources

and not half of it, is realized in the flow confined within the Mach cone. Accordingly,

$$d\varphi' = -Q\, d\sigma/[2\pi \sqrt{x^2 - \alpha'^2 (y^2 + z^2)}] \qquad (8.2.10)$$

In the considered case, the elementary area $d\sigma = d\xi\, d\zeta$ with the sources is at the origin of coordinates. If it is displaced with respect to the origin of coordinates to a point with the coordinates $x = \xi$ and $z = \zeta$, Eq. (8.2.10) has the form

$$d\varphi' = -Q\, d\sigma/\{2\pi \sqrt{(x-\xi)^2 - \alpha'^2 [y^2 + (z-\zeta)^2]}\} \qquad (8.2.11)$$

When studying the flow over a wing, its surface is replaced with a **system of disturbed sources.** To obtain the potential due to these sources at arbitrary point A (x, y, z) (Fig. 8.2.2), we must integrate (8.2.11) over the region σ in which only part of the sources are located. Each of these sources influences point A (x, y, z) if it is inside a Mach cone with its vertex in the source. Hence, the region affected by the sources (the region of integration) is in the zone of intersection with the wing surface of an "inverted Mach cone" with its vertex at point A (x, y, z) being considered.

In a simpler case, point A and the source are located, as can be seen from Fig. 8.2.2, in the same plane $y = 0$. In this case, the affected zone coincides with the region of intersection of the wing and the Mach lines issuing from point M (x, z), while the region of integration σ is on the wing and is the intersection of the wing surface with the inverted plane Mach wave having its vertex at point A (x, z).

Having determined the integration region σ, we can evaluate the total potential at point A (x, y, z):

$$\varphi'(x, y, z) = -\frac{1}{2\pi} \int_\sigma \int \frac{Q(\xi, \zeta)\, d\xi\, d\zeta}{\sqrt{(x-\xi)^2 - \alpha'^2 [y^2 + (z-\zeta)^2]}} \qquad (8.2.12)$$

By calculating the partial derivative of φ' (8.2.12) with respect to x, we find the additional axial velocity component:

$$\frac{\partial \varphi'}{\partial x} = u = \frac{1}{2\pi} \int\int_{\sigma} \frac{Q(\xi, \zeta)(x-\xi)\, d\xi\, d\zeta}{\sqrt{\{(x-\xi)^2 - \alpha'^2 [y^2 + (z-\zeta)^2]\}^3}} \qquad (8.2.13)$$

We use this value to determine the pressure coefficient $\bar{p} = -2u/V_\infty$ at the corresponding point.

Let us introduce the new coordinates

$$x_1 = x/\alpha', \quad y_1 = y, \quad z_1 = z \qquad (8.2.14)$$

In these coordinates, expression (8.2.12) has the form

$$\varphi'(x_1, y_1, z_1) = -\frac{1}{2\pi} \int\int_{\sigma} \frac{Q(\xi, \zeta)\, d\xi\, d\zeta}{\sqrt{(x_1-\xi)^2 - y_1^2 - (z_1-\zeta)^2}} \qquad (8.2.15)$$

In a particular case for points on the wing surface ($y_1 = 0$), the additional potential is

$$\varphi'(x_1, 0, z_1) = -\frac{1}{2\pi} \int\int_{\sigma} \frac{Q(\xi, \zeta)\, d\xi\, d\zeta}{\sqrt{(x_1-\xi)^2 - (z_1-\zeta)^2}} \qquad (8.2.16)$$

where by (8.2.7)

$$Q = 2v_{y_1=0} = 2\,(\partial\varphi'/\partial y_1)_{y_1=0} \qquad (8.2.17)$$

The expressions obtained for the potential function allow us to calculate the distribution of the velocity and pressure over the surface of a thin wing if its planform, airfoil configuration, and the free stream number M are given.

8.3. Wing with a Symmetric Airfoil and Triangular Planform

$(\alpha=0,\ c_{y_a}=0)$

Flow over a Wing Panel with a Subsonic Leading Edge

Let us consider a supersonic flow at a zero angle of attack over a wing panel with a symmetric airfoil that is a triangular surface in which one of the side edges is directed along the x-axis, while the trailing edge is removed to infinity (such a panel is also called an infinite triangular half-wing, Fig. 8.3.1). If such a surface has a *subsonic leading edge*, the Mach line issuing from vertex O is ahead of this edge.

The flow parameters at small angles of attack α can be determined by replacing the surface in the flow with a system of distributed sources on the plane $y = 0$. Let us consider arbitrary point P on the surface and evaluate the velocity potential at this point by add-

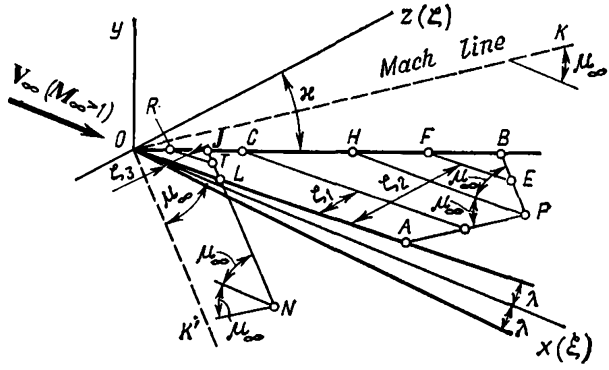

Fig. 8.3.1
Triangular wing with a subsonic leading edge

ing up the action of the sources in region $OAPB$ confined by the leading OA and side OB edges, and also by the Mach lines AP and BP.

We determine the strength $Q(\xi, \zeta)$ of the sources by formula (8.2.7) in which according to the condition of flow without separation we have $v = \lambda V_\infty$, where $\lambda = dy/dx$ is the angular coefficient of the wing surface. Hence

$$Q(\xi, \zeta) = 2\lambda V_\infty$$

The velocity potential at point P is determined by formula (8.2.12). Performing the substitution $Q = 2\lambda V_\infty$ and assuming that $y = 0$, we obtain

$$\varphi' = -\frac{\lambda V_\infty}{\pi} \iint\limits_\sigma \frac{d\xi\, d\zeta}{\sqrt{(x_P - \xi)^2 - \alpha'^2 (z_P - \zeta)^2}} \tag{8.3.1}$$

where x_P and z_P are the coordinates of point P.

This integral takes into account the action on point P of sources located on the area σ equal to region $OAPB$ that can be represented as the sum of two sections: $OAPH$ and HPB. Accordingly, the integral φ' (8.3.1) can be written as the sum of two integrals:

$$\varphi' = \frac{\lambda V_\infty}{\pi} \left[\iint\limits_{OAPH} f(\xi, \zeta)\, d\xi\, d\zeta + \iint\limits_{HPB} f(\xi, \zeta)\, d\xi\, d\zeta \right] \tag{8.3.2}$$

where

$$f(\xi, \zeta) = [(x_P - \xi)^2 - \alpha'^2 (z_P - \zeta)^2]^{-1/2} \tag{8.3.3}$$

On section $OAPH$, integration with respect to ξ for each value of $\zeta = \zeta_1$ must be performed from $\xi = \xi_C = \zeta \tan \varkappa$ to $\xi = \xi_D = x_P - \alpha'(z_P - \zeta)$, and integration with respect to ζ from 0 to z_P. On section HPB, integration with respect to ξ, for which the value of $\zeta = \zeta_2$, must be performed from $\xi = \xi_F = \zeta \tan \varkappa$ to $\xi = \xi_E = x_P - \alpha'(\zeta - z_P)$, and integration with respect to ζ from z_P to

$z_B = (x_P + \alpha' z_P)/(\alpha' + \tan \varkappa)$. Hence,

$$\varphi' = -\frac{\lambda V_\infty}{\pi}\left[\int_0^{z_P} d\zeta \int_{\zeta \tan \varkappa}^{x_P - \alpha'(z_P - \zeta)} f(\xi, \zeta)\, d\xi + \int_{z_P}^{z_B} d\zeta \int_{\zeta \tan \varkappa}^{x_P - \alpha'(\zeta - z_P)} f(\xi, \zeta)\, d\xi\right] \tag{8.3.4}$$

The indefinite integral

$$\int f(\xi, \zeta)\, d\xi = \int \frac{d\xi}{\sqrt{(x_P - \xi)^2 - \alpha'^2 (z_P - \zeta)^2}} = \cosh^{-1} \frac{x_P - \xi}{\alpha' (z_P - \zeta)} \tag{8.3.5}$$

Using this expression and introducing the main value of the integral, we obtain the following formula for the potential function:

$$\varphi' = \frac{\lambda V_\infty}{\pi} \int_0^{z_B} \cosh^{-1} \frac{x_P - \zeta \tan \varkappa}{\alpha' |z_P - \zeta|}\, d\zeta \tag{8.3.6}$$

By calculating the partial derivative $\partial\varphi'/\partial x$, we find the component of the additional velocity at point P in the direction of the x-axis:

$$u = \frac{\partial \varphi'}{\partial x} = \frac{\lambda V_\infty}{\pi} \int_0^{z_B} \frac{d\zeta}{\sqrt{(x_P - \zeta \tan \varkappa)^2 - \alpha'^2 (z_P - \zeta)^2}} \tag{8.3.7}$$

Taking into account that $\tan \varkappa > \alpha'$ $(\cot \mu_\infty)$, we find as a result of integration that

$$u = -\frac{\lambda V_\infty}{\pi \sqrt{\tan^2 \varkappa - \alpha'^2}} \cosh^{-1} \frac{x_P \tan \varkappa - \alpha'^2 z_P}{\alpha' (x_P - z_P \tan \varkappa)} \tag{8.3.8}$$

To facilitate the calculations, we shall introduce the angle θ determined from the condition $\tan \theta = z_P/x_P$, and the nose angle of the leading edge $\gamma = \pi/2 - \varkappa$ (Fig. 8.3.2). In addition, let us introduce the notation

$$n = \tan \varkappa/\alpha' = \tan \mu_\infty/\tan \gamma,$$
$$\sigma = z_P \tan \varkappa/x_P = \tan \theta/\tan \gamma$$

With this taken into account, we have

$$u = -\frac{\lambda V_\infty}{\pi \alpha' \sqrt{n^2 - 1}} \cosh^{-1} \frac{n^2 - \sigma}{n(1 - \sigma)} \tag{8.3.9}$$

and the pressure coefficient is

$$\bar{p} = -\frac{2u}{V_\infty} = \frac{2\lambda}{\pi \alpha' \sqrt{n^2 - 1}} \cosh^{-1} \frac{n^2 - \sigma}{n(1 - \sigma)} \tag{8.3.10}$$

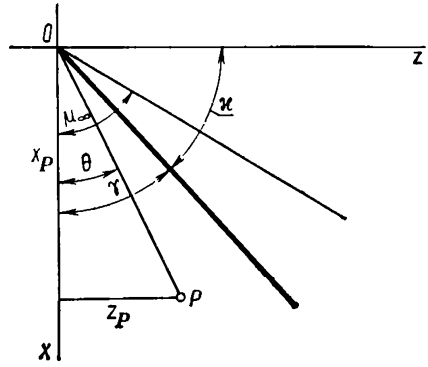

Fig. 8.3.2
Angular parameters for a triangular wing

Now let us consider point N outside of the wing between the Mach line OK' and the x-axis (see Fig. 8.3.1) and calculate for it the velocity that is induced by the sources distributed over the wing surface. To do this, we shall use formula (8.3.1) determining the velocity potential. Taking into account that the action of the sources on point N is confined by the region $\sigma = OLJ$, we obtain the expression

$$\varphi' = -\frac{\lambda V_\infty}{\pi} \iint\limits_{OLJ} f(\xi, \zeta)\, d\xi\, d\zeta \tag{8.3.11}$$

where the function $f(\xi, \zeta)$ is determined by relation (8.3.3). Integration with respect to ξ for each value of $\zeta = \zeta_3$ must be performed from $\xi = \xi_R = \zeta \tan \varkappa$ to $\xi = \xi_T = x_N + \alpha'(z_N - \zeta)$, and integration with respect to ζ, from 0 to z_J. Hence,

$$\varphi' = -\frac{\lambda V_\infty}{\pi} \int_0^{z_J} d\zeta \int_{\zeta \tan \varkappa}^{x_N + \alpha'(z_N - \zeta)} f(\xi, \zeta)\, d\xi \tag{8.3.12}$$

where $z_J = (x_N + \alpha' z_N)/(\alpha' + \tan \varkappa)$.

By integrating and using the main value of the integral, we obtain

$$\varphi' = \frac{\lambda V_\infty}{\pi} \int_0^{z_J} \cosh^{-1} \frac{x_N - \zeta \tan \varkappa}{\alpha' |z_N - \zeta|}\, d\zeta$$

This expression is similar to (8.3.6) with the difference that the coordinate z_J is taken as the upper limit of the integral. By calculating the derivative $\partial\varphi'/\partial x$ and integrating, we obtain relation (8.3.9) for the component of the additional velocity. We must assume in it that $\sigma < 0$ because the coordinate z_N is negative. In calculations, the coordinate z_N may be assumed to be positive, and, consequently, $\sigma > 0$. If we take the magnitudes of $\tan \varkappa$, then to determine the

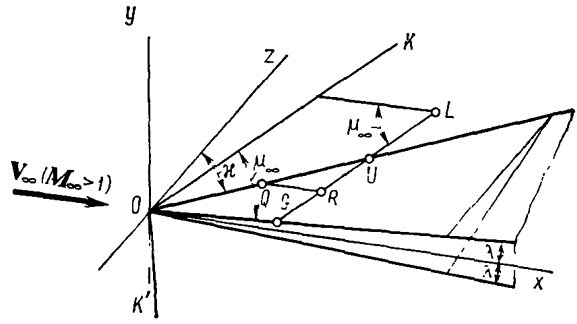

Fig. 8.3.3
Influence of sources on the velocity outside a wing

induced velocity we may use Eq. (8.3.9) in which σ should be taken with the opposite sign. The working relation now becomes

$$u = -\frac{\lambda V_\infty}{\pi\alpha' \sqrt{n^2-1}} \cosh^{-1} \frac{n^2+\sigma}{n(1+\sigma)} \tag{8.3.13}$$

The pressure coefficient in the region being considered is

$$\bar{p} = -\frac{2u}{V_\infty} = \frac{2\lambda}{\pi\alpha' \sqrt{n^2-1}} \cosh^{-1} \frac{n^2+\sigma}{n(1+\sigma)} \tag{8.3.14}$$

The sources distributed over the wing also induce a velocity in the region between the Mach line OK and the leading subsonic edge (Fig. 8.3.3). The magnitude of this velocity at a point L is determined by the sources distributed on region OUG. We find the corresponding potential function by expression (8.3.12) in which we must introduce the coordinate z_L instead of z_J, and replace the quantity $x_N + \alpha'(z_N - \zeta)$ with the value $x_L - \alpha'(z_L - \zeta)$ equal to the longitudinal coordinate of point R (Fig. 8.3.3). Hence,

$$\varphi' = -\frac{\lambda V_\infty}{\pi} \int_0^{z_U} d\zeta \int_{\zeta \tan \varkappa}^{x_L - \alpha'(z_L - \zeta)} f(\xi, \zeta)\, d\xi \tag{8.3.15}$$

where $z_U = (x_L - \alpha' z_L)/(\tan \varkappa - \alpha')$.

Integration yields

$$\varphi' = \frac{\lambda V_\infty}{\pi} \int_0^{z_U} \cosh^{-1} \frac{x_L - \zeta \tan \varkappa}{\alpha' |z_L - \zeta|}\, d\zeta$$

By evaluating the derivative $\partial\varphi'/\partial x$ and then performing integration provided that $\sigma = z_L \tan \varkappa / x_P > 1$, we obtain the following

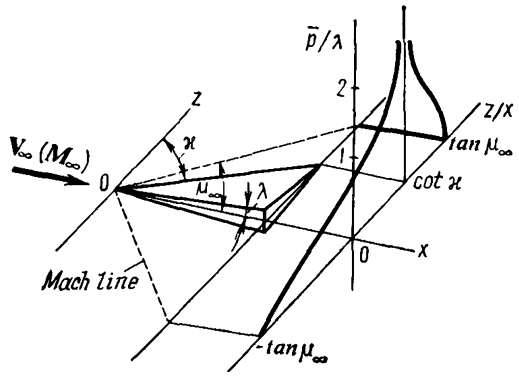

Fig. 8.3.4
Pressure field for a triangular wing with a subsonic leading edge

formula similar to (8.3.9) for the additional velocity component:

$$u = -\frac{\lambda V_\infty}{\pi\alpha' \sqrt{n^2-1}} \cosh^{-1} \frac{n^2-\sigma}{n(\sigma-1)} \qquad (8.3.16)$$

where $n > \sigma$.

We use the value of this velocity to find the pressure coefficient:

$$\bar{p} = -\frac{2u}{V_\infty} = \frac{2\lambda}{\pi\alpha' \sqrt{n^2-1}} \cosh^{-1} \frac{n^2-\sigma}{n(\sigma-1)} \qquad (8.3.17)$$

Figure 8.3.4 shows the field of pressures for a wing with a triangular planform having a subsonic leading edge. The pressure coefficient along the Mach lines is zero. On the leading edge, the theoretical pressure coefficient equals infinity. The physically possible pressure can be considered to be sufficiently high, corresponding to the stagnation pressure at a subsonic velocity whose direction coincides with a normal to the leading edge.

Triangular Wing Symmetric about the x-Axis with Subsonic Leading Edges

The velocity at point P of a triangular wing symmetric about the x-axis and having subsonic leading edges (Fig. 8.3.5) is determined by summating the action of sources in region $OBPA'$ confined by leading edges OA' and OB and by Mach lines PA' and PB. The velocity induced by the sources distributed on section $OAPB$ is determined by formula (8.3.9). The sources distributed in region OAA' produce at point P a velocity that is calculated by expression (8.3.13). The total value of the velocity is

$$u = -\frac{\lambda V_\infty}{\pi\alpha' \sqrt{n^2-1}} \left[\cosh^{-1} \frac{n^2-\sigma}{n(1-\sigma)} + \cosh^{-1} \frac{n^2+\sigma}{n(1+\sigma)} \right]$$

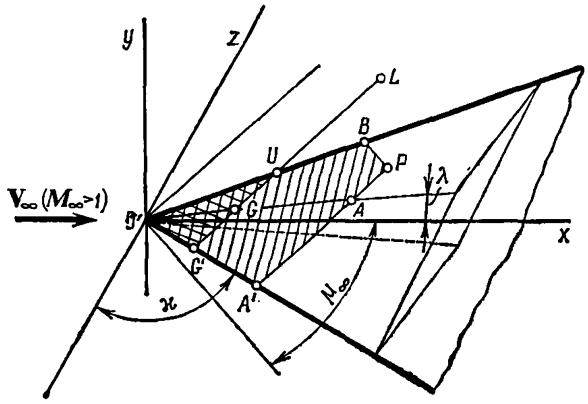

Fig. 8.3.5
Triangular wing symmetric about the x-axis with subsonic leading edges

This expression can be transformed as follows:

$$u = -\frac{2\lambda V_\infty}{\pi\alpha' \sqrt{n^2-1}} \cosh^{-1} \sqrt{\frac{n^2-\sigma^2}{1-\sigma^2}} \tag{8.3.18}$$

Formula (8.3.18) is suitable for the conditions $n > 1 > \sigma$.

We can determine the pressure coefficient with the aid of (6.1.5) according to the known value of the additional velocity component:

$$\bar{p} = -\frac{2u}{V_\infty} = \frac{4\lambda}{\pi\alpha' \sqrt{n^2-1}} \cosh^{-1} \sqrt{\frac{n^2-\sigma^2}{1-\sigma^2}} \tag{8.3.19}$$

Point L located between the leading edge and the Mach wave (Fig. 8.3.5) is influenced by the sources distributed on section OUG' of the wing. The velocity induced by these sources can be calculated as the sum of the velocities induced by the sources in region OUG [formula (8.3.16)] and by the sources distributed in triangle OGG' [formula (8.3.13)].

Consequently,

$$u = -\frac{\lambda V_\infty}{\pi\alpha' \sqrt{n^2-1}} \left[\cosh^{-1} \frac{n^2-\sigma}{n(\sigma-1)} + \cosh^{-1} \frac{n^2+\sigma}{n(1+\sigma)} \right]$$

or after transformations

$$u = -\frac{2\lambda V_\infty}{\pi\alpha' \sqrt{n^2-1}} \cosh^{-1} \sqrt{\frac{n^2-1}{\sigma^2-1}} \tag{8.3.20}$$

The corresponding pressure coefficient is

$$\bar{p} = \frac{4\lambda}{\pi\alpha' \sqrt{n^2-1}} \cosh^{-1} \sqrt{\frac{n^2-1}{\sigma^2-1}} \tag{8.3.21}$$

where $n > \sigma > 1$.

Semi-Infinite Wing with a Supersonic Edge

For such a wing (Fig. 8.3.6), Mach line OK issuing from a vertex is on its surface. Consequently,

$$\pi/2 - \varkappa > \mu_\infty,\ \tan\varkappa < \alpha',\ n = \tan\varkappa/\alpha' < 1\ (\alpha' = \cot\mu_\infty = \sqrt{M_\infty^2 - 1})$$

Let us consider the velocity at point L on the wing between the leading edge and Mach line OK. Since the side edge (tip) of the wing coinciding with the x-axis is outside the Mach line drawn through point L, no influence of the side edge is observed on the flow at this point. This flow is the same as over a flat plate in a flow directed along a normal to its leading edge at the supersonic velocity $V_{n\infty} = V_\infty \cos\varkappa > a_\infty$. By expression (7.6.8) and the formula $\bar{p} = -2u/V_\infty$, the additional velocity component is

$$u = -\lambda V_\infty \cos\varkappa/\sqrt{M_\infty^2 \cos^2\varkappa - 1}$$

Since

$$M_\infty^2 = \alpha'^2 + 1 \quad \text{and} \quad 1 - 1/\cos^2\varkappa = -\tan^2\varkappa$$

we have

$$u = -\lambda V_\infty/\sqrt{\alpha'^2 - \tan^2\varkappa}$$

whence

$$u = -\lambda V_\infty/(\alpha'\sqrt{1 - n^2}) \tag{8.3.22}$$

The relevant value of the pressure coefficient is

$$\bar{p} = -2u/V_\infty = 2\lambda/(\alpha'\sqrt{1 - n^2}) \tag{8.3.23}$$

Formulas (8.3.22) and (8.3.23) may be applied for $n < 1$ and $1 > \sigma > n$.

Let us calculate the velocity and pressure at point P between Mach line OK and the side edge. If we assume that this point belongs to a wing whose vertex is at point C (Fig. 8.3.6), the velocity would be calculated with account taken of the influence of only the leading edge and, consequently, of the sources distributed in region PCH. By (8.3.22), this velocity is

$$u_{PCH} = -\lambda V_\infty/(\alpha'\sqrt{1 - n^2}) \tag{8.3.24}$$

To find the actual velocity at point P belonging to the wing with its vertex at point O, we must subtract from (8.3.24) the velocity induced by sources distributed in triangle ACO and having a strength of the opposite sign. The magnitude of this velocity is determined by means of formula (8.3.7). Substituting $z_C = (x_P - \alpha' z_P)/(\tan\varkappa - \alpha')$

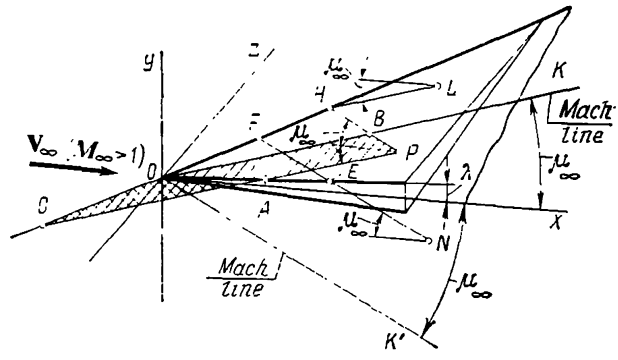

Fig. 8.3.6
Triangular wing with a supersonic edge

for the upper limit z_B of the integral, after integration we obtain

$$u_{AOC} = \frac{\lambda V_\infty}{\pi} \int_0^{z_C} \frac{d\zeta}{\sqrt{\zeta^2(\tan^2\varkappa - \alpha'^2) - 2\zeta(x_P \tan\varkappa - \alpha'^2 z_P) + x_P^2 - \alpha'^2 z_P^2}}$$

$$= -\frac{\lambda V_\infty}{\pi\sqrt{\alpha'^2 - \tan^2\varkappa}} \cos^{-1}\frac{\alpha'^2 z_P - x_P \tan\varkappa}{\alpha'(x_P - z_P\tan\varkappa)} \qquad (8.3.25)$$

Taking into account that $n = \tan\varkappa/\alpha'$ and $\sigma = z_P \tan\varkappa/x_P$, we find

$$u_{AOC} = -\frac{\lambda V_\infty}{\pi\alpha'\sqrt{1-n^2}} \cos^{-1}\frac{\sigma - n^2}{n(1-\sigma)} \qquad (8.3.26)$$

The total value of the additional velocity at point P is

$$u = u_{PCH} - u_{AOC} = -\frac{\lambda V_\infty}{\alpha'\sqrt{1-n^2}}\left[1 - \frac{1}{\pi}\cos^{-1}\frac{\sigma - n^2}{n(1-\sigma)}\right] \qquad (8.3.27)$$

and the pressure coefficient is

$$\bar{p} = -\frac{2u}{V_\infty} = \frac{2\lambda}{\alpha'\sqrt{1-n^2}}\left[1 - \frac{1}{\pi}\cos^{-1}\frac{\sigma - n^2}{n(1-\sigma)}\right] \qquad (8.3.28)$$

where $\sigma < n < 1$.

The induced velocity at point N, between Mach wave OK' and the side edge is determined by summation of the action of the sources distributed on surface section OEF confined by leading edge OF, side edge OE, and Mach line EF drawn through point N.

To calculate the velocity, we shall use formula (8.3.25), in which we shall replace the upper limit z_C of the integral with the quantity $z_F = (x_N + \alpha' z_N)/(\tan\varkappa + \alpha')$, and the coordinates x_P and z_P

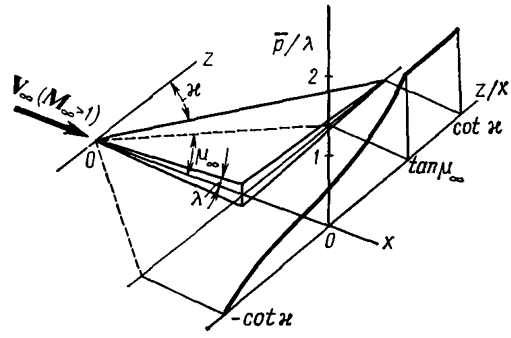

Fig. 8.3.7
Pressure field for a semi-infinite triangular wing with a supersonic leading edge

with the relevant values x_N and z_N. Integration yields

$$u_{OEF} = -\frac{\lambda V_\infty}{\pi \sqrt{\alpha'^2 - \tan^2 \varkappa}} \cos^{-1} \frac{x_N \tan \varkappa - \alpha'^2 z_N}{\alpha' (x_N - z_N \tan \varkappa)} \qquad (8.3.29)$$

Introducing the symbols σ and n, we have

$$u_{OEF} = -\frac{\lambda V_\infty}{\pi \alpha' \sqrt{1-n^2}} \cos^{-1} \frac{n^2 - \sigma}{n(1-\sigma)} \qquad (8.3.30)$$

where $\sigma < 0$, $n < 1$, and $|\sigma| < n$.

If we adopt positive values of z_N and $\sigma = z_N \tan \varkappa / x_N$ and take absolute values for n, the additional velocity is

$$u = -\frac{\lambda V_\infty}{\pi \alpha' \sqrt{1-n^2}} \cos^{-1} \frac{n^2 + \sigma}{n(1+\sigma)} \qquad (8.3.31)$$

and the pressure coefficient is

$$\bar{p} = -\frac{2u}{V_\infty} = \frac{2\lambda}{\pi \alpha' \sqrt{1-n^2}} \cos^{-1} \frac{n^2 + \sigma}{n(1+\sigma)} \qquad (8.3.32)$$

The pressure field for a semi-infinite triangular wing with a supersonic leading edge is shown in Fig. 8.3.7. Between the leading edge and the internal Mach line, the pressure is constant, then it lowers, and on the external Mach line reaches the value of the free-stream pressure ($\bar{p} = 0$).

Triangular Wing Symmetric about the x-Axis with Supersonic Leading Edges

The velocity and the pressure coefficient at point L (Fig. 8.3.8) between Mach wave OK and the leading edge are determined by formulas (8.3.22) and (8.3.23), respectively, because the flow at this point is affected only by edge OR. These formulas may be applied for the conditions $n < 1$ and $1 > \sigma > n$.

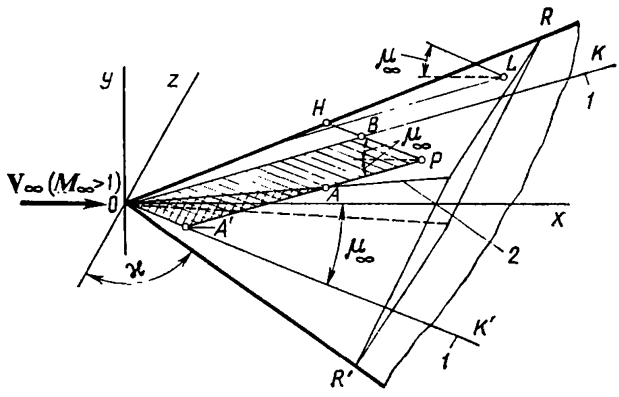

Fig. 8.3.8
Triangular wing symmetric about the x-axis with supersonic leading edges: *1*—Mach line; *2*—maximum thickness line

The velocity at point P that is within the Mach angle is affected not only by the leading edge, but also by the trailing and side edges of the wing. The velocity due to the influence of the leading edge and part OA of the maximum thickness line (Fig. 8.3.8) is determined by formula (8.3.27), while the velocity induced by the sources distributed over region $OA'A$ is evaluated by expression (8.3 31). Adding (8.3.27) and (8.3.31), we obtain the total velocity at point P of a symmetric wing:

$$u = -\frac{\lambda V_\infty}{\alpha' \sqrt{1-n^2}}\left[1 - \frac{1}{\pi}\cos^{-1}\frac{\sigma - n^2}{n(1-\sigma)} + \frac{1}{\pi}\cos^{-1}\frac{n^2+\sigma}{n(1+\sigma)}\right]$$

or after transformations,

$$u = -\frac{\lambda V_\infty}{\alpha' \sqrt{1-n^2}}\left(1 - \frac{2}{\pi}\sin^{-1}\sqrt{\frac{n^2-\sigma^2}{1-\sigma^2}}\right) \qquad (8.3.33)$$

The corresponding pressure coefficient is

$$\bar{p} = -\frac{2u}{V_\infty} = \frac{2\lambda}{\alpha' \sqrt{1-n^2}}\left(1 - \frac{2}{\pi}\sin^{-1}\sqrt{\frac{n^2-\sigma^2}{1-\sigma^2}}\right) \qquad (8.3.34)$$

8.4. Flow over a Tetragonal Symmetric Airfoil Wing with Subsonic Edges at a Zero Angle of Attack

By using the formulas for determining the velocity and pressure on the surface of a triangular wing, we can calculate the flow at a zero angle of attack over wings with a symmetric airfoil and an arbi-

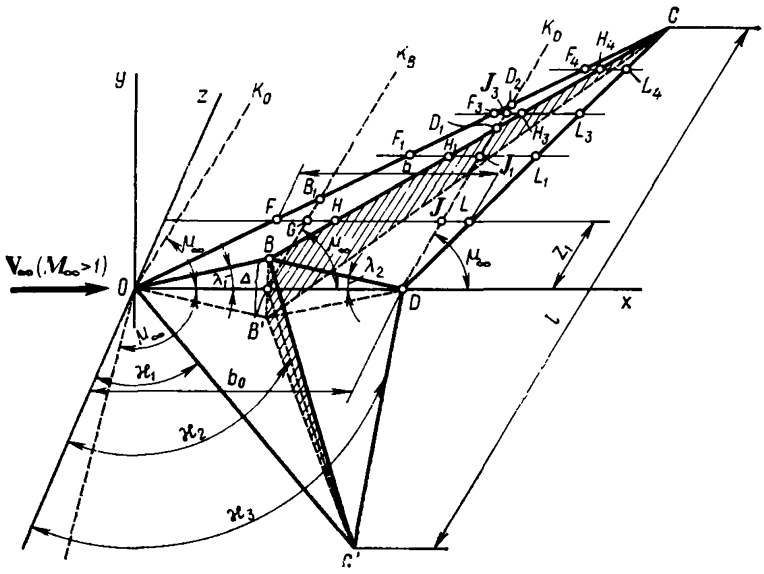

Fig. 8.4.1
Tetragonal wing with a symmetric airfoil and subsonic edges

trary planform. Let us consider the tetragonal wing shown in Fig. 8.4.1. A left-hand system of coordinates has been adopted here and in some other figures to facilitate the spatial depicting of the wing and the arrangement of both the sections being considered and the required notation. We shall assume that for such a wing the *leading* and *trailing edges*, and also *maximum thickness line CBC' are subsonic*. Accordingly, the sweep angles $\varkappa_1$, $\varkappa_3$ of the leading and trailing edges and the angle $\varkappa_2$ of the maximum thickness line are larger than $\pi/2 - \mu_\infty$.

The distribution of the velocity and pressure over an airfoil depends on where the latter is along the wing span, i.e. on the lateral coordinate z of the section.

Airfoil FL $(z = z_1)$. Four flow regions, namely, FG, GH, HJ, and JL, should be considered on the airfoil. Region FG is confined by point F on the leading edge and point G at the intersection of a Mach line with the coordinate plane $z = z_1$. Point G is considered to be on plane zOx and is determined, consequently, as the point of intersection of the Mach line issuing from the projection B' of point B onto plane zOx and of the straight line $z = z_1$ (Fig. 8.4.1). The velocity and pressure coefficient in region FG behind Mach line OK_0 on the surface of the wing are determined with the aid of the distribution of the sources in triangle OCC' by the relevant formulas (8.3.18) and (8.3.19).

Since the inclination of the surface is λ_1 in accordance with (8.3.19) we have

$$\bar{p}_{FG} = \frac{4\lambda_1}{\pi\alpha' \sqrt{n_1^2 - 1}} \cosh^{-1} \sqrt{\frac{n_1^2 - \sigma_1^2}{1 - \sigma_1^2}} \tag{8.4.1}$$

where $n_1 = \tan \varkappa_1/\alpha_1$. $\sigma_1 = z_1 \tan \varkappa_1/x_1$, and x_1 is the running coordinate of the point.

The drag coefficient of the airfoil corresponding to region FG is

$$c_{x,\,FG} = \frac{\lambda_1}{b} \int_{x_F}^{x_G} (\bar{p}_u + \bar{p}_b)\, dx_1 \tag{8.4.2}$$

where b is the local chord of the profile.

Since

$$\bar{p}_u + \bar{p}_b = 2\bar{p}_{FG}, \quad \sigma_1 = \frac{z_1 \tan \varkappa_1}{x_1},$$

$$d\sigma_1 = -\frac{z_1 \tan \varkappa_1}{x_1^2}\, dx_1 = -\frac{dx_1}{z_1 \tan \varkappa_1}\, \sigma_1^2$$

we have

$$c_{x,\,FG} = \frac{-8\lambda_1^2 z_1 \tan \varkappa_1}{b\pi\alpha' \sqrt{n^2 - 1}} \int_{\sigma_{1F}}^{\sigma_{1G}} \cosh^{-1} \sqrt{\frac{n_1^2 - \sigma_1^2}{1 - \sigma_1^2}} \cdot \frac{d\sigma_1}{\sigma_1^2} \tag{8.4.3}$$

where $\sigma_{1F} = z_1 \tan \varkappa_1/x_F = 1$, and $\sigma_{1G} = z_1 \tan \varkappa_1/x_G$.

Region GH is acted upon by the distribution of the sources in triangle OCC' with a strength of $Q = 2\lambda_1 V_\infty$ and in triangle BCC' where the strength of the sources $Q = 2(\lambda_2 - \lambda_1) V_\infty$ (the sign of the angle λ_2 is opposite to that of λ_1).

Since region GH is behind Mach line OK_0 within the limits of the wing, the pressure coefficient due to the distributed sources in region OCC' must be calculated with the aid of formula (8.3.19). The influence of the distribution of sources in triangle BCC' on the pressure coefficient should be taken into account with the aid of relation (8.3.21) because region GH is outside triangle BCC' between Mach wave $B'K_B$ and edge BC. Hence,

$$\bar{p}_{GH} = \frac{4\lambda_1}{\pi\alpha' \sqrt{n^2 - 1}} \cosh^{-1} \sqrt{\frac{n_1^2 - \sigma_1^2}{1 - \sigma_1^2}} + \frac{4(\lambda_2 - \lambda_1)}{\pi\alpha' \sqrt{n_1^2 - 1}} \cosh^{-1} \sqrt{\frac{n_2^2 - 1}{\sigma_2^2 - 1}} \tag{8.4.4}$$

where $n_2 = \tan \varkappa_2/\alpha'$; $\sigma_2 = z_1 \tan \varkappa_2/x_2$, and x_2 is the coordinate measured from point B and equal to $x_2 = x_1 - x_B$.

Using formulas (8.4.2) and (8.4.4), let us determine the drag coefficient corresponding to region GH:

$$c_{x,\,GH} = -\frac{8\lambda_1^2 z_1 \tan \varkappa_1}{b\pi\alpha' \sqrt{n_1^2-1}} \int_{\sigma_{1G}}^{\sigma_{1H}} \cosh^{-1} \sqrt{\frac{n_1^2-\sigma_1^2}{1-\sigma_1^2}} \cdot \frac{d\sigma_1}{\sigma_1^2}$$

$$-\frac{8(\lambda_2-\lambda_1)\lambda_1 z_1 \tan \varkappa_2}{b\pi\alpha' \sqrt{n_2^2-1}} \int_{\sigma_{2G}}^{\sigma_{2H}} \cosh^{-1} \sqrt{\frac{n_2^2-1}{\sigma_2^2-1}} \cdot \frac{d\sigma_2}{\sigma_2^2} \qquad (8.4.5)$$

where σ_{2H} and σ_{2G} are evaluated relative to point B.

Summing (8.4.3) and (8.4.5) and taking into account that

$$\sigma_{1F} = \frac{z_1 \tan \varkappa_1}{x_F} = 1, \quad \sigma_{1H} = \frac{z_1 \tan \varkappa_1}{x_H} = \frac{z_1 \tan \varkappa_1}{x_B + z_1 \operatorname{tg} \varkappa_2}$$

$$\sigma_{2G} = \frac{z_1 \tan \varkappa_2}{x_G} = \tan \mu_\infty \tan \varkappa_2 = \frac{\tan \varkappa_2}{\alpha'} = n_2, \quad \sigma_{2H} = \frac{z_1 \tan \varkappa_2}{x_H} = 1$$

we obtain

$$c_{x,\,FH} = c_{x,\,FG} + c_{x,\,GH}$$

$$= -\frac{8\lambda_1^2 z_1 \tan \varkappa_1}{b\pi\alpha' \sqrt{n_1^2-1}} \int_1^{\frac{z_1 \tan \varkappa_1}{x_B + z_1 \tan \varkappa_2}} \cosh^{-1} \sqrt{\frac{n_1^2-\sigma_1^2}{1-\sigma_1^2}}$$

$$\times \frac{d\sigma_1}{\sigma_1^2} - \frac{8(\lambda_2-\lambda_1)\lambda_1 z_1 \tan \varkappa_2}{b\pi\alpha' \sqrt{n_2^2-1}} \int_{n_2}^{1} \cosh^{-1} \sqrt{\frac{n_2^2-1}{\sigma_2^2-1}} \cdot \frac{d\sigma_2}{\sigma_2^2} \qquad (8.4.6)$$

Let us assume that part of chord HL (we presume that point H is on line BC) equals $\bar{r}b$, where $\bar{r}$ is a dimensionless coefficient of proportionality determined from the condition $\bar{r} = B'D/b_0$ (here b_0 is the central chord). Therefore, for surface OBC, the part of chord FH will be $(1 - \bar{r})\, b$.

Since a part of central chord $B'D$ equals $\bar{r}b_0$, the remaining part OB' equals $(1 - \bar{r})\, b_0$. The angles are

$$\lambda_1 = \bar{\Delta}/2\,(1 - \bar{r}), \quad \lambda_2 = -\bar{\Delta}/(2\bar{r}) \qquad (8.4.7)$$

where $\bar{\Delta} = \Delta/b_0$ is the relative thickness of the airfoil.

Taking into account the values of λ_1 and λ_2 we can write formula (8.4.6) as:

$$c_{x,\,FH} = -\frac{2\bar{\Delta}^2 z_1}{b(1-\bar{r})\pi\alpha'} \left[\frac{\tan \varkappa_1}{\sqrt{n_1^2-1}} \int_1^{\frac{z_1 \tan \varkappa_1}{(1-\bar{r})b_0 + z_1 \tan \varkappa_2}} \cosh^{-1} \sqrt{\frac{n_1^2-\sigma_1^2}{1-\sigma_1^2}} \right.$$

$$\left. \times \frac{d\sigma_1}{\sigma_1^2} + \frac{\operatorname{ta}\, \varkappa_2}{\bar{r}\sqrt{n_2^2-1}} \int_1^{n_2} \cosh^{-1} \sqrt{\frac{n_2^2-1}{\sigma_2^2-1}} \cdot \frac{d\sigma_2}{\sigma_2^2} \right] \qquad (8.4.8)$$

The velocity on line HJ is induced by sources of the strength $Q = 2\lambda_1 V_\infty$ distributed in triangle OCC' and by sources of the strength $Q = 2(\lambda_2 - \lambda_1) V_\infty$ distributed over region BCC'. The first distribution of the sources gives rise to the pressure coefficient calculated by formula (8.3.19) in which we must assume that $\lambda = \lambda_1$, $n = n_1$, and $\sigma = \sigma_1$. The pressure coefficient due to the influence of the second distribution of the sources is also found with the aid of formula (8.3.19) in which we must assume that $\lambda = \lambda_2 - \lambda_1$, $n = n_2$, and $\sigma = \sigma_2$. Summation of the pressure coefficients yields

$$\bar{p}_{HJ} = \frac{4\lambda_1}{\pi\alpha' \sqrt{n_1^2 - 1}} \cosh^{-1} \sqrt{\frac{n_1^2 - \sigma_1^2}{1 - \sigma_1^2}} + \frac{4(\lambda_2 - \lambda_1)}{\pi\alpha' \sqrt{n_2^2 - 1}} \cosh^{-1} \sqrt{\frac{n_2^2 - \sigma_2^2}{1 - \sigma_2^2}} \tag{8.4.9}$$

Using formula (8.4.5) in which we must replace the value of λ_1 with λ_2 and taking into account that

$$\lambda_1 = \bar{\Delta}/[2(1 - \bar{r})], \quad \lambda_2 - \lambda_1 = -\bar{\Delta}^2/[2\bar{r}(1 - \bar{r})], \quad \lambda_2 = -\bar{\Delta}(2\bar{r})$$

$$n_1 = \tan \varkappa_1/\alpha', \quad n_2 = \tan \varkappa_2/\alpha', \quad \sigma_1 = z_1 \tan \varkappa_1/x_1$$

$$\sigma_2 = z_2 \tan \varkappa_2/x_2', \quad x_H \leqslant x_1 \leqslant x_J, \quad x_2' = x_1 - x_H$$

we obtain

$$c_{x,HJ} = \frac{-2\bar{\Delta}^2 z_1}{b\bar{r}(1-\bar{r})\pi\alpha'} \left[\frac{\tan \varkappa_1}{\sqrt{n_1^2 - 1}} \int_{\sigma_{1H}}^{\sigma_{1J}} \cosh^{-1} \sqrt{\frac{n_1^2 - \sigma_1^2}{1 - \sigma_1^2}} \cdot \frac{d\sigma_1}{\sigma_1^2} - \frac{\tan \varkappa_2}{\sqrt{n_2^2 - 1}} \int_{\sigma_{2H}}^{\sigma_{2J}} \cosh^{-1} \sqrt{\frac{n_2^2 - \sigma_2^2}{1 - \sigma_2^2}} \cdot \frac{d\sigma^2}{\sigma_2^2} \right] \tag{8.4.10}$$

where σ_2 is evaluated relative to point B.

On JL, we take into account the influence of three distributions of the sources, namely, on triangular surfaces OCC', BCC' and DCC'. The first two distributions give rise to the pressure coefficient determined with the aid of formula (8.4.9) in which σ_1 and σ_2 are calculated relative to points O and D, respectively. The additional coefficient of pressure induced by the sources distributed over region DCC' with a strength of $-\lambda_2$ is found with the aid of formula (8.3.21) in which we must assume that $\lambda = \lambda_2$, $n = n_3$, and $\sigma = \sigma_3$.

Summing the pressure coefficients due to all three source distributions, we obtain

$$\bar{p}_{JL} = \frac{4\lambda_1}{\pi\alpha' \sqrt{n_1^2 - 1}} \cosh^{-1} \sqrt{\frac{n_1^2 - \sigma_1^2}{1 - \sigma_1^2}} + \frac{4(\lambda_2 - \lambda_1)}{\pi\alpha' \sqrt{n_2^2 - 1}} \times \cosh^{-1} \sqrt{\frac{n_2^2 - \sigma_2^2}{1 - \sigma_2^2}} - \frac{4\lambda_2}{\pi\alpha' \sqrt{n_3^2 - 1}} \cosh^{-1} \sqrt{\frac{n_3^2 - 1}{\sigma_3^2 - 1}} \tag{8.4.11}$$

where $n_3 = \tan \varkappa_3/\alpha'$; the values of σ_1, σ_2, and σ_3 are calculated relative to points O, B and D.

Introducing the value of $\bar{p}_{JL}$ into formula (8.4.2) and substituting λ_2 for λ_1 in it, we obtain

$$c_{x,\,JL} = -\frac{2\bar{\Delta}^2 z_1}{b\bar{r}\pi\alpha'}\left[\frac{\tan\varkappa_1}{(1-\bar{r})\sqrt{n_1^2-1}}\int\limits_{\sigma_{1J}}^{\sigma_{1L}}\cosh^{-1}\sqrt{\frac{n_1^2-\sigma_1^2}{1-\sigma_1^2}}\cdot\frac{d\sigma_1}{\sigma_1^2}\right.$$

$$-\frac{\tan\varkappa_2}{\bar{r}(1-\bar{r})\sqrt{n_2^2-1}}\int\limits_{\sigma_{2J}}^{\sigma_{2L}}\cosh^{-1}\sqrt{\frac{n_2^2-\sigma_2^2}{1-\sigma_2^2}}\cdot\frac{d\sigma_2}{\sigma_2^2}$$

$$\left.+\frac{\tan\varkappa_3}{\bar{r}\sqrt{n_3^2-1}}\int\limits_{\sigma_{3J}}^{\sigma_{3L}}\cosh^{-1}\sqrt{\frac{n_3^2-1}{\sigma_3^2-1}}\cdot\frac{d\sigma_3}{\sigma_3^2}\right] \qquad (8.4.12)$$

Summing (8.4.10) and (8.4.12), we have

$$c_{x,\,HL} = -\frac{2\bar{\Delta}^2 z_1}{b\bar{r}\pi\alpha'}\left[\frac{\tan\varkappa_1}{(1-\bar{r})\sqrt{n_1^2-1}}\int\limits_{\sigma_{1H}}^{\sigma_{1L}}\cosh^{-1}\sqrt{\frac{n_1^2-\sigma_1^2}{1-\sigma_1^2}}\cdot\frac{d\sigma_1}{\sigma_1^2}\right.$$

$$-\frac{\tan\varkappa_2}{\bar{r}(1-\bar{r})\sqrt{n_2^2-1}}\int\limits_{\sigma_{2H}}^{\sigma_{2L}}\cosh^{-1}\sqrt{\frac{n_2^2-\sigma_2^2}{1-\sigma_2^2}}\cdot\frac{d\sigma_2}{\sigma_2^2}$$

$$\left.+\frac{\tan\varkappa_3}{\bar{r}\sqrt{n_3^2-1}}\int\limits_{\sigma_{3J}}^{\sigma_{3L}}\cosh^{-1}\sqrt{\frac{n_3^2-1}{\sigma_3^2-1}}\cdot\frac{d\sigma_3}{\sigma_3^2}\right] \qquad (8.4.13)$$

In this expression

$$\left.\begin{aligned}\sigma_{1H} &= \frac{z_1\tan\varkappa_1}{(1-\bar{r})\,b_0+z_1\tan\varkappa_2}, \quad \sigma_{1L} = \frac{z_1\tan\varkappa_1}{b_0+z_1\tan\varkappa_3}\\ \sigma_{2H} &= 1, \quad \sigma_{2L} = \frac{z_1\tan\varkappa_2}{\bar{r}b_0+z_1\tan\varkappa_3}\\ \sigma_{3J} &= \frac{z_1\tan\varkappa_3}{x_J'} = n_3, \quad \sigma_{3L} = \frac{z_1\tan\varkappa_3}{x_L'} = 1\end{aligned}\right\} \qquad (8.4.13')$$

where $x_J' = z_1\cot\mu_\infty = z_1\alpha'$, and $x_L' = z_1\tan\varkappa_3$.

We take the integrals in formulas (8.4.8) and (8.4.13) by parts. These formulas hold (see Fig. 8.4.1) when

$$0 < z_1 < z_{B_1} < z_{D_1} \qquad (8.4.14)$$

where

$$z_{B_1} = (1-\bar{r})\,b_0/(\tan\varkappa_1 - \alpha'), \quad z_{D_1} = \bar{r}b_0/(\tan\varkappa_2 - \alpha') \qquad (8.4.15)$$

or (Fig. 8.4.2) when

$$0 < z_1 < z_{D_1} < z_{B_1} \tag{8.4.16}$$

The drag coefficient of the airfoil determined by formula (8.4.13) has been related to the local chord b. We calculate the value of the drag coefficient $c_{x,0}$ related to the central chord b_0 by the formula $c_{x,0} = c_x (b/b_0)$.

Airfoil in the Mid-Span Section ($z = 0$). We determine the values of the aerodynamic coefficients for this airfoil as follows. On airfoil section OB (see Fig. 8.4.1) with a length of $(1 - \bar{r})\, b_0$, the velocity is induced by sources having a strength of $Q = 2\lambda_1 V_\infty$ distributed in triangle OCC'.

Accordingly, we evaluate the pressure coefficient by formula (8.3.19). Assuming that $\sigma = z_1 \tan \varkappa_1 / x_1 = 0$, we obtain

$$\bar{p}_{OB} = \frac{4\lambda_1}{\pi\alpha' \sqrt{n_1^2 - 1}} \cosh^{-1} n_1 \tag{8.4.17}$$

Airfoil section DB with a length of $\bar{r}b_0$ experiences the action of sources with a strength of $Q = 2\lambda_1 V_\infty$ distributed over region OCC' and with a strength of $Q = 2(\lambda_2 - \lambda_1) V_\infty$ distributed in triangle BCC'. In accordance with this, we determine the pressure coefficients. Using formula (8.3.19) at $\sigma = 0$, we find

$$\bar{p}_{BD} = \frac{4\lambda_1}{\pi\alpha' \sqrt{n_1^2 - 1}} \cosh^{-1} n_1 + \frac{4(\lambda_2 - \lambda_1)}{\pi\alpha' \sqrt{n_2^2 - 1}} \cosh^{-1} n_2 \tag{8.4.18}$$

The drag coefficient of the airfoil with account taken of the upper and bottom surfaces related to the central chord b_0 is

$$c_x = \frac{2}{b_0} \int_0^{(1-\bar{r})b_0} \bar{p}_{OB}\lambda_1\, dx + \frac{2}{b_0} \int_0^{\bar{r}b_0} \bar{p}_{BD}\lambda_2\, dx \tag{8.4.19}$$

Introducing the value of $\bar{p}_{OB}$ from (8.4.17), of $\bar{p}_{BD}$ from (8.4.18), and having in view that $\lambda_2 = -\bar{\Delta}/(2\bar{r})$, $\lambda_2 - \lambda_1 = -\bar{\Delta}/[2\bar{r}(1 - \bar{r})]$ and also that $(1 - r)\lambda_1 = \bar{\Delta}/2$ and $\bar{r}\lambda_2 = -\bar{\Delta}/2$, we obtain

$$c_x = \frac{2\bar{\Delta}^2}{\pi\alpha' \bar{r}(1-\bar{r}) \sqrt{n_2^2 - 1}} \cosh^{-1} n_2 \tag{8.4.20}$$

where $\cosh^{-1} n_2 = \ln (n_2 + \sqrt{n_2^2 - 1})$.

Airfoil F_1L_1. Let us calculate the drag coefficient of an airfoil (see Fig. 8.4.1) whose coordinate z_1 satisfies the inequality $z_{B_1} < z_1 < z_{D_1}$. Section F_1H_1 of the airfoil experiences the action of sources with the strength $Q = 2\lambda_1 V_\infty$ distributed in region $OCDC'$, and with the strength $Q = 2(\lambda_2 - \lambda_1) V_\infty$ distributed in BCC'. Therefore, we may use formula (8.4.4) to calculate the pressure

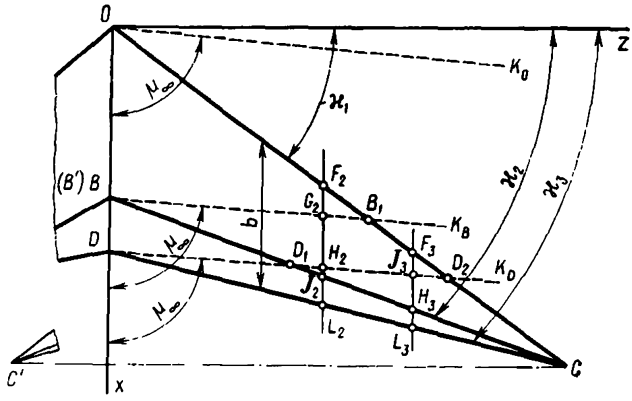

Fig. 8.4.2
Arrangement of Mach lines

coefficient, and relation (8.4.5) to determine the drag coefficient. For airfoil section F_1H_1, relation (8.4.5) has the form

$$c_{x,\,F_1H_1} = -\frac{8\lambda_1^2 z_1 \tan \varkappa_1}{b\pi\alpha' \sqrt{n_1^2-1}} \int_{\sigma_{1F_1}}^{\sigma_{1H_1}} \cosh^{-1} \sqrt{\frac{n_1^2-\sigma_1^2}{1-\sigma_1^2}} \cdot \frac{d\sigma_1}{\sigma_1^2}$$

$$-\frac{8(\lambda_2-\lambda_1)\lambda_1 z_1 \tan \varkappa_2}{b\pi\alpha' \sqrt{n_2^2-1}} \int_{\sigma_{2F_1}}^{\sigma_{2H_1}} \cosh^{-1} \sqrt{\frac{n_2^2-1}{\sigma_2^2-1}} \cdot \frac{d\sigma_2}{\sigma_2^2} \qquad (8.4.21)$$

where σ_1 and σ_2 are calculated relative to points O and B, respectively.

We determine the pressure on airfoil section H_1L_1 in the same way as on HL with the aid of formulas (8.4.9) and (8.4.11). We find the corresponding drag coefficient c_{x_1,H_1L_1} from expression (8.4.13) in which we replace the limits σ_{1H} and σ_{1L} with the quantities σ_{1H_1} and σ_{1L_1}, the limits σ_{2H} and σ_{2L} with the quantities σ_{2H_1} and σ_{2L_1}, and the limits σ_{3J} and σ_{3L} with the quantities σ_{3J_1} and σ_{3L_1}, respectively, determined by formulas (8.4.13'). The overall drag coefficient for the airfoil F_1L_1 related to the central chord b_0 is

$$c_{x,\,F_1L_1} = c_{x,\,F_1H_1} + c_{x,\,H_1L_1}$$

Airfoil F_2L_2. Let us consider the airfoil between points D_1 and B_1 (Fig. 8.4.2) with the coordinate z_1 satisfying the inequality $z_{D_1} < z_1 < z_{B_1}$. The flow over this airfoil is of a more intricate nature. The velocity on section F_2G_2 is induced by sources having the strength $Q = 2\lambda_1 V_\infty$ distributed in triangle OCC'. Consequently, the pressure coefficient on this section is determined with the aid of formula (8.4.1), and the corresponding drag coefficient $c_{x,\,F_2G_2}$ from expression (8.4.3) in which the integral is taken between the limits σ_{1F_2} and σ_{1G_2}.

The pressure on section G_2H_2 depends on the influence of sources having a strength of $Q = 2\lambda_1 V_\infty$ distributed over section OCC', and also of sources having a strength of $Q = 2(\lambda_2 - \lambda_1) V_\infty$ in region BCC'. Consequently, we calculate the pressure coefficient by formula (8.4.4), and the drag coefficient $c_{x,\,G_2H_2}$ from expression (8.4.5) in which we take the first integral between the limits σ_{1G_2} and σ_{1H_2}, and the second between σ_{2G_2} and σ_{2H_2}.

Section H_2J_2 experiences the simultaneous action of sources distributed in region OCC' ($Q = 2\lambda_1 V_\infty$), and also in triangle BCC' [$Q = 2(\lambda_2 - \lambda_1) V_\infty$] and on surface BCC', where the strength $Q = -2\lambda_2 V_\infty$. The first distribution results in a pressure coefficient determined by formula (8.3.19), and the second two distributions result in the coefficient calculated by expression (8.3.21).

The total value of the pressure coefficient on this section of the airfoil is

$$\bar{p}_{H_2J_2} = \frac{4\lambda_1}{\pi\alpha' \sqrt{n_1^2-1}} \cosh^{-1} \sqrt{\frac{n_1^2-\sigma_1^2}{1-\sigma_1^2}} + \frac{4(\lambda_2-\lambda_1)}{\pi\alpha' \sqrt{n_1^2-1}} \times \cosh^{-1} \sqrt{\frac{n_2^2-1}{\sigma_2^2-1}} - \frac{4\lambda_2}{\pi\alpha' \sqrt{n_3^2-1}} \cosh^{-1} \sqrt{\frac{n_3^2-1}{\sigma_3^2-1}} \quad (8.4.22)$$

where σ_1, σ_2, and σ_3 are determined relative to points O, B, and D, respectively.

By using the formula

$$c_{x,\,H_2J_2} = \frac{2}{b_0} \int_{x_{H_2}}^{x_{J_2}} \bar{p}_{H_2J_2} \lambda_2 \, dx \quad (8.4.23)$$

we can calculate the drag coefficient for the section of the airfoil being considered related to the length b_0 of the centre chord.

The flow over the last airfoil section J_2L_2 is the result of induction by the sources distributed in the same regions of the wing as for airfoil section H_2J_2. Here account must be taken of the feature that the velocity induced by the sources in region BCC' is determined by formula (8.3.18), where λ is replaced by the angular coefficient $\lambda_2 - \lambda_1$. Therefore, the pressure coefficient should be calculated by formula (8.4.11), and the drag coefficient $c_{x,\,J_2L_2}$ from expression (8.4.12) in which we take the integrals between the limits σ_{nJ_2} and σ_{nL_2} ($n = 1, 2, 3$).

We obtain the total drag coefficient by summation of the coefficients for all four sections of the airfoil:

$$c_{x,\,F_2L_2} = c_{x,\,F_2G_2} + c_{x,\,G_2H_2} + c_{x,\,H_2J_2} + c_{x,\,J_2L_2}$$

provided that the value of z_1 satisfies the inequality

$$\frac{\bar{r}b_0}{\tan\chi_1 - \alpha'} < z_1 < \frac{(1-\bar{r})\,b_0}{\tan\chi_1 - \alpha'}$$

Airfoil F_3L_3. Let us consider section F_3L_3 (Fig. 8.4.2) with the coordinate z_1 satisfying the inequality

$$z_{D_1} < z_1 < z_{D_2} \tag{8.4.24}$$

where

$$z_{D_2} = b_0/(\tan \varkappa_1 - \alpha') \tag{8.4.25}$$

The pressure on section F_3J_3 of the airfoil is due to the action of sources distributed on the triangular surfaces OCC' ($Q = 2\lambda_1 V_\infty$) and BCC' [$Q = 2(\lambda_2 - \lambda_1) V_\infty$]. We shall therefore calculate the pressure coefficient by expression (8.4.4), and the drag coefficient by formula (8.4.5) in which we replace the limits $\sigma_{n,G}$ and $\sigma_{n,H}$ with the values σ_{n,F_3} and σ_{n,J_3} ($n = 1, 2$).

Airfoil section J_3H_3, in addition to the indicated source distributions in regions OCC' and BCC', also experiences the action of sources having a strength of $Q = -2\lambda_2 V\mathrm{L}$ distributed in triangle DCC'. Consequently, the pressure coefficient equals the value calculated by formula (8.4.4) plus the additional value calculated by formula (8.3.21) in which we assume that $\lambda = -\lambda_2$.

Flow over section H_3L_3 is characterized by the induction of sources distributed in three regions of the wing, namely, OCC', BCC', and DCC'. Accordingly, the pressure coefficient on this section should be calculated with the aid of formula (8.4.11).

By calculating the relevant components of the drag coefficient for all three sections and summing them, we obtain the total drag coefficient:

$$c_{x,F_3L_3} = c_{x,F_3J_3} + c_{x,J_3H_3} + c_{x,H_3L_3}$$

The relevant expression is suitable for calculating the drag coefficient of the airfoil between points D_1 and D_2 (Fig. 8.4.2) with the coordinate z_1 that satisfies the inequality

$$\frac{\bar{r}b_0}{\tan \varkappa_2 - \alpha'} < z_1 < \frac{b_0}{\tan \varkappa_1 - \alpha'} \tag{8.4.26}$$

Airfoil F_4L_4. Let as consider section F_4L_4 (see Fig. 8.4.1) with coordinate

$$z_1 > z_{D_2} \tag{8.4.27}$$

Three source distributions simultaneously act on this section, namely, OCC' ($Q = 2\lambda_1 V_\infty$), BCC' [$Q = 2(\lambda_2 - \lambda_1) V_\infty$], and DCC' ($Q = -2\lambda_2 V_\infty$). Airfoil section F_4H_4 is behind Mach line OK_0 within the confines of the wing, therefore to calculate the pressure produced by the distribution of the sources in OCC' we must use formula (8.3.19) in which we assume that $\lambda = \lambda_1$. The second distribution of the sources in BCC' acts on section F_4H_4 located beyond the confines of the surface between the Mach line and edge BC. Therefore, to calculate the additional pressure due to the influence of the distribution of the sources in BCC', we must use formula (8.3.21) with the substitution of $\lambda_2 - \lambda_1$ for λ.

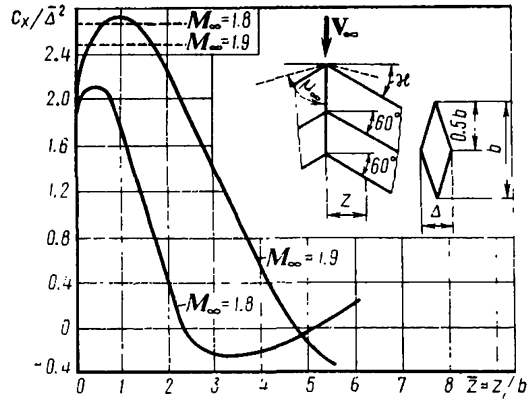

Fig. 8.4.3
Distribution of the drag coefficient over the span of a swept constant chord wing with subsonic edges
(the dashed line shows an unswept wing)

The second section of airfoil H_4L_4 is located within the confines of the wing surface, i.e. at the same side from the Mach lines and the relevant edges OC and BC. Consequently, to determine the pressure coefficient resulting from the distributions of the sources in OCC' and BCC', we use formula (8.3.19) in which the value $\lambda = \lambda_1$ corresponds to the distribution in OCC', and the value $\lambda = \lambda_2 - \lambda_1$ to the distribution in BCC'.

Section H_4L_4 is at both sides of Mach line DK_D and trailing edge DC, i.e. it is beyond the confines of triangular surface DCC' where the strength of the sources is $Q = -2\lambda_2 V_\infty$. Hence, to calculate the pressure coefficient produced by these sources, we should use formula (8.3.21) with the substitution of $-\lambda_2$ for λ.

Using the obtained value of the pressure coefficient, we can determine the relevant drag coefficient for airfoil F_4L_4:

$$c_{x,\,F_4L_4} = c_{x,\,F_4H_4} + c_{x,\,H_4L_4}$$

Figure 8.4.3 shows the results of calculating the distribution of the drag coefficient $c_x/\bar{\Delta}^2$ ($\bar{\Delta} = \Delta/b$) over the span of a swept constant chord (b) wing ($\varkappa_1 = \varkappa_2 = \varkappa_3 = 60°$) with a symmetric rhombiform airfoil ($\bar{r} = 1/2$) for $M_\infty = 1.8$ and 1.9. A glance at the figure reveals that with an increase in the distance from the centre chord, the drag coefficient first grows somewhat, and then sharply drops. For purposes of comparison, the figure shows the value of the function $c_x/\bar{\Delta}^2$ for an airfoil belonging to an unswept wing.

To determine the total drag coefficient of the wing, we must integrate the distribution of the drag coefficients $c_{x,k}$ of the airfoils over the span, using the formula

$$c_x = \frac{2}{l}\int_0^{l/2} c_{x,k}\,dz \qquad (8.4.28)$$

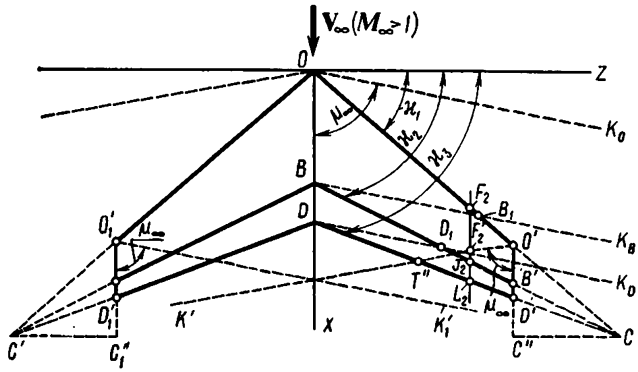

Fig. 8.4.4
Wing with side edges

Influence of a Side Edge on the Flow over a Wing. If a wing has a wide tip or side edge (Fig. 8.4.4), its influence on the pressure distribution and the drag coefficient must be taken into account. The flow over such a hexagonal wing is calculated as follows. First the velocities and pressures in region $OO'D'D$ produced by the distribution of the sources on triangular area OCD are calculated. The calculations in this case are performed similar to those of a wing with a tetragonal planform (see Fig. 8.4.1) having no side edges. Next the calculated velocities and pressures are determined more precisely with account taken of the influence of side edge $O'C''$, which is equivalent to the action of sources distributed in triangle $O'CD'$. The strength of these sources has a sign opposite to that of the sources corresponding to a wing of area $O'CD'$. The action of the sources distributed in triangle $O'CD'$ extends to the wing within the area $O'T''D'$ confined by Mach line $O'K'$, the side edge, and the trailing edge. For example, for airfoil F_2L_2, the action of the sources is confined by section $F_2'L_2$ (point F_2' is at the intersection of chord F_2L_2 and Mach line $O'K'$).

Let us see how the pressure is evaluated on section J_2L_2 of this airfoil. Taking into consideration only the distribution of the sources in region OCC', we can determine the pressure coefficient by formula (8.4.11). We can introduce the correction $\Delta\bar{p}$ for the action of sources of opposite signs in triangle $O'CD'$, so that

$$\bar{p}_{J_2L_2} = \bar{p}_{JL} - \Delta\bar{p} \qquad (8.4.29)$$

When finding the correction $\Delta\bar{p}$ we must take account of the position of airfoil section J_2L_2 relative to Mach line $O_1'K_1'$ that passes through point O_1' belonging to the opposite side edge (Fig. 8.4.4). If this line does not intersect J_2L_2, the latter is influenced only by the distribution of the sources in region $O'CD'$ of one side of the

wing, whereas the influence of the sources in $O_1'C'D_1'$ is excluded. The induced velocity is calculated by formula (8.3.13), and the corresponding additional value of the pressure coefficient by the formula $\Delta\bar{p} = -2u/V_\infty$. We shall write this additional value in the form of the sum

$$\Delta\bar{p} = \Delta\bar{p}_1 + \Delta\bar{p}_2 + \Delta\bar{p}_3 \tag{8.4.30}$$

where $\Delta\bar{p}_1$ depends on the distribution of the sources in $O'CC''$ ($Q = 2\lambda_1 V_\infty$), while $\Delta\bar{p}_2$ and $\Delta\bar{p}_3$ depend on the distribution of the sources in $B'CC''$ [$Q = 2(\lambda_2 - \lambda_1) V_\infty$] and $D'CC''$ ($Q = -2\lambda_2 V_\infty$).

Hence, by using formula (8.3.14), we obtain

$$\begin{aligned}\Delta\bar{p} = &\frac{2\lambda_1}{\pi\alpha' \sqrt{n_1^2-1}} \cosh^{-1} \frac{n_1^2+\sigma_1}{n_1(1+\sigma_1)} \\ &+ \frac{2(\lambda_2-\lambda_1)}{\pi\alpha' \sqrt{n_2^2-1}} \cosh^{-1} \frac{n_2^2+\sigma_2}{n_2(1+\sigma_2)} \\ &- \frac{2\lambda_2}{\pi\alpha' \sqrt{n_3^2-1}} \cosh^{-1} \frac{n_3^2+\sigma_3}{n_3(1+\sigma_3)}\end{aligned} \tag{8.4.31}$$

where σ_1, σ_2 and σ_3 are calculated relative to points O', B', and D'.

If Mach line $O_1'K_1'$ intersects chord F_2L_2, then simultaneously with the action of sources $O'CC''$ account must also be taken of the influence of the sources distributed in triangle $O_1'C'C_1''$ at the opposite side of the wing. The same formula (8.3.13) is used to calculate the induced velocity.

8.5. Flow over a Tetragonal Symmetric Airfoil Wing with Edges of Different Kinds (Subsonic and Supersonic)

Leading and Middle Edges Are Subsonic Trailing Edge Is Supersonic

The disturbances from the trailing supersonic edges of a wing (Fig. 8.5.1*a*) propagate downstream within the confines of the Mach cone with the generatrix DK_D and therefore do not affect the flow over the wing surface. The velocities and pressures depend on the influence of the leading and middle subsonic edges.

Let us consider profile FL with the coordinate $z_1 < z_{B_1}$. The pressure coefficient on section FG, which depends on the action of sources having a strength of $Q = 2\lambda_1 V_\infty$ that are distributed in triangle OCC', is determined from (8.4.1), and the corresponding drag coefficient $c_{x,\,FG}$, from (8.4.3). On the following section GH experiencing the influence of the sources distributed in triangles OCC' ($Q = 2\lambda_1 V_\infty$) and BCC' [$Q = 2(\lambda_2 - \lambda_1) V_\infty$], the pressure

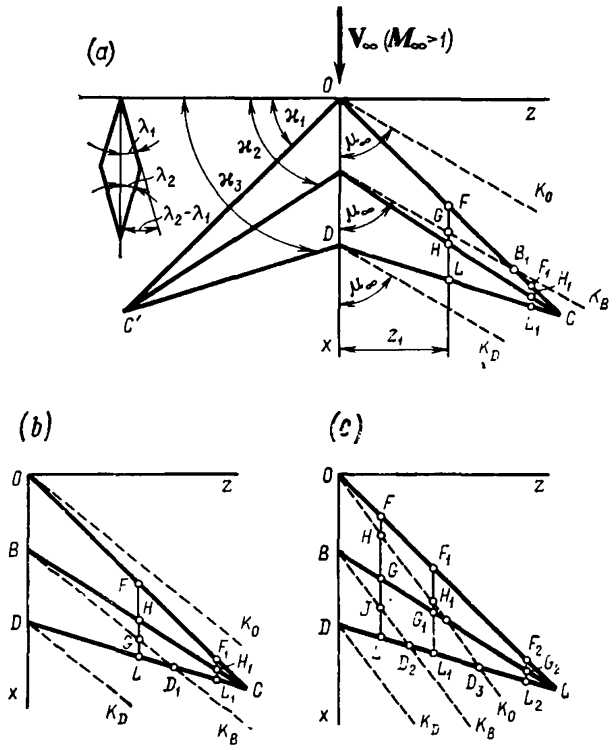

Fig. 8.5.1
Tetragonal wing in a supersonic flow:
a—the leading and middle edges are subsonic, the trailing edge is supersonic; *b*—the leading edge is subsonic, the middle and trailing edges are supersonic; *c*—all the edges are supersonic

coefficient is calculated by (8.4.4). The corresponding value of the drag coefficient $c_{x,\,GH}$ for this section is determined from (8.4.5).

The action of the same source distributions is observed on section HL as on section GH. But taking into account that section HL is below Mach line BK_B (on the wing surface), the pressure coefficient $\bar{p}_{HL}$ must be calculated from (8.4.9), and the drag coefficient $c_{x,\,HL}$, from (8.4.10). The total drag coefficient of the airfoil is

$$c_{x,\,FL} = c_{x,\,FG} + c_{x,\,GH} + c_{x,\,HL} \qquad (8.5.1)$$

When considering section F_1L_1 with the coordinate $z_1 > z_{B_1}$, account must be taken simultaneously of the source distributions in OCC' and BCC'. For section F_1H_1, the drag coefficient $c_{x,\,F_1H_1}$ is determined by formula (8.4.21). For section H_1L_1 the drag coefficient $c_{x,\,H_1L_1}$ is found by expression (8.4.13) in which the third term in the brackets is taken equal to zero, while the limits $\sigma_{n,H}$ and $\sigma_{n,L}$

are replaced with the values $\sigma_{n,\,H_1}$ and $\sigma_{n,\,L_1}(n = 1, 2)$, respectively. The total drag coefficient for airfoil F_1L_1 is

$$c_{x,\,F_1L_1} = c_{x,\,F_1H_1} + c_{x,\,H_1L_1} \tag{8.5.2}$$

Leading Edge Is Subsonic, Middle and Trailing Edges are Supersonic

A feature of the flow over the wing (Fig. 8.5.1*b*) consists in that the sources distributed in region BDD_1 do not affect the distribution of the velocities and pressures on the remaining part of the wing above Mach line BK_B.

Let us consider airfoil FL with the coordinate $z_1 < z_{D_1}$. Section FH of this airfoil is acted upon by the sources distributed in triangle OCC' (Fig. 8.5.1*a*); consequently, the pressure distribution can be found from (8.4.1), and the corresponding drag coefficient $c_{x,\,FH}$, from (8.4.3) in which σ_{1H} is substituted for the upper limit σ_{1G}. The second section HG is influenced by subsonic leading edge OC (and, therefore, the distribution of the sources in OCC') and by supersonic middle edge BC. The corresponding pressure coefficient is determined as the sum of two coefficients, the first of which is evaluated by expression (8.4.1), and the second by (8.3.23) where we assume $\lambda = \lambda_2 - \lambda_1$ and $n = n_2$. Consequently,

$$\bar{p}_{HG} = \frac{4\lambda_1}{\pi\alpha' \sqrt{n_1^2 - 1}} \cosh^{-1} \sqrt{\frac{n_1^2 - \sigma_1^2}{1 - \sigma_1^2}} + \frac{2(\lambda_2 - \lambda_1)}{\alpha' \sqrt{1 - n_2^2}} \tag{8.5.3}$$

On section GL, the velocity is induced by the sources distributed in triangles OCC' and BCC' (Fig. 8.5.1*a*). By using formulas (8.5.3) and (8.3.34), we obtain the following working relation for the pressure coefficient:

$$\bar{p}_{GL} = \frac{4\lambda_1}{\pi\alpha' \sqrt{n_1^2 - 1}} \cosh^{-1} \sqrt{\frac{n_1^2 - \sigma_1^2}{1 - \sigma_1^2}} + \frac{2(\lambda_2 - \lambda_1)}{\alpha' \sqrt{1 - n_2^2}} \left(1 - \frac{2}{\pi} \sin^{-1} \sqrt{\frac{n_2^2 - \sigma_2^2}{1 - \sigma_2^2}}\right) \tag{8.5.4}$$

The drag coefficient of the airfoil is

$$c_{x,\,FL} = \frac{2}{b} \left(\int_{x_F}^{x_H} \bar{p}_{FH}\lambda_1\, dx + \int_{x_H}^{x_G} \bar{p}_{HG}\lambda_2\, dx + \int_{x_G}^{x_L} \bar{p}_{GL}\lambda_2\, dx \right) \tag{8.5.5}$$

Airfoil F_1L_1 is below Mach line OK_O, therefore it is influenced by the distribution of sources with a strength of $Q = 2\lambda_1 V_\infty$ in triangle

OCC'. In addition, section H_1L_1 is acted upon by the distribution of sources with a strength of $Q = 2(\lambda_2 - \lambda_1) V_\infty$ in triangle BCC' that produces an additional pressure evaluated by formula (8.3.23), where we assume $\lambda = \lambda_2 - \lambda_1$. Accordingly, the pressure coefficient $\bar{p}_{F_1H_1}$ on section F_1H_1 is evaluated by expression (8.4.1), and the pressure coefficient $\bar{p}_{H_1L_1}$ on section H_1L_1, with the aid of formula (8.5.3). The drag coefficient of the airfoil is

$$c_{x,\,F_1L_1} = \frac{2}{b}\left(\int_{x_{F_1}}^{x_{H_1}} \bar{p}_{F_1H_1}\lambda_1 dx + \int_{x_{H_1}}^{x_{L_1}} \bar{p}_{H_1L_1}\lambda_2\, dx\right) \qquad (8.5.6)$$

Wing with All Supersonic Edges

For such a wing (Fig. 8.5.1*c*), Mach lines OK_O, BK_B, and DK_D drawn from points O, B, and D are below the corresponding edges OC, BC and DC, therefore formulas (8.3.23) and (8.3.34) are used to calculate the pressure coefficient.

Let us consider airfoil FL with the coordinate $O < z_1 < z_{D_2}$. Section FH is between leading edge OC and Mach line OK_0. Therefore, the other edge OC' (Fig. 8.5.1*a*) does not affect the flow on this section, which is considered as plane supersonic. Taking into account that section FH is influenced by the sources in triangle OCC' having a strength of $Q = 2\lambda_1 V_\infty$, the pressure coefficient $\bar{p}_{FH}$ can be determined by formula (8.3.23) in which we assume $\lambda = \lambda_1$ and $n = n_1$. The additional pressure on section HG is due to the influence of edge OC'. The pressure coefficient $\bar{p}_{HG}$ on this section is found from expression (8.3.34) in which it is assumed that $n = n_1$ and $\sigma = \sigma_1$.

Section GJ, in addition to the distribution of the sources in OCC', is affected by the source distribution in BCC' having a strength of $Q = 2(\lambda_2 - \lambda_1) V_\infty$. Using formulas (8.3.34) and (8.3.23), we obtain an expression for the pressure coefficient:

$$\bar{p}_{GJ} = \frac{2\lambda_1}{\alpha' \sqrt{1-n_1^2}}\left(1 - \frac{2}{\pi}\sin^{-1}\sqrt{\frac{n_1^2-\sigma_1^2}{1-\sigma_1^2}}\right) + \frac{2(\lambda_2-\lambda_1)}{\alpha' \sqrt{1-n_2^2}} \qquad (8.5.7)$$

The last airfoil section JL is influenced additionally by opposite edge BC'. Accordingly, the pressure coefficient on section JL on which sources having a strength of $Q = 2(\lambda_2 - \lambda_1) V_\infty$ act is

$$\bar{p}_{JL} = \frac{2\lambda_1}{\alpha' \sqrt{1-n_1^2}}\left(1 - \frac{2}{\pi}\sin^{-1}\sqrt{\frac{n_1^2-\sigma_1^2}{1-\sigma_1^2}}\right)$$

$$+ \frac{2(\lambda_2-\lambda_1)}{\alpha' \sqrt{1-n_2^2}}\left(1 - \frac{2}{\pi}\sin^{-1}\sqrt{\frac{n_2^2-\sigma_2^2}{1-\sigma_2^2}}\right) \qquad (8.5.8)$$

The drag coefficient of airfoil FL is

$$c_{x,\,FL} = \frac{2}{b}\left(\int_{x_F}^{x_H} \bar{p}_{FH}\lambda_1\,dx + \int_{x_H}^{x_G} \bar{p}_{HG}\lambda_1\,dx + \int_{x_G}^{x_J} \bar{p}_{GJ}\lambda_2\,dx + \int_{x_J}^{x_L} \bar{p}_{JL}\lambda_2\,dx\right) \tag{8.5.9}$$

The pressure coefficient $\bar{p}_{F_1H_1}$ on section F_1H_1 of airfoil F_1L_1 with the coordinate $z_D < z_1 < z_{D_2}$ is determined by formula (8.3.23) in which $\lambda = \lambda_1$ and $n = n_1$. To determine the pressure coefficient $\bar{p}_{H_1G_1}$ for the neighbouring section H_1G_1, we use formula (8.3.34) in which $\lambda = \lambda_1$, $n = n_1$, and $\sigma = \sigma_1$. On the last section G_1L_1, the pressure is due to the influence of source distributions in OCC' ($Q = 2\lambda_1 V_\infty$) and BCC' [$Q = 2(\lambda_2 - \lambda_1)V_\infty$]. Consequently, to calculate the pressure coefficient $\bar{p}_{G_1L_1}$, we can use formula (8.5.7). The drag coefficient of airfoil F_1L_1 is

$$c_{x,\,F_1L_1} = \frac{2}{b}\left(\int_{x_{F_1}}^{x_{H_1}} \bar{p}_{F_1H_1}\lambda_1\,dx + \int_{x_{H_1}}^{x_{G_1}} \bar{p}_{H_1G_1}\lambda_1\,dx + \int_{x_{G_1}}^{x_{L_1}} \bar{p}_{G_1L_1}\lambda_2\,dx\right) \tag{8.5.10}$$

The flow near airfoil F_2L_2 in the section $z_{D_2} < z_1$ is plane supersonic, therefore the pressure coefficient for it is determined by formula (8.3.23). The sources in triangle OCC' having a strength of $Q = 2\lambda_1 V_\infty$ act on section F_2G_2, therefore the pressure coefficient $\bar{p}_{F_2G_2}$ is found by formula (8.3.23) in which $\lambda = \lambda_1$ and $n = n_1$. The second section G_2L_2 is additionally influenced by the sources having a strength of $Q = 2(\lambda_2 - \lambda_1)V_\infty$ distributed in triangle BCC'. Therefore, the pressure coefficient on this section is

$$\bar{p}_{G_2L_2} = \frac{2\lambda_1}{\alpha'\sqrt{1-n_2^2}} + \frac{2(\lambda_2-\lambda_1)}{\alpha'\sqrt{1-n_2^2}} \tag{8.5.11}$$

The drag coefficient for airfoil F_2L_2 is

$$c_{x,F_2L_2} = \frac{2}{b}\left(\int_{x_{F_2}}^{x_{G_2}} \bar{p}_{F_2G_2}\lambda_1\,dx + \int_{x_{G_2}}^{x_{L_2}} \bar{p}_{G_2L_2}\lambda_2\,dx\right) \tag{8.5.12}$$

If a tetragonal wing has an extended tip or side edge ($b_t \neq 0$), the flow parameters are calculated with account taken of the influence of the side edge on them. The part of the wing where this influence is observed is below the Mach line issuing from the front point of the side edge (see Fig. 8.4.4). The velocity and pressure on

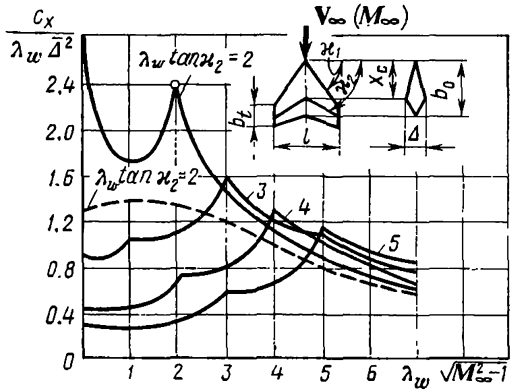

Fig. 8.5.2
Drag coefficient of wings with a symmetric rhombiform airfoil: $\bar{x}_C = x_C/b_0 = 0.5$; $\eta_W = b_0/b_t = 5$; $\lambda_W = l^2/S_W$; $\tan \varkappa_2 = \tan \varkappa_1 - (2/\lambda_W)(\eta_W - 1)/(\eta_W + 1)$; $\bar{\Delta} = \Delta/b_0$ (the dashed curve is an experimental one)

this section are calculated by the method set out in Sec. 8.4 with account taken of the kind of the leading and middle edges (i.e. depending on whether they are subsonic or supersonic) by means of the relevant relations similar to (8.4.31).

By integrating over the span, we can determine the wave-drag coefficients in each of the cases of flow over a hexagonal or tetragonal rhombiform airfoil wing considered in Secs. 8.4 and 8.5. According to the relations obtained, these coefficients depend on the number M_∞ and on the configuration and relative dimensions of the wing:

$$c_x = f_1 (M_\infty, \lambda_w, \varkappa_1, \eta_w, \bar{x}_C, \bar{\Delta}) \qquad (8.5.13)$$

Here in addition to the known notation, we have introduced the quantity $\bar{x}_C = x_C/b$—the dimensionless distance to the spot with the maximum airfoil thickness.

The number of independent variables in (8.5.13) can be reduced by using the relation

$$c_x/(\lambda_w \bar{\Delta}^2) = f_2 (\lambda_w \sqrt{M_\infty^2 - 1}, \lambda_w \tan \varkappa_2, \eta_w, \bar{x}_C) \qquad (8.5.14)$$

where $\tan \varkappa_2$ is the tangent of the sweep angle along the maximum thickness line (i.e. of the middle edge).

Figure 8.5.2 shows a family of curves constructed in accordance with formula (8.5.14) for the following conditions: $\eta_w = b_0/b_t = 5$ and $x_C = 0.5$. The salient points of the curves correspond to sonic edges. Particularly, for the curve corresponding to the value of $\lambda_w \tan \varkappa_2 = 3$, the salient point for the smallest value of $\lambda_w \sqrt{M_\infty^2 - 1}$ corresponds to a sonic trailing edge, and the second and third points to a sonic middle (the maximum thickness line) and trailing edges.

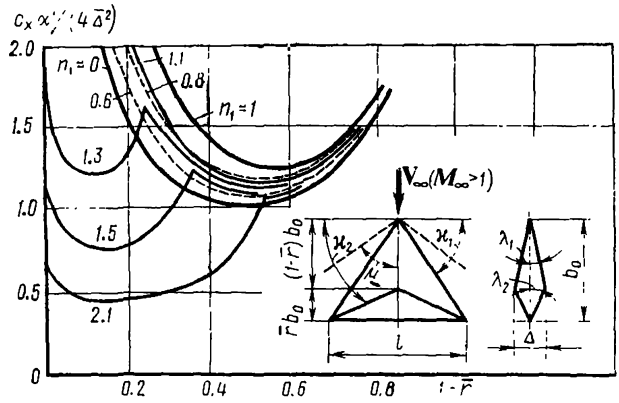

Fig. 8.5.3
Drag of triangular wings with a symmetric rhombiform airfoil in a supersonic flow
($n_1 = \tan \varkappa_1/\alpha'$)

A comparison shows that the experimental and theoretical values of the wave-drag coefficients differ, especially near values of $\lambda_w\sqrt{M_\infty^2 - 1} \approx \lambda_w \tan \varkappa_2$, i.e. when the maximum thickness line becomes sonic. In this case, the linear theory cannot be applied. The discrepancy between the indicated values diminishes when this line is supersonic ($\lambda_w\sqrt{M_\infty^2 - 1} > \lambda_w \tan \varkappa_2$).

From the relations found for a tetragonal planform wing, we can obtain the relations for the aerodynamic characteristics of a triangular wing as a particular case (Fig. 8.5.3). The trailing edge of such a wing is supersonic and straight ($\varkappa_3 = 0$). The leading edge and the maximum thickness line (the middle edge) may be either subsonic or supersonic and, consequently, inclined at different angles $\varkappa_1$ and $\varkappa_2$. Depending on this, we determine the local velocities and pressures, and also the total drag coefficient c_x.

Figure 8.5.3 shows the results of calculating the function $c_x\alpha'/(4\bar{\Delta}^2)$ for triangular wings with a subsonic ($n_1 > 1$) and supersonic ($n_1 < 1$) leading edges depending on $1 - \bar{r}$ for various values of n_1 (the sweep angle $\varkappa_1$). The values of $c_x\alpha'/(4\bar{\Delta}^2)$ at $n_1 = 0$ correspond to a straight wing with a symmetric airfoil.

Figure 8.5.3 can be used to appraise the influence of the location of the maximum airfoil thickness on the drag. We can indicate the value of $\bar{r}$ which the minimum drag coefficient corresponds to. The salient points of the curves correspond to values of $\bar{r}$ at which the maximum thickness line becomes sonic ($n_2 = n_1$ and $\bar{r} = 1$).

General Relation for Calculating the Drag

The total drag coefficient of a wing can be written in the form

$$c_{x_a} = c_{x,\,f} + c_{x,\,w0} + Ac_{y_a}^2 \qquad (8.5.15)$$

where A is a coefficient determined by the kind of the leading edge; if it is supersonic, the coefficient A equals the reciprocal of the derivative of the lift coefficient with respect to the angle of attack $[A = (c_{y_a}^{\alpha})^{-1}]$; with a subsonic edge $A < (c_{y_a}^{\alpha})^{-1}$ because a suction force appears that decreases the drag. The quantity $Ac_{y_a}^2$ is the induced drag depending on the lift force.

The coefficient of friction drag $c_{x,\,f}$ can be evaluated for an equivalent rectangular wing whose chord equals the mean aerodynamic chord of the given lifting surface. We may consider here that the boundary layer near the leading edge of such a wing is laminar and on the remaining part is turbulent.

Let us consider the second component of the total drag coefficient, $c_{x,\,w0}$, which is the wave-drag coefficient of the wing at $\alpha = 0$. We shall use formula (7.5.31) to evaluate it. According to this formula, at $\alpha = 0$, the wave-drag coefficient of an airfoil is $c_{x,\,w} = c_1 K_1 = c_1 \int_0^1 (\beta_b^2 + \beta_u^2)\, d\bar{x}$, therefore for a symmetric wedge we have $c_{x,\,w} = 0.5 c_1 \bar{\Delta}^2$. Such a relation, characterizing the change in the wave-drag coefficient proportional to the square of the relative thickness of the airfoil $[\bar{\Delta}^2 = (\Delta/b)^2]$, can be applied for a thin airfoil of an arbitrary configuration. By comparing the above relation for $c_{x,\,w}$ with (8.5.14), we can determine the ratio

$$c_{x,\,w0}/c_{x,\,w} = f_3\,(\lambda_w \sqrt{M_\infty^2 - 1},\ \lambda_w \tan \varkappa,\ \eta_w,\ \bar{x}_c) \qquad (8.5.16)$$

in which $c_{x,\,w}$ is the wave-drag coefficient of the airfoil oriented in the direction of the oncoming flow (see Sec. 7.5), λ_w and η_w are the speed ratio and taper ratio of the wing, respectively.

The function f_3 in (8.5.16) is similar to the function f_2 in (8.5.14) and is determined with the aid of the method of sources set out above. The quantity $\varkappa$ may be taken equal to one of the characteristic angles of the given wing (the angle of inclination of the leading and trailing edges or of the maximum thickness line).

Figure 8.5.4 shows a curve characterizing the change in the function f_3 for a swept wing with a taper ratio of $\eta_w = 2$ a relative coordinate of $\bar{x}_c = 0.5$ and the quantity $\lambda_w \tan \varkappa_1 = 3.67$. The first

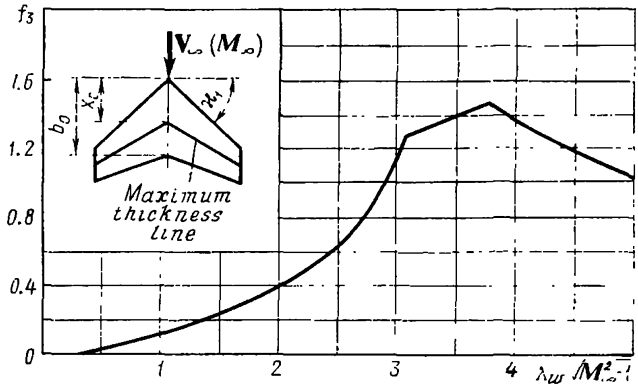

Fig. 8.5.4
Change in drag function f_3 by formula (8.5.16)

salient point corresponds to the transformation of the trailing edge, and the second, of the leading edge into a sonic one.

8.6. Field of Application of the Source Method

The method of sources, as we already know, is used to calculate the flow in order to find the drag force of a wing with a symmetric airfoil at a *zero angle of attack*, i.e. in the absence of a lift force. Investigations reveal that the field of application of this method in aerodynamic research can be extended. Let us consider cases when the method of sources can be used to determine a nearly uniform flow over a thin wing at a *non-zero angle of attack*, and we can thus find the lift force in addition to the drag.

Let us take two wings with different leading edges. One of them has a curved edge with a finite supersonic section (Fig. 8.6.1), while the other has completely subsonic leading edges (Fig. 8.6.2).

In Fig. 8.6.1, the supersonic section is bounded by points E and E' at which a tangent to the contour coincides with the generatrices of the Mach cones. Let us consider the velocity potential at a point M in the region confined by edges ED and the Mach lines drawn in plane xOz from points E, D, D', and E'.

By formula (8.2.16) in which the integration region σ should be taken equal to $\sigma = S_1 + S_2$, the velocity potential at the point being considered is

$$\varphi' = -\frac{1}{2\pi}\iint\limits_{S_1}\frac{Q_1(\xi,\zeta)\,d\xi\,d\zeta}{\sqrt{(x_1-\xi)^2-(z_1-\zeta)^2}} - \frac{1}{2\pi}\iint\limits_{S_2}\frac{Q_2(\xi,\zeta)\,d\xi\,d\zeta}{\sqrt{(x_1-\xi)^2-(z_1-\zeta)^2}} \qquad (8.6.1)$$

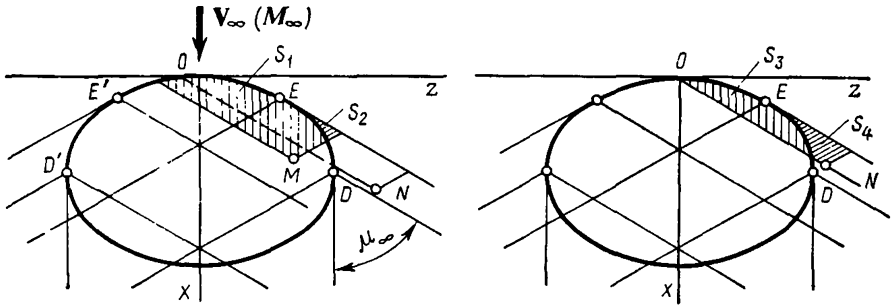

Fig. 8.6.1
Wing with a finite section of a supersonic leading edge

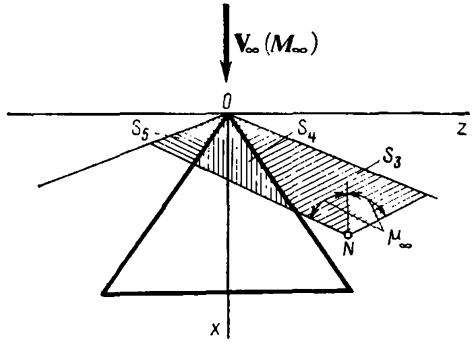

Fig. 8.6.2
Wing with subsonic leading edges

In (8.6.1), the function $Q_1(x, z) = 2(\partial\varphi'/\partial y)_{y=0}$. This follows from (8.2.17). This function is determined from the condition of flow over the wing surface without separation (8.1.12). Since the equation of this surface is given, the function $Q_1(x, z)$ is known. In the particular case of a wing in the form of a plate in a flow at the angle of attack α, the function $Q_1 = 2V_\infty\alpha$. Hence, the determination of φ' by formula (8.6.1) is associated with the finding of the unknown function Q_2 determining the intensity of source distribution on section S_2.

To find this function Q_2, let us take an arbitrary point $N(x, O, z)$ in the region between the Mach lines issuing from points E and D. At this point, according to (8.1.20), the velocity potential is zero, therefore in accordance with the notation (see Fig. 8.6.1), we have

$$0 = -\frac{1}{2\pi}\iint\limits_{S_3}\frac{Q_1(\xi, \zeta)\,d\xi\,d\zeta}{\sqrt{(x_1-\xi)^2-(z_1-\zeta)^2}} + \frac{1}{2\pi}\iint\limits_{S_4}\frac{Q_2(\xi, \zeta)\,d\xi\,d\zeta}{\sqrt{(x_1-\xi)^2-(z_1-\zeta)^2}} \qquad (8.6.2)$$

The first term on the right-hand side of this integral equation is a known function of the coordinates of a point because the strength Q_1 on area S_3 has been determined from the boundary conditions. We can therefore use the equation to determine the unknown function Q_2 that is the strength of the sources in region S_4.

Hence, *if the leading edge of a symmetric airfoil wing is completely or partly supersonic, the method of sources is suitable for investigating the flow over the wing at a non-zero angle of attack.* The same conclusion evidently also relates to a wing with similar edges and a non-symmetric airfoil in a flow either at the angle $\alpha \neq 0$ or at $\alpha = 0$.

Now let us consider a wing with subsonic leading edges. We can derive the following relation for a similar point N (Fig. 8.6.2):

$$0 = -\frac{1}{2\pi}\iint\limits_{S_5}\frac{Q_3(\xi, \zeta)\,d\xi\,d\zeta}{\sqrt{(x_1-\xi)^2-(z_1-\zeta)^2}} - \frac{1}{2\pi}\iint\limits_{S_3}\frac{Q_1(\xi, \zeta)\,d\xi\,d\zeta}{\sqrt{(x_1-\xi)^2-(z_1-\zeta)^2}} - \frac{1}{2\pi}\iint\limits_{S_4}\frac{Q_2(\xi, \zeta)\,d\xi\,d\zeta}{\sqrt{(x_1-\xi)^2-(z_1-\zeta)^2}} \tag{8.6.3}$$

We have obtained an equation with two unknown functions Q_3 and Q_2. Similar to Q_2, the function Q_3 is the strength of the sources on area S_5 belonging to the region located between the left-hand leading edge and the Mach line issuing from the wing vertex.

Hence, *if a wing has a subsonic leading edge, the source method cannot be used to investigate the flow over a thin symmetric airfoil wing at an angle of attack*, or the flow over a non-symmetric airfoil wing at a zero angle of attack or when $\alpha \neq 0$.

8.7. Doublet Distribution Method

It has been established that the application of the source method for investigating supersonic flow is restricted to wings with completely or partly supersonic leading edges. In other cases associated with the investigation of the supersonic aerodynamic characteristics of wings with subsonic leading edges with a non-zero angle of attack (or of similar non-symmetric airfoil wings and at $\alpha = 0$), the **doublet distribution method** must be used.

Let us consider a doublet in a supersonic flow. To do this, we shall determine the velocity potential of the flow produced by an elementary source and an elementary sink of the same strength Q having coordinates $x = \xi$, $z = \zeta$, $y = \varepsilon$, and $x = \xi$, $z = \zeta$, $y = -\varepsilon$, respectively. The chosen source is located above the plane $y = 0$ at the small distance ε from it, and the sink is under this plane at the same small distance $-\varepsilon$. Expressing (8.2.11) as a difference equation, we shall write the potential produced by the source and sink

in the form

$$\Delta\varphi = \frac{Q\Delta\sigma}{2\pi}\left\{\frac{-1}{\sqrt{(x-\xi)^2-\alpha'^2[(y-\varepsilon)^2+(z-\zeta)^2]}} + \frac{1}{\sqrt{(x-\xi)^2-\alpha'^2[(y+\varepsilon)^2+(z-\zeta)^2]}}\right\}$$

Introducing the symbol $\rho = \sqrt{(x-\xi)^2 - \alpha'^2[y^2 + (z-\zeta)^2]}$ and disregarding the quantity $\alpha'^2\varepsilon^2$, we obtain

$$\Delta\varphi = \frac{Q\Delta\sigma}{2\pi\rho}\left(\frac{-1}{\sqrt{1+2\alpha'^2 y\varepsilon/\rho^2}} + \frac{1}{\sqrt{1-2\alpha'^2 y\varepsilon/\rho^2}}\right)$$

Using the expansion of the square roots into a series and deleting the second and higher order infinitesimals, we find

$$\Delta\varphi = \frac{\alpha'^2 Qy\varepsilon\Delta\sigma}{\pi\rho^3} = \frac{\alpha'^2 Qy\varepsilon\, d\sigma}{\pi\{(x-\xi)^2-\alpha'^2[y^2+(z-\zeta)^2]\}^{3/2}}$$

By calculating the limit of $\Delta\varphi$ at $\varepsilon \to 0$ and assuming that the quantity $M = Q\varepsilon$ called the **moment** (or power) of the doublet remains constant, we obtain an expression for the differential of the potential function of a doublet

$$d\varphi_{\text{doub}} = \frac{My\, d\sigma}{\pi\{(x-\xi)^2-\alpha'^2[y^2+(z-\zeta)^2]\}^{3/2}}$$

This expression can be written in the form

$$d\varphi_{\text{doub}} = \frac{M\, d\sigma}{\pi}\cdot\frac{\partial}{\partial y}\left\{\frac{1}{\sqrt{(x-\xi)^2-\alpha'^2[y^2+(z-\zeta)^2]}}\right\}$$

Integrating over the region σ which the influence of the doublets extends to, we obtain for the potential function

$$\varphi_{\text{doub}} = \frac{\partial}{\partial y}\int\int_{\sigma}\frac{M(\xi,\zeta)\, d\xi\, d\zeta}{\sqrt{(x-\xi)^2-\alpha'^2[y^2+(z-\zeta)^2]}} \qquad (8.7.1)$$

where the number π has been included in the doublet distribution function.

It can be shown that function (8.7.1) satisfies Eq. (8.1.7). To do this, let us differentiate (8.1.7) with respect to y:

$$(M_\infty^2-1)\frac{\partial}{\partial y}\left(\frac{\partial^2\varphi'}{\partial x^2}\right) - \frac{\partial}{\partial y}\left(\frac{\partial^2\varphi'}{\partial y^2}\right) - \frac{\partial}{\partial y}\left(\frac{\partial^2\varphi'}{\partial z^2}\right) = 0$$

We can write this equation as

$$(M_\infty^2-1)\frac{\partial^2}{\partial x^2}\left(\frac{\partial\varphi'}{\partial y}\right) - \frac{\partial^2}{\partial y^2}\left(\frac{\partial\varphi'}{\partial y}\right) - \frac{\partial^2}{\partial z^2}\left(\frac{\partial\varphi'}{\partial y}\right) = 0 \qquad (8.7.2)$$

Now let us consider expression (8.7.1) for the potential of a doublet. If we include the quantity $-1/(2\pi)$ into the expression for this

potential, then in accordance with (8.2.12) the double integral can be considered as the potential of sources whose distribution over area σ is set by a function M. Consequently,

$$\varphi_{doub} = \partial\varphi'/\partial y \tag{8.7.3}$$

Comparing (8.7.2) and (8.7.3), we see that the function φ_{doub} does indeed satisfy Eq. (8.1.7) for the velocity potential.

Knowing the configuration of the surface in the flow, the free-stream velocity, and the angle of attack, we can find the doublet distribution function M and thus determine the potential φ_{doub} of the doublets. The derivative of the function φ_{doub} with respect to x yields the additional longitudinal component of the disturbed velocity $u = \partial\varphi_{doub}/\partial x$ that is used to calculate the pressure coefficient $\bar{p} = -2u/V_\infty$ on the lifting surface and the lift force produced by this surface.

8.8. Flow over a Triangular Wing with Subsonic Leading Edges

A plane triangular wing with subsonic leading edges is *inside a Mach cone* (Fig. 8.8.1). To find the lift force of such a wing, we shall use the doublet distribution method and the relevant relation (8.7.1) for the velocity potential of doublets.

It is general knowledge that the additional velocity u induced by sources distributed over an inclined triangular surface with subsonic edges depends only on the function $\sigma = z\alpha'/x$ [see, for example, formula (8.3.18)]. This signifies that along the ray issuing from the salient point of the leading edge of the wing at the angle $\gamma = \tan^{-1}(z/x)$ the velocity is *constant*. This ray can be considered as the generatrix of a cone with its vertex coinciding with the salient point of the leading edge.

A flow retaining a constant velocity and, therefore, other constant parameters along a generatrix of such a conical surface is called a **conical flow**. We can consider that the additional velocity u for such a flow in the plane $y = 0$ is a function of the ratio z/x, i.e. $u = f(z/x)$. It thus follows that the potential produced by the sources for a conical flow also depends on this ratio.

Considering the flow set up by doublets near a triangular surface as a conical one, its potential can be written for point P in the plane $y = 0$ (Fig. 8.8.1) as follows:

$$\varphi_{doub} = xF_{doub}(z/x) \tag{8.8.1}$$

where $F_{doub}(z/x)$ is a function depending only on the angle of the conical surface $\gamma = \tan^{-1}(z/x)$.

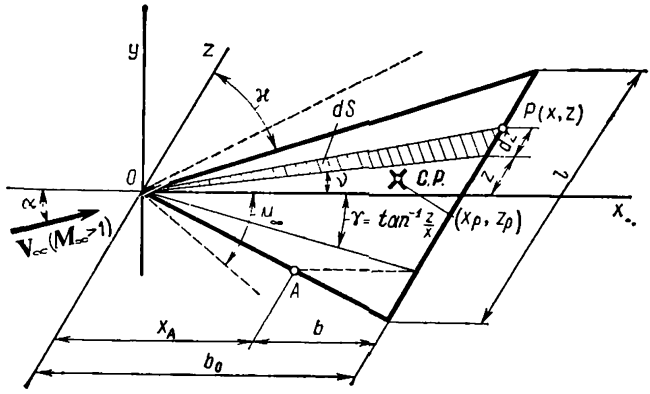

Fig. 8.8.1
Plane triangular wing with subsonic edges

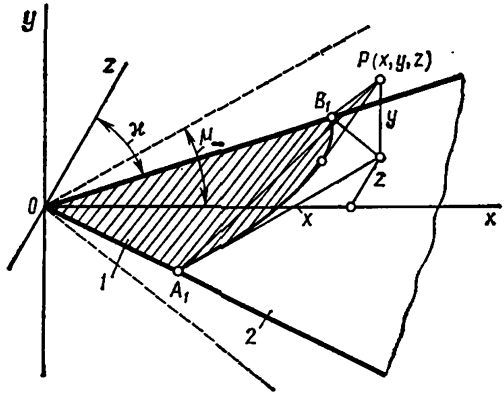

Fig. 8.8.2
Region of doublet influence on the flow over a wing with subsonic leading edges:
1—region of doublet influence; *2*—triangular wing

For a point with the coordinates x, y, z we shall write the potential of a conical flow in a more general form:

$$\varphi_{\text{doub}} = xF_{\text{doub}}\,(z/x,\ y/x) \tag{8.8.2}$$

In accordance with Eq. (8.8.1), the relation characterizing the distribution of the doublets in the plane $y = 0$ (on the wing surface) is such that

$$M\,(\xi,\ \zeta) = \xi m\,(h) \tag{8.8.3}$$

where $h = \zeta/\xi$, and $m\,(h)$ is a function of the argument h.

Let us transform Eq. (8.7.1). We shall express the elementary area occupied by a doublet in the form $d\sigma = d\xi\,d\zeta = \xi\,dh\,d\xi$ because $d\zeta = \xi\,dh$. Therefore

$$\varphi_{\text{doub}} = \int\limits_{-\cot\varkappa}^{\cot\varkappa} m\,(h)\,dh \frac{\partial}{\partial y} \int\limits_{0}^{\xi_1} \frac{\xi^2\,d\xi}{\sqrt{(x-\xi)^2 - \alpha'^2\,[y^2 + (z-h\xi)^2]}} \tag{8.8.4}$$

where ξ_1 is the coordinate of a doublet that may influence the flow at point P (x, y, z). This doublet is on the curve confining the region of doublet influence (Fig. 8.8.2) and obtained as a result of the intersection of the plane $y = 0$ with the Mach cone issuing upstream from point P. This curve is parabola A_1B_1 described by the equation

$$(x - \xi_1)^2 - \alpha'^2 [y^2 + (z - \zeta_1)^2] = 0 \qquad (8.8.5)$$

in the coordinates ξ_1, ζ_1. We shall write the radicand in (8.8.4) in the form

$$(x - \xi)^2 - \alpha'^2 [y^2 + (z - h\xi)^2] = a\xi^2 + b\xi + c \qquad (8.8.6)$$

where

$$a = 1 - \alpha'^2 h^2, \quad b = 2x \left(\alpha'^2 h \frac{z}{x} - 1\right),$$
$$c = x^2 \left[1 - \alpha'^2 \left(\frac{y^2}{x^2} + \frac{z^2}{x^2}\right)\right] \qquad (8.8.7)$$

The integral in the case being considered is

$$\int_0^{\xi_1} \frac{\xi^2 d\xi}{\sqrt{a\xi^2 + b\xi + c}} = \left(\frac{\xi}{2a} - \frac{3b}{4a^2}\right) \sqrt{a\xi^2 + b\xi + c} \Big|_0^{\xi_1}$$
$$+ \frac{3b^2 - 4ac}{8a^2} \int_0^{\xi_1} \frac{d\xi}{\sqrt{a\xi^2 + b\xi + c}} \qquad (8.8.8)$$

Taking into account that $a = 1 - \alpha'^2$ and $h^2 > 0$, we find the integral on the right-hand side of (8.8.8):

$$\int_0^{\xi_1} \frac{d\xi}{\sqrt{a\xi^2 + b\xi + c}} = \frac{1}{\sqrt{a}} \ln [2\sqrt{a(a\xi^2 + b\xi + c)} + 2a\xi + b] \Big|_0^{\xi_1} \qquad (8.8.9)$$

By (8.8.5), the value of $a\xi_1^2 + b\xi_1 + c = 0$, consequently,

$$\int_0^{\xi_1} \frac{\xi^2 d\xi}{\sqrt{a\xi^2 + b\xi + c}} = \frac{3b}{4a^2} \sqrt{c}$$
$$+ \frac{3b^2 - 4ac}{8a^2 \sqrt{a}} [\ln (2a\xi_1 + b) - \ln (2\sqrt{ac} + b)] \qquad (8.8.10)$$

Solving Eq. (8.8.5) in the form

$$a\xi_1^2 + b\xi_1 + c = 0, \qquad (8.8.11)$$

we obtain

$$\xi_1 = (-b + \sqrt{b^2 - 4ac})/2a \qquad (8.8.12)$$

Accordingly,

$$\ln (2a\xi_1 + b) = \ln \sqrt{b^2 - 4ac} \qquad (8.8.13)$$

The difference of the logarithms in (8.8.10) with a view to (8.8.13) is

$$\ln(2a\xi_1+b)-\ln(2\sqrt{ac}+b)=\ln\frac{\sqrt{b^2-4ac}}{2\sqrt{ac}+b}=\frac{1}{2}\ln\frac{b^2-4ac}{(2\sqrt{ac}+b)^2}$$

$$=\frac{1}{2}\ln\frac{b-2\sqrt{ac}}{b+2\sqrt{ac}}=-\operatorname{th}^{-1}\frac{b}{2\sqrt{ac}} \qquad (8.8.14)$$

Therefore,

$$\int_0^{\xi_1}\frac{\xi^2\,d\xi}{\sqrt{a\xi^2+b\xi+c}}=\frac{3b\sqrt{c}}{4a^2}-\frac{3b^2-4ac}{8a^2\sqrt{a}}\operatorname{th}^{-1}\frac{b}{2\sqrt{ac}} \qquad (8.8.15)$$

We calculate the derivative with respect to y from (8.8.15):

$$\frac{\partial}{\partial y}\int_0^{\xi_1}\frac{\xi^2\,d\xi}{\sqrt{a\xi^2+b\xi+c}}=N$$

$$=\frac{1}{2a\sqrt{a}}\cdot\frac{\partial c}{\partial y}\left(\frac{b}{4\sqrt{ac}}\cdot\frac{8ac}{4ac-b^2}+\operatorname{th}^{-1}\frac{b}{2\sqrt{ac}}\right)$$

Introducing the symbol

$$\nu=b/(2\sqrt{ac}) \qquad (8.8.16)$$

and having in view that $\partial c/\partial y=-2y\alpha'^2$ [see formula (8.8.7)], we obtain

$$N=\frac{-y\alpha'^2}{a\sqrt{a}}\left(\frac{\nu}{1-\nu^2}+\operatorname{th}^{-1}\nu\right) \qquad (8.8.17)$$

We introduce this expression into (8.8.4):

$$\varphi_{\text{doub}}=\int_{-\cot\varkappa}^{\cot\varkappa}Nm(h)\,dh \qquad (8.8.18)$$

To determine the form of the doublet distribution function, we shall use the condition of flow without separation, in accordance with which

$$v_{y=0}=V_\infty\alpha=(\partial\varphi_{\text{doub}}/\partial y)_{y=0} \qquad (8.8.19)$$

The partial derivative $(\partial\varphi_{\text{doub}}/\partial y)_{y=0}$ is determined in accordance with (8.8.18) in the form

$$\left(\frac{\partial\varphi_{\text{doub}}}{\partial y}\right)_{y=0}=\int_{-\cot\varkappa}^{\cot\varkappa}\left(\frac{\partial N}{\partial y}\right)_{y=0}m(h)\,dh \qquad (8.8.20)$$

Introducing this expression into (8.8.19), we find

$$V_\infty\alpha=\int_{-\cot\varkappa}^{\cot\varkappa}\left(\frac{\partial N}{\partial y}\right)_{y=0}m(h)\,dh \qquad (8.8.21)$$

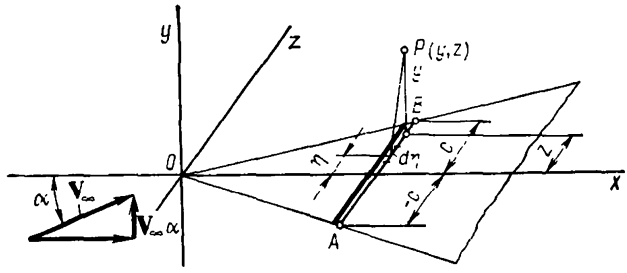

Fig. 8.8.3
Incompressible two-dimensional cross flow at the velocity $V_\infty\alpha$ over flat plate AB belonging to a triangular wing

Differentiation of (8.8.17) with respect to y yields

$$\left(\frac{\partial N}{\partial y}\right)_{y=0} = -\frac{\alpha'^2}{a\sqrt{a}}\left(\frac{\nu}{1-\nu^2} + \mathrm{th}^{-1}\,\nu\right)_{y=0} \qquad (8.8.22)$$

Let us calculate the partial derivative with respect to z/x from (8.8.20) with a view to (8.8.22):

$$0 = \int\limits_{-\cot\varkappa}^{\cot\varkappa} \frac{1}{(1-\nu^2)^2}\cdot\frac{\partial\nu}{\partial\,(z\,x)}\Big|_{y=0} m\,(h)\,dh \qquad (8.8.23)$$

We calculate the value of the derivative $\partial\nu/\partial\,(z/x)\,|_{y=0}$ by (8.8.16) and determine the quantity $(1-\nu^2)^2\,|_{y=0}$ by using (8.8.7) and (8.8.16). After the corresponding substitutions into (8.8.23), we obtain the equation

$$\int\limits_{-\cot\varkappa}^{\cot\varkappa} \frac{m\,(h)\,dh}{\left(h-\dfrac{z}{x}\right)^3} = 0 \qquad (8.8.24)$$

We shall show that this equation has the same form as the one obtained when using the doublet distribution method to solve the problem on the flow of an incompressible fluid over a flat plate of infinite length installed at right angles to the direction of the free-stream velocity. We can determine the velocity potential for a plate that is a part of a wing in section AB with the coordinates $z_A = -c$, $z_B = c$, and over which an incompressible fluid flows in a lateral direction at the velocity $v = V_\infty\alpha$ (Fig. 8.8.3) with the aid of Eq. (2.9.16). We shall write the latter in accordance with the coordinate system chosen in Fig. 8.8.3 in the form

$$\varphi_{\text{doub}} = y/[(z-\eta)^2 + y^2] \qquad (8.8.25)$$

This expression determines the potential at point $P\,(y,\ z)$ produced by a two-dimensional point doublet with a unit moment

($M = 1$). If the moment of the doublet differs from unity and the doublet distribution over the span of the plate is set by the function $M(\eta)$, the velocity potential induced by the doublets on the wing section $d\eta$ is

$$d\varphi_{doub} = M(\eta)\, y\, d\eta/[(z-\eta)^2 + y^2] \tag{8.8.26}$$

The velocity potential at point P due to the influence of the doublets located along the span of the plate on the section from $z_A = -c$ to $z_B = c$ is

$$\varphi_{doub} = \int_{-c}^{c} \frac{M(\eta)\, y\, d\eta}{(z-\eta)^2+y^2} \tag{8.8.27}$$

The vertical component of the velocity $v = \partial\varphi_{doub}/\partial y$ on the surface of the wing is

$$v_{y=0} = \left(\frac{\partial\varphi_{doub}}{\partial y}\right)_{y=0} = \left[\frac{\partial}{\partial y}\int_{-c}^{c} \frac{M(\eta)\, y\, d\eta}{(z-\eta)^2+y^2}\right]_{y=0} = \int_{-c}^{c} \frac{M(\eta)\, d\eta}{(z-\eta)^2} \tag{8.8.28}$$

Since the component $v_{y=0}$ does not change over the span of the plate, we have

$$\left(\frac{\partial v}{\partial z}\right)_{y=0} = \frac{\partial}{\partial z}\int_{-c}^{c} \frac{M(\eta)\, d\eta}{(z-\eta)^2} = 0 \tag{8.8.29}$$

Differentiation yields

$$\int_{-c}^{c} \frac{M(\eta)\, d\eta}{(z-\eta)^3} = 0 \tag{8.8.30}$$

A comparison of Eqs. (8.8.24) and (8.8.30) reveals that they are both of a single type, therefore it is possible to take the doublet distribution function $m(h)$ in a supersonic linearized flow of the same appearance as the corresponding function $M(\eta)$ in an incompressible flow.

To determine the form of the function $M(\eta)$, we shall use the solution of the problem on finding the potential function for a plane plate over which an incompressible fluid flows in a lateral direction (see Sec. 6.2). According to this solution, the velocity potential on the plate is determined by formula (6.2.7). The relevant potential difference on both sides of it is $\Delta\varphi = 2V\sqrt{a^2 - z^2}$. The flow of an incompressible fluid near the plate is considered as the result of superposition of the flow produced by the doublets onto the undisturbed flow [see formula (6.3.6)]. Consequently, *the distribution of doublets for a plane plate in a non-circulatory flow of an incompressible fluid is equivalent to the potential difference* $\Delta\varphi$. Having in view that

the doublet distribution function $m(h)$ in a compressible flow has the same form as for an incompressible one, we can consider the expression for this function in the form

$$m(h) = L\sqrt{H^2 - h^2} \tag{8.8.31}$$

where $H^2 = \cot^2 \varkappa$ and L is a proportionality coefficient.

We shall use Eq. (8.8.21) to find the coefficient L. Inserting (8.8.22) and (8.8.31) into it, we obtain

$$\alpha V_\infty = -\alpha'^2 L \int_{-\cot \varkappa}^{\cot \varkappa} \frac{1}{a\sqrt{a}} \left(\frac{\nu}{1-\nu^2} + \operatorname{th}^{-1} \nu \right)_{y=0} \sqrt{\cot^2 \varkappa - h^2}\, dh \tag{8.8.32}$$

To simplify the calculation of the coefficient L, we can integrate (8.8.32) along a longitudinal coordinate on the wing. Having in view that along the x-axis the coordinates $z = 0$ and $y = 0$, we determine the value of $| \nu/(1 - \nu^2) + \operatorname{th}^{-1} \nu |_{y=0}$ in accordance with (8.8.7) and (8.8.16), and the value of $a\sqrt{a}$ by (8.8.7). Integration yields

$$\alpha V_\infty = \pi L \int_0^{\pi/2} \sqrt{1 - (1 - \alpha'^2 \cot^2 \varkappa) \sin^2 \varphi}\, d\varphi \tag{8.8.33}$$

The integral

$$\int_0^{\pi/2} \sqrt{1 - (1 - \alpha'^2 \cot^2 \varkappa) \sin^2 \varphi}\, d\varphi = E(k) \tag{8.8.34}$$

is a complete elliptic integral of the second order with the parameter

$$k = \sqrt{1 - \alpha'^2 \cot^2 \varkappa} \tag{8.8.35}$$

The values of integral (8.8.34) are determined with the aid of the previously calculated tables depending on the parameter k.

The doublet distribution can be expressed by function (8.8.3) provided that $m(h)$ is replaced by (8.8.31) and with account taken of the value for L determined from (8.8.33). As a result, we have

$$M(\xi, \zeta) = \xi \sqrt{\cot^2 \varkappa - h^2}\, \frac{\alpha V_\infty}{\pi E(k)} \tag{8.8.36}$$

Let us find the component of the induced velocity produced by the doublets on the surface of the wing for $y = 0$. From (8.7.3), we have

$$(\varphi_{\text{doub}})_{y=0} = (\partial \varphi'/\partial y)_{y=0} = (v_{y=0})_{\text{source}} \tag{8.8.37}$$

i.e. the potential of the doublets on the wing is determined by the magnitude of the vertical component of the velocity induced by the

sources. A comparison of (8.2.12) and (8.7.1) reveals that $M(\xi, \zeta)$ can be considered as a function similar to the function $Q(\xi, \zeta)$ determining the distribution of the sources over the surface of a wing having a given planform and angle of attack. Consequently, if we take into account that in (8.7.1) the number π is included in $M(\xi, \zeta)$ in accordance with (8.2.7), (8.8.36), and (8.8.37), we can compile the equation

$$(\varphi_{\text{doub}})_{y=0} = \pi M(\xi, \zeta) = \frac{\alpha V_\infty \xi \sqrt{\cot^2 \varkappa - h^2}}{E(k)} \tag{8.8.38}$$

where $h = \zeta/\xi$ (or $h = z/x$).

The component of the induced velocity due to the doublets is

$$u = \left(\frac{\partial \varphi_{\text{doub}}}{\partial x}\right)_{y=0} = \frac{\alpha V_\infty}{E(k)} \cdot \frac{\partial}{\partial x}\left(x \sqrt{\cot^2 \varkappa - \frac{z^2}{x^2}}\right)$$

$$= \frac{\alpha V_\infty \cot^2 \varkappa}{E(k) \sqrt{\cot^2 \varkappa - h^2}} \tag{8.8.39}$$

The corresponding value of the pressure coefficient with a view to the possible signs in front of the square root is

$$\bar{p} = \frac{2(p - p_\infty)}{\rho_\infty V_\infty^2} = -\frac{2u}{V_\infty} = \frac{\pm 2\alpha \cot^2 \varkappa}{E(k) \sqrt{\cot^2 \varkappa - h^2}} \tag{8.8.40}$$

where the plus sign determines the pressure on the bottom, and the minus sign on the upper side of the wing. *The field of pressures corresponds to a conical flow relative to the vertex of the wing* at which the pressure coefficient $\bar{p} = \text{const}$ for all the values of $z/x = \text{const}$.

The lift force acting on a triangular wing consists of the force produced by the pressure on the bottom surface, and of the suction force equal to it in magnitude and caused by the rarefaction on the upper side. The elementary lift force acting on area $dS = 0.5x dz$ (see Fig. 8.8.1) is

$$dY_a = 2(p - p_\infty)\, dS = (p - p_\infty)\, x\, dz \tag{8.8.41}$$

The total force is obtained as a result of integration over the entire surface of the wing $S_w = x^2 \cot \varkappa$:

$$Y_a = \int_{S_w} 2(p - p_\infty)\, dS \tag{8.8.42}$$

The lift coefficient is

$$c_{y_a} = \frac{2Y_a}{\rho_\infty V_\infty^2 S_w} = \frac{1}{-\cot \varkappa} \int_{-\cot \varkappa}^{\cot \varkappa} |\bar{p}|\, dh$$

$$= \frac{2\alpha \cot \varkappa}{E(k)} \int_{-\cot \varkappa}^{\cot \varkappa} \frac{dh}{\sqrt{\cot^2 \varkappa - h^2}} \tag{8.8.43}$$

After integration, we have

$$c_{y_a} = 2\alpha\pi \cot \varkappa / E(k) \tag{8.8.44}$$

For a conical flow, the centre of pressure of each triangular element issuing from the apex is at a distance of two-thirds of the altitude from the apex. Therefore, the centre of pressure of the entire wing is on the root chord at a point that is at a distance of two-thirds of the chord from the apex. Accordingly, the coefficient of the pitching moment about the wing apex is

$$m_{z_a} = -c_{y_a} c_p = -(4/3)\, \alpha\pi \cot \varkappa / E(k) \tag{8.8.45}$$

For a triangular low aspect ratio wing ($\varkappa \to \pi/2$), the quantity $\alpha' \cot \varkappa \ll 1$, and we can take the value of the elliptic integral $E(k) \approx 1$. Consequently, for such a wing we have

$$c_{y_a} = 2\alpha\pi \cot \varkappa;\ m_{z_a} = -(4/3)\, \alpha\pi \cot \varkappa \tag{8.8.46}$$

Expressing cot $\varkappa$ in terms of the wing aspect ratio $\lambda_w = 4 \cot \varkappa$, we obtain

$$c_{y_a} = \alpha\pi\lambda_w/2;\ m_{z_a} = -(1/3)\, \alpha\pi\lambda_w \tag{8.8.46'}$$

If the sweep angle $\varkappa$ is chosen such that $\varkappa = \pi/2 - \mu_\infty$, and, consequently, the Mach line coincides with the leading edge, we have

$$\cot \varkappa = \tan \mu_\infty \quad \text{and} \quad \alpha' \cot \varkappa = \cot \mu_\infty \cot \varkappa = 1$$

In the given case, the elliptic integral $E(k) = \pi/2$, therefore for a triangular wing with a sonic leading edge, we have

$$c_{y_a} = 4\alpha \cot \varkappa \tag{8.8.47}$$

Since

$$\cot \varkappa = \tan \mu_\infty = 1/\sqrt{M_\infty^2 - 1}$$

we obtain

$$c_{y_a} = 4\alpha/\sqrt{M_\infty^2 - 1} \tag{8.8.48}$$

This value coincides with the lift coefficient for a thin sharp-nosed airfoil in a linearized supersonic flow.

We shall show that the lift coefficient of a triangular wing with supersonic leading edges is expressed by the same relation (8.8.48). In accordance with (8.3.34), the pressure coefficient for the wing in the region between Mach cones is

$$\bar{p}_1 = \frac{\pm 2\alpha}{\alpha' \sqrt{1 - n^2}} \left(1 - \frac{2}{\pi} \sin^{-1} \sqrt{\frac{n^2 - \sigma^2}{1 - \sigma^2}}\right) \tag{8.8.49}$$

and on the section between the leading edge and a Mach cone [see (8.3.23)] it is

$$\bar{p}_2 = \pm 2\alpha/(\alpha' \sqrt{1 - n^2}) \tag{8.8.50}$$

where $n = \tan\varkappa/\alpha'$, and $\sigma = z \tan\varkappa/x = h \tan \varkappa$.

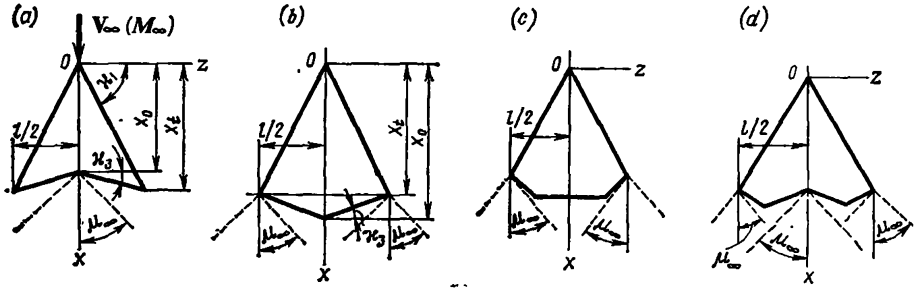

Fig. 8.8.4
Wings with supersonic trailing and side edges ($x_0 = b_0$):
a—tetragonal wing with a dovetail; *b*—tetragonal wing with a vee-shaped appendage (rhombiform plate); *c*—pentagonal wing; *d*—hexagonal wing

According to (8.8.43), (8.8.49), and (8.8.50), the lift coefficient is

$$c_{y_a} = 2\int_0^n |\bar{p}_1|\,d\sigma - 2\int_0^n |\bar{p}_2|\,d\sigma = \frac{4\alpha}{\alpha'\sqrt{1-n^2}} \times \left[\int_0^n \left(1 - \frac{2}{\pi}\sin^{-1}\sqrt{\frac{n^2-\alpha^2}{1-\sigma^2}}\right)d\sigma - \int_1^n d\sigma\right]$$

Integration yields the relation $c_{y_a} = 4\alpha/\alpha'$ that coincides with (8.8.48).

The methods of calculating the flow over triangular (delta) wings can be used to determine the aerodynamic characteristics of lifting surfaces in the form of tetragonal, pentagonal, and hexagonal plates with *supersonic* trailing and side edges (Fig. 8.8.4). The flow over them is characterized by the absence of zones of mutual influence of the tail and side regions confined by the intersection of Mach cones with the wing, i.e. when the flow at the side and trailing edges is supersonic. As a result, the coefficient of the pressure on the wing surface is the same as at the relevant point of a triangular plate. The formula for calculating it is chosen with account taken of the kind of leading edge (subsonic or supersonic). The lift and moment coefficients can be determined by integration according to the pressure distribution.

We shall give the results obtained for a tetragonal wing: with a subsonic leading edge

$$c_{y_a} = \frac{4\alpha\cot\varkappa_1}{(1-\varepsilon)E(k)}\left[(1-\varepsilon)^{-1/2}\cos^{-1}\varepsilon - \varepsilon\right] \qquad (8.8.51)$$

$$m_{z_a} = \frac{-4\alpha\cot\varkappa_1}{3(1-\varepsilon)E(k)}\left[\frac{2+\varepsilon^2}{(1+\varepsilon)^{3/2}}\cos^{-1}\varepsilon - \frac{\varepsilon(4-\varepsilon)^2}{1-\varepsilon^2}\right] \qquad (8.8.52)$$

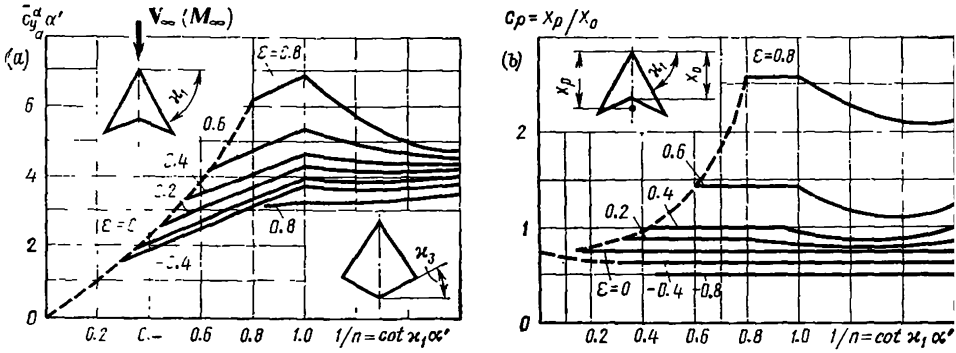

Fig. 8.8.5
Curves characterizing the change in the derivative of the lift coefficient (a) and centre-of-pressure coefficient (b) for a tetragonal wing

with supersonic edges

$$c_{y_a} = \frac{8\alpha}{(1-\varepsilon)\pi\alpha'}\left(\frac{1}{\sqrt{1-n_1^2}}\cos^{-1} n_1 - \frac{\varepsilon}{\sqrt{1-n^2}}\cos^{-1} n\right) \quad (8.8.53)$$

$$m_{z_a} = \frac{-8\alpha}{3(1-\varepsilon)\pi\alpha'}\left[\frac{2-n_1^2(1+\varepsilon^2)}{(1+\varepsilon)^2(1-n_1^2)^{3/2}}\cos^{-1} n_1 - \frac{\varepsilon(3-\varepsilon^2)}{(1+\varepsilon)^2\sqrt{1-n^2}}\cos^{-1} n - \frac{n_1}{1-n_1^2}\right] \quad (8.8.54)$$

where $\varepsilon = (x_t - x_0)/x_t = \tan\varkappa_3/\tan\varkappa_1$; $n_1 = \tan\varkappa_3/\alpha' = \varepsilon n$; x_0 and x_t are the dimensions shown in Fig. 8.8.4.

For dovetail wings (Fig. 8.8.4*a*), the quantity ε is positive, and for rhombiform plates (Fig. 8.8.4*b*), it is negative.

The relations for c_{y_a} and m_{z_a} allow us to determine the centre-of-pressure coefficient $c_p = x_p/x_0 = -m_{z_a}/c_{y_a}$.

Figure 8.8.5 shows curves characterizing the change in $c_{y_a}^{\alpha}$ and c_p in accordance with the above relations. The dashed lines in this figure determine the values of the aerodynamic coefficients in the limiting case when $1/n = \cot\varkappa_1\alpha' = \varepsilon$ (a sonic trailing edge).

A salient point appears on the curves (Fig. 8.8.5) at a value of $n = 1$ (when $\cot\varkappa_1\alpha' = 1$), i.e. when the leading edge is sonic. The coefficients c_{y_a} and c_p behind the salient point (with a supersonic leading edge) diminish with an increasing M_∞.

Let us consider another limiting case corresponding to sufficiently high values of $\cot\varkappa_1\alpha' \gg 1$ ($n \ll 1$, $n_1 \ll 1$) at which the surface of a Mach cone is near the root chord. A glance at formula (8.8.53) reveals that the parameter ε does not virtually affect the coefficient c_{y_a}, and a dovetail or a V-shaped appendage (see the diagrams of the

wings in Fig. 8.8.5) alters the lift force of the wing almost in proportion to the change in the area of the plate.

It is not difficult to see that for $\varepsilon = 0$ formulas (8.8.51)-(8.8.54) yield the values of the relevant coefficients for a triangular wing: $c_{y_a} = c_{y_{a\Delta}}$ and $m_{z_a} = m_{z_{a\Delta}}$. The calculations by these formulas can be simplified if the tetragonal wings differ only slightly from triangular ones. In this case, provided that $|\varepsilon| \ll 1$, we have

$$c_{y_a} = c_{y_{a\Delta}}/(1-\varepsilon),\quad m_{z_a} = m_{z_{a\Delta}}/(1-\varepsilon) \qquad (8.8.55)$$

8.9. Flow over a Hexagonal Wing with Subsonic Leading and Supersonic Trailing Edges

Let us find the aerodynamic characteristics in the more general case of the flow at a small angle of attack over a plane hexagonal wing *with subsonic leading and supersonic trailing edges* (Fig. 8.9.1). Such a kind of the trailing edges excludes the influence of the vortex sheet behind the wing on the flow over it.

To determine the velocity potential, let us use the results of solving the problem on the flow over a triangular wing with subsonic leading edges. Let us consider point A with the coordinates x, z in region *1* confined by the leading edges and the Mach lines issuing from points G and D. The velocity potential at this point can be expressed by analogy with (8.6.1) with the aid of the following formula:

$$\varphi_1' = -\frac{1}{2\pi}\int\int_{\sigma}\frac{Q_1(\xi,\zeta)\,d\xi\,d\zeta}{\sqrt{(x-\varepsilon)^2-\alpha'^2(z-\zeta)^2}} + \Delta\varphi_2 + \Delta\varphi_3 \qquad (8.9.1)$$

in which σ is the region of integration on the wing surface, $\Delta\varphi_2$ and $\Delta\varphi_3$ are the additional potentials determined by expressions similar to the second and third terms on the right-hand side of (8.6.3) when integrating over regions σ_1 and σ_2 (hatched in Fig. 8.9.1).

Taking into account that $Q_1 = 2\lambda V_\infty = 2\alpha V_\infty$, we can write Eq. (8.9.1) as follows:

$$\varphi_1' = -\frac{\alpha V_\infty \Omega}{\pi}\int\int_{\sigma}\frac{d\xi\,d\zeta}{\sqrt{(x-\xi)^2-\alpha'^2(z-\zeta)^2}} \qquad (8.9.2)$$

where in accordance with (8.9.1)

$$\Omega = 1-(\Delta\varphi_2+\Delta\varphi_3)\left[\frac{\alpha V_\infty}{\pi}\int\int_{\sigma}\frac{d\xi\,d\zeta}{\sqrt{(x-\xi)^2-\alpha'^2(z-\zeta)^2}}\right]^{-1} \qquad (8.9.3)$$

For our further transformations, we shall introduce a characteristic system of coordinates whose axes r and s coincide with the

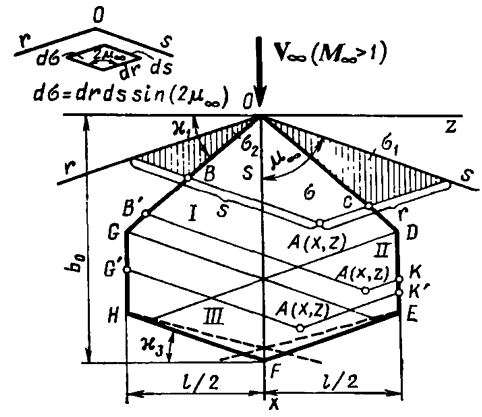

Fig. 8.9.1
Hexagonal wing with subsonic leading and supersonic trailing edges

directions of the Mach lines issuing from the vertex of the wing (Fig. 8.9.1):

$$r = (M_\infty/2\alpha')\,(x - \alpha' z),\quad s = (M_\infty/2\alpha')\,(x + \alpha' z) \tag{8.9.4}$$

The characteristic coordinates of point $A(x_A, z_A)$ are as follows:

$$r_A = (M_\infty/2\alpha')\,(x_A - \alpha' z_A),\quad s_A = (M_\infty/2\alpha')\,(x_A + \alpha' z_A) \tag{8.9.4'}$$

Let us convert Eq. (8.9.2) to the characteristic coordinates r and s. From (8.9.4), we find:

$$r + s = (M_\infty/\alpha')x,\quad r - s = -M_\infty z \tag{8.9.4''}$$

Consequently,

$$\left.\begin{aligned} x - \xi = x_A - x &= (\alpha'/M_\infty)\,[(r_A + s_A) - (r + s)] \\ \alpha'\,(z - \zeta) = \alpha'\,(z_A - z) &= -(\alpha'/M_\infty)\,[(r_A - s_A) - (r - s)] \end{aligned}\right\} \tag{8.9.5}$$

Introducing these expressions into (8.9.2) and taking into account that an area element in the coordinates r and s is $d\sigma = dr\,ds \times \sin(2\mu_\infty)$ (Fig. 8.9.1), and that the integration limits are s_B and s_A, r_C and r_A, we obtain an equation for the potential function:

$$\varphi_I' = -\frac{V_\infty \alpha \Omega}{\pi M_\infty} \int_{r_C}^{r_A} \frac{dr}{\sqrt{r_A - r}} \int_{s_B}^{s_A} \frac{ds}{\sqrt{s_A - s}} \tag{8.9.6}$$

We shall express the coordinates s_B and r_C in terms of the coordinates r_A and s_A of point A. Since the equations of the leading edges in the coordinates z and x are $z = \pm x \tan \varkappa$, then in accordance with (8.9.4'') these equations in the coordinates r and s are

transformed to the form:

$$\left.\begin{array}{l} r = sm \text{ for the starboard leading edge: } z = +x\cot\varkappa \\ r = s/m \text{ for the port leading edge: } z = -x\cot\varkappa \end{array}\right\} \quad (8.9.7)$$

where $m = (n-1)/(n+1)$ and $n = \tan\varkappa_1/\alpha'$.

Therefore the coordinates r_C and s_B can be expressed as follows:

$$r_C = s_C m = s_A m \quad \text{and} \quad s_B = r_B m = r_A m \quad (8.9.8)$$

Substituting $s_A m$ and $r_A m$ for r_C and s_B in (8.9.6), respectively, after integration we obtain

$$\varphi_I' = -\frac{4\alpha V_\infty \Omega}{\pi M_\infty}\sqrt{(r_A - ms_A)(s_A - mr_A)} \quad (8.9.9)$$

Introducing into (8.9.9) the values of r_A and s_A from (8.9.4′) and also the quantity

$$m = (n-1)/(n+1) \quad (8.9.10)$$

we find

$$\varphi_I' = -\frac{4\alpha V_\infty n x_A \Omega}{\pi(n+1)}\sqrt{\cot^2\varkappa - h^2} \quad (8.9.11)$$

where $h = z_A/x_A$ (or $h = \zeta/\xi$).

By comparing Eq. (8.9.11) with relation (8.8.38) for the potential function at the point being considered, we see that for matching of the results, in (8.9.11) we must assume that

$$\Omega = -\frac{\pi}{4}\cdot\frac{n+1}{nE(k)} \quad (8.9.12)$$

Hence, at point A located on the wing in region I, the velocity potential is

$$\varphi_I' = \frac{\alpha V_\infty x_A}{E(k)}\sqrt{\cot^2\varkappa - h^2} \quad (8.9.13)$$

Accordingly, the equation that must be used when determining the potential function on the wing has the following general form:

$$\varphi_I' = \frac{\alpha V_\infty (n+1)}{4nM_\infty E(k)}\int\int_\sigma \frac{dr}{\sqrt{r_A - r}}\cdot\frac{ds}{\sqrt{s_A - s}} \quad (8.9.14)$$

Let us use Eq. (8.9.14) to determine the potential function at point A in region II that is confined by the Mach lines issuing from points D and G, the tips, (side edges) and partly the trailing edges. We shall write Eq. (8.9.14) in the following form:

$$\varphi_{II}' = \frac{\alpha V_\infty (n+1)}{4nM_\infty E(k)}\int_{r_K}^{r_A}\frac{dr}{\sqrt{r_A - r}}\int_{s_{B'}}^{s_A}\frac{ds}{\sqrt{s_A - s}} \quad (8.9.15)$$

By analogy with (8.9.8):

$$s_{B'} = r_{B'} m = r_A m \quad (8.9.16)$$

Point K is on a tip whose equation is $z = l/2$. In the coordinates r and s, the equation of a tip in accordance with (8.9.4″) is

$$r - s = -M_\infty l/2 \tag{8.9.17}$$

Therefore, for point K, the coordinate is

$$r_K = s_K - M_\infty l/2 = s_A - M_\infty l/2 \tag{8.9.18}$$

Taking also into account that $s_{B'} = r_A m$, after integration of (8.9.15) we obtain

$$\varphi'_{II} = \frac{\alpha V_\infty (n+1)}{nM_\infty E(k)} \sqrt{\left[r_A - \left(s_A - \frac{M_\infty l}{2}\right)\right](s_A - r_A m)} \tag{8.9.19}$$

Introducing instead of r_A, s_A and m the relevant values from (8.9.4′) and (8.9.10), we find

$$\varphi'_{II} = \frac{\alpha V_\infty}{nE(k)} \sqrt{\frac{n+1}{2}(l - 2z_A)\left(\frac{x_A}{\alpha'} + nz_A\right)} \tag{8.9.20}$$

The velocity potential for point A in region III is

$$\varphi'_{III} = \frac{\alpha V_\infty (n+1)}{4nM_\infty E(k)} \int_{r_{K'}}^{r_A} \frac{dr}{\sqrt{r_A - r}} \int_{s_{G'}}^{s_A} \frac{ds}{\sqrt{s_A - s}} \tag{8.9.21}$$

Points K' and G' are on the tips whose equations are $z = \pm l/2$ (the plus sign is for the starboard and the minus sign is for the port tip). In the coordinates r and s, the equations of these tips in accordance with (8.9.4) have the form:

$$\left.\begin{aligned} r - s &= -M_\infty l/2 \text{ for the starboard tip} \\ r - s &= M_\infty l/2 \text{ for the port tip} \end{aligned}\right\} \tag{8.9.22}$$

Consequently, for points K' and G', we have, respectively:

$$\left.\begin{aligned} r_{K'} &= s_{K'} - M_\infty l/2 = s_A - M_\infty l/2 \\ s_{G'} &= r_{G'} - M_\infty l/2 = r_A - M_\infty l/2 \end{aligned}\right\} \tag{8.9.23}$$

After the integration of (8.9.21), with a view to the values of the limits (8.9.23), we obtain

$$\varphi'_{III} = \frac{\alpha V_\infty (n+1)}{nM_\infty E(k)} \sqrt{\left(r_A - s_A + \frac{M_\infty l}{2}\right)\left(s_A - r_A \frac{M_\infty l}{2}\right)} \tag{8.9.24}$$

We introduce into (8.9.24) the values of s_A and r_A from (8.9.4′):

$$\varphi'_{III} = \frac{\alpha V_\infty (n+1)}{2nE(k)} \sqrt{l^2 - 4z_A^2} \tag{8.9.25}$$

By calculating the partial derivatives with respect to x_A, we find the components of the disturbed velocity $u = \partial\varphi'_n/\partial x_A$ (n = I, II,

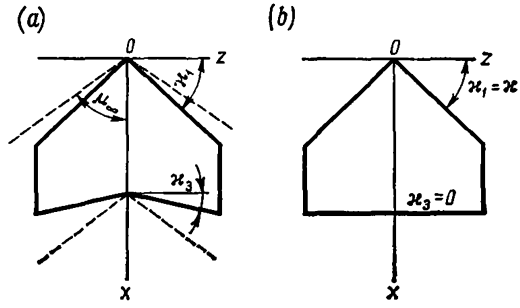

Fig. 8.9.2
Wings with subsonic leading edges and tips and with supersonic trailing edges:
a—hexagonal wing with a dovetail; *b*—plate with a straight trailing edge (a pentagonal wing)

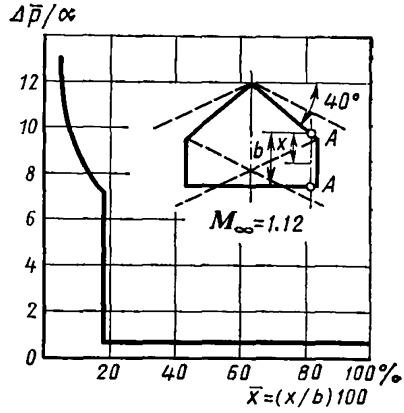

Fig. 8.9.3
Distribution of the quantity $\Delta\bar{p}/\alpha = (\bar{p}_b - \bar{p}_u)/\alpha$ near a tip of a pentagonal wing with subsonic leading edges (section AA)

III) and determine the pressure coefficients in the corresponding regions on the bottom and upper sides of the wing:

$$\left.\begin{aligned}
\bar{p}_{\mathrm{I}} &= -\frac{2}{V_\infty}\cdot\frac{\partial\varphi'_{\mathrm{I}}}{\partial x_{\mathrm{A}}} = \pm\frac{2\alpha\cot^2\varkappa}{E(k)}\cdot\frac{x_{\mathrm{A}}}{\sqrt{x_{\mathrm{A}}^2\cot^2\varkappa - z_{\mathrm{A}}^2}}\\
\bar{p}_{\mathrm{II}} &= -\frac{2}{V_\infty}\cdot\frac{\partial\varphi'_{\mathrm{II}}}{\partial x_{\mathrm{A}}} = \pm\frac{\alpha}{nE(k)}\sqrt{\frac{(n+1)(l-2z_{\mathrm{A}})}{2\alpha'(x_{\mathrm{A}}+z_{\mathrm{A}}\tan\varkappa)}}\\
\bar{p}_{\mathrm{III}} &= -\frac{2}{V_\infty}\cdot\frac{\partial\varphi'_{\mathrm{III}}}{\partial x_{\mathrm{A}}} = 0
\end{aligned}\right\} \quad (8.9.26)$$

Here the plus sign on the right-hand side of the equations corresponds to the bottom side, and the minus sign, to the upper one.

The above relations for calculating the pressure coefficients can be used not only for triangular wings with a V-shaped appendage (Fig. 8.9.1), but also for similar wings with a dovetail and wings with a straight trailing edge (pentagonal plates shown in Fig. 8.9.2).

The change in the quantity $\Delta\bar{p}/\alpha = (\bar{p}_b - \bar{p}_u)/\alpha$ near a tip as a function of the distance from the leading edge (in per cent of the

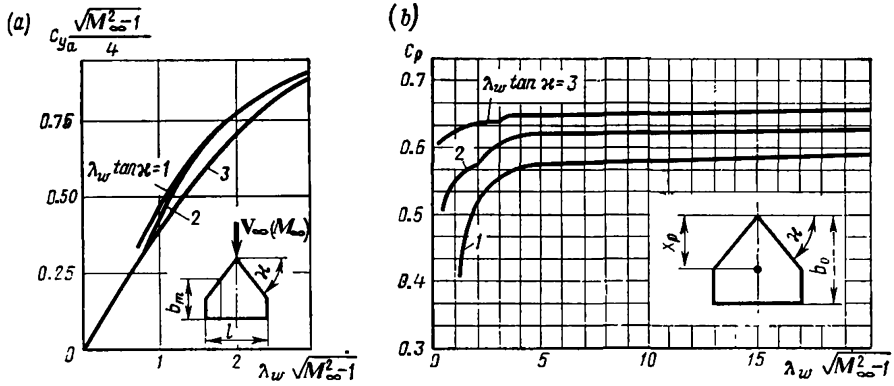

Fig. 8.9.4
Curves characterizing the change in the lift (*a*) and centre-of-pressure (*b*) coefficients for a pentagonal wing

chord) calculated by the above formulas for a pentagonal wing with $M_\infty = 1.12$ is shown in Fig. 8.9.3. On the surface of the tip Mach cone, a pressure discontinuity is observed due to the action of the corner point of the wing. The pressure is constant on the part between the tip and the tip Mach cone.

We use the known pressure to determine the lift and moment coefficients:

$$c_{y_a} = \frac{Y_a}{q_\infty S_w} = \frac{1}{S_w}\int\limits_{S_w}\int (\bar{p}_b - \bar{p}_u)\, dx\, dz \qquad (8.9.27)$$

$$m_{z_a} = \frac{M_{z_a}}{q_\infty S_w b_0} = \frac{-1}{S_w b_0}\int\limits_{S_w}\int (\bar{p}_b - \bar{p}_u)\, x\, dx\, dz \qquad (8.9.28)$$

where S_w and b_0 are the area and the root chord of the wing, respectively, and $\bar{p}_b$ and $\bar{p}_u$ are the coefficients of the pressure on the bottom and upper sides determined by formulas (8.9.26).

According to the values of m_{z_a} and c_{y_a}, we can determine the centre-of-pressure coefficient $c_p = x_p/b_0 = -m_{z_a}/c_{y_a}$. Figure 8.9.4 shows theoretical curves characterizing the change in c_{y_a} and c_p for a wing in the form of a pentagonal plate. In this figure, the parts of the curves for which $\lambda_w\sqrt{M_\infty^2 - 1} \ll \lambda_w \tan\varkappa$ correspond to subsonic leading edges. A feature of the graphs characterizing the change in c_{y_a} is the absence of noticeable salient points on the corresponding curves in the transition to supersonic leading edges (i.e. when $\lambda_w\sqrt{M_\infty^2 - 1} = \lambda_w \tan\varkappa$).

8.10. Flow over a Hexagonal Wing with Supersonic Leading and Trailing Edges

To calculate the flow over arbitrary planform wings (including hexagonal ones with supersonic leading edges) in regions *I* and *II* (Fig. 8.10.1*a*, *b*) we can use the corresponding results for a triangular wing with the same leading edges (see Sec. 8.3).

According to these results, the pressure coefficient for point A (x_A, z_A) in region *I* between the leading edge and the Mach lines issuing from the vertex of the wing and points D and G on its tips is determined by the formula

$$\bar{p}_I = \pm 2\alpha/(\alpha' \sqrt{1 - n^2}) \tag{8.10.1}$$

that has been obtained from (8.3.23) provided that α has been substituted for λ. In the same condition, we find the corresponding relation for the pressure coefficient in region *II* confined by the Mach lines issuing from the vertex and the same points D and G. By (8.3.34), we have

$$\bar{p}_{II} = \pm \frac{4\alpha}{\alpha' \pi \sqrt{1-n^2}} \left(\frac{\pi}{2} - \sin^{-1} \sqrt{\frac{n^2-\sigma^2}{1-\sigma^2}} \right) \tag{8.10.2}$$

The flow over the remaining part of the hexagonal wing (Fig. 8.10.1*c-h*) can be calculated with the aid of Eq. (8.3.1) for the velocity potential of the sources and sinks. We transform this equation to the following form in the new variables r and s [see (8.9.4)]

$$\varphi' = \frac{-\alpha V_\infty}{\pi M_\infty} \int_\sigma \int \frac{dr\, ds}{\sqrt{(r_A - r)(s_A - s)}} \tag{8.10.3}$$

where r_A and s_A are the coordinates of point A on the surface of the hexagonal wing.

The coordinate lines r and s are directed along the Mach lines. The wing surface is divided into eight regions by these Mach lines, as well as by the lines of weak disturbances issuing from points G and D, and also from intersection points G' and D' of the coordinate lines r and s (the Mach lines) with the tips. For each of these eight regions, the velocity potential is calculated with the aid of Eq. (8.10.3).

Let us consider arbitrary point A in region *III* (Fig. 8.10.1*c*). When determining the velocity potential for this region, we must take into account the sources both on the surface of the wing (on areas $S_1 = AD_1D_2A'$ and $S_2 = A'D_2D$) and outside of it (area $S_3 = A'DD''$).

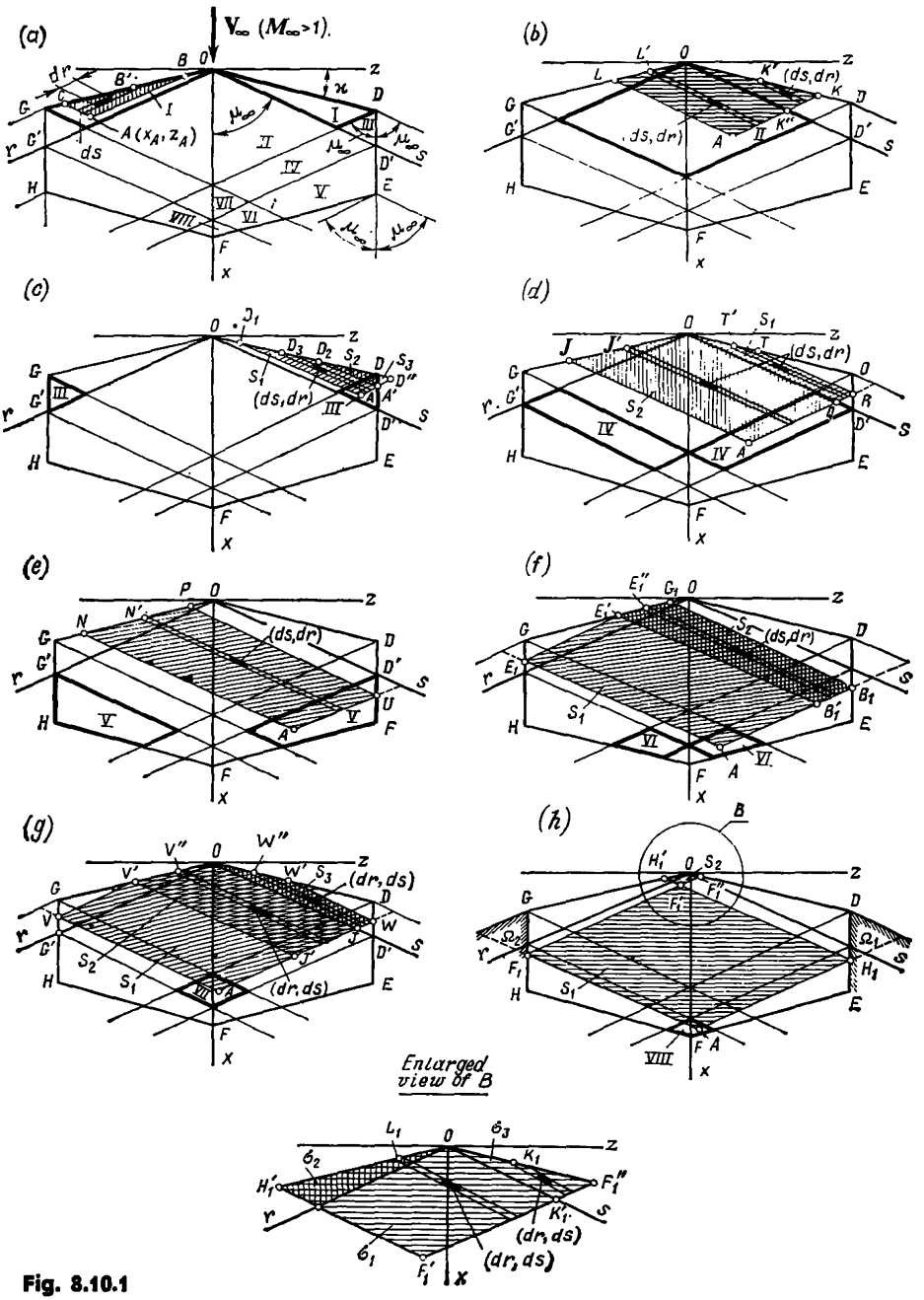

Fig. 8.10.1
Hexagonal wing with supersonic leading and trailing edges

Using (8.2.13), let us write the expression for φ'_{III} at point $A\ (x,\ 0,\ z)$ in the form

$$\varphi'_{III} = -\frac{1}{2\pi} \iint\limits_{S_1+S_2+S_3} \frac{Q(\xi,\ \zeta)\, d\xi\, d\zeta}{\sqrt{(x-\xi)^2 - \alpha'^2 (z-\zeta)^2}} \qquad (8.10.4)$$

On the wing area $S_1 + S_2$, the source strength is known and equals $Q = 2v = 2\alpha V_\infty$, therefore

$$\varphi'_{III} = \frac{-\alpha V_\infty}{\pi} \iint\limits_{S_1} \frac{d\xi\, d\zeta}{\sqrt{(x-\xi)^2 - \alpha'^2 (z-\zeta)^2}} - \frac{\alpha V_\infty}{\pi} \iint\limits_{S_2} \frac{d\xi\, d\zeta}{\sqrt{(x-\xi)^2 - \alpha'^2 (z-\zeta)^2}} - \frac{1}{2\pi} \iint\limits_{S_3} \frac{Q(\xi,\ \zeta)\, d\xi\, d\zeta}{\sqrt{(x-\xi)^2 - \alpha'^2 (x-\zeta)^2}} \qquad (8.10.4')$$

where $Q\ (\xi,\ \zeta)$ is a function determining the law of source distribution in region S_3 outside the wing.

We can perform integration if we know the function $Q\ (\xi,\ \zeta)$. To determine it, let us use the boundary condition (8.1.20), in accordance with which the potential function on plane xOz in the region between the tip and the Mach line issuing from point D is zero. For point A' belonging to this region, the condition of the equality to zero of the potential function by analogy with (8.6.2) has the form

$$0 = \frac{-\alpha V_\infty}{\pi} \iint\limits_{S_2} \frac{d\xi\, d\zeta}{\sqrt{(x-\xi)^2 - \alpha'^2 (z-\zeta)^2}} - \frac{1}{2\pi} \iint\limits_{S_3} \frac{Q(\xi,\ \zeta)\, d\xi\, d\zeta}{\sqrt{(x-\xi)^2 - \alpha'^2 (z-\zeta)^2}}$$

A comparison of this equation with (8.10.4') reveals that to calculate the velocity potential at point $A(x,\ 0,\ z)$, it is sufficient to extend integration to region S_1 in the main formula (8.10.4), i.e.

$$\varphi'_{III} = \frac{-\alpha V_\infty}{\pi} \iint\limits_{S_1} \frac{d\xi\, d\zeta}{\sqrt{(x-\xi)^2 - \alpha'^2 (z-\zeta)^2}} \qquad (8.10.4'')$$

By this formula, the overall action on point A of the sources on sections S_2 of the wing area and S_3 of the area outside the wing equals zero (see [17]).

Using expression (8.10.4'') transformed to the form (8.10.3) in the coordinates r, s, we obtain

$$\varphi'_{III} = \frac{-\alpha V_\infty}{\pi M_\infty} \int\limits_{r_{A'}}^{r_A} \frac{dr}{\sqrt{r_A - r}} \int\limits_{s_{D3}}^{s_A} \frac{ds}{\sqrt{s_A - s}} \qquad (8.10.5)$$

where in accordance with (8.9.8) for point D_3 on the starboard tip, we have

$$s_{D_3} = r_{D_3}/m = r/m \tag{8.10.6}$$

We find the lower limit $r_{A'}$ of the integral from the equation $z = l/2$ for the tip. In the coordinates r and s, this equation has the form of (8.9.17). Consequently, the coordinate

$$r_{A'} = s_{A'} - M_\infty l/2 = s_A - M_\infty l/2 \tag{8.10.7}$$

With a view to (8.10.6), the integral

$$\int_{r/m}^{s_A} \frac{ds}{\sqrt{s_A - s}} = 2\sqrt{s_A - \frac{r}{m}} = \frac{2}{\sqrt{\bar{m}}}\sqrt{r - s_A m}$$

where $m = (n-1)/(n+1)$; $\bar{m} = (1-m)/(n+1)$.

Hence

$$\varphi'_{III} = \frac{-2\alpha V_\infty}{\pi M_\infty \sqrt{\bar{m}}} \int_{r_{A'}}^{r_A} \sqrt{\frac{r - s_A m}{r_A - r}}$$

By calculating the integral, next inserting into it $r_{A'}$ from (8.10.7), and taking into account expressions (8.9.4′) for r_A and s_A, and also the values of m and $\bar{m}$, we find the potential

$$\varphi'_{III} = \frac{-\alpha V_\infty}{\pi\sqrt{1-n^2}} \left\{ \sqrt{(l-2z_A)\left[(x_A + \alpha' z_A) - \alpha' l\,(n+1)\right]\frac{n+1}{\alpha'}} \right.$$
$$\left. + \frac{2\,(x_A - z_A \tan\varkappa_1)}{\alpha'} \tan^{-1} \sqrt{\frac{\alpha'\,(n+1)\,(l-2z_A)}{2\,(x_A + \alpha' z_A) - l\,(n+1)\,\alpha'_1}} \right\} \tag{8.10.8}$$

We determine the derivative $\partial\varphi'_{III}/\partial x_A$ and find the pressure coefficient:

$$\bar{p}_{III} = -\frac{2}{V_\infty} \cdot \frac{\partial \varphi'_{III}}{\partial x_A}$$
$$= \frac{\pm 4\alpha}{\pi\alpha'\sqrt{1-n^2}} \tan^{-1} \sqrt{\frac{\alpha'\,(n+1)\,(l-2z_A)}{2\,(x_A + \alpha' z_A) - l\,(n+1)\alpha'}} \tag{8.10.9}$$

The velocity potential for point A in region IV (Fig. 8.10.1d) is determined by the action of sources distributed over area $AJOTR$. We divide this area into two parts, namely, $S_1 = OTRQ$ and $S_2 = OQAJ$, and find the potential at the point being considered as the sum of the potentials due to the action of the sources on areas S_1 and S_2. By using formula (8.10.3), we obtain

$$\varphi'_{IV} = \frac{-\alpha V_\infty}{\pi M_\infty} \iint_{S_1 + S_2} \frac{dr\,ds}{\sqrt{(r_A - r)\,(s_A - s)}}$$

$$= \frac{-\alpha V_\infty}{\pi M_\infty} \int_{r_R}^{0} \frac{dr}{\sqrt{r_A - r}}$$

$$\times \int_{s_{T'}}^{s_A} \frac{ds}{\sqrt{s_A - s}} - \frac{\alpha V_\infty}{\pi M_\infty} \int_0^{r_A} \frac{dr}{\sqrt{r_A - r}} \int_{s_{J'}}^{s_A} \frac{ds}{\sqrt{s_A - s}} \qquad (8.10.10)$$

We determine the integration limits $s_{T'}$ and $s_{J'}$ with the aid of (8.9.8). For point T' on the starboard leading edge and point J' on the port one, we have

$$s_{T'} = r_{T'}/m = r/m, \quad s_{J'} = r_{J'}m = rm \qquad (8.10.11)$$

With a view to these values of the limits, we calculate the integrals:

$$\int_{s_T}^{s_A} \frac{ds}{\sqrt{s_A - s}} = \frac{2}{\sqrt{m}} \sqrt{r - s_A m}$$

$$\int_{s_{J'}}^{s_A} \frac{ds}{\sqrt{s_A - s}} = 2\sqrt{m} \sqrt{r - \frac{s_A}{m}}$$

Accordingly,

$$\varphi'_{IV} = \frac{-2\alpha V_\infty}{\pi M_\infty \sqrt{m}} \int_{r_R}^{0} \sqrt{\frac{r - s_A m}{r_A - r}}\, dr$$

$$- \frac{2\alpha V_\infty \sqrt{m}}{\pi M_\infty} \int_0^{r_A} \sqrt{\frac{r - s_A/m}{r_A - r}}\, dr$$

where r_R is determined by formula (8.9.23):

$$r_R = s_R - M_\infty l/2 = s_A - M_\infty l/2$$

Integration and substitution of the values for s_A and r_A from (8.9.4'), and also $m = -\bar{m} = (n-1)/(n+1)$ yield

$$\varphi'_{IV} = \frac{-2\alpha V_\infty}{\alpha' \pi \sqrt{1-n^2}} \left\{ (x_A - z_A \tan \varkappa_1) \left[-\tan^{-1} \sqrt{\frac{(n+1)(x_A - \alpha' z_A)}{(1-n)(x_A + \alpha' z_A)}} \right.\right.$$

$$\left. + \tan^{-1} \sqrt{\frac{\alpha'(n+1)(l+2z_A)}{2(x_A + \alpha' z_A) - \alpha' l (n+1)}} \right]$$

$$+ \frac{1}{2} \sqrt{(l-2z_A)[2(x_A + \alpha' z_A) - \alpha' l (n+1)](n+1)\alpha'}$$

$$\left. + (x_A + z_A \tan \varkappa_1) \tan^{-1} \sqrt{\frac{(1-n)(x - \alpha' z_A)}{(n+1)(x_A + \alpha' z_A)}} \right\} \qquad (8.10\ 12)$$

Upon calculating the pressure coefficient $\bar{p}_{IV} = -(2/V_\infty)\,\partial\varphi'_{IV}/\partial x_A$ and using here the formula $\tan^{-1} x - \tan^{-1} y = \tan^{-1}[(x-y)/(1+xy)]$, we find

$$\bar{p}_{IV} = \frac{\pm 4\alpha}{\alpha'\pi\sqrt{1-n^2}}\left[\tan^{-1}\sqrt{\frac{\alpha'(n+1)(l-2z_A)}{2(x_A-\alpha' z_A)-\alpha' l(n+1)}} - \tan^{-1}\sqrt{\frac{n^2-\sigma^2}{1-n^2}}\right] \qquad (8.10.13)$$

Let us consider region V. For point A in this region (Fig. 8.10.1*e*), the potential is

$$\varphi'_V = \frac{-\alpha V_\infty}{\pi M_\infty}\int_{r_U}^{r_A}\frac{dr}{\sqrt{r_A-r}}\int_{s_{N'}}^{s_A}\frac{ds}{\sqrt{s_A-s}} \qquad (8.10.14)$$

By this formula, the velocity at point A is induced by the sources on section $ANPU$ of the wing area. The inner integral in (8.10.14) whose lower limit $s_{N'} = rm$, is

$$\int_{s_{N'}}^{s_A}\frac{ds}{\sqrt{s_A-s}} = 2\sqrt{m}\,\sqrt{r-\frac{s_A}{m}}$$

Consequently,

$$\varphi'_V = \frac{-2\alpha V_\infty\sqrt{m}}{\pi M_\infty}\int_{r_U}^{r_A}\sqrt{\frac{r-s_A/m}{r_A-r}}\,dr$$

Since $r_U = s_A - M_\infty l/2$, then, going over to conventional coordinates x and y and taking into account that $m = (n-1)/(n+1)$ and $\bar{m} = -m$, after integration we find

$$\varphi'_V = \frac{2\alpha V\sqrt{1-n}}{M_\infty\pi\sqrt{n+1}}\left\{M_\infty\sqrt{\left(z_A-\frac{l}{2}\right)\left[(x_A+\alpha' z_A)\frac{1}{\alpha'(n-1)}+\frac{l}{2}\right]}\right.$$
$$\left. - \frac{M_\infty(x_A+z_A\tan\varkappa_1)}{\alpha'(n-1)}\tan^{-1}\sqrt{\frac{z_A-l/2}{(x_A+\alpha' z_A)/\alpha'(n-1)+l/2}}\right\} \qquad (8.10.15)$$

After finding the derivative with respect to x_A, we determine the pressure coefficient:

$$\bar{p}_V = -\frac{2}{V_\infty}\cdot\frac{\partial\varphi'_V}{\partial x_A} = \frac{\pm 4\alpha}{\pi\alpha'\sqrt{1-n^2}}$$
$$\times\tan^{-1}\sqrt{\frac{\alpha'(z_A-l/2)(n-1)}{x_A+\alpha' z_A+(l/2)(n-1)\alpha'}} \qquad (8.10.16)$$

In region VI, the velocity potential is determined as follows (Fig. 8.10.1*f*):

$$\varphi'_{VI} = \frac{-\alpha V_\infty}{\pi M_\infty} \iint\limits_{S_1+S_2} \frac{dr\,ds}{\sqrt{(r_A - r)(s_A - s)}}$$

$$= \frac{-\alpha V_\infty}{\pi M_\infty} \int\limits_{r_{B_1'}}^{r_A} \frac{dr}{\sqrt{r_A - r}}$$

$$\times \int\limits_{s_{E_1}}^{s_A} \frac{ds}{\sqrt{s_A - s}} - \frac{\alpha V_\infty}{\pi M_\infty} \int\limits_{r_{B_1}}^{r_{B_1'}} \frac{dr}{\sqrt{r_A - r}} \int\limits_{s_{E_1''}}^{s_A} \frac{ds}{\sqrt{s_A - s}} \qquad (8.10.17)$$

In accordance with (8.9.4) and (8.9.7), the limits of the integrals in expression (8.10.17) have the form

$$\left.\begin{aligned} &s_{E_1''} = mr, \quad s_{E_1} = r_{E_1} - \frac{M_\infty l}{2} = r_A - \frac{M_\infty l}{2} \\ &r_{B_1'} = r_{E_1'} = s_{E_1'}/m = s_{E_1}/m = (1/m)(r_A - M_\infty l/2) \\ &r_{B_1} = s_A - M_\infty l/2 \end{aligned}\right\} \qquad (8.10.18)$$

As a result of integration, we establish the corresponding relation for φ'_{VI} in the variables r_A, s_A. Using their dependence on x_A and z_A, we find the velocity potential as a function of these coordinates. By calculating the derivative $\partial\varphi'_{VI}/\partial x_A$ and inserting it into the formula $\bar{p}_{VI} = -2\,(\partial\varphi'_{VI}/\partial x_A)/V_\infty$, we obtain the following expression for the pressure coefficient in the region being considered:

$$\bar{p}_{VI} = \frac{\pm 4\alpha}{\pi\alpha' \sqrt{1-n^2}} \left[\tan^{-1} \sqrt{\frac{\alpha'(n-1)(z_A - l/2)}{x_A + \alpha' z_A + \left(\frac{l}{2}\right)(n-1)\alpha'}} \right.$$

$$\left. - \tan^{-1} \sqrt{\frac{(x_A - \alpha' z_A) - (l/2)\alpha'(n+1)}{\alpha'(l/2 + z_A)(n+1)}} \right] \qquad (8.10.19)$$

For point A in region VII (Fig. 8.10.1*g*), we have

$$\varphi'_{VII} = \frac{-\alpha V_\infty}{\pi M_\infty} \iint\limits_{S_1+S_2+S_3} \frac{dr\,ds}{\sqrt{(r_A - r)(s_A - s)}}$$

$$= \frac{-\alpha V_\infty}{\pi M_\infty} \int\limits_{r_{J'}}^{r_A} \frac{dr}{\sqrt{r_A - r}} \int\limits_{s_V}^{s_A} \frac{ds}{\sqrt{s_A - s}}$$

$$-\frac{\alpha V_\infty}{\pi M_\infty}\int_0^{r_{J'}}\frac{dr}{\sqrt{r_A-r}}\int_{s_{V''}}^{s_A}\frac{ds}{\sqrt{s_A-s}}$$

$$-\frac{\alpha V_\infty}{\pi M_\infty}\int_{r_{W'}}^{0}\frac{dr}{\sqrt{r_A-r}}\int_{s_{W''}}^{s_A}\frac{ds}{\sqrt{s_A-s}} \qquad (8.10.20)$$

$$\left.\begin{aligned} &s_V = r_A - M_\infty l/2, \quad r_{J'} = (1/m)\left(r_A - \frac{M_\infty l}{2}\right) \\ &s_{V''} = mr, \quad s_{W''} = r/m, \quad r_W = s_A - M_\infty l/2 \end{aligned}\right\} \qquad (8.10.21)$$

The following pressure coefficient corresponds to the potential (8.10.20) calculated according to the values of the integration limits (8.10.21):

$$\begin{aligned} \bar{p}_{VII}\frac{\pm 4\alpha}{\pi\alpha'\sqrt{1-n^2}}\Bigg[&\tan^{-1}\sqrt{\frac{1+n}{1-n}}\sqrt{\frac{x_A-\alpha' z_A}{x_A+\alpha' z_A}} \\ &-\tan^{-1}\sqrt{\frac{\alpha'(l/2-z_A)(n+1)}{x_A+\alpha' z_A-(l/2)\alpha'(n+1)}} \\ &+\tan^{-1}\sqrt{\frac{(x_A+\alpha' z_A)-(l/2)\alpha'(n-1)}{\alpha'(l/2+z_A)(n+1)}}, \\ &-\tan^{-1}\sqrt{\frac{1-n}{n+1}}\sqrt{\frac{x_A-\alpha' z_A}{x_A-\alpha' z_A}}\Bigg] \end{aligned} \qquad (8.10.22)$$

Let us now consider region *VIII* (Fig. 8.10.1*h*) for whose points the region of integration simultaneously intersects regions Ω_1 and Ω_2; disturbances manifest themselves in these regions that are produced by the flow over both tips DE and GH. To evaluate the velocity potential for point A that belongs to region *VIII*, it is sufficient to extend integration in formula (8.10.3) to the region $S = S_1 + S_2$ hatched in Fig. 8.10.1*h*. Here the integral calculated over region S_2 in formula (8.10.3) must be taken with the opposite sign, i.e. with the plus sign. Accordingly, we have

$$\varphi'_{VIII} = \frac{-\alpha V_\infty}{\pi M_\infty}\iint_{S_1}\frac{dr\,ds}{\sqrt{(r_A-r)(s_A-s)}} + \frac{\alpha V_\infty}{\pi M_\infty}\iint_{S_2}\frac{dr\,ds}{\sqrt{(r_A-r)(s_A-s)}} \qquad (8.10.23)$$

Here

$$\iint_{S_1}\frac{dr\,ds}{\sqrt{(r_A-r)(s_A-s)}} = \int_{r_{H_1}}^{r_A}\frac{dr}{\sqrt{r_A-r}}\int_{s_{F_1}}^{s_A}\frac{ds}{\sqrt{s_A-s}} \qquad (8.10.24)$$

$$\iint\limits_{S_2} \frac{dr\,ds}{\sqrt{(r_A-r)(s_A-s)}} = \iint\limits_{\sigma_1} \frac{dr\,ds}{\sqrt{(r_A-r)(s_A-s)}} + \iint\limits_{\sigma_2} \frac{dr\,ds}{\sqrt{(r_A-r)(s_A-s)}} + \iint\limits_{\sigma_3} \frac{dr\,ds}{\sqrt{(r_A-r)(s_A-s)}}$$

$$= \int\limits_0^{r_{F_1'}} \frac{dr}{\sqrt{r_A-r}} \int\limits_{s_{L_1}}^{s_{F_1'}} \frac{ds}{\sqrt{s_A-s}} + \int\limits_{r_{F_1''}}^{0} \frac{dr}{\sqrt{r_A-r}} \int\limits_{s_{K_1}}^{s_{F_1'}} \frac{ds}{\sqrt{s_A-s}} \qquad (8.10.25)$$

The integration limits have the following values:

$$\left.\begin{aligned} r_{F_1'} &= r_{H_1} = s_A - M_\infty l/2,\ s_{L_1} = mr,\ s_{F_1'} = s_{F_1} = r_A - M_\infty l/2 \\ r_{F_1''} &= m s_{F_1''} = m s_{F_1} = m\,(r_A - M_\infty l/2),\ s_{K_1} = r/m \end{aligned}\right\} \qquad (8.10.26)$$

provided that

$$s_{F_1} = r_A - M_\infty l/2,\quad r_{H_1} = s_A - M_\infty l/2 \qquad (8.10.26')$$

With a view to these values of the limits, we calculate integrals (8.10.24) and (8.10.25), and then find the velocity potential (8.10.23). The following pressure coefficient corresponds to this potential:

$$\bar{p}_{VIII} = \frac{\pm 4\alpha}{\alpha'\pi\sqrt{1-n^2}} \left[\tan^{-1} \sqrt{\frac{1+n}{1-n}} \sqrt{\frac{(x_A-\alpha' z_A)+(l/2)\,\alpha'(n-1)}{\alpha'(l/2+z_A)(n+1)}} \right.$$

$$- \tan^{-1} \sqrt{\frac{1+n}{1-n}} \sqrt{\frac{x_A-\alpha' z_A}{x_A+\alpha' z_A}} + \tan^{-1} \sqrt{\frac{1-n}{1+n}} \sqrt{\frac{x_A-\alpha' z_A}{x_A+\alpha' z_A}}$$

$$\left. - \tan^{-1} \sqrt{\frac{1-n}{1+n}} \sqrt{\frac{\alpha'(l/2-z_A)(n+1)}{x_A+\alpha' z_A+(l/2)\,\alpha'(n-1)}} \right] \qquad (8.10.27)$$

The above method of calculating the pressure distribution can be related not only to hexagonal wings with a V-shaped appendage (see Fig. 8.9.1), but also to other planforms, namely, to a wing with a dovetail and a pentagonal plate (see Fig. 8.9.2) provided that the tips are subsonic, while the leading and trailing edges are supersonic. The corresponding change in the quantity $\Delta\bar{p}/\alpha = (\bar{p}_h - \bar{p}_u)/\alpha$ near a tip with the distance from the leading edge (in per cent of the chord) evaluated for a wing with a pentagonal planform at $M_\infty = 1.61$ is shown in Fig. 8.10.2. The coefficient $\Delta\bar{p}/\alpha$ is constant in the region between the leading edge and the Mach cones issuing from the vertex and tips of the wing, on the section confined by the tips and trailing edges, and also by the Mach wave reflected from a tip. A break in the curve characterizing a change in the pressure drop coefficient occurs on the Mach lines and is a result of the break in the configuration of the wing tip.

The found pressure distribution and formulas (8.9.27) and (8.9.28) are used to determine the lift, moment and centre-of-pressure coefficients. Figure 8.9.4 shows curves characterizing the change in the values of c_{y_a} and c_p for a pentagonal wing. These values should be

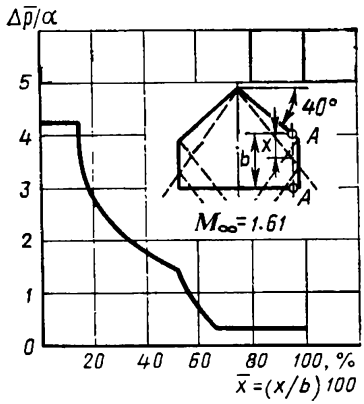

Fig. 8.10.2
Distribution of the quantity $\Delta\bar{p}/\alpha = (\bar{p}_b - \bar{p}_u)/\alpha$ near a tip of a pentagonal wing with supersonic leading edges (section *A-A*)

determined provided that $\lambda_w\sqrt{M_\infty^2 - 1} > \lambda_w \tan \varkappa_1$, i.e. if the leading edge is supersonic. If a wing has subsonic leading edges (see Fig. 8.9.1), the flow over the section of the surface between the edges and the Mach lines issuing from points E and H is affected by a vortex sheet. The calculation of this flow is associated with solution of integral equation (8.2.16) and the use of boundary conditions (8.1.15) and (8.1.16). Such a solution is treated in detail in [17].

8.11. Drag of Wings with Subsonic Leading Edges

Let us consider the calculation of the drag of swept wings with *subsonic leading edges* in a supersonic flow at an angle of attack. We already know that the disturbed flow normal to the leading edge is subsonic near such wings. Such a flow is attended by the *overflow* of the gas from the region of increased pressure into the region where the pressure is reduced and is the cause of the corresponding force action on the wing. To calculate this action, we can use the results of investigating the disturbed flow of an incompressible fluid near an airfoil in the form of a flat plate arranged in the flow at an angle of attack (see Sec. 6.3).

The drag coefficient for a thin wing with subsonic leading edges in a supersonic flow is

$$c_{x_a} = \alpha c_{y_a} - c_{x,T} \tag{8.11.1}$$

in which $c_{x\,T}$ is the coefficient of the wing suction force depending on the sweep angle $\varkappa$ of the leading edge and the number M_∞:

$$c_{x,T} = T/(q_\infty S_w) \tag{8.11.2}$$

where T is the suction force, $q_\infty = \rho_\infty V_\infty/2$ is the velocity head, and S_w is the area of the wing planform.

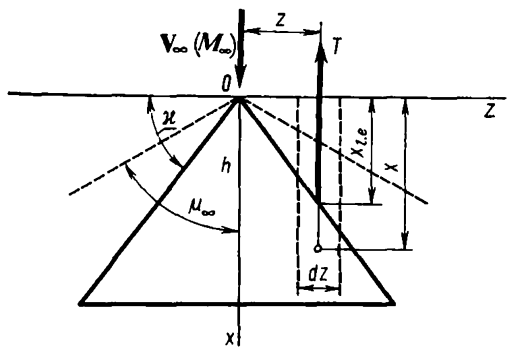

Fig. 8.11.1
To the calculation of the suction force for a triangular wing with subsonic leading edges

To determine the force T, we can use the relations obtained in Sec. 7.6 for an *infinite-span* swept wing. This follows from the fact that in accordance with (7.6.18) and (7.6.19), the suction force depends on the change in the axial component of the velocity in the close vicinity of the leading edge of the airfoil being considered, and also on the local sweep angle, and does not depend on the behaviour of this velocity far from the leading edge.

Using (7.6.18), we obtain

$$T = 2\pi\rho_\infty \sqrt{1+\tan^2\varkappa - M_\infty^2} \int_0^{l/2} c^2\, dz \qquad (8.11.3)$$

where c is a coefficient determined from (7.6.19).

Let us determine the drag for a triangular wing. For this purpose, we shall use expression (8.8.39) for the disturbed velocity. Assuming that $\cot\varkappa = z/x_{l.e}$, we find

$$u = \frac{aV_\infty (z/x_{l.e})^2}{[E(k)\sqrt{1-(x_{l.e}/x)^2}]}$$

where $x_{l.e}$ is the distance to the leading edge, z and x are the coordinates of a point on the wing (Fig. 8.11.1).

Introducing the value of u^2 into (7.6.19) and taking into account that $\lim\limits_{x\to x_{l.e}} (x/x_{l.e}) = 1$, we have

$$c^2 = \left[\frac{\alpha V_\infty}{E(k)}\right]^2 \lim_{x\to x_{l.e}} \frac{z^2 (x/x_{l.e})^2 (x-x_{l.e})}{(x-x_{l.e})(x+x_{l.e})} = \frac{1}{2}\left[\frac{\alpha V_\infty}{E(k)}\right]^2 z\cot\varkappa$$

Introducing this expression into (7.6.18) and integrating, we find

$$T = \frac{\pi\rho_\infty \cot\varkappa}{2}\left[\frac{\alpha V_\infty}{E(k)}\right]^2 2\sqrt{1+\tan^2\varkappa - M_\infty^2} \int_0^{l/2} z\, dz$$

$$= \frac{\pi\rho_\infty \cot\varkappa}{2}\left[\frac{\alpha V_\infty}{E(k)}\right]^2 \frac{l^2}{4}\sqrt{1+\tan^2\varkappa - M_\infty^2}$$

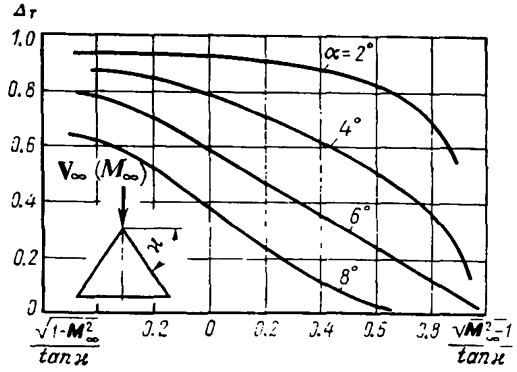

Fig. 8.11.2
Change in the factor Δ_T in formula (8.11.5) for calculating the suction force

The suction force coefficient by (8.11.2) is

$$c_{x,T} = \left[\frac{\alpha \cot \varkappa}{E(k)}\right]^2 \pi \sqrt{1 + \tan^2 \varkappa - M_\infty^2} \qquad (8.11.4)$$

Taking into account expression (8.8.44) for c_{y_a}, we have

$$c_{x,T} = (c_{y_a}^2 / 4\pi) \sqrt{1 + \tan^2 \varkappa - M_\infty^2} \qquad (8.11.4')$$

According to this formula, the suction force coefficient is proportional to $c_{y_a}^2$, i.e. $c_{x,T} = \bar{c}_T c_{y_a}^2$. The proportionality coefficient, equal to $\bar{c}_T = (1/4\pi)\sqrt{1 + \tan^2 \varkappa - M_\infty^2}$ for a triangular wing, changes when going over to another planform and depends not only on $\varkappa$ and M_∞, but also on the taper ratio η_w and the aspect ratio λ_w. Investigations show, however, that the influence of these additional parameters is not great, and the suction force for an arbitrary planform wing can be calculated with the aid of (8.11.4').

With a supersonic leading edge ($M_\infty \cos \varkappa > 1$), and also when the leading edge becomes sonic ($\tan \varkappa = \cot \mu_\infty = \sqrt{M_\infty^2 - 1}$), the suction force coefficient equals zero. With a subsonic leading edge ($M_\infty \cos \varkappa < 1$), the quantity $c_{x,T} = 0$, but experimental investigations show that its actual value is lower than the calculated one. This is especially noticeable at large angles of attack or sweep when local separation of the flow (burble) occurs in the vicinity of the leading edge and no further growth of the suction is observed. The decrease in the suction force can be taken into account by the correction factor Δ_T in accordance with which

$$c_{x,T} = \bar{c}_T \Delta_T c_{y_a}^2 \qquad (8.11.5)$$

Experimental data on the change in the quantity Δ_T are contained in Fig. 8.11.2. According to these data, the suction force at subsonic velocities lowers less than in supersonic flow upon an increase in the

angle of attack because at such velocities the separation of the flow from the leading edge is less noticeable and the suction is greater. According to experimental investigations, at subsonic velocities the correction factor in (8.11.5) is determined by the formula (see [18])

$$\Delta_T = (c^{\alpha}_{y_a w})^{-1} - 1/(\pi\lambda_w) \tag{8.11.6}$$

No suction force appears on wings with a sharp leading edge, i.e. the coefficient $c_{x,\ T} = 0$. Let us consider the total drag of a wing, which in accordance with (8.11.1), (8.11.5), and (8.8.44) can be written as

$$c_{x_a} = \alpha c_{y_a} - c_{x,\ T} = \frac{c^2_{y_a}}{4\pi \cot \varkappa} [2E(k) - \Delta_T \sqrt{1 - \cot^2 \varkappa (M^2_\infty - 1)}]$$

Having in view that the aspect ratio of the wing is

$$\lambda_w = l^2/S_w = 4 \cot \varkappa \tag{8.11.7}$$

we obtain

$$c_{x_a} = \frac{c^2_{y_a}}{\pi\lambda_w} [2E(k) - \Delta_T \sqrt{1 - \cot^2 \varkappa (M^2_\infty - 1)}] \tag{8.11.8}$$

Let us consider sonic flow. If $M_\infty \to 1$, then $E(k) \to 1$, and, consequently, the drag coefficient is

$$c_{x_a} = c^2_{y_a}/(\pi\lambda_w) \tag{8.11.9}$$

Expression (8.11.9) coincides with formula (6.4.16) for the coefficient of the induced vortex drag of a finite-span wing (provided that $\delta = 0$). Hence, *the physical nature of the drag force arising in a flow over a triangular wing with subsonic leading edges is due to induction by the vortices formed behind the wing.* Accordingly, the quantity determined by (8.11.8) is called the **induced drag coefficient.**

If the leading edge is sonic ($\tan \varkappa = \sqrt{M^2_\infty - 1}$), the second term in the brackets in (8.11.8) is zero, while $E(k) = E(0) = \pi/2$; consequently, the induced drag coefficient is

$$c_{x_a} = c_{x,\ i} = c^2_{y_a}/\lambda_w \tag{8.11.10}$$

For a very thin wing ($\varkappa \to \pi/2$), we may assume that $\cot \varkappa \approx 0$ and $E(k) \approx E(1) = 1$. In this case, expression (8.11.8) coincides with (8.11.9).

In addition to triangular wings, formula (8.11.8) may be applied to wings having the form of tetra-, penta-, and hexagonal plates with subsonic leading edges, and supersonic trailing and side edges (tips) (see Fig. 8.8.4). Particularly, for tetragonal wings, the coefficient c_{y_a} in (8.11.8) is found from (8.8.51).

8.12. Aerodynamic Characteristics of a Rectangular Wing

Supersonic flow over a thin finite-span rectangular wing at a small angle of attack is characterized by the influence of the *leading supersonic edge and the subsonic tips* (side edges) on the disturbed flow near the surface. The simultaneous influence of the leading edge and one tip is present within the limits of Mach cones issuing from wing corners O and O' (Fig. 8.12.1*a*) if the generatrices of these cones intersect outside the wing. If these generatrices intersect on the surface of the wing (Fig. 8.12.1*b*), in addition to regions II and II' where the influence of one tip is observed, zone III appears in which both tips act simultaneously on the disturbed flow.

In region I on the wing between the leading edge and the Mach cones, the disturbed flow is due to the influence of only the leading edge. Here the pressure coefficient is determined by the formula for a flat plate:

$$\bar{p}_I = \pm 2\alpha/\sqrt{M_\infty^2 - 1} \tag{8.12.1}$$

We shall use the method of sources to calculate the disturbed flow in region II (Fig. 8.12.1*a*). The velocity at point A in this region is induced by sources distributed over wing section $ACOE$. The total action of sources BCO and OBD on point A is zero, and, consequently, integration in (8.10.3) must be performed over region $ABDE$. Accordingly, the velocity potential at point A is

$$\varphi'_{II} = \frac{-\alpha V_\infty}{\pi M_\infty} \iint\limits_{ABDE} \frac{dr\,ds}{\sqrt{(r_A - r)(s_A - s)}}$$

$$= \frac{-\alpha V_\infty}{\pi M_\infty} \int\limits_{s_B}^{s_A} \frac{ds}{\sqrt{s_A - s}} \int\limits_{r_F}^{r_A} \frac{dr}{\sqrt{r_A - r}} \tag{8.12.2}$$

Point F is on the leading edge whose equation is $x = 0$. Hence, by (8.9.4), for this edge we have

$$r = -(M_\infty/2)\, z, \quad s = (M_\infty/2)\, z \tag{8.12.3}$$

Consequently, the equation of the leading edge in the coordinates r and s has the form

$$r = -s \tag{8.12.4}$$

Therefore, for point F, the coordinate $r_F = r = -s$.

Point B is on the tip whose equation is $z = 0$. Hence, by (8.9.4), for this tip we have

$$r = (M_\infty/2\alpha')x, \quad s = (M_\infty/2\alpha')\, x \tag{8.12.5}$$

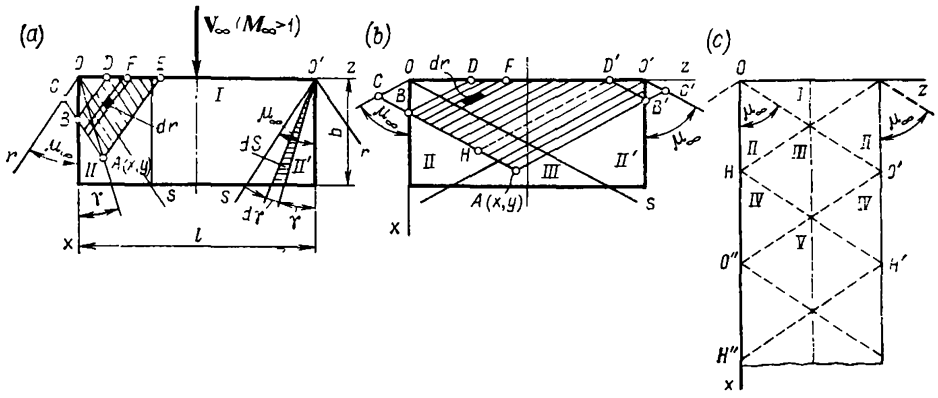

Fig. 8.12.1
Rectangular wing in a linearized supersonic flow

We can thus write the equation of the tip in the form

$$r = s \tag{8.12.6}$$

For point B, the coordinate $s_B = r_B = r_A$.

Performing integration in (8.12.2) with a view to the limits $r_F = -s$ and $s_B = r_A$, after introducing the values of r_A and s_A from (8.9.4′), we obtain

$$\varphi'_{II} = \frac{-2\alpha V_\infty}{\pi}\left[\sqrt{\frac{z_A}{\alpha'}(x_A - \alpha' z_A)} + \frac{x_A}{\alpha'}\tan^{-1}\sqrt{\frac{\alpha' z_A}{x_A - \alpha' z_A}}\right] \tag{8.12.7}$$

Let us calculate the corresponding pressure coefficient:

$$\bar{p}_{II} = -(2/V_\infty)\,\partial\varphi'_{II}/\partial x_A = \frac{\pm 4\alpha}{\pi\alpha'}\tan^{-1}\sqrt{\frac{\alpha' z_A}{x_A - \alpha' z_A}} \tag{8.12.8}$$

On the boundary of the two regions I and II separated by a Mach line, the pressure coefficient determined by (8.12.8) equals the value (8.12.1). Indeed, since the equation of this boundary is $z_A = x_A \tan \mu_\infty = x_A/\alpha'$, from (8.12.8) we find

$$\bar{p}_{II} = \pm(4\alpha/\pi\alpha')\,\pi/2 = \bar{p}_I$$

It follows from (8.12.8) that at the tips of the wing, the pressure at the points along the lines whose equation is z/x = const *is constant*. These lines can be considered as the generatrices of conical surfaces and, consequently, the flow in the indicated region of the wing can be considered *conical*.

Let us calculate the aerodynamic coefficients of a wing. The lift force acting on an element of area of the end part of the wing is

$$dY = (\bar{p}_b - \bar{p}_u)\,(\rho_\infty V_\infty^2/2)\,dS \tag{8.12.9}$$

A glance at Fig. 8.12.1*a* reveals that the elementary area is

$$dS = \frac{1}{2} \cdot \frac{b^2}{\cos^2 \gamma} d\gamma \qquad (8.12.10)$$

where γ is the angle measured from the wing tip.

Introducing into (8.12.9) the values of $\bar{p}_l$ and $-\bar{p}_u$ from (8.12.8), the value of dS from (8.12.10), and substituting $\tan\gamma$ for z_A/x_A, we have

$$dY = \frac{4\alpha b^2}{\pi\alpha'} \cdot \frac{\rho_\infty V_\infty^2}{2} \tan^{-1} \sqrt{\frac{\alpha' \tan\gamma}{1-\alpha' \tan\gamma}} \cdot \frac{d\gamma}{\cos^2\gamma}$$

Dividing this expression by the product of the wing area confined within the Mach cone ($S_{II} = b^2/2\alpha'$) and the velocity head ($q_\infty = \rho_\infty V_\infty^2/2$) and performing integration, we obtain the lift coefficient for the wing tips:

$$c_y'' = \frac{Y_a}{S_{II} q_\infty} = \frac{8\alpha}{\pi} \int_0^{\mu_\infty} \tan^{-1} \sqrt{\frac{\alpha' \tan\gamma}{1-\alpha' \tan\gamma}} \cdot \frac{d\gamma}{\cos^2\gamma}.$$

Integration by parts yields

$$c_y'' = 2\alpha/\alpha' = 2\alpha \sqrt{M_\infty^2 - 1} \qquad (8.12.11)$$

Let us determine the lift coefficient c_{yII} for the end parts of the wing related to its total area $S_w = lb$:

$$c_{yII} = c_y'' \frac{S_{II} + S_{II'}}{S_w} = c_y'' \frac{b^2}{lb\alpha'} = c_y'' \frac{1}{\lambda_w \alpha'} \qquad (8.12.11')$$

where $\lambda_w = l/b$.

The lift coefficient for wing section I related to the area S_I of this section is

$$c_y' = 4\alpha/\alpha' = 4\alpha \sqrt{M_\infty^2 - 1} \qquad (8.12.12)$$

The lift coefficient for this section related to the total wing surface is

$$c_{yI} = c_y' \frac{S_I}{S_w} = c_y' \frac{S_w - (S_{II} + S_{II'})}{S_w} = c_y' \left(1 - \frac{1}{\lambda_w \alpha'}\right) \qquad (8.12.13)$$

The total lift coefficient is

$$c_{y_a} = c_{yII} + c_{yI} = \frac{4\alpha}{\sqrt{M_\infty^2 - 1}} \left(1 - \frac{1}{2\lambda_w \sqrt{M_\infty^2 - 1}}\right) \qquad (8.12.14)$$

The wave drag coefficient is

$$c_{x,\,wave} = \alpha c_{y_a} = \frac{4\alpha^2}{\sqrt{M_\infty^2 - 1}} \left(1 - \frac{1}{2\lambda_w \sqrt{M_\infty^2 - 1}}\right) \qquad (8.12.15)$$

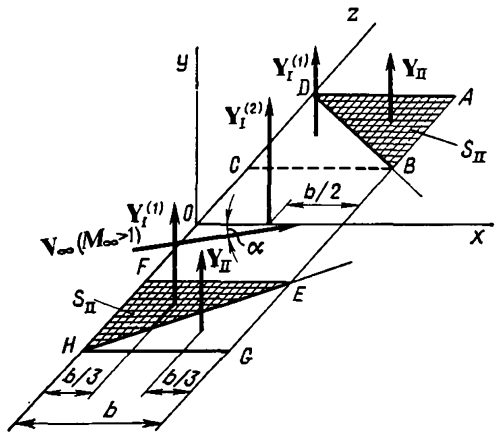

Fig. 8.12.2
To the determination of the aerodynamic moment for a rectangular wing

We can calculate the coefficient of the moment about the z-axis according to the known data on the pressure distribution and the lift coefficients for individual parts of the wing:

$$m_{z_a} = M_{z_a}/(q_\infty S_w b) \tag{8.12.16}$$

The moment M_{z_a} of the pressure forces distributed over the surface of the wing can be found as the sum of the moments of the lift forces about the z-axis acting on various parts of the wing (Fig. 8.12.2). Taking into account that on the triangular parts of the wing the point of application of the lift force coincides with the centre of mass of the area of the relevant part, we have the following expression for the moment:

$$-M_{z_a} = \frac{b}{3} 2Y_I^{(1)} + \frac{b}{2} Y_I^{(2)} + \frac{2b}{3} 2Y_{II} \tag{8.12.17}$$

where $Y_I^{(1)}$, $Y_I^{(2)}$, and Y_{II} are the values of the lift force calculated for parts CDB (HEF), $EFCB$, and ADB (GHE), respectively. By (8.12.11) and (8.12.12), we have

$$\left.\begin{aligned} Y_I^{(1)} &= c_y' \frac{\rho_\infty V_\infty^2}{2} S_{II} = \frac{4\alpha}{\alpha'} \cdot \frac{\rho_\infty V_\infty^2}{2} S_{II} \\ Y_I^{(2)} &= c_y' \frac{\rho_\infty V_\infty^2}{2} S_{EFCB} = \frac{4\alpha}{\alpha'} \cdot \frac{\rho_\infty V_\infty^2}{2} (S_w - 4S_{II}) \\ Y_{II} &= c_y'' \frac{\rho_\infty V_\infty^2}{2} S_{II} = \frac{2\alpha}{2} \cdot \frac{\rho_\infty V_\infty^2}{2} S_{II} \end{aligned}\right\} \tag{8.12.18}$$

Introducing (8.12.7) and (8.12.18) into (8.12.16) and taking into account the value $S_{II} = S_w/(2\lambda_w \alpha')$, we have

$$m_{z_a} = \frac{-2\alpha}{\sqrt{M_\infty^2 - 1}} \left(1 - \frac{2}{3\lambda_w \sqrt{M_\infty^2 - 1}}\right) \tag{8.12.19}$$

The coefficient of the centre of pressure is

$$c_p = \frac{x_p}{b} = \frac{-M_{z_a}}{bY_a} = \frac{-m_{z_a}}{c_{y_a}} = \frac{3\lambda_w \sqrt{M_\infty^2 - 1} - 2}{3(2\lambda_w \sqrt{M_\infty^2 - 1} - 1)} \quad (8.12.20)$$

If the number M_∞ for the flow over the wing shown in Fig. 8.12.1*a* is reduced, then at a certain value of this number the tip Mach cones intersect inside the wing. Here region *III* appears (see Fig. 8.12.1*b*) in which the disturbed flow is affected by the leading supersonic edge and both subsonic tips. The nature of the flow in regions *I* and *II* (*II'*) is the same as in the corresponding zones *I* and *II* (*II'*) of the wing whose diagram is shown in Fig. 8.12.1*a*.

Let us consider the flow at point *A* of region *III* (see Fig. 8.12.1*b*). The region of influence of the sources on this flow coincides with wing section *ABDD'B'*. The latter can be represented as the sum of areas *HBDD'* and *AHD'B'*. With this in view and according to (8.10.3), the velocity potential at point *A* is

$$\varphi'_{III} = \frac{-\alpha V_\infty}{\pi M_\infty} \left[\iint\limits_{HBDD'} \frac{dr\,ds}{\sqrt{(r_A - r)(s_A - s)}} + \iint\limits_{AHD'B'} \frac{dr\,ds}{\sqrt{(r_A - r)(s_A - s)}} \right]$$

We can determine the integration limits directly from Fig. 8.12.1*b*. Hence,

$$\varphi'_{III} = \frac{-\alpha V_\infty}{\pi M_\infty} \left[\int_{s_B}^{s_H} \frac{ds}{\sqrt{s_A - s}} \int_{r_F}^{r_A} \frac{dr}{\sqrt{r_A - r}} + \int_{s_H}^{s_A} \frac{ds}{\sqrt{s_A - s}} \int_{r_{B'}}^{r_A} \frac{dr}{\sqrt{r_A - r}} \right]$$

We calculate the first two integrals by analogy with (8.12.7), and the other two independently of each other because the region of integration is a parallelogram (see Fig. 8.12.1*b*). With this in view, we have

$$\varphi'_{III} = \frac{-2\alpha V_\infty}{\pi M_\infty} \left\{ -\sqrt{(r_A + s_H)(s_A - s_H)} + \sqrt{2r_A(s_A - r_A)} - (s_A + r_A) \left(\tan^{-1} \sqrt{\frac{s_A - s_H}{r_A + s_H}} - \tan^{-1} \sqrt{\frac{s_A - r_A}{2r_A}} \right) + 2\sqrt{(s_A - s_H)(r_A - r_{B'})} \right\} \quad (8.12.21)$$

Examination of Fig. 8.12.1*b* reveals that the coordinate $s_H = s_{D'}$ and in accordance with (8.12.4), the quantity $s_{D'} = -r_{D'}$. Consequently, $s_H = -r_{D'} = -r_{B'}$.

Point B' is on the starboard tip whose equation is $z = l$. From (8.9.4″), we can find the equation of this tip in the coordinates r and s:

$$r - s = -M_\infty l \tag{8.12.22}$$

Hence for point B'

$$r_{B'} = s_{B'} - M_\infty l = s_A + M_\infty l \tag{8.12.23}$$

Accordingly, we have

$$s_H = -r_{B'} = -s_A + M_\infty l \tag{8.12.24}$$

Introducing into (8.12.21) the coordinates r_A and s_A from (8.9.4′) and $r_{B'}$ and s_H from (8.12.23) and (8.12.24), we find

$$\varphi'_{III} = \frac{-2\alpha V_\infty}{\pi\alpha'}\left\{\sqrt{[(x_A - \alpha' z_A) - \alpha' l]\,(l - z_A)\,\alpha'}\right.$$
$$+\sqrt{\alpha' z_A\,(x_A - \alpha' z_A)} - x_A\left[\tan^{-1}\sqrt{\frac{(x_A + \alpha' z_A) - \alpha' l}{(l - z_A)\,\alpha'}}\right.$$
$$\left.\left. - \tan^{-1}\sqrt{\frac{\alpha' z_A}{x_A - \alpha' z_A}}\right]\right\} \tag{8.12.25}$$

Using the formula $\bar{p} = -(2/V_\infty)\,\partial\varphi'_{III}/\partial x_A$, we find the pressure coefficient as a result of simple transformations:

$$\bar{p}_{III} = \frac{\pm 4\alpha}{\pi\alpha'}\tan^{-1}\sqrt{\frac{\alpha' z_A}{x_A - \alpha' z_A}}$$
$$\pm\frac{4\alpha}{\pi\alpha'}\tan^{-1}\sqrt{\frac{(l - z_A)\,\alpha'}{(x_A + \alpha' z_A) - \alpha' l}} \pm \frac{2\alpha}{\alpha'} \tag{8.12.26}$$

The first and second terms in this expression are the pressure coefficients $\bar{p}_{II}$ and $\bar{p}_{II'}$ for the tip parts of the wing, respectively, while the third term is the pressure coefficient $\bar{p}_I$ for region I where there is no influence of the tips.

The flow over a rectangular wing is of a still more intricate nature if it has a low aspect ratio and the quantity $\lambda_w\sqrt{M_\infty^2 - 1} < 1$. In this case (see Fig. 8.12.1*c*), new wave regions appear that are formed as a result of intersection of the disturbance waves incident on and reflected from the tips. For example, the disturbances travelling from section OH of the port tip reach the starboard one on section $O'H'$ and over it propagate along Mach lines $O'O''$-$H'H''$ in the opposite direction. This gives rise to new wave zones IV and V in which the nature of the flow changes substantially. This flow can be calculated by using the method of sources set out above and taking into consideration the indicated intricate nature of formation of the disturbance zones.

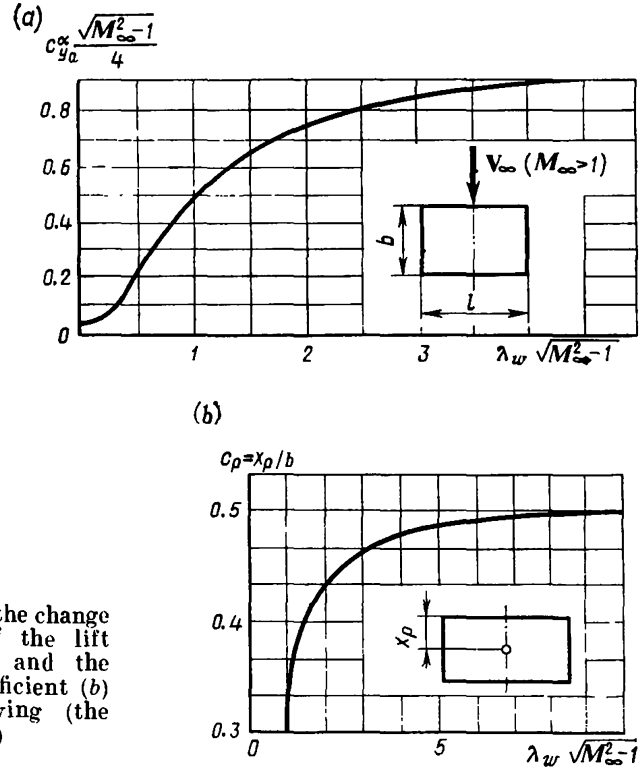

Fig. 8.12.3
Curves characterizing the change in the derivative of the lift force coefficient (*a*) and the centre-of-pressure coefficient (*b*) for a rectangular wing (the aspect ratio $\lambda_w = l/b$)

The known pressure distribution and formulas (8.9.27) and (8.9.28) are used to calculate the coefficients of the lift force and moment, while the expressions $c_p = -m_{z_a}/c_{y_a}$ and $c_{x_a} = \alpha c_{y_a}$ are used to calculate the coefficients of the centre of pressure and drag of the wing being considered. Curves characterizing the change in the lift and centre-of-pressure coefficients of a rectangular wing with a various aspect ratio have been constructed in Fig. 8.12.3 according to the results of such calculations.

8.13. Reverse-Flow Method

Let us consider one of the methods of aerodynamic investigations, the **reverse-flow method**, that establishes relations between the aerodynamic characteristics of thin wings with an identical planform and located in oppositely directed flows.

Let us assume that one of such wings is in a *forward* flow at the angle of attack α_1, and the other in an *reverse* flow at the angle of

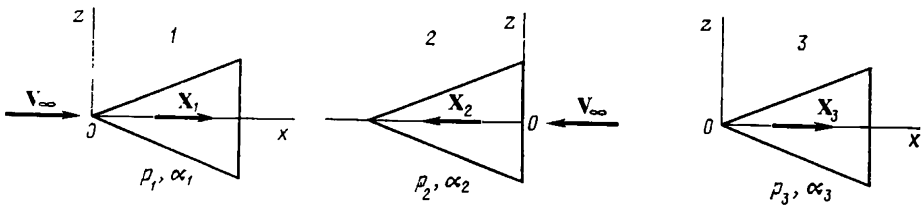

Fig. 8.13.1
To the explanation of the reverse-flow method:
1—forward flow; *2*—reverse flow; *3*—combined flow

attack α_2 (Fig. 8.13.1). According to the theory of linearized flow, the excess pressure at a point of the surface is $p - p_\infty = -\rho_\infty V_\infty u$, while the pressure increment between the bottom and upper sides is

$$\Delta p = p_b - p_u = \rho_\infty V_\infty (u_u - u_b) = \rho_\infty V_\infty \Delta u \qquad (8.13.1)$$

The magnitude of the drag force produced by the pressure increment is $dX_a = \Delta p\, \alpha\, dS$. Accordingly, the force for wing *1* in the forward flow is

$$X_{a1} = \int\int_S \Delta p_1 \alpha_1 \, dS \qquad (8.13.2)$$

and for wing *2* in the reverse flow is

$$X_{a2} = \int\int_S \Delta p_2 \alpha_2 \, dS \qquad (8.13.3)$$

The magnitudes of the pressure increment Δp_1, Δp_2 and of the local angles of attack α_1, α_2 are measured at the same point.

In the following, we shall disregard the suction force that can develop on the subsonic leading edge. This does not change the results. Since the flows in the vicinity of the wings are nearly uniform, by superposing them we can obtain a new flow with parameters satisfying the linearized equation for the velocity potential. We shall perform the superposition so that the free-stream velocities are subtracted. Now the contour of the new wing *3* (Fig. 8.13.1) coincides with the configuration of the given wings *1* and *2*, but the camber of its surface is different.

This camber is determined by the local angle of attack α_3 equal to the sum of the angles of attack:

$$\alpha_3 = v_3/V_\infty = v_1/V_\infty + v_2/V_\infty = \alpha_1 + \alpha_2 \qquad (8.13.4)$$

In accordance with (8.13.4), the vertical components of the velocity v at the corresponding points of the surfaces are added. The horizontal velocity components upon superposition are subtracted, therefore for the combined wing *3* we obtain $\Delta u_3 = \Delta u_1 - \Delta u_2$.

Hence the pressure increment between the bottom and upper sides of this wing is $\Delta p_3 = \rho_\infty V_\infty \Delta u_3 = \rho_\infty V_\infty (\Delta u_1 - \Delta u_2)$, or by (8.13.1):

$$\Delta p_3 = \Delta p_1 - \Delta p_2 \tag{8.13.5}$$

The drag of wing *3* is

$$X_{a3} = \int\int_S (\Delta p_1 - \Delta p_2)(\alpha_1 - \alpha_2)\, dS \tag{8.13.6}$$

A drag in a wing is associated with a disturbed flow behind it. The latter is an infinitely long vortex sheet cast off the trailing edge. It is clear from physical considerations that there is strict correspondence between the disturbed state behind the wing and the drag force. Particularly, the force X_{a1} and the disturbed state behind wing *1*, as well as the force X_{a2} and the disturbed state behind wing *2* are in such correspondence.

The flow near wing *3* obtained as a result of superposition of the flow patterns near wing *1* and wing *2* has the property that the disturbances ahead of it are the same as for wing *2*, and behind it, the same as for wing *3*. Hence, the drag force of combined wing *3* equals the difference between the drags of wings *1* and *2*, i.e.

$$X_{a3} = X_{a1} - X_{a2} = \int\int_S (\Delta p_1 \alpha_1 - \Delta p_2 \alpha_2)\, dS \tag{8.13.7}$$

Equating the right-hand sides of (8.13.6) and (8.13.7), we obtain

$$\int\int_S \Delta p_1 \alpha_2\, dS = \int\int_S \Delta p_2 \alpha_1\, dS \tag{8.13.8}$$

This relation is the *fundamental expression of the reverse-flow method.*

Going over to pressure coefficients in (8.13.8), we can write this relation as

$$\int\int_S \Delta \bar{p}_1 \alpha_2\, dS = \int\int_S \Delta \bar{p}_2 \alpha_1\, dS \tag{8.13.8'}$$

where the pressure increment coefficients are $\Delta \bar{p}_1 = \bar{p}_{1b} - \bar{p}_{1u}$ and $\Delta \bar{p}_2 = \bar{p}_{2b} - \bar{p}_{2u}$.

Using our right to choose the angle of attack arbitrarily, let us adopt the same constant values of α_1 and α_2 for all points on a wing surface, i.e. $\alpha_1 = \alpha_2 = \alpha$. We therefore find from (8.13.8') that

$$\int\int_S \Delta \bar{p}_1\, dS = \int\int_S \Delta \bar{p}_2\, dS, \text{ or } Y_{a1} = Y_{a2}$$

Hence, the reverse-flow method allows us to establish that the lift force of a flat plate in forward (Y_{a1}) and reverse (Y_{a2}) flow *is the same* at identical angles of attack and free-stream velocities.

Aerodynamic Characteristics of Craft in Unsteady Motion

In the steady motion of craft, the aerodynamic forces and moments are independent of time and are determined for fixed rudders and elevators and for a given altitude and velocity only by the orientation of the craft relative to the velocity vector. Unsteady motion, when a craft experiences acceleration or deceleration and vibrates for various reasons, is the most general case. In inverted motion, this is equivalent to an unsteady flow of air over a craft. With such a flow, the aerodynamic properties of a craft are due not only to its position relative to the free-stream velocity, but also depend on the kinematic parameters characterizing motion, i.e. the aerodynamic coefficients are a function of time.

In unsteady flow, a craft experiences additional forces and moments. Their magnitudes in a number of cases are quite small in comparison with those encountered in steady motion. Particularly, in an axial accelerated supersonic flow over a body, the drag grows only insignificantly, which may be disregarded in practice (according to Frankl).

Many important problems relating to the motion of craft, including unsteady motion, can be solved by using the aerodynamic characteristics for a steady flow. A number of problems, however, are solved only by finding the aerodynamic characteristics with account taken of the unsteady nature of the flow.

The major problems include that of the **dynamic stability** of a craft. A craft has dynamic stability in given flight conditions if the deviation of the kinematic parameters produced by disturbing forces diminishes with time so that the disturbed motion attenuates and tends to the initial programmed flight.

If this condition is not realized, we have dynamic instability of a craft. Dynamic stability (or instability) is investigated on the basis of the equations for disturbed motion including time-dependent aerodynamic characteristics (what are called non-stationary aerodynamic characteristics).

The concept of **controllability**, i.e. the ability of a craft to respond to the controls and change its position in space and the corresponding flight characteristics sufficiently rapidly and without appreciable vibrations, is associated with the concept of stability.

The problem of control is solved on the basis of equations of motion including non-stationary characteristics of a craft with account taken of the action of the control surfaces. These problems include the investigation of an unsteady flight for establishing and evaluating the **manoeuvrability** of a craft, i.e. its ability to change its speed, direction of flight, and orientation in space within a given interval of time.

9.1. General Relations for the Aerodynamic Coefficients

The aerodynamic forces or moments acting on a craft depend on the **kinematic variables** characterizing its motion. For a given configuration and altitude H of a craft, these forces and moments are determined by the flight velocity $\mathbf{V} = -\mathbf{V}_\infty$ ($\mathbf{V}_\infty$ is the free-stream velocity in inverted flow), the angular orientation relative to the velocity vector $\mathbf{V}$ (the angles α and β), the angles of deflection of the control surfaces arranged in three mutually perpendicular planes (δ_r, δ_e and δ_a are the rudder, elevator, and aileron angles, respectively), and also the angular velocities of rotation about the body axes (Ω_x, Ω_y, Ω_z, Fig. 9.1.1). In addition, in the general case it is necessary to take into account the influence of the angular and linear accelerations ($\dot{\Omega}_x = d\Omega_x/dt$, $\dot{\Omega}_y = d\Omega_y/dt$, $\dot{\Omega}_z = d\Omega_z/dt$, $\dot{V}_\infty = dV_\infty/dt$), of the rate of change in the angle of attack and the sideslip angle ($\dot{\alpha} = d\alpha/dt$, $\dot{\beta} = d\beta/dt$), and also of the rate of change in the angle of deflection of the control surfaces ($\dot{\delta}_r = d\delta_r/dt$, $\dot{\delta}_e = d\delta_e/dt$, $\dot{\delta}_a = d\delta_a/dt$). Accordingly, the following general relation holds for a force or moment:

$$T = f_1(V_\infty, H, \alpha, \beta, \delta_r, \delta_e, \delta_a, \Omega_x, \Omega_y, \Omega_z, \dot{V}_\infty, \dot{\alpha}, \dot{\beta}, \dot{\delta}_r, \dot{\delta}_e, \dot{\delta}_a, \dot{\Omega}_x, \dot{\Omega}_y, \dot{\Omega}_z) \qquad (9.1.1)$$

The aerodynamic force and moment coefficients are functions of dimensionless variables corresponding to the dimensional quantities in relation (9.1.1). As examples of such variables corresponding to the velocity V_∞ and altitude H, we can consider the Mach number $M_\infty = V_\infty/a_\infty$ and Reynolds number $Re = V_\infty l \rho_\infty/\mu_\infty$ (here a_∞, ρ_∞, and μ_∞ are the speed of sound, the density, and the dynamic viscosity, respectively, of the air at the altitude H, and l is a typical dimension of the craft).

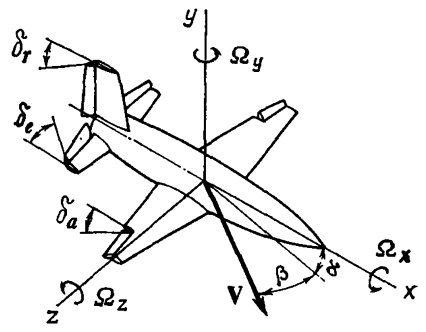

Fig. 9.1.1
Designation of kinematic variables characterizing the motion of a craft

We can write the other dimensionless variables in the following form:

$$\left.\begin{aligned} &\dot{\bar{\delta}}_{r(e.\,a)} = \dot{\delta}_{r(e,\,a)} l/V_\infty, \quad \dot{\bar{\alpha}} = \dot{\alpha} l/V_\infty, \quad \dot{\bar{\beta}} = \dot{\beta} l/V_\infty \\ &\omega_x = \Omega_x l/V_\infty, \quad \omega_y = \Omega_y l/V_\infty, \quad \omega_z = \Omega_z l/V_\infty, \quad \dot{\bar{V}}_\infty = \dot{V}_\infty l/V_\infty \\ &\dot{\omega}_x = \dot{\Omega}_x l^2/V_\infty^2, \quad \dot{\omega}_y = \dot{\Omega}_y l^2/V_\infty^2, \quad \dot{\omega}_z = \dot{\Omega}_z l^2/V_\infty^2 \end{aligned}\right\} \qquad (9.1.2)$$

Hence, for an aerodynamic coefficient in any coordinate system, we have

$$c = f_2(\boldsymbol{M}_\infty, \boldsymbol{Re}_\infty, \alpha, \beta, \delta_r, \delta_e, \delta_a, \omega_x, \omega_y, \omega_z, \dot{\bar{V}}_\infty, \dot{\bar{\alpha}}, \dot{\bar{\beta}}, \dot{\bar{\delta}}_r, \dot{\bar{\delta}}_e, \dot{\bar{\delta}}_a, \dot{\omega}_x, \dot{\omega}_y, \dot{\omega}_z) \qquad (9.1.3)$$

The variables $\boldsymbol{M}_\infty$, α, β, δ_r, δ_e, δ_a, ω_x, ω_y, and ω_z determine the coefficients of the aerodynamic forces and moments due to the instantaneous distribution of the local angles of attack. Here the variables $\boldsymbol{M}_\infty$, α, β, δ_r, δ_e, and δ_a characterize the forces and moments depending on the velocity, the angle of attack, the sideslip angle, and the control surface angles, while the variables ω_x, ω_y, and ω_z determine the forces and moments due to the change in the local angles of attack caused by rotation.

The time derivatives $\dot{\bar{V}}_\infty$, $\dot{\bar{\alpha}}$, $\dot{\bar{\beta}}$, $\dot{\bar{\delta}}_r$, $\dot{\bar{\delta}}_e$, $\dot{\bar{\delta}}_a$, $\dot{\omega}_x$, $\dot{\omega}_y$ and $\dot{\omega}_z$ determine the additional forces of an inertial nature and appearing upon the accelerated motion of a body. This motion accelerates the air particles on the surface in the flow.

When investigating the motion of craft characterized by a small change in the dimensionless kinematic variables, the aerodynamic coefficients are written in the form of a Taylor series in which the second-order infinitesimals may be retained. Assuming the number $\boldsymbol{Re}_\infty$ to be fixed, we shall present, particularly, such a series for the

normal force coefficient:

$$c_y = c_{y0} + c_y^{M_\infty}\Delta M_\infty + c_y^{\alpha}\Delta\alpha + c_y^{\beta}\Delta\beta + c_y^{\delta_r}\Delta\delta_r + c_y^{\delta_e}\Delta\delta_e + c_y^{\delta_a}\Delta\delta_a + c_y^{\omega_x}\Delta\omega_x + c_y^{\omega_y}\Delta\omega_y + c_y^{\omega_z}\Delta\omega_z + c_y^{\dot{V}_\infty}\Delta\dot{\bar{V}}_\infty + c_y^{\dot{\alpha}}\Delta\dot{\bar{\alpha}} - c_y^{\dot{\beta}}\Delta\dot{\bar{\beta}} + c_y^{\dot{\delta}_r}\Delta\dot{\bar{\delta}}_r + c_y^{\dot{\delta}_e}\Delta\dot{\bar{\delta}}_e + c_y^{\dot{\delta}_a}\Delta\dot{\bar{\delta}}_a + c_y^{\dot{\omega}_x}\Delta\dot{\omega}_x + c_y^{\dot{\omega}_y}\Delta\dot{\omega}_y + c_y^{\dot{\omega}_z}\Delta\dot{\omega}_z + \ldots + \frac{1}{2}c_y^{\beta\omega_y}\Delta\beta\,\Delta\omega_x + \ldots + \frac{1}{2}c_y^{\omega_x\omega_y}\Delta\omega_x\Delta\omega_y + \ldots \quad (9.1.4)$$

Here the coefficient c_{y0}, the derivatives $c_y^{M_\infty} = \partial c_y/\partial M_\infty$, $c_y^{\alpha} = \partial c_y/\partial\alpha$, $c_y^{\beta} = \partial c_y/\partial\beta$ and others are calculated for certain initial values of the variables. If these values equal zero, one must assume that $\Delta\alpha = \alpha$, $\Delta\dot{\bar{\alpha}} = \dot{\bar{\alpha}}$, etc.

The derivatives can be considered as the rates of change in a coefficient of any force or moment depending on the number M_∞, the angle of attack or the sideslip angle, the control surface angles, the angular and linear velocities, and also on their time derivatives.

The derivatives being considered are aerodynamic characteristics used in the investigation of a flight and first of all in solving stability problems. This is why such characteristics are usually called **stability derivatives.**

The stability derivatives in (9.1.4) do not depend on the time and are determined by the values of the dimensionless kinematic variables at the point of a trajectory for which the aerodynamic coefficient being considered is expanded into a Taylor series. For unsteady motion, the values of these coefficients are not only determined by the values of the kinematic variables at a given instant, but are also dependent on the history of the motion, i.e. on how it occurred in the preceding period. In an appreciable number of problems of practical interest, we can determine the law of motion beforehand with a high authenticity and thereby substantially simplify the investigation of non-stationary aerodynamic characteristics. The calculations are simplified, particularly, if the kinematic variables determining the nature of motion change **harmonically**, i.e. the values of these parameters can be written in the form

$$q_i = q_i^* \cos p_i t \quad (9.1.5)$$

where q_i is the set of dimensionless kinematic variables, q_i^* is the amplitude, and p_i is the circular frequency of the oscillations.

In accordance with (9.1.5), the time derivative is

$$\dot{q}_i = dq_i/dt = -q_i^* p_i^* \sin p_i t \quad (9.1.6)$$

where we have introduced the **Strouhal number**

$$p_i^* = p_i l/V_\infty \quad (9.1.7)$$

For example, if $q_i = \alpha$, $q_i^* = \alpha_0$ (the amplitude of the oscillations with respect to the angle of attack), $\dot{q}_i = (d\alpha/dt)\, l/V_\infty = \bar{\dot{\alpha}}$, $p_i^* = p_\alpha^*$, and $p_i = p_\alpha$, then

$$\alpha = \alpha_0 \cos p_\alpha t, \quad \bar{\dot{\alpha}} = -\alpha_0 p_\alpha^* \sin p_\alpha t \tag{9.1.8}$$

Important solutions from a practical viewpoint have been obtained for the particular case of harmonic oscillations. They allow one to determine the basic aerodynamic characteristics for the unsteady motion of wings, bodies of revolution, and separate kinds of aircraft.

Expressions (9.1.3) and (9.1.4) for the aerodynamic coefficients relate to a craft with an undeformed (rigid) surface. It must be taken into account here that in real conditions such a surface may deform, for example, because of bending, which leads to an additional change in the non-stationary characteristics. Considered below are problems on the determination of such characteristics without account taken of deformation, i.e. for inelastic bodies in a flow. The results of investigating unsteady-flow aerodynamic characteristics for the more general case of deformed surfaces are given in [4, 19].

9.2. Analysis of Stability Derivatives and Aerodynamic Coefficients

The first seven terms in Eq. (9.1.4) determine the **static**, and the remaining ones, the **dynamic components** of the aerodynamic coefficients. The static components correspond to steady conditions of flow over a craft in which its velocity is constant, while the angle of attack, the sideslip angle, and also the control surface angles are fixed. The dynamic components appear in non-stationary motion attended by acceleration or deceleration of the flow over a craft, its rotation, and a change in time of the control surface angles.

In accordance with the above, the derivatives $c_y^{M_\infty}$, c_y^α, c_y^β, and $c_y^{\delta_r}$ are called **static stability derivatives**, and the remaining ones, ($c_y^{\omega_x}$ $c_y^{\bar{\dot{V}}_\infty}$, $c_y^{\bar{\dot{\alpha}}}$, $c_y^{\bar{\dot{\beta}}}$, $c_y^{\bar{\dot{\delta}}_r}$, etc.), the **dynamic stability derivatives.**

As can be seen from (9.1.4), the aerodynamic coefficients are determined by the corresponding **first** and **second order stability derivatives.** The first order ones include the values of $c_y^{M_\infty}$, c_y^α, $c_y^{\bar{\dot{\alpha}}}$, c_y^β, $c_y^{\bar{\dot{\beta}}}$, and the second order ones, $c_y^{\alpha\beta} = \partial^2 c_y/\partial\alpha\,\partial\beta$, $c_y^{\alpha\omega_x} = \partial^2 c_y/\partial\alpha\,\partial\omega_x$, etc.

An analysis of (9.1.4) reveals that the aerodynamic coefficients are determined by two groups of derivatives, one of which depends on the control surface variables ($c_y^{\delta_r}$, $c_y^{\bar{\dot{\delta}}_r}$, . . .), while the other is not related to them (c_y^α, $c_y^{\bar{\dot{\alpha}}}$, . . .). The magnitude of a coefficient depends on the action of these controls. This is due to the change

in the angle of attack and sideslip angle upon deflection of the control surfaces. The values of the angles α and β correspond to the position of static equilibrium of a craft.

To retain the given flight conditions, the control surfaces must be fixed in place. Such a flight with "fixed" control surfaces becomes uncontrollable. Its conditions are determined completely by the stability derivatives that depend on the intrinsic aerodynamic properties of a craft if controls are absent or are fixed in place.

Derivatives such as c_y^{α}, c_y^{β}, $c_y^{\delta_r}$, . . ., determined as a result of differentiation of the aerodynamic coefficients with respect to α, β, δ_r (static stability derivatives) relate to the first group of derivatives. The partial derivatives of the coefficients with respect to one of the variables ω_x, ω_y, ω_z form the second group of what we call rotary derivatives (for example, $c_y^{\omega_x}$, $c_y^{\omega_y}$, $m_z^{\omega_z}$, . . .). This group also includes derivatives similar to $c_y^{\dot{\alpha}}$, $c_y^{\dot{\beta}}$, $c_y^{\dot{\delta}_r}$, and also *acceleration derivatives* determined as the partial derivatives of the aerodynamic coefficients with respect to one of the parameters $\dot{V}_{\infty}$, $\dot{\omega}_x$, $\dot{\omega}_y$, or $\dot{\omega}_z$.

If the non-stationary disturbances are finite, non-linearity becomes a noticeable feature. It is reflected in expansion (9.1.4) where there are several second-order terms. The latter are determined by stability derivatives of the second order (for example, $c_y^{\alpha\beta}$ and $c_y^{\alpha\omega_y}$) that are in the fourth group.

Investigations show that the influence of the derivatives on the aerodynamic coefficients is not the same and that a practical significance is a feature of only a part of such derivatives, among which second order derivatives form a quite small fraction. This influence is analysed in each specific case depending on the aerodynamic configuration of a craft and the conditions of its motion. As a result, we find the derivatives which the aerodynamic coefficients (or the corresponding forces and moments) depend on and the influence of which of them may be ignored. For each coefficient, we can reveal the characteristic trend associated with such a relation. Let us consider, for example, the longitudinal (axial) force coefficient, the expression for which will be written in the form

$$c_x = c_{x0} + c_x^{\alpha^2}\alpha^2 + c_x^{\alpha\delta_e}\alpha\delta_e + c_x^{\delta_e^2}\delta_e^2 + c_x^{\beta^2}\beta^2 + c_x^{\beta\delta_r}\beta\delta_r + c_x^{\delta_r^2}\delta_r^2 \qquad (9.2.1)$$

where c_{x0} is the value of c_x at $\alpha = \beta = \delta_e = \delta_r = 0$, $c_x^{\alpha^2}$, . . ., $c_x^{\alpha\delta_e}$ are the second-order partial derivatives of the longitudinal force coefficient with respect to α^2, . . ., $\alpha\delta_e$ (for example, $c_x^{\alpha^2} = \partial^2 c_x/\partial\alpha^2$).

In accordance with expression (9.2.1), the longitudinal force coefficient is a quantity not depending on the rotary derivatives or the acceleration derivatives. This quantity is determined in the form

of a quadratic dependence on the angle of attack and the sideslip angle, as well as the elevator and rudder angles. Here the components of the coefficient c_x depending on the derivatives $c_x^{\delta_e^2}$ and $c_x^{\delta_r^2}$ are of significance when control surfaces are present in the form of movable wings or empennage whose deflection may lead to a substantial change in the longitudinal force.

The **normal force coefficient** can be written in the form of the linear relation

$$c_y = c_{y0} + c_y^{\alpha}\alpha + c_y^{\delta_e}\delta \tag{9.2.2}$$

where c_{y0} is the value of c_y at $\alpha = \delta_e = 0$.

Relation (9.2.2) is suitable for small values of α and δ_e. The larger these angles (beginning approximately from values of 10°), the more does the non-linear nature of the dependence of the coefficient c_y on them manifest itself. The non-linear nature increases with a decrease in the aspect ratio of the lifting planes, and also with an increase in the Mach number ($M_\infty > 3$-4). In accordance with (9.2.2), when determining the normal force coefficient, no account is taken of the influence of the sideslip, rudder, elevator, and aileron angles, and also of the rotation of the craft and its acceleration. At the same time, when a movable wing (empennage) is present, the quantity $c_y^{\delta_e}\delta_e$ differs appreciably from that for conventional control surfaces. In the latter case, this quantity may be negligibly small.

The **lateral force coefficient** c_z (in body axes) can be calculated by analogy with the normal force coefficient c_y, i.e. by using formula (9.2.2) in which the angle of attack and the elevator angle must be replaced with the sideslip and rudder angles, respectively:

$$c_z = c_z^{\beta}\beta + c_z^{\delta_r}\delta_r \tag{9.2.3}$$

According to this expression, when $\beta = \delta_r = 0$, the lateral force coefficient equals zero, which corresponds to symmetry of a craft about the vertical plane xOy.

The pitching moment at a given number M_∞ for a flight depends mainly on parameters such as the angle of attack α and the elevator angle δ_e, the rate of change in these angles $\dot{\alpha}$ and $\dot{\delta}_e$, and also the angular velocity Ω_z. The influence of other parameters, in particular of the sideslip angle, the aileron angle, and the angular velocities Ω_y or Ω_x, is not great and is usually disregarded.

In accordance with the above, for the pitching moment coefficient we can obtain the following linear relation suitable for small values of the indicated variables (in a body axis coordinate system):

$$m_z = m_{z0} + m_z^{\alpha}\alpha + m_z^{\delta_e}\delta_e + m_z^{\omega_z}\omega_z + m_z^{\dot{\alpha}}\dot{\alpha} + m_z^{\dot{\delta}_e}\dot{\delta}_e \tag{9.2.4}$$

where m_{z0} is the moment coefficient when $\alpha = \delta_e = \omega_z = \dot{\alpha} = \dot{\delta}_e = 0$.

A glance at the above expression reveals that the pitching moment coefficient is determined by two static stability derivatives m_z^{α}, $m_z^{\delta_e}$ and three rotary derivatives $m_z^{\omega_z}$, $m_z^{\dot{\alpha}}$, $m_z^{\dot{\delta}_e}$.

By analogy with the pitching moment, the yawing moment may be considered to depend mainly on the sideslip and rudder angles β and δ_r, the rates of their change in time $\dot{\beta}$, $\dot{\delta}_r$, and also on the angular velocity Ω_z. Such a relation exists for axisymmetric craft. If symmetry is disturbed, however, account must also be taken of the influence of the angular velocity Ω_x. This can be done, for example, with the presence of a non-symmetric vertical empennage when the upper panel upon rotation about its longitudinal axis creates a lateral (side) force that produces an additional moment about the vertical axis.

Deflection of the ailerons also produces a certain yawing moment, which is associated with the longitudinal forces differing in value on horizontal wings upon deflection of the ailerons (this is similar to the appearance of a small pitching moment upon the deflection of the ailerons on vertical wings). Investigations show that such an additional yawing moment is usually very small in modern aircraft. Accordingly, the yawing moment coefficient may be expressed by the following linear relation:

$$m_y = m_y^{\beta}\beta + m_y^{\delta_r}\delta_r + m_y^{\omega_x}\omega_x + m_y^{\omega_y}\omega_y + m_y^{\dot{\beta}}\dot{\beta} + m_y^{\dot{\delta}_r}\dot{\delta}_r \quad (9.2.5)$$

In accordance with this relation, the yawing moment at $\beta = \delta_r = \ldots = 0$ equals zero. This is always observed in aircraft symmetric about the plane xOy. By (9.2.5), the yawing moment coefficient is determined by two static derivatives m_y^{β}, $m_y^{\delta_r}$ and four rotational derivatives $m_y^{\omega_x}$, $m_y^{\omega_y}$, $m_y^{\dot{\beta}}$, and $m_y^{\dot{\delta}_r}$.

A rolling moment (a moment about the longitudinal axis Ox) is due to the asymmetry of the flow caused by sideslip and control surface deflection angles or rotation of the craft. For a given craft design and a definite flight speed (number M_∞), this moment can be considered as a function of the angle of attack α, the sideslip angle β, the elevator, rudder, and aileron angles δ_e, δ_r, δ_a, and also of the rotational velocities Ω_x, Ω_y, Ω_z. Accordingly, the rolling moment coefficient can be written as

$$m_x = m_x^{\beta}\beta + m_x^{\delta_r}\delta_r + m_x^{\delta_a}\delta_a + m_x^{\alpha\beta}\alpha\beta + m_x^{\alpha\delta_r}\alpha\delta_r + m_x^{\beta\delta_e}\beta\delta_e + m_x^{\omega_x}\omega_x + m_x^{\omega_y}\omega_y + m_x^{\alpha\omega_y}\alpha\omega_y + m_x^{\beta\omega_z}\beta\omega_z \quad (9.2.6)$$

According to this expression, the rolling moment at $\beta = \delta_r = \delta_a = \ldots = 0$ equals zero, which corresponds to an ideal design of the craft produced without any technological errors. When study-

ing the motion of a real craft, particularly rolling motion, account must be taken of the presence of such errors, especially of those associated with inaccurate wing installation, which has the maximum influence on the rolling moment.

Inspection of (9.2.6) reveals that the rolling moment is determined as the function of derivatives not only of the first, but also of the second order (m_x^{β}, $m_x^{\delta_r}$, . . ., $m_x^{\alpha\beta}$, $m_x^{\alpha\delta_r}$, . . .). Therefore, such a function is non-linear, which occurs even with small angular values of α, β, δ_e, δ_r, δ_a, and small velocities ω_x, ω_y, ω_z. At the same time, the rolling moment coefficient when performing approximate calculations may be found without taking into account the influence of the rates of change in the angle of attack and the sideslip angle, and also of the acceleration, this influence being negligible.

All the derivatives determining the aerodynamic coefficients are functions depending mainly on the number M_∞, and also on the geometric configuration and dimensions of the craft. In a more general case, these derivatives depend on the arguments determining the aerodynamic coefficients, particularly on the angle of attack and the sideslip angle, the angular velocities and the relevant accelerations, and also on the acceleration of the translational motion. Such a relation is found separately in each case for a given kind of motion of a craft.

A part of the considered stability derivatives characterize the aerodynamic properties of a craft regardless of the action of the control surfaces (c_y^{α}, m_z^{α}, $m_x^{\omega_x}$, . . .), whereas the other part is associated with their deflection ($c_y^{\delta_e}$, $m_z^{\delta_e}$, $m_x^{\delta_a}$, $m_x^{\delta_e}$. . . .). Each of these derivatives has a physical meaning and may be helpful in studying the motion of a craft.

The static derivatives c_y^{α} and c_z^{β} characterize the property of a craft to change the normal and lateral forces depending on the angle of attack and the sideslip angle, whereas the derivatives $c_y^{\delta_e}$ and $c_z^{\delta_r}$ characterize the same property, but associated with the deflection of the corresponding control surfaces. These derivatives are important for controlling the motion of the centre of mass of a craft in the longitudinal and lateral directions.

The static second-order derivatives $c_x^{\alpha^2}$, $c_x^{\beta^2}$, $c_x^{\delta_e^2}$, and $c_x^{\delta_r^2}$ determine the additional increment of the longitudinal force due to deflection of a craft through the angles α and β, and also to the controlling action of the control surfaces. The derivatives $c_x^{\alpha\delta_e}$ and $c_x^{\beta\delta_r}$ characterize the influence on the longitudinal force of the interaction of the angle of attack and the elevator angle, while $c_x^{\beta\delta_r}$ characterizes the influence of the sideslip and rudder angles [in accordance with this, the quantities $c_x^{\alpha\delta_e}\alpha\delta_e$ and $c_x^{\beta\delta_r}\beta\delta_r$ in (9.2.1) are called **interaction terms**].

The static stability derivatives m_z^{α}, m_y^{β}, and m_x^{β} characterize an important property of a craft such as the stiffness of its longitudinal,

sideslipping, and lateral motions, while the derivatives $m_z^{\delta_e}$, $m_y^{\delta_r}$, $m_x^{\delta_r}$, and $m_x^{\delta_a}$ characterize the effectiveness of the corresponding control surface.

The rotational derivatives act on the motion like damping variables, and they are called, respectively, **longitudinal damping coefficients** ($m_z^{\omega_z}$, $m_z^{\dot{\alpha}}$, $m_z^{\dot{\delta}_e}$), **yawing damping coefficients** ($m_y^{\omega_y}$, $m_y^{\dot{\beta}}$, $m_y^{\dot{\delta}_r}$), and **rolling damping coefficients** ($m_x^{\omega_x}$).

The components $m_y^{\omega_x}\omega_x$ in (9.2.5) and $m_x^{\omega_y}\omega_y$ in (9.2.6) are, respectively, **the coefficients of the spiral yawing and rolling moments.** These moments appear because a craft combines translational motion with rotation about the axes Ox and Oy, i.e. performs spiral motion. The investigation of this complicated motion is associated with the calculation of the rotary (spiral) derivatives $m_y^{\omega_x}$ and $m_x^{\omega_y}$.

Formula (9.2.6) for the rolling moment coefficient includes interaction terms determined by second-order stability derivatives. For example, the derivative $m_x^{\alpha\beta}$ is related to the change in the rolling moment caused by the additional angles of attack on the port and starboard wing panels during flight with side-slipping. A similar effect characterized by the derivative $m_x^{\alpha\delta_r}$ is produced by deflection of the rudder. An additional rolling moment may also be caused by a change in the sideslip angle upon deflection of the elevators. The magnitude of the lateral moment depends on the second derivative $m_x^{\beta\delta_e}$. Rotation of a craft about the Oy or Oz axis may lead to an additional change in the angle of attack and the sideslip angle on opposite panels of lifting surfaces and to the relevant spiral rolling moments characterized by the derivatives $m_x^{\alpha\omega_y}$ and $m_x^{\beta\omega_z}$.

From the more general expression (9.1.4) for the aerodynamic coefficient, we can see that it also depends on the other stability derivatives that were not taken into account in the considered expressions. In separate kinds of motion, the influence of such derivatives may be substantial.

One of these motions is associated with the rolling of a craft at a sufficiently high angular velocity Ω_x. Such rotation produces the **Magnus effect** consisting in that with the presence of an angle of attack and a sideslip angle, forces and moments appear that are proportional to the products $\alpha\Omega_x$ or $\beta\Omega_x$, the direction of the forces coinciding with a normal to the planes containing the angles α and β. Accordingly, the increments of the lateral force coefficients are $\Delta c_z = c_z^{\alpha\omega_x}\alpha\omega_x$, and of the normal force ones are $\Delta c_y = c_y^{\beta\omega_x}\beta\omega_x$. The increments of the yawing and pitching moment coefficients are, respectively, $\Delta m_y = m_y^{\alpha\omega_x}\alpha\omega_x$ and $\Delta m_z = m_z^{\beta\omega_x}\beta\omega_x$. In these expressions, the quantities $c_z^{\alpha\omega_x}$ and $m_y^{\alpha\omega_x}$ are called the **Magnus stability derivatives.**

The origin of still another group of forces and moments is associated with the simultaneous rotation of a craft about two axes and is of a gyroscopic nature. Gyroscopic forces and moments are pro-

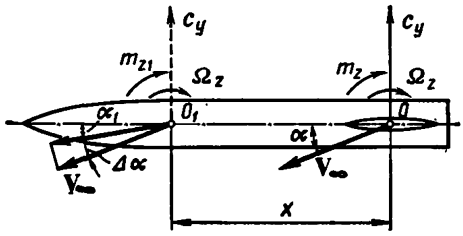

Fig. 9.3.1
To the conversion of the aerodynamic coefficients and their stability derivatives from one reduction centre to another

portional to the product of two angular velocities. For example, upon the simultaneous rotation about the axes Ox and Oy, these additional forces and moments are proportional to the product $\Omega_x\Omega_y$, and the corresponding aerodynamic coefficients, to the product of the dimensionless variables $\omega_x\omega_y$. This is why the derivatives of a coefficient with respect to $\omega_x\omega_y$ ($c_y^{\omega_x\omega_y}$, $m_z^{\omega_x\omega_y}$, etc.) are known as the **gyroscopic stability derivatives**.

9.3. Conversion of Stability Derivatives upon a Change in the Position of the Force Reduction Centre

Let us consider the conversion of the pitching moment and normal force coefficients, and also of the relevant stability derivatives calculated with respect to a reduction centre at point O for a new position O_1 of this centre at a distance of x from O (Fig. 9.3.1). A similar problem is solved, particularly, when determining the aerodynamic characteristics of an empennage relative to the centre of mass that is the centre of rotation of a craft in flight and coincides, consequently, with the centre of moments.

Assuming that the pitching moment coefficient at $\alpha = \Omega_z = 0$ equals zero ($m_{z0} = 0$) and that the airspeed is constant, let us form a general expression for this coefficient relative to the lateral axis passing through point O:

$$m_z = m_z^\alpha \alpha + m_z^{\dot\alpha}\dot\alpha + m_z^{\omega_z}\omega_z + m_z^{\dot\omega_z}\dot\omega_z \qquad (9.3.1)$$

in which the derivatives m_z^α, $m_z^{\dot\alpha}$, . . ., are known.

We can obtain a similar expression for the new reduction centre:

$$m_{z1} = m_{z1}^{\alpha_1}\alpha_1 + m_{z1}^{\dot\alpha_1}\dot\alpha_1 + m_{z1}^{\omega_{z1}}\omega_{z1} + m_{z1}^{\dot\omega_{z1}}\dot\omega_{z1} \qquad (9.3.2)$$

Here the derivatives $m_{z1}^{\alpha_1}$, $m_{z1}^{\dot\alpha_1}$, . . . are to be found in terms of their corresponding values obtained for the reduction centre O.

For this purpose, let us first consider the relations between α, $\dot{\bar{\alpha}}$, ω_z, $\dot{\omega}_z$, and α_1, $\dot{\bar{\alpha}}_1$, ω_{z1}, $\dot{\omega}_{z1}$. A glance at Fig. 9.3.1 reveals that

$$\alpha_1 = \alpha + \Delta\alpha = \alpha - \omega_z \bar{x}$$

where $\bar{x} = x/l$, $\omega_z = \Omega_z l/V_\infty$, and, consequently, $\dot{\bar{\alpha}}_1 = \dot{\bar{\alpha}} - \dot{\omega}_z \bar{x}$. The angular velocities and their derivatives do not change upon a change in the reduction centres, i.e. $\omega_{z1} = \omega_z$, and $\dot{\omega}_{z1} = \dot{\omega}_z$. Using these relations, let us reduce the formula for the moment coefficient:

$$m_z = m_z^{\alpha_1}\alpha_1 + m_z^{\dot{\bar{\alpha}}_1}\dot{\bar{\alpha}}_1 + m_z^{\omega_{z1}}\omega_{z1} + m_z^{\dot{\omega}_{z1}}\dot{\omega}_{z1} \qquad (9.3.3)$$

expressed in terms of the new kinematic parameters (for point O_1) to the form

$$m_z = m_z^{\alpha_1}\alpha + m_z^{\dot{\bar{\alpha}}_1}\dot{\bar{\alpha}} + (m_z^{\omega_{z1}} - m_z^{\alpha_1}\bar{x})\,\omega_z + (m_z^{\dot{\omega}_{z1}} - m_z^{\dot{\bar{\alpha}}}\bar{x})\,\dot{\omega}_z \qquad (9.3.4)$$

By comparing (9.3.1) and (9.3.4) we find

$$m_z^{\alpha_1} = m_z^{\alpha},\quad m_z^{\dot{\bar{\alpha}}_1} = m_z^{\dot{\bar{\alpha}}},\quad m_z^{\omega_{z1}} = m_z^{\omega_z} + m_z^{\alpha}\bar{x},\quad m_z^{\dot{\omega}_{z1}} = m_z^{\dot{\omega}_z} + m_z^{\dot{\bar{\alpha}}}\bar{x}$$

With this in view, expression (9.3.3) acquires the form

$$m_z = m_z^{\alpha}\alpha_1 + m_z^{\dot{\bar{\alpha}}}\dot{\bar{\alpha}}_1 + (m_z^{\omega_z} + m_z^{\alpha}\bar{x})\,\omega_{z1} + (m_z^{\dot{\omega}_z} + m_z^{\dot{\bar{\alpha}}}\bar{x})\,\dot{\omega}_{z1} \qquad (9.3.5)$$

The obtained moment coefficient can be expressed in terms of its value found for the new centre O_1 by means of the formula $m_z = m_{z1} + c_y\bar{x}$ (Fig. 9.3.1). Here formula (9.3.2) can be substituted for m_{z1}, and c_y written in the form of a relation similar to (9.3.5):

$$c_y = c_y^{\alpha}\alpha_1 + c_y^{\dot{\bar{\alpha}}}\dot{\bar{\alpha}}_1 + (c_y^{\omega_z} + c_y^{\alpha}\bar{x})\,\omega_{z1} + (c_y^{\dot{\omega}_z} + c_y^{\dot{\bar{\alpha}}}\bar{x})\,\omega_{z1} \qquad (9.3.6)$$

By comparing the expression obtained for $m_z = m_{z1} + c_y\bar{x}$ with the corresponding relation (9.3.6), we find formulas for the stability derivatives relative to point O_1:

$$\left.\begin{aligned} m_{z1}^{\alpha_1} &= m_z^{\alpha} - c_y^{\alpha}\bar{x}, \quad m_{z1}^{\omega_{z1}} = m_z^{\omega_z} + (m_z^{\alpha} - c_y^{\omega_z})\,\bar{x} - c_y^{\alpha}\bar{x}^2 \\ m_{z1}^{\dot{\bar{\alpha}}_1} &= m_z^{\dot{\bar{\alpha}}} - c_y^{\dot{\bar{\alpha}}}\bar{x}, \quad m_{z1}^{\dot{\omega}_{z1}} = m_z^{\omega_z} + (m_z^{\dot{\bar{\alpha}}} - c_y^{\omega_z})\,\bar{x} - c_y^{\dot{\bar{\alpha}}}\bar{x}^2 \end{aligned}\right\} \qquad (9.3.7)$$

The new stability derivatives of the normal force coefficient are obtained by comparing Eq. (9.3.6) and an equation similar to (9.3.2):

$$c_{y1} = c_{y1}^{\alpha_1}\alpha_1 + c_{y1}^{\dot{\bar{\alpha}}_1}\dot{\bar{\alpha}}_1 + c_{y1}^{\omega_{z1}}\omega_{z1} + c_{y1}^{\dot{\omega}_{z1}}\dot{\omega}_{z1}$$

in which we assume that $c_{y1} = c_y$ (because upon a change in the reduction centre the aerodynamic force does not change). The comparison yields

$$c_{y1}^{\alpha_1} = c_y, \quad \dot{c}_{y1}^{\bar{\alpha}_1} = \dot{c}_y^{\bar{\alpha}}, \quad c_{y1}^{\omega_{z1}} = c_y^{\omega_z} + c_y^{\alpha}\bar{x}$$
$$\dot{c}_{y1}^{\omega_{z1}} = \dot{c}_{y1}^{\omega_z} + \dot{c}_y^{\bar{\alpha}}\bar{x} \tag{9.3.8}$$

Similarly, we can convert the aerodynamic characteristics for a rear arrangement of the new reduction centre.

9.4. Particular Cases of Motion

Longitudinal and Lateral Motions

To simplify our investigation of the motion of a controllable craft and facilitate the finding of the required aerodynamic characteristics, including the stability derivatives, we shall use the method of resolving the total motion into individual components. The possibility of resolution into **longitudinal and lateral motions** in principal is due to the symmetry of a craft about its longitudinal axis. The longitudinal motion (pitching motion), in turn, consists of the translational displacement of the centre of mass *in the vertical flight plane* (the trajectory differs only slightly from a plane one) and rotation about the lateral axis Oz. In such motion, good stability in roll is ensured, and variables such as β, γ, ω_x, and ω_y may be considered negligibly small (the surfaces controlling rolling and yawing are virtually not deflected).

Upon lateral motion in the direction of the axis Oz, the centre of mass moves, and the craft experiences **rotation** about the axes Ox and Oy (here the control surfaces function that ensure yawing and rolling motion).

When investigating longitudinal motion, we usually consider the aerodynamic coefficients in the form of the following functions:

$$\left.\begin{aligned} &c_x = c_x(M_\infty, \alpha, \delta_e), \quad c_y = c_y(M_\infty, \alpha, \delta_e) \\ &c_z = 0, \quad m_x = 0, \quad m_y = 0, \quad m_z = m_z(M_\infty, \alpha, \delta_e, \dot{\bar{\alpha}}, \dot{\bar{\delta}}_e) \end{aligned}\right\} \tag{9.4.1}$$

To study lateral motion, we use the coefficients in the form of

$$\left.\begin{aligned} &c_y = c_y(M_\infty, \alpha, \delta_e), \quad c_z = c_z(M_\infty, \beta, \delta_r) \\ &m_x = m_x(M_\infty, \alpha, \beta, \delta_e, \delta_r, \delta_a, \omega_x, \omega_y, \omega_z) \\ &m_y = m_y(M_\infty, \beta, \delta_r, \omega_x, \omega_y, \dot{\bar{\beta}}, \dot{\bar{\delta}}_r) \end{aligned}\right\} \tag{9.4.2}$$

It must be had in view that longitudinal motion is studied independently of lateral motion, whereas the latter is considered with account taken of the parameters of longitudinal motion, which are determined beforehand. Particularly, the magnitude of the control normal force c_y is found.

Motion of the Centre of Mass and Rotation about It

The division of the total motion of a craft into these two modes is possible if we assume that the control system functions perfectly and during the entire flight ensures the equality of the moments M_x, M_y, and M_z to zero. Such a craft and its control system are considered as *inertiafree* (*fast-response*). The assumption on the absence of inertia signifies that when control surfaces are deflected, the angle of attack and the sideslip angle instantaneously (or sufficiently rapidly) take on values corresponding to a statically stable position of the craft. In these conditions, the motion of its centre of mass in the plane of flight is investigated independently. When performing such investigation, we shall write the aerodynamic coefficients in the form

$$\left.\begin{aligned} &c_x = c_x(M_\infty,\ \alpha,\ \beta,\ \delta_e,\ \delta_r),\ c_y = c_y(M_\infty,\ \alpha,\ \delta_e) \\ &c_z = c_z(M_\infty,\ \beta,\ \delta_r) \\ &m_y = m_y(M_\infty,\ \beta,\ \delta_r),\ m_z = m_z(M_\infty,\ \alpha,\ \delta_e) \end{aligned}\right\} \quad (9.4.3)$$

Assuming that $m_y = m_z = 0$, we can find the elevator and rudder angles corresponding to the required angle of attack and sideslip angle, and to the given trajectory.

The possibility of using such a method of investigation of the trajectory is based on the low sensitivity of displacement of the centre of mass to the rotation of the craft about this centre up to the instant

Table 9.4.1

Motion	Variables							
	α	β	Ω_x	Ω_y	Ω_z	δ_e	δ_r	δ_a
Pitching and rolling	+	−	+	−	+	+	−	+
Pitching without rolling	+	−	−	−	+	+	−	−
Rolling without pitching	−	−	+	−	−	−	−	+
Motion without pitching and rolling	−	−	−	−	−	−	−	−

when the craft occupies a position of statically stable equilibrium. This motion due to deflection of the control surfaces or random disturbances can be studied independently of the longitudinal motion of the craft. Table 9.4.1 shows the different modes of these motions and the corresponding control surface angles δ_e, δ_r, δ_a, the angle of attack α, the sideslip angle β, and also the angular velocities Ω_x, Ω_y, Ω_z.

The investigation of a particular mode of motion can be simplified by excluding the influence of accelerations. This is justified in practice when the motion develops sufficiently slowly. When it is necessary to take the acceleration into account, one can introduce a correction to the aerodynamic coefficient in the form of a term equal to the product of the first stability derivative with respect to the acceleration and the relevant dimensionless acceleration.

Pitching Motion

Of special interest is pitching motion, which is called the **principal mode of motion.** Longitudinal oscillations that are described quite well by a harmonic function such as (9.1.6) usually appear in this motion. According to this law, the time derivatives of the angles of attack and trajectory inclination are

$$\dot{\alpha} = A \sin p_\alpha t, \quad \dot{\vartheta} = \Omega_z = B \sin p_\vartheta t \tag{9.4.4}$$

where A, B are the amplitudes, and p_α, p_ϑ are the frequencies of oscillations of the corresponding derivatives.

We can consider three modes of motion each of which is described by a harmonic function.

The first mode (Fig. 9.4.1*a*) corresponds to the condition $\alpha = 0$, $\dot{\vartheta} = \Omega_z = B \sin p_\vartheta t$. In this mode, the axis of a body, coinciding with the direction of flight ($\alpha = 0$), performs harmonic oscillations along the trajectory.

The second mode of motion (Fig. 9.4.1*b*) is characterized by the fact that the axis of the body retains its orientation along the trajectory so that $\Omega_z = \dot{\vartheta} = 0$. Here, however, the angle of attack changes to follow the harmonic change in its derivative $\dot{\alpha}$.

The third mode of motion (Fig. 9.4.1*c*) is characterized by a rectilinear trajectory with the angle between the axis of the craft and the trajectory changing sinusoidally. In this case, the angles ϑ and α are equal and coincide in phase so that $\dot{\alpha} = \dot{\vartheta} = \Omega_z$. Important derivatives in this motion are $c_y^{\dot{\alpha}} + c_y^{\omega_z}$ and $m_z^{\dot{\alpha}} + m_z^{\omega_z}$.

All these three modes of motion, which are of a quite intricate nature, are encountered comparatively frequently. Two other modes

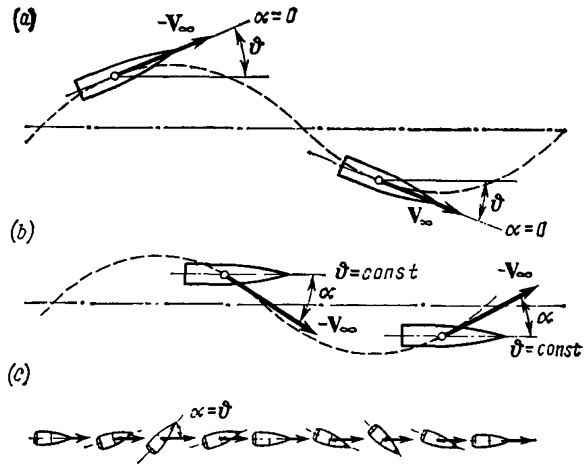

Fig. 9.4.1
Particular cases of motion of a craft:
a—at a zero angle of attack; *b*—with constant orientation of the craft (ϑ = const); *c*—along a straight trajectory

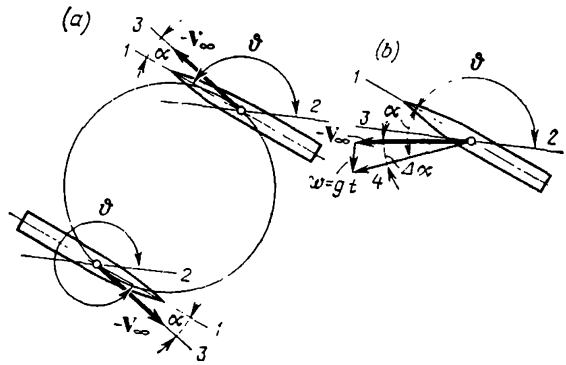

Fig. 9.4.2
Modes of motion of a craft:
a—perfect loop; *b*—free fall

are simpler, but are encountered less frequently. Each of them allows one to understand the distinction between the modes of motion characterized by two conditions: $\dot{\alpha} = 0$, $\Omega_z \neq 0$ and $\dot{\alpha} \neq 0$, $\Omega_z = 0$, and accordingly to gain an idea of the derivatives $m_z^{\dot{\alpha}}$ and $m_z^{\omega_z}$. The three modes of sinusoidal motions indicated above can be treated as combinations of these two modes.

The first of them (Fig. 9.4.2*a*) is characterized by the fact that the angle of attack between the instantaneous direction *3* of the vector

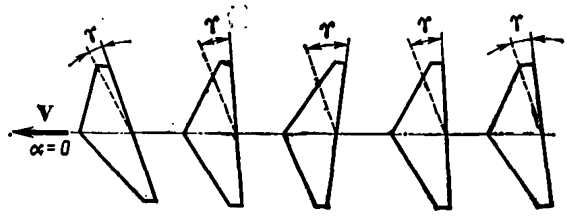

Fig. 9.4.3
Banking of a craft

$-\bar{V}_\infty$ and body axis *1* does not change and, consequently, the derivative $\dot{\alpha} = 0$. In this motion, however, a varying angle ϑ forms between fixed direction *2* and axis *1*. Therefore $\Omega_z = d\vartheta/dt \neq 0$. In a particular case when $\Omega_z = \text{const}$, the trajectory in Fig. 9.4.2*a* characterizes the motion of a craft performing a perfect loop.

Figure 9.4.2*b* shows a second mode of motion corresponding to the conditions $\dot{\alpha} \neq 0$ and $\Omega_z = 0$. This motion may occur if free fall with a velocity of $w = gt$ (where g is the acceleration of free fall) is superposed on the longitudinal motion. Here the angle ϑ between the fixed direction *2* and body axis *1* remains constant, while the angle α changes (between the instantaneous flight direction *4* and axis *1*). Consequently, the derivatives $\dot{\vartheta} = \Omega_z = 0$ and $\dot{\alpha} \neq 0$; in the given case the derivative $\dot{\alpha} = \text{const}$.

In a more general case (for example, in sinusoidal motions), it is necessary to use both derivatives $m_z^{\dot{\alpha}}$ and $m_z^{\omega_z}$. If one of the considered modes of motion dominates, only one derivative is significant, and it is exactly what should be used. Figure 9.4.3 shows a wing for which translational motion along its longitudinal axis, at a zero angle of attack. is supplemented with rotation about this axis at the angular velocity $\Omega_x = d\gamma/dt$. The non-zero variables ω_x and $\dot{\omega}_x$ correspond to this mode of motion. If the rotation about the axis Ox is steady, then $\omega_x \neq 0$, while the derivative $\dot{\omega}_x = 0$.

9.5. Dynamic Stability

Definition

An analysis of the derivatives of the aerodynamic moments with respect to α or β allows us to establish the kind of static stability. This analysis is not sufficient for estimating the flight performance of a moving body, however, because it does not allow one to establish the nature of the body's motion after the removal of a disturbance and to find the variables determining this motion.

Actually, if we know, for example, that the derivative m_z^{α} is negative and that, consequently, the centre of pressure is behind the centre of mass, we can arrive at a conclusion only on longitudinal static stability. But we cannot establish, for example, the amplitude of oscillations of the angle of attack at a certain value of the initial disturbance and how it changes in time. These and other problems are studied by the theory of the **dynamic stability of a craft** or of the **stability of its motion**. This theory makes it possible, naturally, to study not only the oscillations of a craft, but also the general case of the motion of a craft along its trajectory and the stability of this motion. The theory of dynamic stability uses the results of aerodynamic investigations obtained in conditions of unsteady flow in which, unlike static conditions, a body experiences the action of additional time-dependent aerodynamic loads.

The concept of dynamic stability is associated with two modes of motion of a craft, namely, undisturbed (basic) and disturbed. Motion is said to be **undisturbed (basic)** if it occurs along a definite trajectory at a velocity varying according to a given law at standard parameters of the atmosphere and known initial parameters of this motion. This theoretical trajectory described by specific flight equations with nominal parameters of the craft and control system is also said to be undisturbed. Owing to random disturbing factors (gusts of wind, interference in the control system, failure of the initial conditions to correspond to the preset ones, deviation of the actual parameters of a craft and its control system from the nominal ones, deviation of the actual parameters of the atmosphere from the standard ones), and also because of disturbances due to deflection of the control surfaces, the basic motion may be violated. After removal of the random disturbances, a body moves during a certain time according to a law differing from the initial one. This motion is called **disturbed**.

If the forces or moments produced upon a deviation from undisturbed motion are such that they return the craft to its initial trajectory, the motion is **stable**, otherwise it is **unstable**. Figure 9.5.1*a* shows a stable flight in which a craft after leaving its trajectory at point M because of a disturbance continues its motion with a constantly diminishing deviation from the initial direction of flight; Fig. 9.5.1*b* shows an unstable flight characterized by an increasing deviation.

In the general case, the motion of a craft is determined by kinematic parameters that are functions of time such as the velocity $V_{\infty}(t)$, the angle of attack $\alpha(t)$, the sideslip angle $\beta(t)$, the components of the angular velocity $[\Omega_x(t), \Omega_y(t), \Omega_z(t)]$, and the pitching, yawing (course angle) and rolling angles $[\vartheta(t), \psi(t),$ and $\gamma(t)]$.

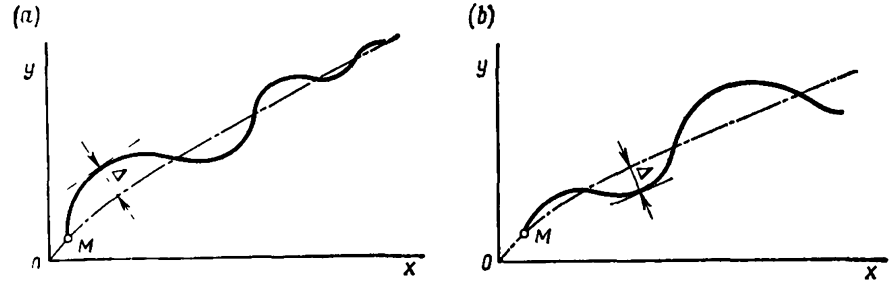

Fig. 9.5.1
Modes of motion of a craft:
1—stable; *2*—unstable; Δ—amplitude of oscillations

Let us assume that the values of the same variables $V_\infty^0(t)$, $\alpha^0(t)$ etc. correspond to a given *undisturbed motion*. If at sufficiently small initial deviations (at the initial disturbances) ΔV_∞^0, $\Delta\alpha^0$, . . . (here $\Delta V_\infty^0 = V_\infty'^0 - V_\infty^0$, $\Delta\alpha^0 = \alpha'^0 - \alpha^0$, . . .) the subsequent deviations $\Delta V_\infty = V_\infty - V_\infty^0$, $\Delta\alpha = \alpha - \alpha^0$ do not exceed certain preset values, the motion is **stable**. If these deviations increase unlimitedly, the motion is **unstable**. A flight may occur when the deviations neither attenuate nor increase: here **neutral** stability of motion is observed.

Such a definition of stability is associated with investigation of the response of a craft to disturbing actions provided that these actions impart initial deviations to the variables of the undisturbed flow, while the following motion is considered already without disturbances. In such motion, the control surfaces remain fixed. This mode of disturbed motion due to initial disturbances of the variables is called **proper** or **free**. The proper motion of a craft can conditionally be considered as a new undisturbed motion.

The stability of free motion of a craft can be investigated by analysing the differential equations describing this motion. If the lateral variables and the time derivatives of the longitudinal variables in the undisturbed flow are not great, we may consider longitudinal and lateral motions independently and, consequently, study the stability of each of them separately. When the nature of motion changes abruptly, for example, when a manoeuver is executed, such a resolution of motion into its components is not justified, and the solution of the system of equations of longitudinal and lateral motion must be considered jointly. This solution makes it possible to establish the nature and influence of the aerodynamic coefficients on stability in the most general form.

If the intensity of action of random factors is not great, the disturbed trajectory differs only slightly from the undisturbed one. This allows one to use the method of small perturbations that is based on linearized equations.

Stability Characteristics

Let us consider the characteristics of dynamic stability, and also the role and place of the aerodynamic coefficients (stability derivatives) in investigating the dynamics of a flight using the example of translational motion of a craft also performing rotation (oscillations) about the axis Oz (Fig. 9.4.1c).

We shall write the equation of such disturbed motion in the form

$$\ddot{\alpha} + (a_1 + a_2)\dot{\alpha} + a_3\alpha = 0 \tag{9.5.1}$$

where

$$\left.\begin{aligned} a_1 &= -m_z^{\Omega_z} q_\infty Sl/J_z, \quad a_2 = -m_z^{\dot{\alpha}} q_\infty Sl/J_z \\ a_3 &= -m_z^{\alpha} q_\infty Sl/J_z \end{aligned}\right\} \tag{9.5.2}$$

Here J_z is the principal central moment of inertia of the craft about the axis Oz that is one of the principal central axes.

Taking into account that $m_z^{\Omega_z} = m_{z1}^{\dot{\alpha}}$, we obtain for the sum of the coefficients

$$a_1 + a_2 = -2m_z^{\dot{\alpha}} q_\infty Sl/J_z \tag{9.5.3}$$

With a view to the value of the coefficient a_3 (9.5.1) can be written as

$$\ddot{\alpha} J_z/(q_\infty Sl) - 2\dot{\alpha} m_z^{\dot{\alpha}} - \alpha m_z^{\alpha} = 0 \tag{9.5.4}$$

Assuming that the coefficients a_i are constant, we find a solution of Eq. (9.5.4) in the following form:

$$\alpha = C_1 e^{p_1 t} + C_2 e^{p_2 t} \tag{9.5.5}$$

Here p_1 and p_2 are the roots of the characteristic equation $p^2 + (a_1 + a_2)\,p + a_3 = 0$ determined by the formula

$$p_{1,2} = -0.5\,(a_1 + a_2) \pm \sqrt{0.25\,(a_1 + a_2)^2 - a_3} \tag{9.5.6}$$

We find the constants C_1 and C_2 from the conditions that can be determined by the derivative $\dot{\alpha} = \dot{\alpha}_0$ and the zero disturbance $\alpha = 0$ at the instant $t = 0$. For these conditions, the constants are

$$C_1 = C_2 = 0.5\dot{\alpha}_0\,[0.25\,(a_1 + a_2)^2 - a_3]^{-1/2}$$

and the solution becomes

$$\alpha = 0.5\dot{\alpha}_0 b^{-1} e^{-\lambda_1 t}\,(e^{bt} - e^{-bt}) \tag{9.5.7}$$

where $b = \sqrt{\lambda_1^2 - a_3}$, $\lambda = 0.5\,(a_1 + a_2)$.

Let us consider static stability when the derivative $m_z^{\alpha} < 0$ and, consequently, $a_3 > 0$. If we have in view here that in real conditions the damping moment is considerably smaller than the stabilizing one and that therefore $|a_3| > \lambda_1^2$, we obtain the relation

$$\alpha = \dot{\alpha}_0 \bar{b}^{-1} e^{-\lambda_1 t} \sin \bar{b}t \tag{9.5.8}$$

in which $\bar{b} = \sqrt{|a_3| - \lambda_1^2}$.

Examination of (9.5.8) reveals that the change in the angle of attack has the nature of periodic oscillations. Since the quantity λ_1 is always positive, these oscillations are damped ones; consequently, we have to do with **oscillatory stability.**

Let us consider the characteristics of this stability. The **period of the oscillations** is

$$T = 2\pi \left(|m_z^{\alpha}| q_{\infty} S l J_z^{-1} - \lambda_1^2\right)^{-1/2} \tag{9.5.9}$$

and their **frequency** is

$$\omega = 2\pi/T = \left(|m_z^{\alpha}| q_{\infty} S l J_z^{-1} - \lambda_1^2\right)^{1/2} \tag{9.5.10}$$

The oscillation frequency is influenced mainly by the degree of static stability, whereas the influence of damping is not great. The nature of action of these factors is different. An increase in the degree of static stability leads to a higher frequency, while an increase in damping, conversely, leads to its diminishing somewhat.

The **logarithmic decrement** is

$$\varepsilon = \lambda_1 T \tag{9.5.11}$$

where

$$\lambda_1 = |m_z^{\dot{\alpha}}| q_{\infty} S l J_z^{-1} \tag{9.5.12}$$

The larger the coefficient m_z^{α} (or $m_z^{\Omega_z}$), the greater is the logarithmic decrement and the more rapidly do the oscillations damp in time.

One of the important characteristics of oscillatory motion is the time to damp to half amplitude:

$$t_2 = \lambda_1^{-1} \ln 2 \tag{9.5.13}$$

When investigating oscillatory stability, the quantity λ_1 can be considered as an independent characteristic of this stability called the **damping coefficient.** A glance at (9.5.12) and (9.5.13) reveals that its magnitude does not depend on the degree of static stability m_z^{α}.

Let us consider the **wavelength of oscillations**

$$\lambda = TV_{\infty} = 2\pi V_{\infty} / \sqrt{|a_3| - \lambda_1^2} \tag{9.5.14}$$

In practice, it is expedient to ensure aerodynamic properties of a moving body such that the damping coefficient is sufficiently great because here the time t_2 is short, although the wavelength grows somewhat, which is not desirable. Good practice dictates decreasing of this length. To do this, it is necessary to increase the stabilizing moment, which, in turn, leads to such a positive phenomenon as a decrease in the amplitude of oscillation.

In the case being considered, a body has static stability that also produces in it **longitudinal oscillatory stability.** A similar analysis can be performed for the case when such static stability is absent, i.e. when the derivative $m_z^\alpha > 0$. Solution of (9.5.4) yields a relation for α indicating the undamping aperiodic nature of motion. Hence, static instability also gives rise to instability of motion.

In this case, agreement can be observed between static and dynamic stability or instability. Such agreement is not obligatory, however, for the general case of motion of a craft. One may have a statically stable craft that, however, does not have dynamic stability and in its tendency to the position of equilibrium will perform oscillations with an increasing amplitude. Such cases are observed in practice in some aircraft at low-speed flight, and also in flying wings with a small sweep of the leading edge.

It must be noted that the overwhelming majority of aircraft owing to special devices have static stability, i.e. the ability to respond to disturbances so as to reduce their magnitude at the initial instant. This property is of major practical significance regardless of how an aircraft behaves in the process of disturbed motion. Free development of the disturbances is usually attended by deflection of the control surfaces to return the craft to its preset flight conditions. The use of these control surfaces is a necessary condition for ensuring the preset motion of a statically unstable (with fixed control surfaces) aircraft.

The concept of stability presumes the existence not of two separate kinds of stability—static and dynamic, but of a single stability reflecting the real motion of a craft in time and its ability to retain the initial flight conditions. Since the dynamic coefficients of the equations depend on the parameters of the undisturbed flight, the same aircraft can have different dynamic properties along a trajectory, for example, its motion may be stable on some sections of the trajectory and unstable on others.

Unsteady motion is described by equations whose dynamic coefficients depend on the design of the craft. Unlike craft of the aeroplane type, such coefficients for bodies without an empennage, or with an only slightly developed empennage (fin assembly), correspond to unstable motion characterized by slow damping of the oscillations. This requires the use of means of stabilization that ensure greater damping.

9.6. Basic Relations for Unsteady Flow

Aerodynamic Coefficients

Let us consider a flat lifting surface moving translationally at a constant velocity in the absence of sideslip ($\beta = 0$) and of an angular velocity Ω_y. The projection of the area of an aircraft or its separate elements (wings, fuselage) onto the plane xOz may be such a surface. The aerodynamic stability derivatives obtained for this surface are very close to those that would have been found for real bodies in an unsteady flow.

The normal aerodynamic force, and also the pitching and rolling moments are due to the pressure difference $\Delta p = p_b - p_u$ on the bottom and upper sides of the lifting surface (Fig. 9.6.1) and are determined by the formulas

$$Y = \iint\limits_{(S)} \Delta p \, dx \, dz, \quad M_z = \iint\limits_{(S)} \Delta \, px \, dx \, dz,$$

$$M_x = -\iint\limits_{(S)} \Delta \, pz \, dx \, dz \tag{9.6.1}$$

in which integration is performed over the area S of the lifting surface.

Let us introduce the pressure coefficient $\bar{p} = (p - p_\infty)/q_\infty = 2\,(p - p_\infty)/(\rho_\infty V_\infty^2)$ and the dimensionless coordinates

$$\xi = x/x_k \text{ and } \zeta = z/x_k \tag{9.6.2}$$

related to the length x_k of the lifting surface.

Now we obtain the following relations for the force and moment coefficients at any unsteady motion of a lifting surface with the dimensions l:

$$\left.\begin{aligned} c_y &= \frac{Y}{q_\infty S} = \frac{2x_k^2}{S} \int\limits_0^{l/(2x_k)} \int\limits_{\xi_0}^{\xi_1} \Delta\bar{p} \, d\xi \, d\zeta \\ m_z &= \frac{M_z}{q_\infty S x_k} = \frac{2x_k^2}{S} \int\limits_0^{l/(2x_k)} \int\limits_{\xi_0}^{\xi_1} \Delta\bar{p}\xi \, d\xi \, d\zeta \\ m_x &= \frac{M_x}{q_\infty S x_k} = -\frac{2x_k^2}{S} \int\limits_0^{l/(2x_k)} \int\limits_{\xi_0}^{\xi_1} \Delta\bar{p}\zeta \, d\xi \, d\zeta \end{aligned}\right\} \tag{9.6.3}$$

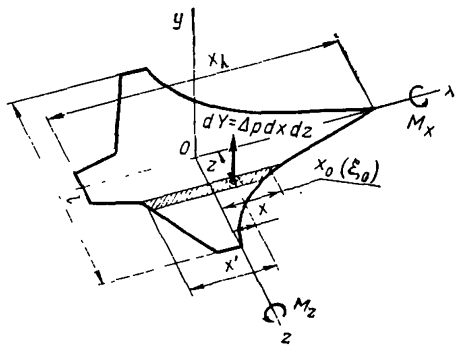

Fig. 9.6.1
To the determination of the aerodynamic coefficients for a lifting surface

Here ξ_0 and ξ_1 are the dimensionless coordinates of the leading and trailing edges of the lifting surface, respectively.

For a non-standard coordinate system in which the axis Ox is directed from the leading edge to the trailing one, the signs in formulas (9.6.3) should be reversed.

Let us find relations for the aerodynamic characteristics of the lifting surface cross sections. For the normal force, longitudinal moment, and rolling moment of a section, we have, respectively

$$dY = \int_{x_0}^{x_1} \Delta p\, dx\, dz, \quad dM_z = \int_{x_0}^{x_1} \Delta p x\, dx\, dz,$$

$$dM_x = -\int_{x_0}^{x_1} \Delta p z\, dx\, dz \tag{9.6.4}$$

The corresponding coefficients are as follows:

$$\left.\begin{aligned} c_y' &= \frac{dY}{q_\infty x'\, dz} = \frac{x_k}{x'} \int_{\xi_0}^{\xi_1} \Delta\bar{p}\, d\xi \\ m_z' &= \frac{dM_z}{q_\infty x'^2\, dz} = \frac{x^2 k}{x'^2} \int_{\xi_0}^{\xi_1} \Delta\bar{p}\xi\, d\xi \\ m_x' &= \frac{dM_x}{q_\infty x'^2\, dz} = -\frac{x_k^2}{x'^2} \int_{\xi_0}^{\xi_1} \Delta\bar{p}\zeta\, d\xi \end{aligned}\right\} \tag{9.6.5}$$

where x' is a chord of a lifting surface element in the section $z =$ $=$ const being considered.

We calculate the integral in (9.6.5) over a given section from the trailing ($\xi_1 = x_1/x_k$) to the leading ($\xi_0 = x_0/x_k$) edges. We can

represent the difference of the pressure coefficients in (9.6.3) and (9.6.5) on the basis of the Taylor formula [see (9.1.4)] in the form of a series expansion in terms of the kinematic variables:

$$\left.\begin{aligned} &q_1 = \alpha(\tau), \quad q_2 = \omega_x(\tau) = \Omega_x(t)\, l/V_\infty \\ &q_3 = \omega_z(\tau) = \Omega_z(t)\, l/V_\infty, \quad \dot{q}_1 = \dot{\bar{\alpha}} = d\alpha/d\tau, \quad \dot{q}_2 = \dot{\omega}_x = d\omega_x/d\tau \\ &\dot{q}_3 = \dot{\omega}_z = d\omega_z/d\tau \quad \tau = V_\infty t/l \end{aligned}\right\} \tag{9.6.6}$$

(here l is the characteristic geometric dimension).

This expansion has the following form:

$$\Delta\bar{p} = \sum_{i=1}^{3} (p^{q_i} q_i + p^{\dot{q}_i}\dot{q}_i) = p^{\alpha}\alpha + p^{\dot{\bar{\alpha}}}\dot{\bar{\alpha}} + p^{\omega_x}\omega_x + p^{\dot{\omega}_x}\dot{\omega}_x + p^{\omega_z}\omega_z + p^{\dot{\omega}_z}\dot{\omega}_z \tag{9.6.7}$$

where $p^{\alpha} = \Delta\bar{p}^{\alpha}$, $p^{\dot{\bar{\alpha}}} = \Delta\bar{p}^{\dot{\bar{\alpha}}}$, etc. are the derivatives of the difference of the pressure coefficients.

By (9.6.7), the aerodynamic coefficients can be written as

$$\left.\begin{aligned} c_y &= \sum_{i=1}^{3} (c_y^{q_i} q_i + c^{\dot{q}_i}\dot{q}_i) \\ m_z &= \sum_{i=1}^{3} (m_z^{q_i} q_i + m_z^{\dot{q}_i}\dot{q}_i) \\ m_x &= \sum_{i=1}^{3} (m_x^{q_i} q_i + m_x^{\dot{q}_i}\dot{q}_i) \end{aligned}\right\} \tag{9.6.8}$$

In formulas (9.6.8) for the non-stationary aerodynamic coefficients expressed in the form of series, the values of the stability derivatives that are coefficients of q_i and $\dot{q}_i$ must correspond to expansion (9.6.7) for the quantity $\Delta\bar{p}$. Accordingly, the relevant derivatives take on the following values:

$$\begin{aligned} &c_y^{q_i} = c_y^{\alpha}, \; c_y^{\omega_x}, \; c_y^{\omega_z}; && c_y^{\dot{q}_i} = c_y^{\dot{\bar{\alpha}}}, \; c_y^{\dot{\omega}_x}, \; c_y^{\dot{\omega}_z} \\ &m_z^{q_i} = m_z^{\alpha}, \; m_z^{\omega_x}; \; m_z^{\omega_z}; && m_z^{\dot{q}_i} = m_z^{\dot{\bar{\alpha}}}, \; m_z^{\dot{\omega}_x}, \; m_z^{\dot{\omega}_z} \\ &m_x^{q_i} = m_x^{\alpha}, \; m_x^{\omega_x}; \; m_x^{\omega_z}; && m_x^{\dot{q}_i} = m_x^{\dot{\bar{\alpha}}}, \; m_x^{\dot{\omega}_x}, \; m_x^{\dot{\omega}_z} \end{aligned}$$

Assuming that the craft length x_k has been adopted as the characteristic geometric dimension, we obtain from (9.6.3), (9.6.7) and (9.6.8) expressions for the derivatives of the aerodynamic coefficients in terms of the derivatives of the difference of the pressure coeffi-

cients:

$$\left.\begin{aligned} c_y^{q_i} &= \frac{2x_k^2}{S}\int_0^{l/(2x_k)}\int_{\xi_1}^{\xi_0} p^{q_i}\,d\xi\,d\zeta, \quad \dot{c}_y^{q_i} = \frac{2x_k^2}{S}\int_0^{l/(2x_k)}\int_{\xi_1}^{\xi_0} \dot{p}^{q_i}\,d\xi\,d\zeta \\ m_x^{q_i} &= -\frac{2x_k^2}{S}\int_0^{l/(2x_k)}\int_{\xi_1}^{\xi_0} p^{q_i}\zeta\,d\xi\,d\zeta, \\ \dot{m}_x^{q_i} &= -\frac{2x_k^2}{S}\int_0^{l/(2x_k)}\int_{\xi_1}^{\xi_0} \dot{p}^{q_i}\zeta\,d\xi\,d\zeta \\ m_z^{q_i} &= \frac{2x_k^2}{S}\int_0^{l/(2x_k)}\int_{\xi_1}^{\xi_0} p^{q_i}\xi\,d\xi\,d\zeta, \quad \dot{m}_z^{q_i} = \frac{2x_k^2}{S}\int_0^{l/(2x_k)}\int_{\xi_1}^{\xi_0} \dot{p}^{q_i}\xi\,d\xi\,d\zeta \end{aligned}\right\} \quad (9.6.9)$$

The above expressions are linear relations between the aerodynamic derivatives and the dimensionless kinematic variables q_i and $\dot{q}_i$ that ensure quite reliable results provided that the values of these variables are small in comparison with unity.

In linearized problems on the unsteady flow over lifting surfaces, such relations are exact for a harmonic law of the change in the kinematic variables (see [4, 19]).

Let us consider some features of the stability derivatives. Since we are dealing with motion in the absence of sideslip and an angular velocity about the axis Oy ($\beta = 0$, $\Omega_y = 0$), here the derivatives of the aerodynamic coefficients with respect to the parameters β and Ω_y evidently equal zero. In addition, we have excluded the coefficients of the longitudinal and lateral forces (c_x, c_z) and also the yawing moment coefficient m_y from our analysis because independent investigations are devoted to them. It must be had in view here that when analysing the stability of a craft, these quantities are of a smaller practical significance.

For a lifting surface that is symmetric about plane xOy and moves translationally in the absence of rotation ($\Omega_x = 0$), the pressure is distributed symmetrically; therefore, the corresponding derivatives equal zero: $m_x^{q_i} = 0$, $\dot{m}_x^{q_i} = 0$ ($i = 1, 3$).

With rotation about the axis Ox, the pressure is distributed asymmetrically about symmetry plane xOy, hence the aerodynamic loads produced by the angular velocity ω_x are also asymmetric, and, consequently, the following stability derivatives equal zero in this case:

$$c_y^{\omega_x} = 0, \quad \dot{c}_y^{\omega_x} = 0, \quad m_z^{\omega_x} = 0, \quad \dot{m}_z^{\omega_x} = 0$$

Cauchy-Lagrange Integral

Let us consider the basic expression of the theory of unsteady flow relating the parameters of the disturbed flow (the velocity, pressure, density) and the potential function Φ. For such a flow, curl $\mathbf{V} = 0$, and, consequently, the local velocity vector can be written in terms of the potential function as $\mathbf{V} = \text{grad}\,\Phi$. With this in view, the equation of motion (3.1.22″) can be given thus

$$\frac{\partial \text{ grad } \Phi}{\partial t} + \text{grad}\,\frac{V^2}{2} = -\frac{1}{\rho}\,\text{grad}\,p \qquad (9.6.10)$$

Considering that the gas flowing over a body is a **barotropic fluid** whose density depends only on the pressure, i.e. $\rho = \rho(p)$, we can introduce a function P, assuming that

$$P = \int dp/\rho(p) \qquad (9.6.11)$$

Accordingly,

$$(1/\rho)\,\text{grad}\,p = \text{grad}\,P \qquad (9.6.12)$$

We can therefore write (9.6.10) as

$$\text{grad}\,(\partial\Phi/\partial t + V^2/2 + P) = 0$$

Hence we obtain an equation suitable for the entire space of a disturbed flow near a lifting surface including the vortex wake:

$$\partial\Phi/\partial t + V^2/2 + P = F(t) \qquad (9.6.13)$$

where $F(t)$ is an arbitrary function of time determined with the aid of the undisturbed flow variables for which $\partial\Phi/\partial t = 0$.

Assuming that $V^2 = V_\infty^2$ and $P = P_\infty$, we find

$$F(t) = V_\infty^2/2 + P_\infty$$

Consequently,

$$\partial\Phi/\partial t + V^2/2 + P = V_\infty^2/2 + P_\infty \qquad (9.6.14)$$

This equation is known as the **Cauchy-Lagrange integral.** For an incompressible medium, we have $\rho_\infty = \rho = \text{const}$. Therefore, $P = p/\rho_\infty$ and $P_\infty = p_\infty/\rho_\infty$. Hence,

$$\partial\Phi/\partial t + V^2/2 + p/\rho_\infty = V_\infty^2/2 + p_\infty/\rho_\infty \qquad (9.6.15)$$

For an isentropic flow of a compressible gas in the region of a continuous change in the thermodynamic properties, we have $p/\rho^k = p_\infty/\rho_\infty^k$ (where $k = c_p/c_v = \text{const}$ is the adiabatic exponent). As a result, we obtain

$$P = \frac{k}{k-1}\cdot\frac{p}{\rho}, \qquad P_\infty = \frac{k}{k-1}\cdot\frac{p_\infty}{\rho_\infty}$$

Therefore, the Cauchy-Lagrange integral will acquire the following form:

$$\frac{\partial \Phi}{\partial t} + \frac{V^2}{2} + \frac{k}{k-1} \cdot \frac{p}{\rho} = \frac{V_\infty^2}{2} + \frac{k}{k-1} \cdot \frac{p_\infty}{\rho_\infty} \qquad (9.6.16)$$

Assuming that the flow over a body is nearly uniform, we linearize Eq. (9.6.16). The square of the velocity is

$$V^2 = V_x^2 + V_y^2 + V_z^2 = (V_\infty + u)^2 + v^2 + w^2$$

where u, v, and w are infinitesimal components of the disturbed velocity ($u \ll V_\infty$, $v \ll V_\infty$, and $w \ll V_\infty$). Excluding the second-order infinitesimals, we obtain $V^2 = V_\infty^2 + 2V_\infty u$. In a nearly uniform flow, the excess pressure $p - p_\infty = p'$ of the gas at any point in space is also small. With this in view, we find the linearized value of the difference of the functions $P - P_\infty$. For an isentropic flow, this difference is

$$P - P_\infty = [k/(k-1)]\,(p/\rho - p_\infty/\rho_\infty)$$

We determine the ratio p/ρ from the adiabat equation $p/\rho^k = p_\infty/\rho_\infty^k$, in accordance with which

$$p/\rho = (p_\infty/\rho_\infty)\,(p/p_\infty)^{(k-1)/k}$$

Introducing $p = p_\infty + p'$ into this expression, we obtain

$$p/\rho = (p_\infty/\rho_\infty)\,(1 + p'/p_\infty)^{(k-1)/k}$$

Expanding this expression into a binomial series, we find with an accuracy within linear terms that

$$\frac{p}{\rho} = \frac{p_\infty}{\rho_\infty}\left(1 + \frac{k-1}{k}\,\frac{p'}{p_\infty}\right)$$

Accordingly,

$$P - P_\infty = p'/\rho_\infty = (p - p_\infty)/\rho_\infty \qquad (9.6.17)$$

Hence, a linearized expression of the Cauchy-Lagrange integral suitable for investigating nearly uniform unsteady flows has the form

$$p - p_\infty = -\rho_\infty\,(V_\infty\,\partial\varphi/\partial x + \partial\varphi/\partial t) \qquad (9.6.18)$$

where $\varphi = \Phi - \Phi_\infty$ is the additional disturbance potential (Φ_∞ is the velocity potential of the undisturbed flow).

In the above form, the Cauchy-Lagrange integral holds both for a compressible and an incompressible fluid. Equation (9.6.18) has been obtained for a coordinate system whose axis Ox is oriented toward the trailing edge. If the axis Ox is oriented in the opposite direction, the sign of the derivative with respect to x has to be reversed:

$$p - p_\infty = \rho_\infty\,(V_\infty\,\partial\varphi/\partial x - \partial\varphi/\partial t) \qquad (9.6.18')$$

Let us introduce the pressure coefficient $\bar{p}$, the difference of its values for the bottom and upper sides $\Delta\bar{p}$, the dimensionless potential $\bar{\varphi}$, and also the relative coordinates and time:

$$\left.\begin{aligned} &\bar{p}=(p-p_\infty)/q_\infty, \quad \Delta\bar{p}=\bar{p}_b-\bar{p}_u \\ &\xi=x/x_k, \quad \eta=y/x_k, \quad \zeta=z/x_k, \quad \tau=V_\infty t/x_k \\ &\varphi(x,\ y,\ z,\ t)=V_\infty x_k\bar{\varphi}(\xi,\ \eta,\ \zeta,\ \tau) \end{aligned}\right\} \tag{9.6.19}$$

When these dimensionless quantities are taken into account, the Cauchy-Lagrange integral becomes

$$\bar{p}=-2\,(\partial\bar{\varphi}/\partial\xi+\partial\bar{\varphi}/\partial\tau) \tag{9.6.20}$$

Having in view that from considerations of symmetry, the velocity potentials on the upper and bottom sides are identical in magnitude, but opposite in sign, i.e. $\varphi(x,\ y,\ z,\ t)=-\varphi(x,\ -y,\ z,\ t)$, we obtain the following formula for $\Delta\bar{p}$:

$$\Delta\bar{p}=\bar{p}_b-\bar{p}_u=-4\,(\partial\bar{\varphi}/\partial\xi+\partial\bar{\varphi}/\partial\tau) \tag{9.6.21}$$

Let us represent the expressions for $\bar{\varphi}$ and $\Delta\bar{p}$ in the form of linear dependences on q_i and $\dot{q}_i$:

$$\bar{\varphi}=\sum_{i=1}^{3}(\bar{\varphi}^{q_i}q_i+\bar{\varphi}^{\dot{q}_i}\dot{q}_i); \quad \Delta\bar{p}=\sum_{i=1}^{3}(p^{q_i}q_i+p^{\dot{q}_i}\dot{q}_i) \tag{9.6.22}$$

We shall insert these relations into (9.6.21) with a view to the aerodynamic coefficients not depending on the time:

$$\sum_{i=1}^{3}(p^{q_i}q_i+p^{\dot{q}_i}\dot{q}_i)=-4\Big[\sum_{i=1}^{3}\Big(\frac{\partial\bar{\varphi}^{q_i}}{\partial\xi}\,q_i+\frac{\partial\bar{\varphi}^{\dot{q}_i}}{\partial\xi}\,\dot{q}_i\Big)+\sum_{i}^{3}\Big(\bar{\varphi}^{q_i}\dot{q}_i+\bar{\varphi}^{\dot{q}_i}\frac{\partial\dot{q}_i}{\partial\tau}\Big)\Big] \tag{9.6.23}$$

For harmonic time dependences of the kinematic variables ($q_i = q_i^* \cos p_i t$), the derivative

$$\partial\dot{q}_i/\partial\tau=\ddot{q}_i=-(p_i^*)^2q_i$$

where $p_i^*=p_i x_k/V_\infty$ is the Strouhal number ($i=1,\ 2,\ 3$).

With a view to the obtained value for $\ddot{q}_i$, we find the following expressions for the derivatives of the difference of the pressure coefficients from (9.6.23):

$$p^{q_i}=-4\,[\partial\bar{\varphi}^{q_i}/\partial\xi+(p_i^*)^2\bar{\varphi}^{\dot{q}_i}]; \quad p^{\dot{q}_i}=-4\,(\partial\bar{\varphi}^{\dot{q}_i}/\partial\xi+\bar{\varphi}^{q_i}) \tag{9.6.24}$$

In accordance with the above relations, the values of p^{qi} and $p^{\dot{q}_i}$ are determined by the derivatives of the dimensionless potential function with respect to the relevant kinematic parameters.

Wave Equation

Let us obtain an equation which the velocity potential φ satisfies. For this purpose, we shall transform the continuity equation (2.4.2) with account taken of the expressions

$$\frac{\partial \rho}{\partial x} = \frac{1}{a^2} \cdot \frac{\partial p}{\partial x}; \quad \frac{\partial \rho}{\partial y} = \frac{1}{a^2} \cdot \frac{\partial p}{\partial y}; \quad \frac{\partial \rho}{\partial z} = \frac{1}{a^2} \cdot \frac{\partial p}{\partial z}$$

$$\frac{\partial \rho}{\partial t} = \frac{1}{a^2} \cdot \frac{\partial p}{\partial t} \tag{9.6.25}$$

These expressions relate to a barotropic fluid for which the density is a function of the pressure [$\rho = \rho(p)$], and the square of the speed of sound $a^2 = dp/d\rho$. By (9.6.25), the continuity equation becomes

$$\frac{1}{\rho} \cdot \frac{\partial p}{\partial t} + a^2 \left(\frac{\partial V_x}{\partial x} + \frac{\partial V_y}{\partial y} + \frac{\partial V_z}{\partial z} \right) + \frac{V_x}{\rho} \cdot \frac{\partial p}{\partial x} + \frac{V_y}{\rho} \cdot \frac{\partial p}{\partial y} + \frac{V_z}{\rho} \cdot \frac{\partial p}{\partial z} = 0 \tag{9.6.26}$$

Let us exclude the dynamic variables from this equation, retaining only the kinematic ones. To do this, we shall use the Cauchy-Lagrange integral (9.6.18′) from which we shall find expressions for the pressure derivatives with respect to the corresponding coordinates x, y, z, and also the time t related to the density:

$$(1/\rho)\, \partial p/\partial x, \quad (1/\rho)\, \partial p/\partial y, \quad (1/\rho)\, \partial p/\partial z$$

For this purpose, we shall differentiate (9.6.18) consecutively with respect to x, y, z, and t:

$$\left.\begin{aligned} \frac{1}{\rho} \cdot \frac{\partial p}{\partial x} &= \frac{\rho_\infty}{\rho} \left[V_\infty \frac{\partial^2 \varphi}{\partial x^2} - \frac{\partial^2 \varphi}{\partial x\, \partial t} \right) \\ \frac{1}{\rho} \cdot \frac{\partial p}{\partial y} &= \frac{\rho_\infty}{\rho} \left(V_\infty \frac{\partial^2 \varphi}{\partial x\, \partial y} - \frac{\partial^2 \varphi}{\partial y\, \partial t} \right) \\ \frac{1}{\rho} \cdot \frac{\partial p}{\partial z} &= \frac{\rho_\infty}{\rho} \left(V_\infty \frac{\partial \varphi}{\partial x\, \partial t} - \frac{\partial^2 \varphi}{\partial z\, \partial t} \right) \\ \frac{1}{\rho} \cdot \frac{\partial p}{\partial t} &= \frac{\rho_\infty}{\rho} \left(V_\infty \frac{\partial^2 \varphi}{\partial x\, \partial t} - \frac{\partial^2 \varphi}{\partial t^2} \right) \end{aligned}\right\} \tag{9.6.27}$$

We shall write the relation for the square of the speed of sound a^2 in a linearized flow on the basis of the Cauchy-Lagrange integral. Since

$$P - P_\infty = \frac{k}{k-1} \left(\frac{p}{\rho} - \frac{p_\infty}{\rho_\infty} \right) = \frac{1}{k-1} (a^2 - a_\infty^2)$$

then with a view to (9.6.17) and (9.6.18'), we have

$$a^2 = a_\infty^2 + (k-1)(V_\infty \partial\varphi/\partial x - \partial\varphi/\partial t) \qquad (9.6.28)$$

We can represent the velocity components in (9.6.26) in the form

$$V_x = V_\infty + \partial\varphi/\partial x, \quad V_y = \partial\varphi/\partial y, \quad V_z = \partial\varphi/\partial z \qquad (9.6.29)$$

Let us introduce (9.6.27)-(9.6.29) into continuity equation (9.6.26). Disregarding second-order infinitesimals and assuming that the density ratio $\rho_\infty/\rho \approx 1$, we obtain

$$(1-M_\infty^2)\frac{\partial^2\varphi}{\partial x^2} + \frac{\partial^2\varphi}{\partial y^2} + \frac{\partial^2\varphi}{\partial z^2} + \frac{2M_\infty}{a_\infty}\cdot\frac{\partial^2\varphi}{\partial x\,\partial t} - \frac{1}{a_\infty^2}\cdot\frac{\partial^2\varphi}{\partial t^2} = 0 \qquad (9.6.30)$$

where $M_\infty = V_\infty/a_\infty$ is the Mach number for an undisturbed flow. The obtained equation is called the wave one. It satisfies the velocity potential φ of an unsteady linearized flow. If in a body-axis system of coordinates, the longitudinal axis Ox is directed from the nose to the tail, the sign of the term $(2M_\infty/a_\infty)\,\partial^2\varphi/\partial x\,\partial t$ in (9.6.30) must be reversed.

With a view to the notation (9.6.19), the wave equation in the dimensionless form can be written as follows:

$$(1-M_\infty^2)\frac{\partial^2\bar{\varphi}}{\partial\xi^2} + \frac{\partial^2\bar{\varphi}}{\partial\eta^2} + \frac{\partial^2\bar{\varphi}}{\partial\zeta^2} + 2M_\infty^2\frac{\partial^2\bar{\varphi}}{\partial\xi\,\partial\tau} - M_\infty^2\frac{\partial^2\bar{\varphi}}{\partial\tau^2} = 0 \qquad (9.6.31)$$

To determine the aerodynamic characteristics of a craft, it is sufficient to solve wave equation (9.6.31), finding the potential of the disturbed velocities $\bar{\varphi}$. The solution for the function $\bar{\varphi}$ must satisfy the boundary conditions on the surface in the flow, the conditions on the vortex sheet, and also at infinity.

The boundary condition on the surface of a craft reflects the requirement of a flow without separation (a smooth flow), in accordance with which the normal component of the velocity on the wall is zero. This signifies that the velocity of the disturbed flow $\partial\varphi/\partial y + \Omega_x z + \Omega_z x$ must cancel the corresponding component αV_∞ of the velocity vector $\bar{V}_\infty$ on the surface in the flow. Consequently,

$$\partial\varphi/\partial y + \Omega_x(t)\,z + \Omega_z(t)\,x + \alpha(t)\,V_\infty = 0 \qquad (9.6.32)$$

or in the dimensionless form

$$\partial\bar{\varphi}/\partial\eta + \omega_x(\tau)\,\zeta + \omega_z(\tau)\,\xi + \alpha(\tau) = 0 \qquad (9.6.32')$$

The condition on the vortex sheet formed behind a craft is stated as the requirement that there be no difference of disturbed pressures on its upper and bottom sides. According to this requirement, we obtain the following expression on the basis of the Cauchy-Lagrange equation:

$$\partial\varphi_b/\partial t - V_\infty\,\partial\varphi_b/\partial x = \partial\varphi_u/\partial t - V_\infty\,\partial\varphi_u/\partial x \qquad (9.6.33)$$

or in the dimensionless form

$$\partial\bar{\varphi}_b/\partial\tau - \partial\bar{\varphi}_b/\partial\xi = \partial\bar{\varphi}_u/\partial\tau - \partial\bar{\varphi}_u/\partial\xi \qquad (9.6.34)$$

In accordance with the *condition at infinity*, we assume that the fluid is undisturbed, i.e. all the disturbances produced by the craft vanish. Accordingly, the potential of the disturbance and its derivatives equal zero, i.e.

$$\varphi = \partial\varphi/\partial x = \partial\varphi/\partial y = \partial\varphi/\partial z = 0 \qquad (9.6.35)$$

9.7. Basic Methods of Solving Non-Stationary Problems

Method of Sources

This method is one of the most widespread ones in the theory of flow over craft or their isolated elements (wings, fin assembly, empennage, body). It establishes expressions relating in the general form the required potential function φ satisfying wave equation (9.6.31) to the geometric parameters of a lifting surface and to the values of the derivatives $\partial\varphi/\partial y$ at points on it. The physical meaning of the method of sources was considered in detail in Chap. 8. We shall give a general scheme of the derivation of a formula for the potential φ as applied to the conditions of supersonic unsteady flow over a preset lifting surface.

The basic idea of the method of sources consists in replacing a flat surface with a system of continuously distributed sources of varying strength that induces the same field of velocities and pressures as in an unsteady flow over the given surface. This method is based on the expression for the **retarded potential** of a stationary fluctuating strength source at the instant t [see (2.9.14)]:

$$\left.\begin{aligned} \varphi^*(x^*, y^*, z^*, t) &= q/r^* \\ r^* &= \sqrt{x^{*2} + y^{*2} + z^{*2}} \end{aligned}\right\} \qquad (9.7.1)$$

Here $q(t)$ is the varying strength of the source determined at the instant $t' = t - r^*/a_\infty$ (where a_∞ is the speed of sound).

Hence, this strength $q(t - r^*/a_\infty)$ is taken for the instant when a sonic disturbance wave emerges from the source and reaches point P with the coordinates x^*, y^*, z^* at the considered instant t (Fig. 9.7.1).

When selecting any doubly differentiable function $\varphi(t')$, expression (9.7.1) satisfies wave equation (9.6.31).

Let us assume that beginning from the instant $t = 0$, point source O begins to move from point O^* at the velocity V_∞. Hence, at any instant t, section OO^* is filled with sources changing according

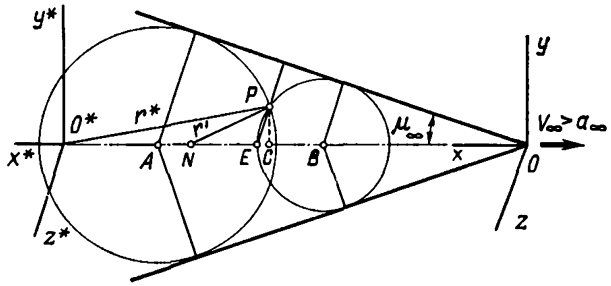

Fig. 9.7.1
To the determination of the velocity potential of non-stationary sources

to the law $q\,(t - t^*)$, where t^* is the instant a source originates at a point N (Fig. 9.7.1). The retarded potential at point $P\,(x^*,\ y^*,\ z^*)$ due to these sources can be written in the form

$$\varphi'(x^*,\ y^*,\ z^*,\ t) = \int_{t_1}^{t_1''} \frac{1}{r'}\, q\left(t - t^* - \frac{r'}{a_\infty}\right) dt^* \qquad (9.7.2)$$

where $r' = \sqrt{(x^* + V_\infty t^*)^2 + y^{*2} + z^{*2}}$ is the distance between points P and N, t_1' and t_1'' are the integration limits taking into account the sources from which the disturbances arrive at point P at the instant t.

Let us consider a moving coordinate system for which $x = x^* + V_\infty t$, $y = y^*$, and $z = z^*$. We shall assume below that $r_2 = a_\infty\,(t - t^*) - r'$. In this case for $V_\infty > a_\infty$, we can find the following expression for the potential:

$$\varphi'(x,\ y,\ z,\ t) = \frac{1}{a_\infty}\int_0^{r_2'} \frac{1}{r_1}\, q_1\left(\frac{r_2}{a_\infty}\right) dr_2 + \frac{1}{a_\infty}\int_0^{r_2'} \frac{1}{r_1}\, q_2\left(\frac{r_2}{a_\infty}\right) dr_2 \qquad (9.7.3)$$

where

$$\left.\begin{aligned} r_1 &= \sqrt{(x - M_\infty r_2)^2 - \alpha'^2 (y^2 + z^2)} \\ M_\infty &= V_\infty / a_\infty, \quad \alpha' = \sqrt{M_\infty^2 - 1} \end{aligned}\right\} \qquad (9.7.4)$$

The upper limit of the integrals $r_2' = a_\infty\,(t - t_1^*) - r'$ is determined by the instant t_1^* at which point O moves to point E on normal PE to the Mach line. The first term in (9.7.3) takes into account the influence on point P of the sources on section AE (the leading front of the sound wave), and the second, on section BE the trailing front of the wave).

Let us consider the case when a source is located only at moving point O, and at the instant t point P is influenced by the disturban-

ces from the spherical waves occurring at the instants t_1' and t_1''. We shall find the potential at point P by formula (9.7.3) as a result of a limiting process, assuming $r_2 \to 0$. We shall presume that

$$q(t_1) = \frac{1}{a_\infty} \int_0^{r_2'} q_1\left(\frac{r_2}{a_\infty}\right) dr_2, \quad q(t_2) = \frac{1}{a_\infty} \int_0^{r_2'} q_2\left(\frac{r_2}{a_\infty}\right) dr_2 \quad (9.7.5)$$

where $t_1 = t - \Delta t_1$; $t_2 = t - \Delta t_2$; Δt_1, Δt_2 are intervals during which the signal is transmitted from the origin of coordinates to a point (x, y, z) with the wave front and its rear surface.

With a view to (9.7.5), we have the following expression for the velocity potential:

$$q(x, y, z, t) = q(t_1)/r + q(t_2)/r; \quad r = \sqrt{x^2 - \alpha'^2 (y^2 + z^2)} \quad (9.7.6)$$

Here $q(t_1)/r$ determines the potential due to the source at point A and $q(t_2)/r$, at point B (Fig. 9.7.1).

We consider that at the instant $t = 0$ sources with a strength of $q(x, z, t)$ appear simultaneously on the entire area occupied by the lifting surface. The potential produced by such sources at a point with the coordinates x_1, y_1, z_1 can be written as

$$\varphi(x_1, y_1, z_1, t) = \int_{\sigma_1} \int \frac{q(x, z, t_1)\, dx\, dy}{r} + \int_{\sigma_2} \int \frac{q(x, z, t_2)\, dx\, dz}{r}$$

where $r = \sqrt{(x_1 - x)^2 - \alpha'^2 [y_1^2 - (z_1 - z)^2]}$ is a conditional distance between the points (x_1, y_1, z_1) and $(x, 0, z)$.

The integration regions $\sigma_1 (x_1, y_1, z_1)$ and $\sigma_2 (x_1, y_1, z_1)$ are the parts of plane xOz confined within the branch of the Mach (characteristic) cone issuing from the point (x_1, y_1, z_1). This branch is determined by the equation

$$\alpha'^2 y_1^2 = (x_1 - x)^2 - \alpha'^2 (z_1 - z)^2$$

As a result of differentiating (9.7.7) with respect to the coordinate y_1, we find an expression for the strength of a source:

$$q(x, z, t) = -\frac{1}{2\pi} \left[\frac{\partial \varphi(x_1, y_1, z_1, t)}{\partial y_1}\right]_{y=0} \quad (9.7.8)$$

The instants $t_1 = t - \Delta t_1$ and $t_2 = t - \Delta t_2$ in (9.7.7) are determined according to the following values:

$$\left.\begin{aligned} \Delta t_1 &= \frac{M_\infty^2}{V_\infty \alpha'^2}\left(x_1 - x - \frac{r}{M_\infty}\right) \\ \Delta t_2 &= \frac{M_\infty^2}{V_\infty \alpha'^2}\left(x_1 - x + \frac{r}{M_\infty}\right) \\ r &= \sqrt{(x_1 - x)^2 - \alpha'^2 [y_1^2 + (z_1 - z)^2]} \end{aligned}\right\} \quad (9.7.9)$$

Relations (9.7.8) and (9.7.9) are derived in [19].

When solving problems on the unsteady flow over flat lifting surfaces, we may assume that $y_1 = 0$ because to determine the aerodynamic characteristics, we must find the values of the potential function on this surface.

The velocity potential φ [see (9.7.7)], in addition to the conditions on the surface of bodies, must satisfy the conditions on the vortex sheet and at infinity, and also the Chaplygin-Zhukovsky condition in accordance with which *a flow does not bend around a trailing subsonic edge, but is cast off it.* In accordance with this condition, disturbed velocities near such edges change continuously, therefore the derivatives $\partial\varphi/\partial x$, $\partial\varphi/\partial y$, and $\partial\varphi/\partial z$ are continuous. The Chaplygin-Zhukovsky condition for the supersonic flow over a lifting surface with subsonic trailing edges is used in the form

$$\left.\begin{aligned} &\lim_{x\to x^*} \frac{\partial\varphi}{\partial y} = \frac{\partial\varphi}{\partial y}\Big|_{x=x^*} \\ &\lim_{x\to x^*} \varphi(x,\ 0,\ z,\ t) = \varphi(x^*,\ 0,\ z,\ t) \end{aligned}\right\} \qquad (9.7.10)$$

where $x^*(z)$ are the coordinates of points on the trailing edges, and $\varphi(x^*, 0, z, t)$ is the value of the potential on these edges.

Vortex Theory

When solving problems on the unsteady incompressible or subsonic compressible flows over a body, it is good practice not to *seek* directly the velocity potential satisfying the wave equation (as in the method of sources for supersonic velocities), but to use what is known as the **vortex theory**, which does not require the finding of φ. According to this theory, the disturbed motion near a lifting surface can be studied with the aid of a vortex pattern including the bound and free vortices that produce the same distribution of the velocities and pressures as the given surface in the flow.

Let us consider a non-stationary vortex pattern using the example of a lifting surface with a rectangular planform (Fig. 9.7.2). The motion of such a surface is characterized by a constant velocity $\mathbf{V}_\infty$ and small velocity increments due to additional translational or rotational modes of motion. These velocities cause a change in the local angles of attack, and also in the angle of attack as a whole, which results in corresponding changes in time of the lift force of the sections and, consequently, according to Zhukovsky's formula, of the circulation $\Gamma(t)$ as well [see formula (6.4.6)]. This circulation is due to the rectilinear bound vortex core used to model the lifting surface with a rectangular planform.

Assume that the circulation during the time Δt changes by the value $\Delta\Gamma$. In accordance with the Helmholtz theorem, in an ideal fluid the circulation of the velocity over closed contour C (Fig. 9.7.2)

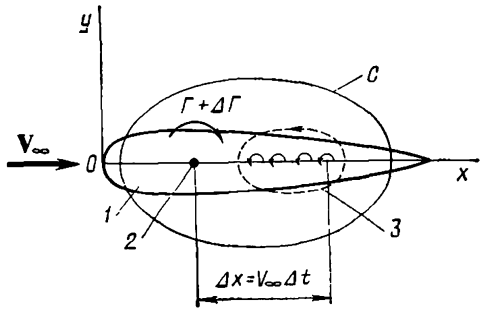

Fig. 9.7.2
Vortex system:
1—lifting surface; *2*—bound vortex with varying circulation; *3*—sheet of non-stationary vortices

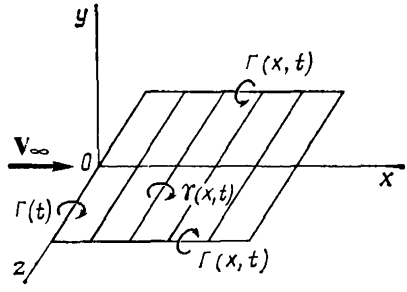

Fig. 9.7.3
Vortex pattern of rectangular lifting surface

passing through the same particles does not depend on the time. Consequently, when the circulation $\Gamma(t)$ changes, a system of free vortices with the circulation $-\Delta\Gamma$ appears behind the lifting surface that compensates the change in the circulation up to its initial value. Accordingly, a vortex sheet forms behind the lifting surface that consists both of longitudinal vortices parallel to the vector $\mathbf{V}_\infty$ and moving along with the flow, and of lateral (bound) vortices that are stationary relative to the lifting surface.

The intensity of vortex filament distribution in the sheet along the longitudinal axis Ox is $\gamma = -d\Gamma/dx = -(1/V_\infty)\, d\Gamma/dt$. It follows from coupling equation (6.4.8) that the circulation is proportional to the lift force coefficient c_y. With a linear dependence of c_y on the angle of attack ($c_y = c_y^\alpha \alpha$), the circulation is also a linear function of α, i.e. $\Gamma = \Gamma^\alpha \alpha$ (where $\Gamma^\alpha = d\Gamma/d\alpha = \text{const}$). Therefore, the strength of the vortex sheet $\gamma = -(\Gamma^\alpha/V_\infty)\, d\alpha/dt$ depends on the rate of change in the angle of attack.

Figure 9.7.3 shows a vortex pattern modelling a rectangular lifting surface. It consists of straight bound vortices with a vortex sheet cast off them.

For a lifting surface of an intricate planform, the vortex pattern consists of a number of bound vortex filaments each of which is replaced with several discrete bound vortices from which a pair

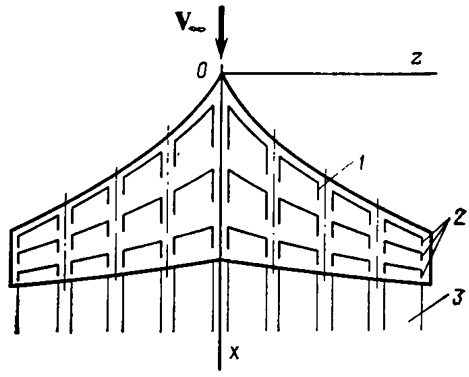

Fig. 9.7.4
Vortex model of intricate lifting surface:
1—discrete oblique horseshoe vortex; *2*—vortex filaments consisting of discrete oblique vortices; *3*—vortex sheet

of free vortex filaments is shed. Such vortex patterns are called **oblique horseshoe vortices** (Fig. 9.7.4)

Let us consider the Kutta-Zhukovsky theorem allowing us to determine the aerodynamic loads acting on a surface element in unsteady flow. This theorem relates to **circulation flow** that is attended by the appearance of a trailing vortex and circulation over the contour enveloping the lifting surface.

According to the Kutta-Zhukovsky theorem, the pressure difference on the bottom and upper sides of a surface element in a linearized flow is

$$\Delta p = p_{\mathrm{b}} - p_{\mathrm{u}} = \rho_\infty \gamma V_\infty \tag{9.7.11}$$

where $\gamma = (1/V_\infty)\,\partial\Gamma/\partial t$ is the **linear strength of the bound vortices**, and V_∞ is the velocity of translational motion.

Formula (9.7.11) is an application of the Kutta-Zhukovsky theorem to an arbitrary unsteady flow over a thin lifting surface and indicates the absence of the influence of free vortices on the aerodynamic loads. From this theorem, particularly, there follows the absence of a pressure difference on a vortex sheet consisting of free vortices.

Let us write the strength of a vortex layer in the form of a series:

$$\gamma = V_\infty \sum_{i=1}^{3} (\gamma^{q_i} q_i + \gamma^{\dot{q}_i} \dot{q}_i) \tag{9.7.12}$$

Introducing this quantity into the formula for calculating the difference of the pressure coefficients

$$\Delta\bar{p} = 2\,(p_{\mathrm{b}} - p_{\mathrm{u}})/(\rho_\infty V_\infty^2) = 2\gamma/V_\infty \tag{9.7.13}$$

we obtain

$$\Delta\bar{p} = 2 \sum_{i=1}^{3} (\gamma^{q_i} q_i + \gamma^{\dot{q}_i} \dot{q}_i) \tag{9.7.14}$$

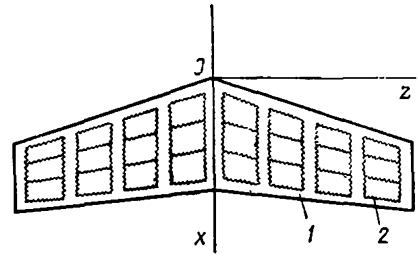

Fig. 9.7.5
Vortex model for non-circulatory flow:
1—lifting surface; *2*—discrete closed attached vortices

Comparing this expression with the second formula (9.6.22), we find expressions for the derivatives of the pressure coefficient difference in terms of the corresponding derivatives of the linear strength of the bound vortex layer:

$$p^{q_i} = 2\gamma^{q_i}, \quad \dot{p}^{q_i} = 2\dot{\gamma}^{q_i} \ (i = 1, 2, 3) \tag{9.7.15}$$

The above relations are exact if the kinematic variables change harmonically.

For circulation problems, the Chaplygin-Zhukovsky condition on the passing off of the flow from the trailing edge of a surface and on the finiteness of the velocity at this edge is satisfied. According to this condition, the strength of the bound vortices on the trailing edges is zero, i.e.

$$\gamma(x, z, t) = 0 \tag{9.7.16}$$

When bodies move at very low speeds, or when oscillations occur in the absence of translational motion, a scheme of non-circulatory flow is realized. Here no wake forms behind a body, and the circulation over an arbitrary contour enveloping the lifting surface is zero.

Accordingly, a vortex layer equivalent to the lifting surface is represented as a system of closed vortex filaments of constant strength (Fig. 9.7.5). Some results of studying non-circulatory flow, in particular the derivation of Zhukovsky's theorem for such flow, are given in [4, 19].

9.8. Numerical Method of Calculating the Stability Derivatives for a Wing in an Incompressible Flow

Velocity Field of an Oblique Horseshoe Vortex

The numerical method of calculating the stability derivatives for a wing in an unsteady flow is based on its replacement by a vortex lifting surface which, in turn, is represented by a system of oblique horsheshoe discrete transient vortices.

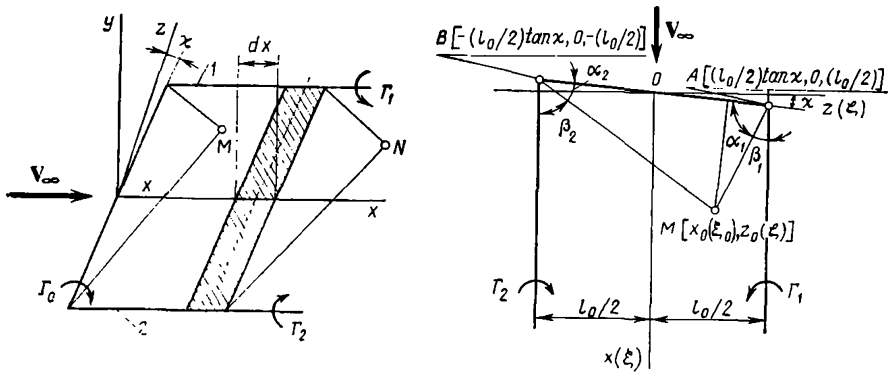

Fig. 9.8.1
Oblique horseshoe vortex in an unsteady flow:
1, 2—free vortices

Let us consider the velocities induced by such vortices. With non-stationary motion of a wing, the circulation (strength) of a bound vortex varies with time, i.e. $\Gamma = \Gamma(t_0)$. In accordance with the condition of constancy of the circulation over a closed contour, this change in the strength is attended by the casting off of free vortices carried away behind the wing together with the flow. The velocity of casting off the free vortices equals the free-stream velocity V_∞, while all the vortices are in the wing plane xOz. The axes of the bound vortices and of the free ones cast off the wing are parallel, while the strength of each of these vortices *1* and *2* (Fig. 9.8.1) at the instant of shedding equals the strength of the bound vortex at this instant.

Let us determine the velocity induced by a bound vortex of strength $\Gamma(t_0) = \Gamma V_\infty b$ (where Γ is the dimensionless magnitude of the circulation, and b is a characteristic linear dimension) at point $M(x_0, 0, z_0)$. According to the Biot-Savart relation, the magnitude of this velocity is

$$W' = \frac{\Gamma_0(t_0)}{4\pi h}(\cos\alpha_1 + \cos\alpha_2) = -\frac{V_\infty \Gamma}{4\pi} \cdot \frac{\cos\alpha_1 + \cos\alpha_2}{\xi_0 \cos\varkappa - \zeta_0 \sin\varkappa} \qquad (9.8.1)$$

where $\xi_0 = x_0/b$, $\zeta_0 = z_0/b$.

The relevant value of the velocity produced by the free vortices is determined by the formula

$$W'' = -\frac{V_\infty \Gamma}{4\pi}\left(\frac{1+\cos\beta_1}{0.5\bar{l}_0 - \zeta_0} + \frac{1+\cos\beta_2}{0.5\bar{l}_0 + \zeta_0}\right) \qquad (9.8.2)$$

where $\bar{l}_0 = l_0/b$.

The total velocity induced by the bound and free vortices is $W = W' + W''$. It will be more convenient in the following to

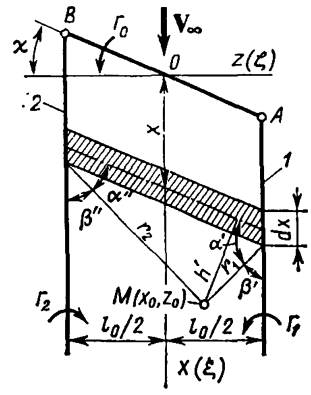

Fig. 9.8.2
To the determination of the velocities induced by a vortex sheet and free vortex filaments of varying strength:
1, 2—free vortices

use the dimensionless value of the velocity:

$$w'(\xi_0, \zeta_0, \varkappa) = W'(4\pi/V_\infty\Gamma) = -\frac{\cos\alpha_1 + \cos\alpha_2}{\xi_0\cos\varkappa - \zeta_0\sin\varkappa} \quad (9.8.3)$$

$$w''(\xi_0, \zeta_0, \varkappa) = W''(4\pi/V_\infty\Gamma) = -\left(\frac{1+\cos\beta_1}{\bar{l}_0 - \zeta_0} + \frac{1+\cos\beta_2}{\bar{l}_0 + \zeta_0}\right) \quad (9.8.4)$$

The corresponding value of the total dimensionless velocity is

$$w(\xi_0, \zeta_0, \varkappa) = W(4\pi/V_\infty\Gamma) = w'(\xi_0, \zeta_0, \varkappa) + w''(\xi_0, \zeta_0, \varkappa) \quad (9.8.5)$$

The values of the geometric parameters determining the induced velocities (the cosines of the angles α_1, α_2, β_1, β_2) depend on the coordinates of point $M[x_0(\xi_0), z_0(\zeta_0)]$ and the angle of inclination $\varkappa$ of an oblique vortex (Fig. 9.8.1). These values are given in [4].

Let us consider an elementary vortex layer of width dx at a distance of x from the bound vortex (Fig. 9.8.2). The linear strength of this layer at the instant t_0 is determined by the magnitude of the derivative

$$\gamma(x, t_0) = -\frac{1}{V_\infty}\cdot\frac{d\Gamma_0(t_1)}{dt_1}; \quad t_1 = t_0 - \frac{x}{V_\infty} \quad (9.8.6)$$

We shall write the strengths of the free vortex filaments $\Gamma_1(x, t_0)$ and $\Gamma_2(x, t_0)$ in the section $x = \text{const}$ as functions:

$$\left.\begin{aligned}\Gamma_1(x, t_0) &= \Gamma_0\left(t_0 - \frac{x - 0.5l_0\tan\varkappa}{V_\infty}\right)\\ \Gamma_2(x, t_0) &= \Gamma_0\left(t_0 - \frac{x + 0.5l_0\tan\varkappa}{V_\infty}\right)\end{aligned}\right\} \quad (9.8.7)$$

The elementary velocity dV' induced at point $M(x_0, \zeta_0)$ by a vortex layer with a strength of $d\Gamma_0 = \gamma(x, t_0)\,dx$ is determined

with the aid of the Biot-Savart formula (9.8.1):

$$dV' = -\frac{d\Gamma_0(x,t_0)}{4\pi h'}(\cos\alpha' + \cos\alpha'') = -\frac{\gamma(x,\ t_0)\,dx\,(\cos\alpha' + \cos\alpha'')}{4\pi\,[(x_0 - x)\cos\varkappa - z_0\sin\varkappa]}$$

By integrating with respect to ξ from 0 to infinity and going over to dimensionless coordinates, we obtain

$$V' = -\frac{1}{4\pi}\int_0^\infty \frac{\gamma\,(x,\ t_0)\,(\cos\alpha' + \cos\alpha'')}{(\xi_0 - \xi)\cos\varkappa - \zeta_0\sin\varkappa}\,d\xi \qquad (9.8.8)$$

Here the cosines of the angles α' and α'' are determined from Fig. 9.8.1 as a function of the dimensionless coordinates ξ_0, ξ, the angle $\varkappa$, and the relative span of a vortex $\bar{l}_0 = l_0/b$.

The velocities dV_1'' and dV_2'' induced by elements of the free vortex filaments *1* and *2* are determined by the Biot-Savart formulas (see Fig. 9.8.1) as follows:

$$dV_1'' = -\frac{\Gamma_1 \sin\beta' dx}{4\pi r_1^2},\quad dV_2'' = -\frac{\Gamma_2 \sin\beta'' dx}{2\pi r_2^2}$$

The geometric variables in these expressions are determined with the aid of Fig. 9.8.2. For example,

$$\sin\beta' = (0.5l_0 - z_0)/r_1,\quad r_1 = \sqrt{(x_0 - x)^2 + (0.5l_0 - z_0)^2}$$

We find the values of $\sin\beta''$ and r_2 in a similar way. Integrating with respect to x from $-0.5l_0\tan\varkappa$ and $0.5l_0\tan\varkappa$ to ∞ and passing over to dimensionless geometric variables, we obtain

$$\left.\begin{aligned} V_1'' &= -\frac{1}{4\pi b}\int_{0.5\bar{l}_0\tan\varkappa}^{\infty} \frac{\Gamma_1\,(x,\ t_0)\,(0.5\bar{l}_0 - \zeta_0)\,d\xi}{[(\xi_0 - \xi)^2 + (0.5\bar{l}_0 - \zeta_0)^2]^{3/2}} \\ V_2'' &= -\frac{1}{4\pi b}\int_{-0.5\bar{l}_0\tan\varkappa}^{\infty} \frac{\Gamma_2\,(x,\ t_0)\,(0.5\bar{l}_0 + \zeta_0)\,d\xi}{[(\xi_0 - \xi)^2 + (0.5\bar{l}_0 + \zeta_0)^2]^{3/2}} \end{aligned}\right\} \qquad (9.8.9)$$

The total velocity induced by the bound vortex, the vortex sheet, and the free vortices is

$$V = W' + V' + V_1'' + V_2'' \qquad (9.8.10)$$

Let us consider a harmonic change in the circulation

$$\Gamma_0(t) = V_\infty b\Gamma\sin pt \qquad (9.8.11)$$

where p is the angular frequency and Γ is a dimensionless constant.

In accordance with this law, we shall write the circulation (9.8.6) in the form

$$\gamma(x,\ t_0) = -b\Gamma p\cos pt_1 = -V_\infty p^*\Gamma\cos(pt_0 - p^*\xi) \qquad (9.8.12)$$

We shall represent formulas (9.8.7) for the circulations as follows:

$$\Gamma_1(x,\ t_0) = V_\infty b\Gamma \sin\left[p\left(t_0 - \frac{x - 0.5l_0 \tan \varkappa}{V_\infty}\right)\right]$$

$$\Gamma_2(x,\ t_0) = V_\infty b\Gamma \sin\left[p\left(t_0 - \frac{x + 0.5l_0 \tan \varkappa}{V_\infty}\right)\right]$$

Introducing the Strouhal number $p^* = bp/V_\infty$ and the dimensionless quantities $\xi = x/b$ and $\bar{l}_0 = l_0/b$, we obtain the generalized expression

$$\Gamma_{1(2)}(x,\ t_0) = V_\infty b\Gamma \sin [pt_0 - p^*(\xi \mp 0.5\bar{l}_0 \tan \varkappa)] \qquad (9.8.13)$$

where the minus sign corresponds to the quantity Γ_1, and the plus sign to Γ_2.

After inserting the obtained values of the strength $\gamma(x,\ t_0)$ and of the circulations $\Gamma_{1(2)}(x,\ t_0)$ into (9.8.8) and (9.8.9), respectively, we find expressions for the induced velocities W', V', V_1'', and V_2'' in the integral form for a harmonic (sinusoidal) change in the circulation. It is not difficult to see that the total induced velocity $V = W' + V' + V_1'' + V_2'$ can be represented in a general form in terms of the dimensionless velocity function $v(\xi_0,\ \zeta_0,\ \varkappa,\ p^*,\ t_0)$:

$$V = \frac{V_\infty \Gamma}{4\pi} v(\xi_0,\ \zeta_0,\ \varkappa,\ p^*,\ t_0) \qquad (9.8.14)$$

where, in turn,

$$\left.\begin{aligned} v &= v^{(1)}(\xi_0,\ \zeta_0,\ \varkappa,\ p^*)\sin pt_0 + v^{(2)}(\xi_0,\ \zeta_0,\ \varkappa,\ p^*)\cos pt_0 \\ v^{(1)} &= w'(\xi_0,\ \zeta_0,\ \varkappa) + p^* v_1'(\xi_0,\ \zeta_0,\ \varkappa,\ p^*) + v_1''(\xi_0,\ \zeta_0,\ \varkappa,\ p^*) \\ v^{(2)} &= p^* v_2'(\xi_0,\ \zeta_0,\ \varkappa,\ p^*) + v_2''(\xi_0,\ \zeta_0,\ \varkappa,\ p^*) \end{aligned}\right\} \qquad (9.8.15)$$

We determine the dimensionless velocity w' from (9.8.3), and we find the functions v_1', v_1'', v_2', and v_2'' from an analysis of integrals (9.8.8) and (9.8.9) after introducing into them, respectively, the harmonically changing quantities $\gamma(x,\ t_0)$ and $\Gamma_{1(2)}(x,\ t_0)$.

The above relations describe a sinusoidal change in the strength of a bound vortex. If this change is cosinusoidal, i.e.

$$\Gamma_0(t) = V_\infty b\Gamma \cos pt \qquad (9.8.16)$$

then we have

$$\left.\begin{aligned} \gamma(x,\ t_0) &= b\Gamma p \sin pt = V_\infty p^* \sin(pt - p^*\xi) \\ \Gamma_{1(2)}(x,\ t_0) &= V_\infty b\Gamma \cos [pt_0 - p^*(\xi \mp 0.5\bar{l}_0 \tan \varkappa)] \end{aligned}\right\} \qquad (9.8.17)$$

With a view to the above, instead of the first of expressions (9.8.15) we have the general relation

$$v = v^{(1)}(\xi_0,\ \zeta_0,\ \varkappa,\ p^*)\cos pt_0 - v^{(2)}(\xi_0,\ \zeta_0,\ \varkappa,\ p^*)\sin pt_0 \qquad (9.8.18)$$

One of the important problems in unsteady aerodynamics is the one on the harmonic oscillations of craft with small Strouhal numbers ($p^* \to 0$). For such numbers

$$v^{(1)}(\xi_0, \zeta_0, \varkappa, 0) = w' + v_1'' \,|_{p^* \to 0} \tag{9.8.19}$$

$$\left.\frac{\partial v^{(2)}}{\partial p^*}\right|_{p^* \to 0} = v_2'(\xi_0, \zeta_0, \varkappa, 0) + \left.\frac{\partial v_2'}{\partial p^*}\right|_{p^* \to 0} \tag{9.8.20}$$

The last derivative is used directly for calculation of unsteady flow parameters. The finding of this derivative, and also of other functions determining the dimensionless induced velocities is described in [4].

Vortex Model of a Wing

A vortex model of a wing in the form of a flat lifting surface in an unsteady circulatory flow is shown in Fig. 9.8.3. If a wing has curved edges, they are replaced approximately with a contour formed of segments of straight lines. Hence, in a most general case, a lifting surface has breaks.

Let us divide the entire area of a wing into zones by drawing sections parallel to the axis Ox through the breaks in the contour. Let us further divide each segment l_δ between the breaks into N_δ^* strips and number their boundaries from right to left (the boundary having the number $p = 0$ coincides with the tip of the wing, and having $p = N$ with the longitudinal axis). Usually the values of the width of a strip $l_{p,p-1}$ differ only slightly from one another.

Let us consider the strip between the sections p and $p - 1$ in any of the zones δ. We shall denote the dimensionless coordinate of the leading edge in the section p by $\xi_{0,p}$, and of the trailing one by ξ_{*p}.

The relative chord of the section is

$$\bar{b}_p = b_p/b_0 = \xi_{*p} - \xi_{0\,p}$$

Let us assume that a strip consists of n cells. For this purpose, we shall divide each chord in the relevant section into n parts by means of points with the coordinates

$$\left.\begin{aligned} \xi_{\nu,p} &= \xi_{0,p} + 0.5\bar{b}_p\left(1 - \cos\frac{\nu\pi}{n}\right) \\ \xi_{\nu,p-1} &= \xi_{0,p-1} + 0.5\bar{b}_{p-1}\left(1 - \cos\frac{\nu\pi}{n}\right) \\ \nu &= 0,\ 1,\ 2,\ \ldots,\ n \end{aligned}\right\} \tag{9.8.21}$$

The cells arranged along the line ν separating them along the span of the wing form panels whose number is the same as that of the cells in a strip (n). We shall designate the boundaries of the panels

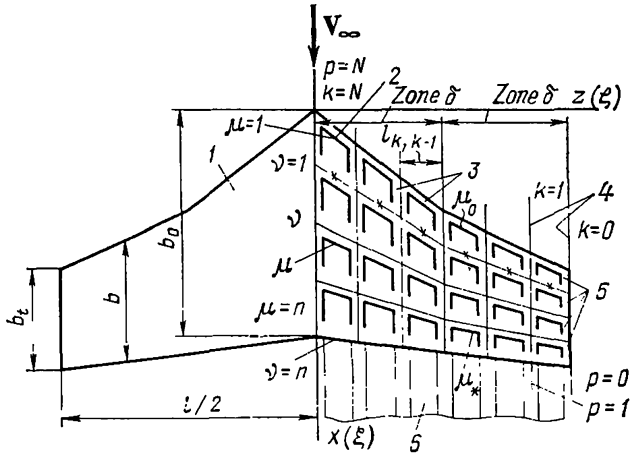

Fig. 9.8.3
Vortex model of a wing in an unsteady circulatory flow:
1—wing; *2*—oblique horseshoe vortex; *3*—cells; *4*—strip; *5*—panels; *6*—vortex wake

by ν (for the leading edge $\nu = 0$, for the trailing one $\nu = \nu_*$). We shall designate the coordinates of points at the intersections of the lines ν and p by the subscripts ν and p.

Hydrodynamically, the plane of the wing is equivalent to a vortex surface that is approximately depicted by a system of bound discrete vortices. Each of such vortices evidently consists of **oblique horseshoe vortices** adjoining one another, while the total number of these vortices coincides with the number of cells in which they are accommodated.

We shall characterize the bound vortex filaments by a serial number μ counted from the nose. Let us introduce for the sections dividing the plane of the wing along its span, in addition to the numbers p, the serial number k counted from a tip where we assume that $k = 0$. Accordingly, $0 \leqslant k \leqslant N$.

We shall denote the points of intersection of the lines μ and k by the same subscripts. We consider here that the coordinates of points on the leading edge in section k and the magnitude of the chord in this section $b_{k(p)}$ of each zone δ are known.

We shall determine the position of discrete vortices as follows. We separate the chords in the sections ζ_k and ζ_{k-1} with points having the coordinates

$$\left.\begin{aligned} \xi_{\mu,k} &= \xi_{0,k} + 0.5\bar{b}_k \left(1 - \cos\frac{2\mu - 1}{2n}\pi\right) \\ \xi_{\mu,k-1} &= \xi_{0,k-1} + 0.5\bar{b}_{k-1}\left(1 - \cos\frac{2\mu - 1}{2n}\pi\right) \\ \mu &= 1, 2, \ldots, n \end{aligned}\right\} \qquad (9.8.22)$$

Points with identical μ's coincide with the ends of discrete vortices. We have the following relations for the dimensionless coordinates of the middles of the oblique bound vortices, their span $l_{k,k-1}$, and sweep angles $\tan \varkappa^{\mu,\ k}_{\mu,\ k-1}$:

$$\left.\begin{aligned}
&\xi^{\mu,\ k}_{\mu,\ k-1} = 0.5\,(\xi_{\mu,\ k} + \xi_{\mu,\ k-1}) = 0.5\,(\xi_{0,\ k} + \xi_{0,\ k-1}) \\
&+ 0.25\,(\bar{b}_k + \bar{b}_{k-1})\left(1 - \cos\frac{2\mu - 1}{2n}\pi\right) \\
&\zeta^{\mu,\ k}_{\mu,\ k-1} = 0.5\,(\zeta_{\mu,\ k} + \zeta_{\mu,\ k-1}),\ \bar{l}_{k,\ k-1} = \frac{l_{k,\ k-1}}{b_0} = \zeta_{\mu,\ k-1} - \zeta_{\mu,\ k} \\
&\tan \varkappa^{\mu,\ k}_{\mu,\ k-1} = (\xi_{\mu,\ k-1} - \xi_{\mu,\ k})/(\zeta_{\mu,\ k-1} - \zeta_{\mu,\ k}) \\
&\mu = 1,\ 2,\ \ldots,\ n;\ k = 1,\ 2,\ \ldots,\ N
\end{aligned}\right\} \qquad (9.8.23)$$

The coordinates of the centre of another vortex symmetric about plane xOy on the port half of the craft and also the sweep angle are as follows:

$$\left.\begin{aligned}
\sigma\xi^{\mu,\ k}_{\mu,\ k-1} = \xi^{\mu,\ k}_{\mu,\ k-1},\ \sigma\zeta^{\mu,\ k}_{\mu,\ k-1} = -\zeta^{\mu,\ k}_{\mu,\ k-1} \\
\sigma\bar{l}_{k,\ k-1} = \bar{l}_{k,\ k-1},\ \sigma\varkappa^{\mu,\ k}_{\mu,\ k-1} = -\varkappa^{\mu,\ k}_{\mu,\ k-1}
\end{aligned}\right\} \qquad (9.8.24)$$

where the variables for the port side of the wing are designated by the factor σ.

For a wing with rectangular edges, the sweep angles of the bound vortices are constant ($\varkappa_\mu$ = const), and each of them transforms into an ordinary straight **horseshoe vortex**. If a wing plane has breaks in its contour, then the corresponding breaks are present in the vortex filaments too.

The circulation of oblique and conventional (straight) horseshoe vortices along the span is constant, while free filaments parallel to the axis Ox are shed off the ends of the bound vortices. The free filaments propagate downstream, and when the flow is circulatory they pass away to infinity. In addition, when the circulation of the bound vortices changes with time, free vortices of the relevant strength are shed off them.

The vortex model being considered is very convenient for computerized calculations of a flow. This is due, first, to the sufficiently simple relations describing the disturbed flow near a wing, and, second, to a number of important properties of the system of algebraic equations which the solution of the problem is reduced to. One of these properties is that the diagonal terms in the matrix of the equation coefficients play a dominating role; the solutions themselves have a great stability relative to the initial conditions.

A significant feature of computerized calculations is also the fact that the use of oblique horseshoe vortices instead of the conventional ones leads to substantial simplification of the calculations and to more accurate results.

Calculation of Circulatory Flow

System of Equations. Let us represent the dimensionless circulation of the oblique horseshoe vortex $\Gamma_{\mu,\,k,\,k-1} = \Gamma'_{\mu,\,k,\,k-1}/(V_\infty b_0)$ in the following form:

$$\left.\begin{aligned}\Gamma_{\mu,\,k,\,k-1}(\tau) = \sum_{i=1}^{3}\left[\Gamma^{q_i}_{\mu,\,k,\,k-1}\,q_i(\tau) + \Gamma^{\dot{q}_i}_{\mu,\,k,\,k-1}\,\dot{q}_i(\tau)\right]\\ q_i = \alpha,\ \omega_x,\ \omega_y;\ \tau = V_\infty t/b_0,\end{aligned}\right\} \tag{9.8.25}$$

or in the expanded form

$$\left.\begin{aligned}\Gamma_{\mu,\,k,\,k-1}(\tau) = \Gamma^{\alpha}_{\mu,\,k,\,k-1}\,\alpha + \Gamma^{\dot{\alpha}}_{\mu,\,k,\,k-1}\,\dot{\alpha} + \Gamma^{\omega_x}_{\mu,\,k,\,k-1}\,\omega_x\\ + \Gamma^{\dot{\omega}_x}_{\mu,\,k,\,k-1}\,\dot{\omega}_x + \Gamma^{\omega_z}_{\mu,\,k,\,k-1}\,\omega_z + \Gamma^{\dot{\omega}_z}_{\mu,\,k,\,k-1}\,\dot{\omega}_z\end{aligned}\right\} \tag{9.8.26}$$

where $\Gamma^{q_i}_{\mu,\,k,\,k-1}$ are dimensionless functions not depending on the time; the only time-dependent variables are q_i and $\dot{q}_i$.

We shall assume that the kinematic variables change according to harmonic relations (9.1.5) and (9.1.6) which can be represented in terms of the dimensionless time τ as follows:

$$q_i = q_i^* \cos p_i^*\tau, \quad \dot{q}_i = -q_i^* p_i^* \sin p_i^*\tau \tag{9.8.27}$$

where q_i^* are the amplitude values of the variables not depending on the time, $p_i^* = p_i b_0/V_\infty$ is the Strouhal number (p_i is the angular frequency), and $\tau = tV_\infty/b_0$.

With a view to (9.8.27). the circulation (9.8.25) is expressed as follows:

$$\Gamma_{\mu,\,k,\,k-1}(\tau) = \sum_{i=1}^{3} q_i^*\left[\Gamma^{q_i}_{\mu,\,k,\,k-1}\cos p_i^*\tau - \Gamma^{\dot{q}_i}_{\mu,\,k,\,k-1}\,p_i^* \sin p_i^*\tau\right] \tag{9.8.28}$$

By (9.8.6)

$$\gamma(\xi^{\mu;\,k}_{\mu;\,k-1},\tau) = V_\infty \sum_{i=1}^{3} q_i^* p_i^* \{\Gamma^{q_i}_{\mu,\,k,\,k-1}\sin[p_i^*(\tau - \xi^{\mu;\,k}_{\mu;\,k-1})] + p_i^*\Gamma^{\dot{q}_i}_{\mu,\,k,\,k-1}\cos[p_i^*(\tau - \xi^{\mu;\,k}_{\mu;\,k-1})]\} \tag{9.8.29}$$

where $\xi^{\mu;\,k}_{\mu;\,k-1}$ is the longitudinal coordinate of the middle of an oblique bound vortex.

The expressions for the circulation of the free vortices (9.8.7) have the form

$$\Gamma_{1\,(2)}(\xi^{\mu;\,k}_{\mu;\,k-1},\tau) = V_\infty b_0 \sum_{i=1}^{3} q_i^*\,[\Gamma^{q_i}_{\mu,\,k,\,k-1}\cos\{p_i^*[\tau - (\xi^{\mu;\,k}_{\mu;\,k-1} \mp 0.5\bar{l}_{k,\,k-1}\tan\varkappa^{\mu;\,k}_{\mu;\,k-1})]\} - \Gamma^{\dot{q}_i}_{\mu,\,k,\,k-1}\,p_i^*\sin\{p_i^*[\tau - (\xi^{\mu;\,k}_{\mu;\,k-1} \mp 0.5\bar{l}_{k,\,k-1}\tan\varkappa^{\mu;\,k}_{\mu;\,k-1})]\}] \tag{9.8.30}$$

Introducing (9.8.28), (9.8.29), and (9.8.30) into (9.8.1), (9.8.8), and (9.8.9), respectively, we obtain for a certain control point $\xi^{\nu,p}_{\nu,p-1}$, $\zeta^{\nu,p}_{\nu,p-1}$ of the wing the induced velocities W', V', V''_1, and V''_2 expressed in terms of derivatives of the circulation. We shall assume that the control points are at the centre of the lines drawn through points with identical values of ν (except for the forward and the rear points), i.e. at an identical distance between the free vortices. Hence the coordinates of the control points (indicated by crosses in Fig. 9.8.3) are determined by the relations

$$\left.\begin{aligned} \xi^{\nu,\ p}_{\nu,\ p-1} &= 0.5\,(\xi_{\nu,\ p} + \xi_{\nu,\ p-1}) = 0.5\,(\xi_{0,\ p} + \xi_{0,\ p-1}) \\ &\quad + 0.25\,(\bar{b}_p + \bar{b}_{p-1})\left(1 - \cos\frac{\nu\pi}{n}\right) \\ \zeta^{\nu,\ p}_{\nu,\ p-1} &= 0.5\,(\zeta_p + \zeta_{p-1}) \\ \nu &= 0,\ 1,\ 2,\ \ldots,\ n-1;\ p = 0,\ 1,\ 2,\ \ldots,\ N \end{aligned}\right\} \quad (9.8.31)$$

The relative value of the total induced velocity at this point $v = (W' + V' + V''_1 + V''_2)/V_\infty$ is determined by the dimensionless velocities $v^{(1)}$ and $v^{(2)}$ that are evaluated in accordance with general relations similar to (9.8.14) and (9.8.15).

Let us designate by $\sigma v^{(1)}$ and $\sigma v^{(2)}$ the additional velocities at the control point being considered produced by an oblique vortex located on the port half of the wing symmetrically about the plane xOy. The coordinates of the middle of such a vortex are $\xi^{\mu,k}_{\mu,k-1}$ and $-\zeta^{\mu,k}_{\mu,k-1}$.! The values of $\sigma v^{(1)}$ and $\sigma v^{(2)}$ are determined with the aid of (9.8.1), (9.8.8) and (9.8.9), account being taken of the change in the direction of the coordinate axes and the transfer of their origin.

We shall add these values of the corresponding dimensionless velocities $v^{(1)}$ and $v^{(2)}$ for symmetric motion (for $q_i = \alpha$, ω_z, and even functions $\Gamma^{q_i}_{\mu,k,k-1}$, $\dot{\Gamma}^{q_i}_{\mu,k,k-1}$) and subtract them for asymmetric motion (for $q_i = \omega_x$ and odd derivatives of the dimensionless circulation). We shall determine the total velocity at a control point with account taken of the influence of all the other vortices, i.e. calculate it by double summation of the induced velocities over the number of strips N and panels n. This velocity is determined by the values of the derivatives of the dimensionless circulation $\Gamma^{q_i}_{\mu,k,k-1}$ and $\dot{\Gamma}^{q_i}_{\mu,k,k-1}$.

To find them, we must use the condition of flow without separation in accordance with which the total dimensionless velocity at a control point induced by the entire vortex pattern of the wing equals the undisturbed component determined by Eq. (9.6.32′):

$$\begin{aligned} v_{\nu,\ p,\ p-1} &= \frac{V_{\nu,\ p,\ p-1}}{V_\infty} = \frac{(W' + V' + V''_1 + V''_2)_{\nu,\ p,\ p-1}}{V_\infty} \\ &= -\omega_x \zeta^{\nu,\ p}_{\nu,\ p-1} - \omega_z \xi^{\nu,\ p}_{\nu,\ p-1} - \alpha \end{aligned} \quad (9.8.32)$$

The kinematic variables in this equation can be represented in the form of a harmonic relation:

$$q_i = q_i^* \cos p_i^* \tau_0 \quad (q_i = \alpha,\ \omega_x,\ \omega_z) \tag{9.8.33}$$

By satisfying Eq. (9.8.32) with a view to (9.8.33), we obtain the following three systems of linear algebraic equations for the required derivatives of the dimensionless circulation $\Gamma^{q_i}_{\mu,k,k-1}$ and $\dot{\Gamma}^{q_i}_{\mu,k,k-1}$:

$$\left.\begin{aligned}
&\frac{1}{4\pi}\sum_{k=1}^{N}\sum_{\mu=1}^{n}\left(v^{(1)\,\mu,\,k,\,k-1}_{\nu,\,p,\,p-1} \pm \sigma v^{(1)\,\mu,\,k,\,k-1}_{\nu,\,p,\,p-1}\right)\Gamma^{q_i}_{\mu,\,k,\,k-1} \\
&\quad + \frac{p_i^*}{4\pi}\sum_{k=1}^{N}\sum_{\mu=1}^{n}\left(v^{(2)\,\mu,\,k,\,k-1}_{\nu,\,p,\,p-1} \pm \sigma v^{(2)\,\mu,\,k,\,k-1}_{\nu,\,p,\,p-1}\right) \\
&\qquad \times \dot{\Gamma}^{q_i}_{\mu,\,k,\,k-1} = v^{q_i}_{\nu,\,p,\,p-1} \\
&\sum_{k=1}^{N}\sum_{\mu=1}^{n}\left(v^{(2)\,\mu,\,k,\,k-1}_{\nu,\,p,\,p-1} \pm \sigma v^{(2)\,\mu,\,k,\,k-1}_{\nu,\,p,\,p-1}\right)\Gamma^{q_i}_{\mu,\,k,\,k-1} \\
&+ p_i^* \sum_{k=1}^{N}\sum_{\mu=1}^{n}\left(v^{(1)\,\mu,\,k,\,k-1}_{\nu,\,p,\,p-1} \pm \sigma v^{(1)\,\mu,\,k,\,k-1}_{\nu,\,p,\,p-1}\right)\dot{\Gamma}^{q_i}_{\mu,\,k,\,k-1} = 0 \\
&\qquad p = 0,\ 1,\ 2,\ \ldots,\ N;\ \nu = 0,\ 1,\ 2,\ \ldots,\ n-1; \\
&\qquad\qquad k = 1,\ 2,\ 3,\ \ldots,\ N
\end{aligned}\right\} \tag{9.8.34}$$

The quantity $v^{q_i}_{\nu,p,p-1}$ is determined in accordance with Eq. (9.8.32) as follows:

$$v^{\alpha}_{\nu,\,p,\,p-1} = -1;\quad v^{\omega_x}_{\nu,\,p,\,p-1} = -\zeta^{\nu,\,p}_{\nu,\,p-1};\quad v^{\omega_z}_{\nu,\,p,\,p-1} = -\xi_{\nu,\,p-1} \tag{9.8.35}$$

We find the dimensionless variables in (9.8.34) with a view to the relations

$$\left.\begin{aligned}
v^{(1)\,\mu,\,k,\,k-1}_{\nu,\,p,\,p-1} &= v^{(1)}\left(\xi^{\mu,\,k,\,k-1}_{\nu,\,p,\,p-1},\ \zeta^{\mu,\,k,\,k-1}_{\nu,\,p,\,p-1},\ \bar{l}_{k,\,k-1},\ \varkappa^{\mu,\,k}_{\mu,\,k-1}, p_i^*\right) \\
v^{(2)\,\mu,\,k,\,k-1}_{\nu,\,p,\,p-1} &= v^{(2)}\left(\xi^{\mu,\,k,\,k-1}_{\nu,\,p,\,p-1},\ \zeta^{\mu,\,k,\,k-1}_{\nu,\,p,\,p-1},\ \bar{l}_{k,\,k-1}, \varkappa^{\mu,\,k}_{\mu,\,k-1},\ p_i^*\right) \\
\sigma v^{(1)\,\mu,\,k,\,k-1}_{\nu,\,p,\,p-1} &= v^{(1)}\left(\xi^{\mu,\,k,\,k-1}_{\nu,\,p,\,p-1},\ \sigma\zeta^{\mu,\,k,\,k-1}_{\nu,\,p,\,p-1},\ \bar{l}_{k,\,k-1},\right. \\
&\qquad \left. -\varkappa^{\mu,\,k}_{\mu,\,k-1},\ p_i^*\right) \\
\sigma v^{(2)\,\mu,\,k,\,k-1}_{\nu,\,p,\,p-1} &= v^{(2)}\left(\xi^{\mu,\,k,\,k-1}_{\nu,\,p,\,p-1},\ \sigma\zeta^{\mu,\,k,\,k-1}_{\nu,\,p,\,p-1},\right. \\
&\qquad \left. \bar{l}_{k,\,k-1}, -\varkappa^{\mu,\,k}_{\mu,\,k-1},\ p_i^*\right)
\end{aligned}\right\} \tag{9.8.36}$$

The dimensionless geometric parameters in these relations are determined in the form

$$\left.\begin{gathered}\xi^{\mu,\,k,\,k-1}_{\nu,\,p,\,p-1}=\xi^{\nu,\,p}_{\nu,\,p-1}-\xi^{\mu,\,k}_{\mu,\,k-1},\quad \zeta^{\mu,\,k,\,k-1}_{\nu,\,p,\,p-1}=\zeta^{\nu,\,p}_{\nu,\,p-1}-\zeta^{\mu,\,k}_{\mu,\,k-1}\\ \bar{l}_{k,\,k-1}=l_{k,\,k-1}/b_0=\zeta_{\mu,\,k-1}-\zeta_{\mu,\,k};\\ \tan\varkappa^{\mu,\,k}_{\mu,\,k-1}=\frac{\xi_{\mu,\,k-1}-\xi_{\mu,\,k}}{\zeta_{\mu,\,k-1}-\zeta_{\mu,\,k}};\quad \sigma\zeta^{\mu,\,k,\,k-1}_{\nu,\,p,\,p-1}\\ =\zeta^{\nu,\,p}_{\nu,\,p-1}+\zeta^{\mu,\,k}_{\mu,\,k-1}\end{gathered}\right\}\quad(9.8.37)$$

Each of the three systems of equations obtained includes $(n-1)N$ linear algebraic equations, whereas the number of unknown derivatives $\Gamma^{q_i}_{\mu,k,k-1}$ and $\dot{\Gamma}^{q_i}_{\mu,k,k-1}$ is nN. To close the system and obtain as many equations as there are unknowns, we must satisfy the Chaplygin-Zhukovsky condition by which the strength of the nearest bound vortex to the trailing edge in each section k, $k-1$ must be zero. Hence, according to this condition, the derivatives can be taken equal to

$$\Gamma^{q_i}_{\mu,\,k,\,k-1}\big|_{\mu=\mu_*}=0,\quad \dot{\Gamma}^{q_i}_{\mu,\,k,\,k-1}\big|_{\mu=\mu_*}=0,\quad q_i=\alpha,\ \omega_x,\ \omega_z\qquad(9.8.38)$$

Proceeding from (9.8.34) and (9.8.38), we shall compile three systems of equations for determining the derivatives of dimensionless circulation, taking into account the specific values of q_i and $\dot{q}_i$.

The first system is used for calculating the derivatives $\Gamma^{\alpha}_{\mu,\,k,\,k-1}$, $\dot{\Gamma}^{\alpha}_{\mu,\,k,\,k-1}$:

$$\left.\begin{gathered}\frac{1}{4\pi}\sum_{k=1}^{N}\sum_{\mu=1}^{n}(v^{(1)\,\mu,\,k,\,k-1}_{\nu,\,p,\,p-1}+\sigma v^{(1)\,\mu,\,k,\,k-1}_{\nu,\,p,\,p-1})\,\Gamma^{\alpha}_{\mu,\,k,\,k-1}\\ -\frac{p^*}{4\pi}\sum_{k=1}^{N}\sum_{\mu=1}^{n}(v^{(2)\,\mu,\,k,\,k-1}_{\nu,\,p,\,p-1}+\sigma v^{(2)\,\mu,\,k,\,k-1}_{\nu,\,p,\,p-1})\,\dot{\Gamma}^{\alpha}_{\mu,\,k,\,k-1}=1\\ \sum_{k=1}^{N}\sum_{\mu=1}^{n}(v^{(2)\,\mu,\,k,\,k-1}_{\nu,\,p,\,p-1}+\sigma v^{(2)\,\mu,\,k,\,k-1}_{\nu,\,p,\,p-1})\,\Gamma^{\alpha}_{\mu,\,k,\,k-1}\\ +p^*\sum_{k=1}^{N}\sum_{\mu=1}^{n}(v^{(1)\,\mu,\,k,\,k-1}_{\nu,\,p,\,p-1}+\sigma v^{(1)\,\mu,\,k,\,k-1}_{\nu,\,p,\,p-1})\,\dot{\Gamma}^{\alpha}_{\mu,\,k,\,k-1}=0\\ \Gamma^{\alpha}_{\mu,\,k,\,k-1}\big|_{\mu=\mu_*}=0,\ \dot{\Gamma}^{\alpha}_{\mu,\,k,\,k-1}\big|_{\mu=\mu_*}=0\\ p=0,\ 1,\ 2,\ \ldots,\ N;\ \nu=0,\ 1,\ 2,\ \ldots,\ n-1;\\ k=1,\ 2,\ 3,\ \ldots,\ N\end{gathered}\right\}\quad(9.8.39)$$

We find the derivatives $\Gamma^{\omega_z}_{\mu,k,k-1}$ and $\dot{\Gamma}^{\omega_z}_{\mu,k,k-1}$ as a result of solving the second system:

$$\left.\begin{aligned}
&\frac{1}{4\pi}\sum_{k=1}^{N}\sum_{\mu=1}^{n}\left(v^{(1)\,\mu,\,k,\,k-1}_{\nu,\,p,\,p-1}+\sigma v^{(1)\,\mu,\,k,\,k-1}_{\nu,\,p,\,p-1}\right)\Gamma^{\omega_z}_{\mu,\,k,\,k-1}\\
&-\frac{p^*}{4\pi}\sum_{k=1}^{N}\sum_{\mu=1}^{n}\left(v^{(2)\,\mu,\,k,\,k-1}_{\nu,\,p,\,p-1}+\sigma v^{(2)\,\mu,\,k,\,k-1}_{\nu,\,p,\,p-1}\right)\dot{\Gamma}^{\omega_z}_{\mu,\,k,\,k-1}\\
&\qquad=-\xi^{\nu,\,p}_{\nu,\,p-1}\\
&\sum_{k=1}^{N}\sum_{\mu=1}^{n}\left(v^{(2)\,\mu,\,k,\,k-1}_{\nu,\,p,\,p-1}+\sigma v^{(2)\,\mu,\,k,\,k-1}_{\nu,\,p,\,p-1}\right)\Gamma^{\omega_z}_{\mu,\,k,\,k-1}\\
&+p^*\sum_{k=1}^{N}\sum_{\mu=1}^{n}\left(v^{(1)\,\mu,\,k,\,k-1}_{\nu,\,p,\,p-1}+\sigma v^{(1)\,\mu,\,k,\,k-1}_{\nu,\,p,\,p-1}\right)\dot{\Gamma}^{\omega_z}_{\mu,\,k,\,k-1}=0\\
&\Gamma^{\omega_z}_{\mu,\,k,\,k-1}\big|_{\mu=\mu^*}=0,\quad \dot{\Gamma}^{\omega_z}_{\mu,\,k,\,k-1}\big|_{\mu=\mu^*}=0\\
&p=0,\ 1,\ 2,\ \ldots,\ N;\quad \nu=0,\ 1,\ 2,\ \ldots,\ n-1;\\
&\qquad k=1,\ 2,\ 3,\ \ldots,\ N
\end{aligned}\right\}\qquad(9.8.40)$$

In Eqs. (9.8.39) and (9.8.40), we have chosen the plus sign in the parentheses because we are considering symmetric motions in which the distribution of the circulation over the span is also symmetric.

The third system of equations allows us to determine the derivatives $\Gamma^{\omega_x}_{\mu,k,\,k-1}$ and $\dot{\Gamma}^{\omega_x}_{\mu,k,k-1}$ characterizing the asymmetric nature of motion of a craft. Choosing the minus sign in (9.8.34), we can write this system as

$$\left.\begin{aligned}
&\frac{1}{4\pi}\sum_{k=1}^{N}\sum_{\mu=1}^{n}\left(v^{(1)\,\mu,\,k,\,k-1}_{\nu,\,p,\,p-1}-\sigma v^{(1)\,\mu,\,k,\,k-1}_{\nu,\,p,\,p-1}\right)\Gamma^{\omega_x}_{\mu,\,k,\,k-1}\\
&-\frac{p^*}{4\pi}\sum_{k=1}^{N}\sum_{\mu=1}^{n}\left(v^{(2)\,\mu,\,k,\,k-1}_{\nu,\,p,\,p-1}-\sigma v^{(2)\,\mu,\,k,\,k-1}_{\nu,\,p,\,p-1}\right)\dot{\Gamma}^{\omega_x}_{\mu,\,k,\,k-1}\\
&\qquad=-\zeta^{\nu,\,p}_{\nu,\,p-1}\\
&\sum_{k=1}^{N}\sum_{\mu=1}^{n}\left(v^{(2)\,\mu,\,k,\,k-1}_{\nu,\,p,\,p-1}-\sigma v^{(2)\,\mu,\,k,\,k-1}_{\nu,\,p,\,p-1}\right)\Gamma^{\omega_x}_{\mu,\,k,\,k-1}\\
&+p^*\sum_{k=1}^{N}\sum_{\mu=1}^{n}\left(v^{(1)\mu,\,k,\,k-1}_{\nu,\,p,\,p-1}-\sigma v^{(1)\,\mu,\,k,\,k-1}_{\nu,\,p,\,p-1}\right)\dot{\Gamma}^{\omega_x}_{\mu,\,k,\,k-1}=0\\
&\Gamma^{\omega_x}_{\mu,\,k,\,k-1}\big|_{\mu=\mu_*}=0,\quad \dot{\Gamma}^{\omega_x}_{\mu,\,k,\,k-1}\big|_{\mu=\mu_*}=0\\
&p=0,\ 1,\ 2,\ \ldots,\ N;\quad \nu=0,\ 1,\ 2,\ \ldots,\ n-1;\\
&\qquad k=1,\ 2,\ 3,\ \ldots,\ N
\end{aligned}\right\}\qquad(9.8.41)$$

We find the dimensionless geometric variables in Eqs. (9.8.39)-(9.8.41) from (9.8.37). The solution of these equations allows us to determine the derivatives of dimensionless circulation for an unsteady flow over a wing at arbitrary Strouhal numbers.

Let us consider the problem of motion *at low Strouhal numbers* ($p_i^* \to 0$), which is of major theoretical and practical significance. In accordance with (9.8.19) and (9.8.20), we have

$$v_{\nu,\,p,\,p-1}^{(1)\,\mu,\,k,\,k-1} = v_{\nu,\,p,\,p-1}^{\mu,\,k,\,k-1};\quad v_{\nu,\,p,\,p-1}^{(2)\,\mu,\,k,\,k-1} = p_i^* \partial v_{\nu,\,p,\,p-1}^{(2)\,\mu,\,k,\,k-1}/\partial p_i^* \qquad (9.8.42)$$

Introducing these expressions into (9.8.34), we obtain the following systems of equations:

$$\left.\begin{aligned} &\frac{1}{4\pi}\sum_{k=1}^{N}\sum_{\mu=1}^{n}\left(v_{\nu,\,p,\,p-1}^{\mu,\,k,\,k-1} \pm \sigma v_{\nu,\,p,\,p-1}^{\mu,\,k,\,k-1}\right)\Gamma_{\mu,\,k,\,k-1}^{q_i} = v_{\nu,\,p,\,p-1}^{q_i} \\ &\Gamma_{\mu,\,k,\,k-1}^{q_i}\big|_{\mu=\mu_*} = 0,\quad p = 1,\ 2,\ \ldots,\ N; \\ &\nu = 1,\ 2,\ \ldots,\ n-1 \quad k = 1,\ 2,\ \ldots,\ N \end{aligned}\right\} \qquad (9.8.43)$$

$$\left.\begin{aligned} &\sum_{k=1}^{N}\sum_{\mu=1}^{n}\left(v_{\nu,\,p,\,p-1}^{\mu,\,k,\,k-1} \pm \sigma v_{\nu,\,p,\,p-1}^{\mu,\,k,\,k-1}\right)\dot{\Gamma}_{\mu,\,k,\,k-1}^{q_i} \\ &\quad = -\sum_{k=1}^{N}\sum_{\mu=1}^{n}\left(\partial v_{\nu,\,p,\,p-1}^{(2)\,\mu,\,k,\,k-1}/\partial p_i^* \pm \sigma \partial v_{\nu,\,p,\,p-1}^{(2)\,\mu,\,k,\,k-1}/\partial p_i^*\right)\Gamma_{\mu,\,k,\,k-1}^{q_i} \\ &\dot{\Gamma}_{\mu,\,k,\,k-1}^{q_i}\big|_{\mu=\mu_*} = 0;\quad p = 1,\ 2,\ \ldots,\ N; \\ &\nu = 1,\ 2,\ \ldots,\ n-1 \quad k = 1,\ 2,\ \ldots,\ N \end{aligned}\right\} \qquad (9.8.44)$$

Consequently, the problem on the oscillations of a wing with low Strouhal numbers reduces to solving six (instead of three) systems of equations but simpler ones than for arbitrary values of p_i^*. The first system of equations (9.8.43) contains no derivatives $\dot{\Gamma}_{\mu,k,k-1}^{qi}$ and is solved independently of system (9.8.44) for the derivative $\Gamma_{\mu,k,k-1}^{qi}$. Its value is used to calculate the right-hand side of the equations of the second system (9.8.44), the solution yielding the derivative $\dot{\Gamma}_{\mu,k,k-1}^{qi}$.

The dimensionless coefficients of equation (9.8.43) and (9.8.44) are determined from the relations

$$\left.\begin{aligned} &v_{\nu,\,p,\,p-1}^{\mu,\,k,\,k-1} = v\left(\xi_{\nu,\,p,\,p-1}^{\mu,\,k,\,k-1},\ \eta_{\nu,\,p,\,p-1}^{\mu,\,k,\,k-1},\ \bar{l}_{k,\,k-1},\ \varkappa_{\mu,\,k-1}^{\mu,\,k}\right) \\ &\sigma v_{\nu,\,p,\,p-1}^{\mu,\,k,\,k-1} = v\left(\xi_{\nu,\,p,\,p-1}^{\mu,\,k,\,k-1},\ \sigma\zeta_{\nu,\,p,\,p-1}^{\mu,\,k,\,k-1},\ \bar{l}_{k,\,k-1},\ -\varkappa_{\mu,\,k-1}^{\mu,\,k}\right) \\ &\frac{\partial v_{\nu,\,p,\,p-1}^{(2)\,\mu,\,k,\,k-1}}{\partial p_i^*} = \frac{\partial v^{(2)}}{\partial p_i^*} \end{aligned}\right\} \qquad (9.8.45)$$

$$\times \left(\xi_{\nu,\ p,\ p-1}^{\mu,\ k,\ k-1},\ \zeta_{\nu,\ p,\ p-1}^{\mu,\ k,\ k-1}\cdot \bar{l}_{k,\ k-1},\ \varkappa_{\mu,\ k-1}^{\mu,\ k}\right)$$

$$\sigma \frac{\partial v_{\nu,\ p,\ p-1}^{(2)\mu,\ k,\ k-1}}{\partial p_i^*} = \frac{\partial v^{(2)}}{\partial p_i^*}$$

$$\times \left(\xi_{\nu,\ p,\ p-1}^{\mu,\ k,\ k-1},\ \sigma\zeta_{\nu,\ p,\ p-1}^{\mu,\ k,\ k-1},\ \bar{l}_{k,\ k-1},\ -\varkappa_{\mu,\ k-1}^{\mu,\ k}\right)$$

Let us write Eqs. (9.8.43) and (9.8.44) with account taken of the specific values of q_i and $\dot{q}_i$, and also of the nature of motion, i.e. symmetric or asymmetric.

The system of equations for determining the derivatives $\Gamma_{\mu,k,k-1}^{\alpha}$ has the following form:

$$\left.\begin{aligned} &\frac{1}{4\pi}\sum_{k=1}^{N}\sum_{\mu=1}^{n}\left(v_{\nu,\ p,\ p-1}^{\mu,\ k,\ k-1}+\sigma v_{\nu,\ p,\ p-1}^{\mu,\ k,\ k-1}\right)\Gamma_{\mu,\ k,\ k-1}^{\alpha}=-1\\ &\Gamma_{\mu,\ k,\ k-1}^{\alpha}\big|_{\mu=\mu_*}=0;\quad p=1,\ 2,\ \ldots,\ N;\ \nu=1,\ 2,\ \ldots,\ n-1;\\ &\qquad k=1,\ 2,\ \ldots,\ N \end{aligned}\right\} \tag{9.8.46}$$

We find the derivative $\dot{\Gamma}_{\mu,k,k-1}^{\alpha}$ by solving a second system of equations:

$$\left.\begin{aligned} &\sum_{k=1}^{N}\sum_{\mu=1}^{n}\left(v_{\nu,\ p,\ p-1}^{\mu,\ k,\ k-1}+\sigma v_{\nu,\ p,\ p-1}^{\mu,\ k,\ k-1}\right)\dot{\Gamma}_{\mu,\ k,\ k-1}^{\alpha}\\ &=-\sum_{k=1}^{N}\sum_{\mu=1}^{n}\left(\frac{\partial v_{\nu,\ p,\ p-1}^{(2)\mu,\ k,\ k-1}}{\partial p_i^*}+\sigma\frac{\partial v_{\nu,\ p,\ p-1}^{(2)\mu,\ k,\ k-1}}{\partial p_i^*}\right)\\ &\qquad\times\Gamma_{\mu,\ k,\ k-1}^{\alpha}\\ &\dot{\Gamma}_{\mu,\ k,\ k-1}^{\alpha}\big|_{\mu=\mu_*}=0;\quad p=1,\ 2,\ \ldots,\ N;\\ &\nu=1,\ 2,\ \ldots,\ n-1;\quad k=1,\ 2,\ \ldots,\ N \end{aligned}\right\} \tag{9.8.47}$$

We use a third system to find the derivative $\Gamma_{\mu,k,k-1}^{\omega z}$:

$$\left.\begin{aligned} &\frac{1}{4\pi}\sum_{k=1}^{N}\sum_{\mu=1}^{n}\left(v_{\nu,\ p,\ p-1}^{\mu,\ k,\ k-1}+\sigma v_{\nu,\ p,\ p-1}^{\mu,\ k,\ k-1}\right)\Gamma_{\mu,\ k,\ k-1}^{\omega z}=-\xi_{\nu,\ p-1}^{\nu,\ p}\\ &\Gamma_{\mu,\ k,\ k-1}^{\omega z}\big|_{\mu=\mu_*}=0;\\ &p=1,\ 2,\ \ldots,\ N;\ \nu=1,\ 2,\ \ldots,\ n-1;\ k=1,\ 2,\ \ldots,\ N \end{aligned}\right\} \tag{9.8.48}$$

A fourth system of equations is intended for calculating $\dot{\Gamma}^{\dot{\omega}_z}_{\mu, k, k-1}$:

$$\left.\begin{aligned}
&\sum_{k=1}^{N}\sum_{\mu-1}^{n}(v^{\mu,\,k,\,k-1}_{\nu,\,p,\,p-1}+\sigma v^{\mu,\,k,\,k-1}_{\nu,\,p,\,p-1})\,\dot{\Gamma}^{\dot{\omega}_z}_{\mu,\,k,\,k-1}\\
&=-\sum_{k=1}^{N}\sum_{\mu=1}^{n}\left(\frac{\partial v^{(2)\mu,\,k,\,k-1}_{\nu,\,p,\,p-1}}{\partial p_i^*}+\sigma\frac{\partial v^{(2)\mu,\,k,\,k-1}_{\nu,\,p,\,p-1}}{\partial p_i^*}\right)\Gamma^{\omega_z}_{\mu,\,k,\,k-1}\\
&\dot{\Gamma}^{\dot{\omega}_z}_{\mu,\,k,\,k-1}\Big|_{\mu=\mu_*}=0;\quad p=1,\,2,\,\ldots,\,N;\quad \nu=1,\,2,\,\ldots,\,n-1;\\
&\qquad\qquad k=1,\,2,\,\ldots,\,N
\end{aligned}\right\}\qquad(9.8.49)$$

We compile a fifth system for determining the derivatives $\Gamma^{\omega_z}_{\mu,\,k,\,k-1}$:

$$\left.\begin{aligned}
&\frac{1}{4\pi}\sum_{k=1}^{N}\sum_{\mu=1}^{n}(v^{\mu,\,k,\,k-1}_{\nu,\,p,\,p-1}-\sigma v^{\mu,\,k,\,k-1}_{\nu,\,p,\,p-1})\,\Gamma^{\omega_z}_{\mu,\,k,\,k-1}=-\zeta^{\nu,\,p}_{\nu,\,p-1}\\
&\Gamma^{\omega_z}_{\mu,\,k,\,k-1}\Big|_{\mu=\mu_*}=0;\quad p=1,\;2,\;\ldots,\,N;\quad \nu=1,\,2,\,\ldots,\,n-1;\\
&\qquad\qquad k=1,\;2,\;\ldots,\,N
\end{aligned}\right\}\qquad(9.8.50)$$

A sixth system of equations, given below, allows us to find $\dot{\Gamma}^{\dot{\omega}_z}_{\mu,\,k,\,k-1}$:

$$\left.\begin{aligned}
&\sum_{k=1}^{N}\sum_{\mu=1}^{n}(v^{\mu,\,k,\,k-1}_{\nu,\,p,\,p-1}-\sigma v^{\mu,\,k,\,k-1}_{\nu,\,p,\,p-1})\,\dot{\Gamma}^{\dot{\omega}_x}_{\mu,\,k,\,k-1}\\
&=-\sum_{k=1}^{N}\sum_{\mu=1}^{n}\left(\frac{\partial v^{(2)\mu,\,k,\,k-1}_{\nu,\,p,\,p-1}}{\partial p_i^*}-\sigma\frac{\partial v^{(2)\mu,\,k,\,k-1}_{\nu,\,p,\,p-1}}{\partial p_i^*}\right)\Gamma^{\omega_x}_{\mu,\,k,\,k-1}\\
&\dot{\Gamma}^{\dot{\omega}_z}_{\mu,\,k,\,k-1}\Big|_{\mu=\mu_*}=0;\quad p=1,\;2,\;\ldots,\,N;\quad \nu=1,\,2,\,\ldots,\,n-1;\\
&\qquad\qquad k=1,\;2,\;\ldots,\,N
\end{aligned}\right\}\qquad(9.8.51)$$

Aerodynamic Characteristics

The values of the circulation derivatives $\Gamma^{qi}_{\mu,k,k-1}$ and $\dot{\Gamma}^{\dot{q}i}_{\mu,k,k-1}$ can be used to calculate the distribution of the pressure coefficients, and according to them, the wing stability derivatives.

Here we calculate the difference of the pressure coefficients for the bottom and upper sides in the form of the series (9.6.22):

$$\Delta\bar{p}=p^{\alpha}\alpha+p^{\dot{\alpha}}\dot{\alpha}+p^{\omega_x}\omega_x+p^{\dot{\omega}_x}\dot{\omega}_x+p^{\omega_z}\omega_z+p^{\dot{\omega}_z}\dot{\omega}_z\qquad(9.8.52)$$

In accordance with Zhukovsky's formula (9.7.15), we have

$$p^{\alpha} = 2\gamma, \quad p^{\dot{\alpha}} = 2\gamma^{\dot{\alpha}}; \quad p^{\omega x} = 2\gamma^{\omega_x}, \quad p^{\dot{\omega}x} = 2\gamma^{\dot{\omega}_x}; \quad p^{\omega_z} = 2\gamma^{\omega_z}, \quad p^{\dot{\omega}_z} = 2\gamma^{\dot{\omega}_z} \tag{9.8.53}$$

Let us consider a cell containing a point with the coordinates $\xi^{\mu,k}_{\mu,k-1}$, $\zeta^{\mu,k}_{\mu,k-1}$ for which we shall calculate the pressure. We determine the strength of a bound vortex at this point by the appropriate value of the circulation related to the interval between the control points $\Delta\xi_{\mu,k,k-1} = \xi^{\nu,p}_{\nu,p-1} - \xi^{\nu-1,p}_{\nu-1,p-1}$ in the section $\zeta^{\mu,k}_{\mu,k-1}$:

$$\gamma(\xi^{\mu,k}_{\mu,k-1}, \zeta^{\mu,k}_{\mu,k-1}) = \Gamma(\xi^{\mu,k}_{\mu,k-1}, \zeta^{\mu,k}_{\mu,k-1})/\Delta\xi_{\mu,k,k-1} \tag{9.8.54}$$

Let us write the strength of the vortex layer and the circulation of a discrete vortex in the form of the series (9.7.12) and (9.8.25):

$$\left.\begin{aligned} \gamma(\xi^{\mu,k}_{\mu,k-1}, \zeta^{\mu,k}_{\mu,k-1}) &= \sum_{i=1}^{3} (\gamma^{q_i}_{\mu,k,k-1} q_i + \gamma^{\dot{q}_i}_{\mu,k,k-1} \dot{q}_i) \\ \Gamma(\xi^{\mu,k}_{\mu,k-1}, \zeta^{\mu,k}_{\mu,k-1}) &= \sum_{i=1}^{3} (\Gamma^{q_i}_{\mu,k,k-1} q_i + \Gamma^{\dot{q}_i}_{\mu,k,k-1} \dot{q}_i) \end{aligned}\right\} \tag{9.8.55}$$

Introducing these expressions into (9.8.54), we obtain relations for the derivatives

$$\gamma^{q_i}_{\mu,k,k-1} = \Gamma^{q_i}_{\mu,k,k-1}/\Delta\xi_{\mu,k,k-1}, \quad \gamma^{\dot{q}_i}_{\mu,k,k-1} = \Gamma^{\dot{q}_i}_{\mu,k,k-1}/\Delta\xi_{\mu,k,k-1} \tag{9.8.56}$$

With account taken of these derivatives, the expressions for the strength of the vortices are determined by the quantities $p^{q_i}_{\mu,k,k-1}$ and $p^{\dot{q}_i}_{\mu,k,k-1}$ (9.8.53). Let us introduce them into formulas (9.6.5) in which Δp is replaced with series (9.8.52), the value of x_k is taken equal to b_0 and x' to the local chord $b_{k,k-1}$:

$$\left.\begin{aligned} c'_y &= \frac{b_0}{b_{k,k-1}} \int_{\xi_0}^{\xi_1} \sum_{i=1}^{3} (p^{q_i} q_i + p^{\dot{q}_i} \dot{q}_i)\, d\xi \\ m'_z &= \frac{b_0^2}{b_{k,k-1}^2} \int_{\xi_0}^{\xi_1} \sum_{i=1}^{3} (p^{q_i} q_i + p^{\dot{q}_i} \dot{q}_i)\, \xi\, d\xi; \\ m'_x &= -\frac{b_0}{b_{k,k-1}} c'_y \zeta \end{aligned}\right\} \tag{9.8.57}$$

Let us replace the coefficients on the left-hand side of (3.8.57) with their expressions in the form of series similar to (9.6.8):

$$\left.\begin{aligned} c_y' &= \sum_{i=1}^{3} (c_y'^{q_i} q_i + c_y'^{\dot{q}_i} \dot{q}_i) \\ m_z' &= \sum_{i=1}^{3} (m_z'^{q_i} q_i + m_z'^{\dot{q}_i} \dot{q}_i) \\ m_x' &= \sum_{i=1}^{3} (m_x'^{q_i} q_i + m_x'^{\dot{q}_i} \dot{q}_i) \end{aligned}\right\} \qquad (9.8.58)$$

As an example, let us write the right-hand side of (9.8.58) for the normal force coefficient in the expanded form:

$$c_y' = c_y'^{\alpha}\alpha + c_y'^{\dot{\alpha}}\dot{\alpha} + c_y'^{\omega_x}\omega_x + c_y'^{\dot{\omega}_x}\dot{\omega}_x + c_y'^{\omega_z}\omega_z + c_y'^{\dot{\omega}_z}\dot{\omega}_z \qquad (9.8.59)$$

Two other coefficients, m_z' and m_x', are expressed similarly. As a result of the indicated replacement of the coefficients c_y', m_z', and m_x' in (9.8.57) with series and of a transition from integrals to sums, we obtain the derivatives of the aerodynamic coefficients of the sections in the following form:

$$\left.\begin{aligned} c_{y,\,k,\,k-1}'^{q_i} &= \frac{2b_0}{b_{k,\,k-1}} \sum_{\mu=\mu_0}^{\mu=\mu_*} \Gamma_{\mu,\,k,\,k-1}^{q_i} \\ c_{y,\,k,\,k-1}'^{\dot{q}_i} &= \frac{2b_0}{b_{k,\,k-1}} \sum_{\mu=\mu_0}^{\mu=\mu_*} \Gamma_{\mu,\,k,\,k-1}^{\dot{q}_i} \end{aligned}\right\} \qquad (9.8.60)$$

$$\left.\begin{aligned} m_{z,\,k,\,k-1}'^{q_i} &= \frac{2b_0^2}{b_{k,\,k-1}^2} \sum_{\mu=\mu_0}^{\mu=\mu_*} \Gamma_{\mu,\,k,\,k-1}^{q_i} \xi_{\mu,\,k-1}^{\mu,\,k} \\ m_{z,\,k,\,k-1}'^{\dot{q}_i} &= \frac{2b_0^2}{b_{k,\,k-1}^2} \sum_{\mu=\mu_0}^{\mu=\mu_*} \Gamma_{\mu,\,k,\,k-1}^{\dot{q}_i} \xi_{\mu,\,k-1}^{\mu,\,k} \end{aligned}\right\} \qquad (9.8.61)$$

$$\left.\begin{aligned} m_{x,\,k,\,k-1}'^{q_i} &= -c_{y,\,k,\,k-1}'^{q_i} \zeta_{\mu,\,k-1}^{\mu,\,k} \frac{b_0}{b_{k,\,k-1}} \\ m_{x,\,k,\,k-1}'^{\dot{q}_i} &= -c_{y,\,k,\,k-1}'^{\dot{q}_i} \zeta_{\mu,\,k-1}^{\mu,\,k} \frac{b_0}{b_{k,\,k-1}} \end{aligned}\right\} \qquad (9.8.62)$$

We obtain the stability derivatives for a wing as a whole by using the following relations for the total aerodynamic characteris-

tics of a wing:

$$\left.\begin{aligned} c_y &= \frac{2b_0}{S_w}\int_0^{l_0/(2b_0)} c_y' b(\zeta)\, d\zeta \\ m_z &= \frac{2}{S_w}\int_0^{l_0/(2b_0)} m_z' b^2(\zeta)\, d\zeta \\ m_x &= \frac{-2b_0}{S_w}\int_0^{l_0/(2b_0)} c_y' b(\zeta)\, d\zeta \end{aligned}\right\} \tag{9.8.63}$$

We can express the coefficients c_y, m_z, and m_x for a wing in the form of series (9.6.8), and their corresponding values c_y', m_z', and m_x' for the sections in the form of (9.8.58). After using the derivatives (9.8.60)-(9.8.62), we obtain the stability derivatives for a wing as a whole ($c_y^{q_l}$, $\dot{c}_y^{q_l}$, $m_z^{q_l}$, $\dot{m}_z^{q_l}$, $m_x^{q_l}$, and $\dot{m}_x^{q_l}$).

Going over from integrals to sums, we obtain for symmetric motions ($q_l = \alpha,\ \omega_z$):

$$m_x^{q_l} = \dot{m}_x^{q_l} = 0 \tag{9.8.64}$$

$$\left.\begin{aligned} c_y^{q_l} &= \frac{4b_0^2}{S_w}\sum_{k=1}^{N} \bar{l}_{k,\,k-1} \sum_{\mu=\mu_0}^{\mu=\mu_*} \Gamma_{\mu,\,k,\,k-1}^{q_l} \\ \dot{c}_y^{q_l} &= \frac{4b_0^2}{S_w}\sum_{k=1}^{N} \bar{l}_{k,\,k-1} \sum_{\mu=\mu_0}^{\mu=\mu_*} \dot{\Gamma}_{\mu,\,k,\,k-1}^{q_l} \end{aligned}\right\} \tag{9.8.65}$$

$$\left.\begin{aligned} m_z^{q_l} &= \frac{4b_0^2}{S_w}\sum_{k=1}^{N} \bar{l}_{k,\,k-1} \sum_{\mu=\mu_0}^{\mu=\mu_*} \Gamma_{\mu,\,k,\,k-1}^{q_l} \xi_{\mu,\,k-1}^{\mu,\,k} \\ \dot{m}_z^{q_l} &= \frac{4b_0^2}{S_w}\sum_{k=1}^{N} \bar{l}_{k,\,k-1} \sum_{\mu=\mu_0}^{\mu=\mu_*} \dot{\Gamma}_{\mu,\,k,\,k-1}^{q_l} \xi_{\mu,\,k-1}^{\mu,\,k} \end{aligned}\right\} \tag{9.8.66}$$

For asymmetric motions ($q_l = \omega_x$):

$$c_y^{q_l} = \dot{c}_y^{q_l} = 0 \tag{9.8.67}$$

$$m_z^{q_l} = \dot{m}_z^{q_l} = 0 \tag{9.8.68}$$

$$\left.\begin{aligned} m_x^{q_l} &= \frac{4b_0^2}{S_w}\sum_{k=1}^{N} \bar{l}_{k,\,k-1} \sum_{\mu=\mu_0}^{\mu=\mu_*} \Gamma_{\mu,\,k,\,k-1}^{q_l} \zeta_{\mu,\,k-1}^{\mu,\,k} \\ \dot{m}_x^{q_l} &= \frac{4b_0^2}{S_w}\sum_{k=1}^{N} \bar{l}_{k,\,k-1} \sum_{\mu=\mu_0}^{\mu=\mu_*} \dot{\Gamma}_{\mu,\,k,\,k-1}^{q_l} \zeta_{\mu,\,k-1}^{\mu,\,k} \end{aligned}\right\} \tag{9.8.69}$$

Let us write these expressions in the expanded form with account taken of the corresponding values of q_i and $\dot{q}_i$, and also of the numbers of the bound vortices $\mu_0 = 1$ and $\mu_* = n$ closest to the leading and trailing edges.

For symmetric motions ($q_i = \alpha,\ \omega_z$):

$$m_x^{\alpha} = m_x^{\dot{\alpha}} = m_x^{\omega_z} = m_x^{\dot{\omega}_z} = 0 \tag{9.8.70}$$

$$\left.\begin{aligned} c_y^{\alpha} &= \frac{4b_0^2}{S_w} \sum_{k=1}^{N} \bar{l}_{k,\,k-1} \sum_{\mu=1}^{n} \Gamma_{\mu,\,k,\,k-1}^{\alpha} \\ c_y^{\dot{\alpha}} &= \frac{4b_0^2}{S_w} \sum_{k=1}^{N} \bar{l}_{k,\,k-1} \sum_{\mu=1}^{n} \Gamma_{\mu,\,k,\,k-1}^{\dot{\alpha}} \end{aligned}\right\} \tag{9.8.71}$$

$$\left.\begin{aligned} c_y^{\omega_z} &= \frac{4b_0^2}{S_w} \sum_{k=1}^{N} \bar{l}_{k,\,k-1} \sum_{\mu=1}^{n} \Gamma_{\mu,\,k,\,k-1}^{\omega_z} \\ c_y^{\dot{\omega}_z} &= \frac{4b_0^2}{S_w} \sum_{k=1}^{N} \bar{l}_{k,\,k-1} \sum_{\mu-1}^{n} \Gamma_{\mu,\,k,\,k-1}^{\dot{\omega}_z} \end{aligned}\right\} \tag{9.8.72}$$

$$\left.\begin{aligned} m_z^{\alpha} &= \frac{4b_0^2}{S_w} \sum_{k=1}^{N} \bar{l}_{k,\,k-1} \sum_{\mu=1}^{n} \Gamma_{\mu,\,k,\,k-1}^{\alpha} \bar{\xi}_{\mu,\,k,\,k-1}^{\mu,\,k} \\ m_z^{\dot{\alpha}} &= \frac{4b_0^2}{S_w} \sum_{k=1}^{N} \bar{l}_{k,\,k-1} \sum_{\mu=1}^{n} \Gamma_{\mu,\,k,\,k-1}^{\dot{\alpha}} \bar{\xi}_{\mu,\,k,\,k-1}^{\mu,\,k} \end{aligned}\right\} \tag{9.8.73}$$

$$\left.\begin{aligned} m_z^{\omega_z} &= \frac{4b_0^2}{S_w} \sum_{k=1}^{N} \bar{l}_{k,\,k-1} \sum_{\mu=1}^{n} \Gamma_{\mu,\,k,\,k-1}^{\omega_z} \bar{\xi}_{\mu,\,k-1}^{\mu,\,k} \\ m_z^{\dot{\omega}_z} &= \frac{4b_0^2}{S_w} \sum_{k=1}^{N} \bar{l}_{k,\,k-1} \sum_{\mu=1}^{n} \Gamma_{\mu,\,k,\,k-1}^{\dot{\omega}_z} \bar{\xi}_{\mu,\,k,\,k-1}^{\mu,\,k} \end{aligned}\right\} \tag{9.8.74}$$

For asymmetric motions ($q_i = \omega_x$)

$$c_y^{\omega_x} = c_y^{\dot{\omega}_x} = m_z^{\omega_x} = m_z^{\dot{\omega}_x} = 0 \tag{9.8.75}$$

$$\left.\begin{aligned} m_x^{\omega_x} &= \frac{4b_0^2}{S_w} \sum_{k=1}^{N} \bar{l}_{k,\,k-1} \sum_{\mu=1}^{n} \Gamma_{\mu,\,k,\,k-1}^{\omega_x} \bar{\zeta}_{\mu,\,k-1}^{\mu,\,k} \\ m_x^{\dot{\omega}_x} &= \frac{4b_0^2}{S_w} \sum_{k=1}^{N} \bar{l}_{k,\,k-1} \sum_{\mu=1}^{n} \Gamma_{\mu,\,k,\,k-1}^{\dot{\omega}_x} \bar{\zeta}_{\mu,\,k-1}^{\mu,\,k} \end{aligned}\right\} \tag{9.8.76}$$

The total values of the aerodynamic coefficients can be determined according to the found stability derivatives, using (9.6.8).

Deformation of a Wing Surface

The above numerical method of aerodynamic calculations related to a wing with an undeformed (rigid) surface. In real conditions, however, such a surface may deform because of bending or deflection of the control surfaces. The flow over a wing with account taken of its deformation is considered in [4, 19].

The magnitude of the deformation can be expressed in the form

$$\eta(\xi, \zeta, \tau) = f_\delta(\xi, \zeta)\,\delta(\tau) \tag{9.8.77}$$

where $f_\delta(\xi, \zeta)$ is a time-independent function determining the changing form of the surface, and $\delta(\tau)$ is a time-dependent kinematic variable characterizing the scale of the deformation.

In addition to q_i ($q_1 = \alpha$, $q_2 = \omega_x$, $q_3 = \omega_z$), we can also adopt the dimensionless time function $q_4 = \delta(\tau)$ as a variable determining the unsteady flow of a deformable wing.

The right-hand side of expression (9.8.26) determining the circulation will additionally include the sum $\Gamma^{\delta}_{\mu,k,k-1}\delta + \Gamma^{\dot{\delta}}_{\mu,k,k-1}\dot{\bar{\delta}}$ [where the derivative $\dot{\bar{\delta}} = (d\delta/dt)\,b_0/V_\infty$]. This will lead to a corresponding change in the aerodynamic coefficients, the general expression for which can be written in the form of a series

$$c = c^{\alpha}\alpha + c^{\dot{\alpha}}\dot{\bar{\alpha}} + c^{\omega_x}\omega_x + c^{\dot{\omega}_x}\dot{\omega}_x + c^{\omega_z}\omega_z + c^{\dot{\omega}_z}\dot{\omega}_z + c^{\delta}\delta + c^{\dot{\delta}}\dot{\bar{\delta}}; \quad c = \Delta\bar{p},\ c_y,\ m_x,\ m_z \tag{9.8.78}$$

The deformation of a wing changes the boundary condition of flow which instead of (9.6.32′) acquires the form

$$\frac{\partial\bar{\varphi}}{\partial\eta} = -\alpha(\tau) - \omega_x(\tau)\,\zeta - \omega_z(\tau)\,\xi + \frac{\partial f_\delta}{\partial\xi}\,\delta(\tau) + f_\delta(\xi, \zeta)\,\dot{\bar{\delta}}(\tau) \tag{9.8.79}$$

where $(\partial f_\delta/\partial\xi)\,\delta(\tau) + f_\delta(\xi, \zeta)\,\dot{\bar{\delta}}(\tau) = v/V_\infty$ is the dimensionless vertical component of the velocity of an undisturbed flow due to deformation of the wing and damped in unsteady flow by the disturbed stream.

With a view to (9.8.79), we shall write a system of algebraic equations for determining the circulation derivatives $\Gamma^{q_i}_{\mu,k,k-1}$ and $\dot{\Gamma}^{q_i}_{\mu,k,k-1}$ which are then used to find the derivatives of the aerodynamic coefficients, and their local and total values with a view to the deformation of the aircraft. The results of solving this problem are given in detail in [4, 19].

Influence of Compressibility (the Number M_∞) on Non-Stationary Flow

In definite conditions, the evaluation of the influence of compressibility on non-stationary linearized flow can be considered by solving the problem of incompressible flow over a fictitious lifting surface. The solution of such a problem allows us to find expressions relating the corresponding aerodynamic characteristics of a wing in an incompressible and compressible flows and take into account the influence of the number M_∞. To consider these conditions, let us use differential equation (9.6.31) for the additional velocity potential $\bar{\varphi}$ of the disturbed non-stationary flow of a compressible fluid [the symbol $\bar{\varphi}$ is given in (9.6.19), where it is assumed that $x_k = b_0$].

We determine the dimensionless coordinates in (9.6.31) in the form $\xi = x/b_0$, $\eta = y/b_0$, and $\zeta = z/b_0$.

Let us express the dimensionless velocity potential $\bar{\varphi}$ equal to $\varphi/(bV_\infty)$ in terms of its derivatives $\varphi^{q_i} = \partial\varphi/\partial q_i$ and $\varphi^{\dot{q}_i} = \partial\varphi/\partial\dot{q}_i$ in the following form (see [4, 19]):

$$\bar{\varphi} = \varphi_0 + \sum_{i=1}^{3} [\varphi^{q_i} q_i(\tau) + \varphi^{\dot{q}_i} \dot{q}_i(\tau)] \tag{9.8.80}$$

where φ_0 is the velocity potential of stationary flow over a wing with a finite airfoil thickness at a zero angle of attack.

Let us introduce the functions ψ, ψ^{q_i}, and $\psi^{\dot{q}_i}$ related to the velocity potential and its derivatives by the following expressions:

$$\left.\begin{aligned} \varphi^{q_i} &= \psi^{q_i}\cos\omega\xi + p_i^* k^{-2}\psi^{\dot{q}_i}\sin\omega\xi \\ \varphi^{\dot{q}_i} &= k^{-2}\psi^{q_i}\cos\omega\xi - p_i^{*-1}\psi^{q_i}\sin\omega\xi \\ \varphi_0 &= \psi_0, \quad \omega = M_\infty^2 k^{-2} p_i^* \end{aligned}\right\} \tag{9.8.81}$$

where $k = \sqrt{1 - M_\infty^2}$.

After the corresponding substitution for the derivatives in (9.8.80) of their values from (9.8.81) and then introducing $\bar{\varphi}$ into (9.6.31), we obtain the following three equations:

$$k^2 \frac{\partial^2\psi_0}{\partial\xi^2} + \frac{\partial^2\psi_0}{\partial\eta^2} + \frac{\partial^2\psi_0}{\partial\zeta^2} = 0 \tag{9.8.82}$$

$$\left.\begin{aligned} k^2 \frac{\partial^2\psi^{q_i}}{\partial\xi^2} + \frac{\partial^2\psi^{q_i}}{\partial\eta_2} + \frac{\partial^2\psi^{q_i}}{\partial\zeta^2} + (p_i^*)^2 M_\infty^2 k^{-2}\psi^{q_i} = 0 \\ k^2 \frac{\partial^2\psi^{\dot{q}_i}}{\partial\xi^2} + \frac{\partial^2\psi^{\dot{q}_i}}{\partial\eta^2} + \frac{\partial^2\psi^{\dot{q}_i}}{\partial\zeta^2} + (p_i^*)^2 M_\infty^2 k^{-2}\psi^{\dot{q}_i} = 0 \end{aligned}\right\} \tag{9.8.83}$$

Considering one of the basic cases of flow that is characterized by low Strouhal numbers ($p_i^* \to 0$), instead of Eq. (9.8.83) we obtain

$$\left.\begin{aligned} k^2 \frac{\partial^2 \psi^{q_i}}{\partial \xi^2} + \frac{\partial^2 \psi^{q_i}}{\partial \eta^2} + \frac{\partial^2 \psi^{q_i}}{\partial \zeta^2} = 0 \\ \cdot \qquad \cdot \qquad \cdot \\ k^2 \frac{\partial^2 \psi^{q_i}}{\partial \xi^2} + \frac{\partial^2 \psi^{q_i}}{\partial \eta^2} + \frac{\partial^2 \psi^{q_i}}{\partial \zeta^2} = 0 \end{aligned}\right\} \tag{9.8.84}$$

Let us consider a rigid lifting surface. Instead of the flow of a compressible fluid over it, we shall study the flow of an incompressible fluid over the transformed surface. The coordinates of points in the incompressible flow are related to the coordinates of the space of the compressible gas by the expressions

$$x_{1c} = x/k, \quad y_{1c} = y, \quad z_{1c} = z \tag{9.8.85}$$

or in the dimensionless form

$$\begin{aligned} \xi_{1c} = x_{1c}/b_{0,1c} = \xi, \quad \eta_{1c} = y_{1c}/b_{0,1c} = \eta k, \\ \zeta_{1c} = z_{1c}/b_{0,1c} = \zeta k \end{aligned} \tag{9.8.86}$$

Let us change the planform of the given lifting surface, using the relations between the coordinates in the form of (9.8.86). In accordance with these relations, the dimensionless geometric variables of the transformed surface can be written as follows:

$$\zeta_{0,1c} = \zeta_0 k, \quad \xi_{0,1c,} = \xi_0 \quad \bar{b}_{1c}(\zeta_{1c}) = \bar{b}(\zeta) \tag{9.8.87}$$

where ξ_0 and ζ_0 are the dimensionless coordinates of the leading edge;

$$\bar{b}_{1c} = b_{1c}/b_{0,1c}, \quad \bar{b} = b/b_0, \quad b_{1c} = b/k$$

For the centre and running chords in (9.8.87), we have introduced the symbols b_0 and b, respectively.

For wings with straight edges, the planform is usually set by dimensionless parameters, namely, the aspect ratio $\lambda_w = l_0/b_m$, the taper ratio $\eta_w = b_0/b_t$, and the sweep angle of the leading edge χ_0. The corresponding dimensionless geometric variables of the transformed wing in an incompressible flow are:

$$\lambda_{1c,w} = k\lambda_w, \quad \eta_{1c,w} = \eta_w, \quad \lambda_{1c,w} \tan \chi_{0,1c} = \lambda_w \tan \chi_0 \tag{9.8.88}$$

where $\lambda_{1c,w} = l_{1c}/b_{m,1c}$, $\lambda_w = l/b_m$, $\eta_{1c,w} = b_{0,1c}/b_{t,1c}$, and $\eta_w = b_0/b_t$.

Figure 9.8.4 shows the given and transformed wing planes. The transformed plane retains its lateral dimensions and is extended in a longitudinal direction in accordance with the relation $x_{1c} = x/\sqrt{1 - M_\infty^2}$.

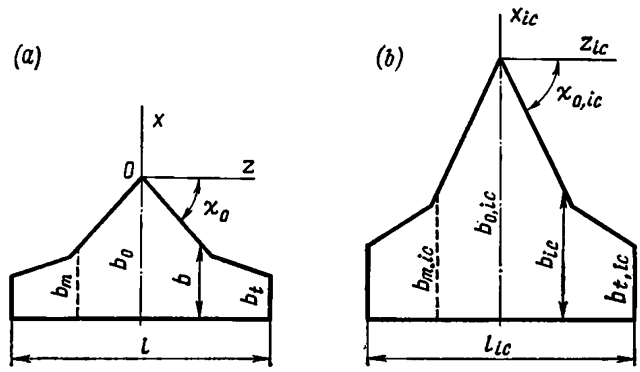

Fig. 9.8.4
Geometric dimensions of a wing:
a—given wing in a compressible flow; *b*—transformed wing in an incompressible flow

Let us go over in Eqs. (9.8.82) and the first equation (9.8.84) to the new variables ξ_{1c}, η_{1c}, and ζ_{1c} related to ξ, η, and ζ by expressions (9.8.86). As a result, we obtain

$$\frac{\partial^2\psi_0}{\partial\xi_{1c}^2}+\frac{\partial^2\psi_0}{\partial\eta_{1c}^2}+\frac{\partial^2\psi_0}{\partial\zeta_{1c}^2}=0 \tag{9.8.89}$$

$$\frac{\partial^2\psi^{q_i}}{\partial\xi_{1c}^2}+\frac{\partial^2\psi^{q_i}}{\partial\eta_{1c}^2}+\frac{\partial^2\psi^{q_i}}{\partial\xi_{1c}^2}=0;\quad \frac{\partial^2\psi^{\dot{q}_i}}{\partial\xi_{1c}^2}+\frac{\partial^2\psi^{\dot{q}_i}}{\partial\eta_{1c}^2}+\frac{\partial^2\psi^{\dot{q}_i}}{\partial\zeta_{1c}^2}=0 \tag{9.8.90}$$

Let us now consider the motion of the transformed lifting surface in an incompressible fluid. Let us write the disturbing potential of the flow over the surface as follows:

$$\Phi_{1c}=k\left[\Phi_0+\sum_{i=1}^{3}\left(\Phi_{1c}^{q_i,\,1c}q_{i,\,1c}+\Phi_{1c}^{\dot{q}_i,\,1c}\dot{q}_{i,\,1c}\right)\right] \tag{9.8.91}$$

where Φ_{1c} is a dimensionless quantity equal to the potential related to the product $b_{0,1c}V_\infty$. Everywhere in the disturbed region of the flow over the surface, the potential must satisfy the continuity equation

$$\frac{\partial^2\Phi_{1c}}{\partial\xi_{1c}^2}+\frac{\partial^2\Phi_{1c}}{\partial\eta_{1c}^2}+\frac{\partial^2\Phi_{1c}}{\partial\zeta_{1c}^2}=0 \tag{9.8.92}$$

Introducing (9.8.91) into this equation, we obtain equations which the derivatives of the potential of the non-stationary incom-

pressible flow over the transformed wing must satisfy:

$$\left.\begin{aligned} &\frac{\partial^2 \Phi_{ic}^{qi,\,ic}}{\partial \xi_{ic}^2}+\frac{\partial^2 \Phi_{ic}^{qi,\,ic}}{\partial \eta_{ic}^2}+\frac{\partial^2 \Phi_{ic}^{qi,\,ic}}{\partial \zeta_{ic}^2}=0; \\ &\frac{\partial^2 \dot{\Phi}_{ic}^{qi,\,ic}}{\partial \xi_{ic}^2}+\frac{\partial^2 \dot{\Phi}_{ic}^{qi,\,ic}}{\partial \eta_{ic}^2}+\frac{\partial^2 \dot{\Phi}_{ic}^{qi,\,ic}}{\partial \zeta_{ic}^2}=0 \end{aligned}\right\} \tag{9.8.93}$$

By comparing Eqs. (9.8.89) and (9.8.92), and also (9.8.90) and (9.8.93), we find that the functions ψ_0, ψ^{qi}, and $\dot{\psi}^{qi}$ determining the velocity potential for a wing in a compressible flow, and the functions Φ_0, $\Phi_{ic}^{qi,ic}$, and $\dot{\Phi}_{ic}^{qi,ic}$ determining the potential for a transformed wing in an incompressible flow satisfy the same differential equations. It is shown in [19] that the boundary conditions are identical. Accordingly, the values of these functions at the points related by conditions (9.8.86) are also identical, i.e.

$$\left.\begin{aligned} &\psi^{qi}(\xi,\ \eta,\ \zeta)=\Phi_{ic}^{qi,\,ic}(\xi_{ic},\ \eta_{ic},\ \zeta_{ic}) \\ &\dot{\psi}^{qi,\,ic}(\xi,\ \eta,\ \zeta)=\dot{\Phi}_{ic}^{qi,\,ic}(\xi_{ic},\ \eta_{ic},\ \zeta_{ic}) \end{aligned}\right\} \tag{9.8.94}$$

where

$$\xi=\xi_{ic},\quad \eta=\eta_{ic}/k,\quad \zeta=\zeta_{ic}/k$$

Consequently, for finding the potential function and its derivatives for a compressible flow over a given lifting surface, we must solve the equivalent problem on the unsteady incompressible flow over a transformed surface with the corresponding boundary conditions. The formulas obtained allow us to directly calculate the relevant values for the given surface in a compressible fluid according to the found aerodynamic characteristics in an incompressible flow for the transformed surface. Particularly, the formulas relating the differences of the pressure coefficients and their derivatives have the following form:

$$\left.\begin{aligned} &\Delta\bar{p}_0=\Delta\bar{p}_{0,\,ic}/k,\quad p^{qi}=p_{ic}^{qi,\,ic}/k \\ &\dot{p}^{qi}=p_{ic}^{qi,\,ic}/k-\xi_{ic}M_\infty^2 p_{ic}^{qi,\,ic}/k^3 \end{aligned}\right\} \tag{9.8.95}$$

We use these data to find the difference of the pressure coefficients at the point of the surface being considered in a compressible flow:

$$\Delta\bar{p}=\Delta\bar{p}_0+\sum_{i=1}^{3}\left(p^{qi}q_i+\dot{p}^{qi}\dot{q}_i\right) \tag{9.8.96}$$

Taking (9.8.96) into account, we can obtain the aerodynamic coefficients of a wing in a compressible flow, while by using (9.8.84)

we can establish the relation between the stability derivatives of this wing and also of the transformed wing in an incompressible fluid:

$$\left.\begin{aligned} c_y^{q_i} &= c_{y,\,\mathrm{ic}}^{q_i,\,\mathrm{ic}}/k, \quad \dot{c}_y^{q_i} = \left(\dot{c}_{y,\,\mathrm{ic}}^{q_i,\,\mathrm{ic}} - M_\infty^2 m_{z,\,\mathrm{ic}}^{q_i,\,\mathrm{ic}}\right)/k^3 \\ m_x^{q_i} &= m_{x,\,\mathrm{ic}}^{q_i,\,\mathrm{ic}}/k^2, \quad \dot{m}_x^{q_i} = \left(\dot{m}_x^{q_i,\,\mathrm{ic}} + M_\infty^2 I_x\right)/k^4 \\ m_z^{q_i} &= m_{z,\,\mathrm{ic}}^{q_i,\,\mathrm{ic}}/k, \quad \dot{m}_z^{q_i} = \left(\dot{m}_{z,\,\mathrm{ic}}^{q_i,\,\mathrm{ic}} - M_\infty^2 I_z\right)/k^3 \end{aligned}\right\} \tag{9.8.97}$$

where

$$\left.\begin{aligned} I_x &= \frac{2b_{0,\,\mathrm{ic}}^2}{S_{\mathrm{w},\,\mathrm{ic}}} \int\limits_{S_{\mathrm{w},\,\mathrm{ic}}} \int p_{\mathrm{ic}}^{q_i,\,\mathrm{ic}} \xi_{\mathrm{ic}} \zeta_{\mathrm{ic}}\, d\xi_{\mathrm{ic}}\, d\zeta_{\mathrm{ic}} \\ I_z &= \frac{2b_{0,\,\mathrm{ic}}^2}{S_{\mathrm{w},\,\mathrm{ic}}} \int\limits_{S_{\mathrm{w},\,\mathrm{ic}}} \int p_{\mathrm{ic}}^{q_i,\,\mathrm{ic}} \xi_{\mathrm{ic}}^2\, d\xi_{\mathrm{ic}}\, d\zeta_{\mathrm{ic}} \end{aligned}\right\} \tag{9.8.98}$$

The following formulas for the coefficients of the normal force and pitching moment for $q_i = \dot{q}_i = 0$ correspond to the relation $\Delta\bar{p}_0 = \Delta\bar{p}_{0,\mathrm{ic}}/k$ between the values of the difference of the pressure coefficients in a compressible and incompressible flows:

$$c_{y0} = c_{y0,\mathrm{ic}}/k, \quad m_{z0} = m_{z0,\mathrm{ic}}/k \tag{9.8.99}$$

With a view to the stability derivatives (9.8.97) and the values (9.8.99), the total normal force and pitching moment coefficients or a wing in a compressible flow have the following form:

$$\left.\begin{aligned} c_y &= c_{y0} + \sum_{i=1}^{3} \left(c_y^{q_i} q_i + \dot{c}_y^{q_i} \dot{q}_i\right) \\ m_z &= m_{z0} + \sum_{i=1}^{3} \left(m_z^{q_i} q_i + \dot{m}_z^{q_i} \dot{q}_i\right) \end{aligned}\right\} \tag{9.8.100}$$

We can write the corresponding rolling moment coefficient m_x in the form of the third of expressions (9.6.8).

9.9. Unsteady Supersonic Flow over a Wing

Let us find the solution of the problem of an unsteady supersonic flow over a wing in the form of the velocity potential $\varphi(x_1, y_1, z_1, t)$ of a transient (pulsating) source (9.7.7) satisfying the wave equation (9.6.30).

Let us consider the expression for such a potential for harmonic oscillations of a wing when the kinematic parameters vary in accord-

ance with the general relation

$$q_j = q_j^* \exp(ipt) \quad (j = \alpha,\ \omega_x,\ \omega_z) \tag{9.9.1}$$

It follows from (9.6.32) that the boundary conditions on a wing also vary harmonically. The derivative of the velocity potential on a wing (9.7.8) (let us call it the flow downwash) can be expressed by the harmonic function

$$\left|\frac{\partial\varphi}{\partial y}(x,\ y,\ z,\ t_{1(2)})\right|_{y=0} = \frac{\partial\varphi}{\partial y}(x,\ y,\ z)\Big|_{y=0} e^{ipt_{1(2)}} \tag{9.9.2}$$

The required disturbance potential is related to the downwashes by formula (9.7.7). The quantities t_1 and t_2 are determined in accordance with formulas (9.7.9) as follows:

$$\left.\begin{aligned} t_1 &= t - \Delta t_1 = t - (x_1 - x)\, M_\infty/(a_\infty \alpha'^2) + M_\infty r/(a_\infty \alpha'^2) \\ t_2 &= t - \Delta t_2 = t - (x_1 - x)\, M_\infty/(a_\infty \alpha'^2) - M_\infty r/(a_\infty \alpha'^2) \end{aligned}\right\} \tag{9.9.3}$$

After introducing (9.9.2) and (9.9.3) into (9.7.7) for a wing (assuming that $y = 0$), we obtain

$$\varphi(x_1,\ y_1,\ z_1,\ t) = -\frac{1}{2\pi}\operatorname{Re} e^{ipt} \iint\limits_{\sigma(x_1,\ z_1)} \left[\frac{\partial\varphi}{\partial y}(x,\ y,\ z)\right]_{y=0} \times e^{-ip\frac{(x_1-x)M_\infty}{a_\infty\alpha'^2}} \left(e^{ip\frac{r}{a_\infty\alpha'^2}} + e^{-ip\frac{r}{a_\infty\alpha'^2}}\right) \frac{dx\,dz}{r}$$

Taking into account that the sum in parentheses on the right-hand side equals $2\cos(pr/a_\infty\alpha'^2)$, and the quantities

$$p^* = pb_0/V_\infty, \quad \omega = p^* M_\infty^2/\alpha'^2 \tag{9.9.4}$$

we obtain the following expression for the velocity potential:

$$\varphi(x_1,\ y_1,\ z_1, t) = -\frac{1}{\pi}\operatorname{Re} q^* e^{ipt} \times \iint\limits_{\sigma(x_1,\ z_1)} \left[\frac{\partial\varphi}{\partial y}(x,\ y,\ z)\right]_{y=0} e^{-\frac{i\omega(x_1-x)}{b_0}} \cos\left(\frac{\omega r}{b_0 M_\infty}\right) \frac{dx\,dz}{r} \tag{9.9.5}$$

where $r = \sqrt{(x_1-x)^2 - \alpha'^2[y_1^2 + (z_1-z)^2]}$.

With a view to the harmonic nature of motion of the wing, we can write the potential function as follows:

$$\varphi(x,\ y,\ z,\ t) = V_\infty b_0 \sum_{j=1}^{3} (\varphi^{q_j} q_j + \varphi^{\dot{q}_j} \dot{q}_j)$$

$$= V_\infty b_0 \operatorname{Re} e^{ipt} \sum_{j=1}^{3} q_j^* [\varphi^{q_j}(x,\ y,\ z) + ip^* \varphi^{\dot{q}_j}(x,\ y,\ z)] \tag{9.9.6}$$

where

$$q_j = q_j^* e^{ipt}, \quad \dot{q}_j = dq_j/d\tau = (dq_j/dt)\, b_0/V_\infty = ip_j^* q_j^* e^{ipt} \qquad (9.9.7)$$

In accordance with (9.9.6), the partial derivative of the potential function with respect to y is

$$\frac{\partial \varphi}{\partial y}(x, y, z, t) = V_\infty b_0 \operatorname{Re} e^{ipt} \sum_{j=1}^{3} q_j^* \left[\frac{\partial \varphi^{q_j}}{\partial y}(x, y, z) + ip^* \frac{\partial \varphi^{\dot{q}_j}}{\partial y}(x, y, z) \right] \qquad (9.9.8)$$

Inserting this derivative into the left-hand side of (9.9.2), we obtain the following relation for $[\partial\varphi\,(x, y, z)/\partial y]_{y=0}$:

$$\left[\frac{\partial \varphi}{\partial y}(x, y, z) \right]_{y=0} = V_\infty b_0 \sum_{j=1}^{3} q_j^* \left[\frac{\partial \varphi^{q_j}}{\partial y}(x, y, z) + ip^* \frac{\partial \varphi^{\dot{q}_j}}{\partial y}(x, y, z) \right] \qquad (9.9.9)$$

Introducing this expression into (9.9.5), substituting (9.9.6) for the velocity potential on the left-hand side, and taking into account that

$$e^{\frac{-i\omega(x_1 - x)}{b_0}} = \cos \frac{\omega (x_1 - x)}{b_0} - i \sin \frac{\omega (x_1 - x)}{b_0}$$

we obtain relations for the derivatives of the potential function:

$$\left.\begin{aligned} \varphi^{q_j}(x, y, z) = -\frac{1}{\pi} \iint\limits_{\sigma(x_1, z_1)} \left\{ \left[\frac{\partial \varphi^{q_j}}{\partial y}(x, y, z) \right]_{y=0} \times \cos \frac{\omega (x_1 - x)}{b_0} + p^* \left[\frac{\partial \varphi^{\dot{q}_j}}{\partial y}(x, y, z) \right]_{y=0} \sin \frac{\omega (x_1 - x)}{b_0} \right\} \times \cos \left(\frac{\omega r}{b_0 M_\infty} \right) \frac{dx\, dy}{r} \\ \varphi^{\dot{q}_j}(x, y, z) = -\frac{1}{\pi} \iint\limits_{\sigma(x_1, z_1)} \left\{ \left[\frac{\partial \varphi^{\dot{q}_j}}{\partial y}(x, y, z) \right]_{y=0} \times \cos \frac{\omega (x_1 - x)}{b_0} - \frac{1}{p^*} \left[\frac{\partial \varphi^{q_j}}{\partial y}(x, y, z) \right]_{y=0} \sin \frac{\omega (x_1 - x)}{b_0} \right\} \times \cos \frac{\omega r}{b_0 M_\infty} \frac{dx\, dz}{r}. \end{aligned}\right\} \qquad (9.9.10)$$

For unsteady motion with small Strouhal numbers ($p^* \to 0$, $\omega \to 0$), Eqs. (9.9.10) acquire the form

$$\left.\begin{aligned}
\varphi^{q_j}(x, y, z) &= -\frac{1}{\pi}\int\int_{\sigma}\left[\frac{\partial\varphi^{q_j}}{\partial y}(x, y, z)\right]_{y=0}\frac{dx\,dz}{r} \\
\dot{\varphi}^{q_j}(x, y, z) &= -\frac{1}{\pi}\int\int_{\sigma}\left\{\left[\frac{\partial\dot{\varphi}^{q_j}}{\partial y}(x, y, z)\right]_{y=0}\right. \\
&\quad \left.-\frac{M_\infty^2(x_1-x)}{\alpha'^2 b_0}\left[\frac{\partial\varphi^{q_j}}{\partial y}(x, y, z)\right]_{y=0}\frac{dx\,dz}{r}\right\}
\end{aligned}\right\} \quad (9.9.10')$$

Let us introduce the dimensionless coordinates (9.6.19), adopting the centre chord ($x_k = b_0$) as the characteristic geometric dimension:

$$\xi = x/b_0, \quad \eta = y/b_0, \quad \zeta = z/b_0 \qquad (9.9.11)$$

Considering that to determine the aerodynamic loads it is sufficient to find the value of the potential function on the wing ($y = 0$), let us express (9.9.10') in terms of the dimensionless coordinates as follows:

$$\left.\begin{aligned}
\varphi^{q_j}(\xi_1, 0, \zeta_1) &= -\frac{1}{\pi}\int\int_{\sigma}\left[\frac{\partial\varphi^{q_j}}{\partial\eta}\right]_{\eta=0}\frac{d\xi\,d\zeta}{\bar{r}} \\
\dot{\varphi}^{q_j}(\xi_1, 0, \zeta_1) &= -\frac{1}{\pi}\int\int_{\sigma}\left\{\left[\frac{\partial\dot{\varphi}^{q_j}}{\partial\eta}\right]_{\eta=0}-\frac{M_\infty^2(\xi_1-\xi)}{\alpha'^2}\right. \\
&\quad \left.\times\left[\frac{\partial\varphi^{q_j}}{\partial\eta}\right]_{\eta-0}\right\}\frac{d\xi\,d\zeta}{\bar{r}}
\end{aligned}\right\} \quad (9.9.12)$$

where $\bar{r} = \sqrt{(\xi_1-\xi)^2-\alpha'^2(\zeta_1-\zeta)^2}$.

We can use the found derivatives φ^{q_j} and $\dot{\varphi}^{q_j}$ to determine the dimensional value of the velocity potential:

$$\varphi(\xi_1, 0, \zeta_1) = V_\infty b_0\sum_{j=1}^{3}[\varphi^{q_j}(\xi_1, 0, \zeta_1)\,q_j+\dot{\varphi}^{q_j}(\xi_1, 0, \zeta_1)\,\dot{q}_j] \qquad (9.9.13)$$

Equations (9.9.12) allow us to find the velocity potential at points on a wing plane if within the entire region of source influence (integration region σ) we know the flow downwashes determined by the derivatives $[\partial\varphi^{q_j}/\partial\eta]_{\eta=0}$ and $[\partial\dot{\varphi}^{q_j}/\partial\eta]_{\eta=0}$. The values of these downwashes must satisfy the boundary condition (9.6.32) on the wing ($\eta = 0$) in accordance with which we have

$$\partial\varphi^{\alpha}/\partial\eta = -1, \quad \partial\dot{\varphi}^{\alpha}/\partial\eta = 0 \quad (j = 1) \qquad (9.9.14)$$

$$\partial\varphi^{\omega_x}/\partial\eta = -\zeta_1, \quad \partial\dot{\varphi}^{\omega_x}/\partial\eta = 0 \quad (j = 2) \qquad (9.9.15)$$

$$\partial\varphi^{\omega_z}/\partial\eta = -\xi_1, \quad \partial\dot{\varphi}^{\omega_z}/\partial\eta = 0 \quad (j = 3) \qquad (9.9.16)$$

In addition, the values of the downwashes being sought must correspond to the value of the potential function on a vortex sheet (9.6.34). In theoretical investigations, (9.6.34) is replaced with the following condition on a vortex sheet:

$$\varphi(\xi, 0, \zeta, \tau) = \varphi(\xi^*, 0, \zeta^*, \tau^*); \quad \tau^* = \tau - (\xi^* - \xi) \quad (9.9.17)$$

that allows us to determine the velocity potential φ at a point of the vortex sheet (x, z) from its value directly behind the trailing edge of the wing (at a point with the coordinates x^* and $z^* = z$), but at a different instant $t^* < t$. It is shown in [19] that condition (9.9.17) corresponds to the requirement of the absence of a pressure difference on the vortex sheet.

Let us expand the left-hand and right-hand sides of (9.9.17) into the series (9.9.6):

$$\sum_{j=1}^{3} [\varphi^{q_j}(\xi, 0, \zeta) q_j(\tau) + \dot{\varphi}^{q_j}(\xi, 0, \zeta) \dot{q}_j(\tau)]$$

$$= \sum_{j=1}^{3} [\varphi^{q_j}(\xi^*, 0, \zeta) q_j(\tau^*) + \dot{\varphi}^{q_j}(\xi^*, 0, \zeta) \dot{q}_j(\tau^*)] \quad (9.9.18)$$

where by (9.9.1), we have

$$q_j(\tau) = q_j^* e^{ipt}, \quad \dot{q}_j(\tau) = i q_j^* p e^{ipt}$$

$$q_j(\tau^*) = q_j^* e^{ip[t-(x^*-x)/V_\infty]}; \quad \dot{q}_j(\tau^*) = i q_j^* p^* e^{ip[t-(x^*-x)/V_\infty]}$$

After introducing the values of q_j and their derivatives into (9.9.18), we obtain (without the summation sign)

$$\varphi^{q_j}(\xi, 0, \zeta) + ip^* \dot{\varphi}^{q_j}(\xi, 0, \zeta)$$

$$= e^{-ip^*(\xi^*-\xi)} \varphi^{q_j}(\xi^*, 0, \zeta) + ip^* e^{-ip^*(\xi^*-\xi)} \dot{\varphi}^{q_j}(\xi^*, 0, \zeta) \quad (9.9.19)$$

Since $e^{-ip^*(\xi^*-\xi)} = \cos[p^*(\xi^*-\xi)] - i \sin[p^*(\xi^*-\xi)]$

or at low Strouhal numbers $(p^* \to 0)$

$$e^{-ip^*(\xi^*-\xi)} = 1 - ip^*(\xi^*-\xi)$$

after introduction into (9.9.19) and separating the real and imaginary parts, we find the following expressions for the derivatives on the vortex sheet (excluding the term with p^{*2}):

$$\left.\begin{aligned} \varphi^{q_j}(\xi, 0, \zeta) &= \varphi^{q_j}(\xi^*, 0, \zeta) \\ \dot{\varphi}^{q_j}(\xi, 0, \zeta) &= \dot{\varphi}^{q_j}(\xi^*, 0, \zeta) - (\xi^* - \xi) \varphi^{q_j}(\xi^*, 0, \zeta) \end{aligned}\right\} \quad (9.9.20)$$

Beyond the limits of the disturbance cones (a Mach cone or wave), the supersonic flow remains undisturbed, hence the potential function is constant. Therefore, the additional disturbance potential

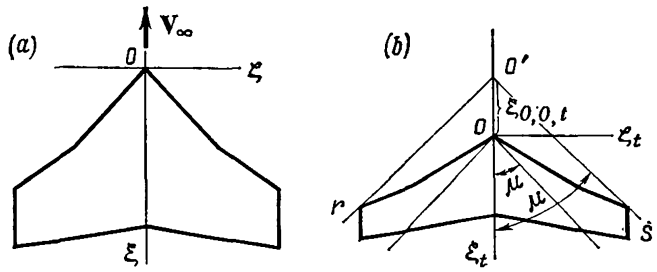

Fig. 9.9.1
Adopted designations of the coordinate systems:
a—conventional (ξ, 0, ζ); *b*—transformed (ξ_t, 0, ζ_t); *s*, *r*—characteristic coordinates

in this region, including the Mach wave, equals zero, i.e.

$$\varphi(\xi, \eta, \zeta, t) = 0 \tag{9.9.21}$$

Simultaneously everywhere in plane xOz except for the wing and the wake vortex behind it, the condition is satisfied that

$$\varphi(\xi, 0, \zeta, t) = 0 \tag{9.9.22}$$

according to which the function φ is continuous and odd relative to the coordinate y (η).

Let us consider Eqs. (9.9.12). Their use for numerical calculations is hindered by that if the equality $\xi_1 - \xi = \pm\alpha'(\zeta_1 - \zeta)$ holds, the integrands have a singularity of the order of $r^{-1/2}$. It is therefore necessary to transform Eqs. (9.9.12) to a form convenient for such calculations. To do this, we shall introduce a new system of coordinates (Fig. 9.9.1):

$$\xi_t = \xi/\alpha', \quad \eta_t = \eta, \quad \zeta_t = \zeta \tag{9.9.23}$$

The wing in the new system of coordinates is shown in Fig. 9.9.1 from which it can be seen that the lifting surface has been made shorter, while the transverse dimensions have been kept unchanged.

Equations (9.9.12) transformed to the coordinates ξ_t, η_t, and ζ_t have the following form:

$$\left.\begin{aligned}
\varphi^{q_j}(\xi_{1,t}, 0, \zeta_{1,t}) &= -\frac{1}{\pi}\int\limits_{\sigma_t}\int \left[\frac{\partial\varphi^{q_j}}{\partial\eta_t}\right]_{\eta_t=0}\frac{d\xi_t\, d\zeta_t}{\bar{r}_t} \\
\dot{\varphi}^{q_j}(\xi_{1,t}, 0, \zeta_{1,t}) &= -\frac{1}{\pi}\int\limits_{\sigma_t}\int \left\{\left[\frac{\partial\dot{\varphi}^{q_j}}{\partial\eta_t}\right]_{\eta_t=0}\right. \\
&\quad \left. -\frac{M_\infty^2(\xi_{1,t}-\xi_t)}{\alpha'}\left[\frac{\partial\varphi^{q_j}}{\partial\eta_t}\right]_{\eta_t=0}\right\}\frac{d\xi_t\, d\zeta_t}{\bar{r}_t} \\
\bar{r}_t &= \sqrt{(\xi_{1,t}-\xi_t)^2-(\zeta_{1,t}-\zeta_t)^2}
\end{aligned}\right\} \tag{9.9.24}$$

To simplify the solution of Eqs. (9.9.24), we shall introduce the following relations for the derivatives of the function φ used for small Strouhal numbers ($p^* \to 0$):

$$\left.\begin{aligned} \varphi^{q_j}(\xi_t,\ 0,\ \zeta_t) &= F^{q_j}(\xi_t,\ 0,\ \zeta_t) \\ \dot{\varphi}^{q_j}(\xi_t,\ 0,\ \zeta_t) &= \dot{F}^{q_j}(\xi_t,\ 0,\ \zeta_t) - \frac{M_\infty^2 \xi_t}{\alpha'} F^{q_j}(\xi_t,\ 0,\ \zeta_t) \end{aligned}\right\} \quad (9.9.25)$$

After inserting the value of φ^{q_j} (9.9.25) into the first of Eqs. (9.9.24), we obtain an integral equation for determining the derivative F^{q_j}:

$$F^{q_j}(\xi_{1,t},\ 0,\ \zeta_{1,t}) = -\frac{1}{\pi} \iint\limits_{\sigma_t} \left[\frac{\partial F^{q_j}}{\partial \eta_t}\right]_{\eta_t=0} \frac{d\xi_t\, d\zeta_t}{\bar{r}_t} \quad (9.9.26)$$

Let us introduce (9.9.25) into the second of Eqs. (9.9.24):

$$\dot{F}^{q_j}(\xi_{1,t},\ 0,\ \zeta_{1,t}) - \frac{M_\infty^2 \xi_{1,t}}{\alpha'} F^{q_j}(\xi_{1,t},\ 0,\ \zeta_{1,t})$$

$$= -\frac{1}{\pi} \iint\limits_{\sigma_t} \left\{ \left[\frac{\partial \dot{F}^{q_j}}{\partial \eta_t}\right]_{\eta_t=0} - \frac{M_\infty^2 \xi_t}{\alpha'} \left[\frac{\partial F^{q_j}}{\partial \eta_t}\right]_{\eta_t=0} \right.$$

$$\left. - \frac{M_\infty^2 (\xi_{1,t} - \xi_t)}{\alpha'} \left[\frac{\partial \varphi^{q_j}}{\partial \eta_t}\right]_{\eta_t=0} \right\} \frac{d\xi_t\, d\zeta_t}{\bar{r}_t}$$

Substituting for the derivative $\dot{F}^{q_j}$ on the left-hand side of the equation its value from (9.9.26) and having in view that by (9.9.25)

$$\left[\frac{\partial \varphi^{q_j}}{\partial \eta_t}\right]_{\eta_t=0} = \left[\frac{\partial F^{q_j}}{\partial \eta_t}\right]_{\eta_t=0}$$

we obtain an expression for finding the derivative $\dot{F}^{q_j}$:

$$\dot{F}^{q_j}(\xi_{1,t},\ 0,\ \zeta_{1,t}) = -\frac{1}{\pi} \iint\limits_{\sigma_t} \left[\frac{\partial \dot{F}^{q_j}}{\partial \eta_t}\right]_{\eta_t=0} \frac{d\xi_t\, d\zeta_t}{\bar{r}_t} \quad (9.9.27)$$

We perform our further transformations in characteristic coordinates (Fig. 9.9.1), namely,

$$r = (\xi_t - \xi_{0,0,t}) - \zeta_t,\quad s = (\xi_t - \xi_{0,0,t}) + \zeta_t \quad (9.9.28)$$

selected so that only positive values of the variables will be used in the calculations. The value of $\xi_{0,0,t}$ representing the displacement of the characteristic system of coordinates is determined as shown in Fig. 9.9.1 (the coordinate lines from the displaced apex O' pass through breaks of the wing at the tips).

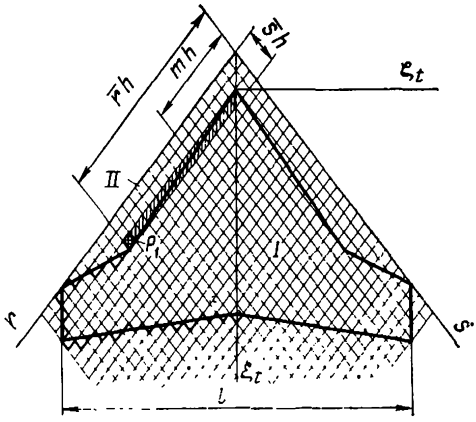

Fig. 9.9.2
To the numerical calculation of a wing with combined leading and supersonic trailing edges in an unsteady flow:
I, II—regions for finding the downwash

Equations (9.9.26) and (9.9.27) acquire the following form in the characteristic coordinates:

$$\left.\begin{aligned} F^{qj}(r_1, 0, s_1) &= -\frac{1}{2\pi}\int_0^{r_1}\int_0^{s_1}\left[\frac{\partial F^{qj}}{\partial \eta_t}\right]_{\eta_t=0}\frac{dr\,ds}{\sqrt{(r_1-r)(s_1-s)}} \\ \dot{F}^{qj}(r_1, 0, s_1) &= -\frac{1}{2\pi}\int_0^{r_1}\int_0^{s_1}\left[\frac{\partial \dot{F}^{qj}}{\partial \eta_t}\right]_{\eta_t=0}\frac{dr\,ds}{\sqrt{(r_1-r)(s_1-s)}} \end{aligned}\right\} \quad (9.9.29)$$

For further transformations allowing us to eliminate the singularity in Eqs. (9.9.29), we shall introduce the variables

$$v = \sqrt{r_1 - r}, \quad u = \sqrt{s_1 - s} \quad (9.9.30)$$

Equations (9.9.29) acquire the following form in the variables (9.9.30)

$$\left.\begin{aligned} F^{qj}(r_1, 0, s_1) &= -\frac{2}{\pi}\int_0^{\sqrt{r_1}}\int_0^{\sqrt{s_1}} D_j\,dv\,du \\ \dot{F}^{qj}(r_1, 0, s_1) &= -\frac{2}{\pi}\int_0^{\sqrt{r_1}}\int_0^{\sqrt{s_1}} E_j\,dv\,du \end{aligned}\right\} \quad (9.9.31)$$

where

$$D_j = \left[\frac{\partial F^{qj}}{\partial \eta_t}\right]_{\eta_t=0}, \quad E_j = \left[\frac{\partial \dot{F}^{qj}}{\partial \eta_t}\right]_{\eta_t=0} \quad (9.9.32)$$

To perform numerical calculations, we shall divide the region occupied by the wing into separate cells as shown in Fig. 9.9.2.

Let h stand for the width of a cell in characteristic axes. This quantity is the dimensionless distance along the r (or s) axis between the edges of a cell for points n, $n + 1$ (or i, $i + 1$), respectively. It is equal to

$$h] = l/(2Nb_0) \tag{9.9.33}$$

where N is the number of parts into which the wing half-span $l/2$ is divided.

Let $\bar{r}$ and $\bar{s}$ be the coordinates of a fixed point (point P_1 in Fig. 9.9.2) at which we are finding the velocity potential (or its derivatives), and m and i be the coordinates of the running points used to perform numerical integration. Accordingly,

$$r_1 = \bar{r}h,\ s_1 = \bar{s}h,\ r = mh,\ s = ih \tag{9.9.34}$$

Assuming that the functions D_j and E_j [see (9.9.32)] within a cell are variable, let us write Eqs. (9.9.31) in terms of the sum of the integrals over all the cells:

$$\left.\begin{aligned} F^{q_j}(r_1, 0, s_1) &= -\frac{2}{\pi}\sum_{m=0}^{\bar{r}-1}\sum_{i=0}^{\bar{s}-1}\int_{\sqrt{mh}}^{\sqrt{(m+1)h}}\int_{\sqrt{ih}}^{\sqrt{(i+1)h}} D_j\,dv\,du \\ \dot{F}^{q_j}(r_1, 0, s_1) &= -\frac{2}{\pi}\sum_{m=0}^{\bar{r}-1}\sum_{i=0}^{\bar{s}-1}\int_{\sqrt{mh}}^{\sqrt{(m+1)h}}\int_{\sqrt{ih}}^{\sqrt{(i+1)h}} E_j\,dv\,du \end{aligned}\right\} \tag{9.9.35}$$

The integration regions including the projection of the wing onto the plane $\eta = 0$, the vortex sheet, and also the sections of the disturbed flow outside the wing and vortex sheet are replaced with a sufficiently large number of whole cells producing a conditional wing with toothed edges (Fig. 9.9.2). A cell should be considered to belong to a section of the integration region if its centre is on this section.

Inside a cell with a sufficiently small area, the derivatives D_j and E_j can be assumed to be constant and equal to their values at the centre of a cell. Accordingly, Eqs. (9.9.35) can be written in a simpler form:

$$\left.\begin{aligned} F^{q_j}(\bar{r}h, \bar{s}h) &= -\frac{2h}{\pi}\sum_{m=1}^{\bar{r}}\sum_{i=1}^{\bar{s}} D_{j,m,i}B_{\bar{r},m,\bar{s},i} \\ \dot{F}^{q_j}(\bar{r}h, \bar{s}h) &= -\frac{2h}{\pi}\sum_{m=1}^{\bar{r}}\sum_{i=1}^{\bar{s}} E_{j,m,i}B_{\bar{r},m,\bar{s},i} \end{aligned}\right\} \tag{9.9.36}$$

where

$$\left.\begin{aligned} D_{j,\,m,\,i} &= D_j[(m-1/2)\,h,\quad (i-1/2)\,h] \\ E_{j,\,m,\,i} &= E_j[(m-1/2)\,h,\quad (i-1/2)\,h] \\ B_{\bar{r},\,m,\,\bar{s},\,i} &= (\sqrt{\bar{r}-m+1}-\sqrt{\bar{r}-m})\,(\sqrt{\bar{s}-i+1}-\sqrt{\bar{s}-1}) \end{aligned}\right\} \quad (9.9.37)$$

Formulas (9.9.36) allow us to determine the values of $F^q{}_j$ and $\dot{F}^q{}_j$ and, consequently, the derivatives of the velocity potential [see expressions (9.9.25)] if within the entire region of source influence (including the wing plane, vortex sheet, and the disturbed flow outside of them) we know the quantities $D_{j,m,i}$ and $E_{j,m,i}$ (the flow downwashes), and also the values of $B_{\bar{r},m,\bar{s},i}$ (the kernel functions).

The downwashes are determined differently for the following three regions: (1) the wing, (2) the disturbed region confined by the leading edges, tips, and surface of the Mach cones issuing from the corresponding points of the wing (end regions), and (3) the vortex sheet.

Let us consider the downwashes in each of these regions, having in view the case of small Strouhal numbers ($p^* \to 0$). For a wing with supersonic (or combined) leading and supersonic trailing edges, it is sufficient to know the downwashes on the lifting surface (section *I* in Fig. 9.9.2). They are determined by boundary conditions (9.9.14)-(9.9.16), in accordance with which

$$\left.\begin{aligned} D^{(I)}_{1mi} &= -1\ (j=1);\quad D^{(I)}_{2mi} = h\,(m-i)/2 \quad (j=2) \\ D^{(I)}_{3mi} &= -\alpha' h\,(m+i-1)/2 - \alpha'\xi_{0,\,0,\,t} \quad (j=3) \end{aligned}\right\} \quad (9.9.38)$$

$$\left.\begin{aligned} E^{(I)}_{1mi} &= M^2_\infty\,[h\,(m+i-1)/2 + \xi_{0,\,0,\,t}]/\alpha' \quad (j=1) \\ E^{(I)}_{2mi} &= \{M^2_\infty\,[h\,(m+i-1)/2 + \xi_{0,\,0,\,t}]/(2\alpha')\} \\ &\qquad \times h\,(m-1) \quad (j=2) \\ E^{(I)}_{3mi} &= -M^2_\infty\,[h\,(m+i-1)/2 + \xi_{0,\,0,\,t}]^2 \quad (j=3) \end{aligned}\right\} \quad (9.9.39)$$

Section *II* (Fig. 9.9.2) between the characteristic axes, the leading edge and the Mach lines issuing from the vertex of the wing is occupied by an undisturbed flow region; hence, all the downwashes equal zero and, consequently,

$$D^{II}_{j,m,i} = E^{II}_{j,m,i} = 0 \quad (9.9.40)$$

Let us determine the flow downwashes in disturbed region *III* between the leading edge, the tip, and the Mach cone issuing from the points of a break in the wing contour (Fig. 9.9.3). The velocity potential in this region (outside of the wing and vortex wake behind

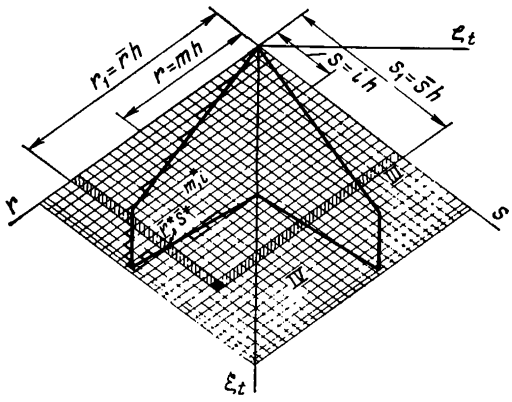

Fig. 9.9.3
To the numerical calculation of a wing with subsonic edges in an unsteady flow:
III, *IV*—regions for finding the downwash

it) in accordance with condition (9.9.22) is zero. Therefore, from (9.9.29), we obtain the conditions for region *III*:

$$\left.\begin{aligned} F^{q_j}(r_1,\ 0,\ s_1) &= -\frac{1}{2\pi}\int_0^{r_1}\int_0^{s_1} D_j \frac{dr\,ds}{\sqrt{(r_1-r)(s_1-s)}} = 0 \\ \dot{F}^{q_j}(r_1,\ 0,\ s_1) &= -\frac{1}{2\pi}\int_0^{r_1}\int_0^{s_1} F_j \frac{dr\,ds}{\sqrt{(r_1-r)(s_1-s)}} = 0 \end{aligned}\right\} \quad (9.9.41)$$

These integrals can be written in a somewhat different form:

$$\int_0^{s_1}\frac{ds}{\sqrt{s_1-s}}\int_0^{r_1} D_j\frac{dr}{\sqrt{r_1-r}}=0;\quad \int_0^{s_1}\frac{ds}{\sqrt{s_1-s}}\int_0^{r_1} E_j\frac{dr}{\sqrt{r_1-r}}=0 \quad (9.9.42)$$

or

$$\int_0^{r_1}\frac{dr}{\sqrt{r_1-r}}\int_0^{s_1} D_j\frac{ds}{\sqrt{s_1-s}}=0;\quad \int_0^{r_1}\frac{dr}{\sqrt{r_1-r}}\int_0^{s_1} E_j\frac{ds}{\sqrt{s_1-s}}=0 \quad (9.9.42')$$

The obtained equalities are Abel equations whose right-hand sides identically equal zero. Hence it follows that the inner integrals for $s = s_1$ [Eqs. (9.9.42)] and for $r = r_1$ [Eqs. (9.9.42')] equal zero. Accordingly, we obtain the following equations for determining the downwashes $D_j^{(III)}$ in region *III* (Fig. 9.9.3):

$$\left.\begin{aligned} \int_{s_1-h}^{s_1} D_j^{(III)}\frac{ds}{\sqrt{s_1-s}} &= -\int_0^{s_1-h} D_j\frac{ds}{\sqrt{s_1-s}} \\ \int_{r_1-h}^{r_1} D_j^{(III)}\frac{dr}{\sqrt{r_1-r}} &= -\int_0^{r_1-h} D_j\frac{ds}{\sqrt{r_1-r}} \end{aligned}\right\} \quad (9.9.43)$$

The equations for the downwashes $E_j^{(III)}$ have a similar form:

$$\left.\begin{aligned}\int_{s_1-h}^{s_1} E_j^{(III)} \frac{ds}{\sqrt{s_1-s}} &= -\int_0^{s_1-h} E_j \frac{ds}{\sqrt{s_1-s}} \\ \int_{r_1-h}^{r_1} E_j^{(III)} \frac{dr}{\sqrt{r_1-r}} &= -\int_0^{r_1-h} E_j \frac{dr}{\sqrt{r_1-r}}\end{aligned}\right\} \quad (9.9.44)$$

Assuming the values of the downwashes in the cells to be constant and going over from integrals to sums, we find in accordance with the variables (9.9.30) the following relations for determining the downwashes in a cell (point) with the coordinates $r_1 = \bar{r}h$ and $s_1 = \bar{s}h$:

$$\left.\begin{aligned}D_j^{(III)}(\bar{r}h, \bar{s}h) &= -\sum_{m=1}^{\bar{r}-1} D_j[(m-0.5)h, \quad (i-0.5)h] B_{\bar{r}, m} \\ E_j^{(III)}(\bar{r}h, \bar{s}h) &= -\sum_{m=1}^{\bar{r}-1} E_j[(m-0.5)h, \quad (i-0.5)h] B_{\bar{r}, m}\end{aligned}\right\} \quad (9.9.45)$$

(for points to the left of the axis ξ_t);

$$\left.\begin{aligned}D_j^{(III)}(\bar{r}h, \bar{s}h) &= -\sum_{i=1}^{\bar{s}-1} D_j[(m-0.5)h, \quad (i-0.5)h] B_{\bar{s}, i} \\ E_j^{(III)}(\bar{r}h, \bar{s}h) &= -\sum_{i=1}^{\bar{s}-1} E_j[(m-0.5)h, \quad (i-0.5)h] B_{\bar{s}, i}\end{aligned}\right\} \quad (9.9.46)$$

(for points to the right of the axis ξ_t).

In Eqs. (9.9.45) and (9.9.46), we have introduced the notation

$$B_{\bar{r}, m} = \sqrt{\bar{r}-m+1} - \sqrt{\bar{r}-m}, \quad B_{\bar{s}, i} = \sqrt{\bar{s}-m+1} - \sqrt{\bar{s}-i} \quad (9.9.47)$$

According to the above relations, the flow downwash at a point is determined by summation of the downwash values in all the cells in the corresponding strip $m = \text{const}$ (or $i = \text{const}$). The calculations are performed consecutively beginning from the cell at the vertex of the wing where the downwash is determined by formulas (9.9.38) and (9.9.39). Let us now calculate the downwashes on the vortex sheet behind the wing (region IV in Fig. 9.9.3). We shall find them from condition (9.9.20), which we shall write in the transformed coordinates

$$\left.\begin{aligned}\varphi^{q_j}(\xi_t, 0, \zeta_t) &= \varphi^{q_j}(\xi_t^*, 0, \zeta_t^*) \\ \dot{\varphi}^{q_j}(\xi_t, 0, \zeta_t) &= \dot{\varphi}^{q_j}(\xi_t^*, 0, \zeta_t^*) - \alpha'(\xi_t^* - \xi_t)\varphi^{q_j}\end{aligned}\right\} \quad (9.9.48)$$

where ξ_t^* and $\zeta_{t1}^* = \zeta$ are the transformed coordinates of points on the trailing edge.

Relations (9.9.48) can be represented with a view to (9.9.25) and the characteristic coordinates (9.9.28) as follows:

$$\left.\begin{aligned}
\varphi^{q_j}(r_1,\ 0,\ s_1) &= F^{q_j}\left(\frac{r^*+s^*}{2},\ \frac{s^*-r^*}{2}\right)\\
\dot{\varphi}^{q_j}(r_1,\ 0,\ s_1) &= \dot{F}^{q_j}\left(\frac{r^*+s^*}{2},\ \frac{s^*-r^*}{2}\right)\\
&-\frac{M_\infty^2}{2\alpha'}(r_1+s_1)\,F^{q_j}\left(\frac{r^*+s^*}{2},\ \frac{s^*-r^*}{2}\right)\\
&+\alpha'\left[\frac{r_1+s_1-(r^*+s^*)}{2}\right]F^{q_j}\left(\frac{r^*+s^*}{2},\ \frac{s^*-r^*}{2}\right)
\end{aligned}\right\} \qquad (9.9.49)$$

These relations hold for the conditions

$$s_1 - r_1 = s^* - r^*,\ r_1 > r^*,\ s_1 > s^* \qquad (9.9.50)$$

where s^* and r^* are characteristic coordinates of points on the trailing edge.

In addition to (9.9.49), we can use Eqs. (9.9.25) for the vortex sheet, which with account taken of (9.9.26) and (9.9.27) have the form

$$\left.\begin{aligned}
\varphi^{q_j}(r_1,\ 0,\ s_1) &= -\frac{1}{2\pi}\int_0^{r_1}\int_0^{s_1} D_j\,\frac{dr\,ds}{\sqrt{(r_1-r)(s_1-s)}}\\
\dot{\varphi}^{q_j}(r_1,\ 0,\ s_1) &= -\frac{1}{2\pi}\int_0^{r_1}\int_0^{s_1} E_j\,\frac{dr\,ds}{\sqrt{(r_1-r)\,(s_1-s)}}\\
&+\frac{M_\infty^2}{4\pi\alpha'}(r_1+s_1)\int_0^{r_1}\int_0^{s_1} D_j\,\frac{dr\,ds}{\sqrt{(r_1-r)\,(s_1-s)}}
\end{aligned}\right\} \qquad (9.9.51)$$

Replacing the derivatives φ^{q_j} and $\dot{\varphi}^{q_j}$ in (9.9.51) with their relevant values from (9.9.49), we obtain integral equations for determining downwashes on a vortex sheet (region IV in Fig. 9.9.3):

$$\left.\begin{aligned}
-\frac{1}{2\pi}\int_0^{r_1}\int_0^{s_1} D_j\,\frac{dr\,ds}{\sqrt{(r_1-r)\,(s_1-s)}} &= F^{q_j}\left(\frac{r^*+s^*}{2},\ \frac{s^*-r^*}{2}\right)\\
-\frac{1}{2\pi}\int_0^{r_1}\int_0^{s_1} E_j\,\frac{dr\,ds}{\sqrt{(r_1-r)\,(s_1-s)}} &= \dot{F}^{q_j}\left(\frac{r^*+s^*}{2},\ \frac{s^*-r^*}{2}\right)\\
+\frac{\alpha'\,[(r_1+s_1)-(r^*+s^*)]}{2}\,F^{q_j}&\left(\frac{r^*+s^*}{2},\ \frac{r^*-s^*}{2}\right)
\end{aligned}\right\} \qquad (9.9.52)$$

Both equations are solved in the same way. Let us consider as an example the first of Eqs. (9.9.52). We shall isolate on section IV a cell with the sides h and the characteristic coordinates $s_1 = \bar{s}h$ and $r_1 = \bar{r}h$. We shall write the left-hand integral of the equation as the sum of four integrals:

$$\int_0^{r_1}\int_0^{s_1} D_j \frac{dr\,ds}{\sqrt{(r_1-r)(s_1-s)}} = \int_0^{s_1-h}\frac{ds}{\sqrt{s_1-s}}\int_0^{r_1-h} D_j\frac{dr}{\sqrt{r_1-r}} + \int_{s_1-h}^{s_1}\frac{ds}{\sqrt{s_1-s}}\int_0^{r_1-h} D_j\frac{dr}{\sqrt{r_1-r}} + \int_0^{s_1-h}\frac{ds}{\sqrt{s_1-s}}\int_{r_1-h}^{r_1} D_j\frac{dr}{\sqrt{r_1-r}} + \int_{s_1-h}^{s_1}\frac{ds}{\sqrt{s_1-s}}\int_{r_1-h}^{r_1} D_j\frac{dr}{\sqrt{r_1-r}} \tag{9.9.53}$$

As we have already indicated, the entire integration region should be divided into cells and the downwashes assumed to be constant in each of them. We determine the coordinates of the cells by means of the integers m, i, $\bar{r}$ and $\bar{s}$ (Fig. 9.9.3). Using (9.9.30), we go over to the variables v and u:

$$v^2 = (\bar{r} - m)\,h, \quad u^2 = (\bar{s} - i)\,h \tag{9.9.54}$$

The first of the integrals (9.9.53) has the following form:

$$\int_0^{s_1-h}\frac{ds}{\sqrt{s_1-s}}\int_0^{r_1-h} D_j\frac{dr}{\sqrt{r_1-r}} = \int_{\sqrt{\bar{s}h}}^{\sqrt{\bar{h}}} 2\,du\int_{\sqrt{\bar{r}h}}^{\sqrt{\bar{h}}} 2D_j\,dv$$

$$= 4\sum_1^{\bar{s}-1}\int_{\sqrt{(\bar{s}-m+1)h}}^{\sqrt{(\bar{s}-m)h}} du\sum_1^{\bar{r}-1}\int_{\sqrt{(\bar{r}-m+1)h}}^{\sqrt{(\bar{r}-m)h}} D_j\,dv$$

$$= 4h\sum_{i=1}^{\bar{s}-1}\sum_{m=1}^{\bar{r}-1} D_j(mh,\ ih)\,B_{\bar{r},\,m,\,\bar{s},\,i} \tag{9.9.55}$$

where $B_{\bar{r},m,\bar{s},i}$ is an influence function determined by the third formula (9.9.37).

For the second and third integrals on the right-hand side of (9.9.53), we obtain the relations:

$$\int_{s1-h}^{s_1}\frac{ds}{\sqrt{s_1-s}}\int_0^{r_1-h} D_j\frac{dr}{\sqrt{r_1-r}} = 4h\sum_{m=1}^{\bar{r}-1} D_j(mh,\ \bar{s}h)\,B_{\bar{r},\,m,\,\bar{s},\,\bar{s}} \tag{9.9.56}$$

$$\int_0^{s_1-h}\frac{ds}{\sqrt{s_1-s}}\int_{r_1-h}^{r_1} D_j\frac{dr}{\sqrt{r_1-r}} = 4h\sum_{i=1}^{\bar{s}-1} D_j(\bar{r}h,\ ih)\,B_{\bar{r},\,\bar{r},\,\bar{s},\,i} \tag{9.9.57}$$

where

$$B_{\bar{r},\,m,\,\bar{s},\,\bar{s}} = \sqrt{\bar{r}-m+1} - \sqrt{\bar{r}-m}; \quad B_{\bar{r},\,\bar{r},\,\bar{s},\,i} = \sqrt{\bar{s}-1+1} - \sqrt{\bar{s}-i} \tag{9.9.58}$$

For the fourth integral (9.9.53), we have the formula

$$\int_{s_1-h}^{s_1} \frac{d\varsigma}{\sqrt{s_1-s}} \int_{r_1-h}^{r_1} D_j \frac{dr}{r_1-r} = 4hD_j(\bar{r}h,\ \bar{s}h) \tag{9.9.59}$$

By summing all the above values of the integrals, from (9.9.52) we obtain relations for numerical calculations of the downwashes in a cell with the coordinates $\bar{r}$ and $\bar{s}$ (Fig. 9.9.3):

$$D_j^{(\mathrm{IV})}(\bar{r}h,\ \bar{s}h) = -\frac{\pi}{2h} F^{q}{}_{j}(\bar{r}^*h,\ \bar{s}^*h) - \sum_{m=1}^{\bar{r}-1}\sum_{i=1}^{\bar{s}-1} D_j(mh,\ ih)\, B_{\bar{r},\,m,\,\bar{s},\,i} \tag{9.9.60}$$

$$E_j^{(\mathrm{IV})}(\bar{r}h,\ \bar{s}h) = -\frac{\pi}{2h}\left[F^{\dot{q}}{}_{j}(\bar{r}^*h,\ \bar{s}^*h) + \frac{\alpha' h}{2}(\bar{r}+\bar{s}-\bar{r}^*-\bar{s}^*) F^{q}{}_{j}(\bar{r}^*h,\ \bar{s}^*h)\right] - \sum_{m=1}^{\bar{r}}\sum_{i=1}^{\bar{s}} E_j(mh,\ ih)\, B_{\bar{r},\,m,\,\bar{s},\,i} \tag{9.9.61}$$

We perform numerical integration by double summation over all the cells within the confines of an inverted Mach cone issuing from the point being considered $(\bar{r}h,\ \bar{s}h)$ excluding the initial cell (at the vertex) at which the downwash is determined. Its magnitude is found consecutively beginning from the cell on the trailing edge with the smallest coordinate $\bar{r}^*$ (for the starboard side) and $\bar{s}^*$ (for the port side). The coordinates of points on the trailing edge are related to the coordinates $\bar{r}$, $\bar{s}$ by the expressions

$$\bar{r}^* - \bar{s}^* = \bar{r} - \bar{s},\ \bar{r}^* < \bar{r},\ \bar{s}^* < \bar{s} \tag{9.9.62}$$

The calculations are performed as follows. The smallest values of the coordinates $\bar{r}^*$ and $\bar{s}^*$ are used to determine the derivatives $F^{q}{}_{j}(\bar{r}^*h,\ \bar{s}^*h)$, $F^{\dot{q}}{}_{j}(\bar{r}^*h,\ \bar{s}^*h)$ for the first cell, next the above relations are used to calculate the downwashes and influence functions for the entire region within the Mach cone issuing from the adjacent cell (with the coordinates $\bar{r}$ and $\bar{s}$).

After this, double summation of the products of the downwashes and the influence functions is performed, and the required values of the downwashes at a point with the coordinates $\bar{r}$ and $\bar{s}$ are found by formulas (9.9.60) and (9.9.61). Passing along a strip $\bar{r}$ = const ($\bar{s}$ = const) to the following cell with the coordinates $[(\bar{s}+1)\bar{h}, \bar{r}]$,

we repeat the calculations and find the corresponding value of the downwash in this cell. By performing similar calculations, the downwashes can be found on the entire vortex sheet behind the wing.

The values of the downwashes are used to determine the derivatives F^{qj} and $\dot{F}^{qj}$ at each point of the lifting surface. Next φ^{qj}, $\dot{\varphi}^{qj}$, and the corresponding values of the velocity potential φ are found (9.9.13). This quantity directly determines the pressure coefficient and the difference between its values on the bottom and upper sides of the wing [see formulas (9.6.20) and (9.6.21)].

The difference of the pressure coefficients (9.6.21) can be written as the series (9.6.7). The derivatives p^{qj} and $\dot{p}^{qj}$ in it are determined in terms of the values of F^{qj} and $\dot{F}^{qj}$; by using (9.6.24) and (9.6.25), we obtain the following relations:

$$\left.\begin{aligned} p^{qj}(\xi, \zeta) &= -\frac{4}{\alpha'}\frac{\partial F^{qj}(\xi_t, \zeta_t)}{\partial \xi_t} \\ \dot{p}^{qj}(\xi, \zeta) &= -\frac{4}{\alpha'^3}\left\{-\alpha' F^{qj}(\xi_t, \zeta_t)\right. \\ &\left. + M_\infty^2 \alpha' \left[\frac{\alpha'}{M_\infty^2}\frac{\partial \dot{F}^{qj}(\xi_t, \zeta_t)}{\partial \xi_t} - \xi_t \frac{\partial F^{qj}(\xi_t, \zeta_t)}{\partial \xi_t}\right]\right\} \end{aligned}\right\} \quad (9.9.63)$$

Hence, to find the derivatives of the difference of the pressure coefficients p^{qj} and $\dot{p}^{qj}$ determining the value of $\Delta\bar{p}$ [see (9.6.21)], it is necessary to calculate the derivatives $\partial F^{qj}/\partial \xi_t$ and $\partial \dot{F}^{qj}/\partial \xi_t$. There are different ways of calculating these derivatives. In aerodynamic calculations, particularly, the method of differences is used, in accordance with which

$$\frac{\partial F^{qj}}{\partial \xi_t} \approx \frac{\Delta F^{qj}}{\Delta \xi_t} = \frac{1}{h}\left[F^{qj}(\bar{r}+1, \bar{s}+1) - F^{qj}(\bar{r}, \bar{s})\right] \quad (9.9.64)$$

The derivative $\partial \dot{F}^{qj}/\partial \xi_t$ is calculated in a similar way. As a result, we can write the following relations for the values of p^{qj} and $\dot{p}^{qj}$:

$$\left.\begin{aligned} p^{qj}(\xi, \zeta) &= \frac{4}{\alpha' h}\left[F^{qj}(\bar{r}+1, \bar{s}+1) - F^{qj}(\bar{r}, \bar{s})\right] \\ \dot{p}^{qj}(\xi, \zeta) &= \frac{4}{\alpha'^3}\left\{-\alpha' F^{qj}(\bar{r}, \bar{s})\right. \\ &+ \frac{\alpha'^2}{h}\left[\dot{F}^{qj}(\bar{r}+1, \bar{s}+1) - \dot{F}^{qj}(\bar{r}, \bar{s})\right] \\ &\left. - \frac{M_\infty^2 \alpha'(\bar{r}+\bar{s})}{2}\left[F^{qj}(\bar{r}+1, \bar{s}+1) - F^{qj}(\bar{r}, \bar{s})\right]\right\} \end{aligned}\right\} \quad (9.9.65)$$

To improve the accuracy of calculating the derivatives (9.9.65), it is necessary that the values of F^{qj} and $\dot{F}^{qj}$ be found in more cells than the number in which p^{qj} and $\dot{p}^{qj}$ are found. Hence, in this case the interval $\Delta\xi_t$ can be increased m times (where m is an integer). Accordingly, the derivative

$$\frac{\partial F^{qj}}{\partial \xi_t} = \frac{1}{mh}\left[F^{qj}(\bar{r}+m,\ \bar{s}+m) - F^{qj}(\bar{r},\ s)\right] \qquad (9.9.66)$$

We determine the derivative $\partial \dot{F}^{qj}/\partial\xi_t$ in a similar way. With a view to the new values of $\partial F^{qj}/\partial\xi_t$ and $\partial \dot{F}^{qj}/\partial\xi_t$, we change formulas (9.9.65) for the derivatives p^{qj} and $\dot{p}^{qj}$. We use these derivatives to find by means of (9.6.9) the derivatives of the lift force, rolling moment, and pitching moment coefficients. As a result of substitutions of (9.9.63) into (9.6.9), where we assume that $x_k = b_0$, we obtain relations for these derivatives that can be written as follows:

$$\left.\begin{aligned} \alpha' c_y^{\alpha} &= c_{y,\,t}^{\alpha}, \quad \alpha'^3 \dot{c}_y^{\alpha} = \dot{c}_{y1,\,t}^{\alpha} + M_\infty^2 \dot{c}_{y2,\,t}^{\alpha} \\ \alpha' c_y^{\omega_z} &= c_{y,\,t}^{\omega_z}, \quad \alpha'^3 \dot{c}_y^{\omega_z} = \dot{c}_{y1,\,t}^{\omega_z} + M_\infty^2 \dot{c}_{y2,\,t}^{\omega_z} \end{aligned}\right\} \qquad (9.9.67)$$

$$\left.\begin{aligned} \alpha' m_z^{\alpha} &= m_{z,\,t}^{\alpha}, \quad \alpha'^3 \dot{m}_z^{\alpha} = \dot{m}_{z1,\,t}^{\alpha} + M_\infty^2 \dot{m}_{z2,\,t}^{\alpha} \\ \alpha' m_z^{\omega_z} &= m_{z,\,t}^{\omega_z}, \quad \alpha'^3 \dot{m}_z^{\omega_z} = \dot{m}_{z1,\,t}^{\omega_z} + M_\infty^2 \dot{m}_{z2,\,t}^{\omega_z} \end{aligned}\right\} \qquad (9.9.68)$$

$$\alpha'^2 m_x^{\omega_x} = m_{x,\,t}^{\omega_x}, \quad \alpha'^4 \dot{m}_x^{\omega_x} = \dot{m}_{x1,\,t}^{\omega_x} + M_\infty^2 \dot{m}_{x2,\,t}^{\omega_x} \qquad (9.9.69)$$

The following symbols have been used in these formulas

$$\left.\begin{aligned} c_{y,\,t}^{\alpha} &= \frac{4b_0^2\alpha'\lambda_w}{l^2} \int_{-l/(2b_0)}^{l/(2b_0)} \int_{\xi_{0,\,t}}^{\xi_t^*} \frac{\partial F^{qj}(\xi_t,\ \zeta_t)}{\partial \xi_t}\, d\xi_t,\ d\zeta_t \\ \dot{c}_{y1,\,t}^{\alpha} &= -\frac{4b_0^2\alpha'^2\lambda_w}{l^2} \int_{-l/(2b_0)}^{l/(2b_0)} \int_{\xi_{0,\,t}}^{\xi_t^*} F^{\alpha}(\xi_t,\ \zeta_t)\, d\xi_t\, d\zeta_t \\ \dot{c}_{y2,\,t}^{\alpha} &= \frac{4b_0^2\alpha'^2\lambda_w}{l^2}\left[\frac{\alpha'}{M_\infty^2} \int_{-l/(2b_0)}^{l/(2b_0)} \int_{\xi_{0,\,t}}^{\xi_t^*} \frac{\partial \dot{F}^{\alpha}(\xi_t,\ \zeta_t)}{\partial \xi_t}\, d\xi_t\, d\zeta_t \right. \\ &\quad \left. - \int_{-l/(2b_0)}^{l/(2b_0)} \int_{\xi_{0,\,t}}^{\xi_t^*} \frac{\partial F^{\alpha}(\xi_t,\ \zeta_t)}{\partial \xi_t}\, \xi_t\, d\xi_t\, d\zeta_t\right] \end{aligned}\right\} \qquad (9.9.70)$$

$$
\left.
\begin{aligned}
c_{y,\,t}^{\omega_z} &= \frac{4b_0^2\alpha'\lambda_w}{l^2}\int\limits_{-l/(2b_0)}^{l/(2b_0)}\int\limits_{\xi_{0,\,t}}^{\xi_t^*}\frac{\partial F^{\omega_z}(\xi_t,\,\zeta_t)}{\partial\xi_t}\,d\xi_t\,d\zeta_t\\
\dot{c}_{y1,\,t}^{\omega_z} &= -\frac{4b_0^2\alpha'^2\lambda_w}{l^2}\int\limits_{-l/(2b_0)}^{l/(2b_0)}\int\limits_{\xi_{0,\,t}}^{\xi_t^*}F^{\omega_z}(\xi_t,\,\zeta_t)\,d\xi_t\,d\zeta_t\\
\dot{c}_{y2,\,t}^{\omega_z} &= \frac{4b_0^2\alpha'^2\lambda_w}{l^2}\left[\frac{\alpha'}{M_\infty^2}\int\limits_{-l/(2b_0)}^{l/(2b_0)}\int\limits_{\xi_{0,\,t}}^{\xi_t^*}\frac{\partial\dot{F}^{\omega_z}(\xi_t,\,\zeta_t)}{\partial\xi_t}\,d\xi_t\,d\zeta_t\right.\\
&\quad\left.-\int\limits_{-l/(2b_0)}^{l/(2b_0)}\int\limits_{\xi_{0,\,t}}^{\xi_t^*}\frac{\partial F^{\omega_z}(\xi,\,\zeta)}{\partial\xi}\,\xi\,d\xi\,d\zeta\right]
\end{aligned}
\right\}\quad(9.9.71)
$$

$$
\left.
\begin{aligned}
m_{z,\,t}^{\alpha} &= \frac{4b_0^2\alpha'^2\lambda_w}{l^2}\int\limits_{-l/(2b_0)}^{l/(2b_0)}\int\limits_{\xi_{0,\,t}}^{\xi_t^*}\frac{\partial F^{\alpha}(\xi_t,\,\zeta_t)}{\partial\xi_t}\,\xi_t\,d\xi_t\,d\zeta_t\\
\dot{m}_{z1,\,t}^{\dot{\alpha}} &= -\frac{4b_0^2\alpha'^3\lambda_w}{l^2}\int\limits_{-l/(2b_0)}^{l/(2b_0)}\int\limits_{\xi_{0,\,t}}^{\xi_t^*}F^{\alpha}(\xi_t,\,\zeta_t)\,\xi_t\,d\xi_t\,d\zeta_t\\
\dot{m}_{z2,\,t}^{\dot{\alpha}} &= -\frac{4b_0^2\alpha'^3\lambda_w}{l^2}\left[\frac{\alpha'}{M_\infty^2}\int\limits_{-l/(2b_0)}^{l/(2b_0)}\int\limits_{\xi_{0,\,t}}^{\xi_t^*}\frac{\partial\dot{F}^{\dot{\alpha}}(\xi_t,\,\zeta_t)}{\partial\xi_t}\,\xi_t\,d\xi_t\,d\zeta_t\right.\\
&\quad\left.-\int\limits_{-l/(2b_0)}^{l/(2b_0)}\int\limits_{\xi_{0,\,t}}^{\xi_t^*}\frac{\partial F^{\alpha}(\xi_t,\,\zeta_t)}{\partial\xi_t}\,\xi_t^2\,d\xi_t\,d\zeta_t\right]
\end{aligned}
\right\}\quad(9.9.72)
$$

$$
\left.
\begin{aligned}
m_{z,\,t}^{\omega_z} &= \frac{4b_0^2\alpha'^2\lambda_w}{l^2}\int\limits_{-l/(2b_0)}^{l/(2b_0)}\int\limits_{\xi_{0,\,t}}^{\xi_t^*}\frac{\partial F^{\omega_z}(\xi_t,\,\zeta_t)}{\partial\xi_t}\,\xi_t\,d\xi_t\,d\zeta_t\\
\dot{m}_{z1,\,t}^{\omega_z} &= -\frac{4b_0^2\alpha'^3\lambda_w}{l^2}\int\limits_{-l/(2b_0)}^{l/(2b_0)}\int\limits_{\xi_{0,\,t}}^{\xi_t^*}F^{\omega_z}(\xi_t,\,\zeta_t)\,\xi_t\,d\xi_t\,d\zeta_t\\
\dot{m}_{z2,\,t}^{\omega_z} &= -\frac{4b_0^2\alpha'^3\lambda_w}{l^2}\left[\frac{\alpha'}{M_\infty^2}\int\limits_{-l/(2b_0)}^{l/(2b_0)}\int\limits_{\xi_{0,\,t}}^{\xi_t^*}\frac{\partial\dot{F}^{\omega_z}(\xi_t,\,\zeta_t)}{\partial\xi_t}\,\xi_t\,d\xi_t\,d\zeta_t\right.\\
&\quad\left.-\int\limits_{-l/(2b_0)}^{l/(2b_0)}\int\limits_{\xi_{0,\,t}}^{\xi_t^*}\frac{\partial F^{\omega_z}(\xi_t,\,\zeta_t)}{\partial\xi_t}\,\xi_t^2\,d\xi_t\,d\zeta_t\right]
\end{aligned}
\right\}\quad(9.9.73)
$$

$$\left.\begin{aligned} m^{\omega_x}_{x,\,t} &= -\frac{4b_0^2\alpha'^2\lambda_w}{l^2}\int\limits_{-l/(2b_0)}^{l/(2b_0)}\int\limits_{\xi_{0,\,t}}^{\xi_t^*}\frac{\partial F^{\omega_x}(\xi_t,\,\zeta_t)}{\partial\xi_t}\,\zeta_t\,d\xi_t\,d\zeta_t \\ \dot{m}^{\omega_x}_{x1,\,t} &= \frac{4b_0^2\alpha'^3\lambda_w}{l^2}\int\limits_{-l/(2b_0)}^{l/(2b_0)}\int\limits_{\xi_{0.\,t}}^{\xi_t^*}F^{\omega_x}(\xi_t,\,\zeta_t)\,\zeta_t\,d\xi_t\,d\zeta_t \end{aligned}\right\} \quad (9.9.74)$$

$$\dot{m}^{\omega_x}_{x2} = -\frac{4b_0^2\alpha'^3\lambda_w}{l^2}\left[\frac{\alpha'}{M_\infty^2}\int\limits_{-l/(2b_0)}^{l/(2b_0)}\int\limits_{\xi_{0,\,t}}^{\xi_t^*}\frac{\partial\dot{F}^{\omega_x}(\xi_t,\,\zeta_t)}{\partial\xi_t}\,\zeta_t\,d\xi_t\,d\zeta_t - \int\limits_{-l/(2b_0)}^{l/(2b_0)}\int\limits_{\xi_{0.\,t}}^{\xi_t^*}\frac{\partial F^{\omega_x}(\xi_t,\,\zeta_t)}{\partial\xi_t}\,\zeta_t\xi_t\,d\xi_t\,d\zeta_t\right] \quad (9.9.75)$$

It must be taken into consideration that the velocity potential on the leading edge is zero. Consequently,

$$F^{q_j}(\xi_{0,\,t},\,\zeta_t) = \dot{F}^{q_j}(\xi_{0,\,t},\,\zeta_t) = 0 \quad (9.9.76)$$

Accordingly,

$$\left.\begin{aligned} &\int\limits_{\xi_{0.\,t}}^{\xi_t^*}\frac{\partial F^{q_j}(\xi_t,\,\zeta_t)}{\partial\xi_t}\,d\xi_t = F^{q_j}(\xi_t^*,\,\zeta_t) \\ &\int\limits_{\xi_{0.\,t}}^{\xi_t^*}\frac{\partial F^{q_j}(\xi_t,\,\zeta_t)}{\partial\xi_t}\,\xi_t\,d\xi_t = \xi_t^*F^{q_j}(\xi_t^*,\,\zeta_t) - \int\limits_{\xi_{0.\,t}}^{\xi_t^*}F^{q_j}(\xi_t,\,\zeta_t)\,d\xi_t \\ &\int\limits_{\xi_{0.\,t}}^{\xi_t^*}\frac{\partial F^{q_j}(\xi_t,\,\zeta_t)}{\partial\xi_t}\,\zeta_t\,d\xi_t = \zeta_tF^{q_j}(\xi_t^*,\,\zeta_t) \\ &\int\limits_{\xi_{0,\,t}}^{\xi_t^*}\frac{\partial F^{q_j}(\xi_t,\,\zeta_t)}{\partial\xi_t}\,\zeta_t\xi_t\,d\xi_t = \zeta_t\xi_t^*F^{q_j}(\xi_t^*,\,\zeta_t) - \int\limits_{\xi_{0,\,t}}^{\xi_t^*}F^{q_j}(\xi_t,\,\zeta_t)\,\zeta_t\,d\xi_t \end{aligned}\right\} \quad (9.9.77)$$

$$\int_{\xi_{0,\,t}}^{\xi_t^*} \frac{\partial F^{q_j}(\xi_t, \zeta_t)}{\partial \xi_t} \xi_t^2 \, d\xi_t = \xi_t^{*2} F^{q_j}(\xi_t^*, \zeta_t) - \int_{\xi_{0,\,t}}^{\xi_t^*} \xi_t F^{q_j}(\xi_t, \zeta_t) \, d\xi_t$$

In a similar way, we shall write the relevant expressions related to the derivatives $F^{\dot{q}j}$. Let us go over in (9.9.70)-(9.9.75) to the characteristic coordinates s and r (9.9.28). Assuming that the velocity potential (or the function D) is constant in the cells and replacing the integrals with sums, with a view to (9.9.77) we obtain relations for numerical calculations of the derivatives of the aerodynamic coefficients.

These relations, used for finding by (9.9.67) the corresponding derivatives of the aerodynamic coefficients of the lift force c_y^{α}, $c_y^{\dot{\alpha}}$, $c_y^{\omega_z}$, $c_y^{\dot{\omega}_z}$, and also for determining from (9.9.68) the derivatives of the pitching moment coefficients m_z^{α}, $m_z^{\dot{\alpha}}$, $m_z^{\omega_z}$, $m_z^{\dot{\omega}_z}$ can be represented by the relations:

$$\left.\begin{aligned}
c_{y,\,t}^{\alpha} &= \frac{4b_0^2\alpha'\lambda_w}{l^2} h \sum_{\bar{r}^*} F^{\alpha}(\bar{r}^*, \bar{s}^*) \\
c_{y1,\,t}^{\dot{\alpha}} &= -\frac{4b_0^2\alpha'^2\lambda_w}{l^2} h^2 \sum_{S} \sum F^{\bar{\alpha}}(\bar{r}, \bar{s}) \\
c_{y,\,2t}^{\dot{\alpha}} &= \frac{4b_0^2\alpha'^2\lambda_w}{l^2} h \left\{ \frac{\alpha'}{M_\infty^2} \sum_{\bar{r}^*} F^{\dot{\bar{\alpha}}}(\bar{r}^*, \bar{s}^*) \right. \\
&\left. - \sum_{\bar{r}^*} [(\bar{r}^* + \bar{s}^*) h/2 + \xi_{0.0.t}] F^{\alpha}(\bar{r}^*, \bar{s}^*) + h \sum_{S} \sum F^{\alpha}(\bar{r}, \bar{s}) \right\}
\end{aligned}\right\} \quad (9.9.78)$$

$$\left.\begin{aligned}
c_{y,\,t}^{\omega_z} &= \frac{4b_0^2\alpha'\lambda_w}{l^2} h \sum_{\bar{r}^*} F^{\omega_z}(\bar{r}^*, \bar{s}^*) \\
c_{y1,\,t}^{\dot{\omega}_z} &= -\frac{4b_0^2\alpha'^2\lambda_w}{l^2} h^2 \sum_{S} \sum F^{\omega_z}(\bar{r}, \bar{s}) \\
c_{y2,\,t}^{\dot{\omega}_z} &= \frac{4b_0^2\alpha'^2\lambda_w}{l^2} h \left\{ \frac{\alpha'}{M_\infty^2} \sum_{\bar{r}^*} F^{\dot{\omega}_z}(\bar{r}^*, \bar{s}^*) \right.
\end{aligned}\right\} \quad (9.9.79)$$

$$
\left.
\begin{aligned}
&- \sum_{\bar{r}^*} [(\bar{r}^* + \bar{s}^*)\, h/2 + \xi_{0.\,0,\,t}]\, F^{\omega_z}(\bar{r}^*,\ \bar{s}^*) \\
&\qquad + h \sum_{S} \sum F^{\omega_z}(\bar{r},\ \bar{s}) \Big\} \\
m^{\alpha}_{z,\,t} = \frac{4b_0^2 \alpha'^2 \lambda_w}{l^2}\, h \Big\{ &\sum_{\bar{r}^*} [(\bar{r}^* + \bar{s}^*)\, h/2 + \xi_{0,\,0,\,t}]\, F^{\alpha}(\bar{r}^*,\ \bar{s}^*) \\
&\qquad - h \sum_{S} \sum F^{\alpha}(\bar{r},\ \bar{s}) \Big\} \\
m^{\dot{\bar{\alpha}}}_{z1,\,t} = -\frac{4b_0^2 \alpha'^3 \lambda_w}{l^2}\, h^2 &\sum_{S} \sum [(\bar{r} + \bar{s})\, h/2 + \xi_{0,\,0,\,t}]\, F^{\alpha}(\bar{r},\ \bar{s}) \\
m^{\dot{\bar{\alpha}}}_{z2,\,t} = \frac{4b_0^2 \alpha'^3 \lambda_w}{l^2}\, h \Big\{ &+ \frac{\alpha'}{M_\infty^2} \sum_{\bar{r}^*} [(\bar{r}^* + \bar{s}^*)\, h/2 \\
&+ \xi_{0,\,0,\,t}]\, F^{\dot{\bar{\alpha}}}(\bar{r}^*,\ \bar{s}^*) + 2h \sum_{S} \sum [(\bar{r} + \bar{s})\, h/2 \\
&+ \xi_{0,\,0,\,t}]\, F^{\alpha}(\bar{r},\ \bar{s}) - \frac{\alpha' h}{M_\infty^2} \sum_{S} \sum F^{\dot{\bar{\alpha}}}(\bar{r},\ \bar{s}) \\
&- \sum_{\bar{r}^*} [(\bar{r}^* + \bar{s}^*)\, h/2 + \xi_{0,\,0,\,t}]^2\, F^{\alpha}(\bar{r}^*,\ \bar{s}^*) \Big\}
\end{aligned}
\right\} \quad (9.9.80)
$$

The aerodynamic derivatives of the rolling moment coefficient are calculated by the following formulas:

$$
\left.
\begin{aligned}
m^{\omega_x}_{x,\,t} &= -\frac{4b_0^2 \alpha'^2 \lambda_w}{l^2}\, h \sum_{\bar{r}^*} [(\bar{s}^* - \bar{r}^*)\, h/2]\, F^{\omega_x}(\bar{r}^*,\ \bar{s}^*) \\
m^{\dot{\omega}_x}_{x1,\,t} &= \frac{4b_0^2 \alpha'^3 \lambda_w}{l^2}\, h^2 \sum_{S} \sum [(\bar{s} - \bar{r})\, h/2]\, F^{\omega_x}(\bar{r},\ \bar{s}) \\
m^{\dot{\omega}_x}_{x2,\,t} &= -\frac{4b_0^2 \alpha'^3 \lambda_w}{l^2}\, h \Big\{ \frac{\alpha'}{M_\infty^2} \sum_{\bar{r}^*} [(\bar{s}^* - \bar{r}^*)\, h/2]\, F^{\dot{\omega}_x}(\bar{r}^*,\ \bar{s}^*) \\
&- \sum_{\bar{r}^*} [(\bar{s}^* - \bar{r}^*)\, h/2]\, [(\bar{r}^* + \bar{s}^*)\, h/2 + \xi_{0,\,0,\,t}]\, F^{\omega_x}(\bar{r}^*,\ \bar{s}^*) \\
&\qquad + h \sum_{S} \sum [(\bar{s} - \bar{r})\, h/2]\, F^{\omega_x}(\bar{r}^*,\ \bar{s}^*) \Big\}
\end{aligned}
\right\} \quad (9.9.81)
$$

If we take the wing span l as the characteristic dimension when calculating the rolling moment coefficient, and the half-span $l/2$ when determining the kinematic parameter ω_x, then the new values of the rolling moment coefficient and the corresponding derivatives are determined by the relations

$$m_{x1}=m_x b_0/l,\quad m_{x1}^{\omega_{x1}}=2m_x^{\omega_x}(b_0/l)^2,\quad \dot{m}_{x1}^{\omega_{x1}}=4\dot{m}_x^{\omega_x}(b_0/l)^3 \tag{9.9.82}$$

By analogy with (9.9.69), we shall give the following working formulas for the derivatives:

$$\alpha' m_{x1}^{\omega_{x1}}=m_{x1,\,t}^{\omega_{x1}},\quad \alpha'^2\dot{m}_{x1}^{\omega_{x1}}=(\dot{m}_{x1,\,t}^{\omega_{x1}})_1+M_\infty^2(\dot{m}_{x1,\,t}^{\omega_{x1}})_2 \tag{9.9.83}$$

$$\left.\begin{aligned}
m_{x1,\,t}^{\omega_{x1}} &= -8\alpha'\lambda_w(b_0/l)^4 h\sum_{\bar r^*}[(\bar s^*-\bar r^*)h/2]F^{\omega_x}(\bar r^*,\ \bar s^*)\\
(\dot m_{x1,\,t}^{\omega_{x1}})_1 &= 16\alpha'\lambda_w(b_0/l)^5 h^2\sum_S\sum[(\bar s-\bar r)h/2]F^{\omega_x}(\bar r,\ \bar s)\\
(\dot m_{x1,\,t}^{\omega_{x1}})_2 &= -16\alpha'\lambda_w(b_0/l)^5 h\Big\{\frac{\alpha'}{M_\infty^2}\sum_{\bar r^*}[(\bar s^*-\bar r^*)h/2]\\
&\quad\times F^{\omega_x}(\bar r,\ \bar s)-\sum_{\bar r^*}[(\bar s^*-\bar r^*)h/2]\,|(\bar r^*+\bar s^*)h/2\\
&\quad+\xi_{0,\,0,\,t}|F^{\omega_x}(\bar r^*,\ \bar s^*)+h\sum_S\sum[(\bar s-\bar r)h/2]F^{\omega_x}(\bar r,\ \bar s)\Big\}
\end{aligned}\right\} \tag{9.9.84}$$

In the above relations, the symbol $\sum_{\bar r^*}$ signifies summation over the cells along the trailing edge, and the symbol $\sum_S\sum$, double summation over all the cells on the lifting surface.

When performing calculations of the total aerodynamic characteristics, one must have in view that these calculations are carried out in the system of coordinate axes depicted in Fig. 9.6.1 (with the rule of signs indicated in this figure). All the geometric quantities are measured and the pressure coefficients are found in the system of coordinates whose axis Oz passes through the vertex of the wing (see Fig. 9.11.1). When the mean aerodynamic chord b_0 is taken as the characteristic dimension, the aerodynamic coefficients and derivatives are found by converting the values of c_y, m_x, m_z, and their derivatives by the following formulas:

$$\left.\begin{aligned}
c_{y,\,A}&=c_y,\quad c_{y,\,A}^{\alpha}=c_y^{\alpha},\quad \dot c_{y,\,A}^{\dot\alpha}=\dot c_y^{\dot\alpha}b_0/b_A\\
c_{y,\,A}^{\omega_z}&=c_y^{\omega_z}b_0/b_A,\quad \dot c_{y,\,A}^{\omega_z}=\dot c_y^{\omega_z}(b_0/b_A)^2
\end{aligned}\right\} \tag{9.9.85}$$

$$\left.\begin{aligned} &m_{z,\,A} = m_z b_0/b_A,\quad m^{\alpha}_{z,\,A} = m_z b_0/b_A,\quad m^{\dot{\bar{\alpha}}_A}_{z,\,A} = m^{\dot{\bar{\alpha}}}_z (b_0/b_A)^2 \\ &m^{\omega_z,\,A}_{z,\,A} = m^{\omega_z}_z (b_0/b_A)^2,\quad m^{\dot{\omega}_z,\,A}_{z,\,A} = m^{\dot{\omega}_z}_z (b_0/b_A) \end{aligned}\right\} \quad (9.9.86)$$

$$m_{x,\,A} = m_x b_0/b_A,\quad m^{\omega_x,\,A}_{x,\,A} = m_x (b_0/b_A)^2,\quad m^{\dot{\omega}_x,\,A}_{x,\,A} = m^{\dot{\omega}_x}_x (b_0/b_A)^3 \quad (9.9.87)$$

In the above expressions, it is assumed that

$$\left.\begin{aligned} &\dot{\bar{\alpha}}_A = (d\alpha/dt)\, b_A/V_\infty,\quad \omega_{z,\,A} = \Omega_z b_A/V_\infty \\ &\dot{\omega}_{z,\,A} = (d\Omega_z/dt)\, b_A^2/V_\infty^2,\quad \dot{\omega}_{x,\,A} = (d\Omega_x/dt)\, b_0^2/V_\infty^2 \end{aligned}\right\} \quad (9.9.88)$$

9.10. Properties of Aerodynamic Derivatives

Let us consider the general properties of the aerodynamic derivatives as applied to finite-span wings with a constant leading and trailing-edge sweep. Investigations show that at low Strouhal numbers ($p^* \to 0$) the value of a derivative is a function of three arguments: $k\lambda_w = \lambda_w \sqrt{1 - M_\infty^2}$, $\tan \chi_0$, and η_w. These arguments, called similarity criteria, are determined, as can be seen, by the aspect ratio λ_w, the leading-edge sweep angle χ_0, the taper ratio η_w, and the Mach number M_∞. For an incompressible fluid, there are two such arguments: $\lambda_w \tan \chi_0$ and η_w. If a rectangular wing is being considered, it is necessary to assume that $\lambda_w \tan \chi_0 = 0$ and $\eta_w = 1$; for a triangular wing, $\eta_w = \infty$.

Diagrams characterizing the dependence of the stability derivatives on the similarity criteria for wings with a taper ratio of $\eta_w = 2$ in a *subsonic flow* are shown in Figs. 9.10.1-9.10.10 as illustrations.

The mean aerodynamic chord b_A has been taken as the characteristic dimension when calculating the data in these figures (the kinematic variables $\dot{\bar{\alpha}}_A$, $\omega_{z,A}$, $\dot{\omega}_{z,A}$, the coefficient $m_{z,A}$). This makes the dependence of the aerodynamic derivatives on the geometric parameters of the wing more stable, the results approaching the relevant quantities for rectangular wings.

When calculating the rolling moment m_{x1}, we chose the wing span l as the characteristic geometric dimension, while for the kinematic variables ω_{x1} and $\dot{\omega}_{x1}$ we took the half-span $l/2$. The origin of coordinates is on the axis of symmetry, while the axis Oz passes through the beginning of the mean aerodynamic chord b_A. When necessary, we can convert the obtained derivatives to another characteristic dimension and to a new position of the axis Oz.

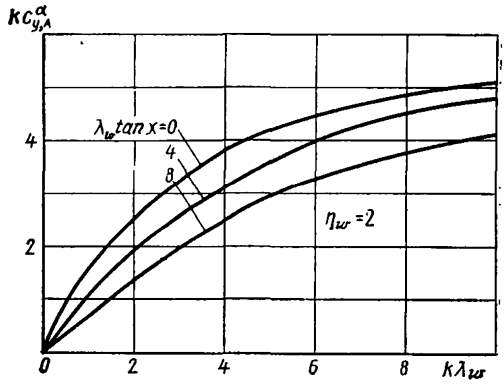

Fig. 9.10.1
Change in the quantity $kc^{\alpha}_{y,A}$ used in calculating the stability derivative c^{α}_{y} for a wing in a subsonic flow

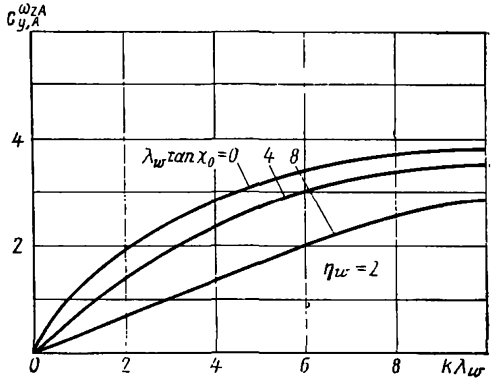

Fig. 9.10.2
Change in the quantity $kc^{\omega_z, A}_{y, A}$ determining the derivative $c^{\omega_z, A}_{y, A}$ for a wing at subsonic velocities

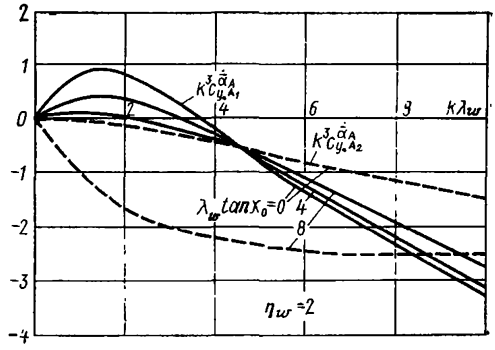

Fig. 9.10.3
Values of $k^3 c^{\dot{\alpha}_A}_{y, A1}$ and $k^3 c^{\dot{\alpha}_A}_{y, A2}$ characterizing the change in the derivative of the coefficient c_y with respect to $\dot{\alpha}_A$ for a lifting surface at $M_\infty < 1$

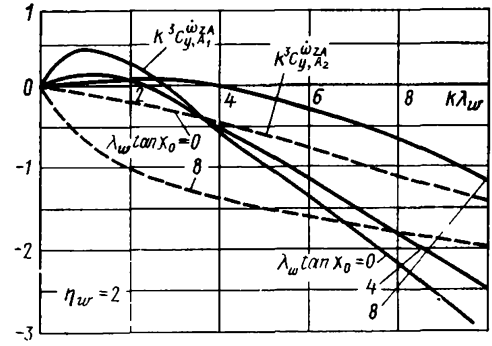

Fig. 9.10.4

Values of $k^3 c_{y,A1}^{\dot{\omega}_z}$ and $k^3 c_{y,A}^{\dot{\omega}_z}$ determining the derivative of $c_{y,A}$ with respect to $\omega_{z,A}$ for a subsonic flow over a wing

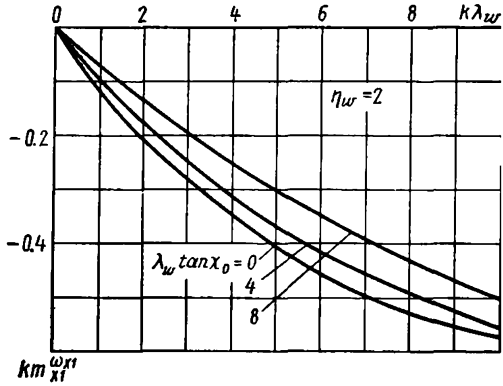

Fig. 9.10.5

Change in the variable $km_{x1}^{\dot{\omega}_{x1}}$ determining the derivative of the rolling moment coefficient with respect to ω_{x1} for a wing at $M_\infty < 1$

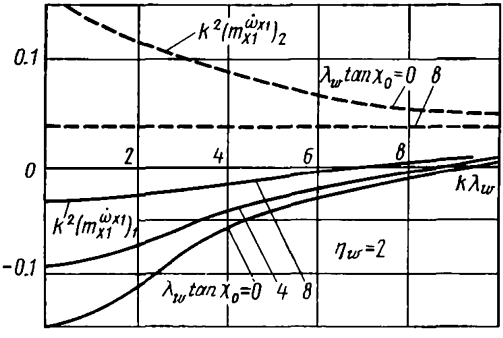

Fig. 9.10.6

Values of $k^2(m_{x1}^{\dot{\omega}_{x1}})_1$ and $k^2(m_{x1}^{\dot{\omega}_{x1}})_2$ characterizing the change in the rolling moment coefficient with respect to $\dot{\omega}_{x1}$ for a wing in a subsonic flow

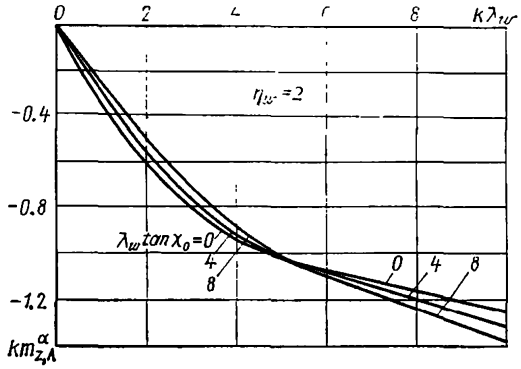

Fig. 9.10.7
Function $km^{\alpha}_{z,\,A}$ determining the derivative $m^{\alpha}_{z,\,A}$ for a wing in a subsonic flow

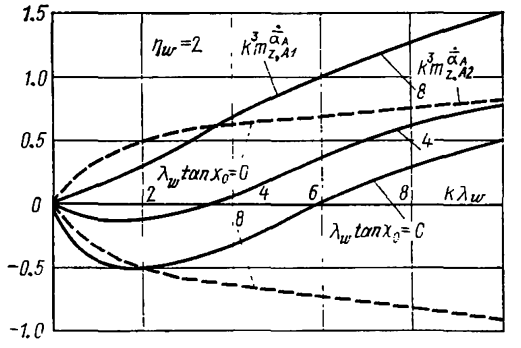

Fig. 9.10.8
Values of $k^3 m^{\dot{\alpha}}_{z,\,A1}$ and $k^3 m^{\dot{\alpha}}_{z,\,A2}$ determining the derivative $m^{\dot{\alpha}}_{z,\,A}$ for a wing at subsonic velocities

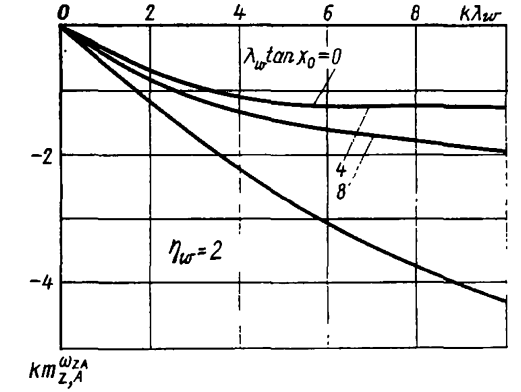

Fig. 9.10.9
Values of $km^{\omega_z}_{z,\,A}$ determining the derivative $m^{\omega_z}_{z,\,A}$ for a wing at $M_\infty < 1$

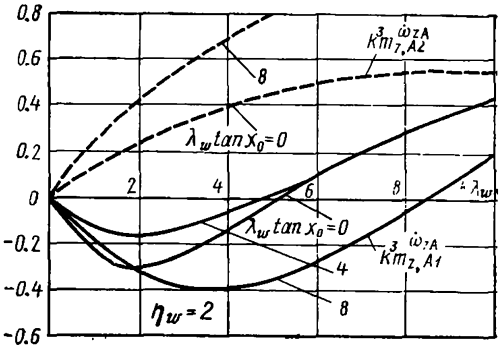

Fig. 9.10.10

Variables $k^3 m^{\dot{\omega}_{z,A}}_{z,A1}$ and $k^3 m^{\dot{\omega}_{z,A}}_{z,A2}$ characterizing the change in the derivative $m^{\dot{\omega}_{z,A}}_{z,A}$ for a wing at $M_\infty < 1$

According to the data shown in Figs. 9.10.1-9.10.10, the aerodynamic derivatives are determined as follows:

$$c_y^{\alpha} = (kc_y^{\alpha})/k, \quad \dot{c}_{y,A}^{\dot{\alpha}_A} = [(k^3 \dot{c}_{y,A1}^{\dot{\alpha}_A}) + M_\infty^2 (k^3 \dot{c}_{y,A2}^{\dot{\alpha}_A})]/k^3 \quad (9.10.1)$$

$$c_{y,A}^{\omega_{z,A}} = (kc_{y,A}^{\omega_{z,A}})/k, \quad \dot{c}_{y,A}^{\dot{\omega}_{z,A}} = [(k^3 \dot{c}_{y,A1}^{\dot{\omega}_{z,A}}) + M_\infty^2 (k^3 \dot{c}_{y,A2}^{\dot{\omega}_{z,A}})]/k^3 \quad (9.10.2)$$

$$m_{x1}^{\omega_{x1}} = (km_{x1}^{\omega_{x1}})/k, \quad \dot{m}_{x1}^{\dot{\omega}_{x1}} = [(k^2 \dot{m}_{x1}^{\dot{\omega}_{x1}})_1 + M_\infty^2 (k^2 \dot{m}_{x1}^{\dot{\omega}_{x1}})_2]/k^2 \quad (9.10.3)$$

$$m_{z,A}^{\alpha} = (km_{z,A}^{\alpha})/k, \quad \dot{m}_{z,A}^{\dot{\alpha}_A} = [(k^3 \dot{m}_{z,A1}^{\dot{\alpha}_A}) + M_\infty^2 (k^3 \dot{m}_{z,A2}^{\dot{\alpha}_A})]/k^3 \quad (9.10.4)$$

$$m_{z,A}^{\omega_{z,A}} = (km_{z,A}^{\omega_{z,A}})/k, \quad \dot{m}_{z,A}^{\dot{\omega}_{z,A}} = [(k^3 \dot{m}_{z,A1}^{\dot{\omega}_{z,A}}) + M_\infty^2 (k^3 \dot{m}_{z,A2}^{\dot{\omega}_{z,A}})]/k^3 \quad (9.10.5)$$

We can use the graphs (Figs. 9.10.1-9.10.10) to find the stability derivatives for the entire range of subsonic numbers M_∞, including an unsteady incompressible flow ($M_\infty = 0$, $k = 1$). The data of these graphs point to the increase in the lifting capacity of the wings when going over from an incompressible ($M_\infty = 0$) to a compressible fluid ($M_\infty < 1$). Here the stability derivatives at $M_\infty < 1$ can be calculated sufficiently accurately according to the Prandtl-Glauert compressibility rule $c = c_{1c}(1 - M_\infty^2)^{-1/2}$, where c and c_{1c} are aerodynamic variables in a compressible and incompressible fluid, respectively. The lower the aspect ratio, the smaller is the action of the compressibility, i.e. the smaller is the influence of the number $M_\infty < 1$. This is due to the fact that the disturbances introduced into a flow attenuate with a decrease in the cross-sectional dimensions of a wing, i.e. with a decrease in the aspect ratio.

Near the tips of a wing in a subsonic flow, the air flows from the bottom side where the pressure is higher to the upper one. This leads

to lowering of the lifting capacity of the wing. The intensity of such overflow grows with a decrease in the aspect ratio of a wing; consequently, an increase in this aspect ratio improves the lifting capacity.

An analysis of the influence of the leading-edge sweep angle χ_0 shows that its growth leads to an appreciable diminishing of the derivative c_y^{α} for a wing with a high aspect ratio. At small aspect ratios. the influence of the angle χ_0 is virtually absent because in this case even an insignificant change in χ_0 leaves the planform of the wing almost unchanged.

A change in the taper ratio η_w at given values of λ_w and χ_0 has a slight effect on the lifting capacities, especially for low aspect ratios of a wing. The explanation is that at $M_\infty < 1$ most of the lift force is produced by the lifting surface near the leading edges, which is especially noticeable with low aspect ratios. A large value of the taper ratio η_w (at $\chi_0 = \text{const}$) corresponds, as it were, to cutting off a part of the poorly lifting tail surface of the wing.

An analysis of the found values of the centre of pressure coefficient $c_p = x_p b_0 = m_{z,A} \cdot c_{y,A}$ (where x_p is the distance to the centre of pressure from the front of the mean aerodynamic chord) allows us to conclude that the quantity c_p grows with an increase in the sweep angles (the centre of pressure is displaced more noticeably to the tail). The aspect ratio affects c_p in the same way as the angle χ_0. At low values of λ_w, however (of the order of 0.5 and below), the position of the centre of pressure does not virtually change.

The derivatives $m_{z,A}^{\dot{\omega}_z}$ and $m_{x1}^{\dot{\omega}_{x1}}$ that characterize damping in oscillatory motion grow with an increase in the aspect ratio λ_w. This indicates an increase in the damping upon longitudinal unsteady motion and rolling of the wing. The above graphs allow us to conclude that the influence of the sweep angle and taper ratio on the damping of low-aspect-ratio wings is relatively small. The above-mentioned derivatives together with the quantity $m_{z,A}^{\alpha}$ characterizing the longitudinal static stability grow with increasing subsonic numbers M_∞.

Aerodynamic derivatives capped with dots depend greatly on the aspect ratio λ_w in the subsonic region. The values of the derivatives grow with an increasing number M_∞. The change in the dotted derivatives, i.e. in the aerodynamic characteristics that are purely unsteady, is especially great at near-sonic velocities. At numbers $M_\infty \to 1$, the magnitudes of the derivatives with dots grow appreciably, and their signs change. A typical feature here is the growing influence of the wing planform on the aerodynamic variables for a non-stationary unsteady flow.

The data characterizing the change in the non-stationary derivatives for a wing at *supersonic velocities* are presented in Figs. 9.10.11-9.10.20. According to these data, the stability derivatives are deter-

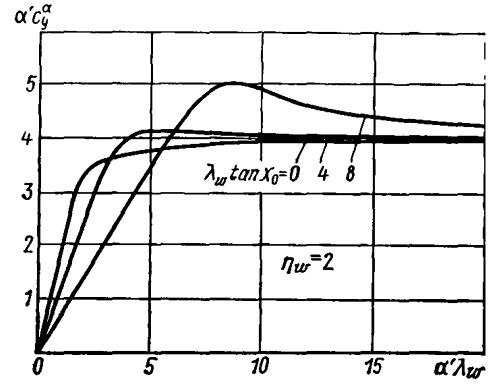

Fig. 9.10.11
Values of $\alpha' c_y^\alpha$ determining the stability derivative c_y^α for a wing in a supersonic flow

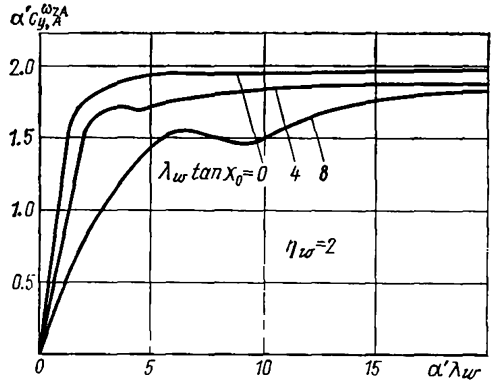

Fig. 9.10.12
Change in the quantity $\alpha' c_{y,A}^{\omega_{z,A}}$ determining the derivative $c_{y,A}^{\omega_{z,A}}$ for a wing at supersonic velocities

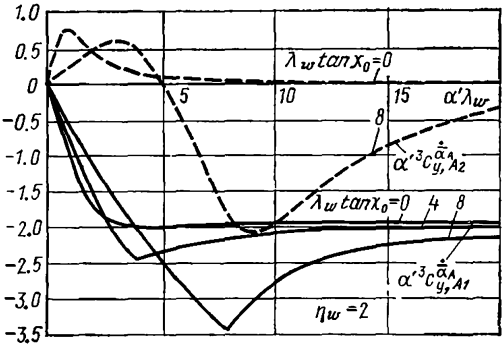

Fig. 9.10.13
Relations for $\alpha'^3 c_{y,A1}^{\dot{\bar{\alpha}}_A}$ and $\alpha'^3 c_{y,A2}^{\dot{\bar{\alpha}}_A}$ characterizing the change in the derivative of the coefficient c_y with respect to $\dot{\bar{\alpha}}_A$ for a wing at $M_\infty > 1$

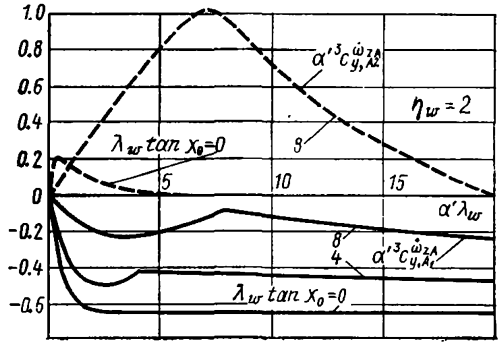

Fig. 9.10.14

Values of $\alpha'^3 c_{y,A1}^{\dot{\omega}_{z,A}}$ and $\alpha'^3 c_{y,A2}^{\dot{\omega}_{z,A}}$ determining the derivative of c_y with respect to $\dot{\omega}_{z,A}$ in a supersonic flow over a wing

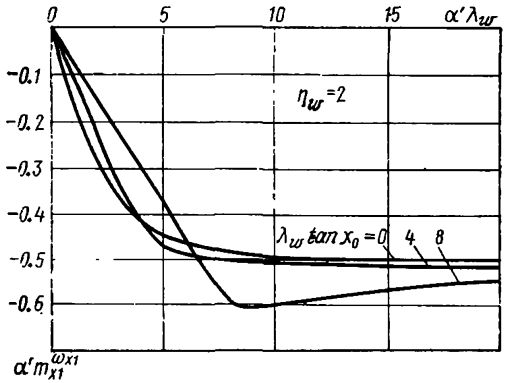

Fig. 9.10.15

Function $\alpha' m_{x1}^{\dot{\omega}_{x1}}$ characterizing the change in the derivative of the rolling moment coefficient with respect to ω_{x1} for a wing at $M_\infty > 1$

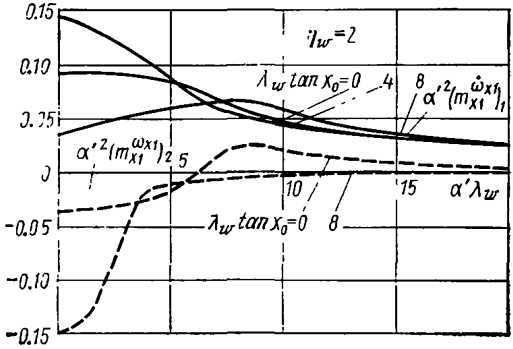

Fig. 9.10.16

Values of $\alpha'^2 (m_{x1}^{\dot{\omega}_{x1}})_1$ and $\alpha'^2 (m_{x1}^{\dot{\omega}_{x1}})_2$ characterizing the change in the derivative of the rolling moment coefficient with respect to $\dot{\omega}_{x1}$ for a wing in a supersonic flow

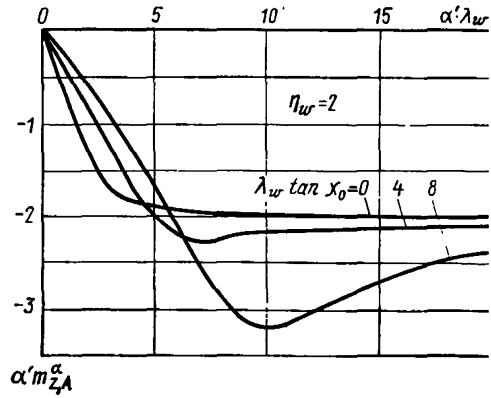

Fig. 9.10.17
Variable $\alpha' m^{\alpha}_{z,A}$ determining the derivative $m^{\alpha}_{z,A}$ for a wing at $M_\infty > 1$

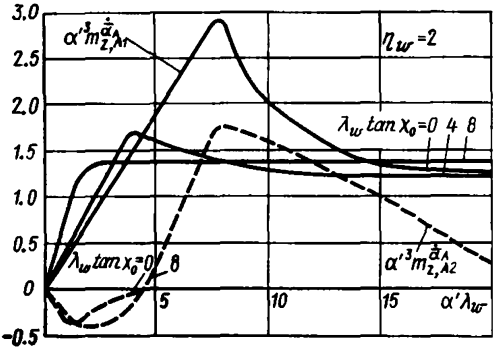

Fig. 9.10.18
Values of $\alpha'^3 m^{\dot{\alpha}_A}_{z,A1}$ and $\alpha'^3 m^{\dot{\alpha}_A}_{z,A2}$ determining the derivative $m^{\dot{\alpha}_A}_{z,A}$ for a wing in a supersonic flow

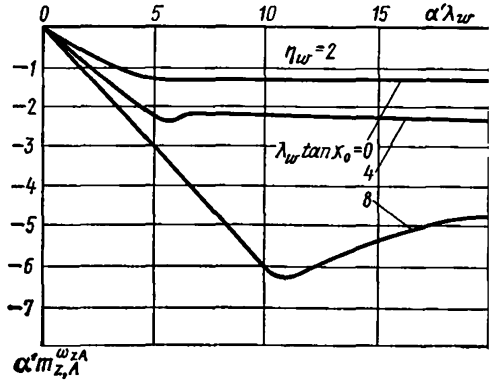

Fig. 9.10.19
Function $\alpha' m^{\omega_z, A}_{z,A}$ determining the derivative $m^{\omega_z, A}_{z,A}$ for a wing at $M_\infty > 1$

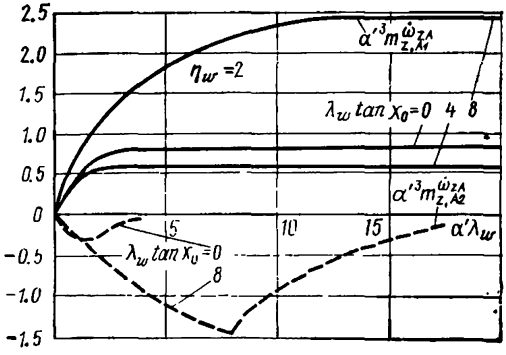

Fig. 9.10.20

Variables $\alpha\, {}^3m^{\dot{\omega}_{z,A}}_{z,A_1}$ and $\alpha'^3 m^{\dot{\omega}_{z,A}}_{z,A_2}$ characterizing the change in the derivative $m^{\dot{\omega}_{z,A}}_{z,A}$ in a supersonic flow

mined with the aid of formulas (9.10.1)-(9.10.5) in which the quantity $k = \sqrt{1 - M_\infty^2}$ is replaced with $\alpha' = \sqrt{M_\infty^2 - 1}$.

The graphs allow us to arrive at the conclusion that the lifting capacities of wings at $M_\infty > 1$ grow with an increase in the aspect ratio. although to a smaller extent than at subsonic velocities. Particularly, for a rectangular wing ($\chi_0 = 0$), the increase in c_y^α when $M_\infty > 1$ occurs only up to $\lambda_w = 3$-4, and then the derivative c_y^α remains virtually constant. For triangular wings, the constancy of c_y^α is observed beginning from $\alpha'\lambda_w \geqslant 4$, i.e. when the leading edges transform from subsonic into supersonic ones.

The derivatives of longitudinal and lateral damping ($m^{\omega_{z,A}}_{z,A}$ and $m^{\omega_{x1}}_{x1}$), as with subsonic velocities, grow (in magnitude) with an increase in the aspect ratio. Their change for low-aspect-ratio wings is only slightly influenced by the sweep angle and the taper ratio. Unlike the case when $M_\infty < 1$, at supersonic velocities the derivatives $m^{\omega_{z,A}}_{z,A}$ and $m^{\omega_{x1}}_{x1}$, and also m_z^α decrease when M_∞ increases.

The dotted aerodynamic derivatives change to a smaller extent under the influence of the wing aspect ratio at $M_\infty > 1$. But they grow in magnitude at supersonic flow near values of $M_\infty > 1$. For these velocities, as when $M_\infty < 1$, a sharp change in the magnitude of the non-stationary derivatives is also attended by a change in their signs.

At large numbers M_∞ ($M_\infty \geqslant 2.5$-3.0), the aerodynamic derivatives with dots decrease, tending to zero at $M_\infty \to \infty$. The influence of the planform on their values is not so great at the usual velocities (sub- or supersonic), but becomes considerably greater in the transonic region where the number M_∞ equals unity or is somewhat larger than it.

9.11. Approximate Methods for Determining the Non-Stationary Aerodynamic Characteristics

Hypotheses of Harmonicity and Stationarity

The harmonicity of oscillations, which is the basis of the method of calculating non-stationary aerodynamic characteristics set out above, reflects only a partial, idealized scheme of unsteady flow over a craft. In the general form, such flow may be characterized by other time dependences of the kinematic parameters. At present, methods have been developed that can be used for unsteady flows described by any functions. But owing to their great intricacy, it is not always possible to use them in practice.

It is therefore necessary to have less strict and sufficiently simple methods of calculating the total and local non-stationary aerodynamic characteristics. One such method is based on what is called the **hypothesis of harmonicity** (see [19]). By this hypothesis, an aerodynamic coefficient for unsteady flow is represented by series (9.6.8) in which the stability derivatives c^{q_j}, $c^{\dot{q}_j}$, and others are functions of the mean angle of attack α_0, the Mach, Reynolds, and Strouhal numbers for a given wing.

In the linear theory of flow of an ideal fluid, such a relation is limited to the Mach and Strouhal numbers. According to this theory, the aerodynamic derivatives depend very slightly on the Strouhal number for low-aspect-ratio wings of any planform at all numbers M_∞ when the latter are large. We can assume that in a first approximation this is also true for any other time dependence of the kinematic variables. But now with any function describing wing motion, the stability derivatives can be taken from the results of calculations or experiments obtained for a harmonic change in the kinematic variables, and the values of these variables can be determined on the basis of their true time dependences for the given mode of motion.

This is the essence of the harmonicity hypothesis. It allows us to obtain more accurate results when the stability derivatives depend less on the Strouhal number. When solving problems on the flight stability of craft, the Strouhal numbers p^* quite rarely exceed values of 0.05-0.07. Consequently, in practice, we may use the non-stationary characteristics for $p^* \to 0$ with sufficient accuracy and, therefore, proceed in our calculations from the harmonicity hypothesis.

The harmonicity hypothesis allows us to obtain more accurate results if the change in the kinematic variables can be represented by a smaller number of terms in the Fourier series corresponding to a narrower spectrum of frequencies characterizing this change.

When studying non-stationary flow over craft, researchers use rather widely what is known as the steadiness hypothesis. The content of this hypothesis consists in that all the aerodynamic characteristics are determined only by instantaneous values of the angle of attack.

The local values of the pressure coefficients are the same as in stationary flow at an angle of attack equal to its true value at the given instant. According to this hypothesis used in the linear theory, the aerodynamic coefficient is

$$c_y\ (t) = c_y^{\alpha}\alpha\ (t) \tag{9.11.1}$$

where $\alpha\ (t)$ is the true angle of attack at the given instant, and c_y^{α} is the stability derivative in steady flow.

If a craft rotates about its lateral axis at the angular velocity Ω_z, the expanded hypothesis of steadiness is used according to which

$$c_y(t) = c_y^{\alpha}\alpha\ (t) + c_y^{\omega_z}\omega_z\ (t) \tag{9.11.2}$$

Experimental investigations show that the hypothesis of harmonicity yields more correct results than that of steadiness. This is especially noticeable for wings with low aspect ratios. An increase in the aspect ratios is attended by larger errors because at large values of λ_w the dependence of the aerodynamic derivatives on the Strouhal number becomes more appreciable. This is not taken into account in the approximate methods.

Tangent-Wedge Method

According to this method, in a stationary supersonic linearized flow over a thin sharp-nosed airfoil, the pressure coefficient at a certain point is determined according to the local angle of inclination of a tangent to the airfoil contour $\alpha - \beta_N$ (for the upper side), and $\alpha - \beta_L$ (for the bottom side), i.e. the corresponding value of this coefficient is the same as that of a local tangent surface of a wedge. By formulas (7.5.20) and (7.5.20′), in which we assume that $\beta_N = \beta$ on the bottom and $\beta_L = -\beta$ on the upper side of the airfoil, at the corresponding points we have

$$\bar{p}_b = 2(\alpha+\beta)/\sqrt{M_\infty^2 - 1},\quad \bar{p}_u = -2(\alpha-\beta)/\sqrt{M_\infty^2 - 1} \tag{9.11.3}$$

where β is the local angle of inclination of the contour calculated with a view to the sign for the upper side of the airfoil.

With account taken of these data, the difference of the pressure coefficients on the bottom and upper sides is

$$\Delta\bar{p} = \bar{p}_b - \bar{p}_u = 4\alpha/\alpha' \tag{9.11.4}$$

where $\alpha' = \sqrt{M_\infty^2 - 1}$.

It is presumed that formula (9.11.4) for $\Delta\bar{p}$ can also be applied to non-stationary flow if instead of α we adopt the value of the local summary angle of attack determined from boundary condition (9.6.32) in the form

$$\alpha_\Sigma = -v/V_\infty = \alpha + \omega_{x1}\bar{z} - \omega_z\bar{x} \tag{9.11.5}$$

where $\bar{x} = x/b_0$, $\bar{z} = 2z/l$, and $\omega_{x1} = \Omega_x l/(2V_\infty)$ [with a view to the chosen coordinate system, the sign of $\omega_z x$ has been changed in comparison with (9.6.32)].

Let us write $\Delta\bar{p}$ in the form of a series:

$$\Delta\bar{p} = p^{\alpha}\alpha + p^{\omega_{x1}}\omega_{x1} + p^{\omega_z}\omega_z \tag{9.11.6}$$

Substituting for $\Delta\bar{p}$ in (9.11.6) its value from (9.11.4), but using α_Σ from (9.11.5) instead of α, we find the aerodynamic derivatives:

$$p^{\alpha} = 4/\alpha', \quad p^{\omega_{x1}} = 4\bar{z}/\alpha', \quad p^{\omega_z} = -4\bar{x}/\alpha' \tag{9.11.7}$$

According to the tangent-wedge method, for all wings we have

$$c_y^{\dot{\alpha}} = c_y^{\dot{\omega}_z} = m_z^{\dot{\alpha}} = m_z^{\dot{\omega}_z} = m_{x1}^{\dot{\omega}_{x1}} = 0 \tag{9.11.8}$$

Knowing the quantity (9.11.7), we can find the stability derivatives:

$$\left.\begin{aligned} c_y^{\alpha} &= \frac{\lambda_w b_0}{l}\int_0^1\int_{\bar{x}_0}^{\bar{x}_1} p^{\alpha}\,d\bar{x}\,d\bar{z}; \quad c_y^{\omega_z} = \frac{\lambda_w b_0}{l}\int_0^1\int_{\bar{x}_0}^{\bar{x}_1} p^{\omega_z}\,d\bar{x}\,d\bar{z} \\ m_{x1}^{\omega_{x1}} &= -\frac{\lambda_w}{2}\int_0^1\int_{\bar{x}_0}^{\bar{x}_1} p^{\omega_{x1}}\bar{z}\,d\bar{x}\,d\bar{z} \\ m_z^{\alpha} &= \frac{\lambda_w b_0}{l}\int_0^1\int_{\bar{x}_0}^{\bar{x}_1} p^{\alpha}\bar{x}\,d\bar{x}\,d\bar{z}; \quad m_z^{\omega_z} = \frac{\lambda_w b_0}{l}\int_0^1\int_{\bar{x}_0}^{\bar{x}_1} p^{\omega_z}\bar{x}\,d\bar{x}\,d\bar{z} \end{aligned}\right\} \tag{9.11.9}$$

We locate the origin of the coordinates at the nose of the centre chord of a wing (Fig. 9.11.1). We adopt the centre chord b_0 as the characteristic dimension for m_z and ω_z, and the span l and half-span $l/2$, respectively, for m_{x1} and ω_{x1}. For such a wing, the equations of the leading and trailing edges in the dimensionless form are as follows:

$$\left.\begin{aligned} \bar{x}_0 &= \frac{x_0}{b_0} = -\frac{(\eta_w+1)\,\eta_w \tan\gamma_0}{4\eta_w}\,\bar{z} \\ \bar{x}_1 &= \frac{x_1}{b_0} = -1 + \left(\frac{\eta_w-1}{\eta_w} - \frac{\eta_w+1}{\eta_w}\,\frac{\lambda_w\tan\chi_0}{4}\right)\bar{z} \end{aligned}\right\} \tag{9.11.10}$$

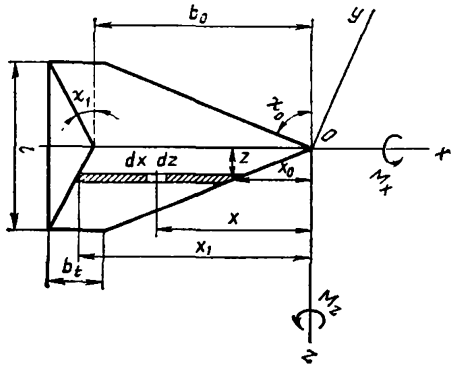

Fig. 9.11.1
Diagram of a wing in the calculation of stability derivatives according to the method of local wedges

Let us write the ratio of the centre chord to the span and the aspect ratio of a wing:

$$b_0/l = 2\eta_w/[\lambda_w(\eta_w + 1)], \quad \lambda_w = l^2/S = 2\eta_w l/[(\eta_w + 1)\, b_0] \tag{9.11.11}$$

The tangent of the sweep angle along the trailing edge is

$$\tan\chi_1 = \tan\chi_0 - (2b_0/l)(1 - 1/\eta_w) \tag{9.11.12}$$

Introducing (9.11.10) and (9.11.7) into (9.11.9), we obtain the stability derivatives of a wing:

$$c_y^{\alpha} = \frac{4}{\alpha'}, \quad c_y^{\omega_z} = \frac{4}{\alpha'}\left[\frac{\eta_w^2+\eta_w+1}{3\eta_w(\eta_w+1)} + \frac{\eta_w+2}{3\eta_w}\cdot\frac{\lambda_w\tan\chi_0}{4}\right] \tag{9.11.13}$$

$$m_{x1}^{\omega_{x1}} = -\frac{1}{3\alpha'}\,\frac{\eta_w+3}{\eta_w+1} \tag{9.11.14}$$

$$m_z^{\alpha} = -c_y^{\omega_z}, \quad m_z^{\omega_z} = -\frac{2}{3\alpha'}\left[\frac{\eta_w^2+1}{\eta_w^2} + \frac{\eta_w^2+2\eta_w+3}{\eta_w^2}\cdot\frac{\lambda_w\tan\gamma_0}{4}\right.$$
$$\left. + \frac{\eta_w^2+4\eta_w+3}{\eta_w^2}\left(\frac{\lambda_w\tan\gamma_0}{4}\right)^2\right] \tag{9.11.15}$$

In the particular case of rectangular wings for which $\tan\chi_0 = 0$ and $\eta_w = 1$, we have

$$c_y^{\alpha} = 4/\alpha', \quad c_y^{\omega_z} = 2/\alpha' \tag{9.11.16}$$

$$m_{x1}^{\omega_{x1}} = -2/(3\alpha') \tag{9.11.17}$$

$$m_z^{\alpha} = -2/\alpha', \quad m_z^{\omega_z} = -4/(3\alpha') \tag{9.11.18}$$

For triangular wings ($\eta_w = \infty$ and $\lambda_w \tan \chi_0 = 4$), we have

$$c_y^{\alpha} = 4/\alpha', \quad c_y^{\omega_z} = 8/(3\alpha') \tag{9.11.19}$$

$$m_{x1}^{\omega_{x1}} = -1/(3\alpha') \tag{9.11.20}$$

$$m_z^{\alpha} = -8/(3\alpha'), \quad m_z^{\omega_z} = -2/\alpha' \tag{9.11.21}$$

It must be noted that the tangent-wedge method makes it possible to determine only the aerodynamic derivatives without dots. The results obtained coincide with the accurate solutions according to the linear theory for infinite-span rectangular wings, and also for triangular wings with supersonic leading edges, at small Strouhal numbers ($p^* \to 0$). For finite-aspect-ratio wings, the tangent-wedge method yields more accurate solutions when the numbers M_∞ and the aspect ratios λ_w are larger.

References

1. Sedov, L.I. *Similarity and Dimensional Methods in Mechanics*, trans. by Kisin, Mir Publishers, Moscow (1982).
2. Sedov, L.I. *A Course of Continuum Mechanics*, Vols. I-IV. Croningen, Wolters-Noorthoff (1971-1972).
3. Khristianovich, S.A. *Obtekanie tel gazom pri bol'shikh skorostyakh* (High-Speed Flow of a Gas over a Body), Nauch. trudy TsAGI, vyp. 481 (1940).
4. Belotserkovsky, S.M. and Skripach, B.K. *Aerodinamicheskie proizvodnye letatel'nogo apparata i kryla pri dozvukovykh skorostyakh* (Aerodynamic Derivatives of a Craft and a Wing at Subsonic Velocities), Nauka, Moscow (1975).
5. Loitsyansky, L.G. *Mekhanika zhidkosti i gaza* (Fluid Mechanics), Nauka, Moscow (1970).
6. Predvoditelev, A.S., Stupochenko, E.V., Ionov, V.P., Pleshanov, A.S., Rozhdestvensky, I.B., and Samuĭlov, E.V. *Termodinamicheskie funktsii vozdukha dlya temperatur ot 1000 do 12 000 K i davlenii ot 0.001 do 1000 atm—grafiki funktsii* (Thermodynamic Functions of Air for Temperatures from *1000 to 12 000* K and Pressures from 0.001 to 1000 atm—Graphs of Functions), Izd. AN SSSR, Moscow (1960).
7. Predvoditelev, A.S., Stupochenko, E.V., Samuĭlov, E.V., Stakhanov, I.P., Pleshanov, A.S., and Rozhdestvensky, I.B. *Tablitsy termodinamicheskikh funktsii vozdukha (dlya temperatur ot 6000 do 12 000 K i davlenii ot 0.001 do 1000 atm)* [Tables of Thermodynamic Functions of Air (for Temperatures from 6000 to 12 000 K and Pressures from 0.001 to 1000 atm)], Izd. AN SSSR, Moscow (1957).
8. Kibardin, Yu.A., Kuznetsov, S.I., Lyubimov, A.N., and Shumyatsky, B.Ya. *Atlas gazodinamicheskikh funktsii pri bol'shikh skorostyakh i vysokikh temperaturakh vozdushnogo potoka* (Atlas of Gas-Dynamic Functions at High Velocities and High Temperatures of an Air Stream), Gosenergoizdat, Moscow (1961).
9. Kochin, N.E., Kibel, I.A., and Roze, N.V. *Teoreticheskaya gidromekhanika* (Theoretical Hydromechanics), Parts I, II, Fizmatgiz, Moscow (1963).
10. Fabrikant, I.Ya. *Aerodinamika* (Aerodynamics), Nauka, Moscow (1964).
11. Arzhanikov, N.S. and Sadekova, G.S. *Aerodinamika bol'shikh skorostei* (High-Speed Aerodynamics), Vysshaya shkola, Moscow (1965).
12. Irov, Yu.D., Keil, E.V., Pavlukhin, B.N., Porodenko, V.V., and Stepanov, E.A. *Gazodinamicheskie funktsii* (Gas-Dynamic Functions), Mashinostroenie, Moscow (1965).
13. Mkhitaryan, A.M. *Aerodinamika* (Aerodynamics), Mashinostroenie, Moscow (1976).

14. Krasnov, N.F., Koshevoi, V.N., Danilov, A.N., and Zakharchenko, V.F. *Aerodinamika raket* (Rocket Aerodynamics), Vysshaya shkola, Moscow (1968).
15. Rakhmatulin, Kh.A., Sagomonyan, A.Ya., Bunimovich, A.I., and Zverev, I.N. *Gazovaya dinamika* (Gas Dynamics), Vysshaya shkola, Moscow (1965).
16. Arzhanikov, N.S. and Mal'tsev, V.N. *Aerodinamika* (Aerodynamics), Oborongiz, Moscow (1956).
17. Krasilshchikova, E.A. *Krylo konechnogo razmakha v szhimaemom potoke* (A Finite-Span Wing in a Compressible Flow), Gostekhizdat, Moscow (1962).
18. Lebedev, A.A. and Chernobrovkin, L.S. *Dinamika poleta* (Flight Dynamics), Mashinostroenie, Moscow (1973).
19. Belotserkovsky, S.M., Skripach, B.K., and Tabachnikov, V.G., *Krylo v nestatsionarnom potoke gaza* (A Wing in an Unsteady Gas Flow), Nauka, Moscow (1971).

Supplementary Reading

Courant, R. and Friedrichs, K.O. *Supersonic Flow and Shock Waves*. New York, Interscience (1948).
Ginzburg, I.P. *Aerodinamika* (Aerodynamics). Moscow, Vysshaya shkola (1966).
Hayes, W.D. and Probstein, R.F. *Hypersonic Flow Theory*. New York, Academic Press (1959).
Krasnov, N.F. (Ed.). *Prikladnaya aerodinamika* (Applied Aerodynamics). Moscow, Vysshaya shkola (1974).
Kuethe, S. *Foundations of Aerodynamics*, 3rd ed. New York, Wiley (1976).
Landau, L.D. and Lifshits, E.M. *Mekhanika sploshnykh sred* (Continuum Mechanics). Moscow, Gostekhizdat (1968).
Liepmann, H.W. and Puckett, A.E. *Introduction to Aerodynamics of a Compressible Fluid*. New York, Wiley; London, Chapman & Hall (1948).
Liepmann, H.W. and Roshko, A. *Elements of Gasdynamics*. New York, Wiley (1957).
Milne-Thomson, L.M. *Theoretical Aerodynamics*. London, MacMillan (1958).
Mironer, A. *Engineering Fluid Mechanics*. New York, McGraw-Hill (1979).
Oswatitsch, K. *Gas Dynamics* (English version by G. Kuerti). New York, Academic Press (1956).
Schlichting, H. *Boundary Layer Theory*, 6th ed. New York, McGraw-Hill (1968).
Sedov, L. *Two-Dimensional Problems in Hydrodynamics and Aerodynamics*. New York, Wiley (1965).

Name Index

Arzhanikov, N. S., 111, 238, 255, 256, 275, 276, 493, 494

Babenko, K. I., 2
Belotserkovsky, O. M., 23
Belotserkovsky, S. M., 22, 23, 398, 419, 427, 431, 433, 436, 451, 452, 455, 460, 488, 493, 494
Bernoulli, D., 13
Bunimovich, A. I., 209, 494
Burago, G. F., 275

Chaplygin, S. A., 15, 21, 22, 250, 269
Chernobrovkin, L. S., 384, 494
Cherny, G. G., 2
Copal, Z., 22
Courant, R., 494

Danilov, A. N., 193, 494
Dorodnitsyn, A. A., 19, 21, 23

Euler, L., 13, 11

Fabrikant, I. Ya., 95, 493
Falkovich, S. V., 22
Frankl, F. I., 21, 22, 206, 394
Friedrichs, K. O., 494

Garabedian, P., 23
Ginzburg, I. P., 494
Glauert, H., 21
Golubev, V. V., 21
Gromeka, I. S., 134, 136

Hayes, W. D., 494
Helmholtz, H. L. F., 251

Ionov, V. P., 61, 62, 66, 165, 188, 493
Irov, Yu. D., 153, 157, 493
Iyevlev, V. M., 19

Joukowski, *see* Zhukovsky

Kalikhman, L. E., 19
Karman, T. von, 19
Karpovich, E. I., 22
Keil, E. V., 153, 157, 493
Keldysh, M. V., 21, 22
Khristianovich, S. A., 21, 269, 270, 271, 273, 493
Kibardin, Yu. A., 62, 63, 67, 188, 493
Kibel, I. A., 19, 22, 82, 111, 493
Kochin, N. E., 19, 82, 111, 493
Koshevoi, V. N., 193, 494
Krasilshchikova, E. A., 22, 269, 381, 494
Krasnov, N. F., 193, 494
Kuethe, S., 494
Kuznetsov, S. I., 62, 63, 67, 188, 493

Landau, L. D., 494
Lavrentyev, M. A., 21, 22
Lebedev, A. A., 384, 494
Lenin, V. I., 15
Liepmann, H. W., 494
Lifshits, E. M., 494
Lighthill, M., 23
Loitsyansky, L. G., 19, 30, 493
Lyubimov, A. N., 62, 63, 67, 188, 493

Mal'tsev, V. N., 238, 255, 256, 275, 276, 494
Melnikov, A. P., 19
Meyer, T., 279
Milne-Thomson, L. M., 494
Mironer, A., 494
Mkhitaryan, A. M., 165, 255, 256, 493

Navier, A., 19
Nekrasov, A. I., 22
Newton, I., 32

Oswatitsch, K., 494

Pavlukhin, B. N., 153, 157, 493
Petrov, G. I., 19
Pleshanov, A. S., 61, 62, 66, 67, 165, 188, 493
Porodenko, V. V., 153, 157, 493
Prandtl, L., 19, 21, 32, 279
Predvoditelev, A. S., 61, 62, 66, 67, 165, 188, 493
Probstein, R. F., 494
Puckett, A. E., 494

Rakhmatulin, Kh. A., 209, 494
Reynolds, O., 19
Roshko, A., 494
Roze, N. V., 82, 111, 493
Rozhdestvensky, I. B., 61, 62, 63, 67, 165, 188, 493

Sadekova, G. S., 111, 493
Sagomonyan, A. Ya, 209, 494
Samuĭlov, E. V., 61, 62, 66, 67, 165, 188, 493
Schlichting, H., 494
Sedov, L. I., 17, 20, 21, 22, 493, 494
Shumyatsky, B. Ya., 62, 63, 67, 188, 493
Skripach, B. K., 23, 398, 419, 427, 431, 433, 436, 451, 452, 455, 460, 488, 493, 494
Stakhanov, I. P., 61, 62, 66, 67, 165, 188, 493
Stepanov, E. A., 153, 157, 493
Stokes, G. G., 19
Struminsky, V. V., 19
Stupochenko, E. V., 61, 62, 66, 165, 188, 493

Tabachnikov, V. G., 398, 419, 427, 431, 451, 452, 455, 460, 488, 494
Taylor, G. I., 32

Voskresensky, G. P., 22

Zakharchenko, V. F., 193, 494
Zhukovsky, N. E., 15, 21, 250
Zverev, I. N., 209, 494

Subject Index

Ablation, 15
Acceleration,
  resultant, 72f
  vector, 72, 113
Adiabat, shock, 172, 184
Aerodynamic coefficients,
  airfoil, 294
  conversion from one aspect ratio to another, 258ff
  dynamic components, 398
  and similarity method, 139ff
  static components, 398
  unsteady flow, 416ff
Aerodynamics,
  ablating surfaces, 23
  blunt-nosed bodies, 23
  bodies of revolution, 22
  boundary layer, 19
  classification, 17
  continuum, 19f
  controls, 22
  definition, 13
  development, 13
  experimental, 15
  force, 17f
  high-speed, 14f, 18, 59
  hulls, 22
  hypersonic, 18
  ideal fluid, 18
  incompressible fluid, 18
  interference, 23
  low-speed, 14
  optimal shapes, 24
  radiating gas, 131
  rarefied gases, 20
  steady-state, 20
  subsonic, 18
  supersonic, 18, 59
  transonic, 18
Aerodynamics,
  unsteady, 20, 436
  wing, 21f
Aerohydrodynamics, 14
Aerothermodynamics, 18
Air, *see also* Flow(s), Gas
  diatomic model, 67, 69
  dissociating, equation of state, 65
  dissociation and ionization, 192f
  motion at high speeds, 14
  structure in dissociation, 67
Aircraft, 20, *see also* Craft
Airfoil,
  aerodynamic forces, 293f
  arbitrary configuration, 285ff
  in compressible flow, 264ff
  drag, 278
  fictitious, 270f
  in hypersonic flow, 291f, 297
  longitudinal force, 293
  in mid-span section, 337
  polar, 296
  sharp-nosed, 285f
    curved, 290f
  sideslipping wing, 299ff
  in supersonic flow, 285ff
  symmetric, 297ff, 317ff, 321ft
  thin,
    in incompressible flow, 234ff
    in nearly uniform flow, 293
    in subsonic flow, 264ff,
  total drag, 275
  wedge-shaped, 297f
Angle(s),
  attack, 38f
    balance, 52
    in normal section, 301f
    optimal, 47
    true, 252

Angle(s),
balance rudder, 58
banking, 39
control surface, 407f
course, 39
downwash, 251f
span-averaged, 252f, 255, 257
total, 253
elevator, 407
flow deflection, 220f
behind shock, 166, 176f, 189
critical, 176f, 182
hypersonic velocities, 221
and shock angle, 182f
flow deviation, *see* Angle, flow deflection
Mach, 161, 212
pitching, 39f
rolling, 39f
rudder, 407
setting, 252, 260f
shock, 167f
oblique, 176ff
and velocity, 189
sideslip, 38f, 52
sweep, 299f, 363
ultimate flow, 221f
yawing, 39f
zero lift, 240
Approach,
Eulerian, 72
Lagrangian, 71f
Axis,
doublet, 102
flight path, 37
lateral, 37
lateral body, 38
lift, 37
longitudinal body, 38
normal, 38

Backpressure, 155f
Balancing, longitudinal, 56f
Boundary conditions, 132ff, 424
dimensionless equations, 145
linearized flow, 310ff
unsteady flow, 451
on vortex sheet, 312, 424
and wall temperature, 145
Boundary layer, 34ff
thickness, 36
turbulent core, 36

Centering, 55
central, 55
Centering,
neutral, 56
Centre,
aerodynamic, 50f, 55
angle-of-attack, 51
coordinate, 240
elevator deflection, 51
sideslip angle, 58
force reduction, 404
moments, 36f
pressure, 48
and aerodynamic centre, 51
conical flow, 363
Centre-of-pressure coefficient, 49, 295, 297, 389, 483
compressible flow, 274
nearly uniform flow, 240
pentagonal wing, 371
sideslipping wing, 302
symmetric airfoil, 297ff
tetragonal wing, 365
wedge-shaped airfoil, 298
Characteristics, 208ff
aerodynamic,
rectangular wing, 385ff
triangular wing, 349
unsteady motion, 394ff
conjugate, 210, 212
determination, 209f
in hodograph, 214, 282
first family, 210ff, 216, 219, 222f
kind, 209f
nodal point, 227
orthogonality, 213f
in physical plane, 210f
second family, 210ff, 216, 219, 222f
stability, 413ff
Chord,
local, wing, 259
mean aerodynamic, 45, 262
mean geometric, 45
wing, 45
in wing section with optimal planform, 258
Circulation,
flow, 103f, 243, 430
intensity, of vortex, 236f
velocity, 91ff, 236, 311, 428f, 434
in vortex-free flow 92
vortex, 439, 447
Coefficient(s),
aerodynamic, *see* Aerodynamic coefficients
centre-of-pressure, *see* Centre-of-pressure coefficient
correlation, 30
one-point, 31
two-point, 30

Coefficient(s),
damping, 414f
longitudinal, 403
rolling, 403
yawing, 403
drag, *see* Drag coefficient
Lame's, 82f, 85, 87
lateral-force, 44, 400
lateral linear deformation, 109
lateral motion, 406
lift, *see* Lift coefficient
longitudinal-force, 44, 296, 399
longitudinal moment, 297
compressible flow, 303
longitudinal motion, 406
moment, *see* Moment coefficient
normal-force, 44, 51, 56f, 296, 397, 448f, 456
compressible flow, 303
and stability derivatives, 400, 405f
pitching-moment, 43, 49, 51, 363, 401, 404f, 416ff, 448f, 456
body axis, 44
pressure, *see* Pressure coefficient
pressure-drop, 284
rolling-moment, 43, 401, 416ff, 448f
body axis, 44
spiral, 403
side-force, 43
stagnation pressure, behind shock, 175
static lateral stability, 57
static longitudinal stability, 54f
suction force, 306f, 383f
vortex drag, 315
wave drag, 277f, 283, 350, 387
induced, 315
wing drag, 315
yawing-moment, 43, 401
body axis, 44
spiral, 403
Compressibility, gas, 14, 16, 58f
influence on non-stationary flow, 452ff
Conditions,
boundary, *see* Boundary conditions
Chaplygin-Zhukovsky, 428, 431
compatability, 209
at infinity, 425
initial, 132
Cauchy's, 206
Conductivity, thermal, 63f
and pressure, 63
and temperature, 63f
Cone,
disturbance, 160, 315, 319
Cone,
Mach, 160, 315, 319
inverted, 319
tip, 371
Contour,
multiply connected, 94
simply connected, 94
Controllability, craft, 395
Controls,
fast-response, 407
inertiafree, 407
Coordinate systems,
body axis, 37
curvilinear, 82ff
cylindrical, 82f
fixed, 37
flight path, 37
local geographic, 39
normal earth-fixed, 39
spherical, 82f
wind, 38
Core(s),
turbulent, 36
vortex, 256
semi-infinite, 253
Correction, Prandtl-Glauert, 268
Cosines, direction, 40
Craft,
banking, 410
controllability, 395
fast-response, 407
inertiafree, 407
manoeuvrability, 395
thermal protection, 23
Criterion(a), similarity, 17, 140ff, 187
hypersonic, 284f
Curl, velocity, 78
Curves,
characteristic, *see* Characteristics
equipotential, 90

Decrement, logarithmic, 414
Deformation, *see also* Strain
relative linear, 108f
relative volume, 109
wing surface, 451
Degree(s),
dissociation, 60
equilibrium, 69
and pressure, 60
and temperature, 60
freedom, inert, 194
ionization, 60f
static lateral stability, 57
static longitudinal stability, 54f
Density(ies),
characteristic, for dissociation, 69

Density(ies),
critical, 152, 154
in jet, 153
ratio, 165, 172f, 184, 188, 189ff
limiting, 186
reduced mass, 157
source distribution, 316f
stagnation, 151, 153, 192
Derivatives,
aerodynamic,
and aspect ratio, 483
properties, 478ff
circulation, 466
stability, *see* Stability derivatives
time, 396f
Diagram,
enthalpy-entropy, 66f
phase, caloric, 67
Diffusion, gas, 121
Diffusivity, thermal, 128
Dimensions, characteristic, 44f
Dissociation, 60, 189ff
Disturbance(s), 159
cone, 160
propagation, 159f
source, 159
in subsonic flow, 160
supersonic, 319
in supersonic flow, 160
Divergence, velocity, 86
Doublet, 102f
axis, 102
distribution function, 354, 358, 360
incompressible flow, 360f
supersonic linearized flow, 360
moment, 102, 354
potential function, 354f
power, 354
in supersonic flow, 353ff
velocity potential, 103
Downwash(es), 250ff, 465f
disturbed region, 465ff
semi-rate, 77
on vortex sheet, 467ff
wing, 468
Drag, 38, 42
friction, 44
induced, 252
nose, 44
overall, 44
pressure, 44
profile, 275
total, 275, 314, 384
wave, 276f, 283
wing, 381ff
total, 384
Drag coefficient, 42, 140, 296
airfoil, 333f
Drag coefficient,
dimensionless, 145
distribution over wing span, 341
friction, 350
induced, 252f, 256f, 261, 384
and lift coefficient, 296
minimum, 47
overall, 44, 339, 341, 350
sideslipping wing, 302, 304
symmetric airfoil, 298f
tetragonal wing, 337ff, 345ff
thin wing, 381
wedge-shaped airfoil, 298

Edge(s),
combined, 463
leading, *see* Leading edge(s)
side, *see* Tip(s)
trailing, *see* Trailing edge(s)
Effect,
Magnus, 403
mid-span, 301
sideslip, 300
tip, 301
Energy,
dissipation, 127
equation, 124ff
particle, 124ff
supplied by conduction, 125
supplied by diffusion, 125f
supplied by radiation, 126
Enthalpy, 65
stagnation, 151, 185
Entropy,
gradient, 216
non-dissociating perfect gas, 170
at stagnation point, 191
Epicycloids, 219f
Equation(s), *see also* Formula
Abel, 468
adiabat, shock, 172, 184
Bernoulli, 137f
Cauchy-Riemann, 97
Chaplygin, 269
characteristic, 208, 218
in hodograph, 219ff
non-isentropic flow, 219
roots, 209f
vortex-free flow, 219
continuity, 80ff, 164, 200f, 423f
in Cartesian coordinate system, 81f
in dimensionless variables, 142f
flow along curved surface, 88
incompressible flow, 81
linearized flow, 309
for potential motion, 81, 85f

Equation(s),
continuity,
steady flow, 81, 85, 88f
two-dimensional flow, 81, 88
unsteady flow, 81
coupling, 254, 257
diffusion, 121
in Cartesian coordinate system, 123
in cylindrical coordinate system, 122f
dimensionless, 142f
and boundary conditions, 145
energy, 124ff, 175
conservation, 165
in dimensionless variables, 143
two-dimensional plane motion, 127
Euler, 113, 136
flow rate, 89
gas dynamics,
fundamental, 129, 201, 309
system, 129ff, 144
Gromeka's, 134, 36
hodograph, 180
Hugoniot, 172f
integro-differential, 254
kinematics, fundamental, 201
Lagrange, 135
Laplace, 81f, 266
mass flow rate, 156ff
momentum conservation, 164
motion,
axisymmetric form, 117
curvilinear coordinates, 114f
cylindrical coordinates, 116f
in dimensionless variables, 142
disturbed, 413
ideal gas, 134
inviscid fluid, 113, 200f
linearized flow, 308
particle, 106
potential, 81, 85f
spherical coordinates, 118ff
steady flow, 117
two-dimensional, 119, 200f
vector form, 113f
viscous fluid, 113
Navier-Stokes, 112f
oblique shock, 163ff, 169f
basic, 171
pathline, 71
potential function, 367ff
speed of sound, 264
state,
diatomic gas mixture, 69f
dissociating gas, 65
perfect gas, 65
Equation(s),
steady flow, 136
stream function, differential, 205
two-dimensional flow, near curved surface, 120f
velocity potential, 201f, 264, 309f, 372ff
linearization, 264f
vortex, 203f
vortex lines, 91
wave, 423ff
Equilibrium,
stable, 52
static, 52f
trim, of craft, 52
unstable, 52
Exponent, adiabatic, 26, 61f

Factor, local friction, 42
Fall, free, 409f
Fan, Prandtl-Meyer (expansion), 280, 285f
Field,
pressure, 326, 330
velocity, 71
Filament,
stream, 74
vortex, 429
strength, 433f
Fineness, 284, *see also* Ratio, lift-to-drag
Flow(s), *see also* Motion(s)
at angle of attack, 243ff, 351ff
axisymmetric, 117, 200f, 222
basic kinds, 17
boundary condition, 451
in boundary layer, 17, 19
circulation (circulatory), 103f, 243, 430
calculations, 439ff
compressible, 264ff, 274, 302f, 306
over circular cylinder, 241
conical, 355ff, 386
cross, 359
along curved surface, 88
disturbed, 420
from supersonic source, 319f
downwash, 457, *see also* Downwash
equilibrium, 194ff
expanding radial, 231
expansion, 220
fictitious incompressible, 270f
forward, 391f
plane-parallel, 98f
free, 17
external, 35
streamline, 132

Flow(s),
over hexagonal wing, 366ff
hypersonic, over thin airfoil, 291f
incompressible, 90, 240ff, 249ff, 360f
cross, 359
over flat plate, 243ff
velocity potential, 105
inviscid, 17, 35, 200f
isentropic, 138, 149ff, 222, 290f, 420f
isotropic, 31
laminar, 28
lateral, 299
linearized, 264f, 297, 308ff, 360
longitudinal, 299
nearly uniform, 235, 282, 293
at angle of attack, 351ff
linearized, 264
pressure, 235
velocity, 235
non-circulatory, 242f, 431
non-equilibrium, 193ff
behind shock, 197f
non-isentropic, 219, 222
one-dimensional, 158
parallel, 98, 249f
stream function, 98
streamlines, 98
velocity potential, 98
plane, 123, 222
over plate, 241ff
potential, 79, 104, 201f, 356
Prandtl-Meyer, 279, 285
at hypersonic velocities, 281f
limiting case, 286
purely subsonic, 275
from reservoir, 154ff
reverse, 391f
without separation, 132f, 145
two-dimensional, plane, 133
velocity ratio, 133
behind shock, 174f
steady, 73, 117, 122f, 200f
non-potential, 136f
potential, 136f
subcritical, 176
subsonic, 302f
stability derivatives, 478ff
over thin airfoil, 264f
supercritical, 177, 274ff
supersonic, 211, 282, 308ff, 353ff
over airfoil, 285ff
disturbed, 222ff
over finite-span wing, 308ff, 385
over rectangular wing, 385
over sharp-nosed airfoil, 285f, 290f
Flow(s),
stability derivatives, 483ff
over tetragonal wing, 344
over thin plate, 269ff
over thin wing, 315f, 385
unsteady, 425, 456ff
over wings, 315f
over symmetric airfoil wing, 312
tetragonal, 331ff, 343ff
over tetragonal wing, 331ff, 343ff
over thin plate, 243
three-dimensional,
disturbed, 308
steady, 309
transverse, 359
over thin plate, 240ff
over triangular wing, 355ff
two-dimensional, 89f
axisymmetric, 200f
near curved surface, 120f
isentropic, 222
non-isentropic, 222
plane, 200f, 211, 264
spatial, 119, 211
supersonic, 211
vortex, 202
vortex-free, 219
turbulent, 28ff
quasi-steady, 31
unsteady, 73, 146, 394, 416ff, 425, 456ff
deformable wing, 451
nearly uniform, 421
velocity, in jet, 150f
viscous, 17, 19
in boundary layer, 134
pressure, 110
vortex, 78, 202, 309
steady, 89
vortex-free, 79ff, 92, 219, 309
Fluid,
barotropic, 420, 423
ideal,
integrals of motion, 134ff
pressure, 26ff
incompressible, 158
inviscid, *see* Fluid, ideal
viscous, 127
Fluid mechanics, 14, 18
Force(s),
aerodynamic, airfoil, 293f
body, 27
complex, 246f
conversion to another coordinate system, 40f
dissipative, 127
drag, 38, 42, *see also* Drag
gyroscopic, 403f

Force(s),
lateral, 38
lift, 38, 42, 250f, 254
flat plate, 248, 393
maximum, 47
nearly uniform flow, 236
rectangular wing, 386
total, 315
triangular wing, 362
longitudinal, 38, 44, 293
mass, 27
external, work, 124
on moving body, 25ff
normal, 38, 416f
produced by pressure, 293
ponderomotive, 27
side, 38, 42
suction, 249, 382ff
correction factor, 383f
sideslipping wing, 305ff
triangular wing, 362
surface, 25f, 107f
work, 124f
viscous, 146
Formula, *see also* Equation(s)
Biot-Savart, 95
conversion, coordinate systems, 82ff
Euler, 97
Karman-Tsien, 268
Prandtl-Glauert, 268, 302, 306
Reynolds generalized, 33f
Sutherland's, 63
Zhukovsky, 248
Zhukovsky-Chaplygin, 247
Frequency, oscillations, 414
Friction, *see also* Viscosity
in turbulent flow, 32ff
Function,
conformal, 240f
dissipative, 127
doublet distribution, 354, 358, 360f
potential, 79, 243, 354f, 367ff, 457, *see also* Velocity potential
derivatives, 458
doublet, 354f
gradient, 80
stream, 89f, 98, 202

Gas, *see also* Air, Flow(s), Fluid
compressibility, 14, 16, 58f, 452ff
conduction of electricity, 19
diatomic, mean molar mass, 70
diffusion, 121
dissociation, 60, 189ff
dynamics, 14f, *see also* Aerodynamics, high-speed
Gas,
equations, 129ff, 144
flow from reservoir, 154ff
heating, 59ff
ideal, 134, 149, *see also* Gas, perfect
interaction with body, 15f, 18
ionization, 189f
jet, configuration, 149f
kinetic coefficients, 63f
mixture, 67
mean molar mass, 70
parameters, at stagnation point, 191
perfect, *see also* Gas, ideal
calorically, 65
equation of state, 65
thermally, 65
recombination, 60
stream, configuration, 149f
viscous, flow in boundary layer, 134
Gradient,
entropy, 216
normal velocity, 32
potential function, 80
pressure, 107
velocity, 34

Half-wing, infinite triangular, 321
Heat, specific, 61f
Heating, aerodynamic, 15, 18, 23
Hodograph, 179ff
Hypothesis,
absence of reverse influence, 17
continuum, 16, 20
harmonicity, 488f
Khristianovich's, 273
Newton's, 32
plane sections, 253f
Prandtl's, 32f
steadiness, 17, 489
expanded, 489
stress-strain proportionality, 108
Zhukovsky-Chaplygin, 244

Instability,
dynamic, 394
static, 53, 415
directional, 57f
lateral, 57
longitudinal, 54f
Integral(s),
Bernoulli, 138
Couchy-Lagrange, 420ff
linearized expression, 421

Integral(s)
Lagrange, 135
motion, 134ff
Intensity,
source distribution, 318
turbulence, 29
vortex circulation, 236f
Interaction,
body-plasma, 19
chemical, 15, 18
force, 15
mechanical, 15
terms, 402
thermal, 15, 18
Interference, aerodynamic, 20f
Ionization, 60, 189f
thermal, 60
Isobars, 66f
Isochors, 66f
Isotherms, 66f

Law,
Dalton's, 69
elliptic, circulation distribution, 258f
energy conservation, 124, 165
Fourier, 125
mass conservation, 80
momentum conservation, 164
Newton's friction, 32
thermodynamics, second, 181
Layer, boundary, *see* Boundary layer
Leading edge(s), 367
sonic, 316, 363, 365, 384
subsonic, 303ff, 316, 326f, 331ff, 351ff, 355ff, 366ff, 381ff
supersonic, 303f, 316, 330f, 351f, 372ff, 385
sweep parameter, 316f
Length,
mixing, 34
relaxation, 198
Level, turbulence, 29
Lift, 38, 42, *see also* Force, lift
Lift coefficient, 43, 253ff, 296, 315
compressible flow, 274
and drag coefficient, 296
nearly uniform flow, 236, 238
pentagonal wing, 371
sideslipping wing, 302, 304
symmetric airfoil, 298f
tetragonal wing, 364f
total, 387
triangular wing, 362ff
wedge-shaped airfoil, 298f
wing tips, 387

Line(s),
disturbance, 160
Mach, 160, 211
waximum thickness, 348f
vortex, 90f
weak disturbances, 161, 182, 211
Loop, perfect, 409f

Magnetogasdynamics, 19
Manoeuvrability, craft, 395
Margin, static stability, 55
Method,
Burago's, 275ff
characteristics, 22, 200ff
calculation of supersonic flow parameters, 285ff
and wind tunnel nozzle shaping, 230ff
conformal transformations, 240ff
doublet distribution, 353ff
Glauert-Trefftz, 255
Khristianovich, 269ff
mapping, 240
reverse-flow, 391ff
similarity, 139
small perturbations, 412
sources, 317ff, 425ff
field of application, 351ff
tangent wedges, 292, 489ff
stability derivatives, 490f
Model, vortex,
intricate lifting surface, 430
non-circulatory flow, 431
Modulus,
longitudinal elasticity, 108
shear, 109
Moment(s),
conversion to another coordinate system, 40f
destabilizing, 53f
doublet, 102
gyroscopic, 403f
pitching, 38, 400f, 404f, 416f
positive, 38
rolling, 38, 401f, 416f
stabilizing, 52
tilting, 53
yawing, 38, 401
Moment coefficient, 284, 295, 388
see also Coefficient(s): longitudinal moment, pitching-moment, rolling-moment, yawing-moment
compressible flow, 274
nearly uniform flow, 236, 239
pentagonal wing, 371
sideslipping wing, 302, 304
symmetric airfoil, 298f

Moment coefficient,
tetragonal wing, 364f
wedge-shaped airfoil, 298
Motion(s), *see also* Flow(s)
air, at high speeds, 14
asymmetric, 449f
basic, 411
centre of mass, 407
disturbed, 411
equations, 114ff
fluid,
inviscid compressible, 113f
viscous incompressible, 113
free, 412
stability, 412
integrals, ideal fluid, 134ff
irrotational, 79
lateral, 406f
longitudinal, 406f
at low Strouhal numbers, 444
oscillatory, 414f, *see also* Oscillations
damping, 483
particle, 106
fluid, 75ff
pitching, 406, 408ff
modes, 408ff
proper, 412
sinusoiadal, 410
spiral, 403
stable, 411f
symmetric, 449f
undisturbed, 411
unstable, 411f
unsteady, 415, 459
aerodynamic characteristics, 394ff
vortex-free, 79ff

Neutrality, 55, 57f
Nose, blunted, 23
Nozzle,
critical section area, 231
two-dimensional supersonic, 231ff
shaped, 232f
unshaped, 231
wind tunnel, for supersonic flow, 230f
Number(s),
dimensionless, 17
Froude, 142, 146f
Mach, 47, 141f, 147, 395
critical, 303
initial value, 271, 273f
limiting value, 186f
behind normal shock, 184, 186f
Number(s),
Prandtl, 143, 146f
Reynolds, 47, 141f, 146f, 395
Strouhal, 142, 146, 397f

Operator, Laplacian, 111, 117, 119
Oscillations,
damped, 414
frequency, 414
harmonic, 398
longitudinal, 408
period, 414
periodic, 414
wavelength, 414

Paradox, Euler-D'Alembert, 248
Parameter(s), *see also* Characteristics, Variables
averaged, 31
disturbed supersonic flow, 222ff
stagnation, 191
behind normal shock, 184f
supersonic flow, calculation by method of characteristics, 285ff
sweep, leading edge, 316f
Particle, fluid,
angular strain, 76, 78
energy, 125f
internal, 124
kinetic, 124
linear strain, 76, 78
motion, 75ff
relative volume deformation, 109
Pathline, particle, 71, 74
equation, 71
Pattern, wing,
Chaplygin's horseshoe, 250
vortex, *see also* Model, vortex
non-stationary, 428f
Period, oscillations, 414
Plane,
independent variables, 205
physical, 205
Plate, 241ff, *see also* Wing(s)
fineness, 284
potential, 243
rhombiform, 364
thin, 240ff
at angle of attack, 243ff
Point,
nodal, characteristics, 227
stagnation, 185f, 191f, 268
Polar,
airfoil, 296

Polar,
craft, 46ff
first kind, 46
second kind, 47
shock, 180, 182
Potential,
additional, 310f, 313, 321
complex, 97, 104
circulatory-forward flow, 243
cylinder, 244f
flow over circular cylinder, 241
flow over plate, 241f
non-circulatory flow, 243
parallel flow, 98
disturbance, 457
disturbed velocities, 424
doublet region, 356
elementary source, 318ff
retarded, 425
total, 313f
velocity, *see* Velocity potential
Pressure(s),
absolute, 272
critical, 152, 154f
dimensionless, 145
excess, 235, 265
gradient, 107
in ideal fluid, 26ff
in jet, 152f
linearized flow, 265
nearly uniform flow, 235
ratio, 166, 172f, 189f,
behind shock, 175
normal shock, 184
stagnation, 151, 153, 191f, 224
flow behind shock, 174f
Pressure coefficient, 42, 172, 187f, 281f, 390, 416
compressible flow, 268, 306
conical flow, 362
conversion to various Mach numbers, 271f
hexagonal wing, 370, 372
hypersonic flow, 292, 297
limiting value, 186
nearly uniform flow, 235, 293
ratio, 166, 172f, 186
rectangular wing, 385f
behind shock, 291
sideslipping wing, 302, 304
at stagnation point, 185f, 191, 268
tetragonal wing, 337, 339, 345f
triangular wing, 325ff, 363
Principle,
flow superposition, 105
freezing, 196
inverted flow, 16
Problem, Cauchy, 206ff
Rate, mass flow, 156ff
specific, 156f
Ratio,
aspect,
influence on aerodynamic derivatives, 483
and wing lifting capacity, 482f, 487
density, 165, 172f, 184, 188
dissociation and ionization, 189ff
limiting, 186
lift-to-drag, 46f, *see also* Fineness
maximum, 47
mass velocity, 156f
pressure, 166, 172f, 186
dissociation and ionization, 189f
normal shock, 184
behind shock, 175
pressure coefficient, 186
pressure recovery, across shock, 174
taper, and wing lifting capacity, 483
temperature, 166, 172f, 184, 189ff
dissociation and ionization, 189ff
velocity (speed), 152, 156, 271
flow without separation, 133
and Mach number, 152
Recombination, 60
Region,
doublet,
influence, 356f
potential, 356
integration, 320
multiply connected, 94
simply connected, 94
source influence, 319f
Relaxation, 194
dissociative, 194f
length, 198
in shock waves, 196ff
time, 194, 199
dissociative, 194f
vibrational, 194f
vibrational, 194f
Resistance, *see* Drag
Rotation, about centre of mass, 407
Rule, Prandtl-Glauert compressibility, 482

Scale, turbulence, 30f
Sheet, vortex, *see* Vortex sheet
Shock (s), 156, 159, *see also* Wave(s), shock

Shock(s)
adiabat, 172, 184
angle, 159
attached, 183f, 187
curved, 159f
straight, 159f
curved, 159f, 178f
density ratio, 165, 172f
detached,
curved, 159f
flow over sharp-nosed cone, 177
expansion, 181, 211, 281
at hypersonic velocities, 186ff
lambda-shaped, 275
local, 275
normal, 159, 168f, 184ff
in dissociated and ionized gas, 189ff
oblique, 159, 163ff, 171
in dissociated and ionized gas, 189
formation, 161f
polar, 180, 182
possibility, 182
pressure ratio, 166, 172f
strength, 172
temperature behind, 170, 172
temperature ratio, 166, 172f
thickness, 163
and Mach number, 163
velocity behind, 166, 171
Similarity,
aerodynamic, 138ff
dynamic, 139, 144f
full-scale and model flows, 146f
complete, 147
partial, 146
geometric, 139
Sink,
point,
three-dimensional, 100
two-dimensional, 100
strength, 100
Sound, speed, 67f, 142f, 151f, 155, 264
critical, 151f, 155
local, 152
and pressure, 67f
stagnation conditions, 151
and temperature, 67f
in undisturbed flow, 142f
Source,
distribution density, 318f
disturbances, 159
elementary, potential, 318ff
point,
three-dimensional, 100
Source,
two-dimensional, 99
region of influence, 319f
strength, 100, 427
varying, 425f
vortex, two-dimensional, 103
Span, characteristic dimension, 262
Specific heats,
and pressure, 61f
and temperature, 61f
Speed, *see also* Velocity
fluctuation, 29
sound, *see* Sound, speed
Stability,
dynamic, 394f, 410ff
free motion, 412
motion, 411
neutral, 412
longitudinal, oscillatory, 415
oscillatory, 414
static, 52ff, 415
axisymmetric craft, 54
lateral, 53, 57f
directional, 57f
rolling, 57
longitudinal, 53ff
and elevator deflection, 56
margin, 55
Stability derivatives, 397f, 418f
acceleration, 399
and aerodynamic coefficients, 399
and control surfaces, 402f
conversion, 404ff
dynamic, 398
first order, 398
groups, 399
gyroscopic, 404
Magnus, 403
potential function, 458
rotary, 399
second order, 398
static, 398, 402f
in subsonic flow, 478ff
in supersonic flow, 483ff
wing, 449
Strain, *see also* Deformation
angular 76, 78
linear, 76, 78
specific volume, rate, 78
Stream,
filament, 74
free, 25
function, 89f, 98, 202
Streamlines, 73f, 98, 104f
family, 74, 104
zero, 104f
Strength,
bound vortex, 435

Strength,
free vortex filaments, 433f
shock, 172
sink, 100
source, 100, 425ff
vortex, 430, 433, 435, 447
vortex layer, 430, 433, 447
vortex sheet, 429f
vortex tube, 91
Stress,
friction, *see* Stress, shear
normal, 107ff
shear, 31ff, 107f
in laminar flow, 31f
in turbulent flow, 32ff
Strophoid, 180f
Sublayer,
laminar, 35
viscous, 35
Surface(s),
control, 402f
angles, 407f
discontinuity, 156, *see also* Shock(s)
lifting,
flat, 428
intricate planform, 429f
rectangular, 428f
wave, 211
wing, deformation, 451
System(s),
coordinate, *see* Coordinate systems
disturbed sources, 320
vortex, 429

Temperature,
characteristic, dissociation, 69
critical, 154
ratio, 166, 172f, 184, 189ff
behind shock, 170, 172
stagnation, 153, 191f
Terms, interaction, 402
Theorem,
equivalence, 209
Helmholtz, 78, 91
Kutta-Zhukovsky, 430
Stokes, 93f
Theory,
aerodynamic, of wing, 21
boundary layer, 19
finite-span wing, 21
heat transfer, gas-dynamic, 19
infinite-span wing, 21
linearized, supersonic flow over finite-span wing, 308ff
"loaded line", 253
second-order aerodynamic, 293, 296, 298
Theory,
shock wave, 159ff
vortex, 428ff
Time,
relaxation, 194, 199
dissociative, 194f
vibrational, 194f
Tip(s),
influence on flow over wing, 342f
rounding, 260
sonic, 317
subsonic, 317, 385
supersonic, 317, 364
Trailing edge(s),
sonic, 317, 365
subsonic, 317, 428
supersonic, 317, 364, 366ff, 372ff
Trajectory, particle, *see* Pathline
Triangle, definiteness, 232
Trim, lateral, 58
Trimming, 55
Tube,
stream, 74
vortex, 91
strength, 91
Tunnels, wind, 15
aerodynamic, 29
Turbulence,
homogeneous, 31
initial, 29f
intensity, 29
isotropic, 31
scale, 30f

Variables,
dimensionless, 141f, *see also* Criteria, similarity
Eulerian, 72
kinematic, 395f, 441
Vector,
acceleration, 72
total, 113
aerodynamic forces, resultant, 36f, 252
moment of aerodynamic forces, resultant, 36f
principal, hydrodynamic pressure forces, 246
velocity, 72
divergence, 78, 86
Velocity(ies),
actual, 28
additional, 323, 325f, 328ff, 355
average, 28
calculation, 226ff
at characteristic-shock intersection, 227ff

Velocity,
at characteristic-surface intersection, 227ff
circulation, 91ff
complex, 97, 245, 247
curl, 78
dimensionless, 433, 435
divergence, 78, 86
fictitious, 266
fluctuation, 28
component, 28
free-stream, 25
in gas jet, 150f
induced, 251, 440
by bound vortex, 432, 434
compound due to doublets, 362
by free vortices, 432, 434
by vortex sheet, 434
local, 154
nearly uniform flow, 235
potential, *see* Velocity potential
ratio, 152, 156, 271
fictitious, 266
flow without separation, 133
and Mach number, 152
relative, 152, *see also* Velocity, ratio
behind shock, 166, 171
supersonic, 275, 303f
total, 245
vector, 72
vortex flow, 89
vortex-induced, 94ff
Velocity potential, 79, 98, 103, 105, 201f, 264f, 372ff, 457
dimensionless, 452
doublet, 103
elementary source, 318ff
hexagonal wing, 366, 368f
incompressible flow, 266
induced by doublets, 360
linearized flow, 264f
non-stationary sources, 426f
on plate, 243
rectangular wing, 385f, 389
supersonic unsteady flow, 425
two-dimensional flow, 264
on vortex sheet, 460
Viscosity,
dynamic, 32, 63
and pressure, 63
and temperature, 63f
and fluid flow, 28ff
Volume, relative rate of change, 78
Vortex(ices), 103
bound, 250, 311, 429
strength, 435
linear, 430
velocity induced by, 432, 434
Vortex(ices),
circulation, 439, 447
intensity, 236f
components, 78
core(s), 256
semi-infinite, 253
strength, 253
curvilinear, 95
equivalent, 250
filament, distribution, 429
free, 250, 429
strength, 433f
velocity induced by, 432, 434
horseshoe, 256, 438
oblique, 430ff, 437
infinite, 95f
interaction, 96
layer, strength, 430, 433, 447
line, 95f
model (pattern), 428ff
point, 104
semi-infinite, 96
sheet, *see* Vortex sheet
source, two-dimensional, 103
strength, 430, 433, 435, 447
system, 429
theory, 428ff
tube, 91
strength, 91
Vortex sheet, 251, 256, 312, 429
boundary conditions, 424
strength, 429f
velocity induced by, 312, 434
velocity potential, 460
Vorticity, 91, 93

Warp, geometric, 259
Wave(s),
Mach, 161
three-dimensional, 211
shock, 159, *see also* Shock(s)
formation, 159ff
infinitesimal, 182
weak, 161
simple pressure, 161
spherical, 427
stationary, 159
surface, 211
Wavelet, *see* Line(s), weak disturbances
Wing(s),
conditional, with toothed edges, 464
downwashes, 465
finite-span, 249ff, 254, 258ff, 300f, 308ff
in incompressible flow, 249ff

Wing(s),
finite-span 301
in supersonic flow, 308ff
hexagonal, 364, 366ff, 372ff
with dovetail, 370
infinite-span,
in plane parallel flow, 249f
swept, 299
lift force, 21, 362, 386
lifting capacity,
and aspect ratio, 482f, 487
and taper ratio, 483
in linearized flow, 310ff
non-elliptical planform, 260
optimal planform, 258ff
pentagonal, 364, 370
rectangular, 260, 385ff
aerodynamic characteristics, 385ff
in linearized flow, 386
in supersonic flow, 386
semi-infinite, 328ff
sideslipping, 299f, 302, 304ff
in subsonic compressible flow, 302f
in supersonic flow, 308ff, 315, 344
surface deformation, 451
swept, 300, 341
symmetric airfoil, 312, 317ff
idealized, 313, 317
Wing(s),
taper ratio, 263
tetragonal, 364f
with dovetail, 364f
in supersonic flow, 344
symmetric airfoil, 331ff
with vee-shaped appendage, 364f
thin, 315f
at angle of attack, 351ff
in nearly uniform flow, 351ff
symmetric airfoil, 317ff
trapezoidal, 260, 262
aerodynamic characteristics, 349
lift force, 362f
pressure field, 326, 330
semi-infinite, 328ff
suction force, 362
symmetric about x-axis, 326f, 330f
vortex model, 436ff
zero-thickness, 312f
Work,
external mass forces, 124
surface forces, 124f

Zone, non-equilibrium, 197

TO THE READER

Mir Publishers would be grateful for your comments on the content, translation and design of this book.

We would also be pleased to receive any other suggestions you may wish to make.

Our address is:

Mir Publishers
2 Pervy Rizhsky Pereulok
I-110, GSP, Moscow, 129820, USSR

Printed in the Union of Soviet Socialist Republics

ALSO FROM MIR PUBLISHERS

Similarity and Dimensional Methods in Mechanics

L. I. SEDOV

The book presents the general theory of dimensions of physical quantities, the theory of mechanical and physical scaling, and the theory of modelling.
Typical examples of applications of the similarity and dimensions theory are given, illustrating how the fundamental mechanical relationships are obtained in ship hydrodynamics, aviation, explosion technology, astrophysics, and some other fields. The book presents the general theory of self-similar motions of continuum, the theory of shock wave propagation through gases, the theory of one-dimensional unsteady motions in a gas, the fundamentals of the gas dynamics theory of atomic explosion in the atmosphere, the theory of averaging gas flow characteristics in ducts, the modelling and dimensionless characteristics of compressors, the theory of thrust of jet engines, and the theory of efficiency of the ideal propeller both at subsonic and supersonic flight velocities.

Nikolai F. Krasnov, D.Sc. (Engineering), is a professor and the head of the department of aerodynamics at the N. E. Bauman Higher Engineering College (Moscow, USSR). He graduated from the college in 1946 and completed a post-graduate course, receiving a candidate's degree in 1950. Starting work at the college as a senior instructor, he was appointed an associate professor in 1952, and after receiving his doctor's degree in 1960, a full professor. In addition to teaching at the college, he worked for many years at a research institute.

Nikolai Krasnov is an outstanding scientist in the field of aerodynamics. His numerous monographs have gained deserved popularity and become reference works for college instructors and engineers at aerodynamic laboratories, research institutions, and design offices. He has published important results on determining the velocity and pressure distribution in supersonic flows over bodies of revolution, a method for calculating the flow over bodies in a non-linear formulation based on the method of local cones, relations for calculating the base drag at subsonic and supersonic velocities and the aerodynamic characteristics of elongated bodies of revolution at hypersonic velocities. He has also dealt with non-stationary supersonic flow over slender bodies, "inviscid" flow, and skin friction and heat transfer on blunt curved surfaces. His monographs include *Rocket Aerodynamics*, *Applied Aerodynamics*, *Fundamentals of Aerodynamic Calculations* (in Russian), and *Aerodynamics of Bodies of Revolution* (translated into English).

Dr. Krasnov has worked particularly on finding engineering methods of calculating aerodynamic parameters. He has proposed approximating relations for finding a number of aerodynamic parameters of craft elements, and also interference characteristics.

His latest interests involve aerodynamic control. Some of his results in this field were published in *Control and Stabilization in Aerodynamics* (in Russian). Nikolai Krasnov received the USSR State Prize in 1982 for the textbook *Aerodynamics*.